

B. STOCK ASSESSMENT FOR ATLANTIC SEA SCALLOPS IN 2014, UPDATED THROUGH 2013

Invertebrate Subcommittee¹

B1. TERMS OF REFERENCE

- 1) Estimate removals from all sources including landings, discards, incidental mortality, and natural mortality. Describe the spatial and temporal distribution of landings, discards, and fishing effort. Characterize the uncertainty in these assumptions and sources of data. If possible using sensitivity analyses, consider the potential effects that changes in fishing gear, fishing behavior, and management may have on the assumptions.
- 2) Present the survey data being used in the assessment (e.g., regional indices of relative or absolute abundance, recruitment, size data, etc.). Characterize the uncertainty and any bias in these sources of data.
- 3) Investigate the role of environmental and ecological factors in determining recruitment success. If possible, integrate the results into the stock assessment.
- 4) Estimate annual fishing mortality, recruitment and stock biomass for the time series, and estimate their uncertainty. Report these elements for both the combined resource and by sub-region. Include a historical retrospective analysis to allow a comparison with previous assessment results and previous projections.
- 5) State the existing stock status definitions for “overfished” and “overfishing”. Then update or redefine biological reference points (BRPs; point estimates or proxies for B_{MSY} , $B_{THRESHOLD}$, F_{MSY} and MSY) and provide estimates of their uncertainty. Comment on the scientific adequacy of existing BRPs and the “new” (i.e., updated, redefined, or alternative) BRPs.
- 6) Evaluate stock status with respect to the existing model (from previous peer reviewed accepted assessment) and with respect to a new model or model formulation developed for this peer review.
 - a. Update the existing model with new data and evaluate stock status (overfished and overfishing) with respect to the existing BRP estimates.
 - b. Then use the newly proposed model and evaluate stock status with respect to “new” BRPs and their estimates (from TOR-5).
- 7) Evaluate the realism of stock and catch projections and compute the statistical distribution (e.g., probability density function) of the OFL (overfishing level).
 - a. Provide numerical annual projections (through 2016). Each projection should estimate and report annual probabilities of exceeding threshold BRPs for F , and probabilities of falling below threshold BRPs for biomass. Use a sensitivity analysis approach in which a range of assumptions about the most important uncertainties in the assessment are considered (e.g., terminal year abundance, variability in recruitment).
 - b. Comment on the realism of the projections. Consider the major uncertainties in the assessment as well as sensitivity of the projections to various assumptions. Describe this stock’s vulnerability (see “Appendix to the SAW TORs”) to becoming overfished, and how this could affect the choice of ABC.

¹ See Appendix B1 for meetings and members of the Invertebrate Subcommittee who helped prepare this assessment.

- 8) Review, evaluate and report on the status of the SARC and Working Group research recommendations listed in most recent SARC reviewed assessment and review panel reports. Identify new research recommendations.

B2. EXECUTIVE SUMMARY

TOR-1 (Estimate removals from landings, discards, incidental mortality, and natural mortality...) U.S. sea scallop landings were high and stable during 2003-2012, averaging about 25,000 mt meats, almost three times higher than the long-term 1950-1999 mean. Landings in 2013 declined to 18,641 mt meats, the lowest since 2000, but still over twice the long-term mean. About 65% of landings during 2003-2012 were from the Mid-Atlantic region, 32% from Georges Bank, 2% from Southern New England and under 1% from the Gulf of Maine; the proportion from the Mid-Atlantic was higher than in earlier periods. A shift in the fishery towards Georges Bank occurred in 2013, when 64% of the landings were from Georges Bank, 32% from the Mid-Atlantic, 2% from Southern New England and 3% from the Gulf of Maine. Discards were highly variable with year and region. Maximum discards were 2553 mt meats in 2003. Discards have decreased since 2004, likely due to changes in gear regulations; estimated discards in 2013 were 437 mt meats. Incidental fishing mortality (mortality of scallops that interact with the gear but are not caught) is highly uncertain; based on two studies from the 1970s and 1980s, incidental fishing mortality on small scallops was estimated as 0.2 times fully recruited fishing mortality on Georges Bank, and 0.1 times fully recruited fishing mortality in the Mid-Atlantic. Natural mortality for all but the largest size group was estimated at 0.16 for Georges Bank and 0.2 for the Mid-Atlantic, an increase from 0.12 and 0.15, respectively, in the last assessment. Plus group natural mortality was estimated as 1.5 times that of smaller scallops.

TOR-2 (Survey data). A scallop survey using a lined scallop dredge and a random-stratified design has been conducted every year since 1979 on Georges Bank and the Mid-Atlantic Bight. Based on this survey, biomass and abundance remained relatively low from 1979-1995 on Georges Bank and 1979-1998 in the Mid-Atlantic. The indices rose dramatically starting in 1995 on Georges Bank and 1998 in the Mid-Atlantic, and were fairly stable from 2003-2009. Decreases have been observed in both regions in recent years, although the indices are still well above levels observed previous to 1995. Paired tows experiments that compared dredge catches to densities observed using the HabCam towed camera system estimated the efficiency of the dredge as 0.41 on sand and 0.27 on gravel/cobble habitat (Appendix B4).

A video drop camera survey was conducted between 2003 and 2012 on Georges Bank and the Mid-Atlantic, using a systematic grid design. This survey generally shows declining trends, with biomass and abundance somewhat less than the expanded dredge survey.

A towed camera (“HabCam”) survey was used for the first time in this assessment (Appendix B6). The survey was conducted during 2011-2013 on Georges Bank and 2012-2013 in the Mid-Atlantic. HabCam is towed behind a vessel, taking rapid-fire photographs of the sea bottom. Estimates from HabCam were obtained using a model-based approach, using a zero-inflated generalized additive model combined with kriging of the residuals. Biomass and abundance estimates from HabCam were similar to those from the dredge.

TOR-3 (Environmental effects on recruitment). Two putative environmental factors were

explored as predictors of recruitment in the Mid-Atlantic Bight (Appendix B8). A tentative relationship was found between food supply (phytoplankton) and recruitment. Additionally, the spatio-temporal distribution of the sea star *Astropecten americanus*, a predator of small invertebrates, including juvenile sea scallops, appear to correlate to the spatio-temporal patterns of scallop recruitment in the southern Mid-Atlantic Bight.

TOR-4 (Estimation of F, Biomass, Recruitment). A forward projecting size-structured estimation model (CASA) was used for estimation of biomass, fishing mortality and recruitment. Growth in the model was based on growth increment data from shell growth ring analysis. Three models were used, one each for the open and closed portions of Georges Bank, and a model for the Mid-Atlantic. The models appeared to give good estimation for some years, but in the Georges Bank Closed and Mid-Atlantic models, estimates of abundance and biomass had poor diagnostics in years associated with very strong year classes. Model estimated biomass and abundance generally declined, and fishing mortality increased, during 1975-1995. The biomass in the Georges Bank closed areas increased rapidly after these areas were closed to fishing in 1994. Estimated biomass in Georges Bank open and the Mid-Atlantic increased more gradually as fishing mortality was slowly reduced starting around 1998. Estimated overall fully recruited fishing mortality in 2013 was 0.32, and biomass was estimated at 132,561 mt meats. This was slightly higher than direct expanded estimates from the dredge survey (129,113 mt meats) and HabCam (111,157 mt meats). Explorations were made in incorporating density-dependent mortality on juvenile scallops into the CASA model in order to better model the population dynamics of large year classes, and initial results appear to be promising.

TOR-5 (Stock status definition). The SYM (Stochastic Yield Model) was used to estimate reference points. This model explicitly takes into account parameter uncertainty, including key uncertainties in natural mortality and stock-recruit relationships, when estimating maximal sustainable yield (MSY) and the associated biomass and fishing mortality reference points B_{MSY} and F_{MSY} . Estimated whole stock MSY, F_{MSY} and B_{MSY} were 23,798 mt meats, 0.48 and 96,480 mt meats, respectively.

TOR-6 (Evaluate stock status). The estimated fishing mortality in 2013 was 0.32, which was below both the previous and new F_{MSY} estimates (0.38 and 0.48, respectively). The estimated biomass in 2013 is 132,561 mt meats. The stock is considered overfished if the biomass is less than half of B_{MSY} . B_{MSY} was estimated as 125,358 in the previous assessment and 96,480 mt meats in this assessment. Thus, the 2013 stock biomass was above both B_{MSY} estimates. Therefore, it can be concluded that the sea scallop stock was neither overfished nor was overfishing occurring in 2013, regardless of whether the previous or new reference points are used.

TOR-7 (Projections) Projections were conducted using the SAMS (Scallop Area Management Simulator), which models scallops on a relatively fine spatial scale in order to model effects such as closures and reopenings of areas. Example simulations, based on expected management during 2014-2016, predicts gradual increases in biomass and landings.

B3. INTRODUCTION AND LIFE HISTORY

The Atlantic sea scallop, *Placopecten magellanicus*, is a bivalve mollusk that occurs on the eastern North American continental shelf from Cape Hatteras to the Gulf of St. Lawrence and Newfoundland. Major aggregations in US waters occur in the Mid-Atlantic from Virginia to Long Island, on Georges Bank, in the Great South Channel, and, to a lesser extent, in the Gulf of Maine (Hart and Chute 2004). In Georges Bank and the Mid-Atlantic, sea scallops are harvested primarily at depths of 30 to 100 m, whereas the bulk of landings from the Gulf of Maine are from near-shore waters. This assessment focuses on the two main portions of the sea scallop stock and fishery, Georges Bank in the north and the Mid-Atlantic in the south (Figure B3.1). Results for Georges Bank and the Mid-Atlantic are combined to evaluate the stock as a whole.

US landings during 2003-2012 exceeded 24,000 mt each year, roughly twice the long-term mean, but declined to 18,641 mt in 2013.² US ex-vessel sea scallop revenues were over \$500 million in 2011-2012 and \$465 million in 2013, making the sea scallop fishery the most valuable fishery in the US during these years. Unusually strong recruitment in the Mid-Atlantic Bight area and increased yield per recruit due to effort reduction, area rotation, and gear restrictions were the key contributors to high landings during the most recent period. The drop off in 2013 reflects weaker recruitment in the Mid-Atlantic during 2009-2011 (2007-2009 year classes). The mean meat weight of landed scallops was over 25 g after 2005 (when the Amendment 10 management plan went into effect), compared to less than 14 g during the early to mid 1990s.

Access area closures and openings used for rotational fishery management have had a strong influence on sea scallop population dynamics (Figure B3.1). Roughly 40% of the productive scallop grounds on Georges Bank and Nantucket Shoals were closed to both groundfish and scallop gear during most of the time since December 1994. Portions of the closed areas have been reopened to limited fishing during 1999-2000 and since 2004. In the Mid-Atlantic, there have been four rotational scallop areas. These areas are generally closed for two to three years, and then reopened to allow harvesting. The areas are closed again after observations of strong recruitment until the small scallops grow to fishable size.

Sea scallops in U.S. waters have been assessed using forward projecting size-structured models since 2007. Fishing mortality, biomass and recruitment are estimated using a version of the CASA (Catch-At-Size Analysis) model based loosely on Sullivan et al. (1990). Forecasts are done using the SAMS (Scallop Area Management Simulator) model, which models the scallop fishery and population on a relatively fine regional scale, in order to help understand the effects of area management such as closing and reopening areas to fishing. Reference points are calculated using the SYM model (Stochastic Yield Model, Hart 2013). All of these models were specifically developed for use with sea scallops.

² In this assessment, landings and biomass are reported in metric tons (mt) of scallop meats, unless otherwise indicated.

Life History and Distribution

Sea scallops are found in the Northwest Atlantic Ocean from North Carolina to Newfoundland along the continental shelf typically on firm sand and gravel bottoms (Hart and Chute 2004). Sea scallops feed by filtering phytoplankton, microzooplankton, and detritus particles. Sea scallops are broadcast spawners with separate sexes. Sea scallops mature at about age 2 (~40-75 mm SH³), but gamete production is limited until age 4. Larvae are planktonic for 5-8 weeks before settling to the bottom. Scallops fully recruit to the NEFSC lined dredge survey at 40 mm SH, and to the current commercial fishery at around 90-105 mm SH, although sea scallops between 70-90 mm were common in landings prior to 2000.

According to Amendment 10 of the Atlantic Sea Scallop Fishery Management Plan, all sea scallops in the US EEZ belong to a single stock but there are two principal stock assessment regions (Mid-Atlantic and Georges Bank). The US sea scallop stock can be divided into Georges Bank, Mid-Atlantic, Southern New England, and Gulf of Maine regional components based on survey data, fishery patterns, and other information (NEFSC 2004, Figure B3.1). However, Southern New England is considered to be part of the Georges Bank region for assessment modeling purposes. Most of the scallops in the Gulf of Maine lie in state waters, and are managed by the states of Maine and Massachusetts. See Appendix B7 for an assessment of sea scallops in the Northern Gulf of Maine federal management area.

Growth

Sea scallop growth can be inferred using visible “rings” laid down on the shell. These rings have been confirmed as annual marks, although the year one ring is typically missing (Stephenson and Dickie 1954, Merrill et al. 1966, Hart and Chute 2009a, Chute et al. 2012). Studies in Canadian waters indicated that the rings are laid down during the winter (Stephenson and Dickie 1954, Tan et al. 1988) but a recent stable isotope study showed that the rings from scallops in US waters are laid down near the temperature maximum, likely coinciding with the fall spawn (Chute et al. 2012).

Obtaining absolute age from shell rings can be problematic for some scallops because the first few rings may be missing or obscure, especially on older scallops (Claereboudt and Himmelman, 1996). For this reason, Hart and Chute (2009b) treated the distance between rings as annual growth increments, with age unknown. They introduced a method to estimate von Bertalanffy growth parameters from such data which includes random effects on both L_{∞} and K to take into account variation in growth among individuals. This method gives estimates of mean von Bertalanffy coefficients and the variance of these parameters among individuals in the population. These parameters and variances are used to estimate growth transition matrices for CASA. The von Bertalanffy parameter t_0 cannot be estimated using growth increments, but estimates of this parameter are not required in a size-structured assessment.

The growth estimates in Hart and Chute (2009b) were based on scallops collected between 2001 and 2007. NEFSC (2010) added additional data from shells collected in 2008. New data from

³ Scallop body size is measured as shell height (SH), the maximum distance between the umbo and shell margin.

shells collected during 1988, 1993 and 2009-2012 are used in this assessment (Table B3-1). Growth on Georges Bank showed little temporal variability during the 2001-2012 time period, but the shells collected in 2010-2012 in the Mid-Atlantic appear to grow slightly faster than those from 2001-2009 (Figure B3.2).

Scallop growth during 1988 and 1993 was substantially slower than in recent years (Figure B3.3). A comparison of the growth increments from these years to 2001-2012 indicate little difference between these periods for scallops less than 76 mm, the ring size for commercial dredge gear before 1994 (Figure B3.3). However, there appears to have been less and less fast growing scallops as shell height increased. This pattern is consistent with preferential removal of faster growing scallops by the fishery. In part, this may be due to a “Lee’s effect”, where the faster growing scallops recruit earlier to the fishery and die sooner. However, spatial fishery patterns likely also play a role because areas containing faster growing scallops were likely fished harder. Similarly, commercial-sized scallops in the Georges Bank closed areas grow faster and have a greater asymptotic size than in the areas opened to fishing (Table B3-1; Figure B3.2; Hart and Chute 2009b).

Maturity and fecundity

Scallops reach sexual maturity at about age 2. Sea scallops > 40 mm SH are reliably detected in surveys used in this assessment and are all considered mature individuals. Thus biomass estimates for scallops 40+ mm in this assessment are effectively spawning biomass estimates. However, individuals younger than 4 years may contribute little to total egg production because fecundity increases rapidly with age (MacDonald and Thompson 1985; NEFSC 1993).

Sea scallop spawning generally occurs in late summer or early autumn throughout their range. Spring spawns and minor “dribble” spawns may also occur at other times. The spring spawn is often strong in the Mid-Atlantic Bight (DuPaul et al. 1989). Spring spawns on Georges Bank are less substantial but may be increasing in strength with warmer winter water temperatures (Almeida et al. 1994, Dibacco et al. 1995, Thompson et al. 2014). Out of 14 scallops (6 from Georges Bank and 8 from the Mid-Atlantic) analyzed by stable isotopes, only one, from Delmarva in the southern Mid-Atlantic, was found to be spring-spawned, while the others were fall spawned (Chute et al. 2012). No assumption regarding timing of spawning is made in this assessment, as it is not required for size-structured models.

Shell height/meat weight relationships

Shell height-meat weight relationships allow conversion from numbers of scallops at a given size to meat weights. For sea scallops $W = \exp(\alpha + \beta \ln(H))$, where W is meat weight in grams and H is shell height in mm (Appendix B3). Meat weights depend on factors which affect feeding and metabolic rates, including depth and location. Meat weights decrease with depth, probably because of reduced food (phytoplankton) supply.

Shell height/meat weight data were collected during annual NEFSC sea scallop surveys during 2001-2013. Unlike previous studies, where meats were either frozen or brought in live and then weighed on land, meats were weighted at sea just after they were shucked (Hennen and Hart

2012). These data have been used in scallop assessments since 2007, and were updated for this assessment (Appendix B3).

Depth and subarea had a significant effect on the shell height/meat weight relationships (Appendix B3). In this assessment, covariate-adjusted shell height/meat weight relationships were used to calculate survey biomass, while simple relationships (depth omitted) were used in modeling (CASA, SAMS and SYM) where depth is not explicit (Table B3.2).

Meat weights for scallops in the commercial fishery may differ from those predicted from research survey data for a number of reasons. First, the shell height-meat weight relationship varies seasonally, in part due to the reproductive cycle, so that meat weights collected during the NEFSC survey in July and August may differ from those in the rest of year (Hennen and Hart 2012). Additionally, commercial fishers concentrate on speed, and often leave some meat on the shell during shucking (Naidu 1987, Kirkley and DuPaul 1989). On the other hand, meats in fishery catches may gain weight due to water uptake during storage on ice (DuPaul et al. 1990). Finally, fishers may target areas with relatively large meat weight at shell height, and thus may increase commercial meat weights compared to that collected on the research vessel.

Observer data were used to adjust predicted meat weights based on survey data for seasonal variation and for commercial fishing practices. Annual commercial meat weight anomalies were computed based on the seasonal patterns of landings together with the mean monthly commercial meat weight at shell height. The average annual meat weight anomalies are used in assessment modeling to calculate fishery meat weights.

Shell height/Meat weight relationships

	Mid-Atlantic		Georges Bank	
	a	B	a	b
NEFSC (2014)	-9.33	2.66	-8.79	2.55
NEFSC(2014) , open areas			-9.37	2.65
NEFSC (2014), closed areas			-8.26	2.45
Hennen Hart (2012)/NEFSC 2010	-10.8	2.97	10.25	2.85
Lai and Helser (2004)	-12.34	3.28	11.44	3.07
Serchuk and Rak (1983)	-12.16	3.25	-11.77	3.17
Haynes (1966)	-11.09	3.04	-10.84	2.95

Natural mortality

Assessments prior to 2010 assumed a natural mortality rate of $M = 0.1$ based on Merrill and Posgay (1964). A reanalysis of the Merrill and Posgay study indicated that an unbiased estimate for M was approximately 0.12 (NEFSC 2010), with a corresponding estimate in the Mid-Atlantic of 0.15. Hart et al. (2013) estimated M within the CASA stock assessment model as 0.16 in the Georges Bank closed areas.

No direct estimate of M is available for Mid-Atlantic sea scallops. The ratio of the growth coefficient K to M is generally regarded as a life history invariant that should be approximately constant for similar organisms (Beverton and Holt 1959, Chernov 1993). Applying this idea and using updated growth parameter estimates indicates that sea scallop natural mortality in the Mid-Atlantic should be about 0.53/0.44 that of Georges Bank (see the estimates of growth coefficients above). Using $M = 0.16$ in Georges Bank, M is about 0.2 in the Mid-Atlantic. These are the estimates used in this assessment for all but the largest size group (plus group).

MacDonald and Thompson (1986) directly observed sea scallop natural mortality in a near-shore population off of Newfoundland. They found that mortality was low from 60-130 mm SH, but increased substantially for scallops larger than 130 mm. A large cohort of 2 year old scallops (1997 cohort) was observed in 1999 at a station in the Nantucket Lightship Closed Area in an area where recruitment is rare and sporadic and which has been closed to scallop fishing since 1994. A second, smaller cohort of 2 year olds was observed there in the 2000 survey, but almost no recruitment has been observed at this site since. This station has been sampled using the NEFSC survey dredge every year since 2003. The catches at this station indicate low mortality until the dominant 1997 cohort reached 11 years old, after which numbers caught declined substantially. Both these studies thus suggest that natural mortality of very old scallops may be higher than younger ones. Likelihood profiles from the Georges Bank closed CASA model, discussed in section 6, suggest the mortality of the plus group is most likely about 1.5 times that of smaller scallops. Therefore, for this assessment, the plus group natural mortality was assumed to be 1.5 times that of smaller sizes, (0.24 on Georges Bank and 0.3 in the Mid-Atlantic).

MacDonald and Thompson (1986) observed scallops as old as 19 years. The oldest observed in the NEFSC age and growth program are at least 18 years old on Georges Bank and 15 years old in the Mid-Atlantic. These oldest ages are consistent with the natural mortality assumptions given above.

Table B3.1. Regional von Bertalanffy growth parameter estimates from mixed-effects models for sea scallops. SD L_{∞} and SD K are the estimated standard deviation of these parameters among individuals in the population.

Source	Region	Years	L_{∞}	SE	K	SE	SD L_{∞}	SD K
NEFSC (2014)	Mid-Atlantic	2010-2012	138.0	0.5	0.522	0.005	12.7	0.05
	Mid-Atlantic	2001-2009	131.7	0.3	0.535	0.003	13.6	0.13
	Mid-Atlantic	1988,1993	118.9	2	0.551	0.02	20.8	0.15
	Georges Bank (All)	2001-2012	144.0	0.2	0.44	0.002	13.9	0.11
	Georges Bank (All)	1988,1993	133.4	1.4	0.498	0.013	9.2	0.09
	Georges Bank (Closed)	2001-2012	147.6	0.3	0.426	0.002	12.8	0.11
	Georges Bank (Open)	2001-2012	137.4	0.3	0.442	0.002	11.4	0.11
NEFSC (2010)	Mid-Atlantic	2001-2008	132.1	0.3	0.527	0.004	13.3	0.14
	Georges Bank	2001-2008	144.0	0.3	0.429	0.002	14.5	0.11
Hart & Chute (2009)	Mid-Atlantic	2001-2007	133.3	0.4	0.508	0.004	13.4	0.13
	Georges Bank (All)	2001-2007	143.9	0.3	0.427	0.002	14.8	0.11
	Georges Bank (Open)	2001-2007	136.3	0.5	0.457	0.004	15.1	0.12
	Georges Bank (Closed)	2001-2007	147.8	0.3	0.413	0.003	13.2	0.1
Serchuk et al (1979)	Mid-Atlantic	?	151.8		0.300			
	Georges Bank	?	152.5		0.337			

Table B3.2. Simple shell height-meat weight relationships $W = \exp(\alpha + \beta \ln(H))$ for sea scallops. W is meat weight in grams and H is shell height in mm.

	Mid-Atlantic		Georges Bank	
	a	b	a	b
NEFSC (2014)	-9.33	2.66	-7.46	2.61
NEFSC(2014), open areas			-9.37	2.65
NEFSC (2014), closed areas			-8.26	2.45
Hennen & Hart (2012)/NEFSC 2010	-10.8	2.97	10.25	2.85
Lai and Helser (2004)	-12.34	3.28	11.44	3.07
Serchuk and Rak (1983)	-12.16	3.25	-11.77	3.17
Haynes (1966)	-11.09	3.04	-10.84	2.95

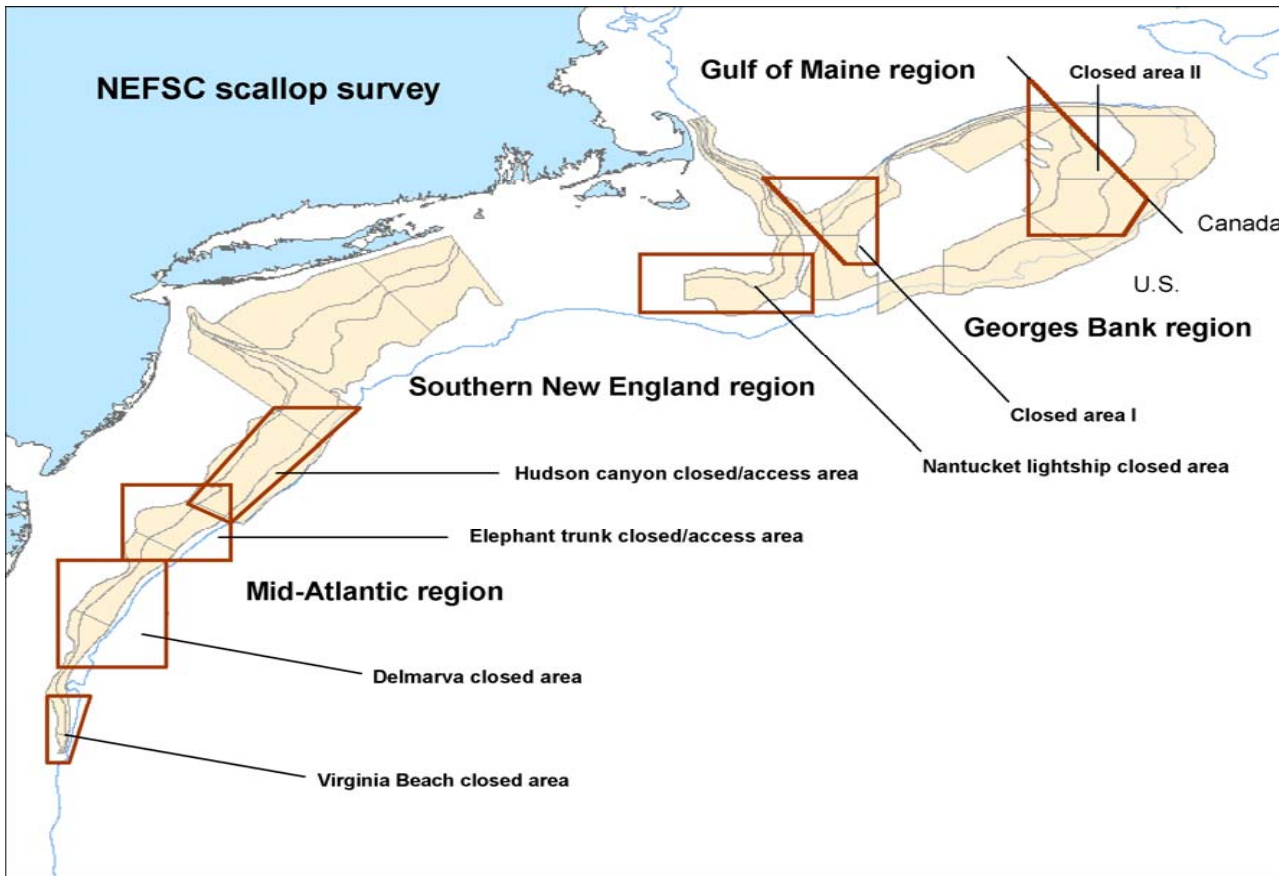


Figure B3.1 Stock assessment and management areas for sea scallops in US waters. The NEFSC scallop survey strata shown in yellow are the areas that are regularly surveyed by the NEFSC dredge survey, which have with appreciable scallop densities.

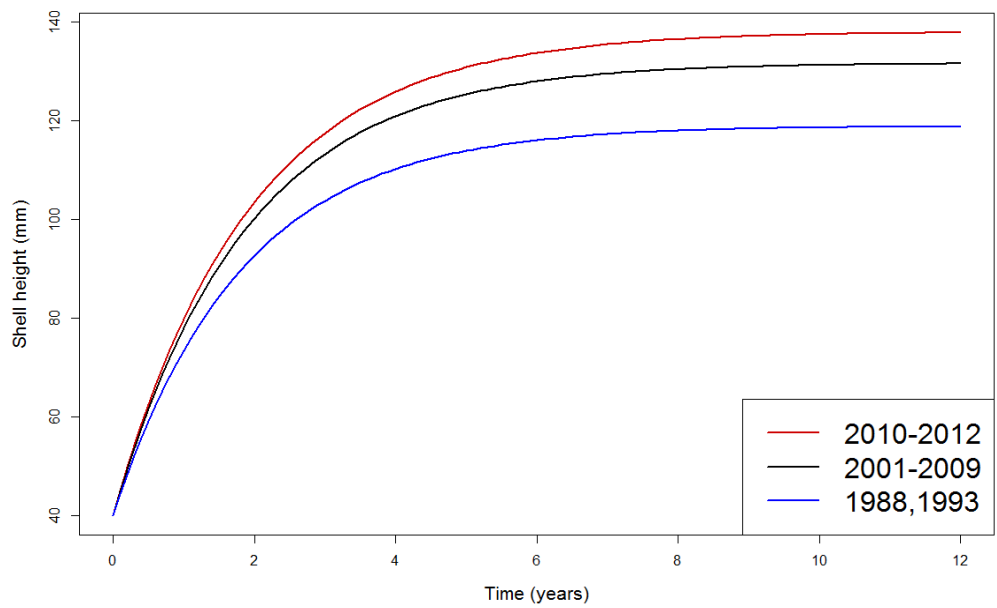
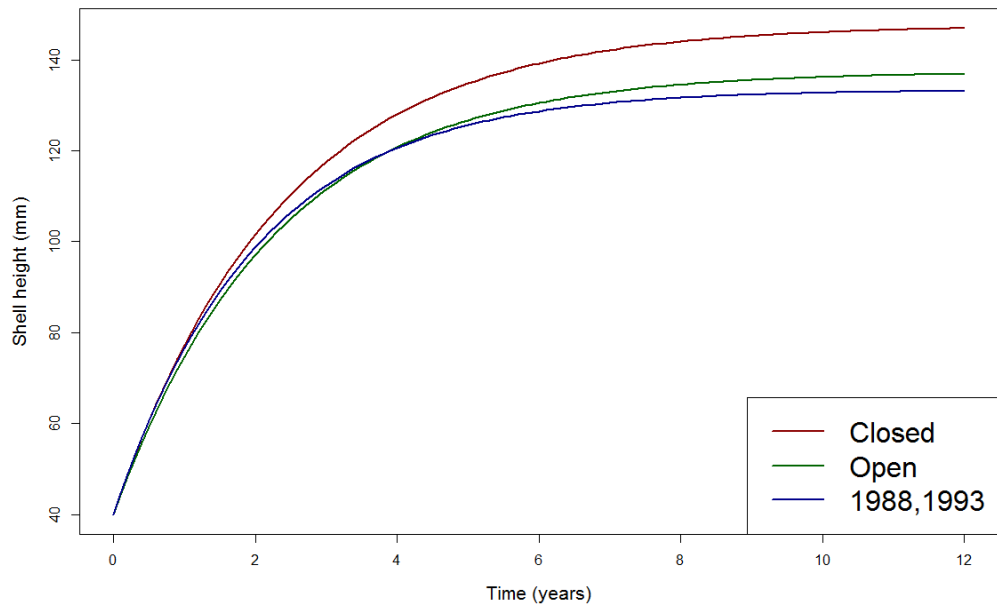


Figure B3.2. Growth curves for sea scallops in the Georges Bank (top) and Mid-Atlantic regions (bottom) for various areas and time periods. The Georges Bank open and closed area growth curves were based on shells collected between 2001-2012.

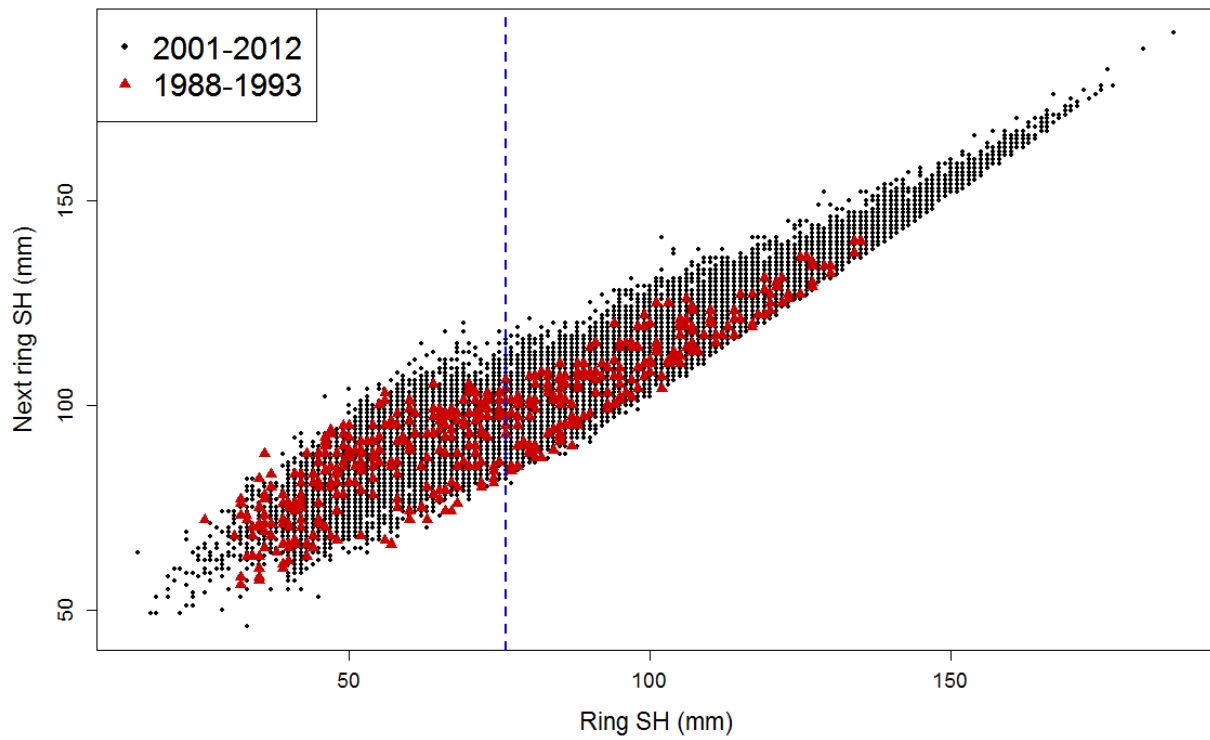


Figure B3.3. Comparison of growth increments from shells collected on Georges Bank between 2001 and 2012 and those collected which fishing effort was much higher (1988,1993). The dashed blue line is at 76 mm, the diameter of most commercial dredge rings prior to 1994.

B4. COMMERCIAL AND RECREATIONAL CATCH (TOR-1)

The US sea scallop fishery is conducted mainly by about 350 vessels with limited access permits. Two types of allocations are given to each limited access vessel. The first is a number of trips to rotational access areas that had been closed to scallop fishing in the past (with a trip limit, typically 12,000-18,000 lbs or 5,443-8,165 kg meats). The second is days at sea (DAS), which can be used in areas outside the closed and access areas. Vessels fishing under days at sea allocations are restricted to a 7 man crew and must shuck their scallops at sea in order to limit their processing power.

The remainder of landings come from vessels operating under "General Category" permits that are currently restricted to 272 kg meats (600 lbs) per trip, with a maximum of one trip per day. Landings from these vessels were less than 1% of total landings in the late 1990s, but increased to about 10% of landings during 2007-2009, and currently constitute about 6-7% of total landings. This type of permit had been open access, but was converted to an individual transferable quota (ITQ) fishery in March 2010.

Principal ports in the sea scallop fishery are New Bedford, MA, Cape May, NJ, and Hampton Roads, VA, but lesser amounts of scallops are landed in many ports from North Carolina to Maine. Toothless offshore (New Bedford style) scallop dredges are the main gear type in all regions, although some scallop fishing is done with otter trawls in the Mid-Atlantic, and a small fraction of the catch in the Gulf of Maine comes from divers. A typical limited access vessel tows two 4-4.6 m dredges, but some limited access vessels are restricted to a single 3.2 m dredge, and most general category vessels also use a single smaller dredge. Recreational catch is negligible.

Management history

The sea scallop fishery in the US EEZ is managed under the Atlantic Sea Scallop Fishery Management Plan (FMP) which was implemented on May 15, 1982. From 1982 to 1994, the primary management control was a minimum average meat weight requirement for landings. In 1984, Georges Bank was divided into US and Canadian EEZs; prior to this time, US and Canadian vessels fished on both sides of the current boundary.

FMP Amendment 4 (NEFMC 1993), implemented in 1994, changed the management strategy from meat count regulation to limited access combined with effort control and gear regulations. Limited access permits were issued to vessels with a history in the fishery; no new permits have been issued since. Incremental restrictions were made on days-at-sea (DAS), minimum ring size, and crew limits; DAS has been reduced from over 200 in 1994 to 31 in open areas in 2014. The minimum size of the rings in the dredge bag was gradually been increased from 76 mm in 1994 to 102 mm since December 2004. The minimum size of the twine top mesh has also been gradually increased from 6" to 10" since December 2004; while this measure was intended mainly to allow better escapement of finfish, it also likely improves the escapement of small scallops.

In addition to these measures, three large areas on Georges Bank and Nantucket Shoals were closed to groundfish and scallop fishing in December 1994 (Figure B3-1). Scallop biomass

rapidly increased in these areas between 1994-2004 (Hart and Rago 2006). Two areas in the Mid-Atlantic were closed to scallop fishing in April 1998 for three years in order to similarly increase scallop biomass and mean weight.

Sea scallops were formally declared overfished in 1997, and Amendment 7 was implemented during 1998 with more stringent days-at-sea limitations and a mortality schedule intended to rebuild the stocks within ten years. Subsequent analyses considering effects of closed areas indicated that the stocks would rebuild with less severe effort reductions than called for in Amendment 7, so the days at sea limitations were relaxed. A combination of the closures, effort reduction, gear and crew restrictions led to a rapid increase in biomass (Hart and Rago 2006), and sea scallops were rebuilt by 2001.

Prior to 2004, there were a number of ad hoc area management measures, including the Georges Bank and Mid-Atlantic closures in 1994 and 1998, limited reopenings of portions of the Georges Bank closed areas between June 1999 and January 2001, and reopening of the first Mid-Atlantic rotational areas in 2001. A new set of regulations was implemented as Amendment 10 during 2004. This amendment formalized an area based management system, with provisions and criteria for new rotational closures, and separate allocations (DAS or TACs) for reopening closed areas (rotational areas) and general open areas. The three Georges Bank closed areas have been divided into access areas, where fishing is periodically permitted, and long-term closures, where no scallop fishing is permitted (Figure B3.1). In most years, one or two of the three Georges Bank access areas are open to fishing, limited by a fixed number of trips and a trip limit.

Unlike the Georges Bank closed areas, which are generally closed to all scallop and groundfish fishing, the Mid-Atlantic rotational areas are specific to the scallop fishery (Figure B3.1). Two areas (Hudson Canyon South and Virginia Beach) were closed in 1998 and then reopened in 2001. Although the small Virginia Beach closure in the far south of the scallops' range was unsuccessful, scallop biomass built up in Hudson Canyon Closed Area while it was closed, and substantial landings were obtained from Hudson Canyon during 2001-2007. This area was again closed in 2008, reopened in 2011 and closed for a third time in 2014. A third rotational closure, the Elephant Trunk area east of Delaware Bay, was closed in 2004 after extremely high densities of small scallops were observed in surveys during 2002 and 2003. About 30,000 mt of scallops worth about \$500 million were landed from that area after it was reopened in 2007. It was closed again in December 2012 after high numbers of small scallops were again observed in surveys. A fourth closed area, Delmarva, directly south of the Elephant Trunk area, was closed in 2007, reopened in 2009, closed in 2012 and reopened in 2014.

Landings

Sea scallop landings in the US increased substantially after the mid-1940's (Figure B4.1), with peaks occurring around 1960, 1978, 1990, and 2004. Maximum landings were 29,109 mt meats in 2004. Landings during 2001-2012 were all over 20,000 mt, whereas the maximum in the 20th century was 17,107 mt in 1990. Landings in 2013 were 18,641 mt, their lowest since 2000, but still higher than any year prior to 2001.

Landings from the Georges Bank and the Mid-Atlantic regions have dominated the fishery since 1964 (Table B4-1; Figure B4.2). Proration of total commercial sea scallop landings into Georges Bank, Mid-Atlantic, Southern New England, and Gulf of Maine used standard allocation procedures (Wigley et al. 2008).

US Georges Bank landings had peaks during the early 1960's, around 1980 and 1990, but declined precipitously during 1993 and remained low through 1998 (Figure B4-2). Landings in Georges Bank during 1999-2004 were fairly steady, averaging almost 5000 mt annually, and then increased in 2005-2006, primarily due to reopening of portions of the groundfish closed areas to scallop fishing. Georges Bank landings increased again in 2012-2013, mainly due to shift of "open" effort from the Mid-Atlantic to Georges Bank

Prior to the mid-1980s, Mid-Atlantic landings were generally lower than those on Georges Bank. Mid-Atlantic landings during 1962-1982 averaged less than 1800 mt per year (Figure B4.2). An upward trend in both recruitment and landings has been evident in the Mid-Atlantic since the mid-eighties. Landings peaked in 2004 at 24,494 mt. Mid-Atlantic landings declined after 2011, reflecting the poor 2007-2009 year classes there and concomitant effort shifts onto Georges Bank.

Landings from other areas (Gulf of Maine and Southern New England) are minor in comparison (Table B4-1). Most of the Gulf of Maine stock is assessed and managed by the State of Maine because it is primarily in state waters. However, the Northern Gulf of Maine management area is managed by the New England Fishery Management Council with separate regulations (see Appendix B7 for an updated assessment). Gulf of Maine landings were less than 1% of the total US sea scallop landings in most recent years. Maximum landings in the Gulf of Maine were 1,614 mt during 1980.

Fishing effort and LPUE

Prior to 1994, landings and effort data were collected during port interviews by port agents which was combined with dealer data. Since 1994, commercial data are available in dealer reports (DR) and in vessel trip report (VTR) logbooks. DR give landings, but not area fished, and have reported landings by market category since 1998. VTR data contain information about area fished, fishing effort, and retained catches of sea scallops. Ability to link DR and VTR reports in data processing is reduced by incomplete data reports and other problems, although there have been significant improvements recently. A standardized method (Wigley et al. 2008) for matching DR to VTRs and assigning landings to fishing areas was used in this assessment for 1994-2013.

Landings per unit effort (LPUE, Figure B4.3) was computed as landings per day fished (days fished represent the time in days that gear was fishing). This was obtained from the port interview records for larger vessels prior to 1994 and from at-sea observers on limited access vessels afterwards. LPUE shows a general downward trend from the beginning of the time series to around 1998, with occasional spikes upward due to strong recruitment events. LPUE increased considerably since then as the stock recovered. Note the close correspondence in most years between the LPUE in the Mid-Atlantic and Georges Bank, probably reflecting the mobility of the scallop fishing fleet; if one area has higher catch rates, it is fished harder until the rates are equalized. Although comparisons of LPUE before and after the change in data collection procedures need to be made cautiously, there is no clear break in the LPUE trend in 1994.

Fishing effort (days fished) was computed as the product of LPUE and landings (Figure B4.4). This effort metric reflects the days fished that would have been required to obtain the reported total landings with limited access vessels. General category vessels, which usually fish with one small dredge would likely fish for several days to account for a single “day fished” of effort. Effort in the US sea scallop fishery generally increased from the mid-1970s to about 1991, and then decreased during the 1990s, first because of low catch rates, and later as a result of effort reduction measures. Effort increased in the Mid-Atlantic during 2000-2005, initially due to reactivation of latent effort among limited access vessels, and then to increases in general category effort. Total effort since 2005 has remained fairly stable, although there have been shifts between regions.

Discards and discard mortality

Sea scallops are sometimes discarded on directed scallop trips because they are too small to be economically profitable to shuck, or because of high-grading, particularly during access area trips (Figure B4.5). Ratios of discard to total catch (by weight) were recorded by sea samplers aboard commercial vessels since 1992 and used to estimate discarded scallops (Appendix B2). Sampling intensity on non-access area trips was low until 2003.

Discarded sea scallops may suffer mortality on deck due to crushing, high temperatures, or desiccation. There may also be mortality after they are thrown back into the water from physiological stress and shock, or from increased predation due to shock and inability to swim or shell damage (Veale et al. 2000, Jenkins and Brand 2001). Murawski and Serchuk (1989) estimated that about 90% of tagged scallops were still living several days after being tagged and placed back in the water. Total discard mortality of discarded scallops (including mortality on deck) is uncertain but has been estimated as 20% in previous assessments (e.g., NEFSC 2010). However, discard mortality may be higher during the Mid-Atlantic during the summer due to high water and deck temperatures, and likely strongly depends in both regions on fishing practices. Scallops returned to the water promptly have much higher chances of survival than ones left on deck for longer periods.

Incidental mortality

Scallop dredges likely kill and injure some scallops that are contacted by the gear but not caught, primarily due to damage (e.g., crushing) to the shells by the dredge. Caddy (1973) estimated that

15-20% of the scallops remaining in the track of a dredge were killed. Murawski and Serchuk (1989) estimated that less than 5% of the scallops remaining in the track of a dredge suffered non-landed mortality. Caddy's study was done in a relatively hard bottom area in Canada, while the Murawski and Serchuk study was in sandy bottom off the coast of New Jersey. It is possible that the difference in indirect mortality estimated in these two studies was due to different bottom types (Murawski and Serchuk 1989).

In order to use these studies to relate landed and non-landed fishing mortality in stock assessment calculations, it is necessary to know the efficiency e of the dredge (the probability that a fully recruited scallop in the path of a dredge is captured). Denote by c the fraction of scallops that suffer mortality among sea scallops in the path of the dredge but not caught. The best available information indicates that $c = 0.15-0.2$ (Caddy 1973), and $c < 0.05$ (Murawski and Serchuk 1989). The ratio R of scallops in the path of the dredge that were caught, to those killed but not caught is:

$$R = e/[c(1-e)] \quad (4.1)$$

If scallops suffer direct (i.e., landed) fishing mortality at rate F_L , then the rate of indirect (non-landed) fishing mortality will be (Hart 2003):

$$F_I = F_L / R = F_L c (1-e)/e. \quad (4.2)$$

If, for example, the commercial dredge efficiency e is 50%, then $F_I = F_L c$, where F_L is the fully recruited fishing mortality rate for sea scallops. Assuming $c = 0.15$ to 0.2 (Caddy 1973) gives $F_I = 0.15 F_L$ to $0.2 F_L$. With $c < 0.05$ (Murawski and Serchuk 1989) $F_I < 0.05 F_L$. For this assessment, incidental mortality was assumed to be $0.2 F_L$ in Georges Bank and $0.1 F_L$ in the Mid-Atlantic.

Prior assessments applied the incidental mortality F_I from equation (4.2) to all sizes of scallops. However, the observations of Caddy (1973) and Murawski and Serchuk (1989) were in terms of mortality of scallops remaining after a pass of a dredge. Thus, the incidental fishing mortality as a function of shell height h should be:

$$F_{Ih}(h) = F_I (1 - q(h)) \quad (4.3)$$

where $q(h)$ is the catchability of commercial gear on a scallop of shell height h . We took $q(h)$ to be:

$$q(h) = q_0 s(h) \quad (4.4)$$

where q_0 is 0.5 on Georges Bank and 0.6 in the Mid-Atlantic (commercial gear is more efficient on large scallops than the survey dredge, see e.g., Yochum and DuPaul 2008), and $s(h)$ is commercial size selectivity estimated by the CASA model. All of these calculations take place in the assessment model itself.

Commercial shell height data

Since most sea scallops are shucked at sea, it has sometimes been difficult to obtain reliable commercial size compositions. Port samples of shells brought in by scallopers have been collected, but there are questions about whether the samples were representative of the landings and catch. Port samples taken during the meat count era often appear to be selected for their size rather than being randomly sampled, and the size composition of port samples from 1992-1994 differed considerably from those collected by at-sea observers during this same period. For this reason, commercial size compositions from port samples after 1984 when meat count regulations were in force are not used in this assessment.

Sea samplers (observers) have collected shell heights of kept scallops from commercial vessels since 1992, and discarded scallops since 1994. Although these data are likely more reliable than that from port sampling, they still must be interpreted cautiously for years prior to 2003 due to limited observer coverage (except for the access area fisheries, which always have had good observer coverage). Except for 2006, observer coverage rates have been over 5% since 2003, and were over 10% during 2012-2013.

Shell heights from port and sea sampling data indicate that sea scallops between 70-90 mm often made up a considerable portion of the landings during 1975-1998, but sizes selected by the fishery have increased since then, so that scallops less than 90 mm were rarely taken since 2002 (Figure B4.6).

Dealer data (landings) have been reported by market categories (under 10 meats per pound, 10-20 meats per pound, 20-30 meats per pound etc) since 1998 (Figure B4.7). These data also indicate a trend towards larger sea scallops in landings in recent years. While nearly half the landings in 1998 were in the smaller market categories (more than 30 meats per pound), 75% or more of recent landings were below 20 count and about 99% were below 30 count.

Table B4.1. US scallop landings 1964-2013 (mt meats), by region and gear type. Dredge gear was recorded as “other” prior to 1978.

Year	Gulf of Maine				Georges Bank				S. New England				Mid Atlantic Bight				Total				
	dredge	trawl	other	sum	dredge	trawl	other	sum	dredge	trawl	other	sum	dredge	trawl	other	sum	dredge	trawl	other	sum	
1964		0	208	208		0	6,241	6,241		52	3	55		0	137	137		52	6,590	6,642	
1965		0	117	117		3	1,478	1,481		2	24	26		0	3,974	3,974		5	5,592	5,598	
1966		0	102	102		0	883	884		0	8	8		0	4,061	4,061		1	5,055	5,056	
1967		0	80	80		4	1,217	1,221		0	8	8		0	1,873	1,873		4	3,178	3,182	
1968		0	113	113		0	993	994		0	56	56		0	2,437	2,437		0	3,599	3,599	
1969		1	122	123		8	1,316	1,324		0	18	19		5	846	851		14	2,302	2,317	
1970		0	132	132		5	1,410	1,415		0	6	6		14	459	473		19	2,006	2,026	
1971		4	358	362		18	1,311	1,329		0	7	7		0	274	274		22	1,949	1,971	
1972		1	524	525		5	816	821		0	2	2		5	653	658		11	1,995	2,006	
1973		0	460	460		15	1,065	1,080		0	3	3		4	245	249		19	1,773	1,792	
1974		0	223	223		15	911	926		0	4	5		0	937	938		16	2,076	2,091	
1975		6	741	746		13	844	857		8	42	50		52	1,506	1,558		80	3,132	3,212	
1976		3	364	366		38	1,723	1,761		4	3	7		819	2,972	3,791		361	5,061	5,422	
1977		4	254	258		27	4,709	4,736		1	10	11		255	2,564	2,819		58	7,536	7,595	
1978	242	1	0	243	5,532	37	0	5,569		25	2	0	27	4,435	207	0	4,642	10,234	247	0	10,481
1979	401	5	1	407	6,253	25	7	6,285		61	5	0	66	2,857	29	1	2,888	9,572	64	9	9,645
1980	1,489	122	3	1,614	5,382	34	2	5,419		130	3	0	133	2,202	85	79	2,366	9,204	245	83	9,532
1981	1,225	73	7	1,305	7,787	56	0	7,843		68	1	0	69	772	14	2	788	9,852	144	9	10,005
1982	631	28	5	664	6,204	119	0	6,322		126	0	0	126	1,602	6	2	1,610	8,562	153	7	8,723
1983	815	72	7	895	4,247	32	4	4,284		243	1	0	243	3,092	19	10	3,121	8,398	124	21	8,542
1984	651	18	10	678	3,011	29	3	3,043		161	3	0	164	3,695	53	2	3,750	7,518	103	14	7,635
1985	408	3	10	421	2,860	34	0	2,894		77	4	0	82	3,230	49	2	3,281	6,575	90	12	6,677
1986	308	2	6	316	4,428	10	0	4,438		76	2	0	78	3,407	386	6	3,799	8,218	400	12	8,631
1987	373	0	9	382	4,821	30	0	4,851		67	1	0	68	7,639	1,168	1	8,808	12,900	1,199	10	14,109
1988	506	7	13	526	6,036	18	0	6,054		65	4	0	68	6,071	938	8	7,017	12,678	966	21	13,666
1989	600	0	44	644	5,637	25	0	5,661		127	11	0	138	7,894	534	5	8,433	14,258	570	49	14,876
1990	545	0	28	574	9,972	10	0	9,982		110	6	0	116	6,364	541	10	6,915	16,991	558	38	17,587
1991	527	3	75	605	9,235	77	0	9,311		55	16	0	71	6,408	878	14	7,300	16,225	973	89	17,288
1992	676	2	45	722	8,230	7	0	8,238		119	5	0	124	4,562	570	5	5,137	13,587	584	50	14,221
1993	763	2	32	797	3,637	18	0	3,655		65	1	0	66	2,412	393	3	2,808	6,878	413	36	7,327
1994	410	6	9	425	1,182	7	0	1,189		29	1	0	30	5,211	754	0	5,965	6,832	768	9	7,609
1995	342	6	13	361	992	4	1	997		41	2	0	43	5,786	798	7	6,591	7,161	810	21	7,992
1996	544	5	12	561	2,126	7	4	2,137		59	5	0	64	4,467	653	4	5,124	7,196	670	20	7,886
1997	673	5	21	699	2,347	9	1	2,357		81	11	3	95	2,703	378	1	3,082	5,804	403	26	6,233
1998	392	5	15	412	2,045	19	1	2,065		103	3	0	106	2,411	564	6	2,981	4,951	591	22	5,564
1999	267	2	2	271	5,172	6	1	5,179		78	1	0	79	3,629	959	1	4,589	9,146	968	4	10,118
2000	162	21	43	226	4,910	40	5	4,955		85	3	1	89	8,139	1,210	2	9,351	13,296	1,274	51	14,621
2001	335	7	1	343	4,879	58	6	4,943		28	37	0	65	14,144	1,543	16	15,703	19,386	1,645	23	21,054
2002	386	18	1	405	5,967	33	11	6,011		20	12	0	32	15,981	1,426	36	17,443	22,354	1,489	48	23,891
2003	197	3	1	201	4,859	22	2	4,883		53	4	0	57	19,040	1,226	10	20,276	24,149	1,255	13	25,417
2004	165	12	0	177	4,249	146	11	4,406		830	151	11	992	22,313	1,194	26	23,533	27,557	1,503	48	29,108
2005	163	12	12	187	8,958	69	15	9,042		845	13	40	898	14,361	1,096	109	15,566	24,327	1,190	176	25,693
2006	147	3	5	155	15,688	51	21	15,760		2,029	10	8	2,047	7,944	782	46	8,772	25,808	846	80	26,734
2007	97	8	12	117	9,419	45	18	9,482		335	18	7	360	16,234	345	55	16,634	26,085	416	92	26,593
2008	103	12	5	120	6,405	24	11	6,440		303	6	16	325	16,819	556	13	17,388	23,630	598	45	24,273
2009	81	0	3	84	6,451	8	16	6,475		216	1	3	220	17,487	12	1,851	19,350	24,235	21	1,873	26,129
2010	148	13	6	168	5,826	18	47	5,890		254	9	26	290	19,172	281	97	19,550	25,400	321	177	25,898
2011	193	17	2	212	8,159	14	135	8,309		338	24	24	386	17,224	318	205	17,747	25,914	373	366	26,653
2012	392	22	3	417	13,671	37	16	13,724		118	4	32	154	11,172	272	176	11,620	25,353	334	228	25,915
2013	449	43	6	498	11,823	27	25	11,875		308	13	5	326	5,683	229	54	5,966	18,263	311	89	18,664

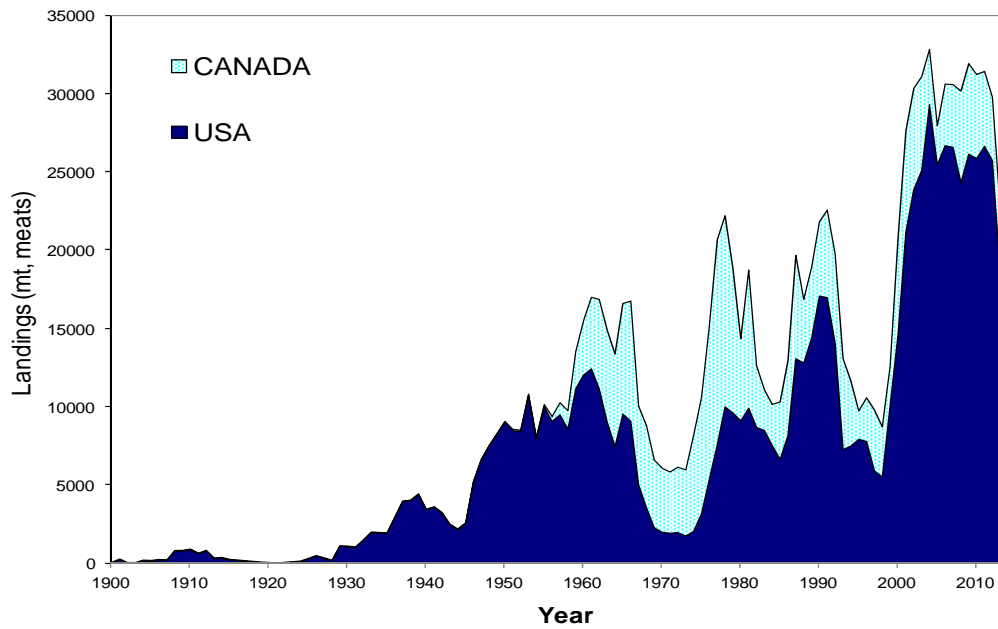


Figure B4.1. Sea scallop landings in NAFO areas 5-6 (North Carolina to Georges Bank).

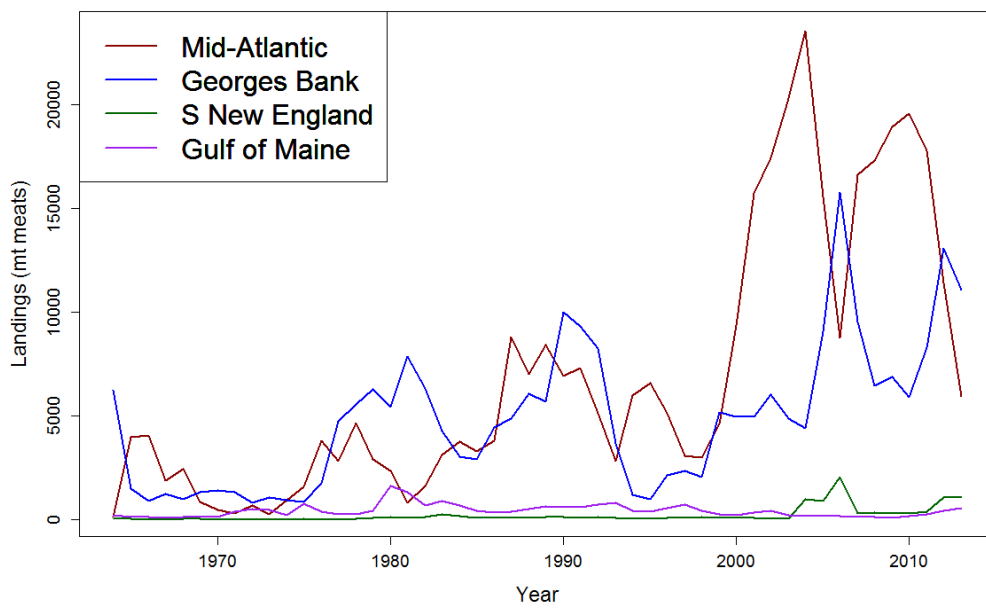


Figure B4.2. US sea scallop landings during 1964-2013, by region.

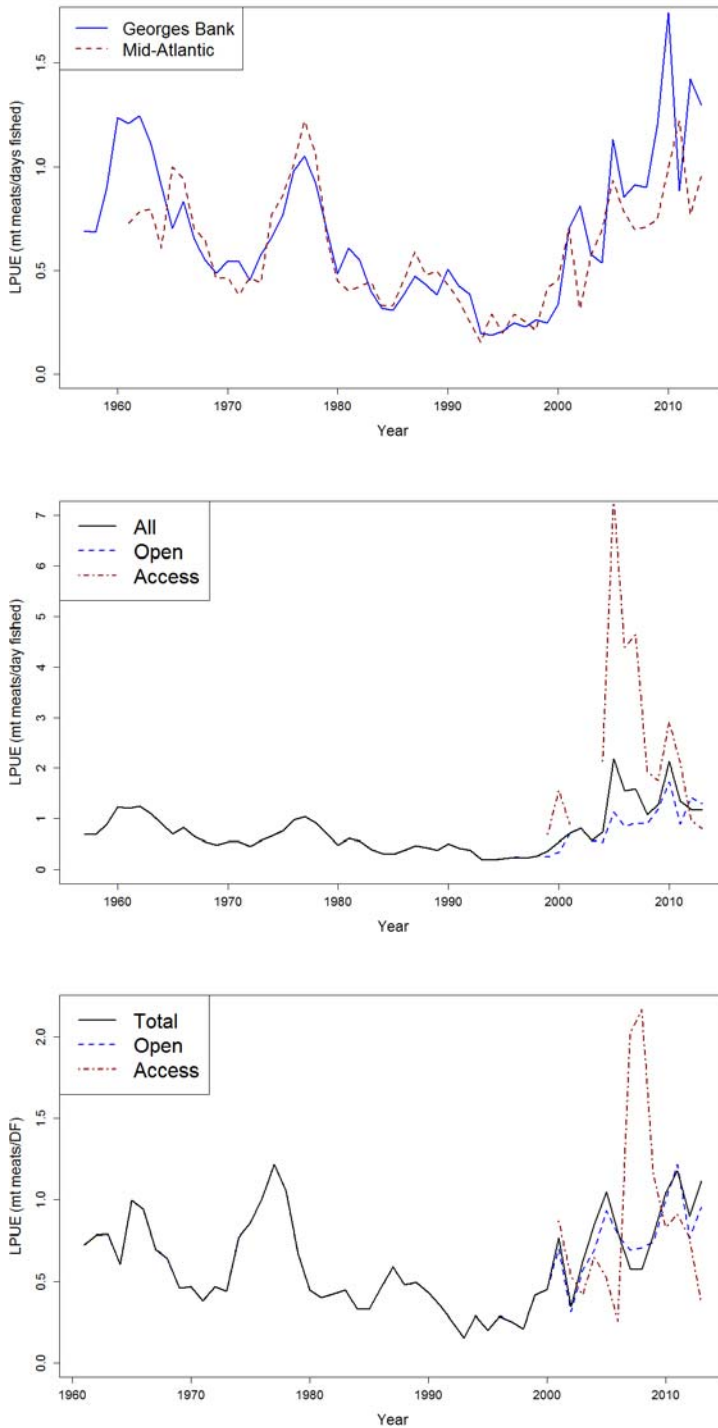


Figure B4.3 *Top*: landings per unit effort (LPUE) on Georges Bank and the Mid-Atlantic, excluding access area trips. *Middle*: LPUE on Georges Bank, separated into access and open areas and combined. *Bottom*: LPUE in the Mid-Atlantic, separated into access and open areas and combined.

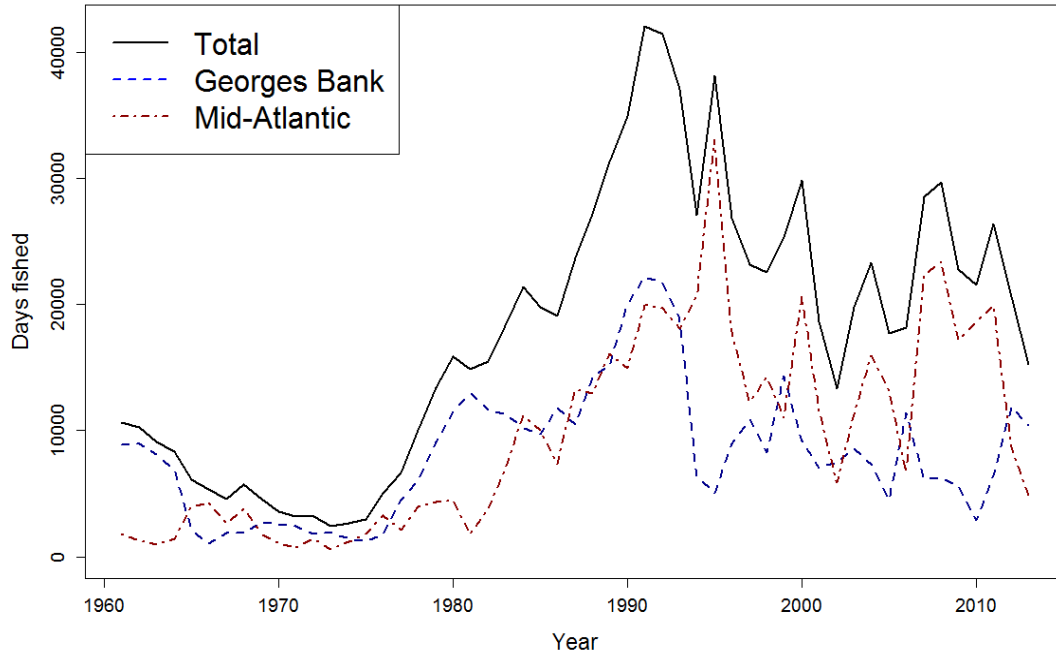


Figure B4.4 Sea scallop fishing effort in the US, 1961-2013.

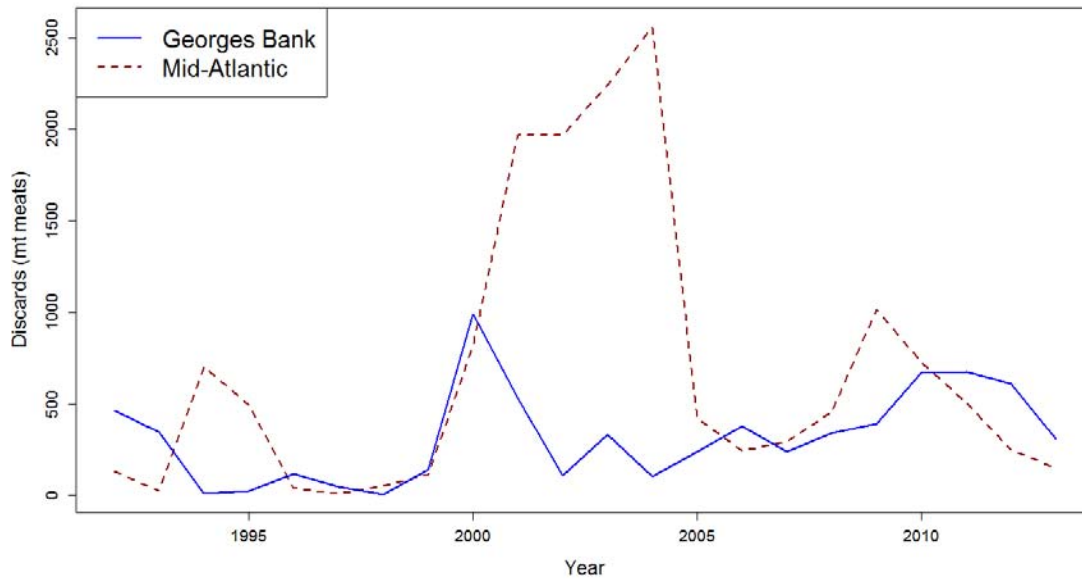


Figure B4.5. Estimated discards in the US scallop fishery, 1992-2013.

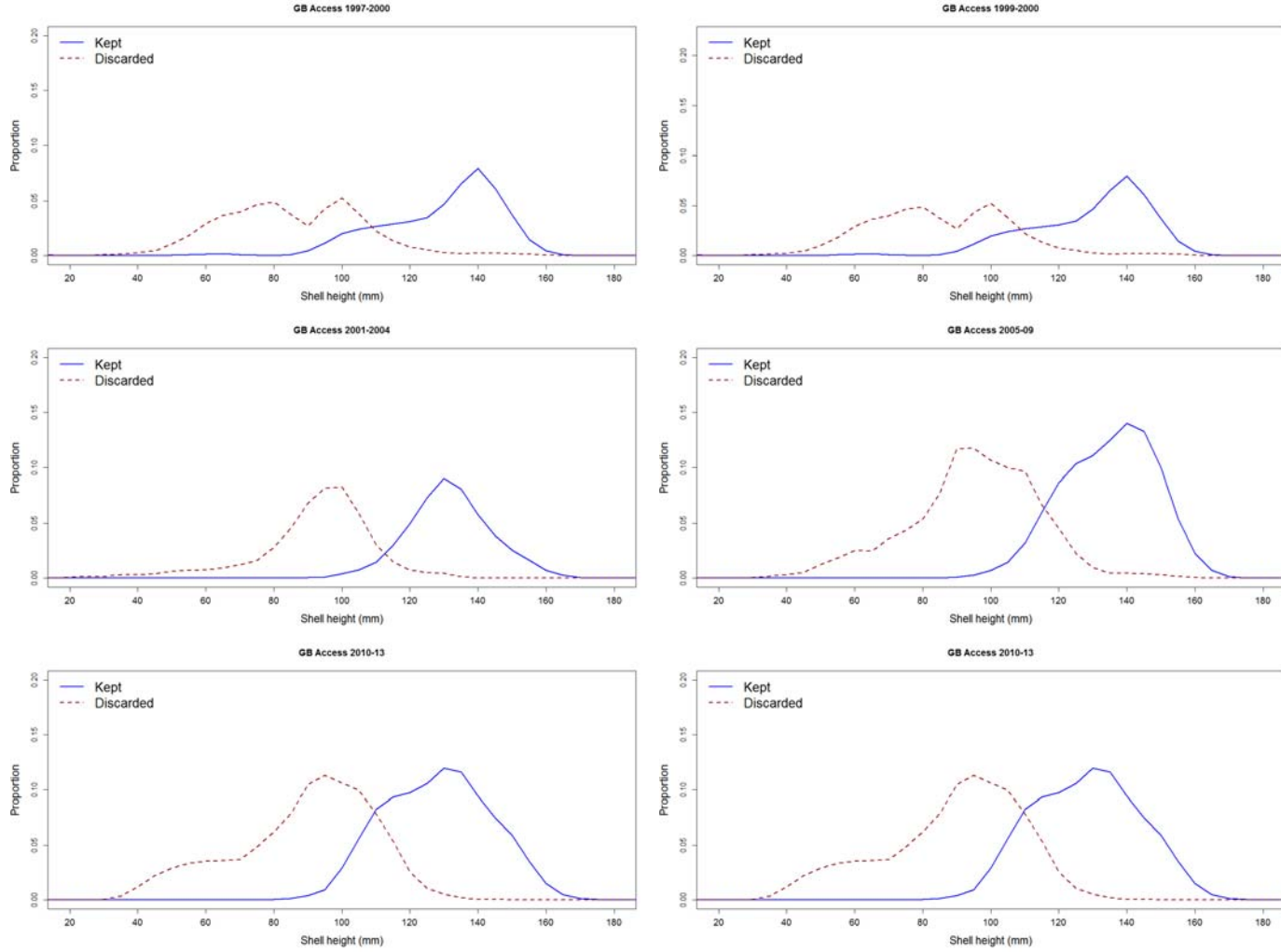


Figure B4.6. Shell heights of commercial kept (solid line) and discarded (dashed line) sea scallops from Georges Bank access areas, based on data from sea samplers.

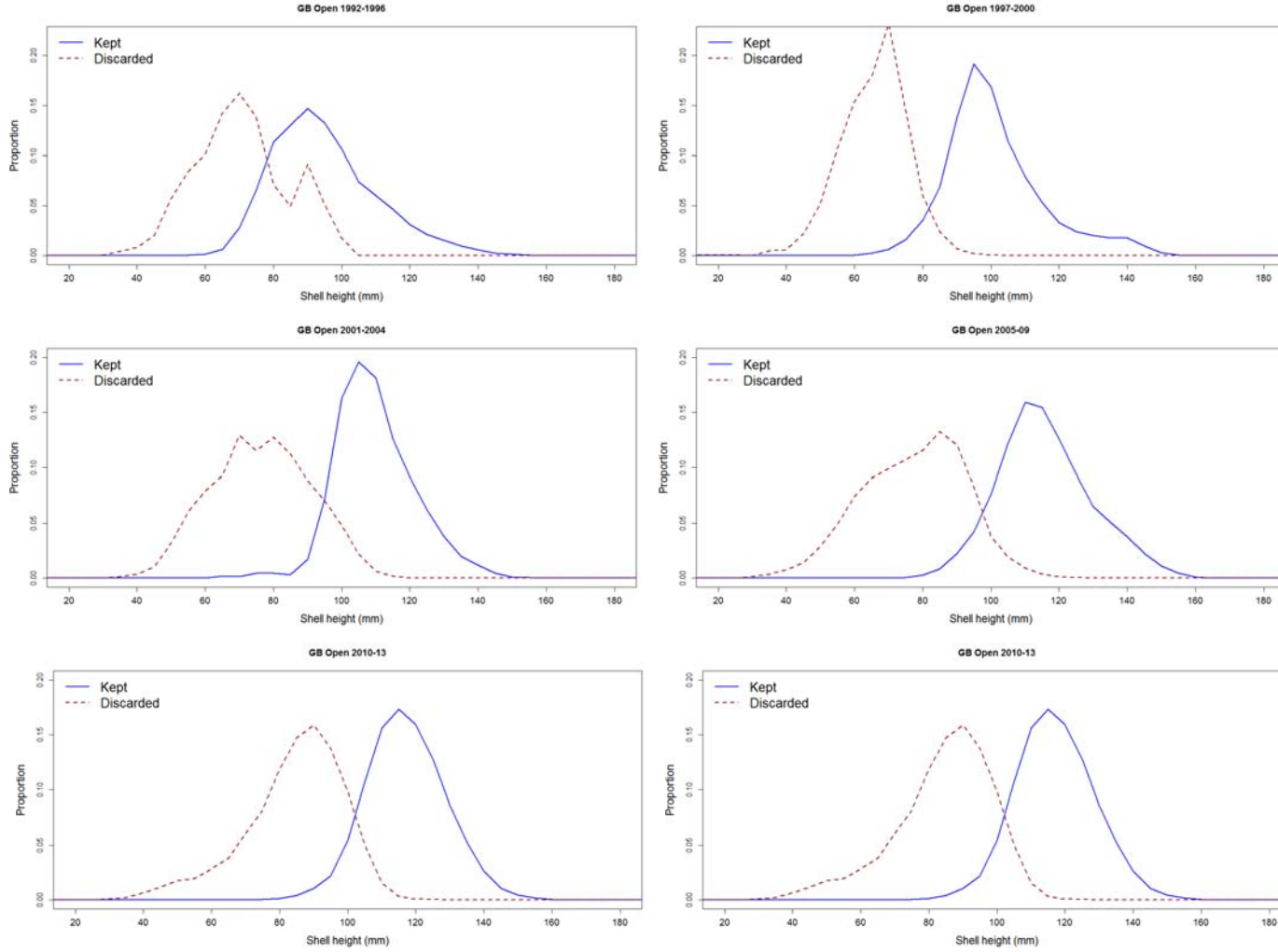


Figure B4.6 (cont). Shell heights of commercial kept (solid line) and discarded (dashed line) sea scallops from Georges Bank open areas.

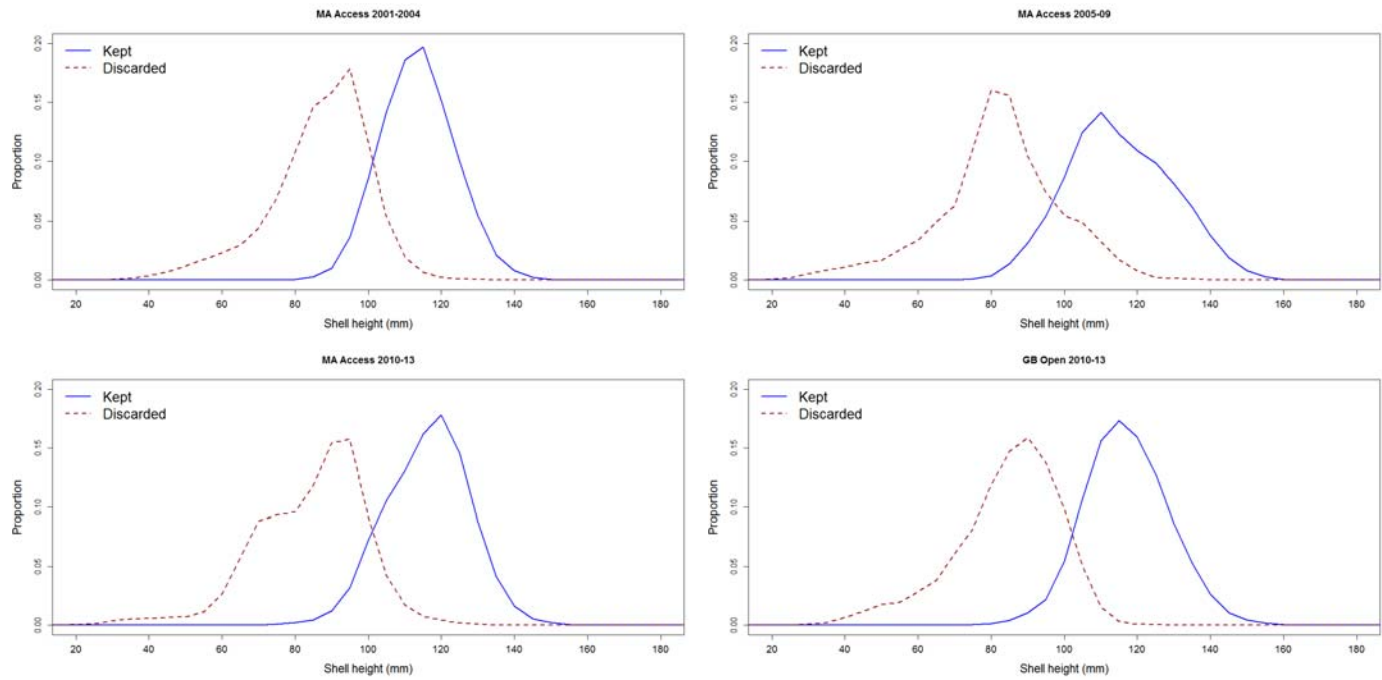


Figure B4.6 (cont.). Shell heights of commercial kept (solid line) and discarded (dashed line) sea scallops from Mid-Atlantic Bight access areas.

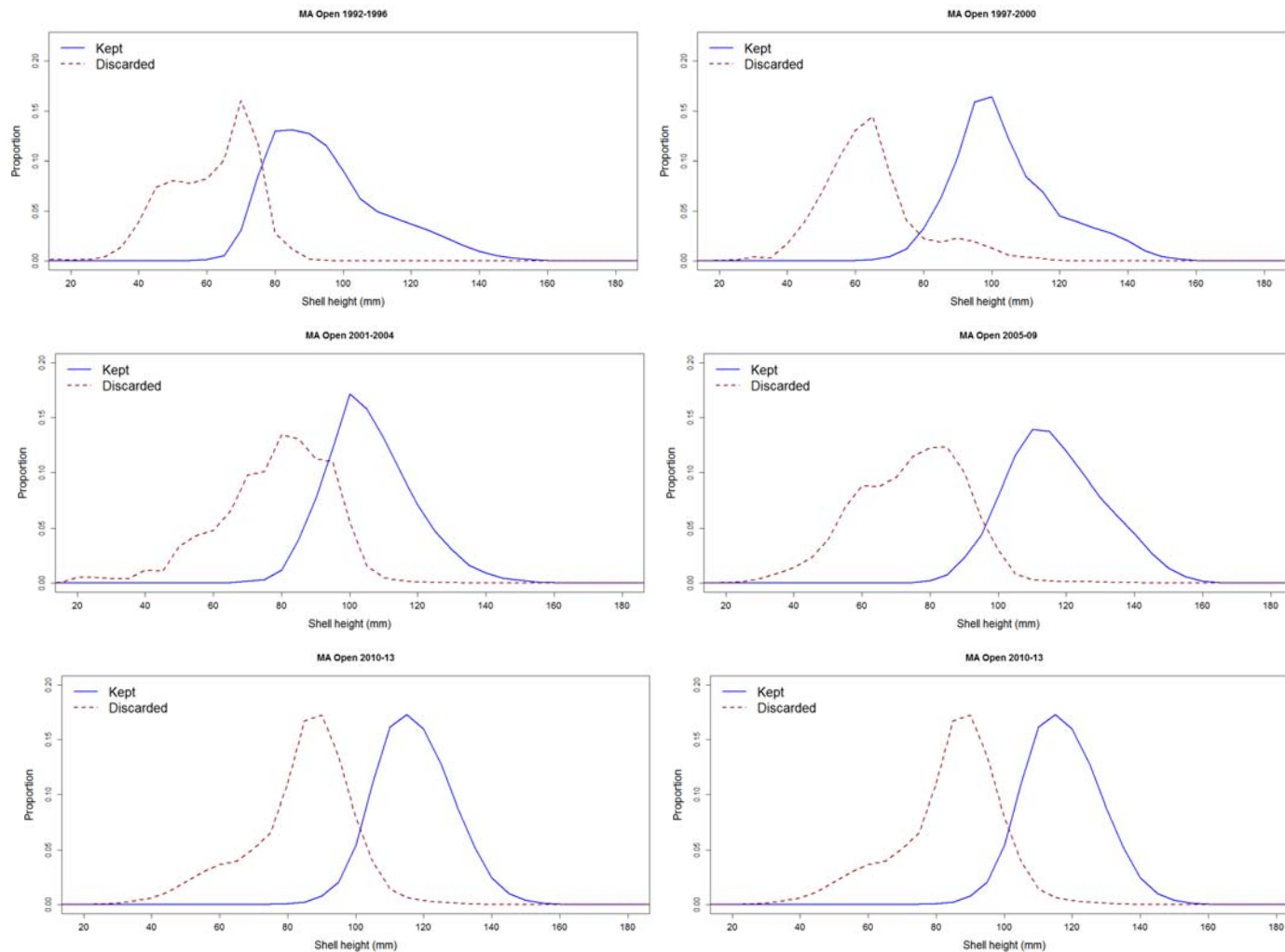


Figure B4.6 (cont.). Shell heights of commercial kept (solid line) and discarded (dashed line) sea scallops from Mid-Atlantic Bight open areas.

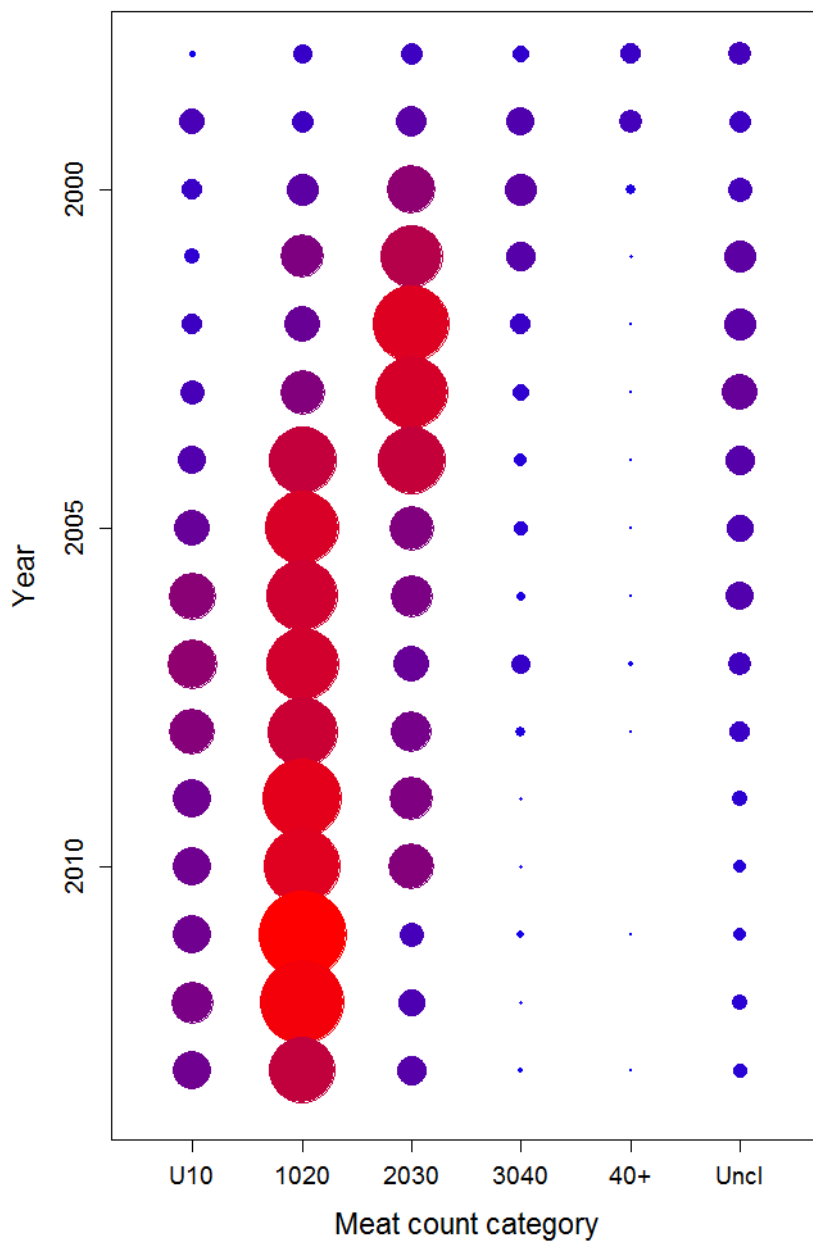


Figure B4.7. Landings by commercial meat count category (U10 = less than 10 meats per lb, 1020 = between 10-20 meats per pound, 2030 = between 20-30 meats per pound, 40+ = over 40 meats per pound, and Uncl = unclassified). The areas of the bubbles are proportional to landings.

B5. SURVEY DATA (TOR-2)

Dredge surveys

Sea scallop dredge surveys were conducted by NEFSC in 1975 and annually after 1977 to measure abundance and size composition of sea scallops in the Georges Bank and Mid-Atlantic regions (Figures B3-1 and B5-1). Means and standard errors were calculated using standard methods for stratified random surveys (Cochran 1977, Serchuk and Wigley 1989; Wigley and Serchuk 1996; Smith 1997).

The 1975-1978 surveys used a 3.08 m (10') unlined New Bedford scallop dredge with 54 mm rings. A 2.44 m New Bedford survey dredge with 54 mm rings and a 38 mm plastic liner has been used since 1979. Based on comparisons between camera and dredge data, scallops greater than 40 mm are considered fully selected by the lined survey dredge gear (NEFSC 2007). The survey covers Georges Bank and the Mid-Atlantic, using a random-stratified design. At each station, the dredge is deployed for 15 minutes. Caught scallops are counted and measured, and subsamples are weighed (meat weight, gonad weight, whole weight, see Hennen and Hart 2012). The shells from the subsamples are brought to shore for growth analysis.

The *R/V Albatross IV* was used for all NEFSC scallop surveys from 1975-2007, except during 1990-1993, when the *R/V Oregon* was used instead. Surveys by the *R/V Albatross IV* during 1989 and 1999 were incomplete on Georges Bank. In 1989, the *R/V Oregon* and *R/V Chapman* were used to sample the South Channel and a section of the Southeast Part of Georges Bank. Serchuk and Wigley (1989) did not find significant differences in catch rates between the *R/V Albatross IV*, *R/V Oregon* and *R/V Chapman*. The *F/V Tradition* was used to complete the 1999 survey on Georges Bank. NEFSC (2001) found no statistically significant differences in catch rates between the *F/V Tradition* and *R/V Albatross IV* from 21 comparison stations after adjustments were made for tow path length. Therefore, survey dredge tows from these other vessels were used without adjustment except for normalizing for tow distance as discussed below. The northern edge of Georges Bank was not covered by the NEFSC survey until 1982. Data from the Canadian scallop survey during 1979-1981, which used the same gear as the NEFSC survey, was used to cover the northern edge in those years (NEFSC 2010).

In 2008-2013, the NEFSC scallop survey was conducted on the *R/V Hugh Sharp*. Direct and indirect comparisons between the catches by the *R/V Hugh Sharp*, *R/V Albatross IV* and commercial vessels towing the lined survey dredge were not significantly different (NEFSC 2010). However, average catches were slightly greater (~5%) on the *R/V Hugh Sharp*. Comparison of tow distance data from dredge sensor data indicate that tow lengths from the *R/V Hugh Sharp* were about 8% longer on average than those on the *R/V Albatross IV* or commercial vessels (Figure B5.2).

In NEFSC (2010), tows on the *R/V Hugh Sharp* were reduced by 5% to compensate for the apparent differences among survey vessels. For this assessment, each tow was normalized to a tow length of 1 nm. Because dredge sensor data is only available for a subset of the tows, regression equations were developed based on tows where the sensor data is available to predict tow distance using nominal tow distance and depth as predictors. Nominal tow distance is the

nominal tow time (i.e., the time elapsed after the winch is locked at the beginning of the tow to the time when haul back begins) times the mean vessel speed between these times. Separate relationships were developed for the *R/V Albatross IV* (which was assumed to also apply to the other vessels used from 1989-1999), and the *R/V Hugh Sharp*:

Tow length = $-0.0388 + 0.001484 * \text{Depth} + 1.061 * \text{Nominal length}$ (*R/V Hugh Sharp*)

Tow length = $0.0864 - 0.000444 * \text{Depth} + 0.972 * \text{Nominal length}$ (*R/V Albatross IV*)

where tow length is in nautical miles and depth is in meters.

Rock excluder chains have been used on NEFSC sea scallop survey dredge since 2004 in certain hard bottom strata to enhance safety at sea and increase reliability (NEFSC 2004). Based on paired tow trials with and without excluders, the best overall estimate was that rock chains increased survey catches on hard grounds by a factor of 1.31 (CV = 0.2). To accommodate rock chain effects in hard bottom areas, survey data collected prior to 2004 from strata 49-52 and in the portions of strata 651, 661, 71 and 74 within Closed Area II were multiplied by 1.31 prior to calculating stratified random means for larger areas. Variance calculations in these strata include a term to account for the uncertainty in the adjustment factor (NEFSC 2007).

The survey area on Georges Bank used in conducting the survey and to tabulate survey data for assessment purposes was modified in this assessment to eliminate marginal scallop habitat. The modified survey area was used to calculate stratified mean catch per tow for the dredge in all years in this assessment. Stratum 72 comprises a shallow area on the northern portion of Georges Bank (Figure B5-3). Most of this stratum has few scallops, but there is a small deep portion where larger catches are often observed. Using the entire stratum induces high variability in the mean number in this stratum, depending primarily on how many tows were in the productive portion. For this reason, stratum 72 was reduced to contain the productive portion of the stratum only (Figure B5-3). Similarly, scallops are more abundant in the northern portion of stratum 74 than in the southern portion. Therefore, only the northern portion of Stratum 74 was used in the survey index. Finally, stratum 631, where the density of scallops is very low, was eliminated from the Georges Bank survey index completely. These changes resulted in a reduction in the total surveyed area on Georges Bank from 7,281 nm² to 6,416 nm².

Relatively high abundance of sea scallops in closed areas makes it necessary to further post-stratify survey data by splitting NEFSC shellfish strata that cross open/closed area boundaries. After re-stratification, the original and new strata were combined into open, closed or other areas as required for assessment and management purposes (NEFSC 1999, Figures B3-1 and B5-1).

The Virginia Institute of Marine Science (VIMS) has conducted intensive dredge surveys of selected regions on commercial vessels since 2005, using partially randomized grid designs (Figure B5.1). These surveys use two dredges fished side-by-side; the NEFSC lined survey dredge is deployed on one side while a commercial dredge is used on the other side.

Comparisons between commercial vessels and the *R/V Albatross IV* indicate suggest that the survey dredge has the same fishing power on these vessels (NEFSC 2010). In the last several years, VIMS has conducted several hundred tows per year.

All VIMS data for fully covered strata (original or post-stratified) were treated in the same way

as NEFSC tows. The partially randomized grid design was treated as random when calculating variances. This likely slightly overstates the true sample variance.

A relatively small number of unsurveyed strata were filled by imputation. Imputation procedures were similar to those in NEFSC (2010). In brief, GAM models were fit to estimate trends in average catch rates over time for individual survey strata with strata nested within subregions. Length composition data for such strata was estimated by the stratified mean length composition for other strata in the same region.

Capture efficiency of the survey dredge was estimated by comparing dredge catches to densities observed by the HabCam system towed at the same location (Appendix B4). The best estimates of dredge efficiency were 0.41 on sand substrates, and 0.27 on rougher gravel/cobble substrates. These, together with estimates of tow path length and stock area (see above) were used to expand mean catch per tow and estimate stock size in absolute terms. For these purposes, the South Channel and northern portion of Closed Area II are considered to have gravel/cobble bottom while the northern edge of Georges Bank, west of Closed Area II are considered mixed sand with gravel/cobble, where dredge efficiency average 0.34. All other areas, including all of the Mid-Atlantic are assumed to be predominately sand and are expanded assuming a survey dredge efficiency of 0.41.

Dredge survey stock size was increased by 10% in the Mid-Atlantic and 4% on Georges Bank to account for scallops at low densities outside the survey strata set used to calculate mean catch per tow. NEFSC (2010) estimated that about 10% of the scallops in the Mid-Atlantic and 3% of the scallops on Georges Bank lie outside the regular dredge survey strata. The new adjustment for Georges Bank was increased from 3% to 4% to also account for scallops in the areas that were dropped from the survey strata set.

Dredge survey results

Biomass and abundance trends for the dredge survey are presented in Table B5-1 and Figure B5-4. Based on dredge survey estimates, biomass and abundance on Georges Bank were generally low until around 1995. Very large increases were observed during 1995-2000 after implementation of closures and effort reduction measures. Biomass has remained high since, although some decreases have occurred during the last several years.

In the Mid-Atlantic Bight, dredge abundance and biomass indices were at low levels during 1979-1997, and then increased rapidly during 1998-2003 due to area closures, reduced fishing mortality, changes in fishery selectivity, and strong recruitment. Biomass was relatively stable during 2003-2008, but then declined, in part due to poor recruitment and fishing down of rotational areas. A slight increase was observed in 2013 due to growth of the large 2010 year class. Survey shell height frequencies show a trend to larger shell heights in both regions since 1995.

SMAST Video Survey

Video survey data was collected by the School for Marine Sciences and Technology (SMAST), University of Massachusetts, Dartmouth between 2003 and 2012 (Table B5-2, Stokesbury et al. 2004). This survey is conducted using drop video cameras; each station consists of clusters of

four drops, and stations are placed on a grid generally 3 m apart. Although there are several cameras on the camera pyramid, the survey index is based on the “large” camera, a standard definition video camera which was mounted 1.575 m above the bottom in the center of the sampling frame. Each drop quadrat covers about 2.8 m².

The precision of measurements must be considered in interpreting shell height data from video. Based on tank experiments, Jacobson et al. (2010) estimated the error associated with shell height measurements from the large video camera had a standard deviation of 6.1 mm. Field measurements are likely less precise than in a tank. For this reason, measurement error was estimated in this assessment by fitting SMAST shell heights to dredge shell heights from the same year and region that were convolved with a Gaussian kernel with mean 0 and standard deviation σ . The standard deviation that best fit the SMAST shell heights over all years and regions was 11 mm. This is the value used in modeling for this assessment.

Video survey data are expressed as densities (number m⁻²). Variances for estimated densities are approximated using the estimator for a simple random survey applied to station means. There was some variability in the areas covered during each year.

HabCam Towed Camera Survey

HabCam is an underwater towed digital camera system (Appendix B6). The camera(s) take rapid-fire still photos of the sea floor (typically 6/sec) as it is towed at typical speeds between 5-7 knots at roughly 2 m above the bottom. Camera output is sent to the vessel using a fiber optic cable, where it is recorded on hard disk together with related metadata.

Two HabCam vehicles are in operation (Figure B5-5). The first, known as “v2”, carries a single camera, and has been in operation since 2005. The second, known as “v4” carries two cameras to allow 3D viewing and more precise measurements, as well as a side-scan sonar and a full array of oceanographic sensors (e.g., CTD, chlorophyll, dissolved oxygen, pH, CDOM, water spectrometer, etc.), and was first deployed in 2012. “v1” and “v3” were prototypes that have not seen routine use.

Region-scale HabCam surveys were conducted on Georges Bank in 2011 using the v2 system, and on both Georges Bank and the Mid-Atlantic in 2012 and 2013 using the v4 system. All broadscale HabCam survey were conducted on the *R/V Hugh Sharp*. The broadscale survey was supplemented in all three years by intensive surveys of selected areas using the v2 system deployed on the *F/V Kathy Marie*. Because of the large number of images collected, only subsets were examined for sea scallop measurements and counts; typically between 1/50 to 1/200 photographs were analyzed, corresponding to about one every 25 to 100 meters. These were expanded to large scales using a zero-inflated generalized additive model followed by ordinary kriging of the residuals (Table B5-3; Figure B5-6; Appendix B6). An alternative method, taking stratified means of the main transects, gave similar results. More details on the HabCam survey and the associated geostatistical methodologies can be found in Appendix B6.

Measurement error was estimated for HabCam by comparing the shell heights to dredge data, as was done for the SMAST survey. Best fit occurred at a standard deviation of 12.7 mm, which is

what was used in the modeling.

The expanded dredge survey time series together with the two optical surveys are shown in Figures B5-7 and B5-8.

Table B5.1. Dredge survey data for sea scallops on Georges Bank (below), in the Mid-Atlantic (next page) and whole stock (3rd page).

Year	Abundance (mean N/tow)	CV	Biomass index (kg/tow meats)	CV	Number of tows	Proportion positive tows	Mean meat weight (g)	Expanded abundance (millions)	Expanded biomass (mt meats)
1979	87.4	0.41	1.697	0.34	108	0.89	19.4	1,269	24,628
1980	75.8	0.24	0.920	0.16	118	0.81	12.1	1,031	12,498
1981	61.2	0.13	1.079	0.13	82	0.83	17.6	753	13,272
1982	132.9	0.46	1.080	0.32	118	0.83	8.1	2,076	16,876
1983	61.2	0.22	0.810	0.21	126	0.88	13.2	890	11,785
1984	39.3	0.11	0.577	0.10	128	0.85	14.7	536	7,887
1985	61.8	0.15	0.731	0.16	154	0.90	11.8	830	9,816
1986	116.8	0.13	1.070	0.10	153	0.90	9.2	1,445	13,237
1987	120.1	0.17	1.173	0.16	170	0.86	9.8	1,619	15,815
1988	98.7	0.16	0.993	0.14	175	0.80	10.1	1,289	12,967
1989	63.6	0.11	0.631	0.08	120	0.78	9.9	806	7,999
1990	184.1	0.24	1.511	0.22	175	0.81	8.2	2,415	19,823
1991	257.9	0.37	1.633	0.25	176	0.89	6.3	3,678	23,292
1992	232.0	0.44	2.020	0.43	171	0.89	8.7	3,300	28,737
1993	61.8	0.24	0.577	0.16	164	0.87	9.3	753	7,027
1994	46.7	0.20	0.518	0.16	177	0.84	11.1	561	6,217
1995	111.8	0.20	0.873	0.16	176	0.88	7.8	1,637	12,774
1996	133.6	0.20	1.617	0.19	171	0.90	12.1	1,855	22,458
1997	89.4	0.15	1.606	0.17	190	0.88	18.0	1,292	23,212
1998	283.0	0.26	4.003	0.32	195	0.87	14.1	3,646	51,566
1999	193.5	0.15	3.391	0.16	173	0.98	17.5	2,663	46,663
2000	766.7	0.29	8.198	0.22	164	0.91	10.7	9,996	106,882
2001	408.9	0.13	6.761	0.13	208	0.95	16.5	5,560	91,938
2002	334.5	0.14	7.195	0.14	214	0.93	21.5	4,498	96,764
2003	277.9	0.12	6.749	0.13	207	0.94	24.3	3,839	93,236
2004	291.5	0.11	8.301	0.12	218	0.94	28.5	3,959	112,749
2005	265.6	0.12	6.792	0.09	343	0.95	25.6	3,888	99,436
2006	221.3	0.13	6.123	0.13	236	0.94	27.7	3,258	90,145
2007	224.8	0.10	4.722	0.07	363	0.97	21.0	3,453	72,533
2008	321.8	0.10	6.460	0.08	239	0.97	20.1	4,805	96,444
2009	362.7	0.15	6.151	0.11	214	0.97	17.0	5,497	93,229
2010	413.1	0.21	7.652	0.09	268	0.97	18.5	6,407	118,682
2011	279.4	0.12	6.971	0.08	225	0.96	25.0	3,946	98,469
2012	225.3	0.13	5.034	0.08	224	0.97	22.3	3,488	77,936
2013	336.5	0.23	4.856	0.14	213	0.94	14.4	4,416	63,723

Table B5.1. (continued – dredge survey data for the Mid Atlantic region)

Year	Abundance (mean N/tow)	CV	Biomass index (kg/tow meats)	CV	Number of tows	Proportion positive tows	Mean meat weight (g)	Expanded abundance (millions)	Expanded biomass (mt meats)
1979	34.7	0.10	0.665	0.10	166	0.92	19.2	590	11,329
1980	42.8	0.12	0.577	0.08	167	0.94	13.5	755	9,829
1981	32.1	0.16	0.457	0.13	167	0.91	14.3	565	7,791
1982	33.5	0.11	0.497	0.08	185	0.91	14.8	591	8,458
1983	32.3	0.10	0.458	0.08	193	0.89	14.2	569	7,794
1984	32.2	0.11	0.444	0.09	204	0.91	13.8	567	7,560
1985	74.1	0.12	0.739	0.09	201	0.94	10.0	1,307	12,582
1986	129.6	0.09	1.295	0.08	226	0.93	10.0	2,285	22,057
1987	131.9	0.08	1.177	0.07	226	0.93	8.9	2,326	20,054
1988	147.8	0.10	1.738	0.08	227	0.91	11.8	2,606	29,610
1989	172.8	0.09	1.553	0.07	244	0.93	9.0	3,047	26,452
1990	215.2	0.22	1.789	0.18	216	0.89	8.3	3,794	30,463
1991	81.0	0.10	0.945	0.10	228	0.92	11.7	1,428	16,100
1992	43.5	0.11	0.526	0.07	229	0.87	12.1	767	8,956
1993	135.6	0.10	0.852	0.08	214	0.96	6.3	2,391	14,513
1994	145.1	0.13	1.141	0.09	227	0.94	7.9	2,558	19,430
1995	173.4	0.13	1.605	0.11	227	0.96	9.3	3,057	27,333
1996	58.8	0.08	0.747	0.07	211	0.89	12.7	1,037	12,718
1997	43.2	0.13	0.504	0.06	225	0.93	11.7	762	8,590
1998	168.4	0.15	1.343	0.12	215	0.92	8.0	2,969	22,872
1999	238.3	0.24	2.239	0.20	226	0.92	9.4	4,202	38,143
2000	292.1	0.14	3.719	0.13	229	0.88	12.7	5,152	63,348
2001	308.4	0.11	4.124	0.12	227	0.90	13.4	5,438	70,236
2002	284.0	0.10	4.224	0.11	206	0.89	14.9	5,009	71,952
2003	654.5	0.16	7.007	0.10	201	0.90	10.7	11,541	119,339
2004	471.0	0.12	6.093	0.08	248	0.89	12.9	8,305	103,772
2005	344.6	0.08	6.048	0.07	278	0.94	17.5	6,077	103,005
2006	386.6	0.09	6.917	0.07	302	0.95	17.9	6,818	117,810
2007	314.6	0.06	6.097	0.06	304	0.94	19.4	5,549	103,852
2008	373.7	0.09	6.258	0.08	259	0.97	16.7	6,591	106,586
2009	370.5	0.12	7.007	0.10	196	0.92	18.9	6,533	119,343
2010	250.3	0.08	5.115	0.07	281	0.94	20.4	4,414	87,126
2011	172.7	0.10	3.840	0.10	298	0.96	22.2	3,045	65,396
2012	260.2	0.12	3.194	0.06	269	0.94	12.3	4,589	54,407
2013	256.1	0.10	3.746	0.08	309	0.98	14.6	4,517	63,796

Table B5.1. (continued – dredge survey data for the whole stock)

Year	Abundance (mean N/tow)	CV	Biomass index (kg/tow meats)	CV	Number of tows	Proportion positive tows	Mean meat weight (g)	Expanded abundance (millions)	Expanded biomass (mt meats)
1979	57.6	0.27	1.113	0.23	274	0.91	19.3	1,859	35,957
1980	57.2	0.15	0.726	0.09	285	0.89	12.6	1,786	22,327
1981	44.7	0.10	0.727	0.09	249	0.88	16.4	1,318	21,063
1982	76.7	0.35	0.750	0.20	303	0.88	9.6	2,667	25,334
1983	44.8	0.14	0.611	0.13	319	0.88	13.6	1,459	19,579
1984	35.3	0.08	0.502	0.07	332	0.89	14.3	1,103	15,447
1985	68.8	0.09	0.735	0.08	355	0.92	10.8	2,137	22,398
1986	124.0	0.08	1.197	0.06	379	0.92	9.6	3,730	35,294
1987	126.8	0.09	1.176	0.08	396	0.90	9.3	3,945	35,869
1988	126.5	0.08	1.415	0.07	402	0.86	11.1	3,895	42,577
1989	125.3	0.07	1.153	0.06	364	0.88	9.2	3,853	34,451
1990	201.7	0.16	1.668	0.14	391	0.85	8.3	6,209	50,286
1991	157.8	0.27	1.244	0.15	404	0.91	7.7	5,106	39,392
1992	125.4	0.35	1.175	0.32	400	0.88	9.3	4,067	37,693
1993	103.6	0.10	0.733	0.08	378	0.92	7.2	3,144	21,540
1994	102.4	0.11	0.870	0.08	404	0.90	8.6	3,119	25,647
1995	146.6	0.11	1.287	0.09	403	0.92	8.7	4,694	40,107
1996	91.3	0.13	1.125	0.12	382	0.90	12.3	2,892	35,176
1997	63.3	0.10	0.983	0.12	415	0.91	15.8	2,054	31,802
1998	218.2	0.16	2.498	0.22	410	0.90	11.7	6,615	74,438
1999	218.8	0.16	2.739	0.13	399	0.95	12.8	6,865	84,806
2000	498.2	0.20	5.664	0.15	393	0.89	11.3	15,148	170,230
2001	352.0	0.09	5.269	0.09	435	0.93	15.1	10,998	162,174
2002	305.9	0.08	5.514	0.09	420	0.91	18.3	9,507	168,716
2003	490.9	0.12	6.895	0.08	408	0.92	14.5	15,380	212,575
2004	393.0	0.09	7.051	0.07	466	0.91	18.5	12,264	216,521
2005	310.3	0.07	6.371	0.05	621	0.95	20.8	9,965	202,441
2006	314.8	0.08	6.572	0.06	538	0.95	21.2	10,076	207,955
2007	275.6	0.05	5.500	0.04	667	0.95	20.0	9,002	176,385
2008	351.2	0.07	6.346	0.06	498	0.97	18.2	11,396	203,030
2009	367.1	0.09	6.635	0.08	410	0.95	18.0	12,030	212,572
2010	321.0	0.12	6.217	0.06	549	0.95	19.3	10,821	205,808
2011	219.0	0.08	5.199	0.06	523	0.96	23.8	6,991	163,865
2012	245.0	0.09	3.993	0.05	493	0.96	16.7	8,077	132,343
2013	291.0	0.12	4.228	0.08	522	0.96	14.5	8,933	127,519

Table B5.2. SMAST Large Camera survey data for sea scallops on Georges Bank, the Mid-Atlantic and combined.

Year	Density (N/m ²)	CV	N stations	Survey area (km ²)	Number (millions)	Mean wt (g)	Biomass (mt)
Georges Bank							
2003	0.147	0.08	929	28,677	4,213	21.9	92,343
2004	0.122	0.12	935	28,863	3,513	26.6	93,341
2005	0.116	0.11	902	27,844	3,235	24.5	79,370
2006	0.110	0.11	939	28,986	3,177	20.9	66,527
2007	0.142	0.11	912	28,153	3,989	17.8	70,858
2008	0.098	0.09	910	28,091	2,744	13.9	38,113
2009	0.157	0.11	899	27,751	4,351	12.1	52,779
2010	0.116	0.10	939	27,937	3,241	18.1	58,682
2011	0.147	0.12	918	28,338	4,169	15.6	64,885
2012	0.129	0.14	892	27,535	3,555	14.7	52,184
Mid-Atlantic							
2003	0.483	0.17	804	24,819	11,995	8.7	103,889
2004	0.224	0.10	840	25,930	5,801	12.9	75,032
2005	0.210	0.12	864	26,671	5,598	14.0	78,141
2006	0.191	0.10	897	27,690	5,292	13.7	72,312
2007	0.179	0.09	941	29,048	5,202	14.5	75,227
2008	0.184	0.10	931	28,739	5,288	14.3	75,356
2009	0.134	0.06	928	28,647	3,844	15.1	57,904
2010	0.109	0.08	988	30,499	3,324	20.6	68,363
2011	0.066	0.06	1,359	41,951	2,756	23.3	64,305
2012	0.111	0.08	1,168	35,999	3,996	9.3	37,187
Whole stock							
2003	0.303	0.12	1,733	53,496	16,208	12.1	196,232
2004	0.170	0.08	1,775	54,793	9,313	18.1	168,374
2005	0.162	0.08	1,766	54,515	8,834	17.8	157,512
2006	0.149	0.07	1,836	56,676	8,468	16.4	138,839
2007	0.161	0.07	1,853	57,201	9,192	15.9	146,085
2008	0.141	0.07	1,841	56,830	8,032	14.1	113,469
2009	0.145	0.06	1,827	56,398	8,196	13.5	110,683
2010	0.112	0.07	1,927	58,436	6,565	19.4	127,045
2011	0.099	0.08	2,277	70,289	6,925	18.7	129,189
2012	0.119	0.08	2,060	63,534	7,551	11.8	89,372

Table B5.3. Summary of HabCam abundance and biomass data for sea scallops used in this assessment. “Images” is the number of images annotated. “Images w/scallops” is the number of images in which scallops were observed. “GAM + kriging” results were estimated using the preferred approach (zero-inflated GAM models with ordinary kriging of residuals). Alternative stratified mean estimates are also shown. See Appendix B6 for further details.

Stock	Year	Annotated Images	Images w/scallops	Number (millions)				Biomass (mt)			
				Stratified random	CV	GAM + kriging	CV	Stratified random	CV	GAM + kriging	CV
GB	2011	202,257	21,428	3,992	0.02	3,832	0.31	110,204	0.02	102,819	0.12
	2012	36,304	7,189	4,003	0.03	4,642	0.14	94,025	0.03	94,040	0.08
	2013	33,864	4,671	3,562	0.03	4,049	0.09	54,683	0.03	49,671	0.29
MAB	2012	20,969	2,095	4,166	0.03	4,902	0.13	50,574	0.04	49,196	0.12
	2013	42,213	3,627	5,064	0.05	4,611	0.07	62,315	0.04	61,485	0.13
Total	2012	57,273	9,284	8,169	0.02	9,545	0.10	144,598	0.02	143,236	0.07
	2013	76,077	8,298	8,627	0.03	8,659	0.06	116,998	0.03	111,157	0.15

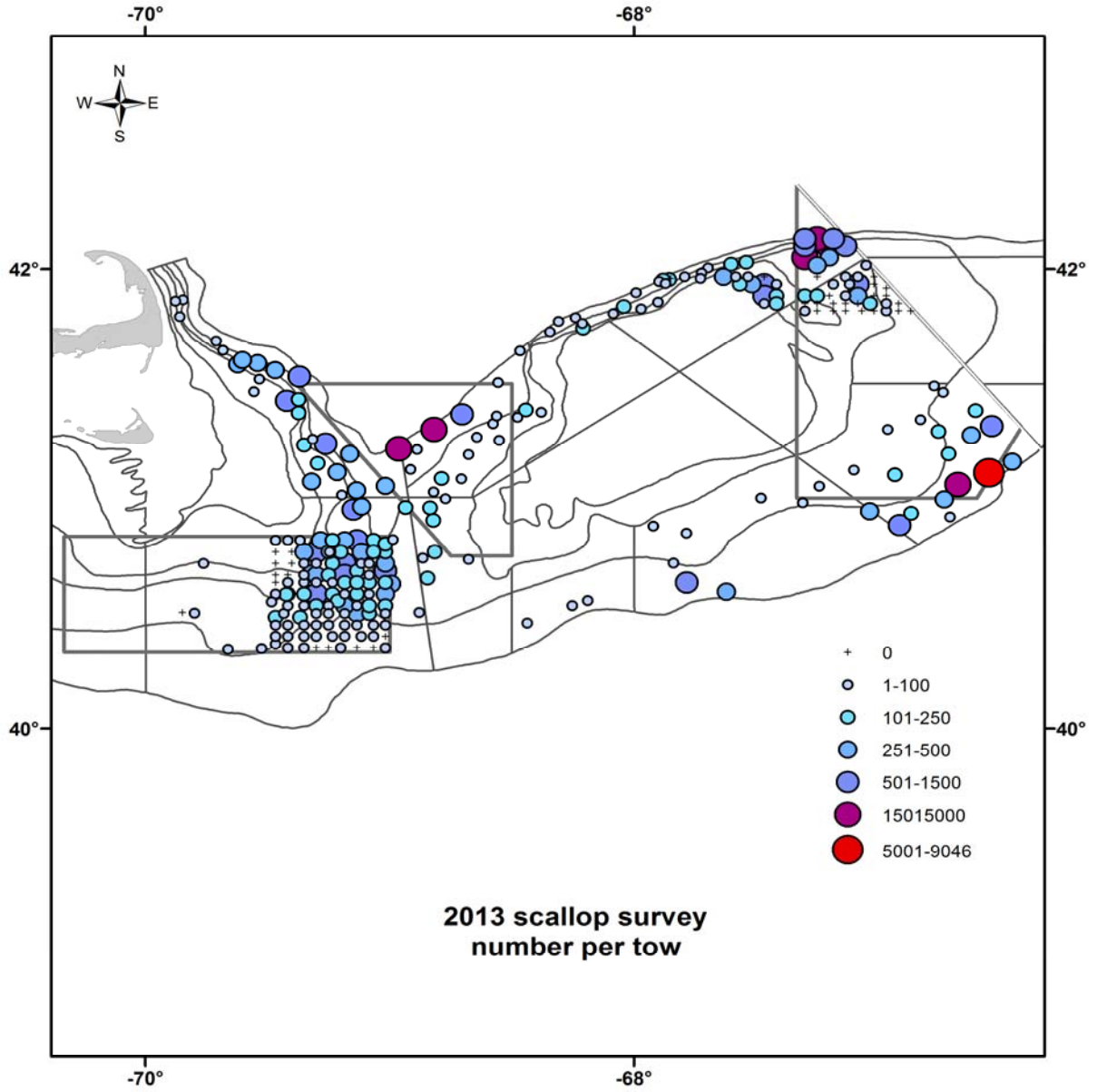


Figure B5.1(a). Dredge survey (NEFSC and VIMS) scallop dredge survey catch number in numbers per tow for Georges Bank.

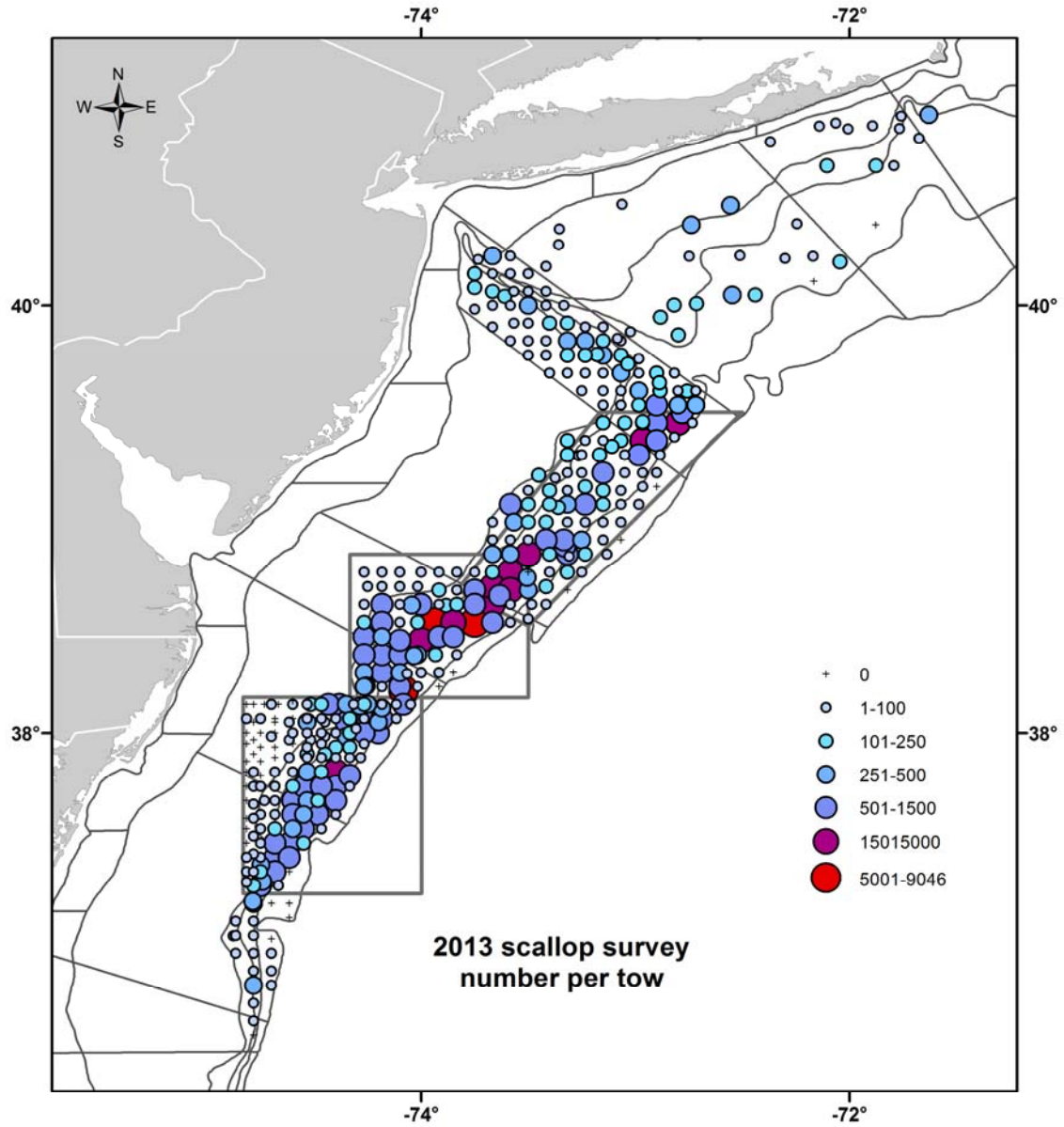


Figure B5.1(b). Dredge survey (NEFSC and VIMS) scallop catch number in numbers per tow for the Mid-Atlantic Bight.

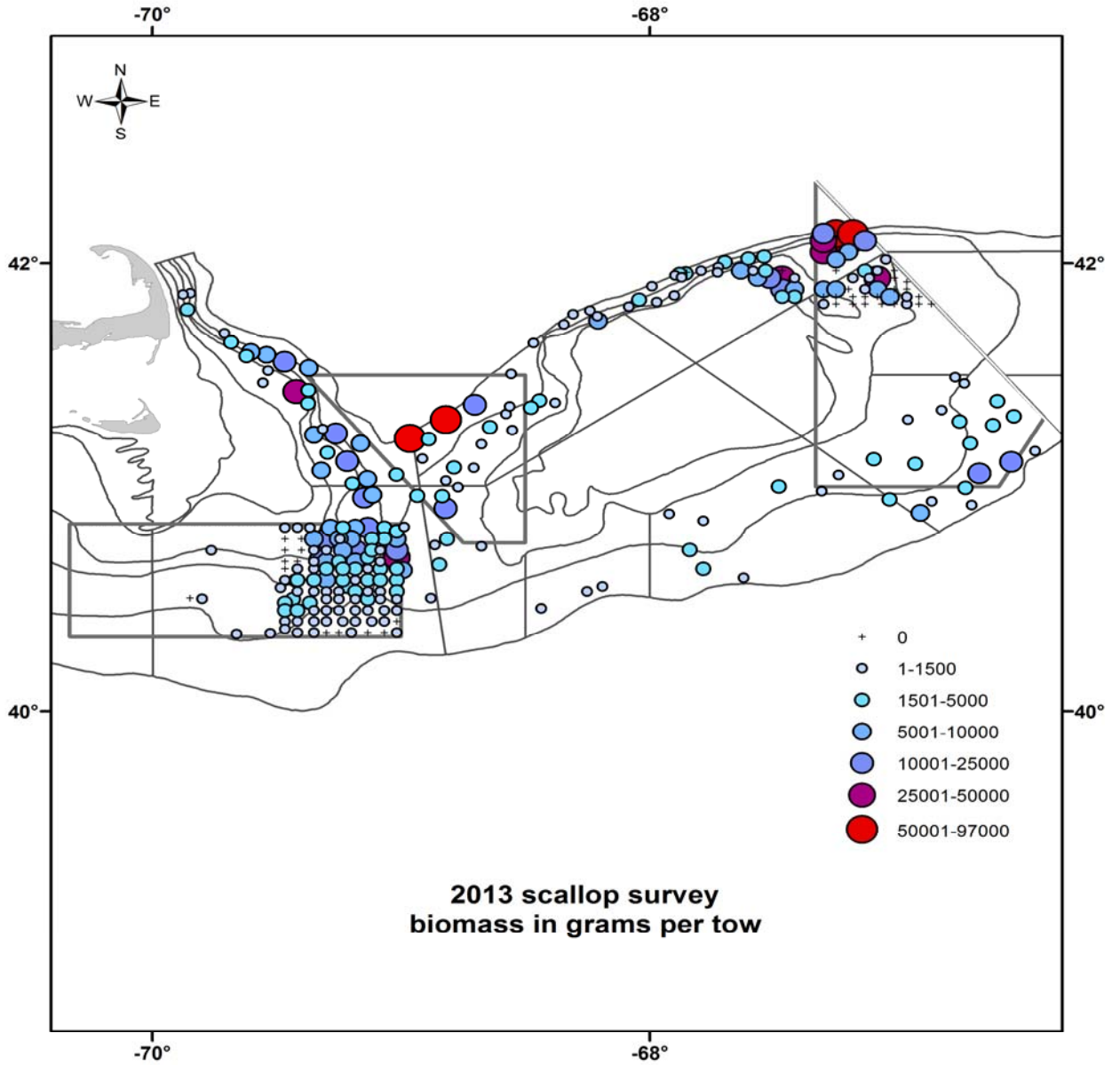


Figure B5.1(c). . Dredge survey (NEFSC and VIMS) scallop catch biomass in grams meats per tow for biomass in grams meat per tow, Georges Bank.

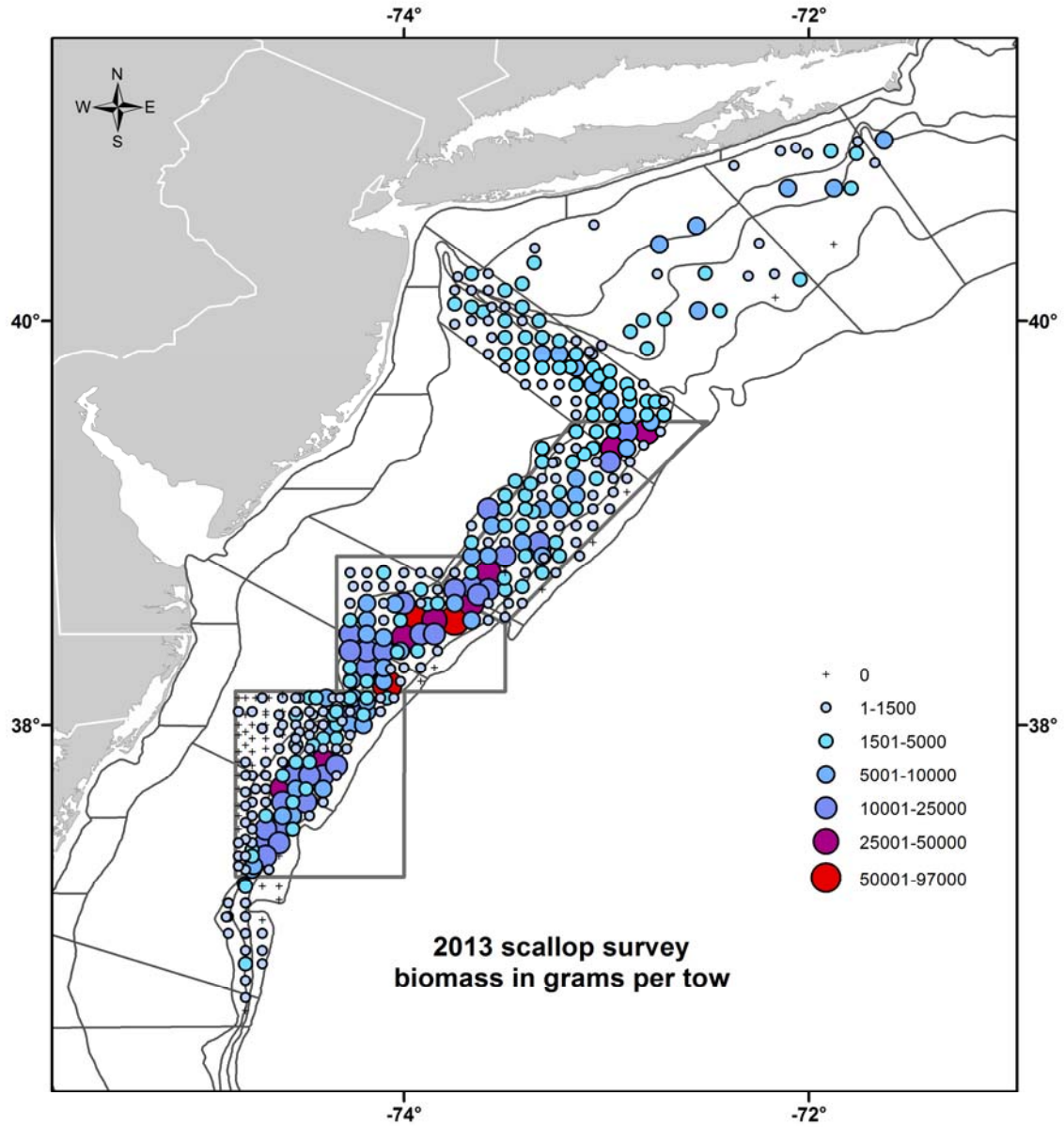


Figure B5.1 (d). Dredge survey (NEFSC and VIMS) scallop catch biomass in grams meats per tow for the Mid-Atlantic Bight.

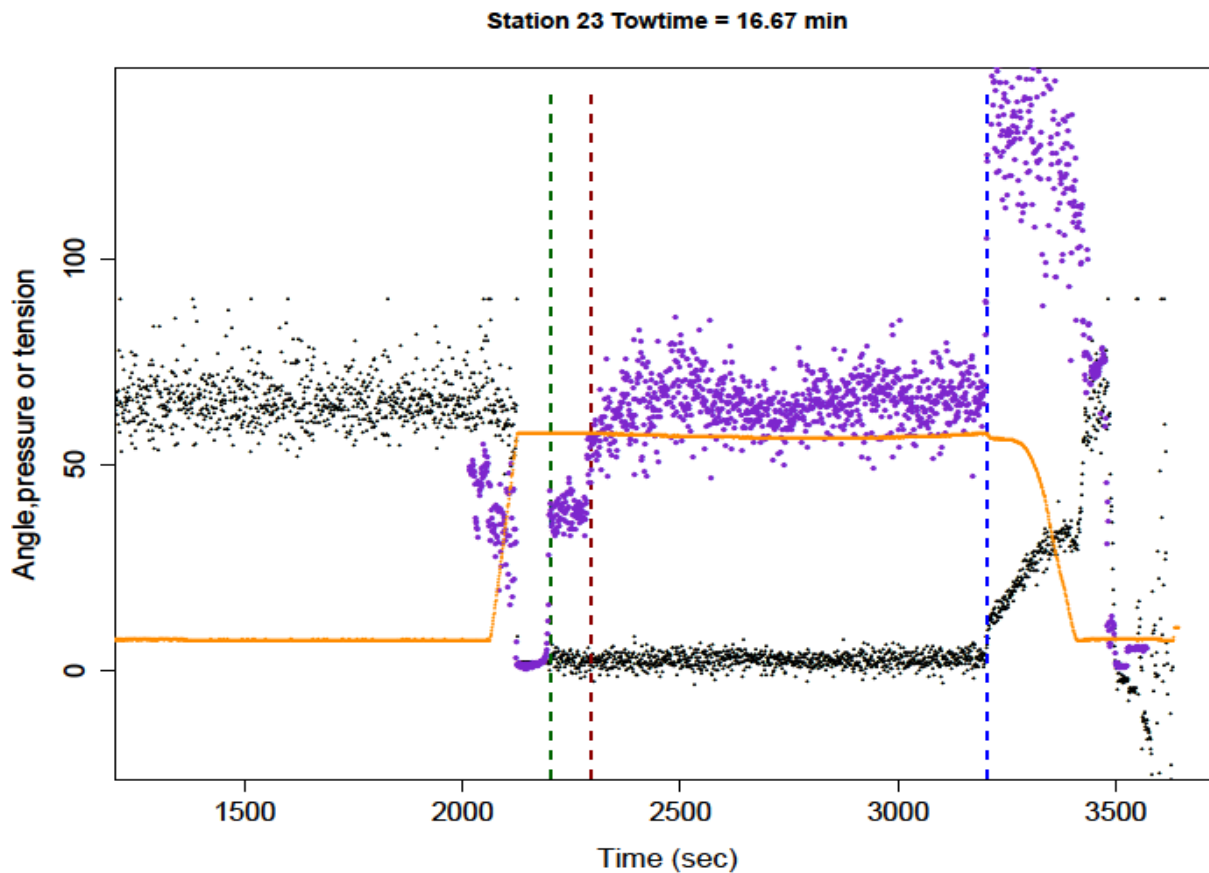


Figure B5.2. Dredge sensor data for an example tow on the *R/V Hugh Sharp* in 2013. The small black dots represent dredge angle, the orange line is pressure (a surrogate for water depth), and the purple dots are cable tension. When the dredge first hits the bottom, cable tension is zero, indicating that the dredge is not moving. The sudden increase in cable tension occurs when the tow has begun (green line), which typically is before the winch is locked (nominal tow start, red line). At tow end (blue line), sudden changes are seen in dredge angle, cable tension, and pressure.

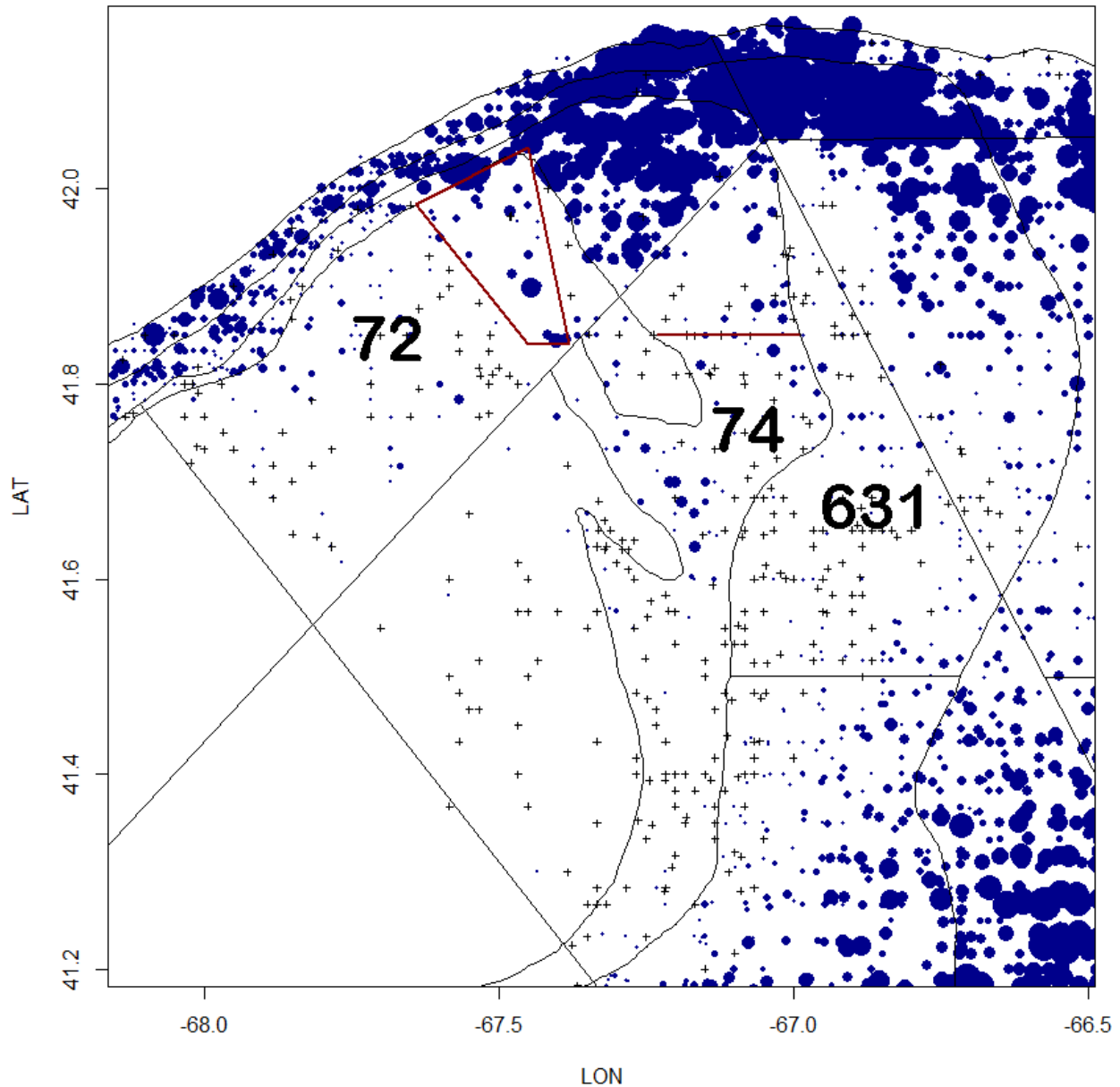


Figure B5.3 Scallop catches (in weight per tow) for all NEFSC dredge tows 1979-2013 in the northeast portion of Georges Bank, showing the two strata (72 and 74) whose areas were modified and the stratum (631) that was dropped. The red polygon in stratum 72 shows the portion of the stratum that is retained in the survey index. The portion of stratum 74 retained in the survey index is the area north of the red line. Catches with zero scallops are shown by plus marks.

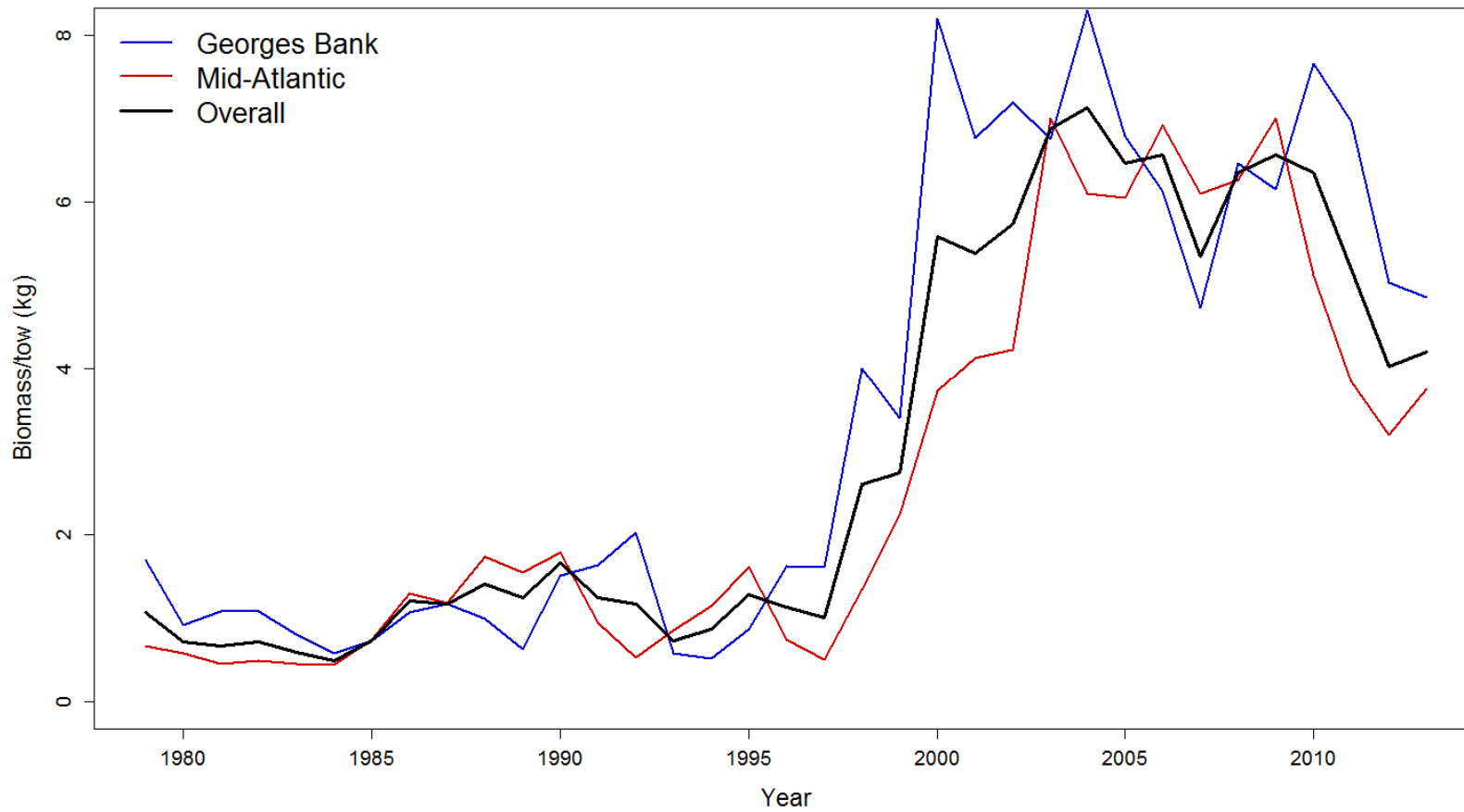


Figure B5.4. Mean stratified biomass from dredge surveys on Georges Bank, the Mid-Atlantic, and overall, 1979-2013.



Figure B5.5. The “v2” (top left) and “v4” (top right) HabCam systems, with an example image taken by v4 in the Elephant Trunk area of the Mid-Atlantic in 2013.

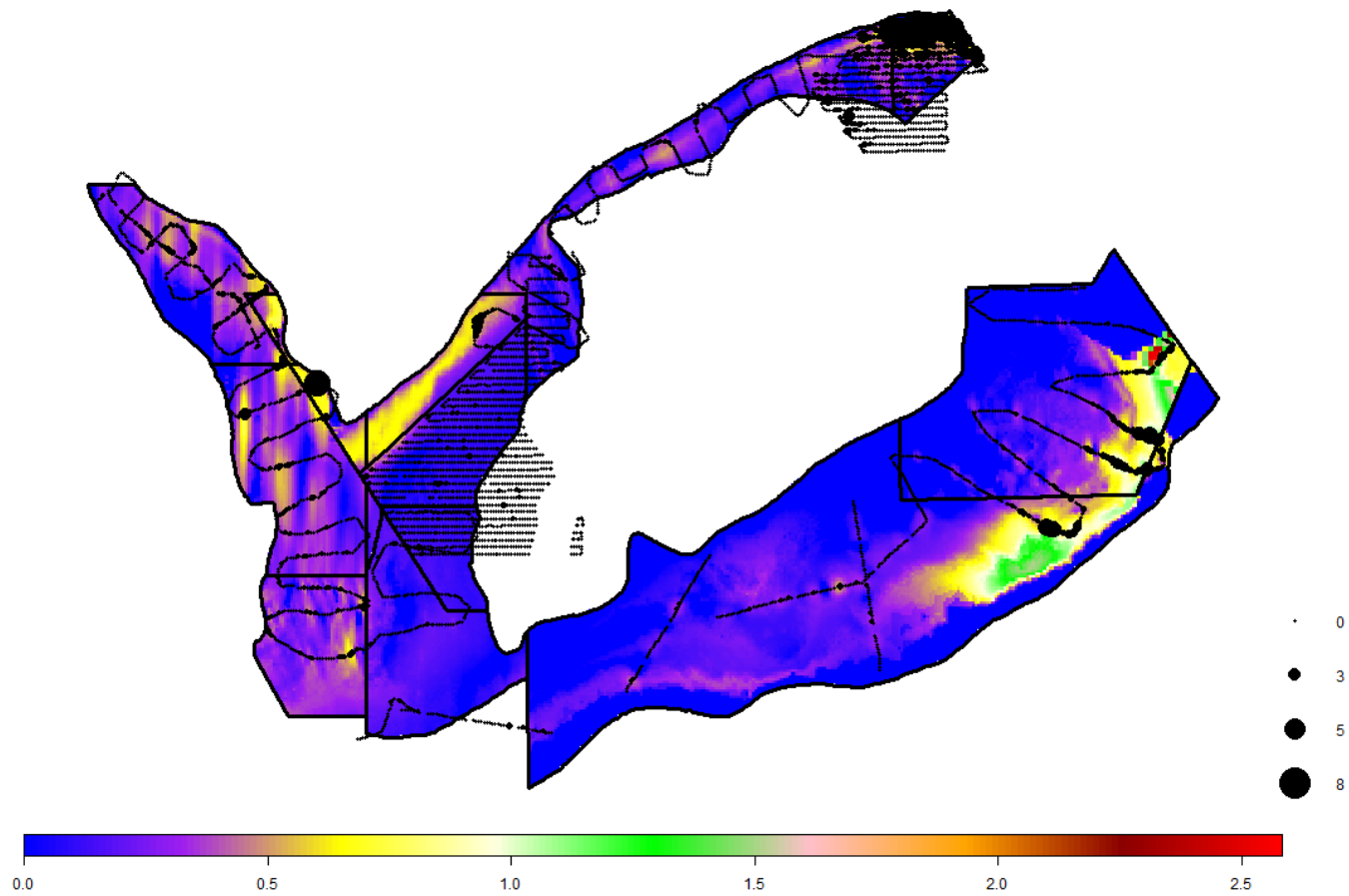


Figure B5.6(a). Estimated scallop densities ($\# \text{ m}^2$) on Georges Bank in 2013 based on HabCam data using the GAM plus ordinary kriging method. The survey trackline (black line) together with observations of scallops (black dots) are also shown.

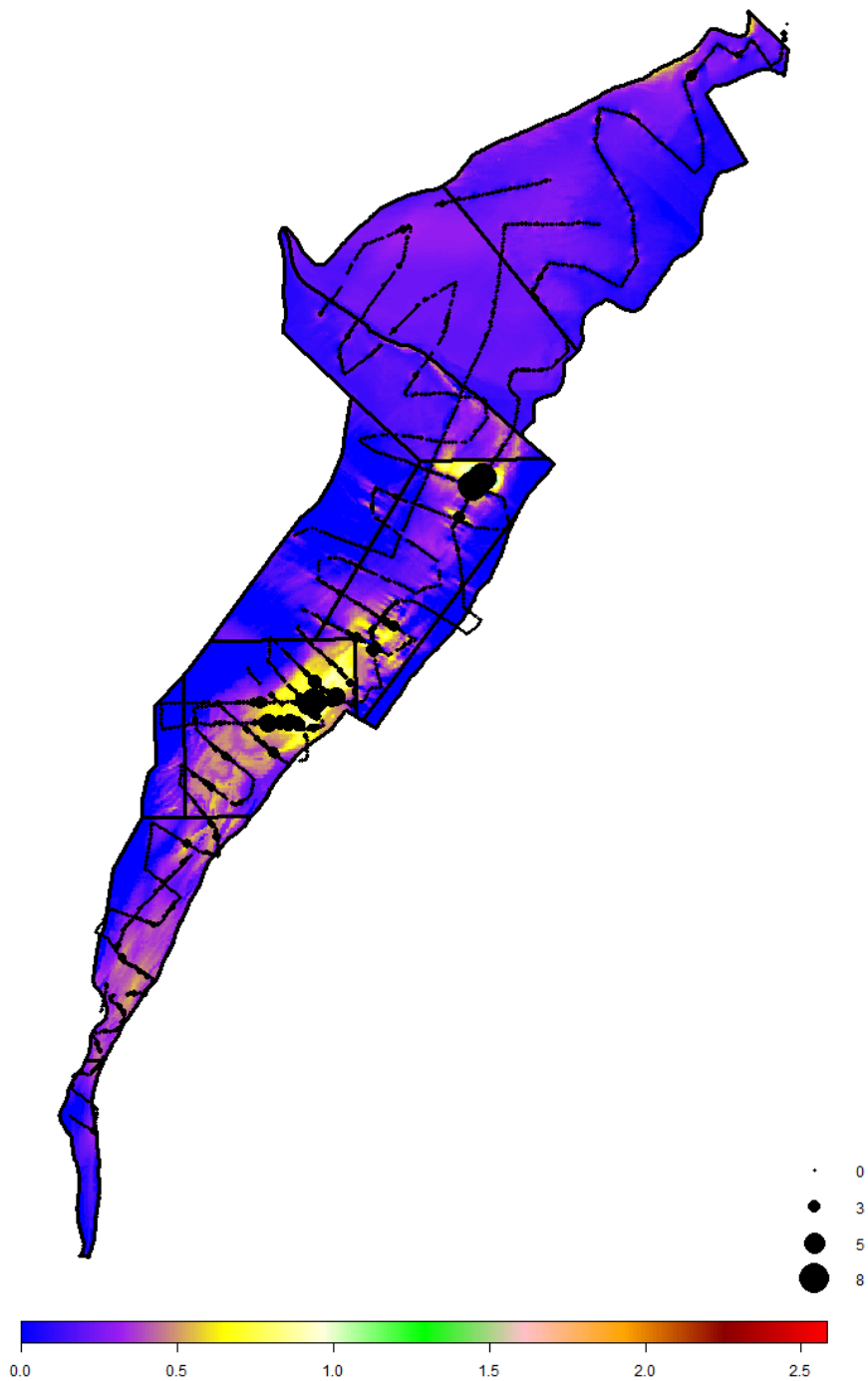


Figure B5.6(b). Estimated scallop densities ($\# \text{ m}^2$) in the Mid-Atlantic in 2013 based on HabCam data using the GAM plus ordinary kriging method. The survey trackline (black line) together with observations of scallops (black dots) are also shown.

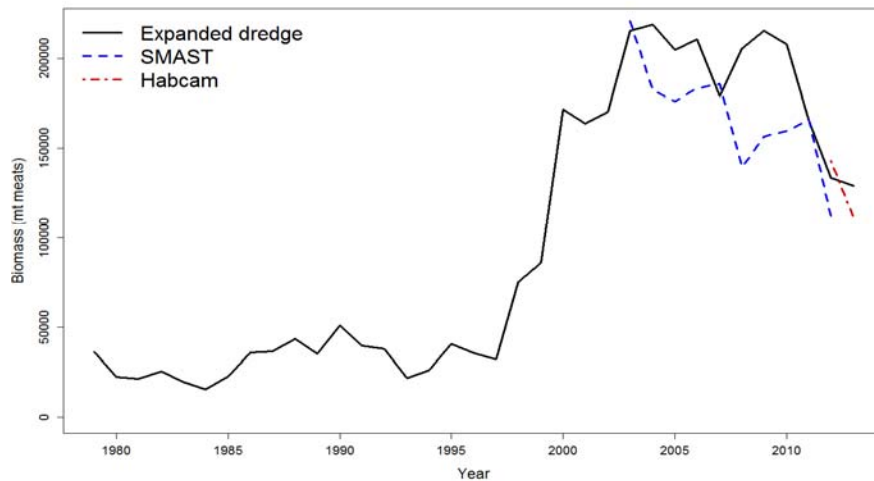
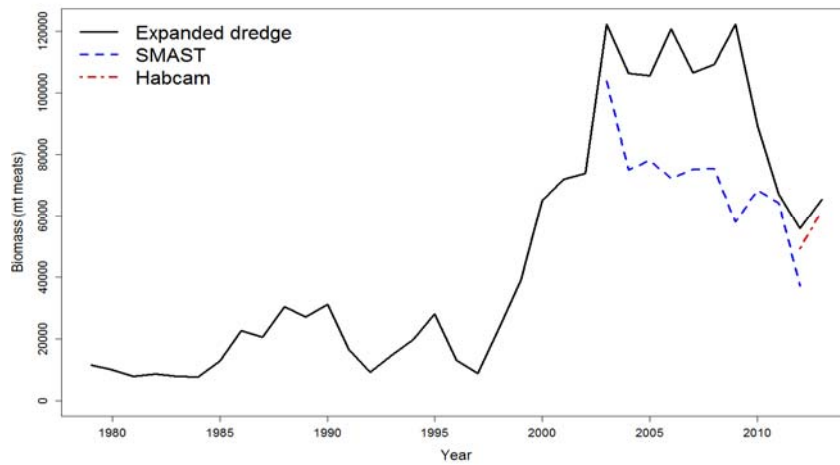
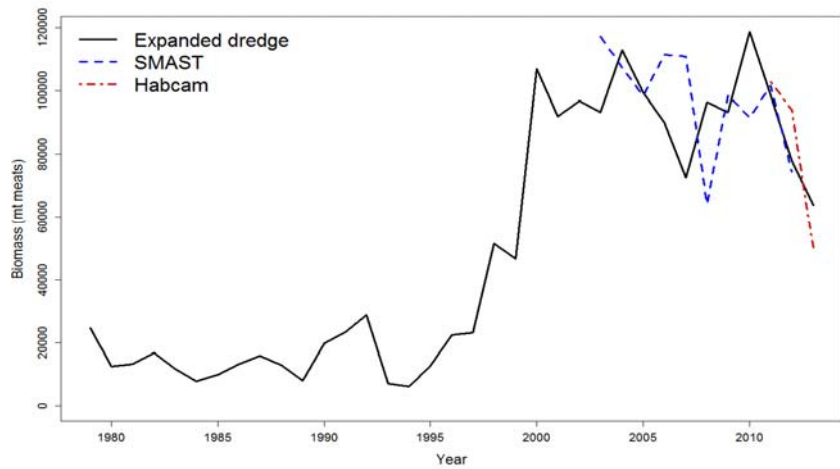


Figure B5.7. Comparison of dredge, SMAST video and HabCam survey biomass estimates for Georges Bank (top), Mid-Atlantic (middle), and combined stock (bottom).

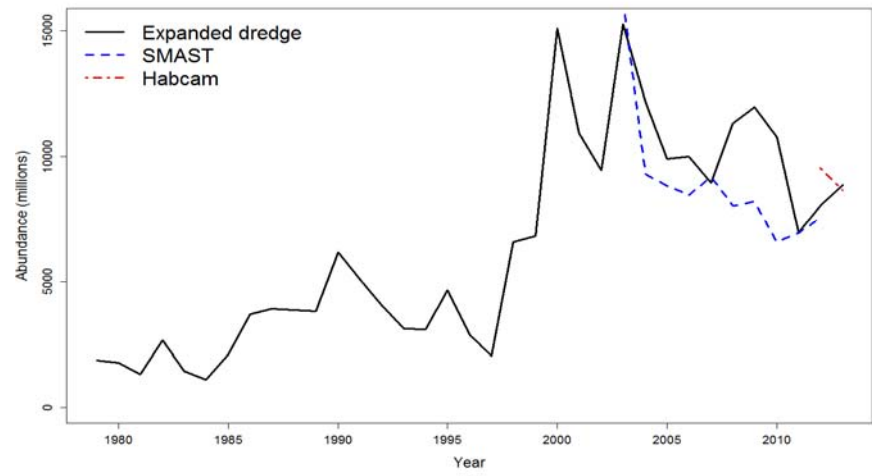
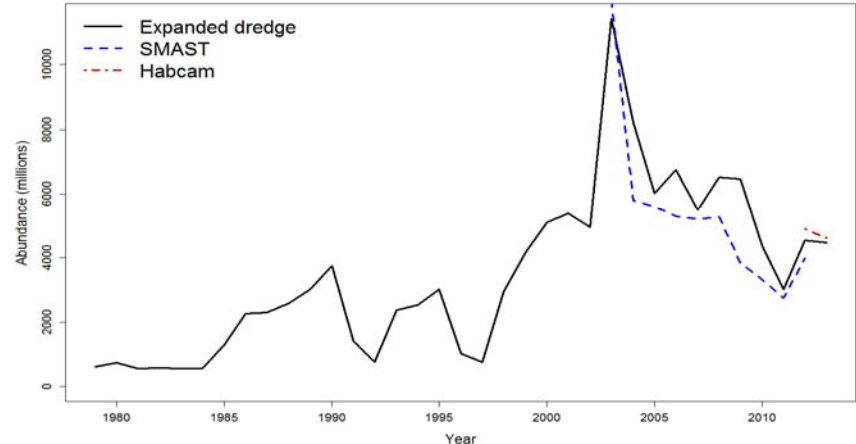
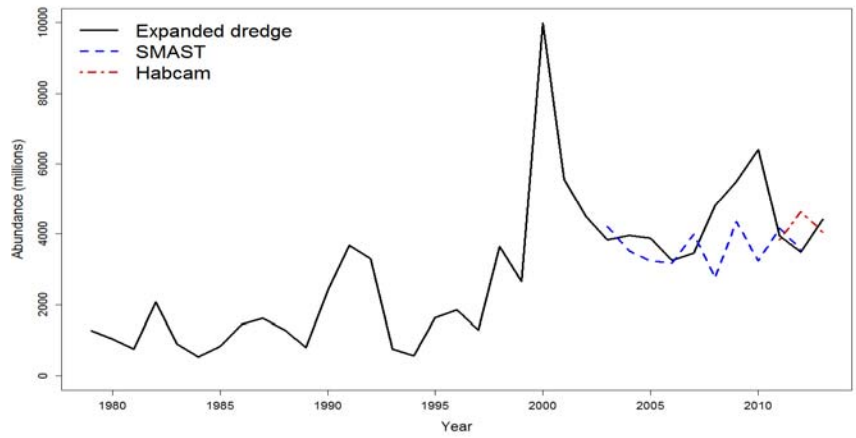


Figure B5.8. Comparison of dredge, SMAST video and HabCam survey abundance estimates for Georges Bank (top), Mid-Atlantic (middle), and combined stock (bottom).

B6. FISHING MORTALITY, BIOMASS, AND RECRUITMENT ESTIMATES (TOR 4)

A catch-at-size-analysis (CASA, Sullivan et al 1990) was used as the primary assessment estimation model. This model has been used for US sea scallop assessments since 2007 (NEFSC 2007, 2010). It performed well in simulation testing using the SAMS model as the operating model (NEFSC 2007; Hart et al. 2013). An additional and simpler “empirical” modeling approach was used for comparison to CASA results (see below and Appendix B9).

For the first time in this assessment, Georges Bank sea scallops were assessed using separate CASA models for open and closed areas. In previous sea scallop assessments, Georges Bank was modeled as a single region containing open, closed and rotational areas. Domed fishery selectivity patterns were used for the Georges Bank stock when there was no fishing in closed areas because large scallops are most common in the closed areas and thus experience less fishing mortality on average than smaller commercial-sized scallops. Using simulated and real data, Hart et al. (2013) concluded that splitting Georges Bank into open and closed areas gave more stable and likely more precise results, probably due to problems modeling complicated and ephemeral domed selectivity patterns. Separating the open and closed areas allows the use of simple logistic selectivity models for fishery size data, rather than domes. As in previous assessments, scallops in the Mid-Atlantic were assessed using single CASA model.

All three CASA models (Georges Bank open, Georges Bank closed and Mid-Atlantic Bight) were run from 1975-2013. Shell heights were modeled with 5mm shell height bins starting at 20mm, but only scallops larger than 40mm were used in tuning because smaller scallops are not fully selected in any of the surveys. The lined dredge and HabCam surveys were assumed to have flat selectivity for scallops 40+ mm. Selectivity of the SMAST large camera and unlined dredge surveys was fixed at experimentally determined values (NEFSC 2007). Selectivity of the winter trawl survey, used in the Mid-Atlantic model only, was assumed logistic with parameters estimated by the model.

Population shell height/meat weight conversions used parameters estimated from 2001-2013 research vessel survey data. Fishery meat weights were adjusted based on estimated seasonal anomalies and the seasonal distribution of landings in that year (see Appendix B3). Commercial shell height (size composition) data for 1975-1984 was from port samples, and 1992-2013 data were from sea samples (observers). The final (plus) group included L_{∞} . The meat weights for the plus group bin in a given year were the mean observed weight of scallops in the plus group in the dredge survey (for the population) or in port or sea samples (for the fishery, Figure B6.1).

CASA models growth using stochastic growth transition matrices that describe the probabilities for each starting size group of reaching new size groups after one year of growth. In previous assessments, transition matrices were derived directly from shell increment data, and a single transition matrix was used for the entire time series (Hart and Chute 2009a). Several growth transition matrices were used in this assessment to represent growth in different time periods because of new evidence indicating that apparent growth has changed over time. The fishery tends to select large, fast growing individuals so that smaller and relatively slow growing individuals are over-represented in the residual population; the extent of the reduced growth depends on the level of fishing effort.

The growth matrices were based on von Bertalanfy growth parameters and their variances (that measure variability among individual scallops) estimated from growth increment data

using mixed-effects models (Hart and Chute 2009b, see life history section). The matrix was constructed by drawing L_{∞} and K values from independent normal distributions with means and variances among individuals estimated by the mixed-effect model. One thousand parameters were drawn for each 0.05 mm interval within each 5 mm starting size bin and used to simulate one year of growth. The resulting binned scallop shell heights were converted to proportions that estimate the desired transition probabilities. Transition matrices constructed in this way were smoother, but similar, to matrices derived directly from growth increments in past assessments.

Prior probabilities (also known as likelihood constraints) are used to incorporate knowledge regarding absolute scale from the surveys. Priors on survey catchability were used for the lined dredge, the SMAST large camera, and HabCam surveys. Priors were calculated assuming that catchability parameters for these surveys have a beta distribution with specified mean and coefficient of variation (CV). The assumed CVs for catchability priors were 0.15 for SMAST and the dredge survey and 0.1 for HabCam. The CV for HabCam is smaller because it is expected to give the most accurate scaling.

For use with priors, the dredge survey was expanded to an absolute scale assuming flat selectivity, experimentally derived estimates of capture efficiency and best estimates of stock area and areas swept by the dredge tows (Appendix B4). SMAST large camera data were expanded after using the experimentally derived selectivity curve to adjust for reduced selectivity of small scallops. After this adjustment, SMAST abundance and size data were expanded assuming flat selectivity and 100% capture efficiency. Expansion of the HabCam survey assumed 100% detectability of scallops > 40mm by the camera.

The estimated catchability parameters from CASA are useful diagnostics when compared to their priors. In the CASA model, $I=qN$ where I is a survey abundance observation, N is abundance available to the survey and q (with expected value 1.0) is the catchability parameter. Relatively high estimates of q indicate relatively low estimated abundance and *vice-versa* because abundance $N=I/q$.

The catchability parameters estimates described above could, in principal, be larger or smaller than one but beta distributions in CASA do not allow values larger than one. Moreover, we wanted to use a symmetrical beta distribution so that the probability of being slightly larger or smaller than the expected value was the same. We met these objectives in a convenient fashion and without additional programming by multiplying the survey abundance data in the model by 0.5 so that the mean of the prior distributions and expected catchability values were 0.5. This rescaling is simply for convenience; it replaces the target 1.0 for catchability by 0.5 with no other effect on model estimates.

CVs for survey data and effective samples sizes for length data were tuned in preliminary model runs so that the median of assumed values used in tuning were similar to expected values based on goodness of fit. Asymptotic delta method variances calculated in CASA with AD-Model Builder software were used to compute variances and CVs. Sensitivity and profile analyses were also used to describe uncertainty.

CASA model for Georges Bank Open

The model was tuned to the lined dredge survey (1979-2013), the SMAST large video camera survey (2003-2012), the HabCam survey (2011-2013) and the unlined dredge survey (1975

and 1977). The commercial fishery selectivity periods were 1975-1998, 1999-2004, and 2005-2013 so that there was separate fishery selectivity curve during each period.

Two growth matrices were used: one derived from shells collected from the Georges Bank open areas from 2001-2012, and the other from shells collected from all of Georges Bank during 1988 and 1993. The first growth matrix is from a period of moderate fishing pressure while the second is from a period of high fishing pressure. The first transition matrix was used during 1975-1985 and 1999-2013 when fishing effort was moderate and the second matrix was used from 1986-1998, when fishing effort was the highest. Natural mortality was set at $M = 0.16$ ($M = 0.24$ on the plus group) and incidental fishing mortality was set at 0.2 times fully recruited fishing mortality for the smallest size group as described elsewhere in this report. Results are shown in Figures B6.2 to B6.15.

The resulting basecase model fit survey abundance, trends and size data reasonably well (Figures B6.2 to B6.5). Mean estimated posterior efficiencies for the dredge, SMAST and HabCam surveys ranged from 0.53-0.66 (compared to the prior mean 0.5), indicating that CASA abundance estimates were slightly lower than the survey abundance data on average (Figure B6.7). Model estimates of fishing mortality were consistent in scale with the Beverton-Holt (1956) length-based equilibrium estimator (Figure B6.13).

Fishery selectivity strongly shifted over time toward larger shell heights, reflecting changes in gear and targeting practices (Figure B6.8). The size at 50% selectivity moved from about 75 mm before 1999, to 90 mm during 1999-2004, and 100 mm since 2005.

Biomass and abundance generally declined and fishing mortality increased during 1975-1995, with these trends reversing themselves after 1995. As a result of the changes in selectivity and fully recruited fishing mortality, survival to large shell heights has increased substantially in recent years (Figures B6.10-11).

The Georges Bank Open runs show very little retrospective pattern with a seven year peel (Figure B6.15). However, over the last three years, there has been a tendency for the model to overestimate biomass and underestimate fishing mortality.

CASA model for Georges Bank Closed

The model was tuned to the same surveys as used for Georges Bank open areas. There were three growth periods in the model. The first, from 1975-1986, used data from shells collected in the open areas during 2001-2012 that reflected moderate fishing pressure. The second 1987-1995 used data from shells collected from all of Georges Bank during 1988 and 1993 when fishing pressure was high. The third period 1996-2013 is based on shells from the Georges Bank Closed Areas during 2001-2012 when fishing was low or zero. Natural and incidental fishing mortality assumptions were the same as the open area model (i.e., $M = 0.16$ and $M = 0.24$ on the plus group). Incidental fishing mortality was set at 0.2 times fully recruited fishing mortality for the smallest size group. Results are shown in Figures B6-16 to B6-25.

Model abundance estimates generally track dredge survey abundance data well during 1979-1997, but are below survey abundance for 1998-2010. Mean posterior efficiencies for catchability were 0.68 for the dredge, 0.74 for SMAST and 0.39 for HabCam so that the dredge and SMAST surveys were above the prior mean of 0.5 while HabCam was below

(Figure B6.21). The discrepancy between the surveys is likely due to the fact that the HabCam survey was only conducted in 2011-2013, when estimated abundance tended to be above the surveys, whereas there were years that the model was well below expanded estimates from both the other surveys. The model estimated abundance and biomass for 2013 above both the dredge and HabCam surveys.

The model generally fit shell height data and survey data, except for years with very strong recruitment events, when the model tended to be below the survey data (Figures B6.17 to B6.19). CASA model estimates of fishing mortality about the same scale as Beverton-Holt estimates (Figure B6.27).

Estimated fishing mortality increased from 1975-1993 (Figures B6.23 and B6.25) and were low or zero afterward. This resulted in a dramatic increase in biomass during 1994-2004, and a build-up of large scallops (Figure B6.23 and B6.24). Fishery selectivity since 1999 shifted strongly to large scallops (Figure B6.22), even more so than in the open areas, because scallop fishermen tend to select the largest market category (U-10s, i.e., over 45 g meat weight) which usually commands a premium price.

The model for Georges Bank closed areas has a moderate retrospective pattern (Figure B6.29, Mohn's $\rho = 0.33$), where estimates of biomass decrease, and fishing mortality increase, as more years of data are added.

When 6 or 7 years of data are removed, the model fits the survey data well (Figure B6.28). However, the declines in biomass observed in surveys in recent years cannot be fully explained by fishery removals and the assumed natural mortality, so that the model lowers the biomass for previous years as more years of data are added.

CASA model for combined Georges Bank open and closed areas

Biomass and fishing mortality estimates for Georges Bank open and closed combined (Figure B6.30) show generally decreasing biomass and increasing fishing mortality from 1975-1992, with peak fishing mortality of 1.69 in 1992, and minimum biomass of 5,903 mt in 1993. Fishing mortality since 1995 has generally been between 0.2 and 0.4, and biomass increased substantially between 1994 and 2003. Estimated 2013 biomass and fishing mortality for Georges Bank combined is 86,460 mt and $F = 0.30$, respectively. Retrospective scores for the entire Georges Bank region fell between the scores for the open and closed portions only (Figure B6.30b).

CASA Model for the Mid-Atlantic

The Mid-Atlantic CASA model uses the surveys also used for Georges Bank plus the NEFSC winter bottom trawl survey which was conducted between 1992 and 2007. The winter survey used flatfish trawl gear similar to commercial scallop trawls and should have caught scallops fairly reliably. Preliminary runs with potentially domed selectivity for the winter trawl survey did not indicate that selectivity was reduced for large scallops, so selectivity was modeled using a logistic curve with parameters estimated by the model. Survey efficiency priors and selectivity assumptions for the other three surveys were the same as for Georges Bank. The fishery selectivity periods were 1975-1979, 1980-1997, 1998-2001, 2002-2004 and 2005-2013. The first period was modeled as domed (double logistic) selectivity, due to indications in the data of higher mortality on intermediate sized scallops. This was likely caused by fishing effort that was concentrated in only a portion of the stock, so that most large scallops

were in areas outside the intensively fished area where densities were lower. All the other periods were assumed to have logistic selectivity. Natural mortality was set at $M = 0.2$ with $M = 0.3$ for the plus group, and incidental fishing mortality was set at 0.1 times fully recruited fishing mortality for the smallest size group.

Three growth periods were used: the 1975-1985 and 1998-2008 periods were modeled based on shells collected during 2001-2009 when fishing pressure was moderate. Growth during 1986-1997 was based on shells collected in 1988 and 1993 when fishing effort was high. Growth during 2009-2013 was based on shells collected during 2010-2012 when growth was apparently somewhat faster than during 2001-2009.

Preliminary runs using the effective sample size tuned to match model fits for the dredge survey gave unrealistic results with the model estimating lower fishing mortality in the early 1990s, when fishing effort was the highest, than ten years later. In addition, the model predicted a build-up of scallops in the plus group during the early 1990s contrary to dredge survey shell heights. Estimated fishing mortalities conflicted with those from the Beverton-Holt equilibrium estimator.

For these reasons, the effective sample size of the dredge shell heights was increased to an average of about 800 so that the dredge size data fit the model more closely (Figures B6-31 to B6-43). This resulted in much more realistic fishing mortality and shell height estimates (Figure B6.40). The increased effective sample size is ad-hoc but corresponds to an effective sample size of about 4 scallops per tow which is not unreasonable. Results are shown in Figures B6.33 to B6-44.

The final model fit survey abundance data well for some years, but was often below survey estimates during and after strong recruitment events (Figures B6.31). This was especially apparent starting in 2003, when a very strong year class was observed in both the dredge and SMAST surveys. Because of this conflict, posterior efficiencies were high and near the upper bounds of their priors (over 0.8 for the dredge and SMAST surveys and over 0.6 for HabCam relative to the prior target 0.5, Figure B6.37). Model estimates of shell heights generally fit the data well, except the model estimates of some strong year classes were below those of surveys (Figures B6.32 to B6.35).

Fishery selectivity was strongly domed during 1975-1979 but shifted to a logistic shape and moved father to the right during subsequent periods as would be expected based on management and fishery changes (Figure B6.38). By 2005-2013, only the plus group was fully selected. Model estimated fishing mortality on larger scallops generally increased during 1975-1995, reaching a maximum fully recruited fishing mortality of about 1.5 in 1995, and then declined (Figure B6.39 and B6.41). This decline was much greater for small scallops, which were affected by the shifting selectivity as well as the decline in fully recruited fishing mortality. Abundance and biomass were relatively low during 1975-1998, and then rapidly increased from 1998-2003 (Figures B6.39). Biomass and abundance declined during 2009-2012, primarily as a result of poor recruitment. Recruitment appears to have been substantially stronger since 1998 (Figure B6.39).

The model for sea scallops in the Mid-Atlantic Bight showed a fairly strong retrospective pattern for the earliest three years, with biomass decreasing and fishing mortality increasing as more years of data were added (Figure B6.44). However, this pattern has disappeared during the last several years and has reversed directions slightly.

Whole stock biomass, abundance and mortality

Biomass, egg production, abundance, recruitment and fishable mean abundance were estimated for the whole stock and for Georges Bank as a whole by adding estimates for the Mid-Atlantic Bight and Georges Bank Open and Closed (Table B6.1). For example, whole stock fishing mortality rates for each year were calculated:

$F = (C_M + C_{Go} + C_{Gc}) / (\bar{N}_M + \bar{N}_{Go} + \bar{N}_{Gc})$ where C_M , C_{Go} , C_{Gc} are catch numbers for the Mid-Atlantic Bight, Georges Open and Georges Closed areas. Terms in the denominator are average fishable abundances during each year calculated in the CASA model as

$\bar{N} = \sum_L \frac{N_L(1 - e^{-Z_L})}{Z_L}$. The simple ratio formula used to calculate whole stock F is an “exact”

solution because the catch equation can be written $C = F\bar{N}$.

Whole stock variances were calculated assuming that estimation errors for Georges Bank open and closed, and the Mid-Atlantic Bight were independent. In particular, variances for biomass, abundance and catch estimates were the sum of the variances for Georges Bank open and closed and the Mid-Atlantic Bight. CVs for the ratios estimating whole stock F were approximated $CV_F = \sqrt{CV_C^2 + CV_{\bar{N}}^2}$, which is exact if catch number C_N and average abundance \bar{N} are independent and lognormally distributed (Deming 1960). The CV for measurement errors in catch for each region $CV_C=0.05$ is the same as assumed in fitting the CASA model. Variances for the stock as a whole depend on the assumption that model errors in Georges Bank and the Mid-Atlantic are independent. These variances would be higher if a positive correlation between model errors exists, and lower if they are negatively correlated.

Like the trends for smaller areas, whole-stock fishing mortality generally increased from 1975-1992 and then declined (Table B6.1 and Figure B6.45). Whole stock biomass, abundance and fishing mortality in 2013 were respectively 132,561 mt meats, 8014 million and 0.32. The biomass and abundance in 2013 were the highest in the 1975-2013 time series. Retrospective scores for the entire sea scallops stock were in the same range as scores for individual regions (Figure B.45b).

The standard errors estimated by the CASA model in this assessment are too small and do not capture all of the underlying uncertainties. The long time series of relatively precise dredge survey data and recent optical survey data, assumptions that survey selectivity is known and prior information on survey efficiencies likely contribute to the underestimation of uncertainty. It is also possible that the survey catchability estimates near the bounds of their priors artificially reduce variance. Comparisons with expanded survey data, retrospective and sensitivity analyses as well as likelihood profiles shown below better describe the uncertainties in the assessment.

Historical retrospective analysis

The current CASA model estimates can be compared to those from the last two benchmark assessments (SARC-45/NEFSC 2007 and SARC-50/NEFSC 2010), and also updates of the SARC-50 model configurations through 2011 and 2012 (Figures B6.46). While the estimates have been fairly stable, there has been a tendency for biomass and recruitment to be revised downward, and fishing mortality upward over time.

It is also of interest to compare the SARC-50 configuration updated through 2013 to the present model. There is a more substantial difference in the Georges Bank models, where the stock was assessed as a whole in the SARC-50 and using separate models for open and closed areas in the current assessment (Hart et al. 2013). The biomass plots indicate modest differences between the two configurations (Figure B6.47). Fishing mortality estimates for the two models are not completely comparable because of differences in estimated selectivity between the models.

Likelihood profile analysis

Likelihood profiles were constructed for natural mortality (Figure B6.48) with plus group natural mortality was fixed at 1.5x that of smaller scallops. For both Georges Bank open and closed, total -log likelihood was minimized at about $M = 0.22$. For the open areas, the survey trend component of the likelihood (sum over all surveys) was smallest at lower M values, whereas the likelihood for the size data (sum of fishery and all surveys) and Q priors were minimized at larger M values. There was a similar pattern for Georges Bank closed, although the survey trend likelihood component was minimized at about $M = 0.18$. For Mid-Atlantic sea scallops, the total -log likelihood was minimized near the assumed $M = 0.2$. The likelihood component for size composition was minimized at a lower natural mortality, whereas the component for the Q prior was minimized at higher M . Effects on stock estimates were evaluated by sensitivity analysis (see below).

Another likelihood profile analysis was constructed for natural mortality of the plus group. Because of the limited number of scallops in the plus groups in the other two models, this was conducted for the Georges Bank closed area model only. Natural mortality for the smaller size groups was fixed at $M = 0.16$ as in the basecase model. The size composition data component of the likelihood was minimized at low plus group mortality, whereas the -log likelihood of the survey trends and q priors decreased and fit improved as plus group mortality increased (Figure B6.49). Total -log likelihood was minimized at a plus group M of about 0.24, or 1.5 times that of smaller size groups. The latter is the assumption of natural mortality on the plus group made in all the models.

Profiles over dredge survey catchability

A final set of likelihood profile analyses were used to explore differences between CASA model abundance estimates and survey swept-area abundance data as well as the tendency for dredge, SMAST and HabCam survey catchability estimates to fall near the upper bound of their prior distributions (Tables B6-2 to B6-4).

Models for the Mid-Atlantic Bight, Georges Bank closed and Georges Bank open areas were run with the catchability parameter (Q) for the dredge survey fixed at a range of values between 0.4 and 1.2. Goodness of fit (unweighted negative log likelihood) for each type of data as well as measures of stock biomass and fishing mortality were recorded after each run. The profiles were run with catchability priors turned off so that they would not interfere with fit to any of the data in the model.

If the survey swept-area abundance data and model agree about stock size, then the CASA model's catchability estimates for the dredge, SMAST and HabCam data should be in the lower end of the range ($Q=0.4-0.6$) because of the way the survey data in CASA are scaled. At higher values of Q , the model estimates stock sizes lower than the swept-area abundance

data and *vice-versa*.

Results indicate that the most of the data for all three areas fit best when dredge survey Q is higher than its expected value and estimated abundance is lower on average than indicated by the survey swept-area abundance data (Tables B6-2 to B6-4). This tendency is most pronounced in the Mid-Atlantic Bight area. The cause of these discrepancies is not clear.

Sensitivity analysis

To test the sensitivity of the model outputs to key assumptions, CASA model runs were conducted with alternative assumptions regarding natural mortality, survey priors and incidental mortality. Alternative assumptions about natural mortality on Georges Bank were $M = 0.12$ (as in SARC-50) and $M = 0.20$, and $M = 0.15$ (SARC-50) and $M = 0.25$ in the Mid-Atlantic. Runs were conducted with the survey priors turned off, at twice the assumed CVs (“loose priors”: 0.3 for dredge and SMAST, and 0.2 for HabCam) and at half the assumed CVs (“tight priors”: 0.075 for the dredge and SMAST, and 0.05 for HabCam). Alternative assumptions for incidental mortality were either zero or twice the assumed value (0.4 for Georges Bank and 0.2 for the Mid-Atlantic).

Variations in the assumed natural mortality had little effect on Georges Bank Open runs. Assumptions about survey priors had modest effects only in the last several years (Figure B6.50). The assumed value of natural mortality had a stronger effect on Georges Bank Closed runs, especially in the first 15 years after the closures. The higher natural mortality rate allowed the model to estimate a biomass closer to that estimated by the surveys during the 1998-2008 period. However, the value of natural mortality had little influence on the 2013 estimated biomass. Tighter survey priors induced higher biomass estimates, mainly from 2002-2013, whereas loose or no priors induced lower estimates.

The assumed natural mortality rate also had limited effects in the Mid-Atlantic Bight runs, and primarily affected the estimated biomass during 2000-2010. Loose or no survey priors decreased biomass estimates in the Mid-Atlantic, mainly in the last 5 years of the time series. Effects on fishing mortality were generally modest and in the reverse direction of effects on biomass (Figure B6.51). The assumed level of incidental mortality had little effect on model estimates of biomass (Figure B6.52).

Experimental runs with density-dependent natural mortality on juvenile scallops

Scallop abundance estimates from the CASA model were typically below those of the surveys when strong recruitment was observed in the surveys. This suggests that natural mortality of juveniles may increase at high density. If this is the case, CASA models would be below the surveys for those years because observations of the strong year class in subsequent years would indicate less scallops than would be expected based on the initial survey observations and assumptions regarding natural and incidental mortality. High natural mortality on large year classes of juveniles ignored in modeling would induce retrospective patterns like that observed, where estimates of strong year classes and abundance would decline as more years of data were added.

There is also experimental evidence of density-dependent natural mortality on juvenile sea scallops. Wong et al. (2005) seeded juvenile scallops in experimental plots at densities of 1, 6

or 69 m^{-2} . Scallop density in the high-density sites declined markedly due to both predation (and in particular predation by *Cancer* spp. crabs) and dispersal, resulting in final densities of about 1 m^{-2} regardless of treatment. Predation rates of *Cancer* crabs on juvenile sea scallops appear to be greater when scallops are more common than alternative prey species, and increase with increasing scallop density (Barbeau et al. 1998, Wong and Barbeau 2005). Thus, *Cancer* crabs are potential agents of density dependence in juvenile sea scallops; they primarily consume scallops less than 70 mm, and almost all less than 90 mm (Elner and Jamieson 1979, Lake et al. 1987).

In order to model density-dependent juvenile mortality, we defined the number of juveniles as the $J = L(H)$, where H is scallop numbers at shell height and L is a declining logistic function. For this initial exploration, the inflection point L_{50} of the logistic function was set at 80 mm, and the slope of the logistic function was also fixed (Figure B6.53). Natural mortality of juveniles of shell height H was assumed to be $M_0(H) + kL(H)J$, where M_0 is a fixed constant and k is a parameter estimated by the model. For this preliminary work, M_0 was set at half of the adult natural mortality (i.e., 0.08 for Georges Bank and 0.1 for the Mid-Atlantic) at small sizes, and increases to full adult natural mortality at large sizes (i.e., $M_0(H) = M[2-L(H)]/2$, where M is the natural mortality on adults).

Example runs are shown here for Georges Bank Open and Closed; density-dependence in the Mid-Atlantic model was difficult to estimate. Both Georges Bank models showed improved fits to the survey data, especially Georges Bank Closed (Figures B6.53 and B6.54). Estimated natural mortality of juveniles ranged between about 0.15 and 1. The working group thought these preliminary model runs were promising and recommended further development of this approach.

Empirical Assessment

The empirical assessment used simple techniques to estimate sea scallop stock abundance, biomass and fishing mortality in the Mid-Atlantic, Georges Bank and combined stock areas without using a stock assessment model (Appendix B5). The purpose was to evaluate the accuracy of CASA estimates as independently as possible by taking advantage of the three surveys (dredge, SMAST and HabCam) that can be used to estimate stock size directly. However, empirical results could be used in place of CASA model estimates if the later were unavailable. The data and various parameters used in the empirical analysis are a subset of those also used in the CASA model and were all obtained independently in field studies or other analyses rather than from a stock assessment model.

Empirical and CASA model estimates of abundance and fishing mortality show similar trends in all regions (Tables 3-4 and Figure 7 all in Appendix B5). However, empirical abundance estimates were usually higher reflecting the tension in CASA models between matching the scale of the abundance data (matching the prior on Q) versus fitting the survey and fishery data which was evident in likelihood profile analysis over a ranges of dredge survey catchability (Tables B6-2 to B6-4). As expected, fishing mortality estimates show the inverse pattern with empirical generally lower than CASA estimates.

Table B6.1. CASA model estimates and standard errors for July 1 abundance and biomass (40+mm SH), and fully recruited fishing mortality for George Bank open, closed, and total. (See following pages).

Year	Georges Bank Open						Georges Bank Closed						Georges Bank Total					
	Abund (millions)	SE	Biomass (mt)	SE	F	SE	Abund (millions)	SE	Biomass (mt)	SE	F	SE	Abund (millions)	SE	Biomass (mt)	SE	F	SE
1975	969	37	16322	622	0.08	0.01	537	23	10625	461	0.09	0.01	1507	623	26946	622	0.09	0.01
1976	1023	35	17449	666	0.19	0.01	601	23	11952	478	0.14	0.01	1624	667	29401	666	0.17	0.01
1977	859	32	16389	634	0.30	0.02	502	20	11651	464	0.28	0.02	1361	635	28040	634	0.29	0.02
1978	752	27	14047	567	0.34	0.02	460	18	10155	412	0.34	0.02	1212	568	24202	567	0.34	0.03
1979	602	24	11299	482	0.45	0.03	312	15	7504	353	0.58	0.04	914	483	18803	482	0.50	0.04
1980	678	25	9484	394	0.43	0.03	359	17	5948	291	0.49	0.04	1037	395	15432	394	0.45	0.03
1981	575	22	8118	313	0.63	0.04	299	15	5160	265	0.58	0.04	875	314	13279	313	0.61	0.05
1982	500	19	6080	249	0.87	0.06	241	15	4371	276	0.49	0.04	741	250	10451	249	0.73	0.06
1983	358	17	4632	230	0.74	0.05	206	18	3667	314	0.56	0.04	565	231	8298	230	0.67	0.05
1984	314	18	3978	244	0.54	0.03	230	21	3682	352	0.26	0.02	543	245	7660	244	0.43	0.04
1985	334	21	3792	257	0.61	0.04	265	26	4034	408	0.47	0.03	598	258	7827	257	0.54	0.05
1986	490	26	3676	239	1.19	0.08	392	35	4551	433	0.72	0.05	883	240	8227	239	0.95	0.09
1987	524	25	4389	239	0.84	0.05	440	45	5005	541	0.89	0.06	964	240	9394	239	0.86	0.08
1988	393	23	4233	270	0.95	0.06	804	62	7335	605	0.87	0.06	1197	271	11568	270	0.91	0.14
1989	451	26	3803	266	0.98	0.06	816	57	10092	728	0.52	0.04	1268	267	13895	266	0.65	0.09
1990	535	26	4033	229	1.21	0.08	674	44	9074	570	1.10	0.08	1209	230	13108	229	1.13	0.13
1991	634	26	4293	188	1.49	0.10	583	30	6445	313	1.44	0.10	1217	190	10738	188	1.46	0.14
1992	376	15	3366	135	1.69	0.11	352	24	4070	269	1.70	0.12	728	136	7435	135	1.69	0.16
1993	222	11	2270	119	1.13	0.07	343	34	3633	368	0.92	0.07	564	120	5903	119	1.02	0.13
1994	220	14	2200	143	0.53	0.03	351	37	4890	546	0.13	0.01	571	143	7090	143	0.26	0.04
1995	440	19	3278	166	0.55	0.04	522	44	7743	726	0.00	0.00	962	167	11022	166	0.17	0.04
1996	466	20	4369	196	0.77	0.05	629	48	11235	905	0.00	0.00	1095	197	15603	196	0.26	0.05
1997	451	22	4456	225	0.81	0.05	691	52	15342	1142	0.00	0.00	1142	226	19798	225	0.24	0.05
1998	637	33	5260	259	0.67	0.04	1014	64	20416	1347	0.00	0.00	1651	261	25676	259	0.30	0.04
1999	1015	44	7770	325	0.90	0.06	988	65	23875	1552	0.20	0.01	2003	328	31645	325	0.44	0.06
2000	1306	45	11600	404	0.60	0.04	1687	86	29443	1689	0.15	0.01	2993	406	41043	404	0.35	0.04
2001	1328	42	14741	468	0.59	0.04	1900	84	38707	1881	0.03	0.002	3229	469	53448	468	0.31	0.04
2002	1174	39	15006	478	0.65	0.04	1918	80	47889	2063	0.00	0.00	3092	480	62895	478	0.29	0.04
2003	1210	37	14775	481	0.53	0.03	2058	79	55666	2216	0.00	0.00	3268	482	70441	481	0.19	0.03
2004	1149	37	16192	521	0.27	0.02	1860	72	58707	2292	0.07	0.005	3008	523	74899	521	0.14	0.02
2005	1257	43	18019	576	0.34	0.02	1676	70	55653	2303	0.15	0.01	2933	577	73672	576	0.21	0.03
2006	1213	47	16459	558	0.85	0.05	1380	66	47466	2251	0.25	0.02	2593	560	63925	558	0.44	0.06
2007	1562	61	16564	605	0.60	0.04	1359	72	41169	2219	0.16	0.01	2921	608	57733	605	0.30	0.04
2008	1694	73	19653	800	0.57	0.04	1376	77	39837	2245	0.07	0.005	3070	803	59489	800	0.25	0.04
2009	1838	91	22826	1101	0.48	0.03	1565	89	41774	2358	0.05	0.004	3403	1105	64600	1101	0.24	0.03
2010	1862	105	26747	1485	0.24	0.01	1689	101	44361	2558	0.09	0.01	3551	1488	71109	1485	0.16	0.02
2011	1994	127	31320	1924	0.17	0.01	1928	127	46717	2908	0.18	0.01	3923	1928	78037	1924	0.17	0.02
2012	1871	140	32374	2400	0.36	0.02	2077	154	48792	3423	0.21	0.02	3948	2404	81166	2400	0.29	0.03
2013	2006	211	29533	2834	0.54	0.03	2756	251	56926	4275	0.06	0.00	4762	2842	86460	2834	0.30	0.04

Figure B6.1 continued. CASA model estimates and standard errors for July 1 abundance and biomass (40+mm SH), and fully recruited fishing mortality for Mid-Atlantic and Total (GB and MA combined).

Year	Mid-Atlantic						Total					
	Abund (millions)	SE	Biomass (mt)	SE	F	SE	Abund (millions)	SE	Biomass (mt)	SE	F	SE
1975	516	26	5890	305	0.56	0.05	2023	50	32837	832	0.17	0.02
1976	632	22	6709	355	1.02	0.10	2256	47	36110	893	0.31	0.03
1977	644	21	8372	307	0.53	0.05	2004	43	36412	844	0.35	0.03
1978	496	15	7821	246	1.07	0.10	1708	36	32023	743	0.49	0.04
1979	328	10	6108	194	0.97	0.09	1241	30	24911	628	0.59	0.04
1980	318	10	4820	172	0.46	0.04	1355	32	20252	519	0.45	0.03
1981	417	12	5601	192	0.17	0.02	1292	30	18880	453	0.50	0.04
1982	473	14	6912	226	0.29	0.03	1215	28	17363	435	0.56	0.04
1983	528	15	7093	236	0.56	0.05	1092	29	15391	455	0.62	0.05
1984	573	18	7021	249	0.68	0.07	1116	33	14681	496	0.54	0.05
1985	799	24	8002	286	0.61	0.06	1397	41	15829	561	0.58	0.05
1986	1087	32	11482	382	0.44	0.04	1969	54	19708	625	0.65	0.05
1987	1270	37	12113	393	0.93	0.09	2234	63	21506	711	0.90	0.08
1988	1230	40	12613	445	0.77	0.07	2427	77	24181	798	0.84	0.07
1989	1212	35	11149	368	1.20	0.12	2480	72	25044	858	0.87	0.08
1990	1097	30	10541	326	1.06	0.10	2306	60	23649	695	1.10	0.09
1991	735	21	8520	263	1.10	0.11	1952	45	19258	450	1.30	0.10
1992	515	18	5733	213	1.12	0.11	1242	34	13168	369	1.47	0.11
1993	941	35	6381	257	0.90	0.09	1505	50	12284	464	0.97	0.08
1994	1405	59	9885	465	1.38	0.13	1976	71	16975	731	0.78	0.10
1995	1044	30	10031	306	1.51	0.15	2007	57	21052	805	0.81	0.11
1996	583	18	7737	246	0.81	0.08	1678	55	23340	958	0.46	0.05
1997	649	25	6606	257	0.61	0.06	1790	62	26404	1191	0.33	0.03
1998	1484	49	9934	364	1.08	0.10	3135	87	35610	1419	0.46	0.04
1999	2655	74	22092	691	0.80	0.08	4658	108	53736	1730	0.57	0.05
2000	3275	84	36301	1025	0.66	0.06	6268	128	77344	2016	0.51	0.06
2001	3355	80	43631	1155	0.69	0.07	6583	123	97079	2257	0.51	0.06
2002	3076	73	44862	1165	0.68	0.07	6168	115	107757	2417	0.47	0.05
2003	3991	87	45517	1109	0.75	0.07	7259	124	115958	2524	0.43	0.05
2004	3801	88	50849	1198	0.93	0.09	6809	120	125748	2638	0.43	0.06
2005	3790	92	52694	1334	0.80	0.08	6723	123	126366	2723	0.41	0.04
2006	3856	99	61284	1650	0.35	0.03	6449	128	125209	2846	0.40	0.03
2007	3681	92	62298	1673	0.62	0.06	6602	132	120031	2844	0.46	0.05
2008	3879	88	58561	1504	0.70	0.07	6948	138	118050	2818	0.47	0.06
2009	3209	74	54706	1272	0.82	0.08	6612	147	119306	2897	0.49	0.06
2010	2343	61	44283	1215	0.85	0.08	5894	158	115392	3197	0.43	0.05
2011	1675	57	33973	1159	0.87	0.08	5598	188	112010	3674	0.39	0.05
2012	2808	134	30516	1468	0.74	0.07	6756	248	111682	4431	0.40	0.03
2013	3253	182	46101	2649	0.39	0.04	8014	375	132561	5772	0.32	0.03

Table B6.2. CASA model likelihood profile analysis over a range of values for dredge survey catchability (Q) in the MAB region. Catchability priors were turned off in profile runs. The basecase run (with priors turned on) is colored yellow, runs with Q in the 0.4-0.6 expected range based on swept-area abundance are blue, and the run with the best fit to the data are salmon in color. The best fit occurs where the likelihood is zero (bold face).

Dredge survey Q	0.40	0.50	0.60	0.70	0.80	0.87	1.00	1.09	1.19
Total unweighted	618.500	480.800	264.000	137.200	48.800	166.600	0.000	200.100	336.100
Catch weight	208.349	194.825	183.041	153.940	44.222	2.902	0.000	37.589	124.802
Recruitment deviations	15.023	10.032	6.819	3.128	0.000	0.054	0.145	0.275	0.981
Survey trends-all	133.689	73.315	34.576	14.634	0.000	0.036	4.412	8.122	13.144
Length data-all	295.900	237.100	74.000	0.000	39.100	43.600	29.900	188.600	231.600
Survey trends									
Dredge	116.668	61.413	27.035	10.436	0.238	0.000	3.760	6.556	10.062
SMAS.T.LrgCam	3.447	2.008	1.269	1.253	0.000	0.135	2.860	4.160	5.381
Winter.BTS	11.039	7.668	5.160	3.130	0.366	0.372	0.124	0.070	0.000
Unlined.Dredge	0.000	0.001	0.216	0.265	0.260	0.286	0.314	0.118	0.176
HabCam	5.317	5.007	3.677	2.333	1.918	2.025	0.137	0.000	0.307
Length data									
Commercial.Fishery	152.900	152.930	35.200	0.000	11.880	24.840	29.840	190.150	211.040
Dredge	144.700	87.300	42.700	4.700	37.600	28.600	3.600	0.000	15.000
SMAS.T.LrgCam	10.061	9.551	8.364	6.129	0.110	0.000	6.562	11.919	16.906
Winter.BTS	0.000	0.080	0.750	1.200	1.960	1.860	2.150	2.030	2.280
Unlined.Dredge	0.297	0.299	2.289	5.140	5.039	5.258	5.197	0.093	0.000
HabCam	5.450	4.350	2.190	0.290	0.000	0.420	0.020	1.860	3.870
Mean 2011-2014 biomass (mt)	434,402	218,487	105,529	60,996	54,785	49,710	28,262	23,758	20,395
Mean 2011-2014 abun. wtd. F	0.01	0.02	0.06	0.12	0.14	0.15	0.31	0.38	0.45

Table B6.3 CASA model likelihood profile analysis over a range of values for dredge survey catchability (Q) in the GBK-open region. Catchability priors were turned off in profile runs. The basecase run (with priors turned on) is colored yellow, runs with Q in the 0.4-0.6 expected range based on swept-area abundance are blue, and the run with the best fit to the data are salmon in color. The best fit occurs where the likelihood is zero (bold face).

Dredge survey Q	0.40	0.50	0.60	0.66	0.75	0.84	0.98	1.09	1.09
Total unweighted	146.13	56.34	6.89	122.74	0.00	37.65	140.49	195.09	236.24
Catch weight	9.32	5.35	1.20	0.00	1.78	11.45	16.86	10.53	11.29
Recruitment deviations	20.90	13.53	6.54	3.36	0.00	0.08	4.44	7.02	8.19
Survey trends-all	116.68	49.64	11.75	1.74	0.00	6.88	3.63	0.92	3.91
Length data-all	11.83	0.41	0.00	2.43	10.82	31.84	128.17	189.19	224.95
Survey trends									
Dredge	89.48	35.27	7.60	0.94	0.25	4.54	1.07	0.00	2.89
SMAST.LrgCam	28.16	15.34	5.11	1.66	0.00	0.57	0.45	0.24	0.27
Unl.10ft.Dredge.40+mm	0.88	0.89	0.90	0.91	0.92	0.89	0.47	0.14	0.00
HabCam	0.02	0.00	0.01	0.09	0.70	2.75	3.51	2.42	2.61
Length data									
Commercial.Fishery	1.59	0.00	3.40	7.49	13.81	27.06	48.45	62.18	72.65
Dredge	15.04	8.82	4.18	1.25	0.00	4.28	64.41	99.38	118.23
SMAST.LrgCam	3.04	0.00	1.16	2.75	6.27	9.52	22.83	33.86	39.59
Unl.10ft.Dredge.40+mm	0.05	0.07	0.09	0.09	0.08	0.00	0.29	1.06	1.36
HabCam	1.44	0.86	0.51	0.18	0.00	0.31	1.52	2.03	2.44
Mean 2011-2014 biomass (mt)	181,251	97,471	53,744	38,653	25,051	19,297	18,282	18,897	18,377
Mean 2011-2014 abun. wtd. F	0.03	0.05	0.10	0.15	0.27	0.46	0.53	0.49	0.52

Table B6.4. CASA model likelihood profile analysis over a range of values for dredge survey catchability (Q) in the GBK-closed region. Catchability priors were turned off in profile runs. The basecase run (with priors turned on) is colored yellow, runs with Q in the 0.4-0.6 expected range based on swept-area abundance are blue, and the run with the best fit to the data are salmon in color. The best fit occurs where the likelihood is zero (bold face).

Dredge survey Q	0.40	0.50	0.60	0.68	0.75	0.85	1.00	1.10	1.20
Total unweighted	36.04	22.05	11.81	142.32	2.40	0.00	2.50	8.54	18.41
Catch weight	0.01	0.02	0.02	0.10	0.00	0.05	0.47	1.15	2.32
Recruitment deviations	14.95	11.32	8.32	5.56	4.77	2.96	1.04	0.30	0.00
Survey trends-all	14.33	7.22	3.06	0.00	1.19	2.59	8.51	14.94	23.17
Length data-all	14.60	11.33	8.26	8.96	4.30	2.26	0.33	0.00	0.77
Survey trends									
Dredge	8.53	3.90	1.53	0.00	0.58	1.13	3.28	5.48	8.25
SMAST.LrgCam	5.35	2.93	1.20	0.00	0.41	1.37	5.35	9.73	15.33
Unl.10ft.Dredge.40+mm	0.00	0.00	0.00	0.00	0.00	0.00	0.00	0.00	0.00
HabCam	0.85	0.80	0.73	0.40	0.60	0.49	0.28	0.13	0.00
Length data									
Commercial.Fishery	1.06	1.22	1.18	2.51	0.89	0.61	0.17	0.00	0.21
Dredge	10.72	8.59	6.68	4.52	4.22	2.87	1.31	0.55	0.00
SMAST.LrgCam	5.82	4.37	3.05	4.95	1.44	0.66	0.02	0.00	0.42
Unl.10ft.Dredge.40+mm	0.08	0.10	0.12	0.14	0.13	0.12	0.09	0.05	0.00
HabCam	0.08	0.22	0.40	0.00	0.79	1.16	1.91	2.57	3.31
Mean 2011-2014 biomass (mt)	125,498	88,137	64,526	50,812	42,317	32,537	22,304	17,508	13,888
Mean 2011-2014 abun. wtd. F	0.06	0.08	0.12	0.15	0.19	0.25	0.37	0.49	0.62

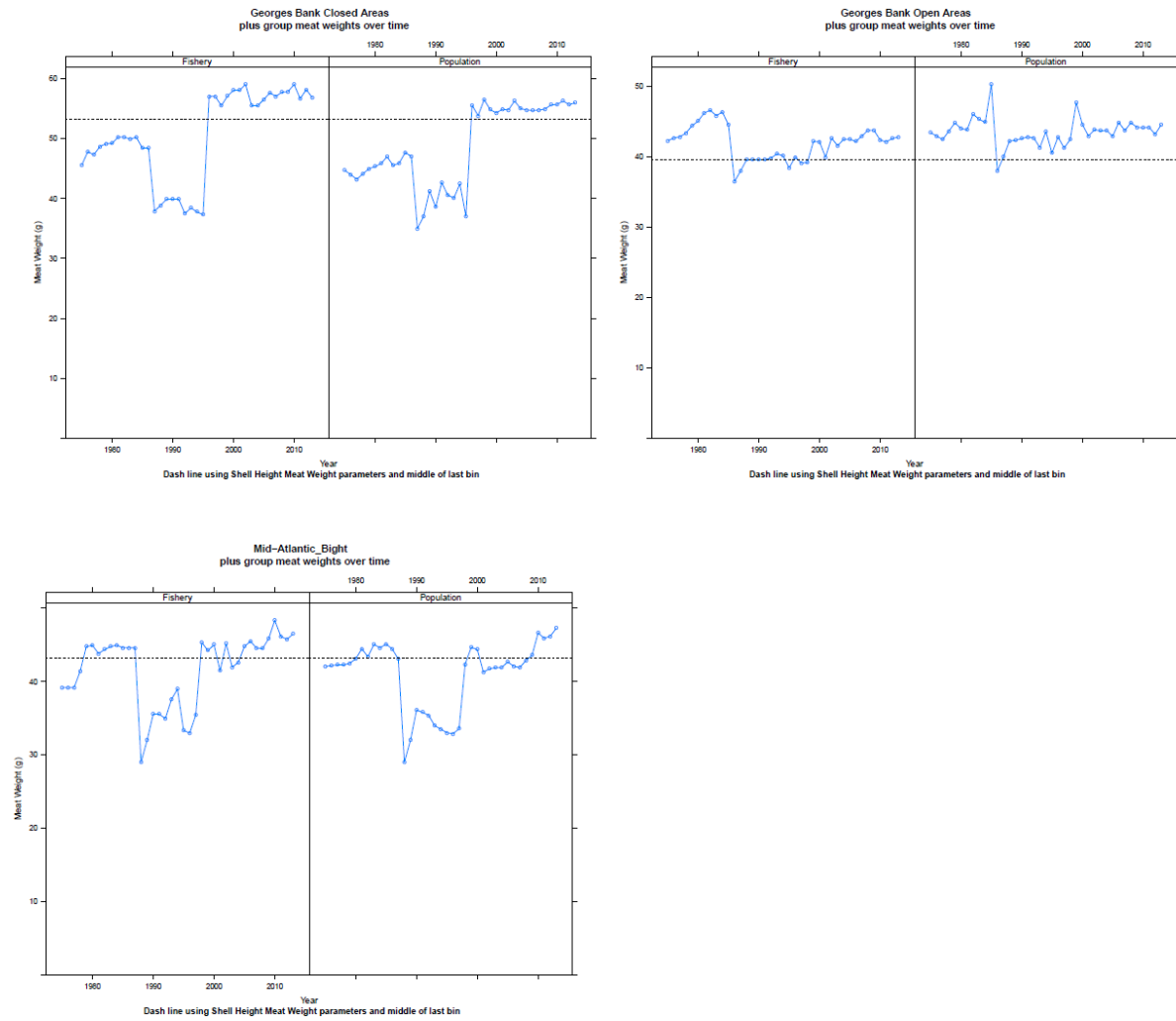


Figure B6.1. Estimated plus group meat weights for the population and the fishery in the open and closed portions of Georges Bank, and in the Mid-Atlantic Bight. The plus group represents scallops in the largest bin which contained L_{∞} .

(A)

(B)

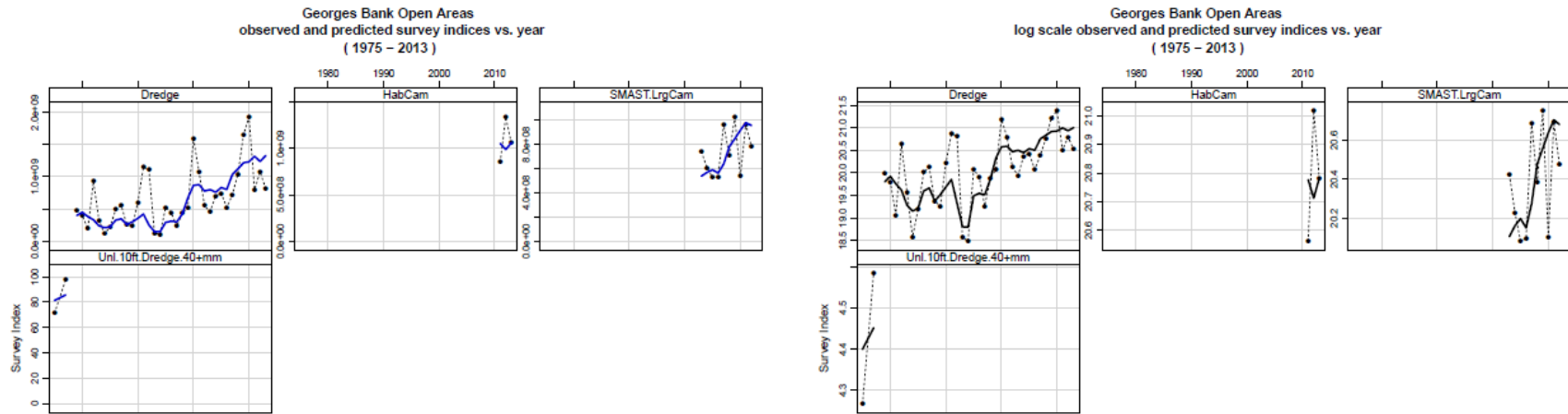


Figure B6.2. Observed survey trend (solid circles) and corresponding model estimates (lines) for the NEFSC lined dredge survey, the HabCam survey, the SMAST large camera survey and the NEFSC unlined dredge survey on Georges Bank open areas. Results are shown on a linear scale (A) and a log scale (B).

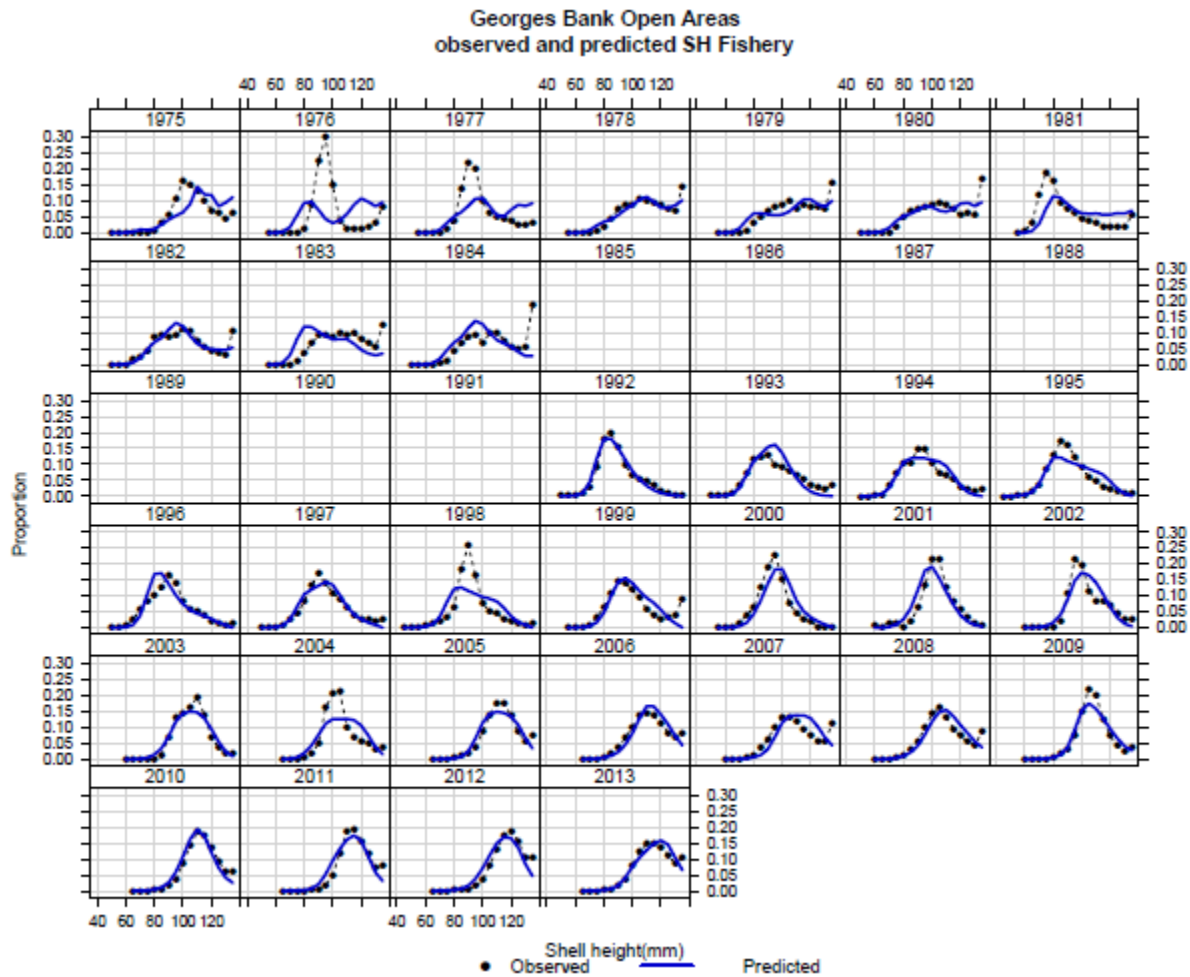


Figure B6.3. Comparison of observed fishery shell height proportions (solid circles) and model estimated fishery shell height proportions (lines) for Georges Bank open areas.

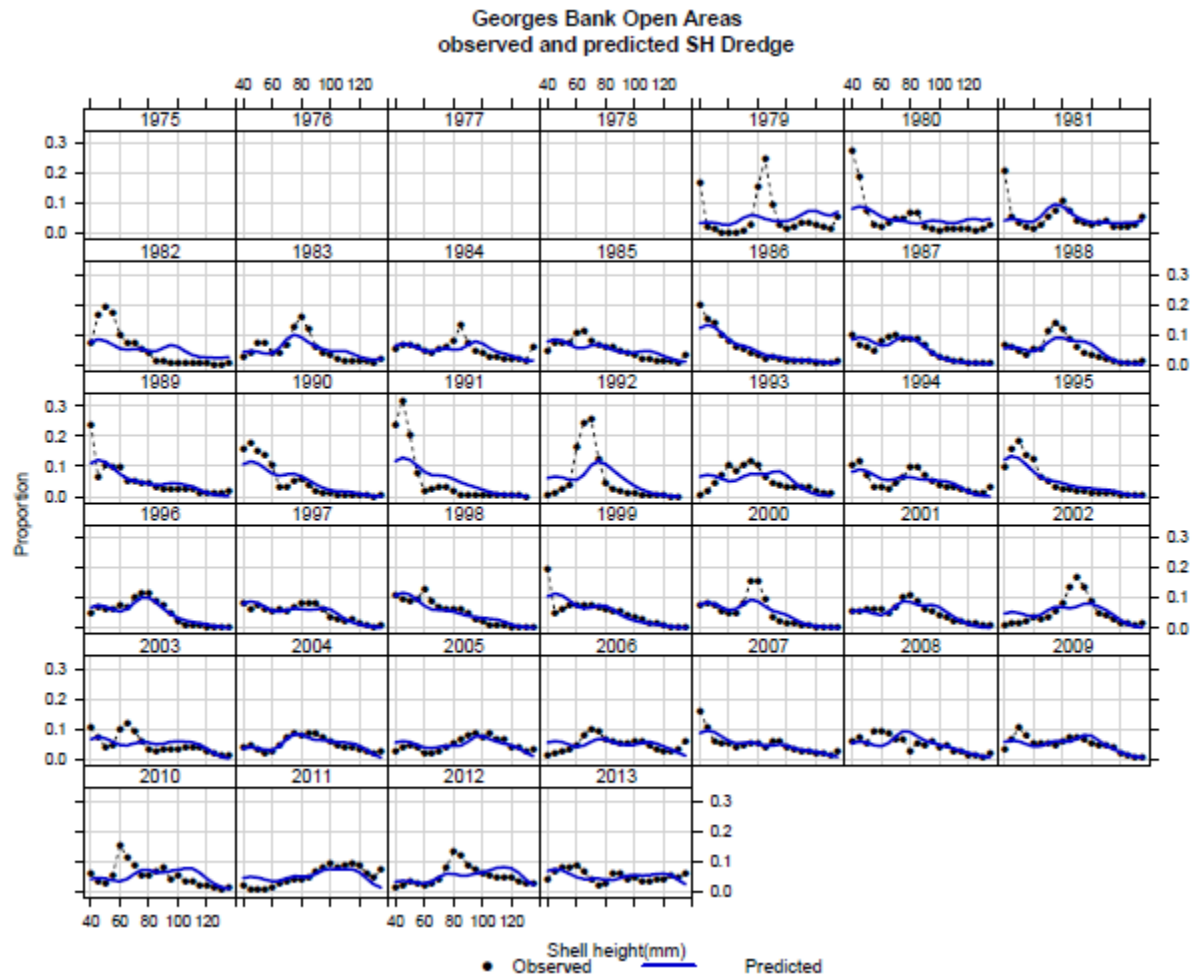


Figure B6.4. NEFSC lined dredge survey shell height proportions (solid circles) and model estimated shell height proportions (lines) for Georges Bank open areas.

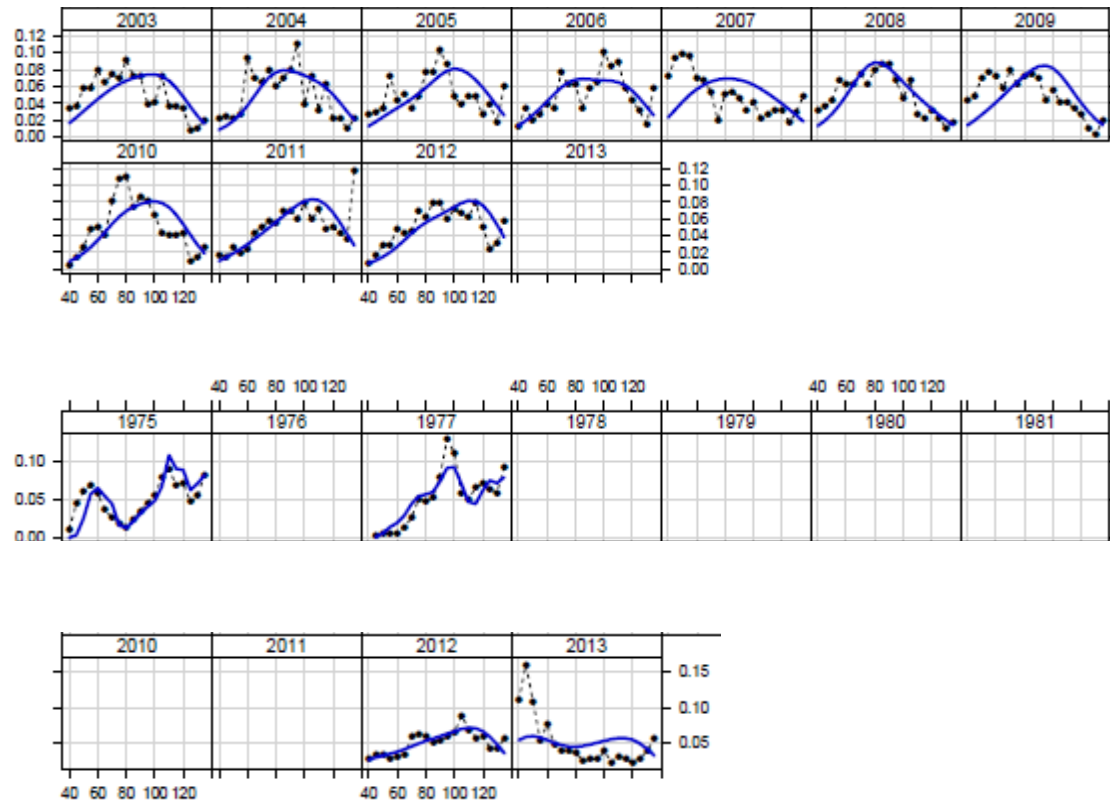


Figure B6.5. Shell height proportions for the SMAST large camera survey (top), the NEFSC unlined dredge survey (middle) and the HabCam survey (bottom) with model predicted proportions (lines) for Georges Bank.

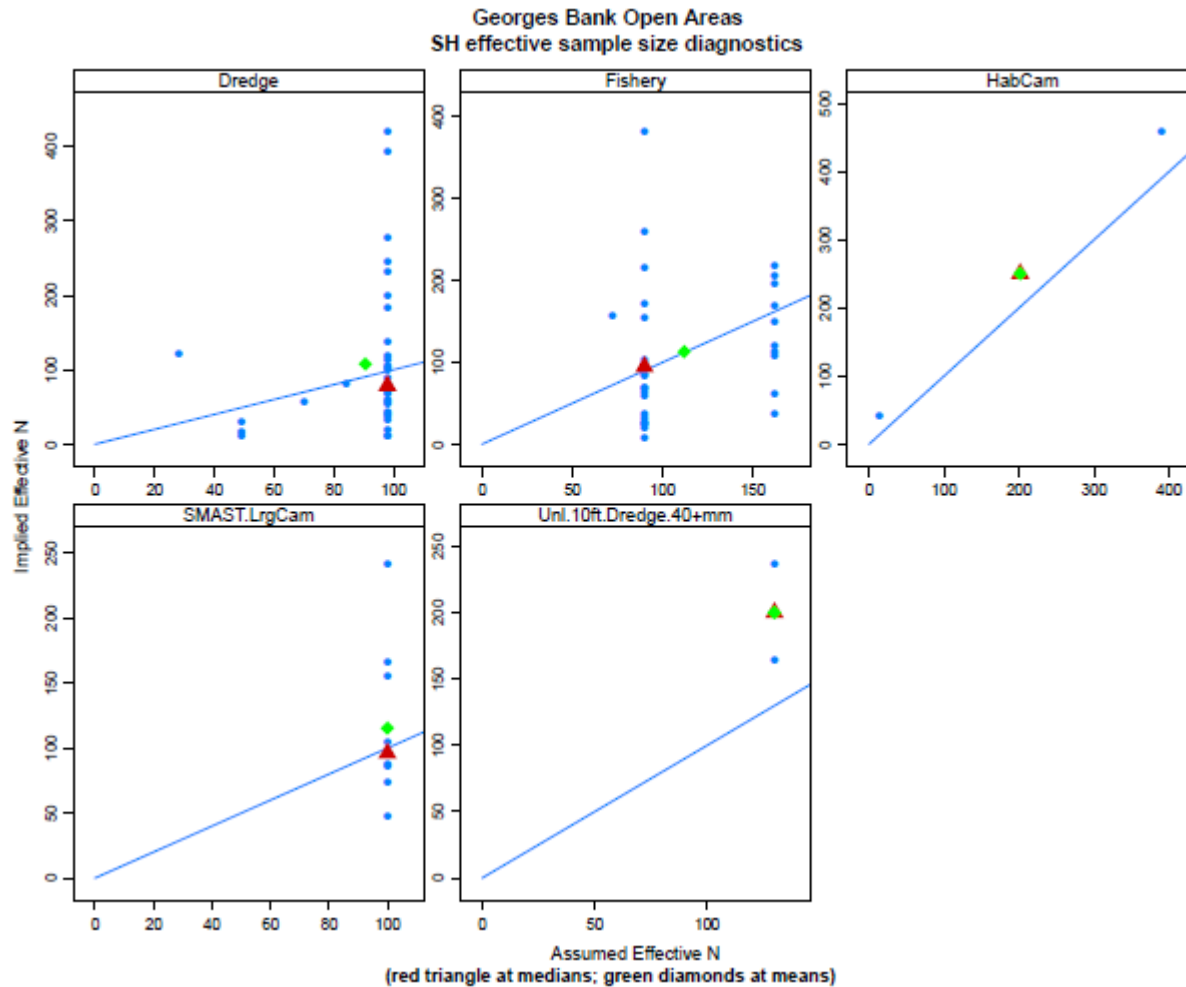


Figure B6.6. Assumed and model implied effective sample sizes for the four surveys (NEFSC unlined dredge, HabCam, SMAST large camera, NEFSC unlined dredge) and the fishery shell height compositions for Georges Bank open areas. The triangle is the median and the diamond is the mean.

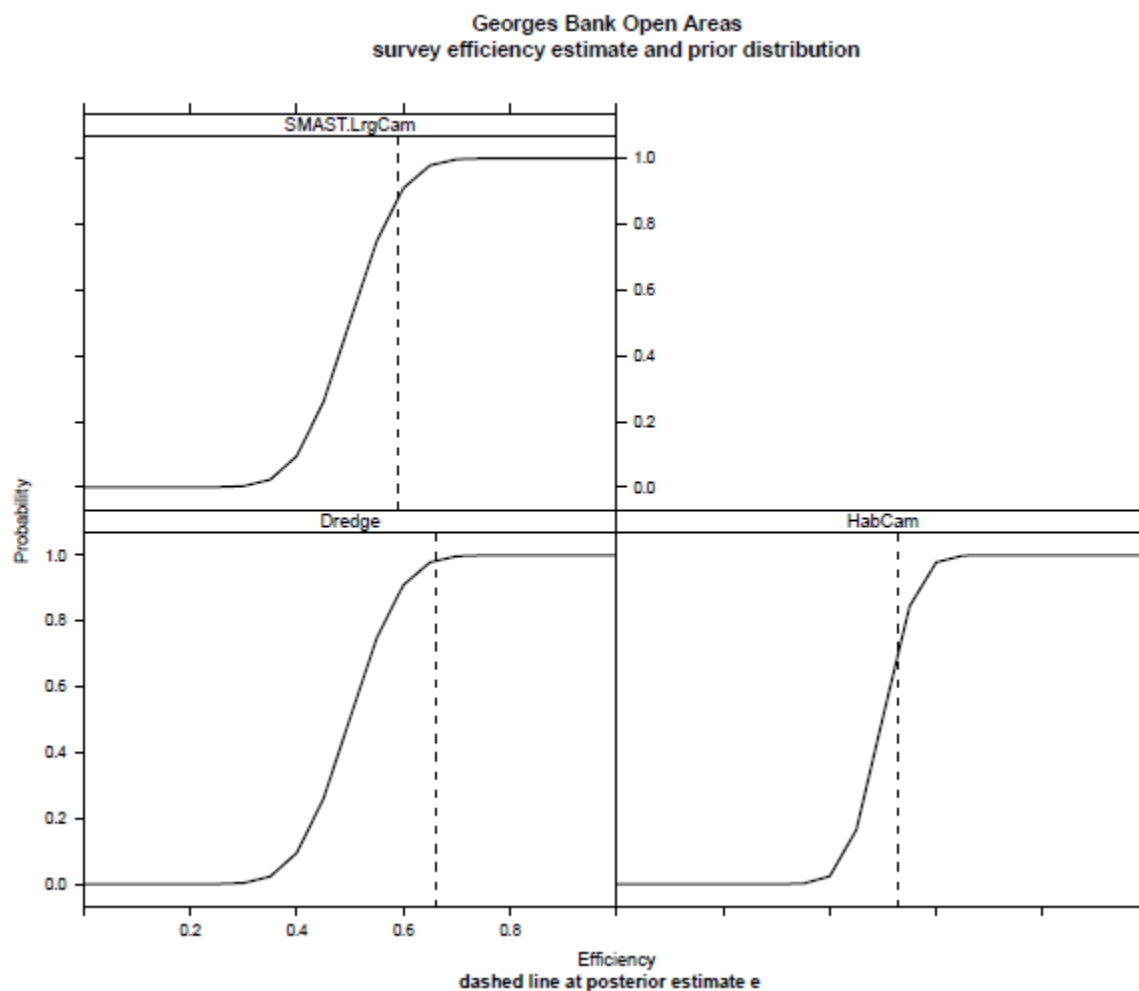


Figure B6.7. Prior cumulative distributions for catchability of the large camera video survey (top) lined dredge survey (bottom left) and HabCam survey (bottom right) for Georges Bank open areas. The dashed lines are the mean posterior estimate for survey catchability. For the purposes of this plot, the surveys were adjusted to have a mean prior catchability of 0.5

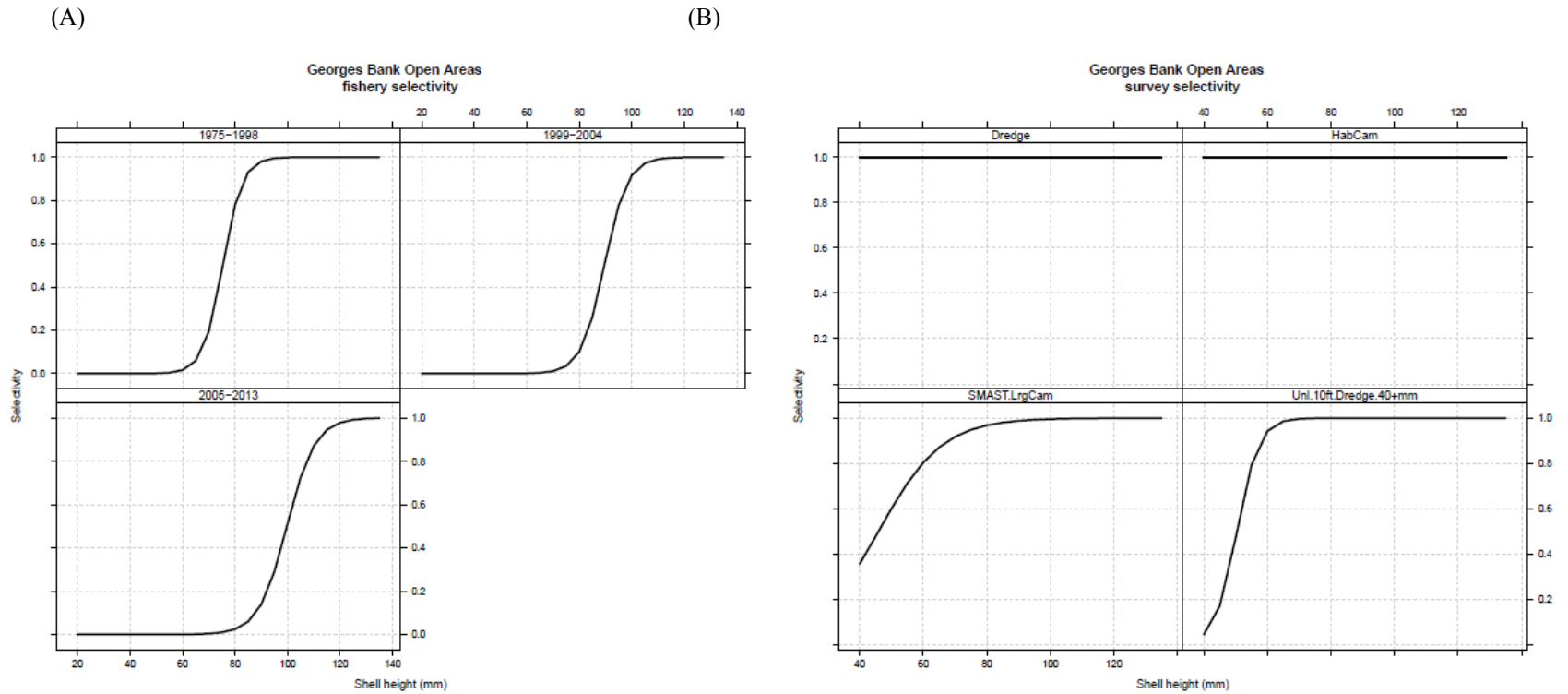


Figure B6.8. (A) Estimated fishery selectivity curves and (B) assumed survey selectivity curves (lined dredge top left, HabCam top right, large camera bottom left, and unlined dredge bottom right) for Georges Bank open areas.

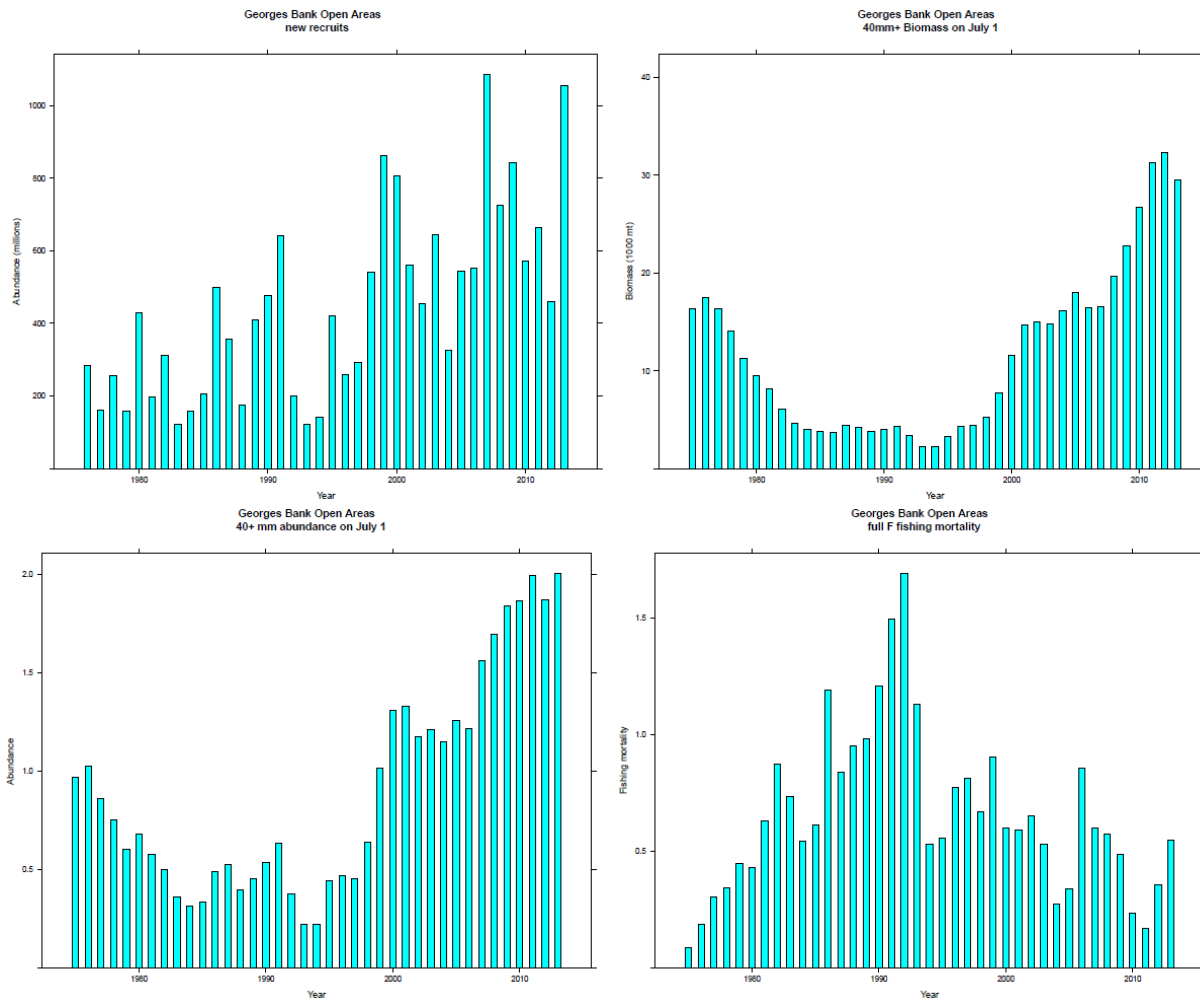


Figure B6.9. CASA model estimated recruitment (top left), July 1 biomass (top right), July 1 abundance (bottom left) and fully recruited fishing mortality (bottom right) for Georges Bank open areas.

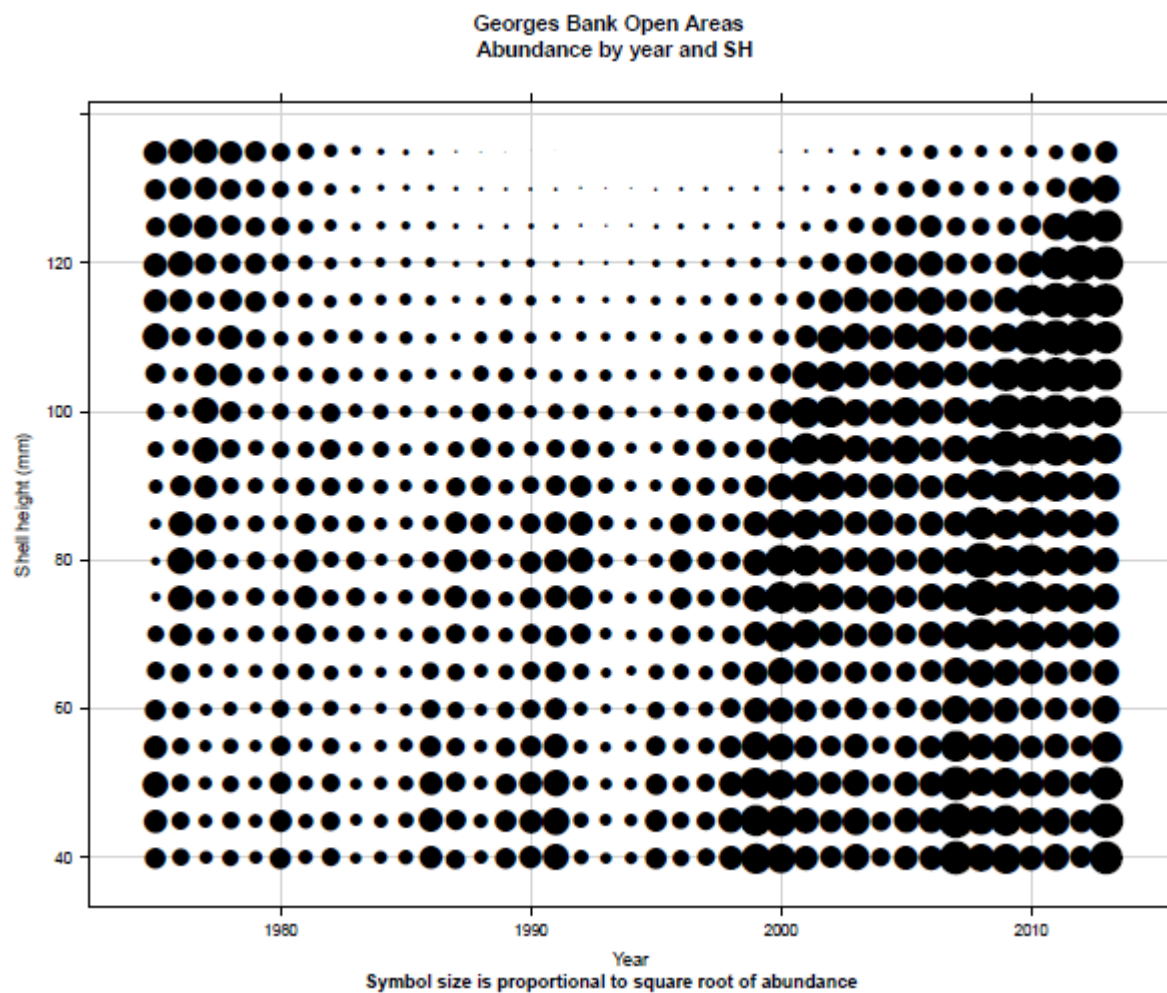


Figure B6.10. Model estimated abundances at shell height for Georges Bank open areas. Symbol areas are proportional to abundance.

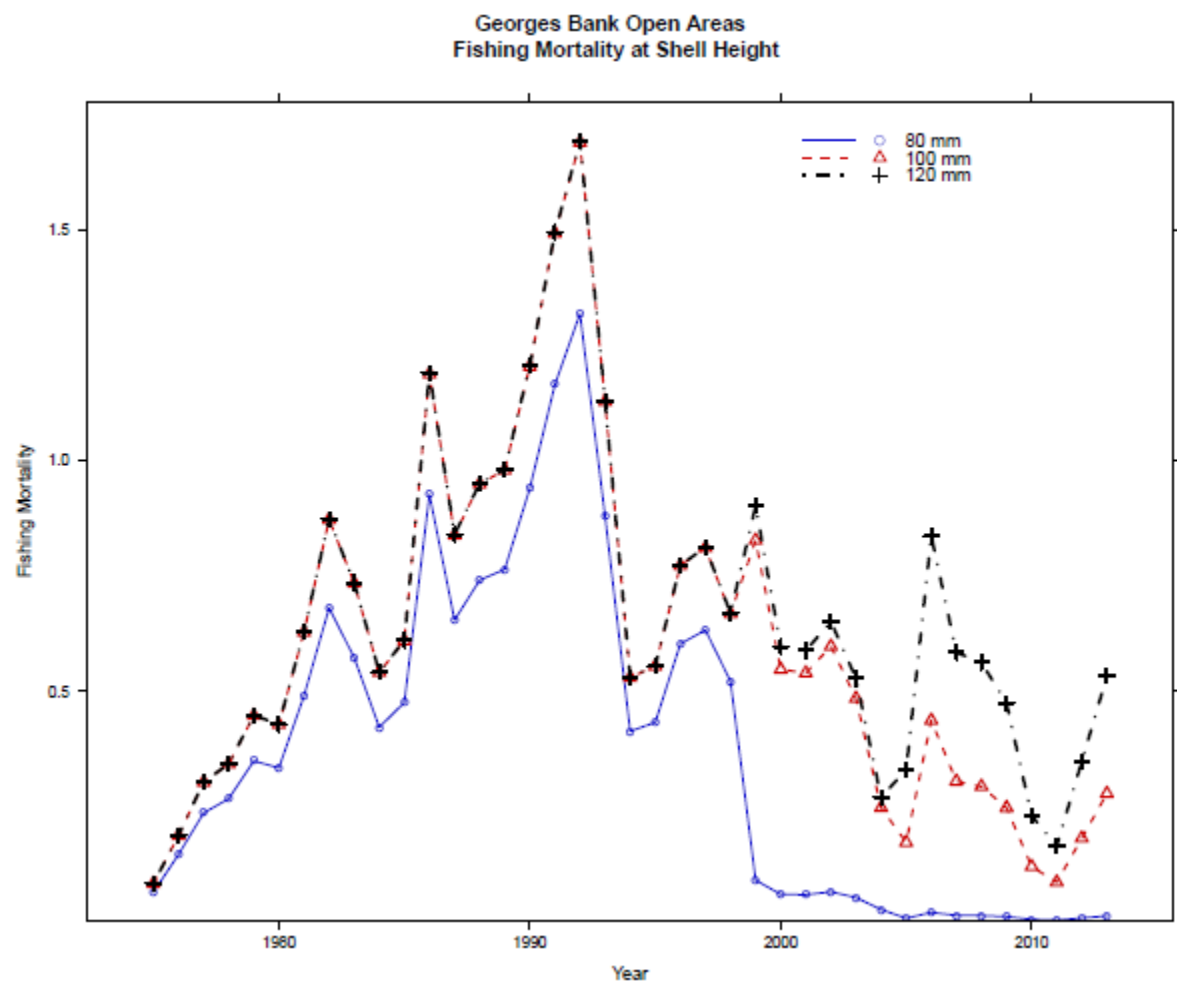


Figure B6.11. CASA model estimated fishing mortality at 80 mm (solid line with circles), 100 mm (dashed line with triangles) and 120 mm SH (dashed line with crosses) for Georges Bank open areas.

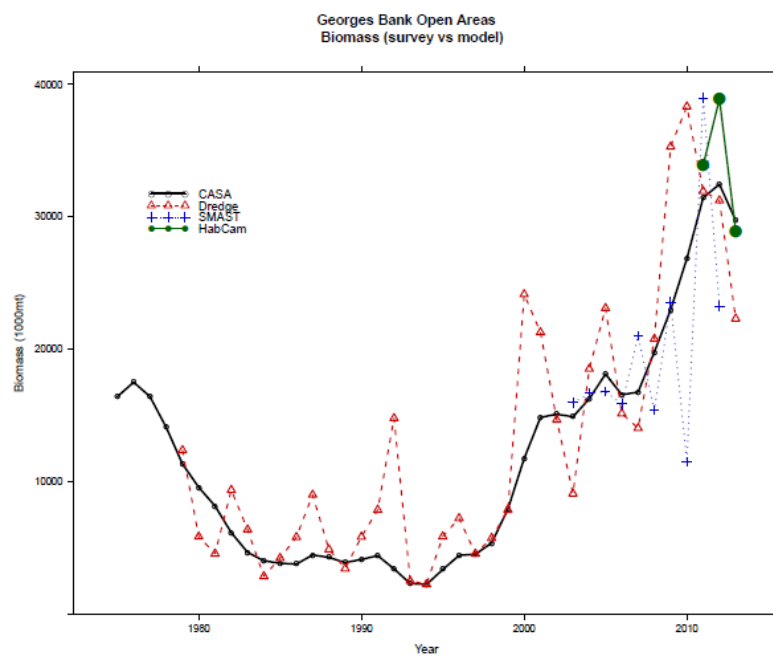
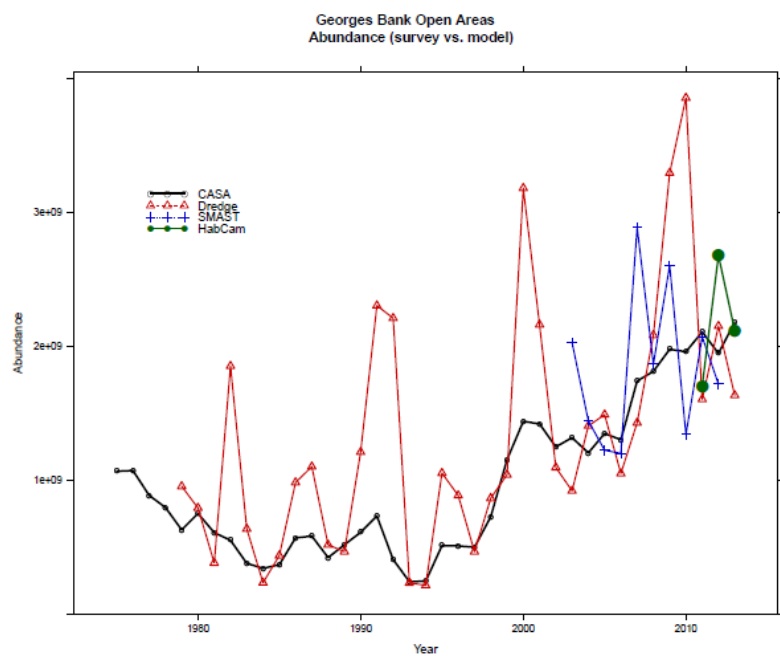


Figure B6.12. Comparison of CASA model estimated abundance (left) and biomass (right) with expanded estimates from the lined dredge survey (dashed red line with triangles), SMAST large camera survey (dotted blue line with crosses) and HabCam (solid line with circles) for Georges Bank open areas.

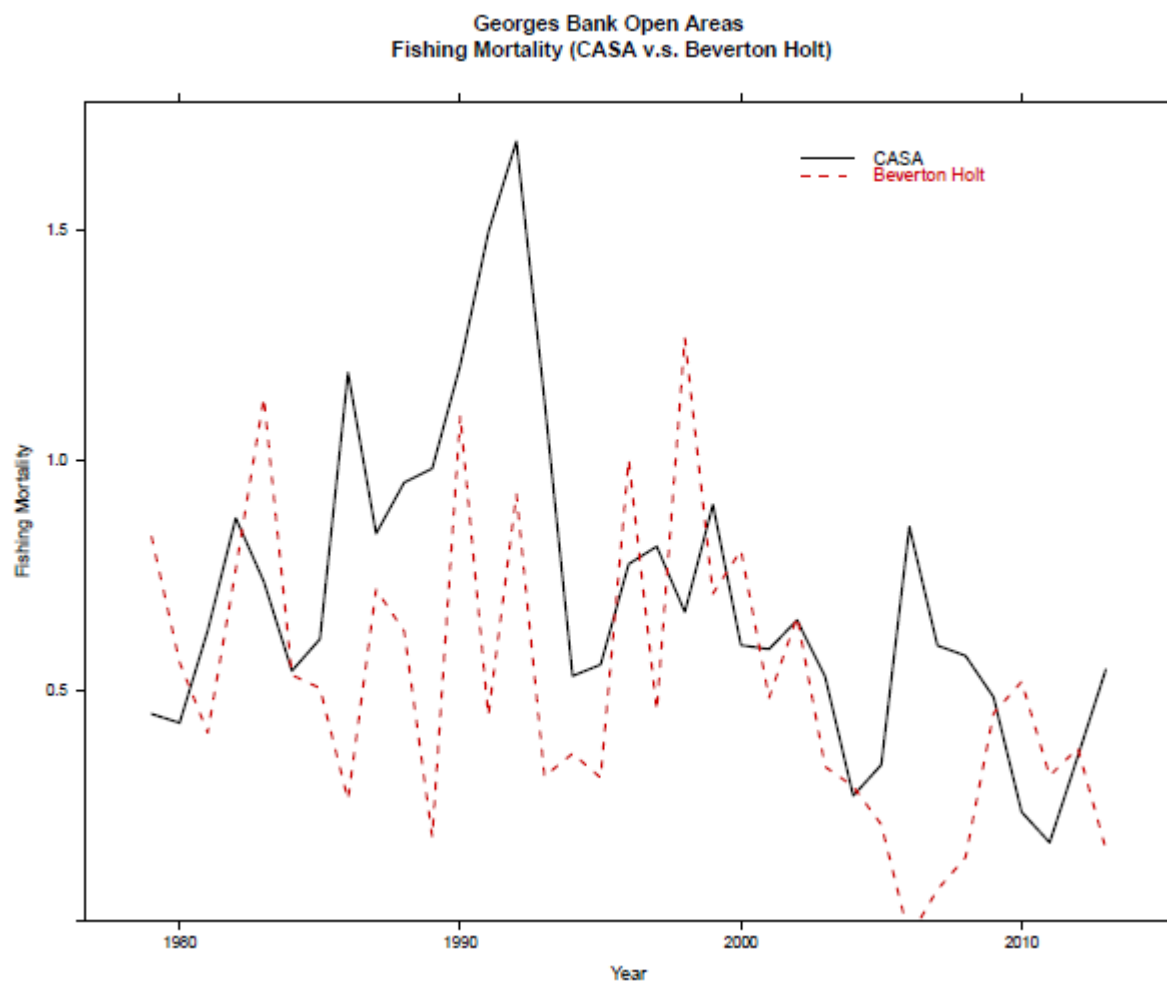


Figure B6.13. Comparison of fully recruited CASA fishing mortality with those calculated from the Beverton-Holt equilibrium length-based estimator for Georges Bank open areas.

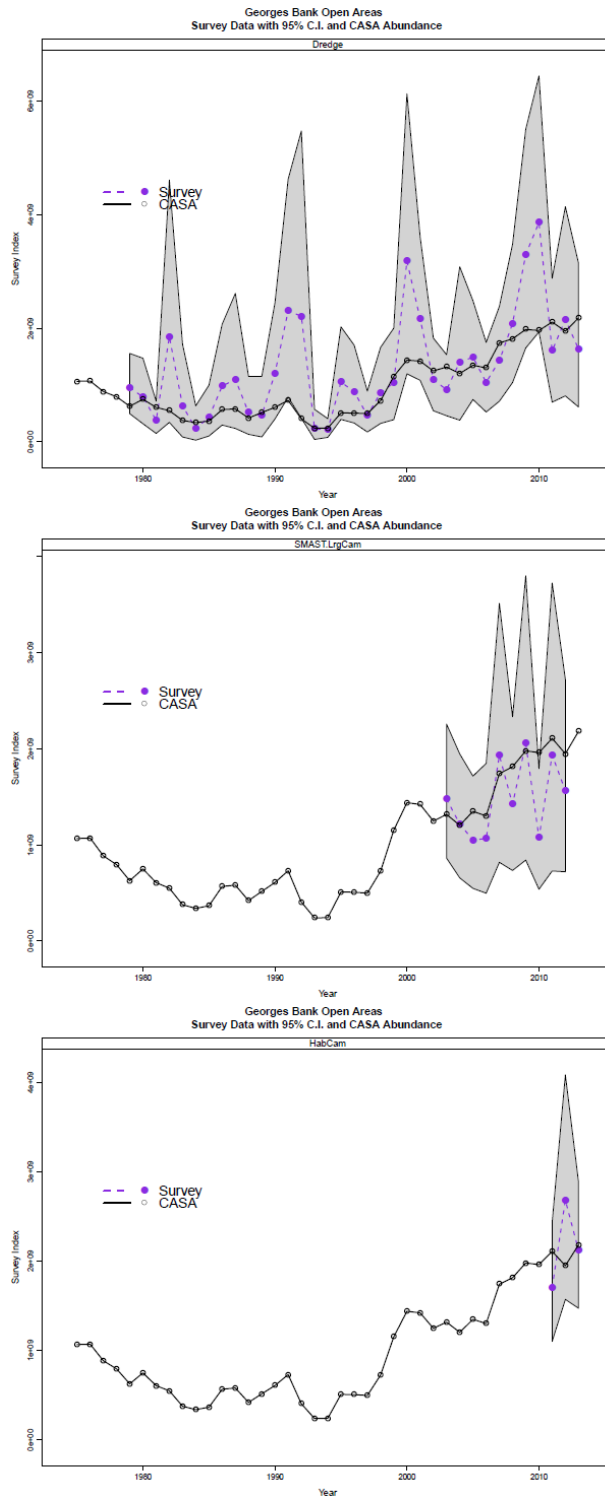


Figure B6.14. CASA model (black line with solid circles) for Georges Bank open areas compared to expanded survey estimates with their 95% C.I.s: dredge (top), SMAST (middle), and HabCam (lower)

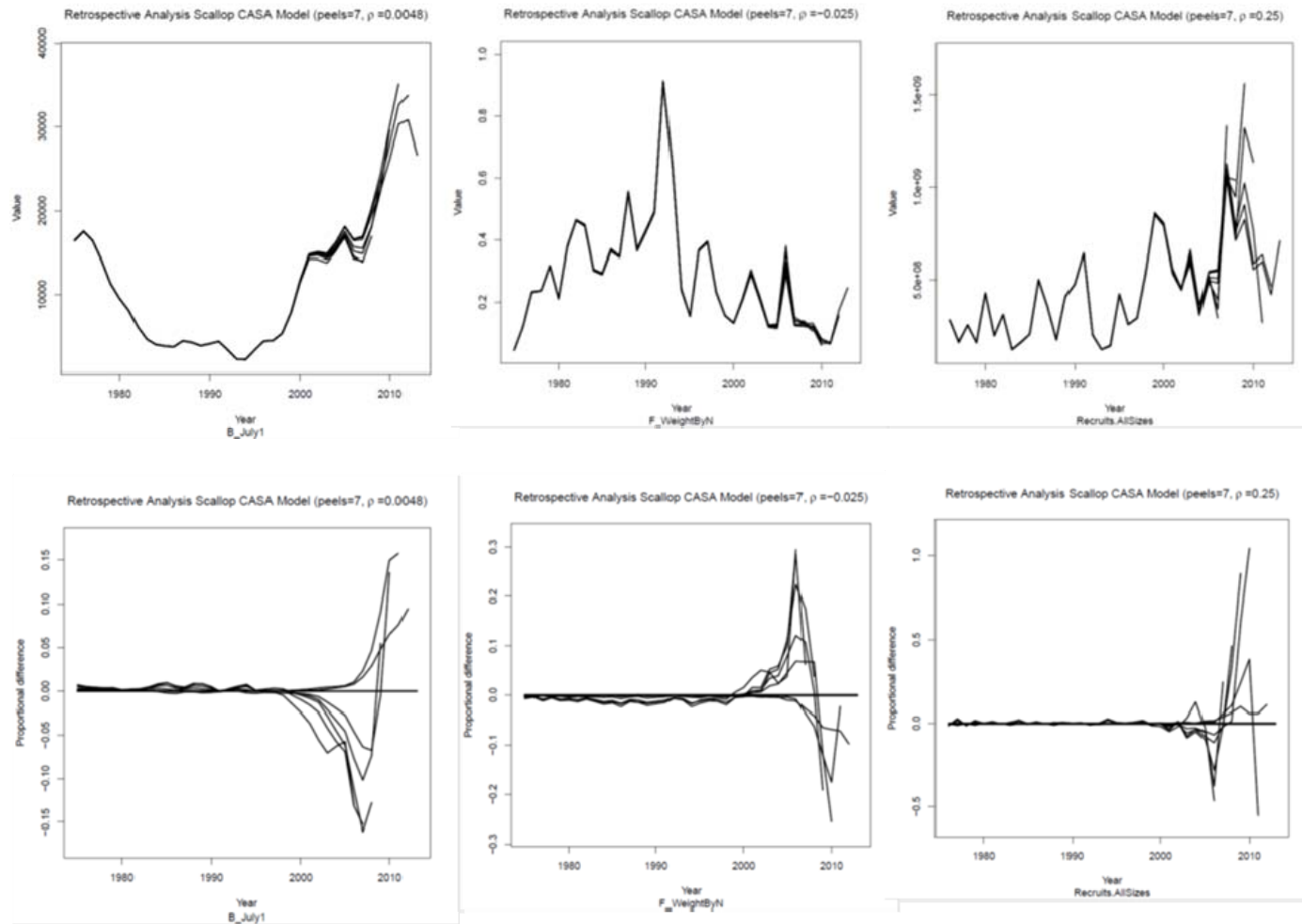
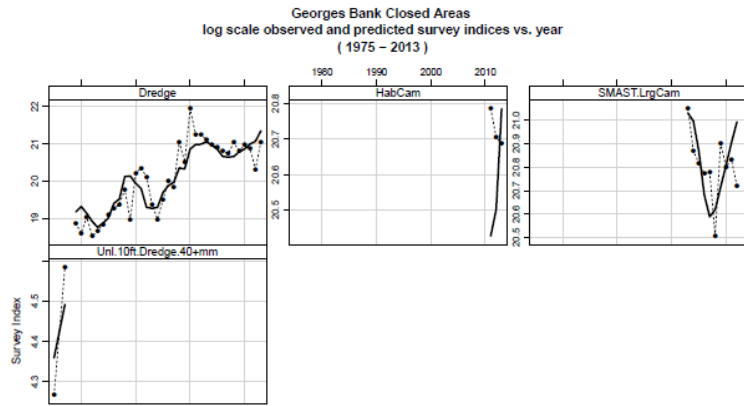


Figure B6.15. Retrospective plots for biomass, fishing mortality and recruitment, shown both on absolute and relative scales for Georges Bank open areas.

(A)



(B)

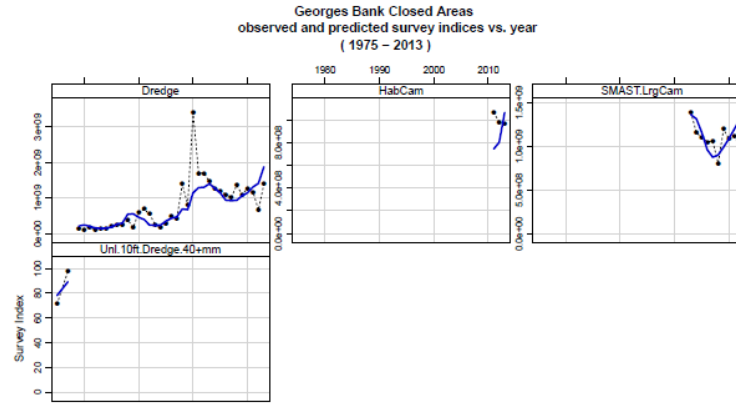


Figure B6.16. Comparison between survey trend (solid circles) and corresponding model estimates (lines) for the NEFSC lined dredge survey, the HabCam survey, The SMAST large camera survey and the NEFSC unlined dredge survey in the Georges Bank closed areas. Results are shown on a linear scale (A) and a log scale (B).

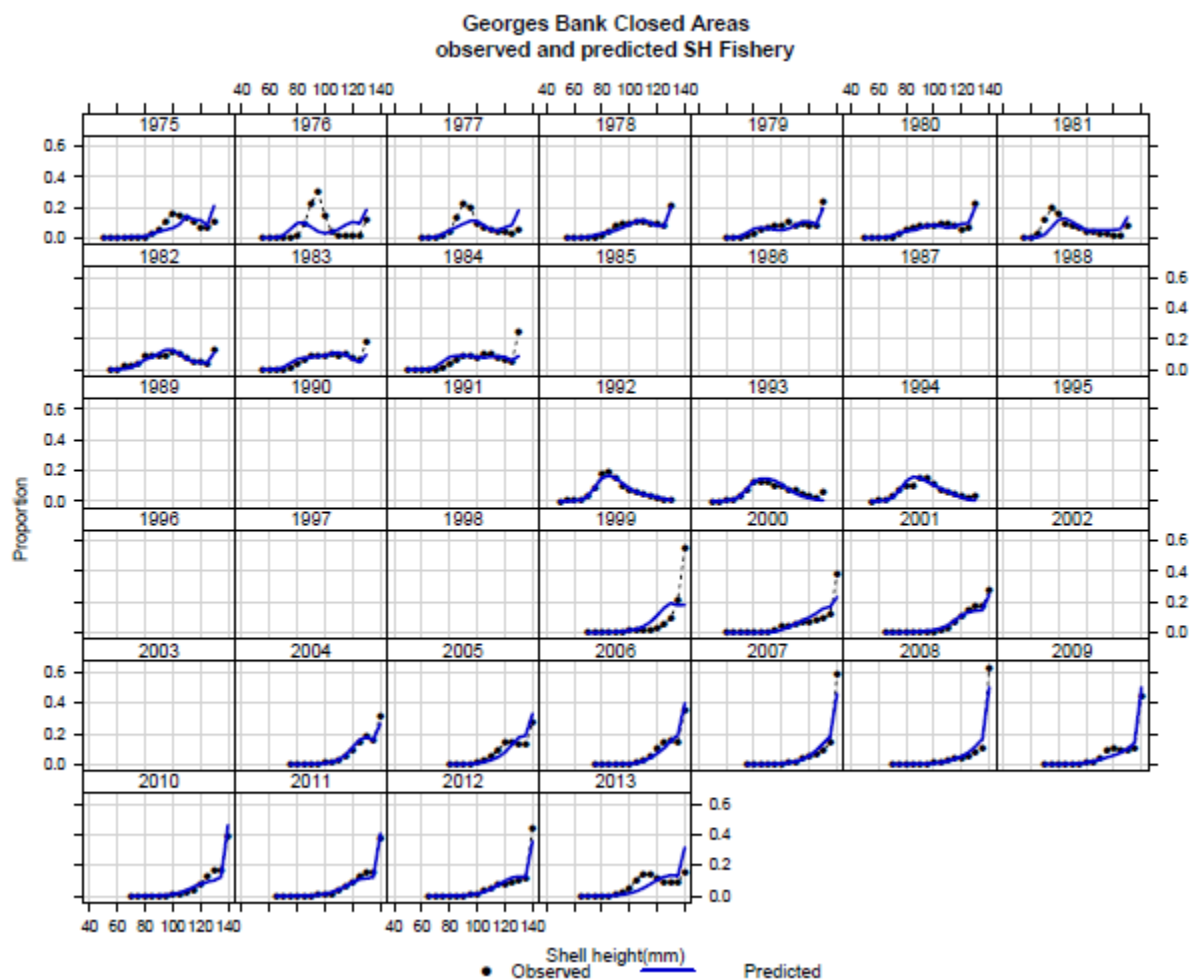


Figure B6.17. Comparison of fishery shell height proportions (solid circles) and model estimated fishery shell height proportions (lines) for Georges Bank closed areas.

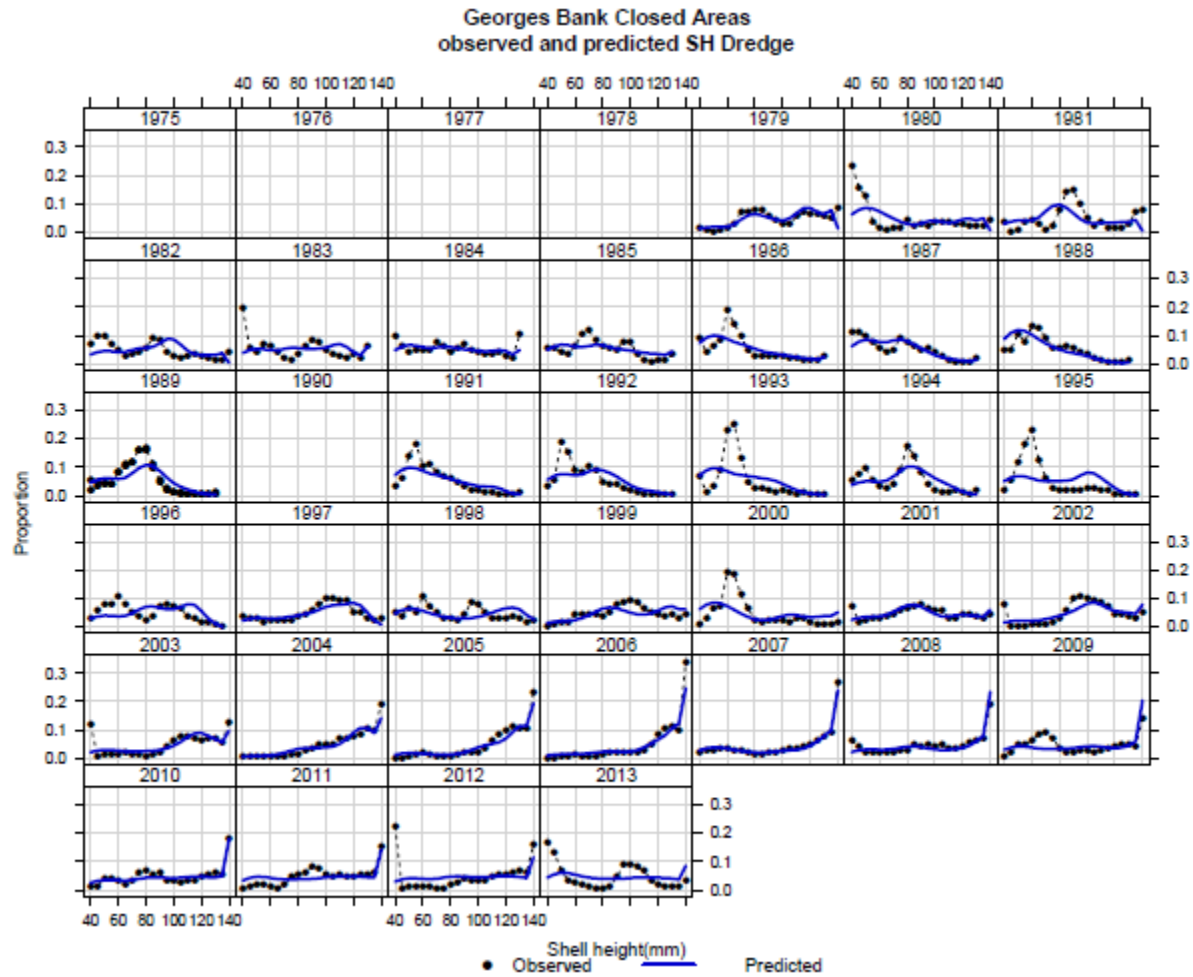


Figure B6.18. NEFSC lined dredge survey shell height proportions (solid circles) and model estimated shell height proportions (lines) for Georges Bank closed areas.

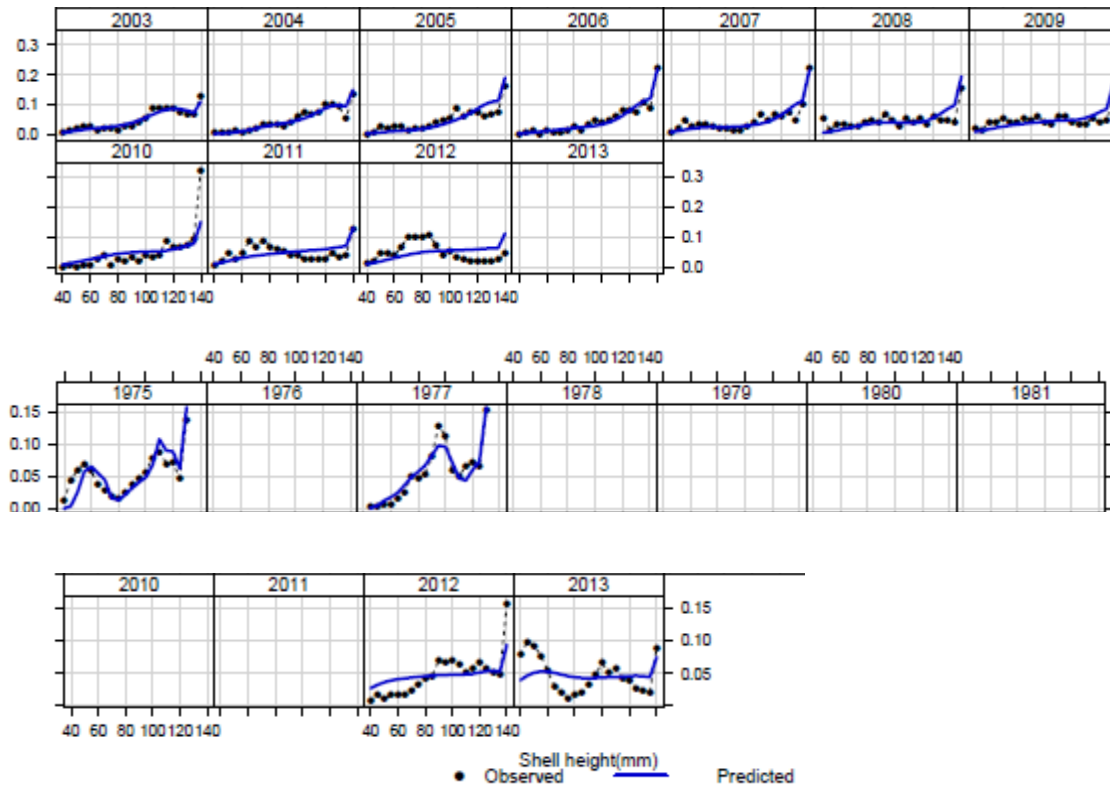


Figure B6.19. Shell height proportions for the SMAST large camera survey (top), the NEFSC unlined dredge survey (middle) and the HabCam survey (bottom) with model predicted proportions (lines) for Georges Bank closed areas.

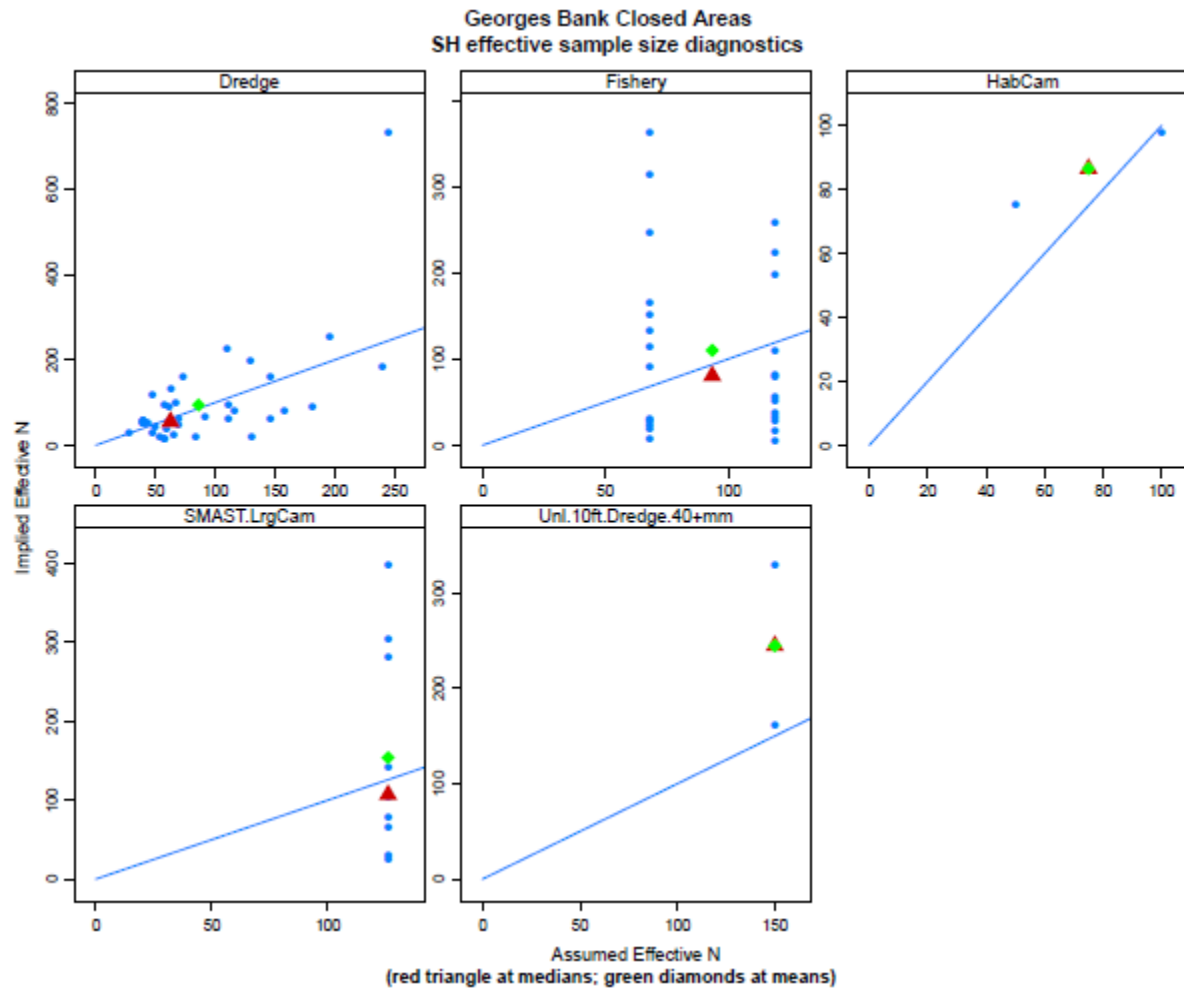


Figure B6.20. Assumed and model implied effective sample sizes for the four surveys (NEFSC unlined dredge, HabCam, S Mast large camera, NEFSC unlined dredge) and the fishery shell height compositions for Georges Bank closed areas. The triangle is the median and the diamond is the mean.

Georges Bank Closed Areas
survey efficiency estimate and prior distribution

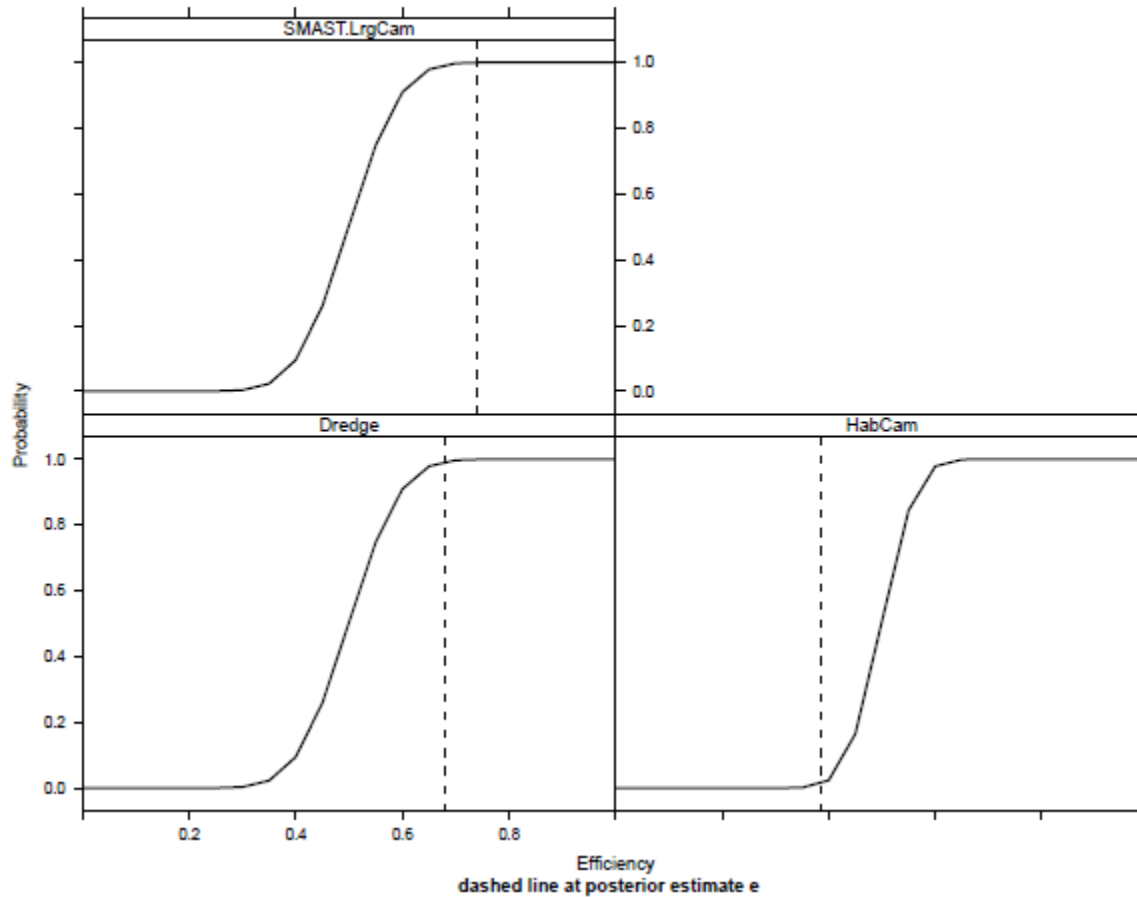


Figure B6.21. Prior cumulative distributions for catchability of the large camera video survey (top) lined dredge survey (bottom left) and HabCam survey (bottom right) for Georges Bank closed areas. The dashed lines are the mean posterior estimate for survey catchability. For the purposes of this plot, the surveys were adjusted to have a mean prior catchability of 0.5

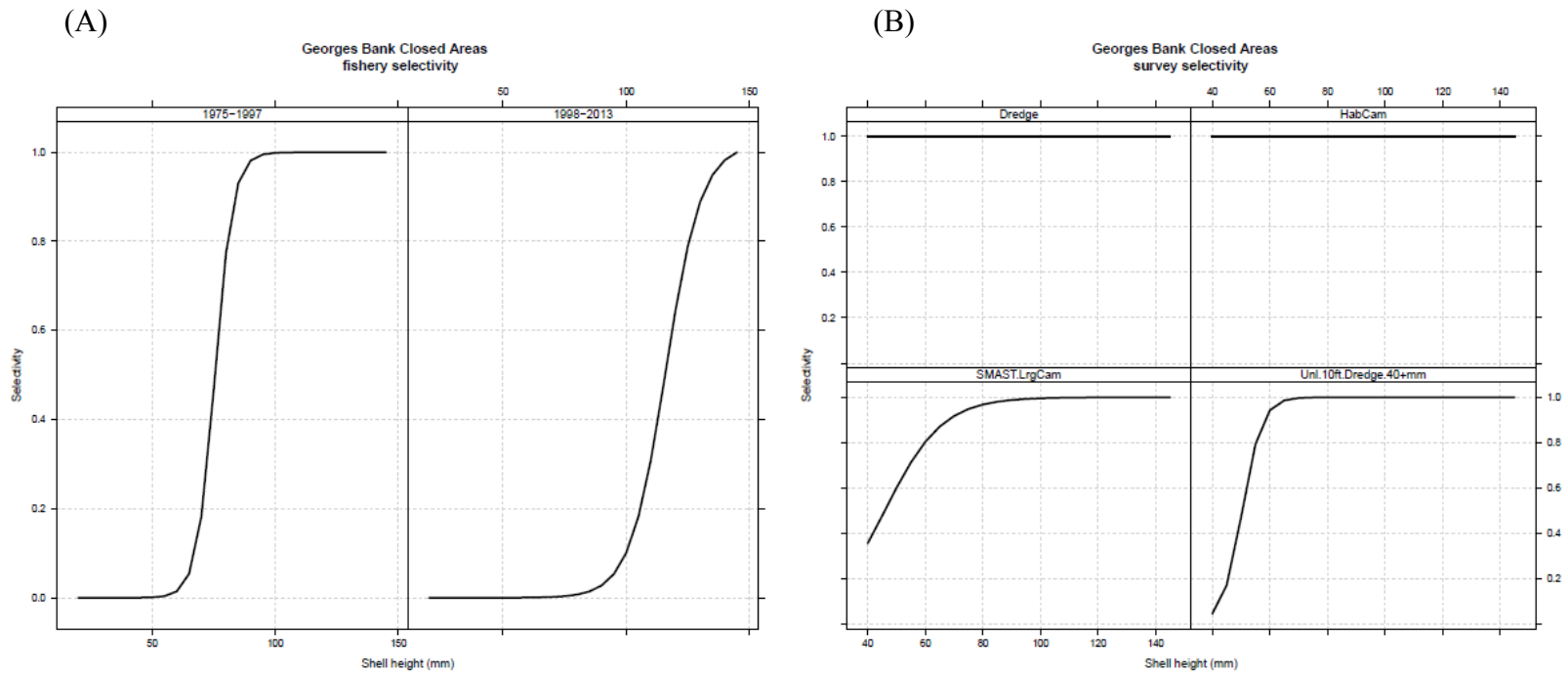


Figure B6.22. (A) Estimated fishery selectivity curves and (B) assumed survey selectivity curves (lined dredge top left, HabCam top right, large camera bottom left, and unlined dredge bottom right) for Georges Bank closed areas.

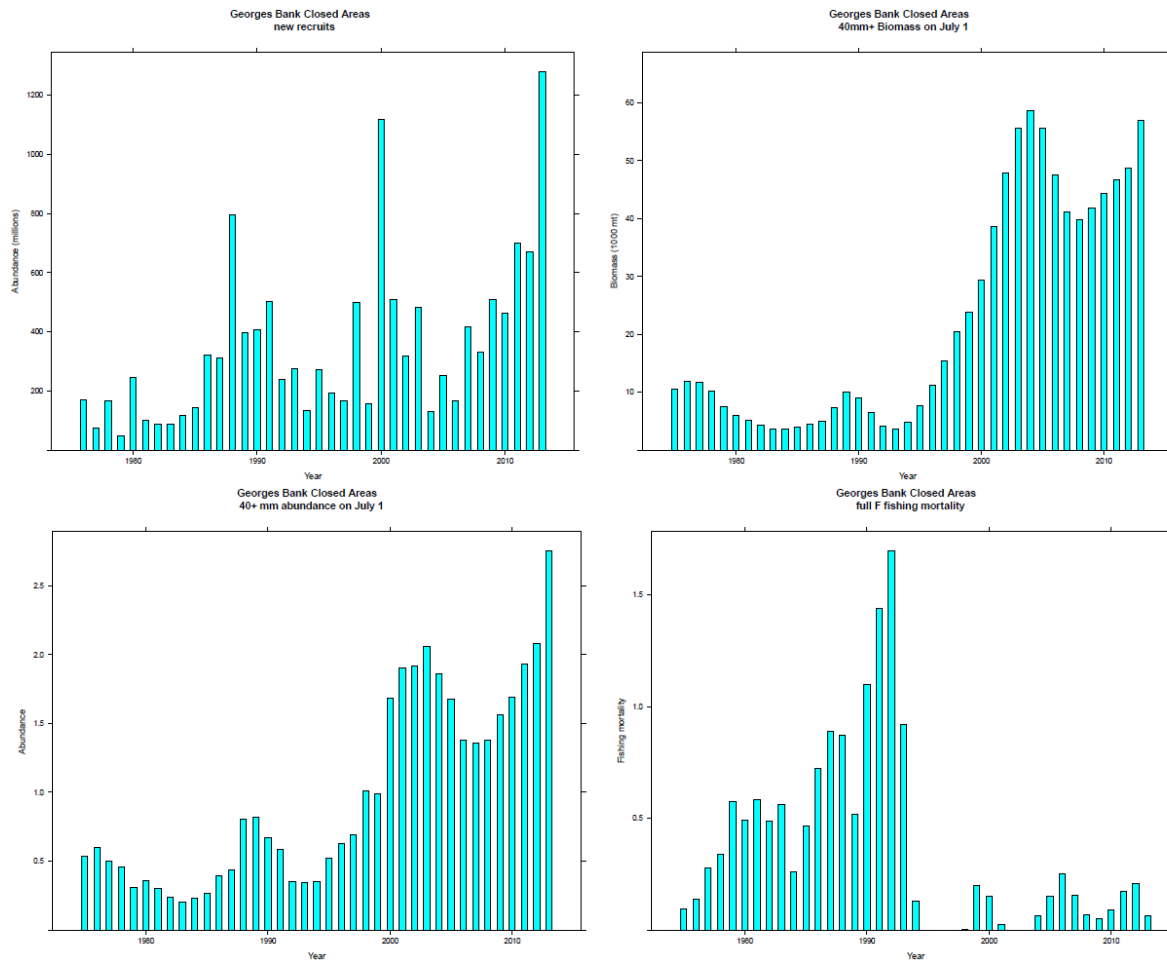


Figure B6.23. CASA model estimated recruitment (top left), July 1 biomass (top right), July 1 abundance (bottom left) and fully recruited fishing mortality (bottom right) for Georges Bank closed areas.

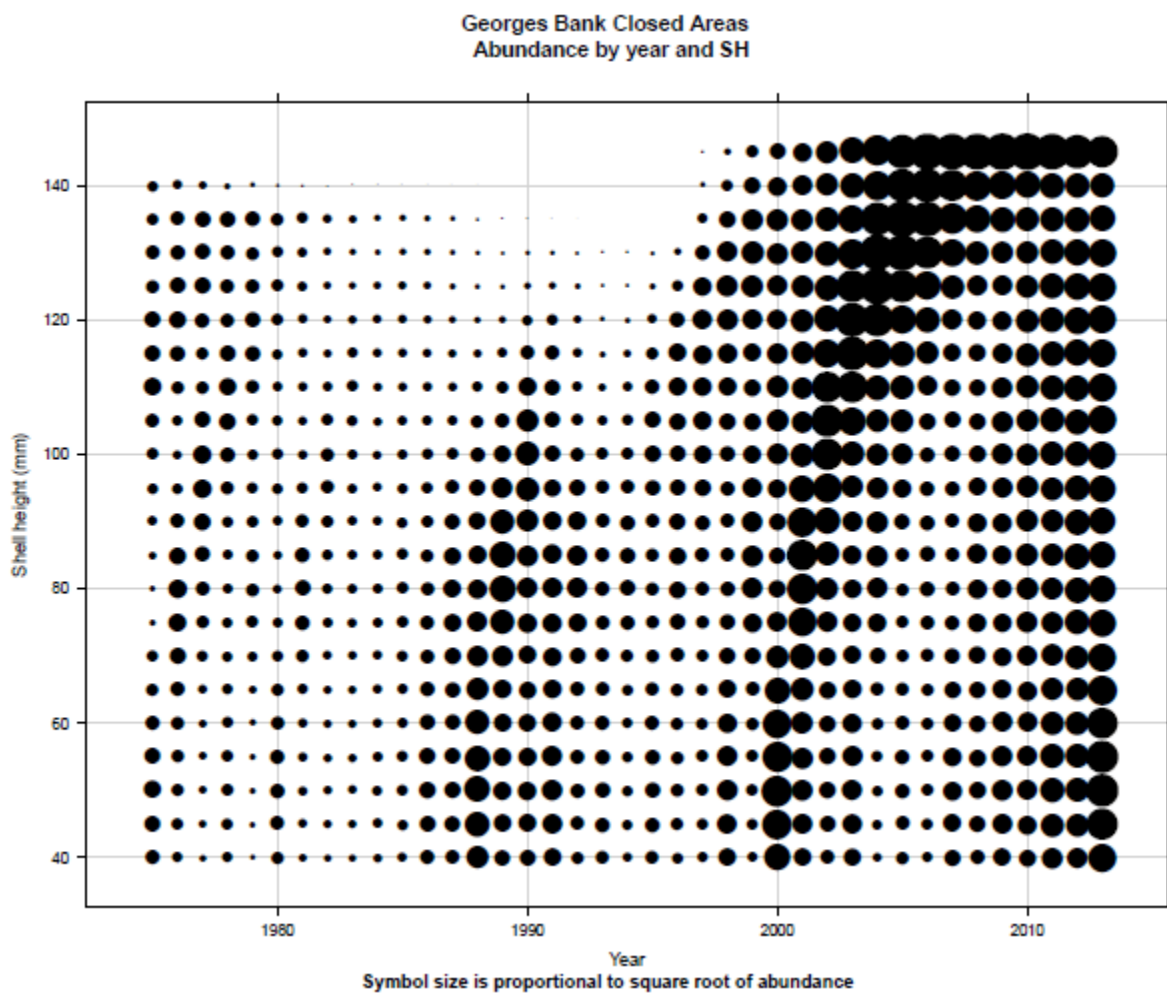


Figure B6.24. Model estimated abundances at shell height for Georges Bank closed areas. Symbol areas are proportional abundance.

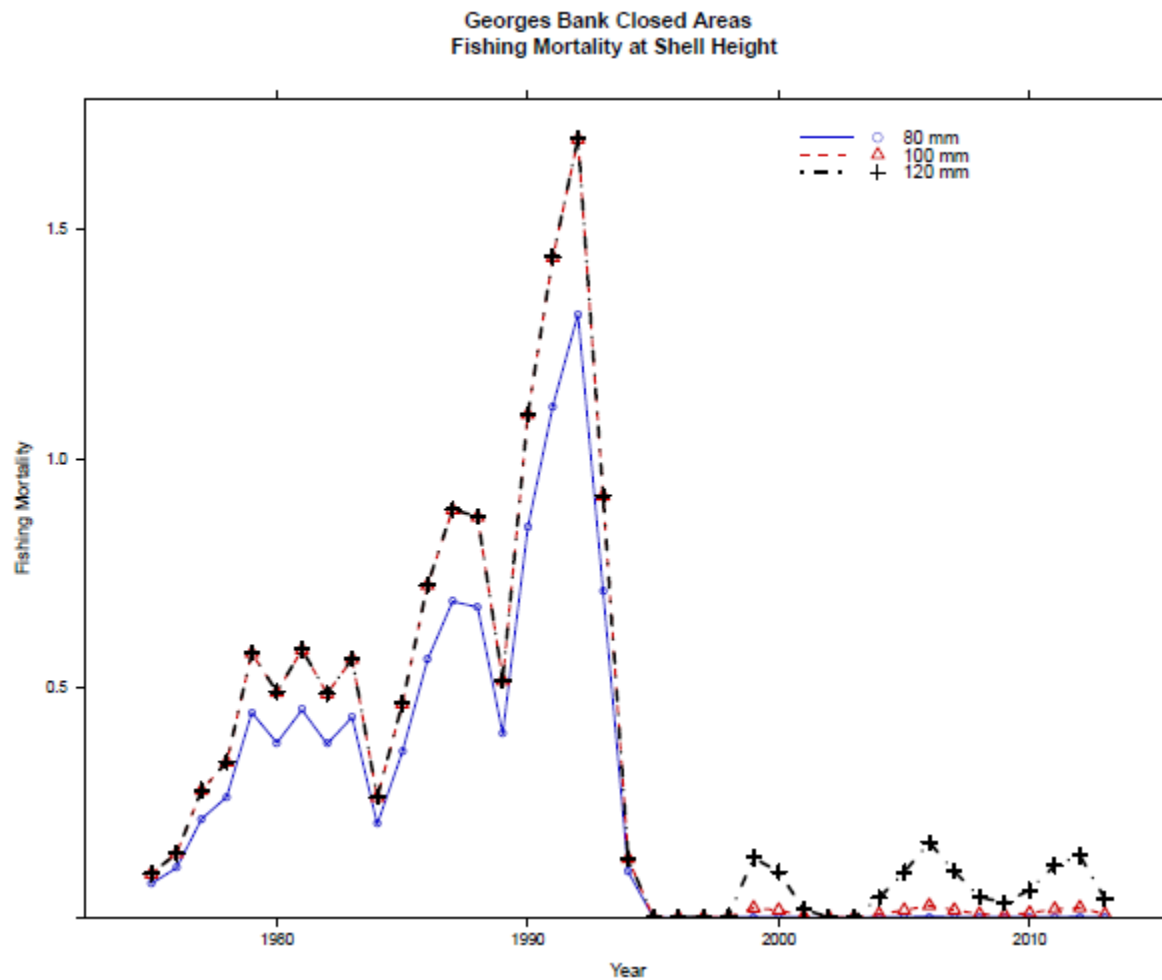


Figure B6.25. CASA model estimated fishing mortality at 80 mm (solid line with circles), 100 mm (dashed line with triangles) and 120 mm SH (dashed line with crosses) for Georges Bank closed areas.

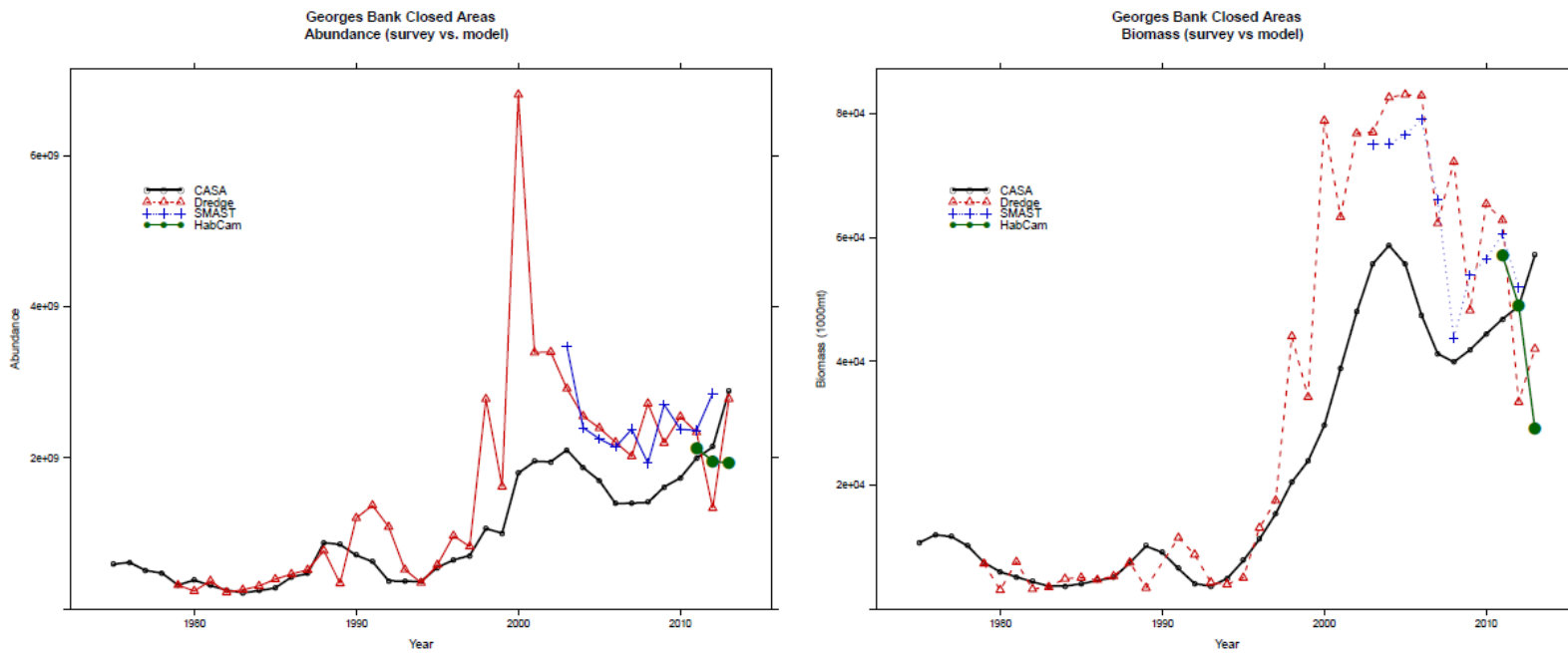


Figure B6.26. Comparison of CASA model estimated abundance (left) and biomass (right) with estimates from the lined dredge survey (dashed line with triangles), SMAST large camera survey (dotted line with crosses) and HabCam (solid line with circles) for Georges Bank closed areas. The dredge survey was expanded assuming an efficiency of 0.41 on sand and 0.27 on gravel/cobble.

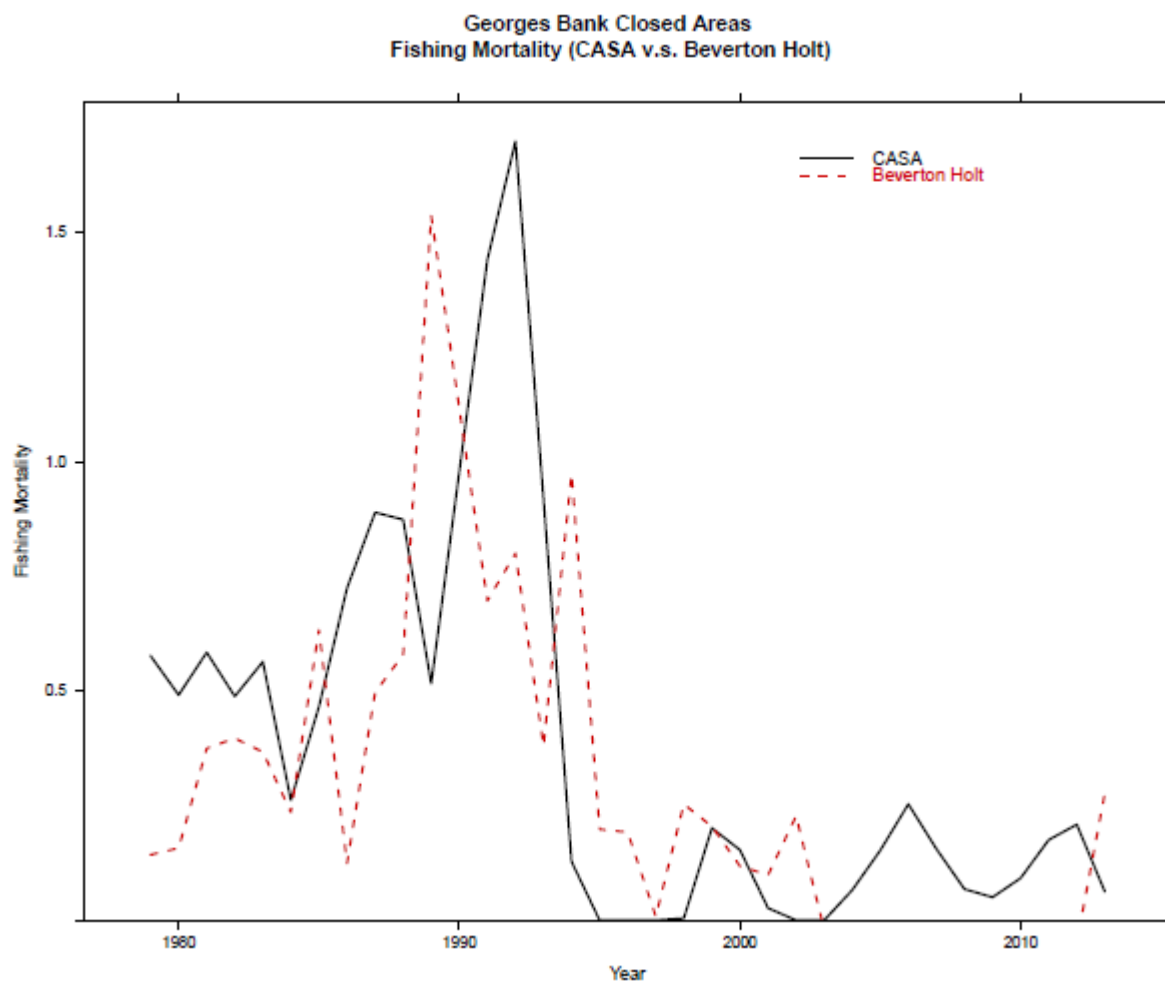


Figure B6.27. Comparison of fully recruited CASA fishing mortality with those calculated from the Beverton-Holt equilibrium estimator for the Georges Bank closed areas.

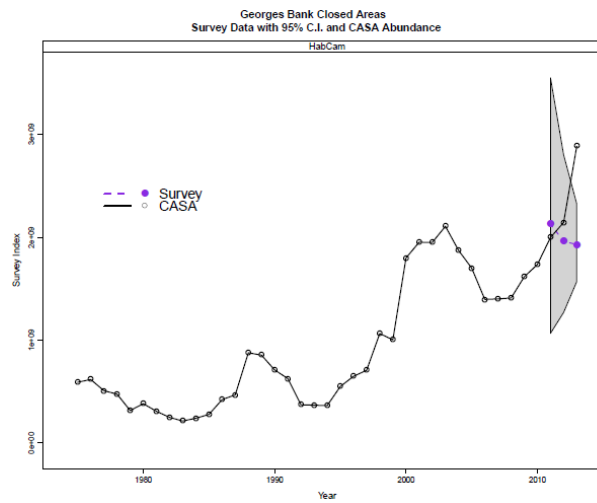
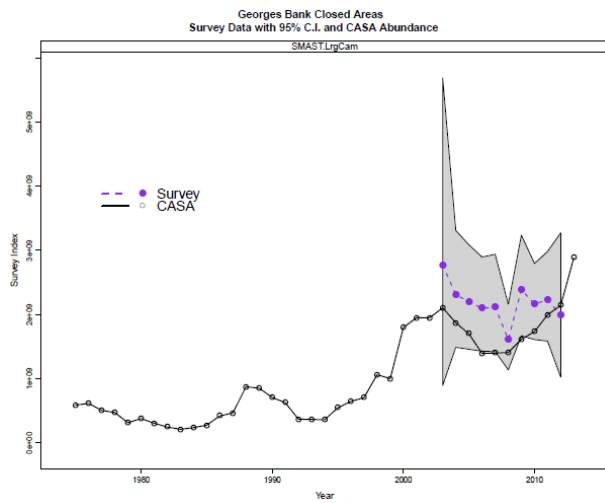
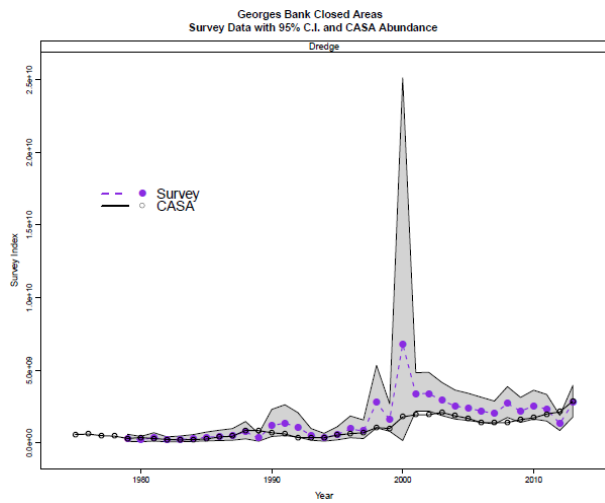


Figure B6.28. CASA estimated abundance compared to that from the dredge survey (top), the SMAST survey (left bottom), and the HabCam survey (right bottom), for Georges Bank closed areas.

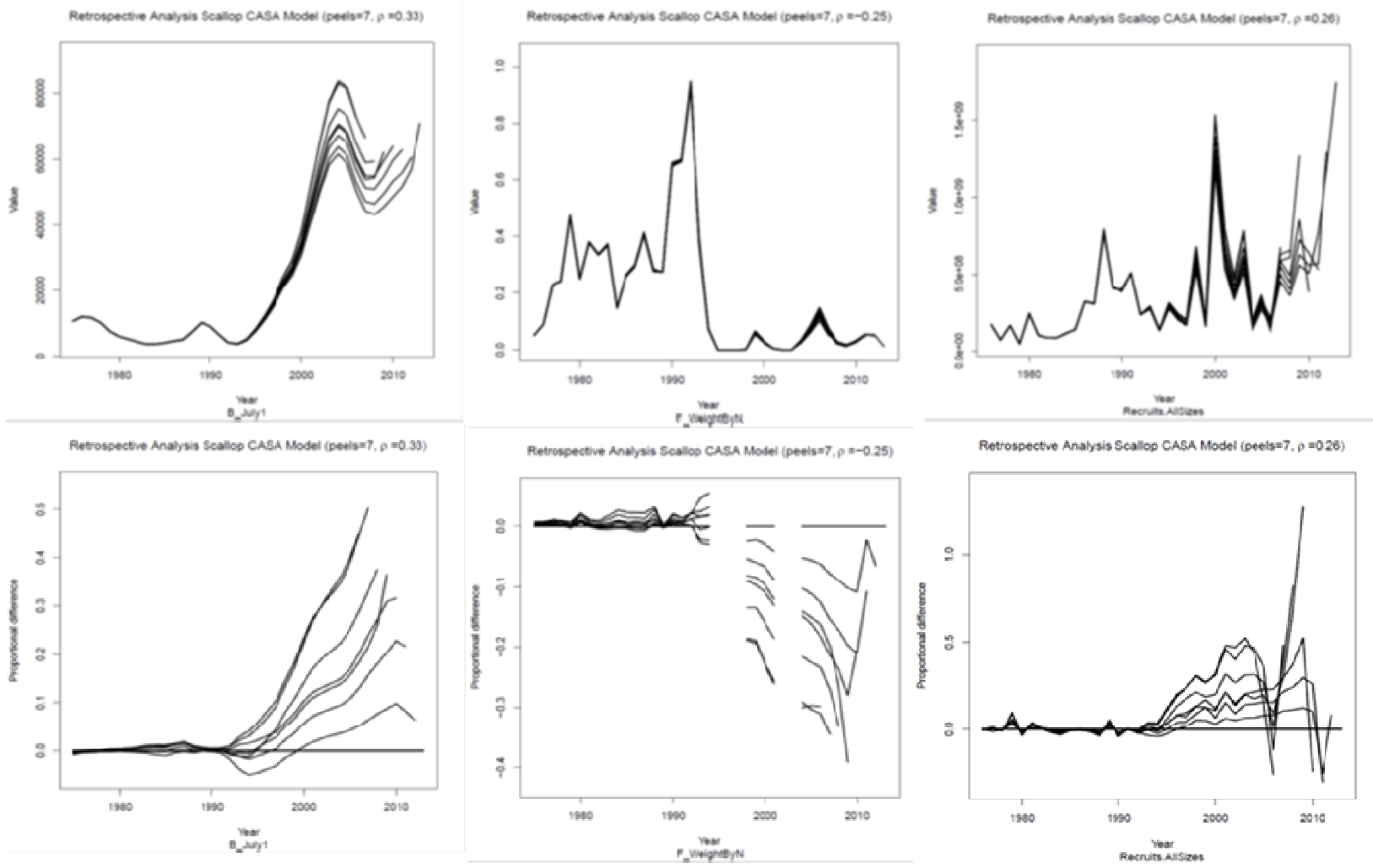


Figure B6.29. Retrospective plots for biomass, fishing mortality and recruitment for Georges Bank closed areas. Retrospectives are shown on both absolute and relative scales.

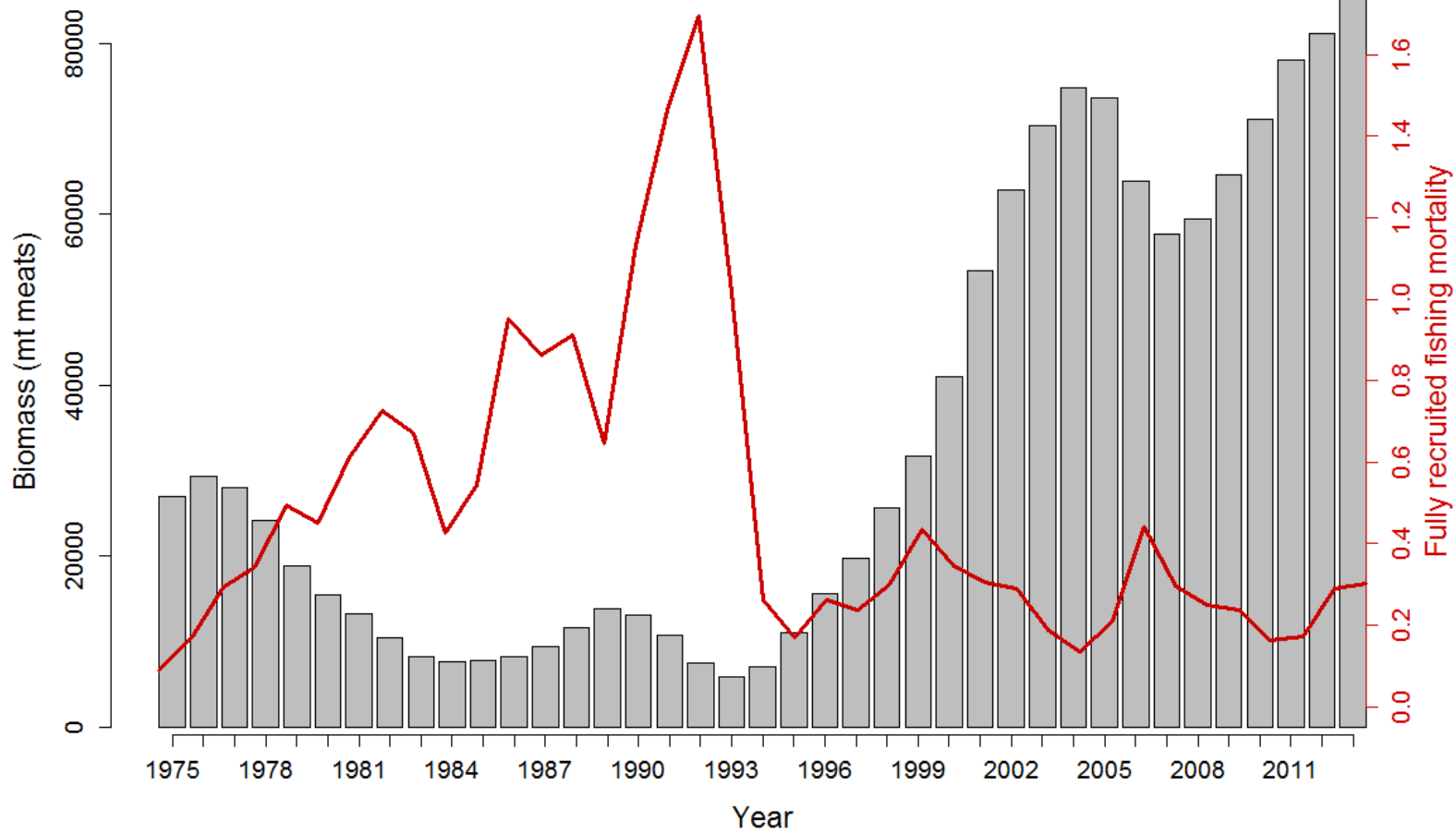


Figure B6.30. Estimated biomass and fully recruited fishing mortality for Georges Bank sea scallops (open and closed combined).

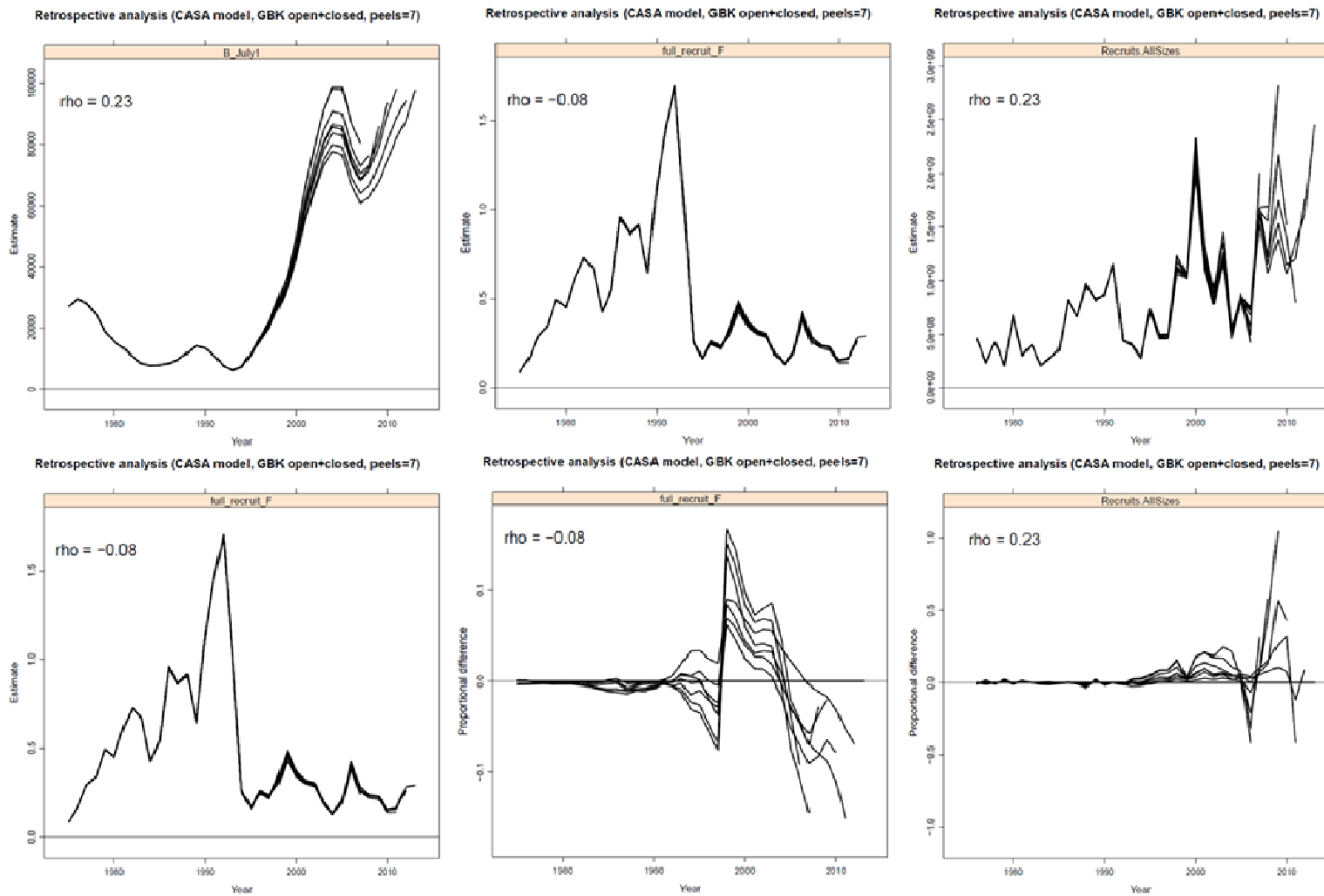
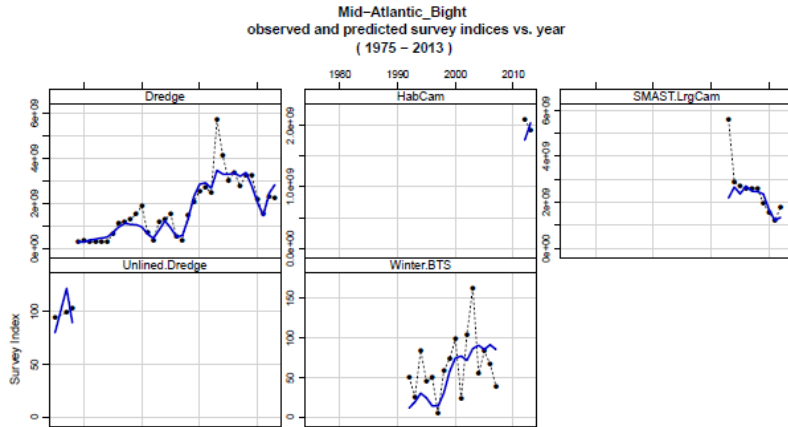


Figure B6.30b. Retrospective plots for the combined Georges Bank open and closed areas.

(A)



(B)

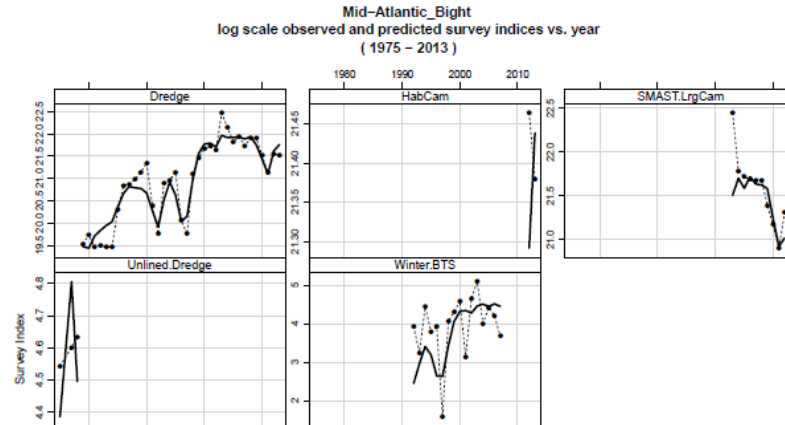


Figure B6.31. Survey trend (solid circles) and corresponding model estimates (lines) for the NEFSC lined dredge survey, the HabCam survey, The SMAST large camera survey, the NEFSC unlined dredge survey, and the NEFSC winter bottom trawl survey in the Mid-Atlantic Bight. Results are shown on a linear scale (A) and a log scale (B).

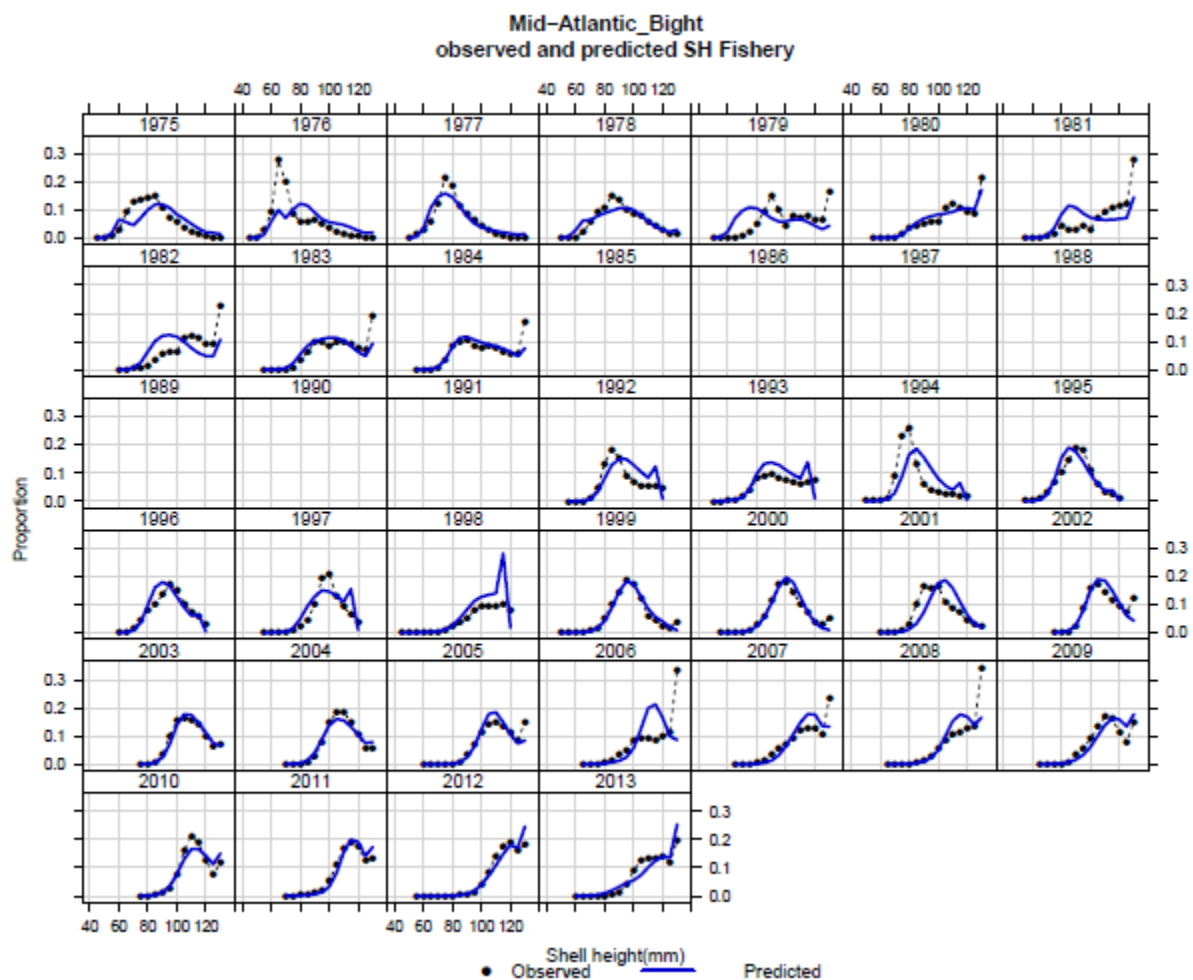


Figure B6.32. Comparison of fishery shell height proportions (solid circles) and model estimated fishery shell height proportions (lines) for the Mid-Atlantic Bight.

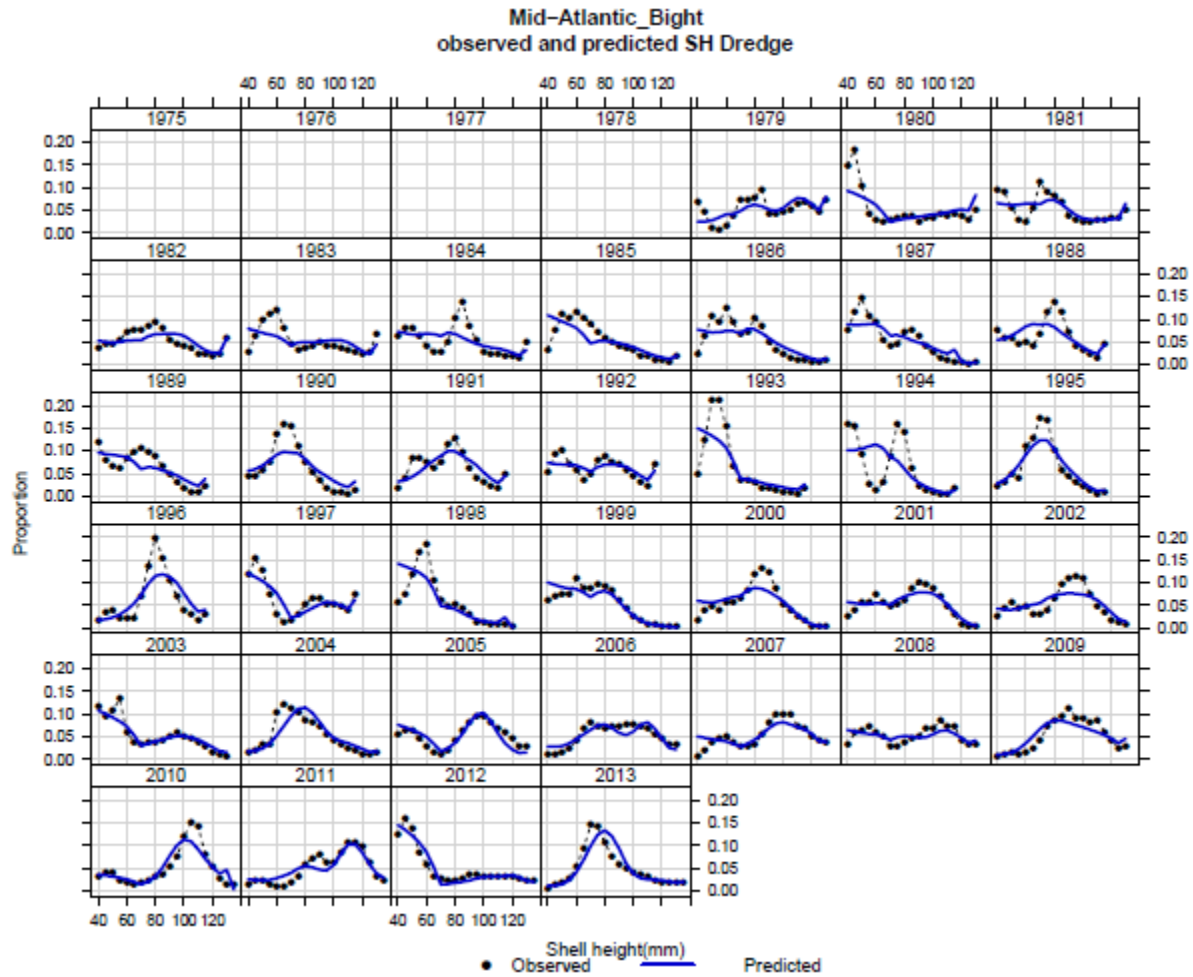


Figure B6.33. NEFSC lined dredge survey shell height proportions (solid circles) and model estimated shell height proportions (lines) for the Mid-Atlantic Bight.

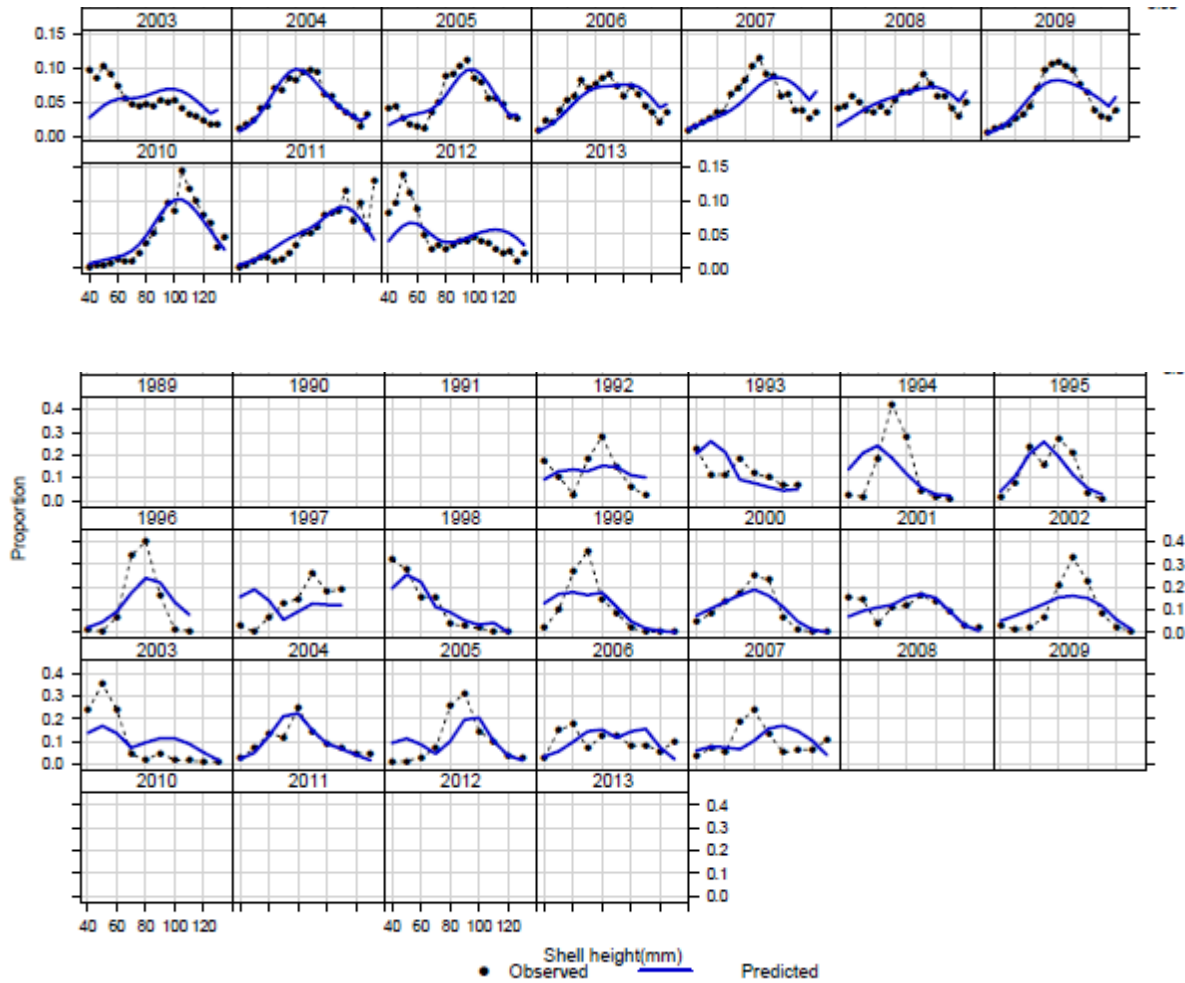


Figure B6.34. Shell height proportions for the SMAST large camera survey (top), and the NEFSC winter bottom trawl survey (bottom) with model predicted proportions (lines) for the Mid-Atlantic Bight.

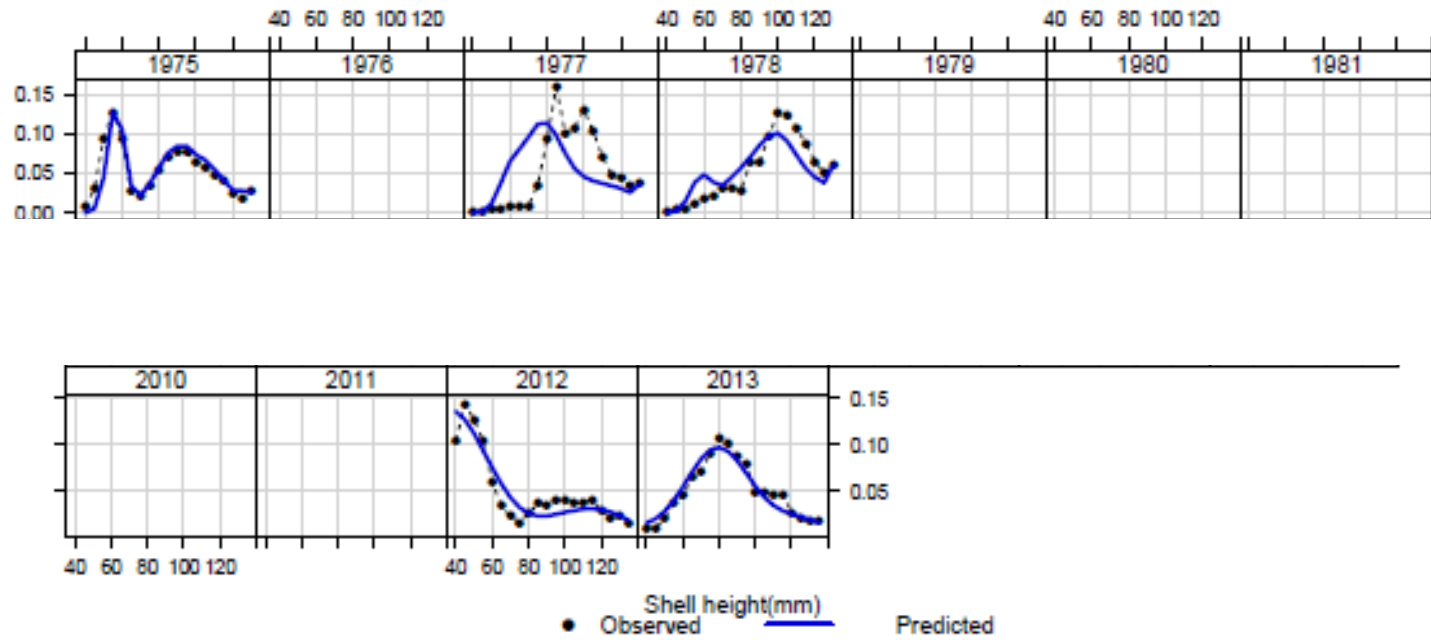


Figure B6.35. Shell height proportions for the NEFSC unlined dredge survey (top) and the HabCam survey (bottom) with model predicted proportions (lines) for the Mid-Atlantic Bight.

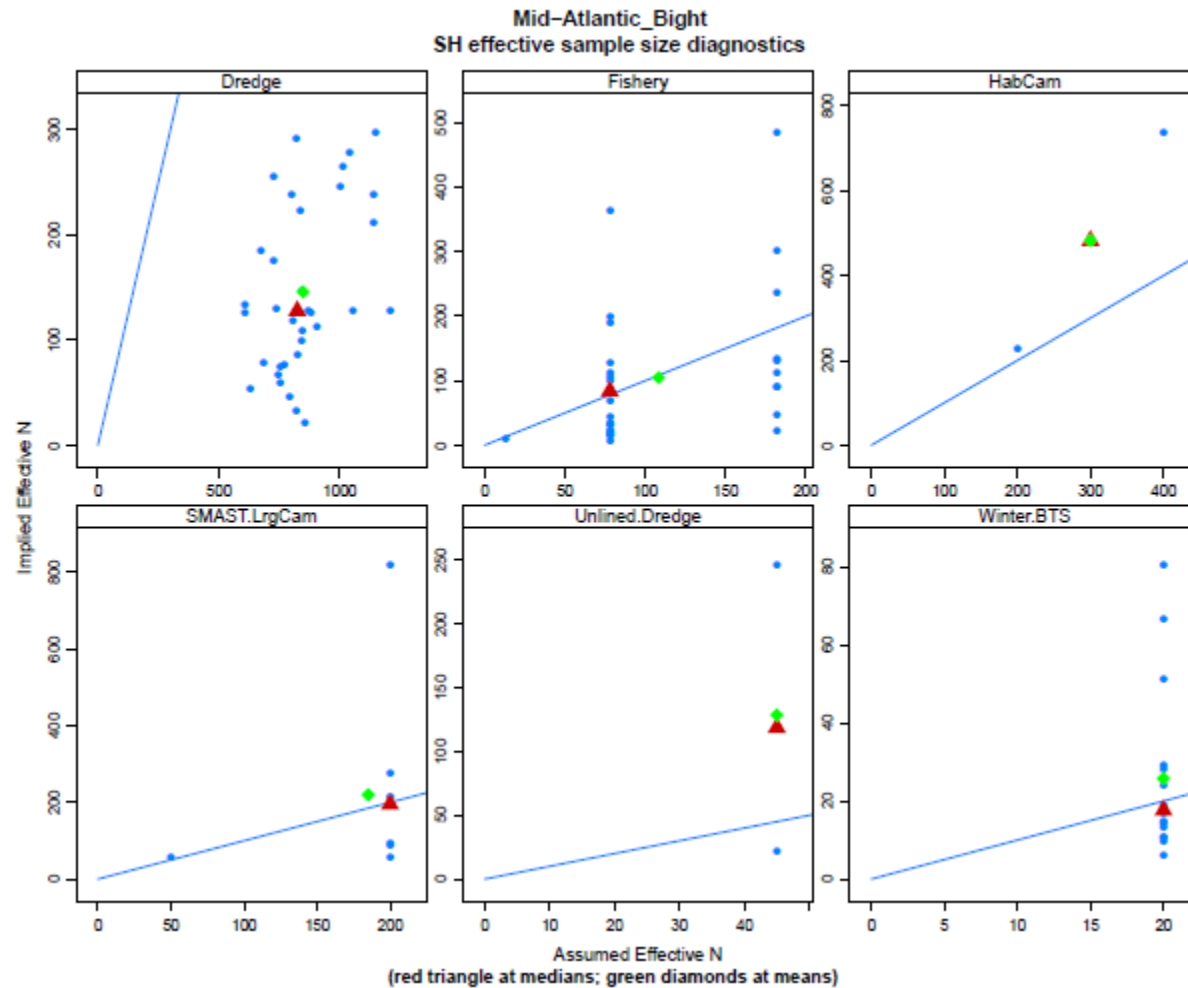


Figure B6.36 Assumed and implied effective sample sizes for the five surveys (NEFSC unlined dredge, HabCam, SMAST large camera, NEFSC unlined dredge, winter bottom trawl survey) and the fishery shell height compositions for the Mid-Atlantic Bight. The triangle is the median and the diamond is the mean.

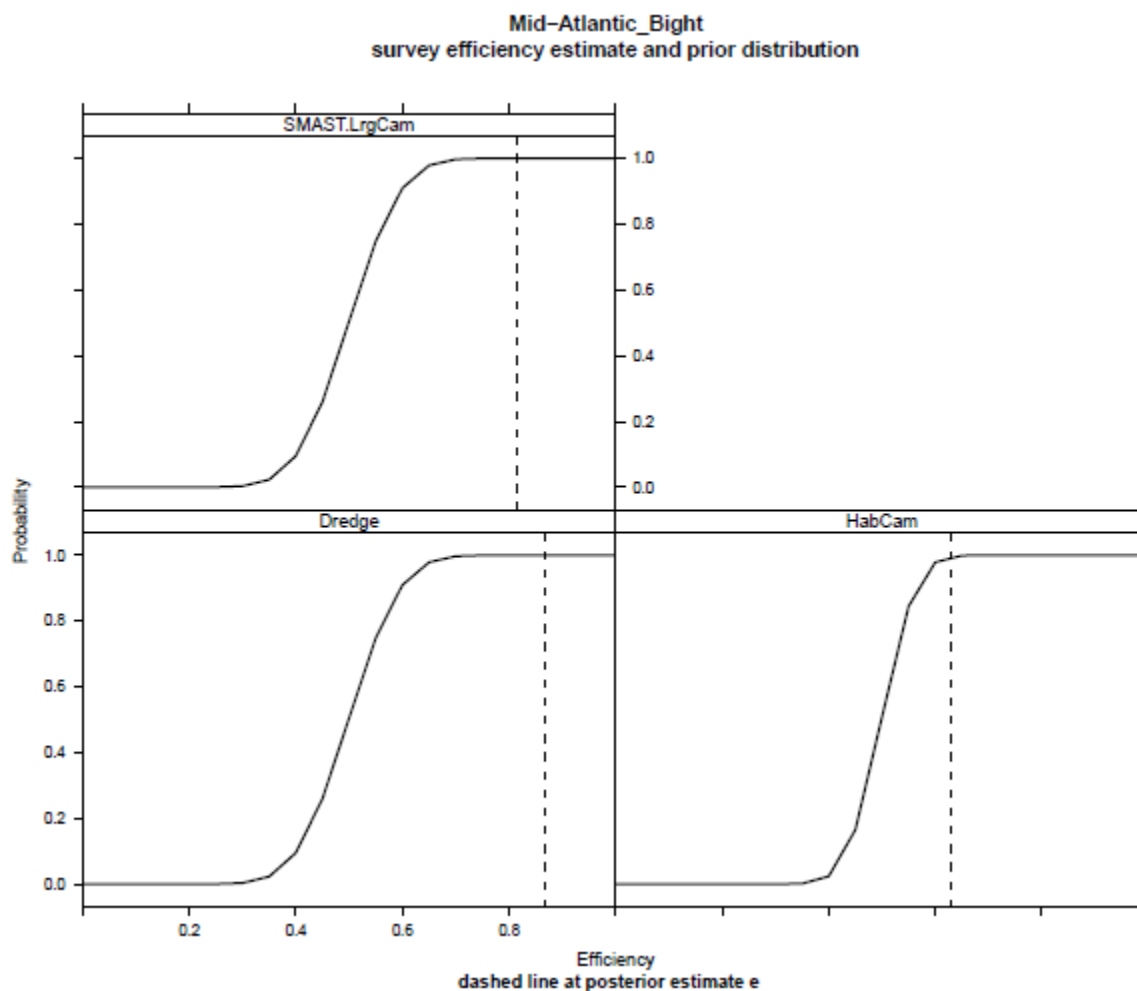


Figure B6.37. Prior cumulative distributions for catchability of the large camera video survey (top) lined dredge survey (bottom left) and HabCam survey (bottom right) for the Mid-Atlantic Bight. The dashed lines are the mean posterior estimate for survey efficiency. For the purposes of this plot, the surveys were adjusted to have a mean prior catchability of 0.5

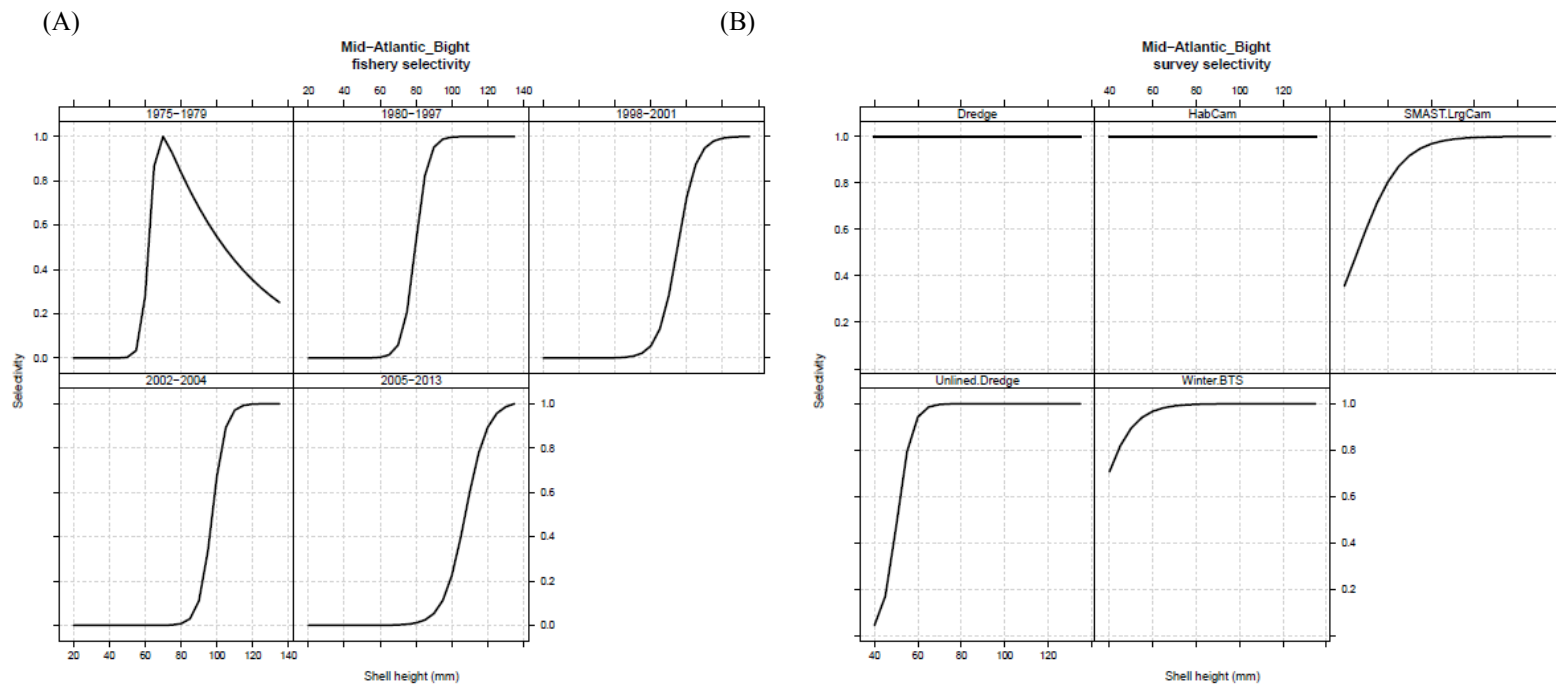


Figure B6.38. (A) Estimated fishery selectivity curves and (B) survey selectivity curves (lined dredge top left, HabCam top middle, large camera top right, unlined dredge bottom left, and winter bottom trawl bottom middle) for the Mid-Atlantic Bight.

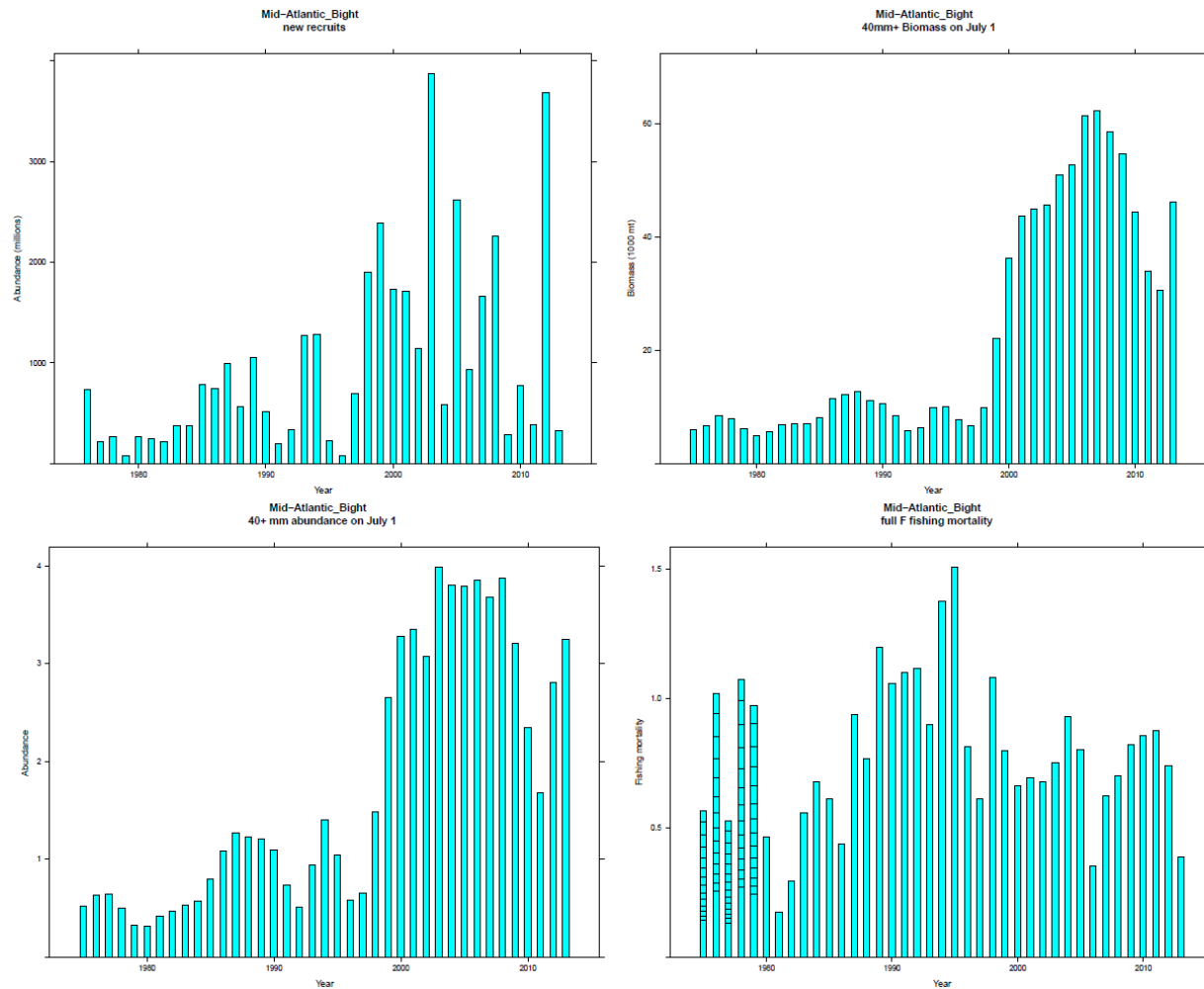


Figure B6.39. CASA model estimated recruitment (top left), July 1 biomass (top right), July 1 abundance (bottom left), and fully recruited fishing mortality (bottom right) for the Mid-Atlantic Bight.

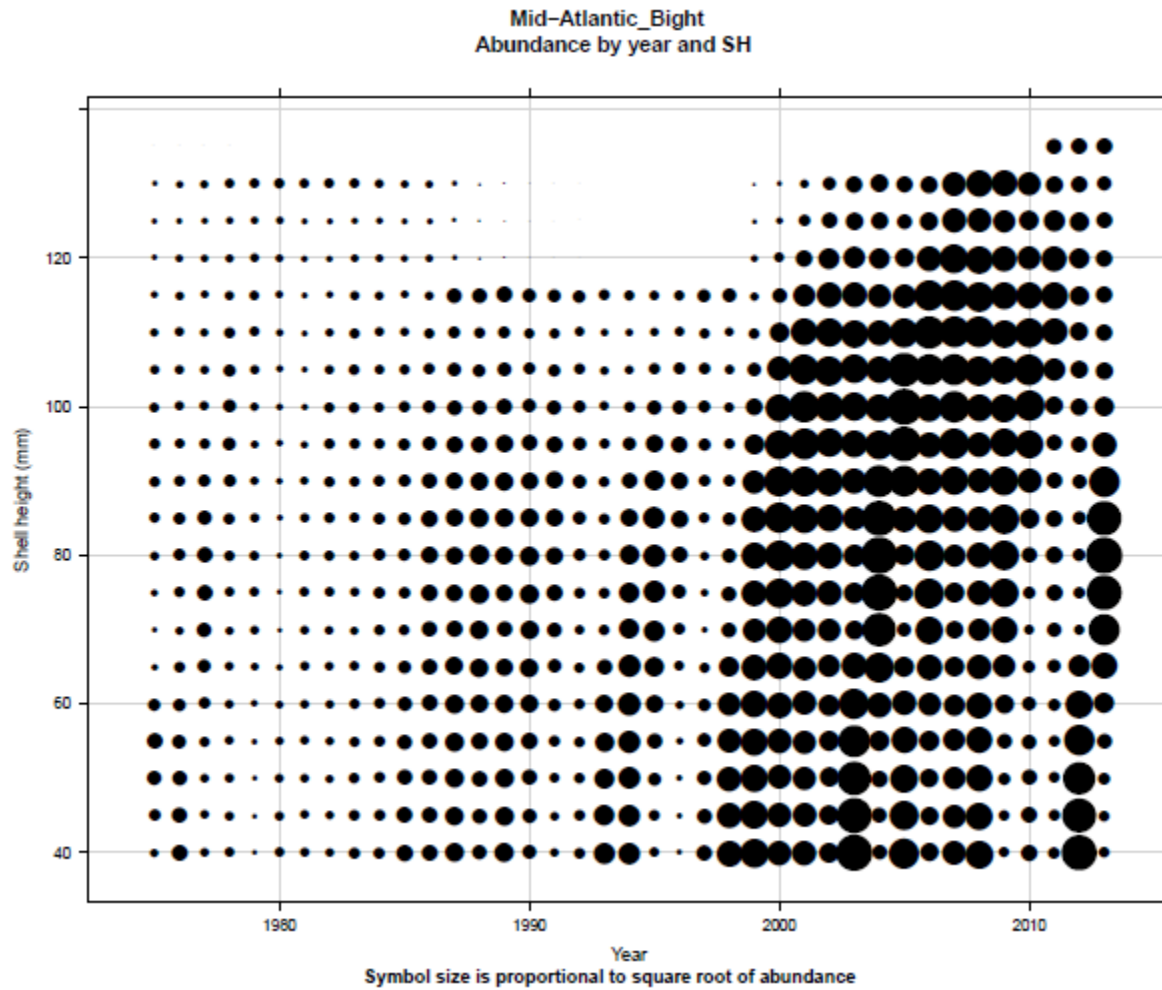


Figure B6.40. Model estimated abundances at shell height for the Mid-Atlantic Bight. Symbol areas are proportional to abundance.

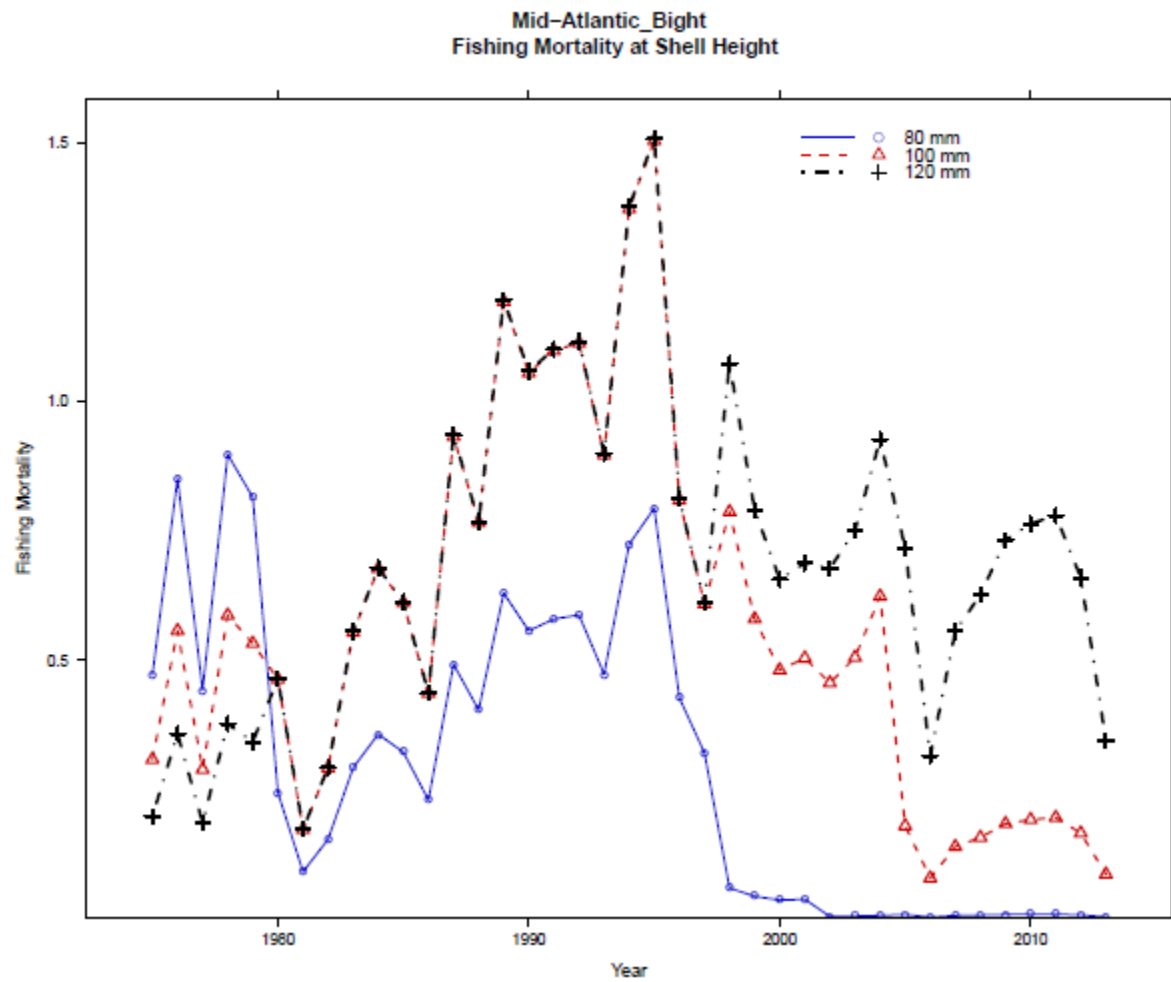


Figure B6.41. CASA model estimated fishing mortality at 80 mm (solid line with circles), 100 mm (dashed line with triangles) and 120 mm SH (dashed line with crosses) for the Mid-Atlantic Bight.

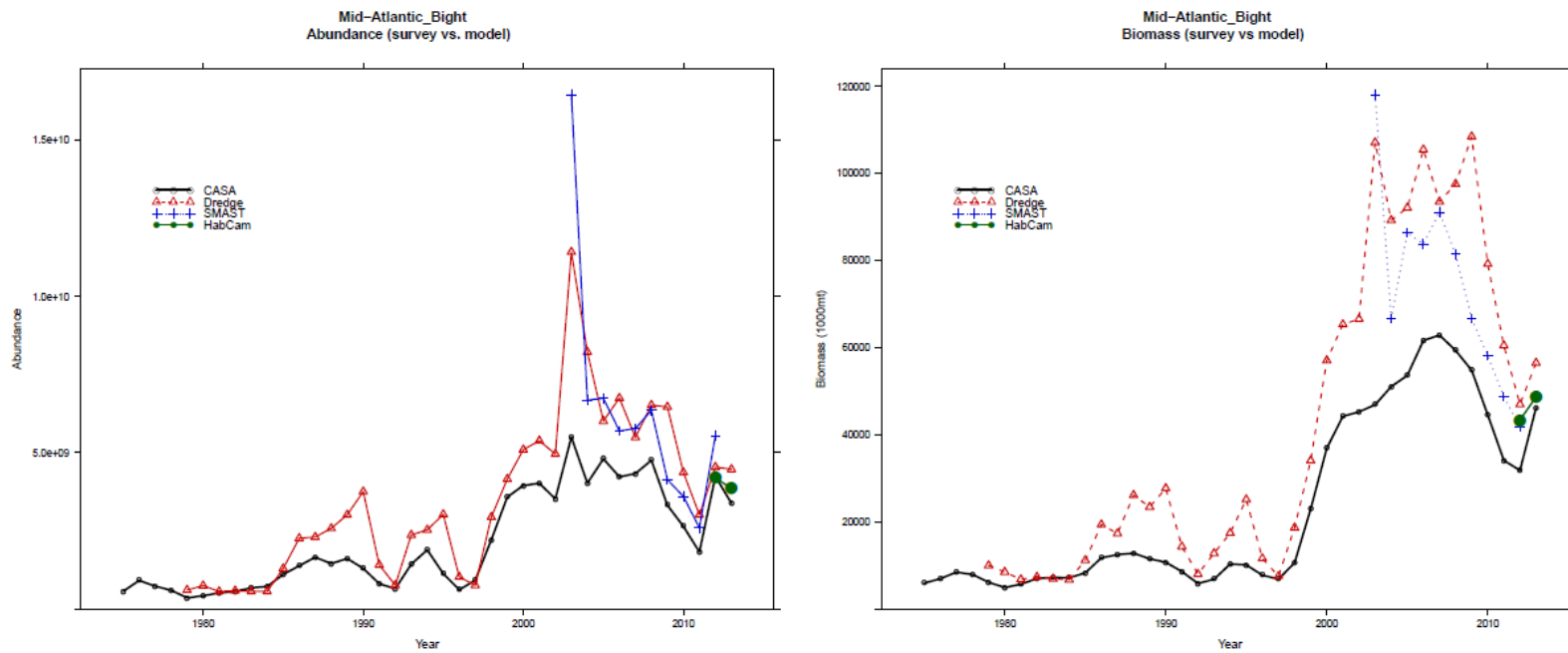


Figure B6.42. Comparison of CASA model estimated abundance (left) and biomass (right) with estimates from the lined dredge survey (dashed line with triangles), S Mast large camera survey (dotted line with crosses) and HabCam (solid line with circles) for the Mid-Atlantic Bight. The dredge survey was expanded assuming an efficiency of 0.41.

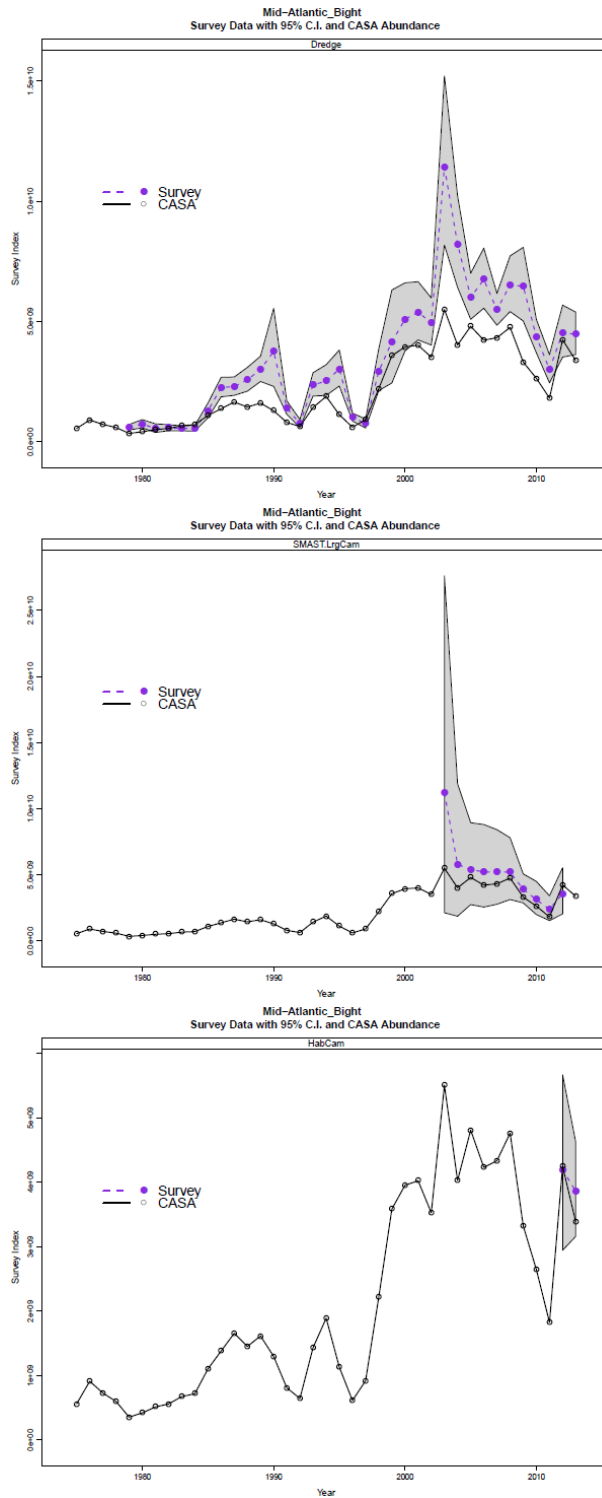


Figure B6.42b. CASA estimated abundance compared to that from the dredge survey (top), the SMAST survey (middle), and the HabCam survey (bottom), for the mid-Atlantic bight.

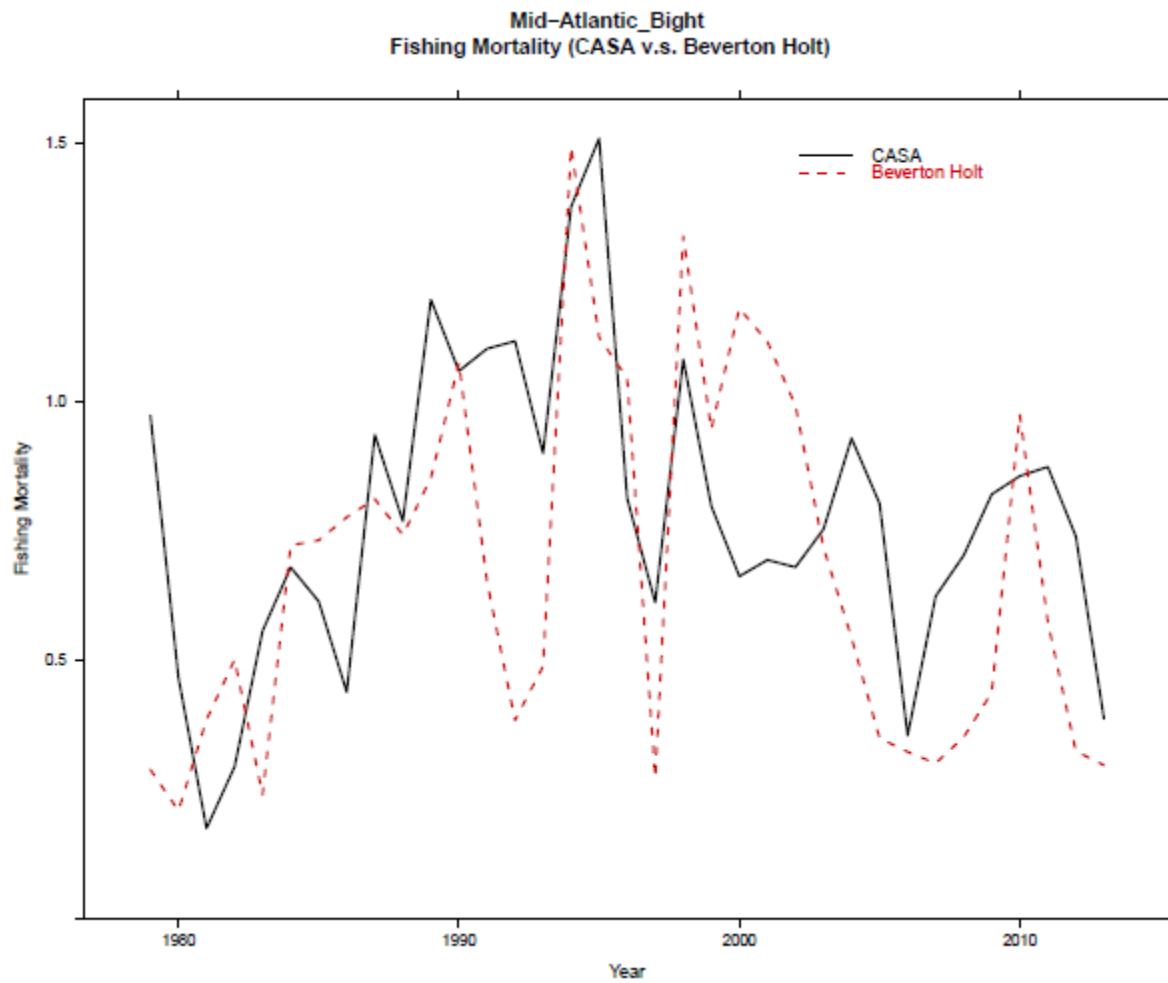


Figure B6.43. Comparison of fully recruited CASA fishing mortality with those calculated from the Beverton-Holt equilibrium estimator for the Mid-Atlantic Bight.

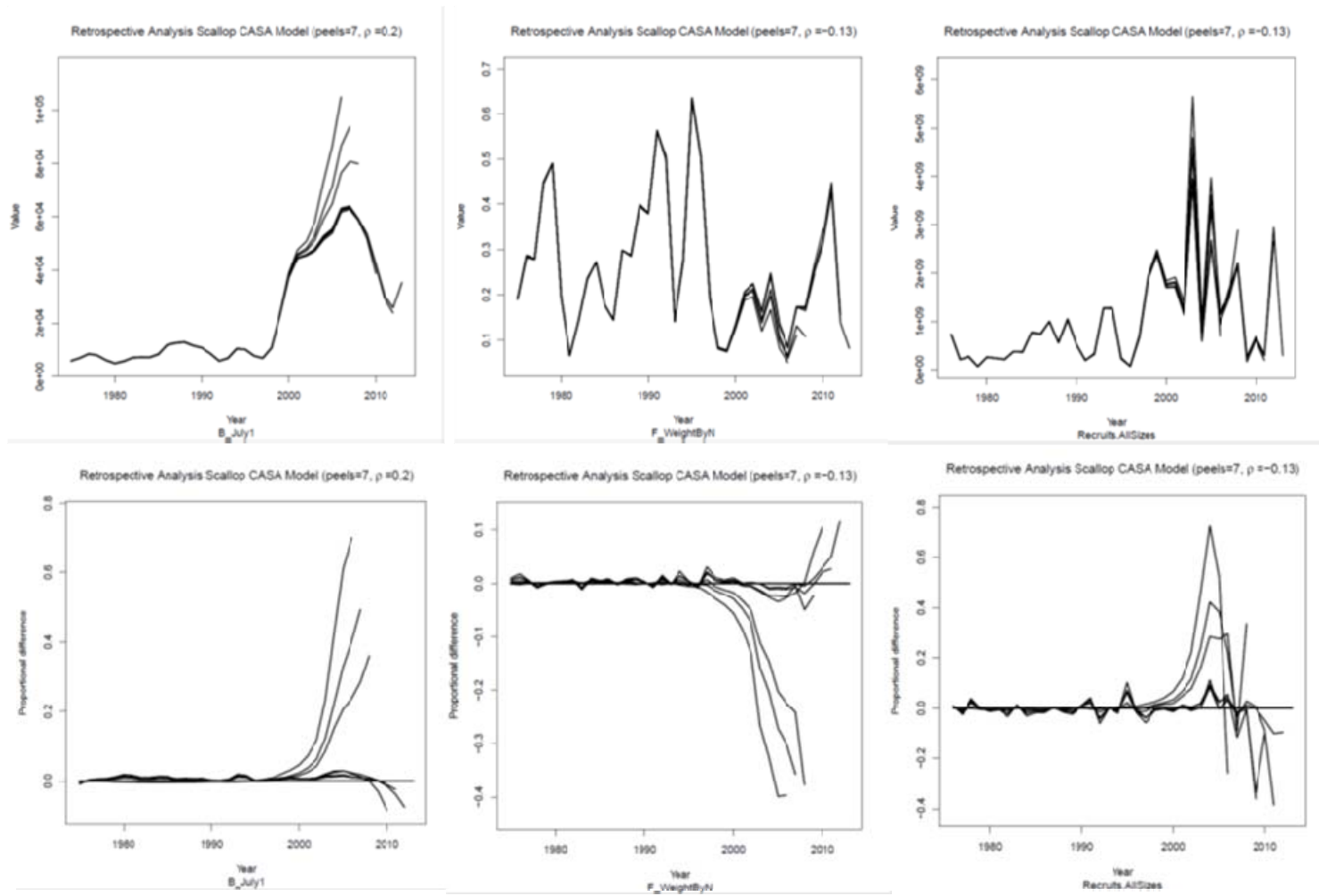


Figure B6.44. Retrospective plots for biomass, fishing mortality and recruitment for the Mid-Atlantic Bight. Retrospective patterns are shown on both absolute and relative scales.

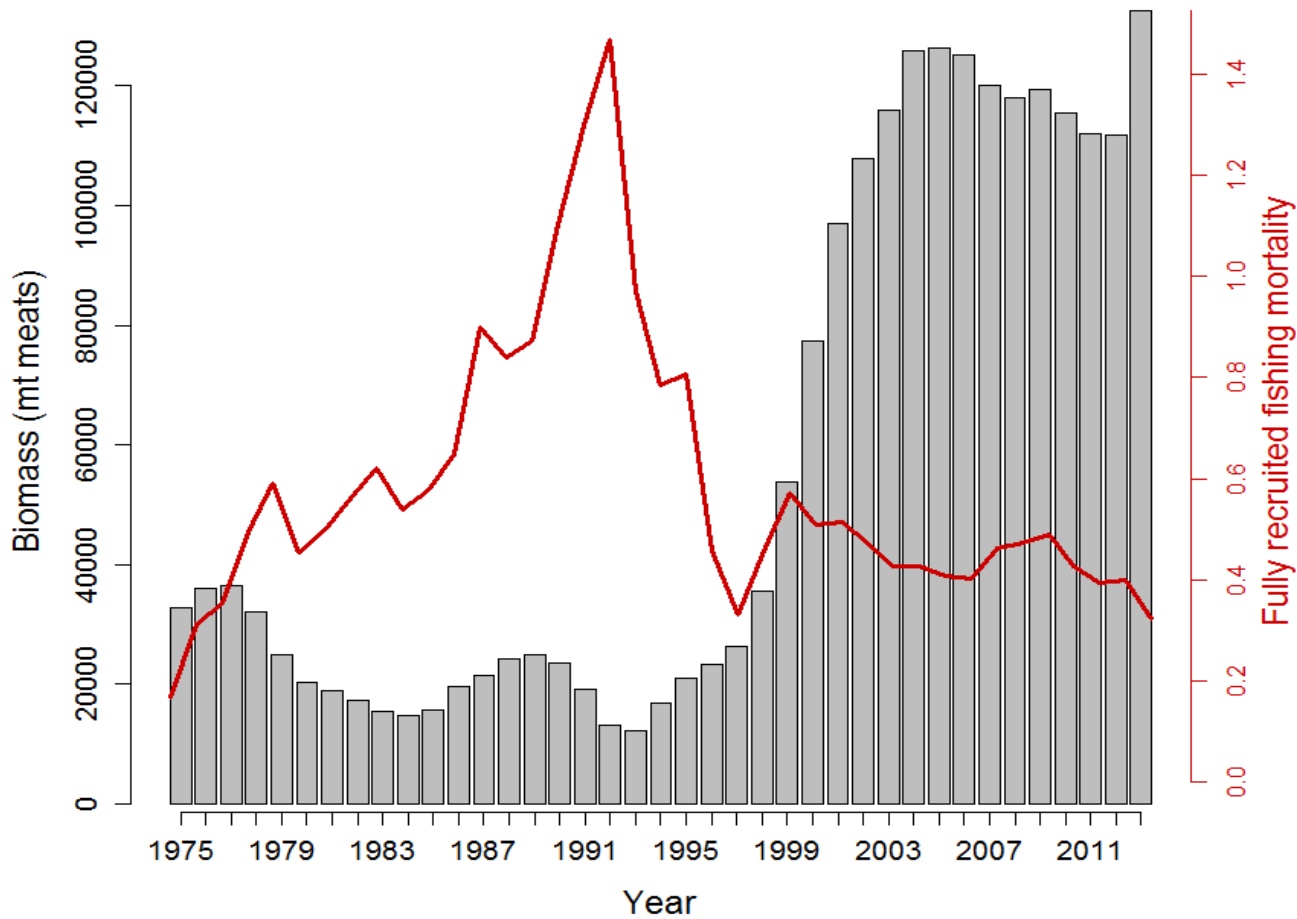


Figure B6.45. Total estimated biomass and fully recruited fishing mortality for Georges Bank and Mid-Atlantic combined.

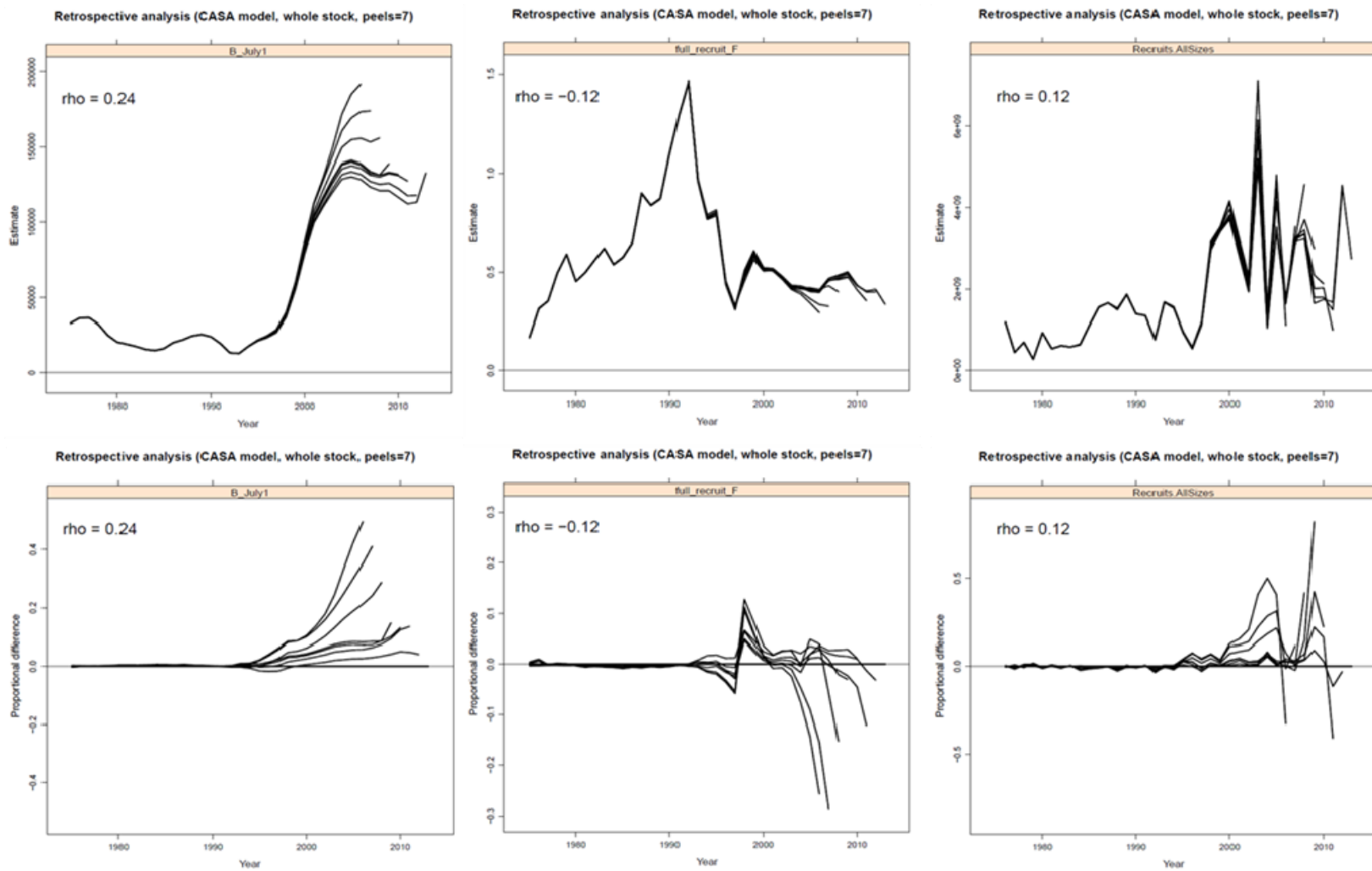


Figure B6.45b. Retrospective plots for the entire sea scallop stock.

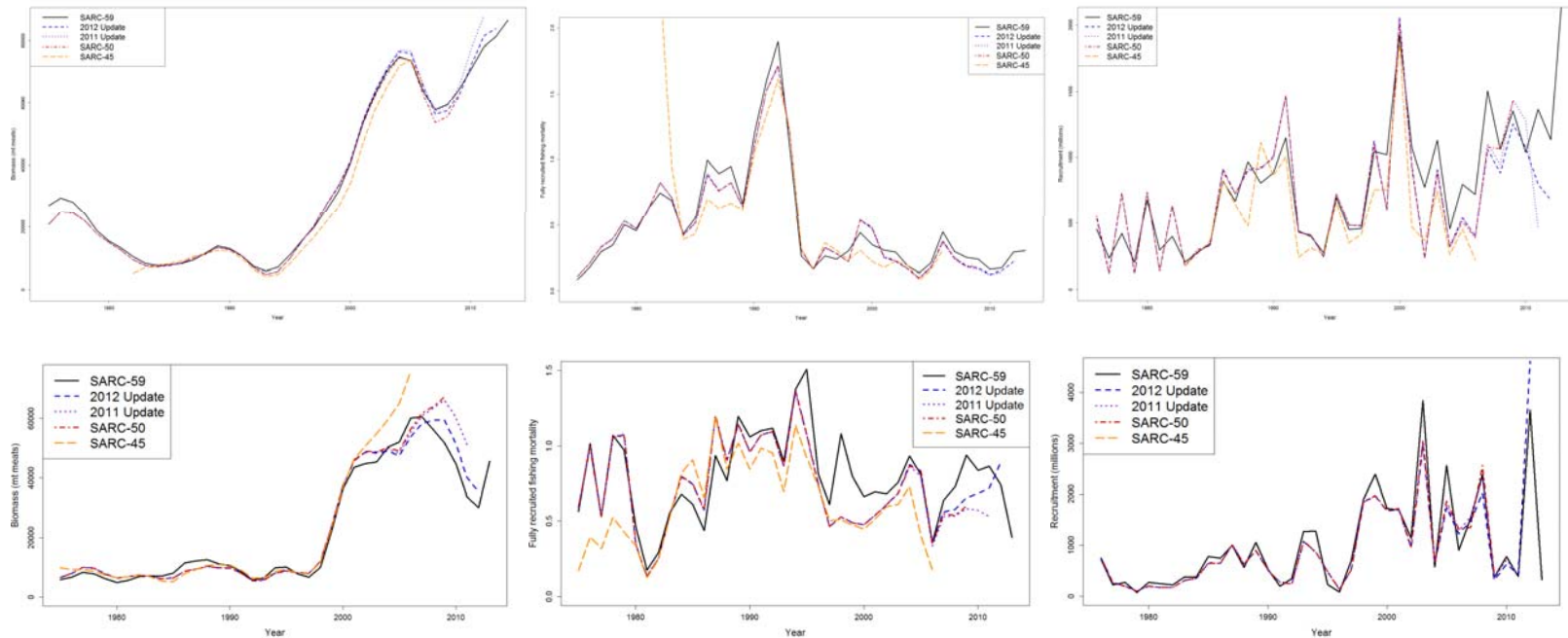


Figure B6.46. Comparison of current CASA model estimates of biomass (left), fishing mortality (middle), and recruitment (right) to previous CASA model estimates for Georges Bank (top) and the Mid-Atlantic (bottom) sea scallops.

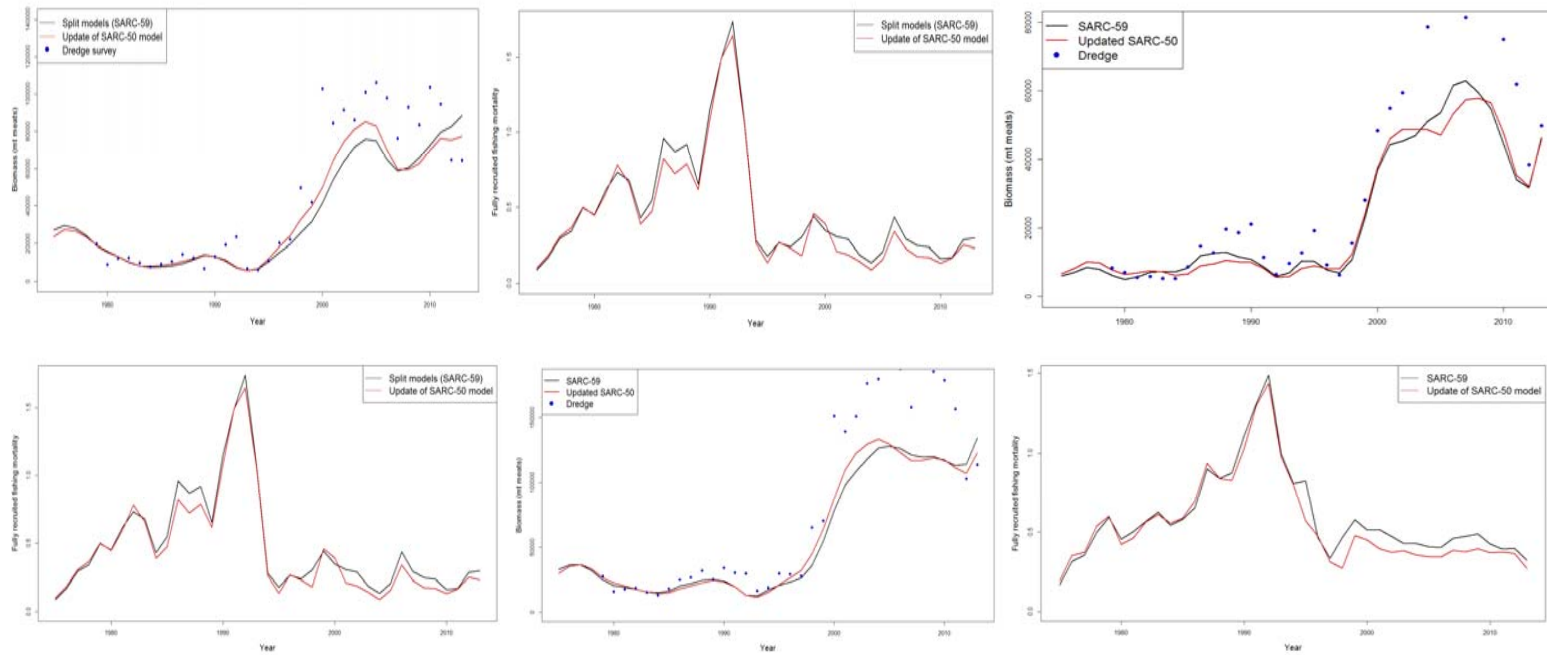


Figure B6.47. Comparisons of biomass and F estimates for the current configurations of the CASA model with the SARC-50 configurations, updated through 2013, for Georges Bank (top left and middle), Mid-Atlantic (top right and bottom left) and total (bottom middle and right). Expanded dredge survey estimates are also given for the biomass plots.

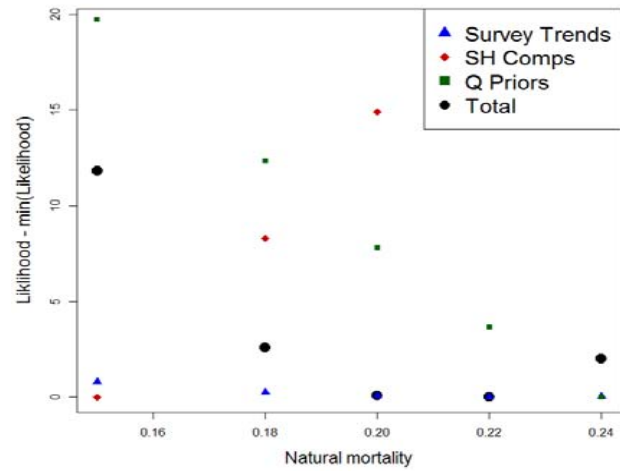
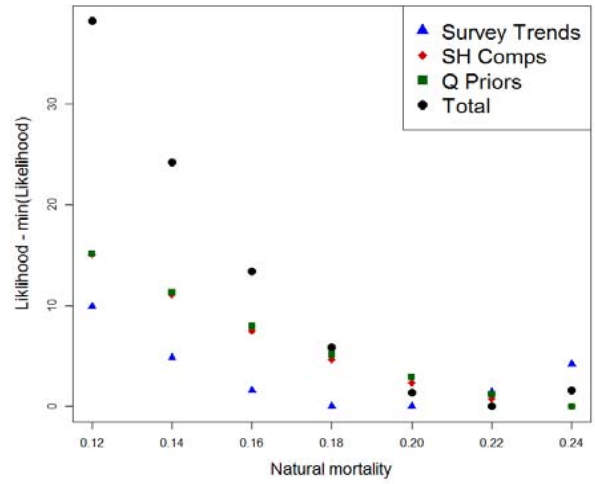
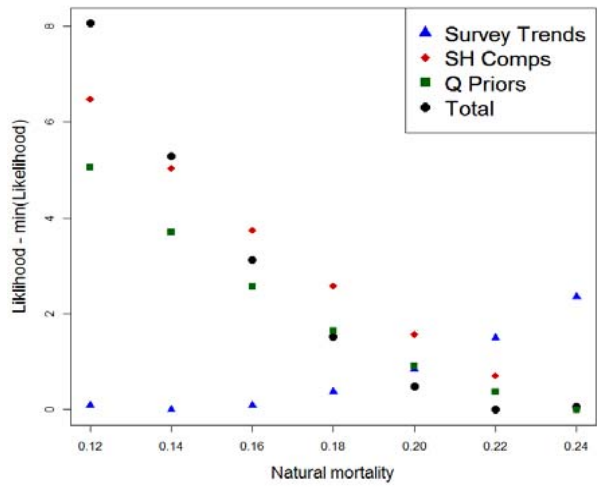


Figure B6.48. Likelihood profiles over the assumed natural mortality for all but the largest size bin (plus group mortality is 1.5x smaller sizes) for (top left) Georges Bank Open, (top right) Georges Bank Closed, (bottom) Mid-Atlantic sea scallops.

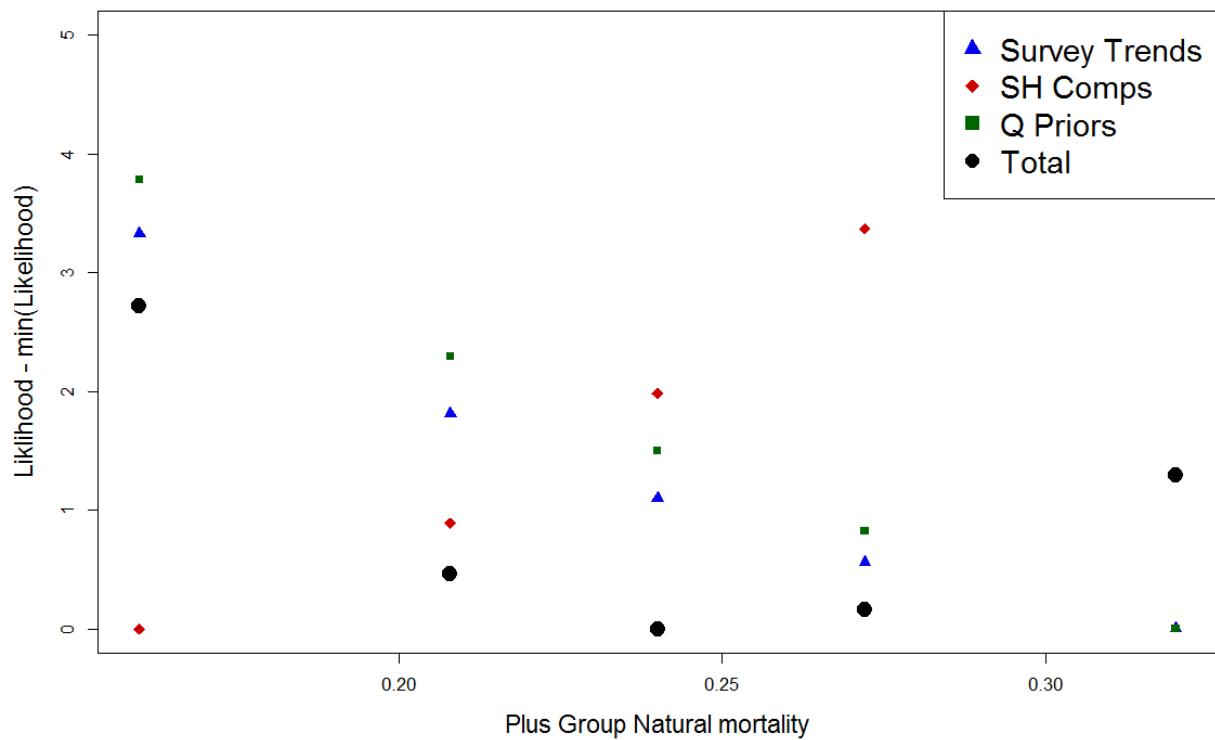


Figure B6.49. Likelihood profile analysis for the assumed plus-group natural mortality in the CASA model for sea scallops in Georges Bank closed areas. Natural mortality on the smaller size classes was fixed at 0.16.

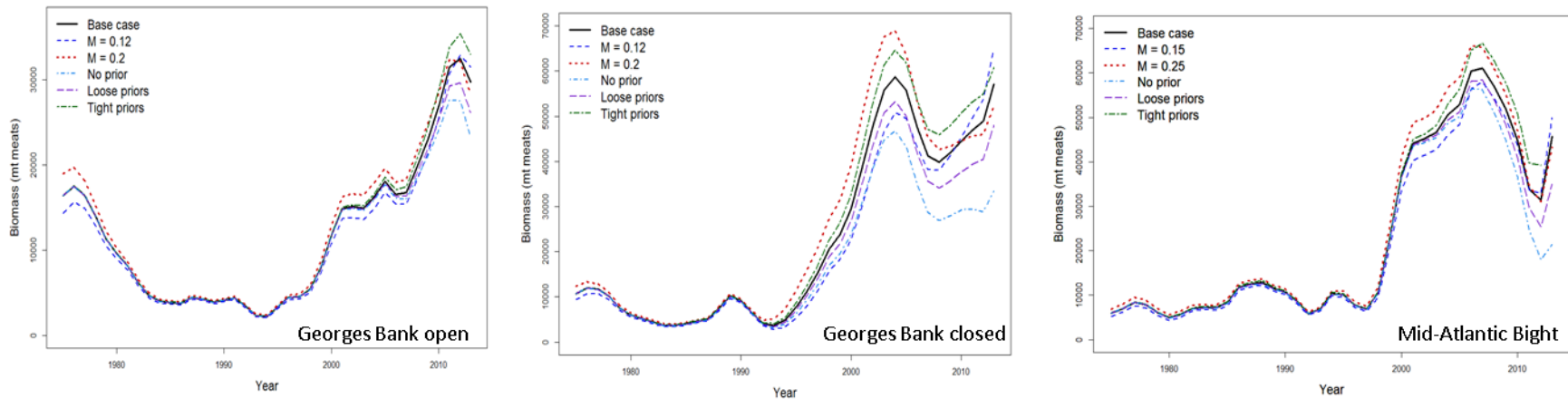


Figure B6.50. Sensitivity of estimated biomass to assumptions about natural mortality and survey efficiency priors in CASA models for Georges Bank open (left), Georges Bank closed (middle), and the Mid-Atlantic Bight (right).

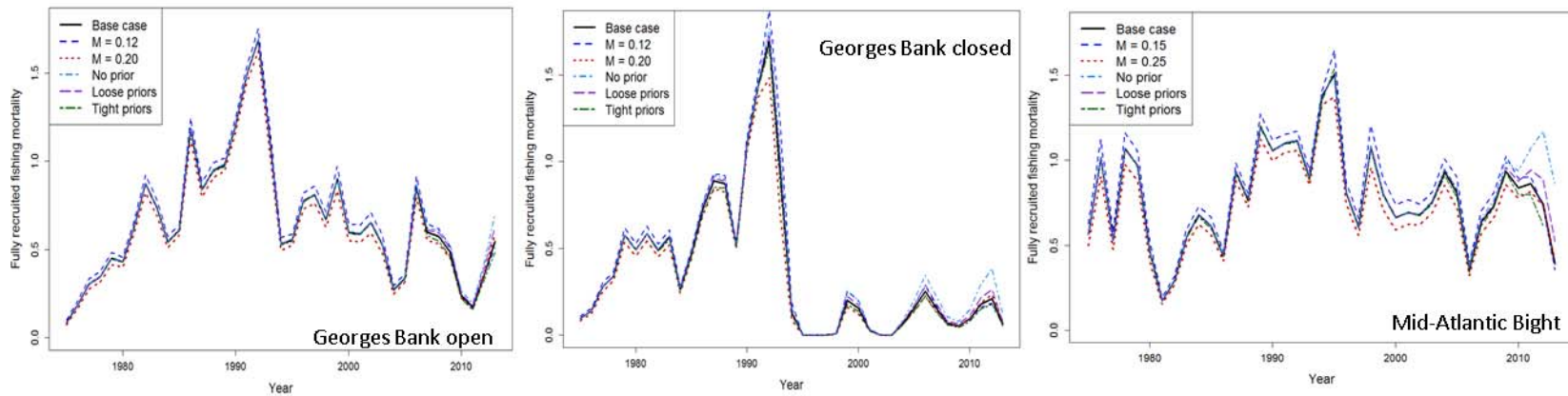


Figure B6.51. Sensitivity of estimated fishing mortality to assumptions regarding natural mortality and survey efficiency priors in CASA models for Georges Bank open (left), Georges Bank closed (middle), and the Mid-Atlantic Bight (right).

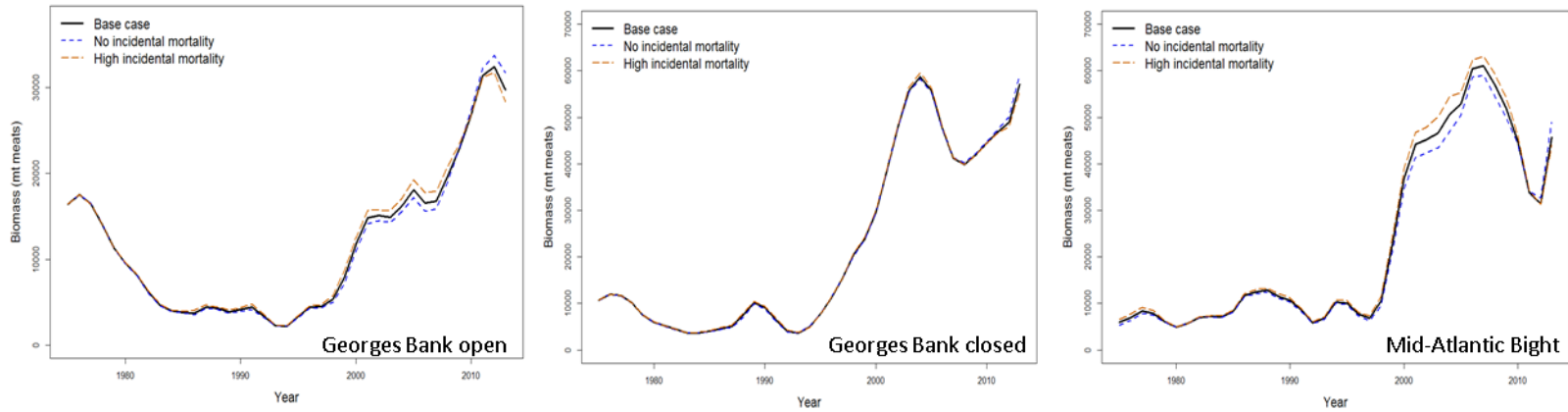
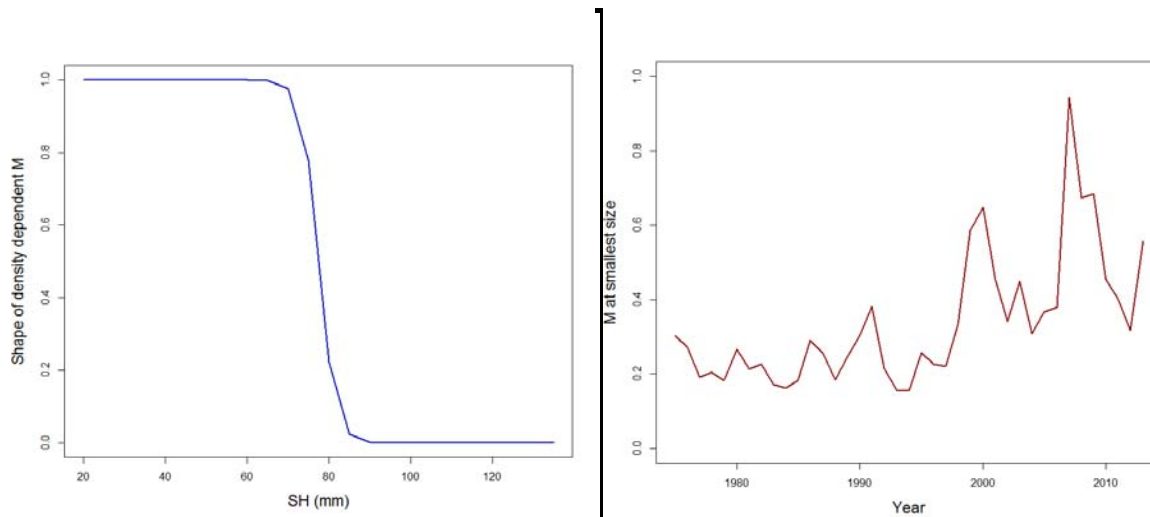


Figure B6.52. Sensitivity of estimated biomass to assumptions regarding incidental fishing mortality in CASA models for Georges Bank open (left), Georges Bank closed (middle), and the Mid-Atlantic Bight (right).



B6.53. (continued). Form of logistic curve used to define juveniles in an experimental model for density-dependent natural mortality in the Georges Bank open area.

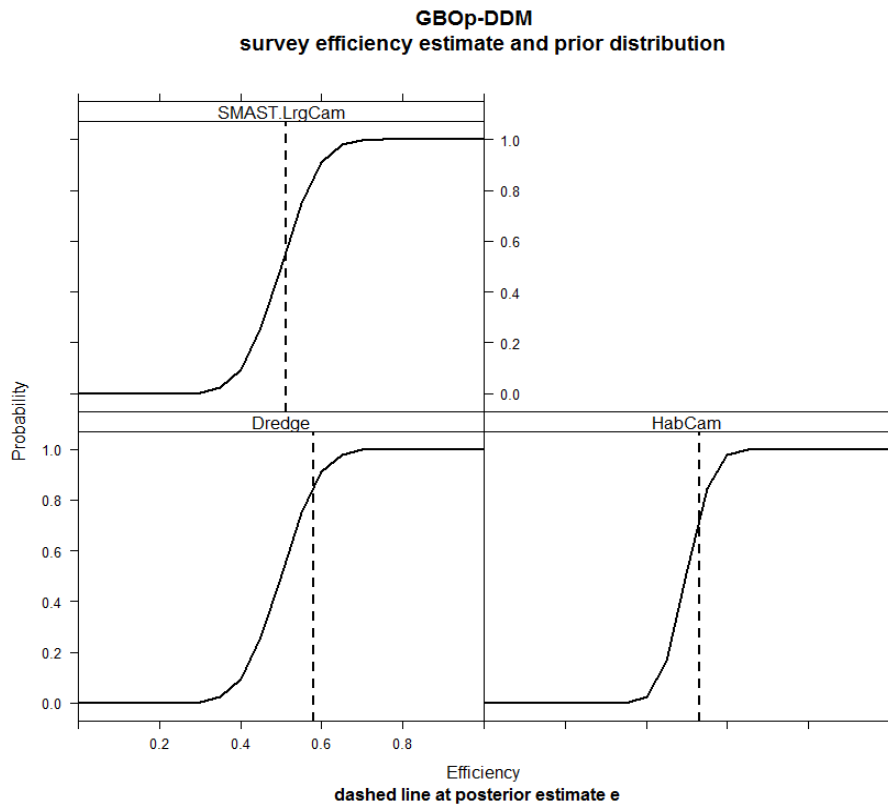


Figure B6.53. Output from experimental density-dependent natural mortality model for Georges Bank open. *Above:* Efficiency priors for three main surveys in an experimental model for density-dependent natural mortality in the Georges Bank open area.

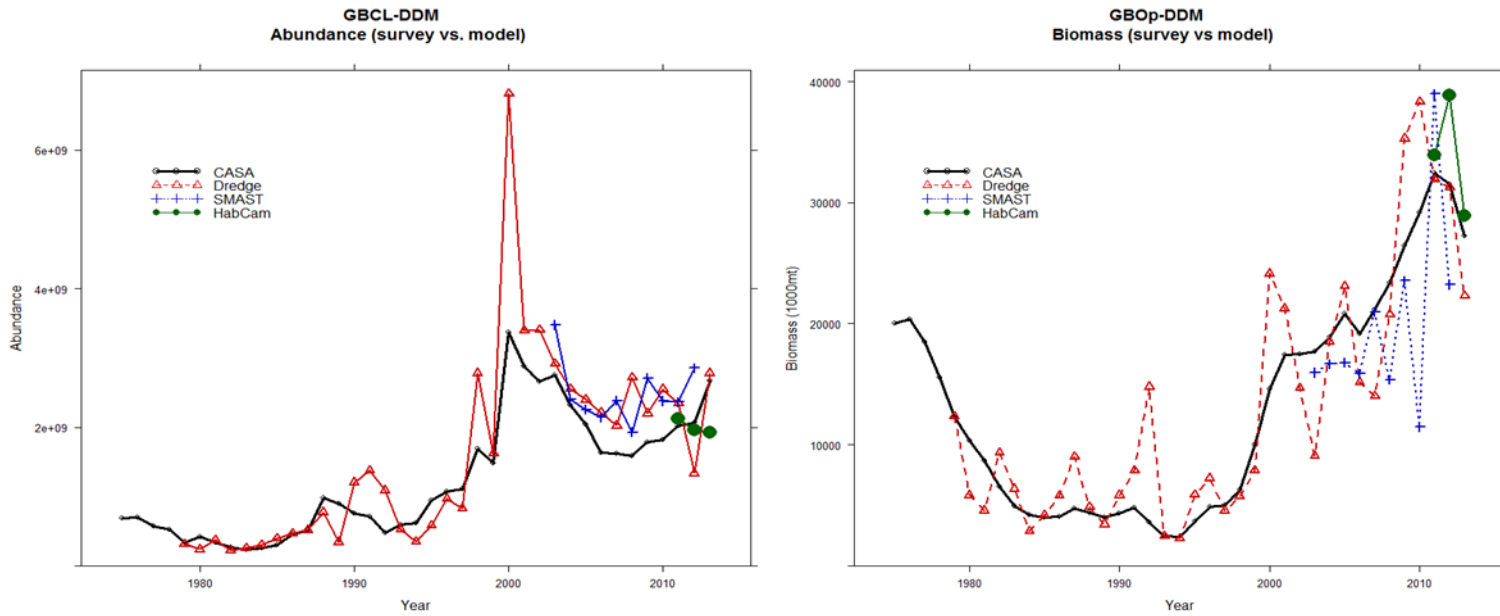


Figure B6.53. (continued). Model estimates of abundance (above) and biomass (below), together with survey stock size estimates from the dredge, SMAST and HabCam surveys in an experimental model for density-dependent natural mortality in the Georges Bank open area.

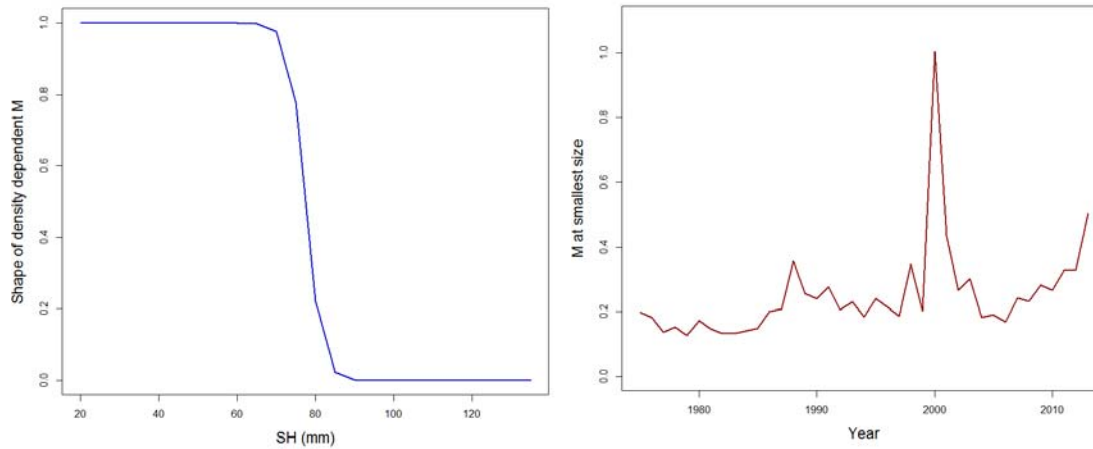


Figure B6.54. Output from experimental density-dependent natural mortality model for Georges Bank open. *Above:* Form of logistic curve used to define juveniles, and estimated natural mortality in the smallest size bin in an experimental model for density-dependent natural mortality in the Georges Bank closed area.

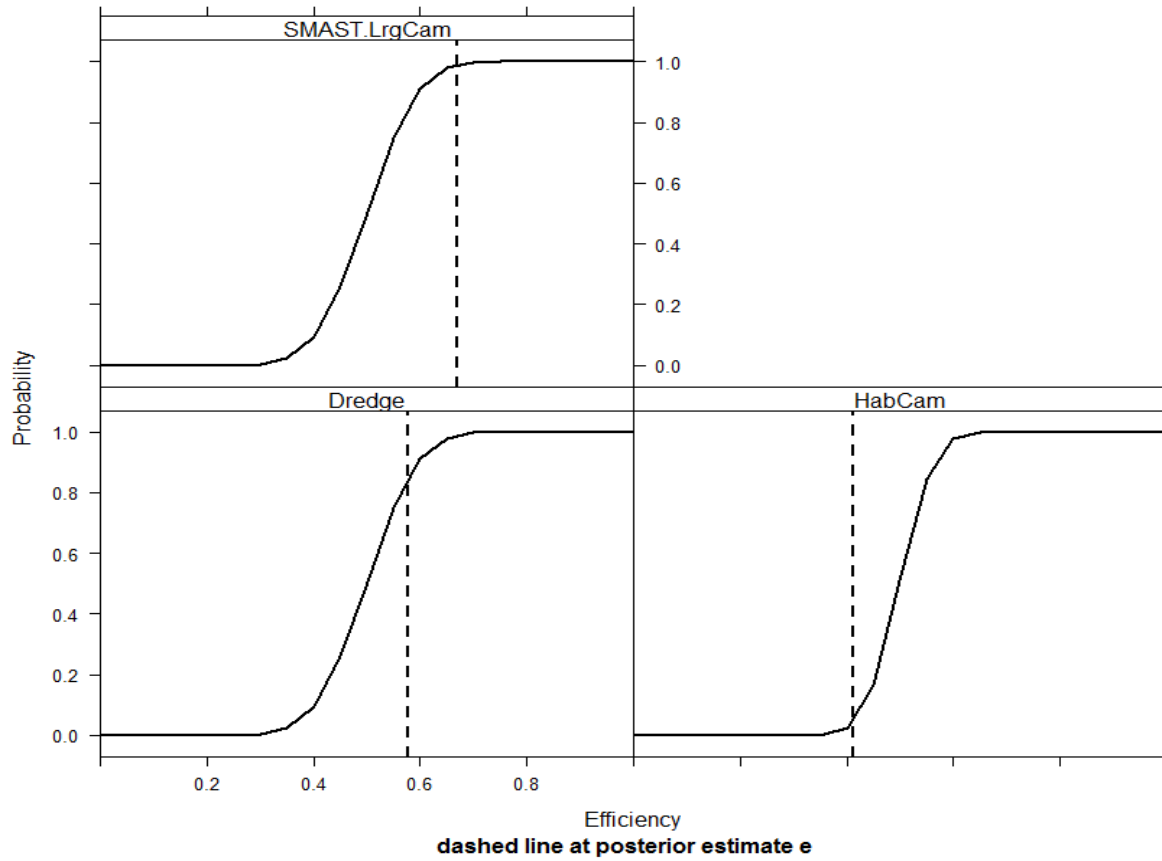


Figure B6.54. (continued). Efficiency priors for three main surveys in an experimental model for density-dependent natural mortality in the Georges Bank open area.

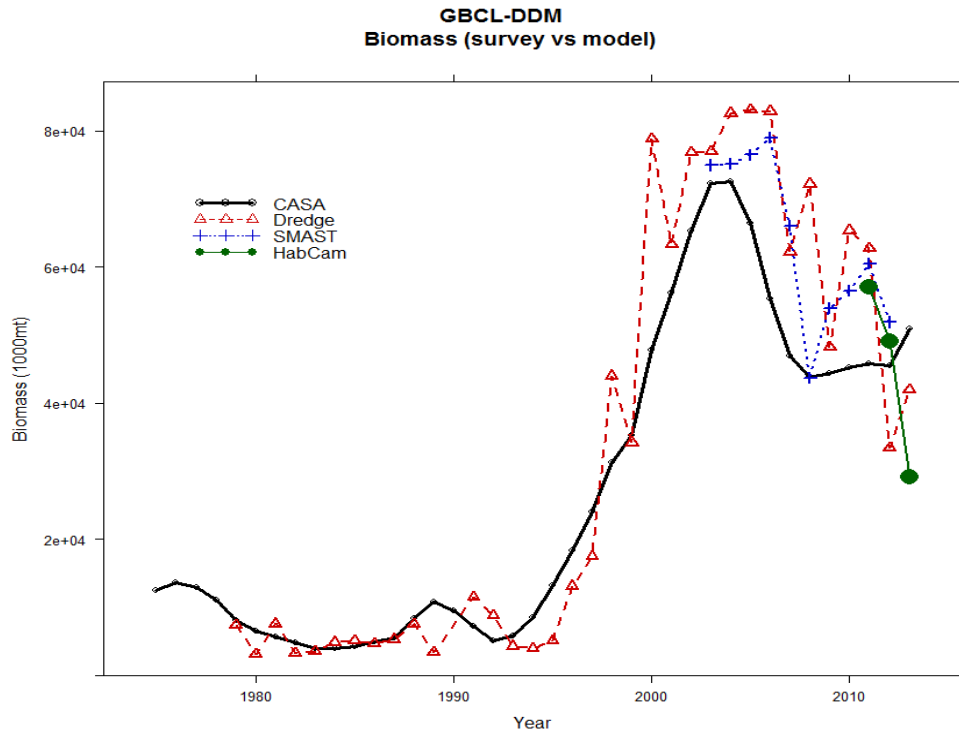


Figure B6.54. (continued). Model estimates of biomass, together with survey stock size estimates from the dredge, SMAST and HabCam surveys in an experimental model for density-dependent natural mortality in the Georges Bank open area.

B7. REFERENCE POINTS (TOR 5)

Per recruit reference points F_{MAX} and B_{MAX} were used as proxies for F_{MSY} and B_{MSY} in assessments prior to 2010 (SARC-50). F_{MAX} is the fishing mortality rate for fully recruited scallops that generates maximum yield-per-recruit. B_{MAX} was defined as the product of BPR_{MAX} (biomass per recruit at $F = F_{MAX}$ from yield-per-recruit analysis) and median numbers of recruits. As selectivity has shifted to larger scallops, yield per recruit curves have become increasingly flat, particularly in the Mid-Atlantic, making per-recruit reference points unstable. Additionally, recruitment has been stronger during the recent period when biomass has been high, suggesting that spawner-recruit relationships should be included. Finally, risk-based reference points are needed to calculate Acceptable Catch Levels/Allowable Biological Catch (ACLs/ABCs) and target fishing mortalities.

To address these issues, the SARC-50 assessment introduced a stochastic model (SYM – Stochastic Yield Model; Hart 2013) for calculating reference points and their uncertainty. It uses Monte-Carlo simulations to propagate the uncertainty in per recruit and stock-recruit calculations while calculating yield curves. B_{MSY} and F_{MSY} reference points are estimated at points where the (trimmed mean) yield curve peaks.

Stochastic yield model

The SYM model combines per-recruit calculations with stock-recruit relationships in order to estimate yield curves, as discussed in Beverton and Holt (1957) and Shepherd (1982). However, the SYM approach treats both the per-recruit and the stock-recruit relationships as being uncertain, and takes this uncertainty into account.

Although the SYM model is separate from CASA, efforts were made to make the two models as compatible as possible. Recruits are initially spread out over 10 size bins (20-70 mm). Growth was modelled using the same stochastic growth matrices used in the CASA model for the most recent period.

Per recruit calculations depend on a number of parameters that each carry a level of uncertainty:

- 1) Shell height/meat weight parameters a and b
- 2) Natural mortality rate M
- 3) Fishery selectivity parameters α and β
- 4) The cull size of the catch and the fraction of discards that survive
- 5) The level of incidental fishing mortality, i.e., non-catch mortality caused by fishing.

Details for each of these parameters are given below.

Shell height/meat weight relationships - Meat weight W at shell height H is calculated using:

$$W = \exp(a + b \ln(H))$$

The means, variances and covariance of parameters a and b were taken from Appendix B3. Similar to the growth parameters, the estimates of a and b have a strong negative correlation. This means that the predicted meat weight at a given shell height carries less uncertainty than it would appear from the variances of the individual parameters. Meat weights vary seasonally, with the greatest meat weights during the late spring and early summer (Appendix B3; Hennen and Hart 2012). However, Haynes (1966) constructed a number of monthly shell height/meat weight relationships, and did not find any significant trend in the slopes indicating that seasonality should not affect the F_{MAX} or F_{MSY} reference point. For this reason, seasonal variability was not considered a source of uncertainty for this analysis.

Natural mortality M - Natural mortality for sea scallops was estimated by Merrill and Posgay (1964) as

$$M = \frac{1}{S} \frac{C}{L} \quad (1)$$

where L is the number of live scallops, S is the mean clapper separation time and C is the number of clappers. Probably the greatest uncertainty in this calculation is the mean separation time S . For example, Dickie (1955) estimated S to be 100 days (14.3 weeks), less than half that estimated by Merrill and Posgay (33 weeks). Reflecting this uncertainty, it was assumed S was distributed as a gamma random variable, with mean set to match the assumed mean natural mortality for each region ($S=20.625$ weeks on Georges Bank and 16.5 weeks in the Mid-Atlantic) and standard deviation 12 weeks. The resulting distribution of M has the desirable characteristic of being skewed to the right. The skew is reasonable because, for example, a natural mortality of $M = 0.3$ is possible, but an $M = 0$, or even close to zero, is not. Note that because S appears in the denominator of the formula above, the expected value of M is not equal to applying equation (1) with the mean value of S .

Fishery selectivity - Fishery selectivity s was estimated using an ascending logistic curve of the form:

$$s = \frac{1}{1 + \exp(\alpha - \beta H)}$$

where H is shell height. The means and covariances of the α and β parameters were taken as estimated by the CASA stock assessment model during the most recent selectivity period. For Georges Bank, we used the open area selectivity in the most recent period, since reference points are calculated under the assumption that all areas are fished. Note that fishery selectivity reflects targeting and discarding as well as gear selectivity.

Cull size and discard mortality - Sea scallops that are caught but are less than 90 mm are assumed to be discarded, based on observer data. Sea scallops likely tolerate discarding fairly well, provided they are returned to the water relatively promptly and they are not damaged by the capture process or their time on deck. Here, discard mortality was simulated as a gamma distribution, with a mean of 0.2 and a standard deviation of 0.15, reflecting the high uncertainty in this parameter. This feature is also included in the SAMS projection model but not in the CASA model.

Incidental fishing mortality - Incidental fishing mortality occurs when scallops are killed but not captured by the gear. Consistent with the assumptions of the CASA model, incidental mortality F_I was estimated as 0.2 on Georges Bank and 0.1 in the Mid-Atlantic for the smallest size group. Because of the considerable uncertainty in these numbers, incidental mortality was simulated here with a gamma distribution with these means and coefficients of variation of 0.75.

Stock-recruit relationships - Beverton-Holt stock-recruit curves were fitted to spawning stock and recruitment estimates from basecase CASA model runs:

$$R = \frac{sB}{\gamma + B},$$

assuming square-root-normal errors (Figure B7.1). Here R is recruitment, B is spawning stock biomass (or egg production), and s and γ are parameters, representing the asymptotic recruitment when B is large, and the spawning stock biomass where the expected recruitment is half its asymptotic value, respectively. Standard errors of the stock-recruit parameters and their correlation were estimated using the delta method.

Calculation of equilibrium yield per recruit and yield

At each iteration of the simulation model, parameter values were drawn from their corresponding distribution and per recruit and yield curves were calculated. This was repeated $n = 100,000$ times and the results of each iteration were stored. The stock-recruit parameters were simulated as correlated square-root normals (chi-squared with 1 df).

For each run, equilibrium recruitment at fishing mortality F is given by

$$R = s - \gamma/b(F)$$

where b is biomass per recruit. Total yield is therefore

$$Y(F) = y(F)R = y(F)[(s - \gamma)/b(F)]$$

where y is yield per recruit.

Although simulation results in this assessment were stable, mean yield curves calculated by this method can be disproportionately influenced by outliers (Hart 2013). For this reason, a 10% trimmed mean was used to obtain the central tendency of per recruit and yield curves as a function of fishing mortality. The probabilistic F_{MSY} (and F_{MAX}) were taken as the fishing mortality that maximizes the trimmed mean yield curve (yield per recruit curve). The probabilistic MSY and B_{MSY} are the trimmed mean yield and biomass at F_{MSY} over all runs.

Results

Stock-recruit curves were better defined on Georges Bank than in the Mid-Atlantic (Figure B7.1). While Y_{MAX} and B_{MAX} values were generally well defined, F_{MAX} was highly uncertain in both regions, and hit the $F = 1$ bound in a majority of the simulations in the Mid-Atlantic (Figures B7.2 to B7.4). MSY based reference points were better defined, as potential stock-recruit relationships tend to reduce F_{MSY} to well below F_{MAX} (Figures B7.5 and B7.7).

MSY estimates for the combined Georges Bank and Mid-Atlantic areas range from 10,000 mt to 40,000 mt meats, and B_{MSY} between about 40,000 to 150,000 mt (Figures B7.8 to B7.10). F_{MSY} values for the combined stock are highly uncertain.

Trimmed mean yield curves have a maximum at $F_{MSY} = 0.3$ on Georges Bank, and $F_{MSY} = 0.74$ in the Mid-Atlantic, with corresponding MSY values of 9,148 and 15,737 mt meats, respectively (Table B7.1, Figure B7.11). Trimmed mean estimates for the combined stock are $F = 0.48$, $MSY = 23,798$ mt, and $B_{MSY} = 96,480$ mt. The entire distribution of yield for the combined stock is shown in Figure B7-12).

Special considerations for sedentary resources under area management

The above reference point calculations are based on the assumption that fishing mortality risk does not vary among individuals. For sedentary organisms such as sea scallops, these assumptions are never even approximately true. With closed and rotational area management, the assumption of uniform fishing mortality is strongly violated (Hart 2001, 2003; Smith and Rago 2004). In such situations, mean yield-per-recruit, averaged over all recruits, may be different than yield-per-recruit obtained by a conventional per-recruit calculation performed on a recruit that suffers the mean fishing mortality risk (Hart 2001). In these types of situations, estimates of fishing mortality may be biased low, because individuals with low mortality risk are overrepresented in the population (Hart 2001, 2003).

Reference point	SARC-50	SARC-59
F_{MSY}	0.38	0.48
$B_{TARGET}=B_{MSY}$ (mt, meats)	125,358	96,480
$B_{THRESHOLD}=1/2 B_{MSY}$ (mt, meats)	62,679	48,240
MSY (mt, meats)	24,975	23,798

Table B7-1. Previous (SARC-50) and revised (SARC-59) reference points for sea scallops.

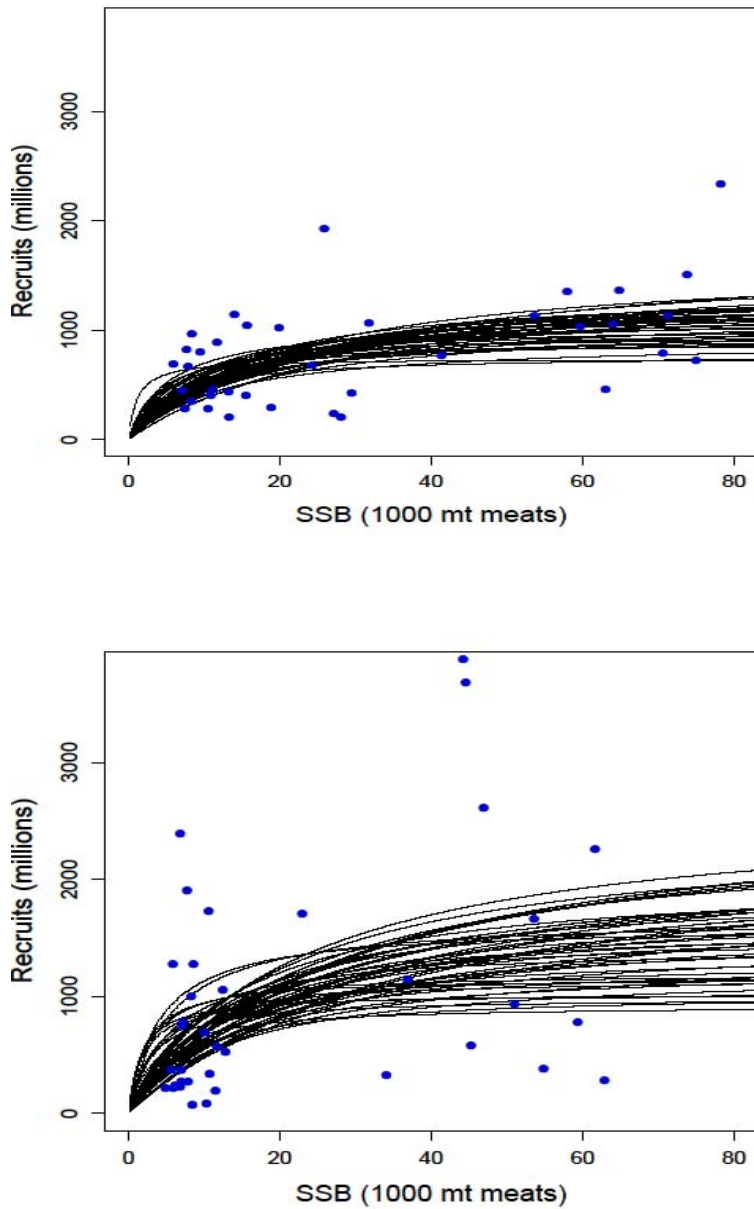


Figure B7.1 Stock-recruit relationships for Georges Bank (top) and the Mid-Atlantic (bottom) showing spawner-recruit estimates from the CASA model (blue dots) and 50 example fitted Beverton-Holt curves.

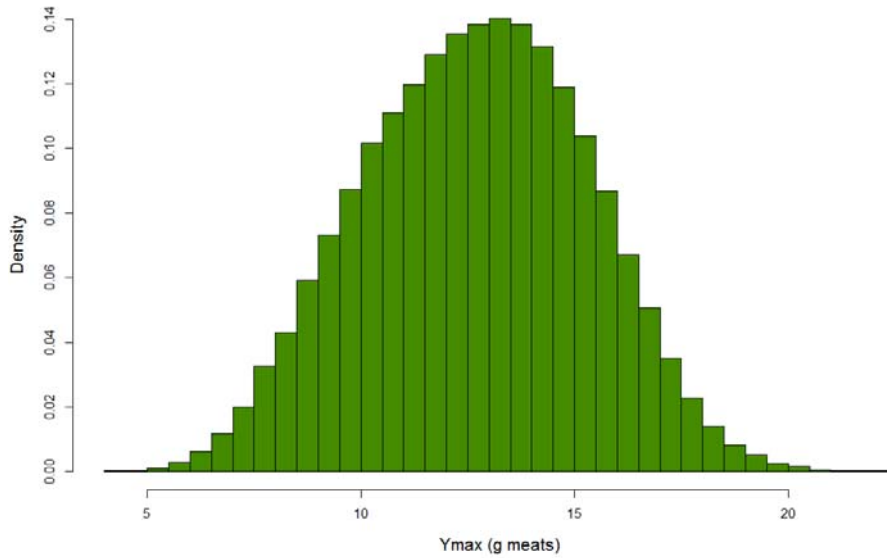
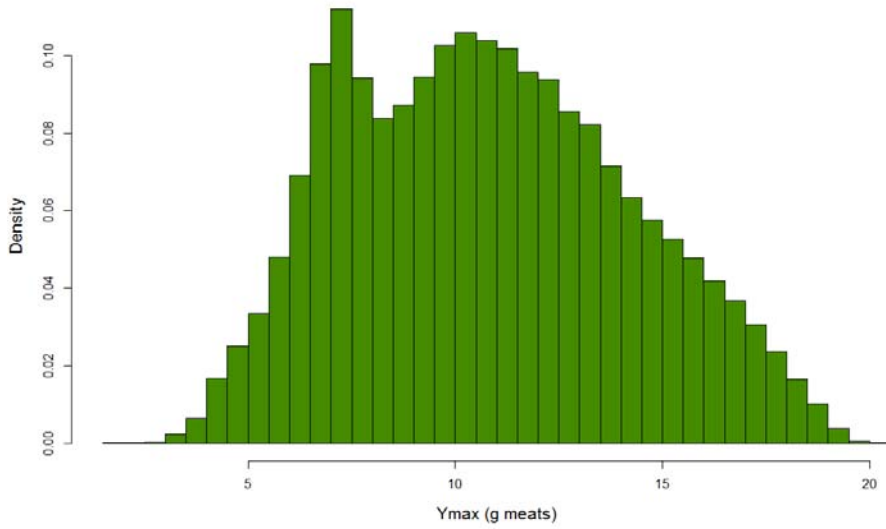


Figure B7.2. Probability distributions for maximum yield per recruit Y_{\max} in the Georges Bank (top) and Mid-Atlantic (bottom) regions.

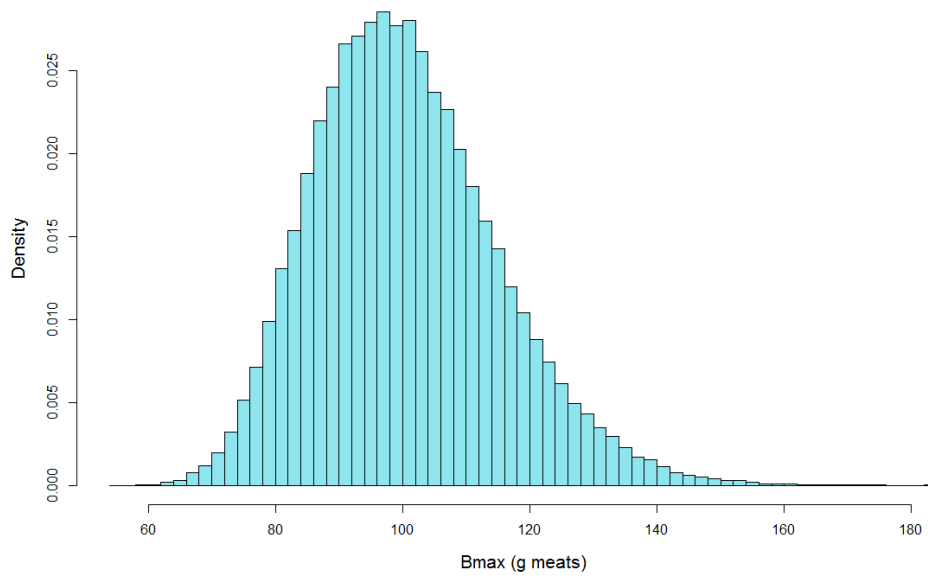
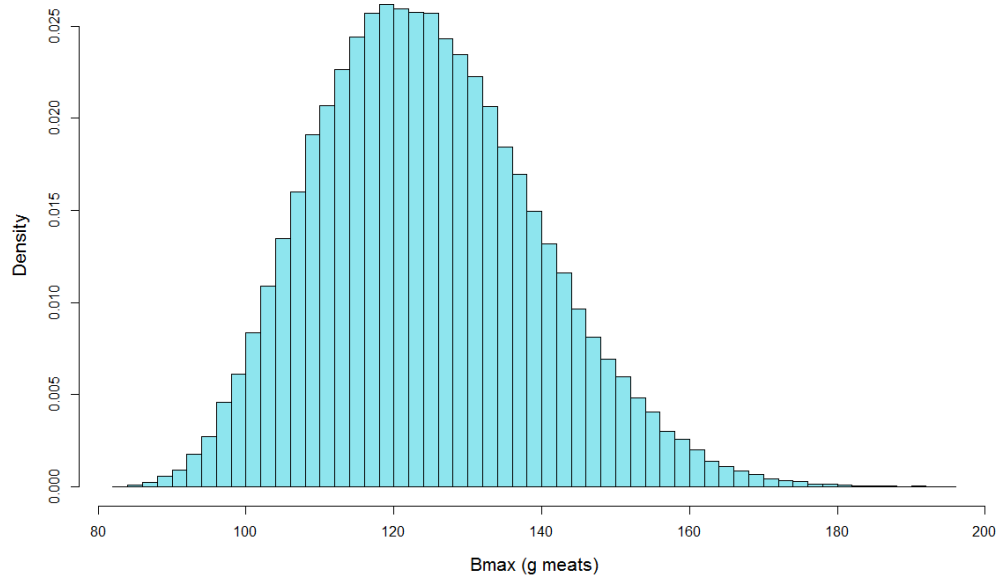


Figure B7.3. Probability distributions for biomass per recruit at B_{max} in the Georges Bank (top) and the Mid-Atlantic (bottom) regions.

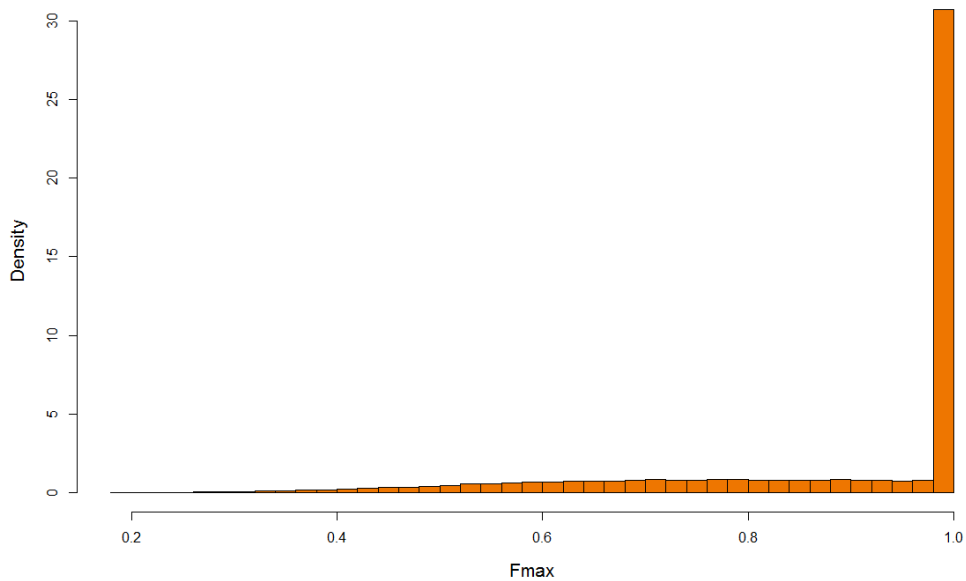
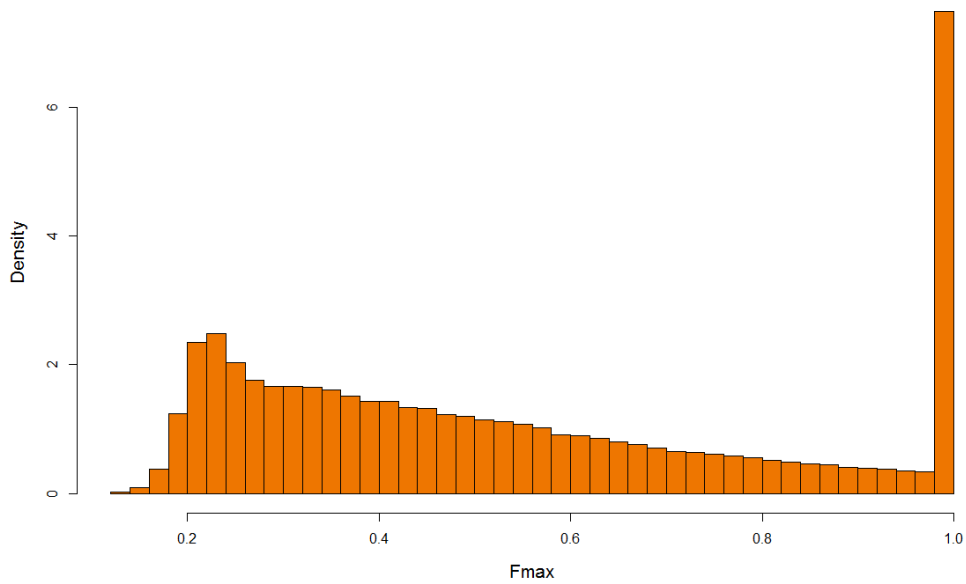


Figure B7.4. Probability distributions for the fishing mortality that gives maximum yield per recruit (F_{max}) in the Georges Bank (top) and Mid-Atlantic Bight (bottom) regions.

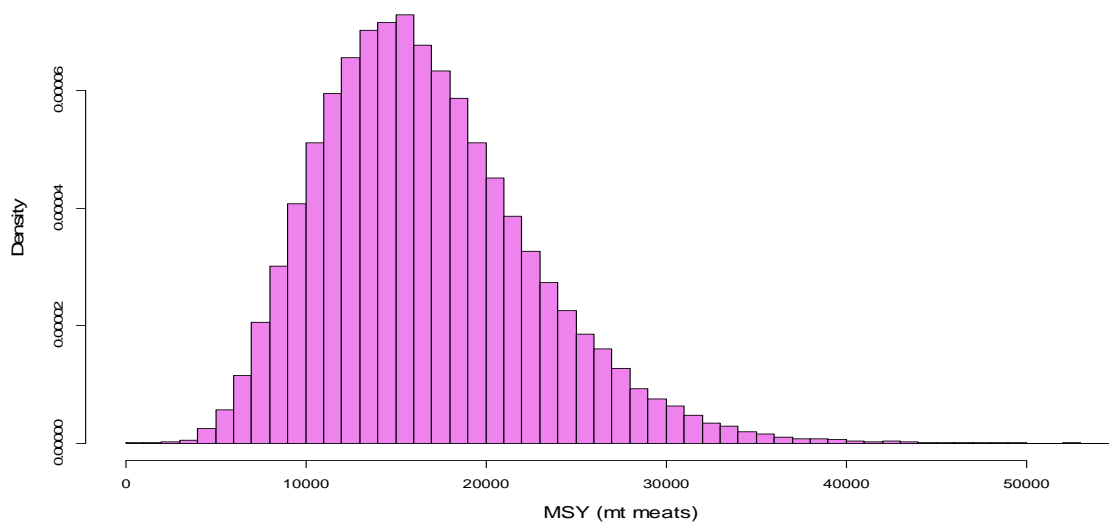
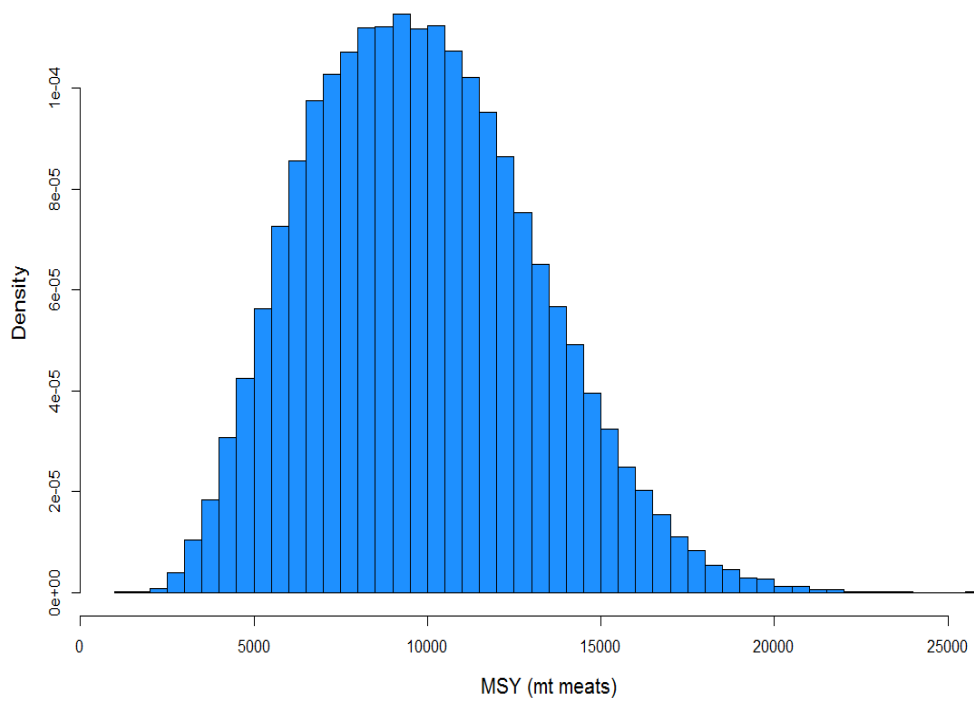


Figure B7.5. Probability distributions for MSY in the Georges Bank (top) and Mid-Atlantic (bottom) regions.

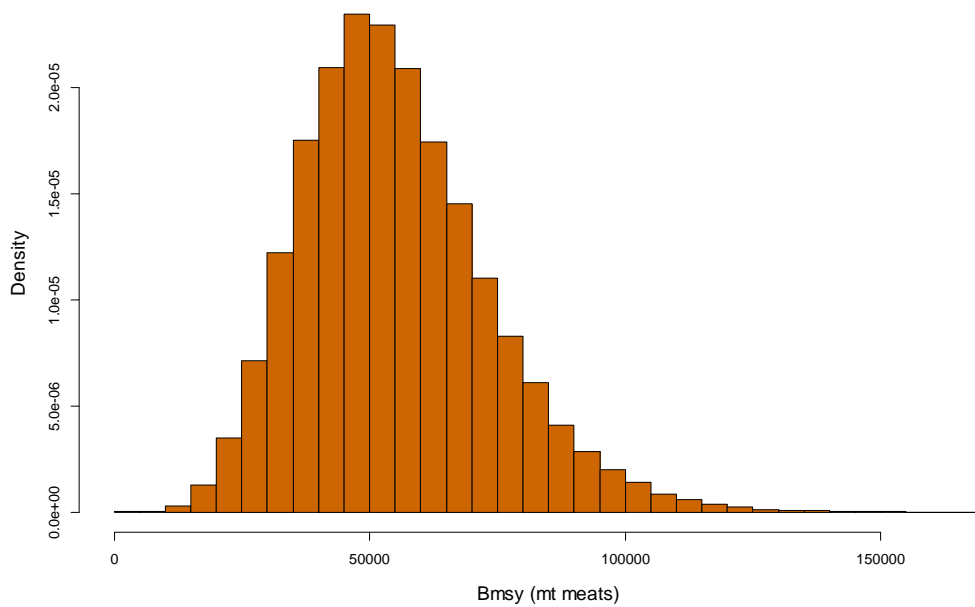
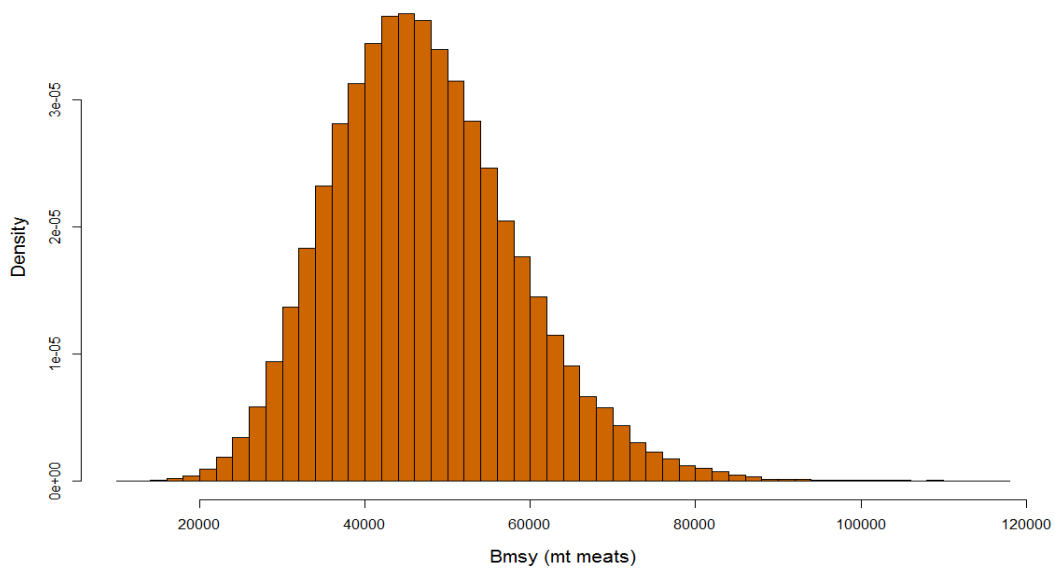


Figure B7.6. Probability distributions for B_{MSY} in the Georges Bank (top) and Mid-Atlantic (bottom) regions.

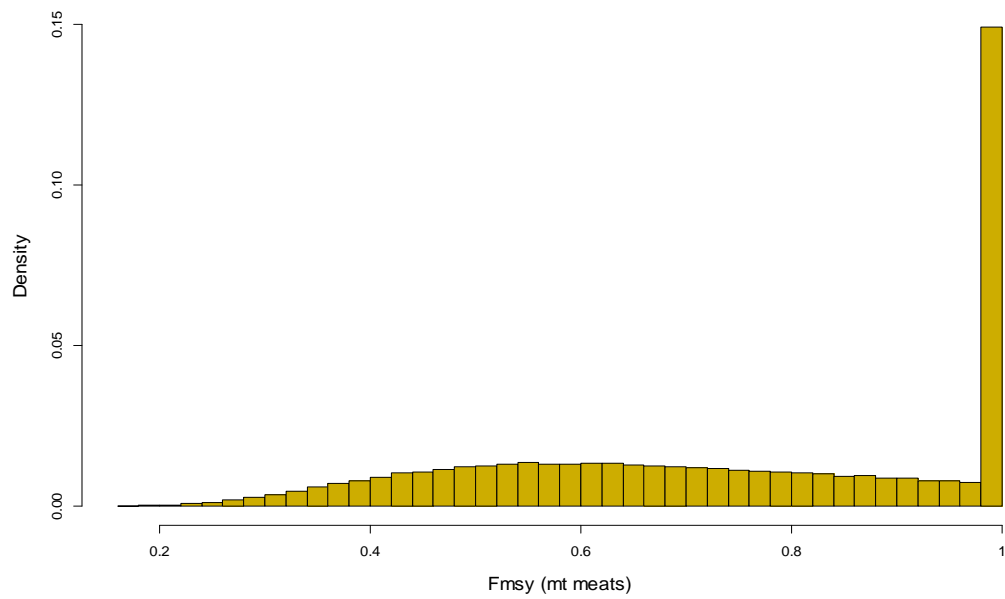
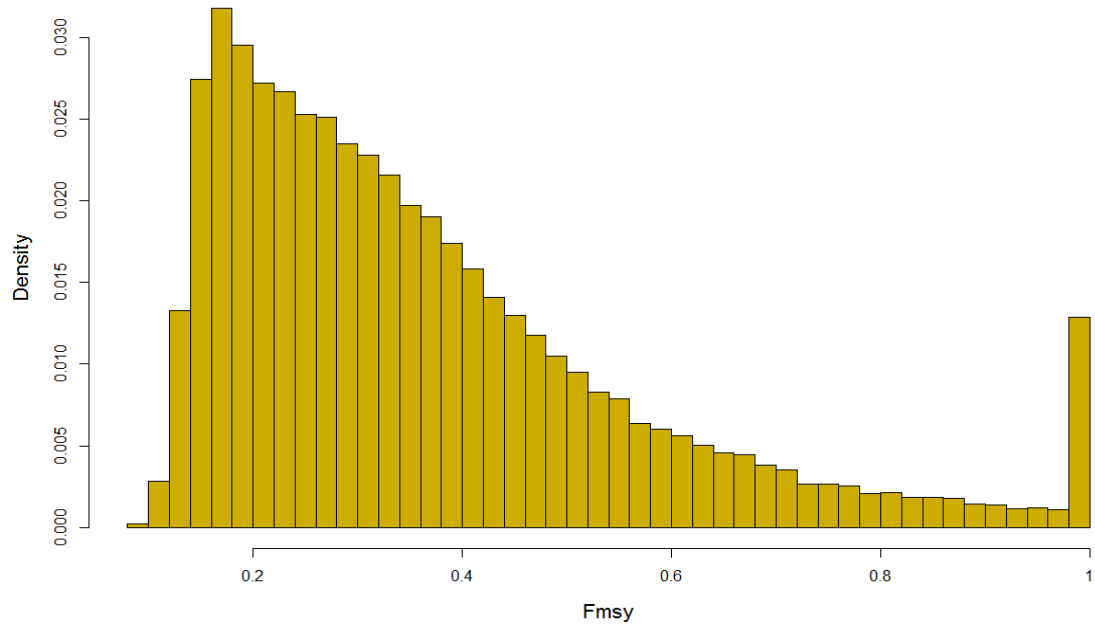


Figure B7.7 Probability distributions for F_{msy} in the Georges Bank (top) and Mid-Atlantic (bottom) regions.

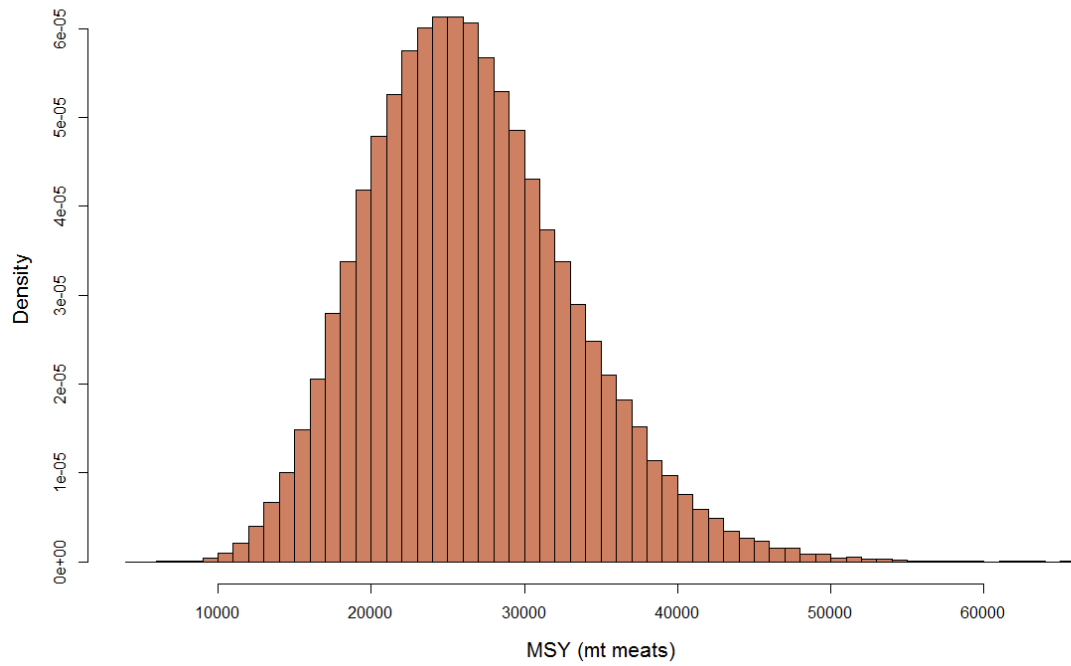


Figure B7.8. Probability distribution for MSY in the combined Georges Bank and Mid-Atlantic region.

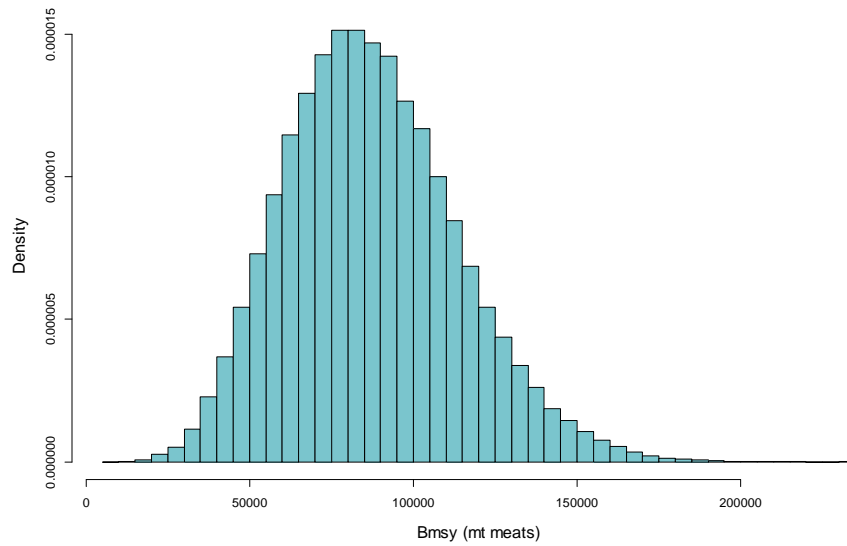


Figure B7.9. Probability distribution for B_{MSY} in the combined Georges Bank and the Mid-Atlantic region.

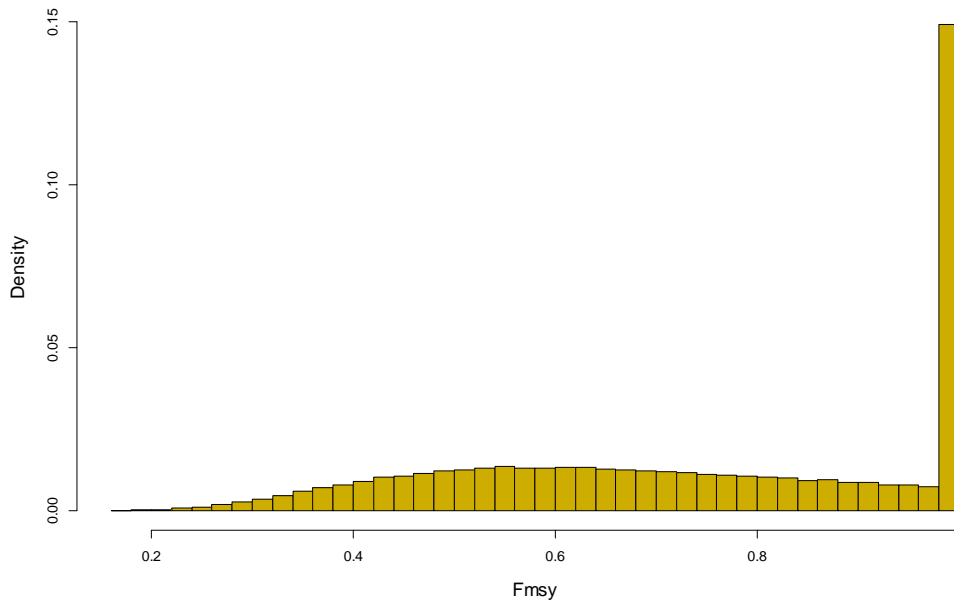


Figure B7.10. Probability distribution for F_{MSY} in the combined Georges Bank and the Mid-Atlantic region.

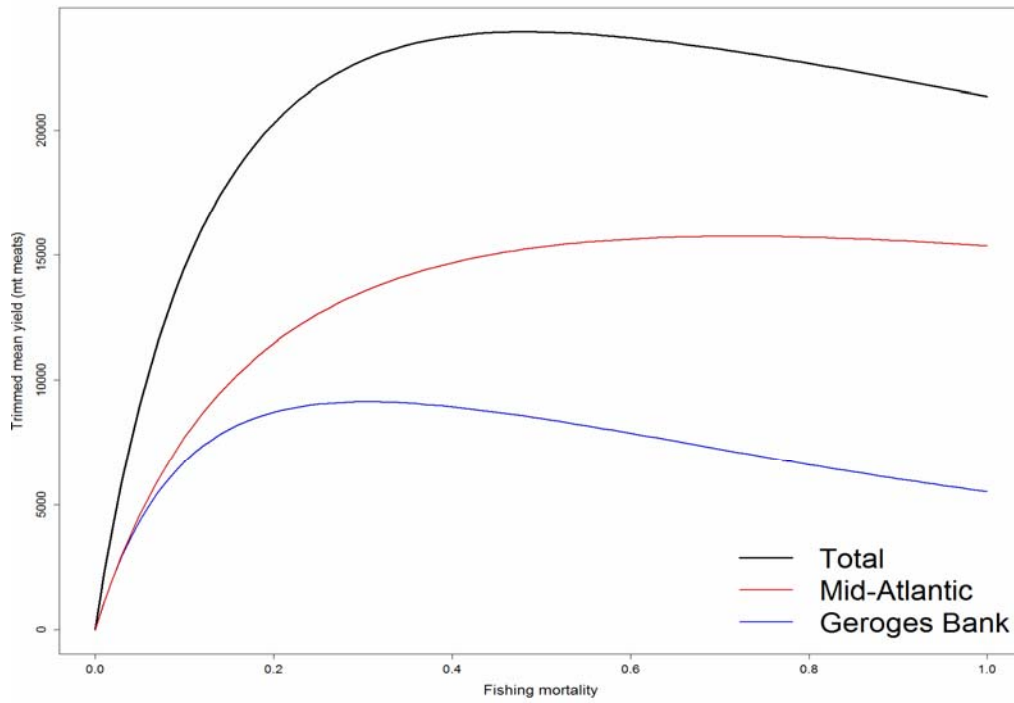


Figure B7.11. Trimmed mean yield as a function of fishing mortality for Georges Bank, the Mid-Atlantic, and combined areas.

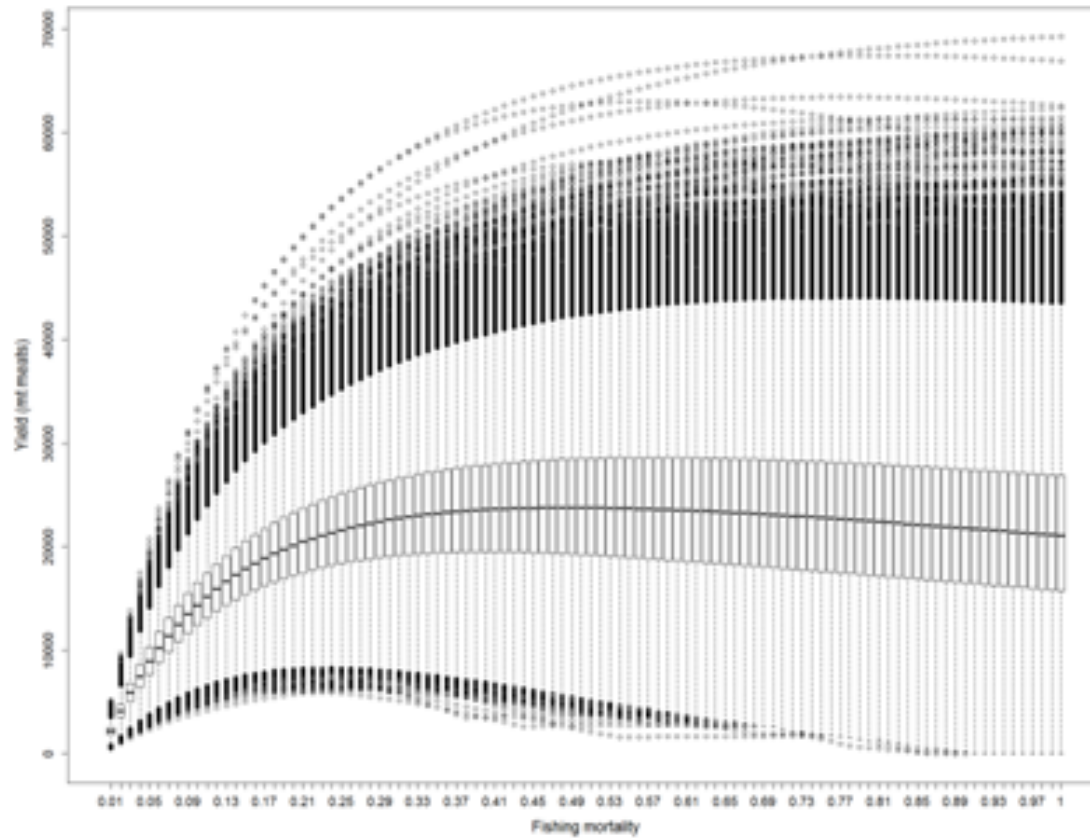


Figure B7.12. Boxplots for yield in the combined Georges Bank and Mid-Atlantic region as a function of fishing mortality.

B8 - Status Determination (TOR 6)

According to the Amendment 10 overfishing definition (NEFMC 2003), sea scallops are overfished when the survey biomass index for the whole stock falls below $1/2 B_{TARGET}$, with B_{TARGET} set equal to B_{MSY} or its proxy (see table below). The current $B_{THRESHOLD}$ is 62,679 mt (NEFSC 2010) and the recommended value in this assessment is 48,240 mt. The estimated combined stock biomass in 2013 was 132,561 mt, which is above both $B_{THRESHOLD}$ reference point values. Thus, the stock is not overfished based on either criterion.

None of the 100,000 simulations done for the SYM model estimated a B_{MSY} that was greater than twice the CASA estimated 2013 biomass. The standard error in the 2013 CASA biomass was estimated at 5772 mt, which is likely underestimates the uncertainty. However, given that both surveys estimated biomasses over 110,000 mt in 2013, it is highly likely that the actual biomass in 2013 was above 100,000 mt. Because less than 1% of the SYM runs estimated a B_{MSY} greater than 200,000 mt, it can be concluded that the chances that the stock is overfished is very small, probably less than 1% (Figure B8.1).

The current $F_{MSY} = 0.38$ (NEFSC 2010) and the recommended F_{MSY} in this assessment is 0.48. The estimated fishing mortality for the whole stock in 2013 was 0.32, which is below both F_{MSY} reference points. Therefore, overfishing was not occurring in 2013 based on either criterion.

Based on SYM model results, there is about a 12% chance that F_{MSY} is below 0.32. The standard error for fishing mortality in 2013 was 0.03 from the CASA model. Combining these results indicate that the probability of overfishing in 2013 was about 13% (Figure B8.1). This probability of overfishing is likely understated because CASA is probably underestimating uncertainty.

Type	2013 stock estimate	Reference point	NEFSC (2010)		Recommended this assessment	
			BRP	Overfished, overfishing?	BRP	Overfished, overfishing?
Biomass (mt)	132,561	$B_{target}=B_{MSY}$	125,358	No	96,480	No
		$B_{Threshold}=B_{Target}/2$	62,679		48,240	
Fishing mortality	0.32	F_{MSY}	0.38	No	0.48	No

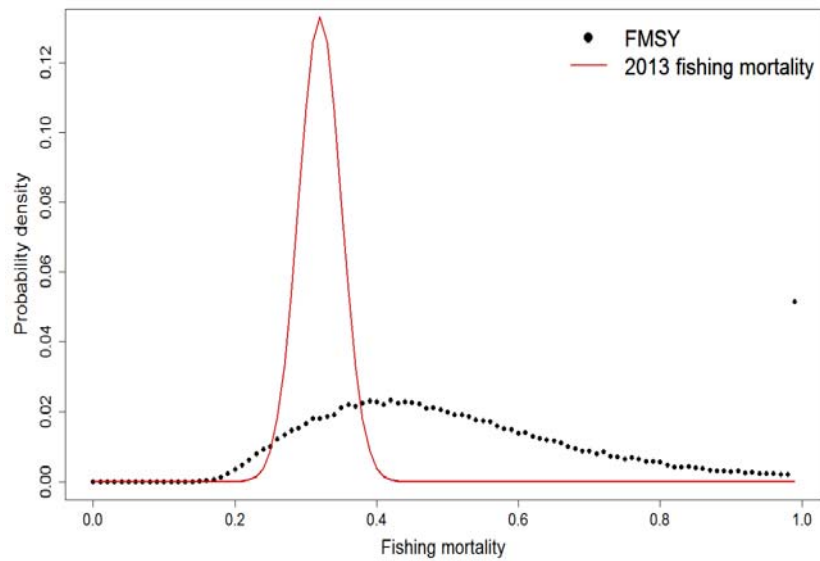
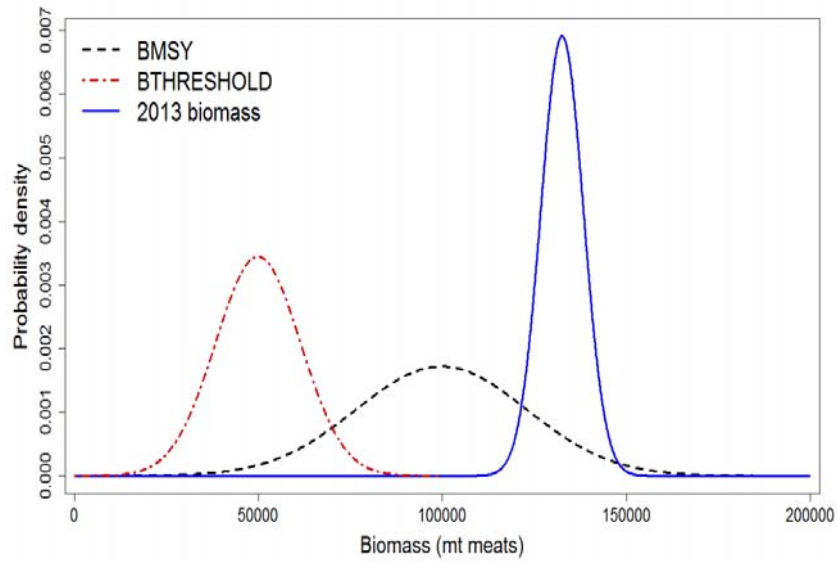


Figure B8.1. *Top*: Probability distributions for B_{MSY} , $B_{THRESHOLD}$ and 2013 biomass. *Bottom*: Probability distributions of F_{MSY} and 2013 fishing mortality.

B9 STOCK PROJECTIONS (TOR 7)

Because of the sedentary nature of sea scallops, fishing mortality can vary considerably in space even in the absence of area specific management (Hart 2001). Rotational management and long-term closures exacerbate this heterogeneity. Projections that ignore spatial variation can be unrealistic and misleading. For example, suppose 80% of the stock biomass is in areas closed to fishing (as occurred in some years in Georges Bank). A stock projection that ignored the closure and assumed an overall F of 0.2 would forecast landings nearly equal to the entire stock biomass in the areas open to fishing. Thus, using a non-spatial forecasting model could lead to unsustainable harvest levels under area management. For these reasons, a spatial forecasting model (the Scallop Area Management Simulator, SAMS) was developed for use in sea scallop management (Appendix B10). Various versions of SAMS have been used since 1999.

Growth is modeled in SAMS and CASA in a similar manner, except that each subarea of Georges Bank and the Mid-Atlantic in SAMS has its own stochastic growth transition matrix derived from the shell increments collected in that area. Mortality and recruitment are also area-specific. Fishing mortality can either be explicitly specified in each area, or calculated using a simple fleet dynamics model that assumes fishing effort is proportional to estimated LPUE.

Projected recruitment is modeled stochastically with the log-transformed mean and covariance for recruitment in each area matching that observed in NEFSC dredge survey time series. In the example projection shown here, initial conditions are based on regional shell height data from the 2013 dredge surveys, with mean regional biomass (Georges Bank open and closed, and Mid-Atlantic) set to match CASA estimates for 2013. Initial values in each subarea are varied according to specified uncertainties. Natural mortality for each run is selected from the same distributions used in the SYM reference point model. Further details regarding the SAMS model are given in Appendix B10.

One set of example runs are used in this assessment to demonstrate of the utility of the SAMS model. Projections used to manage the fishery are carried out by the Scallop Plan Development Team while evaluating potential management measures. For example, SAMS runs for management in 2015-2016 will be updated with 2014 survey data in the fall of 2014 after this assessment is complete.

Example SAMS runs

For the example simulations, the stock area was split into 16 subareas (Figure B3-1), seven in the Mid-Atlantic (Virginia Beach, Delmarva, Elephant Trunk, Hudson Canyon South, New York Bight, Long Island, and New York Bight inshore) and ten on Georges Bank (Closed Area I, II and Nantucket Lightship EFH closures, Closed Area I, II and Nantucket Lightship access areas, Great South Channel proposed closure and the remainder of the Great South Channel, Northern Edge and Peak, and Southeast Part).

The EFH (Essential Fish Habitat) closures on Georges Bank were assumed to be closed for the duration of the simulations. The Georges Bank access areas were assumed to be fished on a rotating basis corresponding to actual management in 2013-2014, and probable management in

2015 (Closed Area I is fished in 2013, 2016, 2017, Closed Area II in 2013, 2014, 2016 and 2017, Nantucket Lightship in 2013, 2014, 2016, and 2017). The Hudson Canyon South rotational closure area was assumed to be fished in 2013, closed in 2014-2015, and fished 2016-2017. The Elephant Trunk rotational area was assumed closed in 2013-2014, and fished in 2015-2017. Delmarva was closed in 2013 and fished in 2014-2017. All other areas (Virginia Beach, New York Bight, Long Island, South Channel, Northern Edge and Peak, Southeast Part) were part of the open areas, where scallop fishermen may chose where to fish, subject to a day at sea limit. These days at sea limits were set at 33 days in 2013, 31 days in 2014, and the number of days that will result in an open area $F=F_{MSY} = 0.48$ in 2015-2017. The effort distribution in the open areas was assumed proportional to projected catch rates.

A total of $n=1000$ projection runs were performed in this example with stochastic initial conditions, recruitment, and natural mortality. Example result indicate that projected mean biomass in both regions would increase modestly from 2013-2016 (Figure B9.1). Fishing mortality is projected to increase in the Mid-Atlantic, primarily due to reopening of the Elephant Trunk and Hudson Canyon South rotational areas. Fishing mortality is expected to be fairly steady and low on Georges Bank. Landings are expected to rise from about 17,000 mt in 2014 to 23,000 mt in 2017, due to reopening rotational areas. While there is some uncertainty in projected biomass, fishing mortality and landings (Figure B9.2), the example projections indicate almost no chance of either overfishing or the stock becoming overfished in the near future under the assumed management conditions. Results from the SAMS model include projected biomass for each management area as well as for the Georges Bank and Mid-Atlantic and combined areas (Figure B9.3).

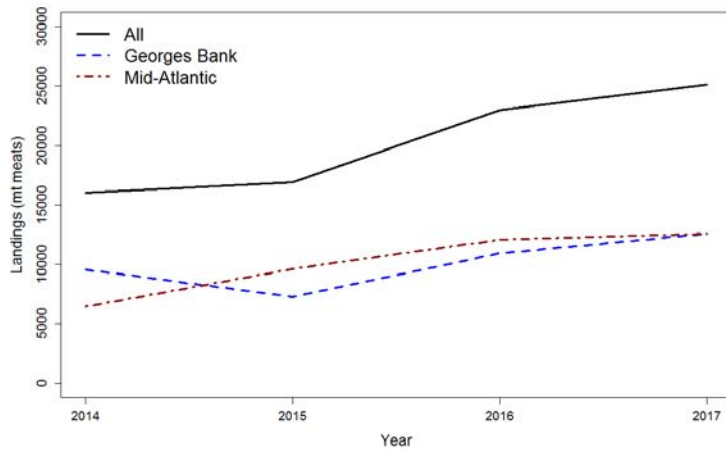
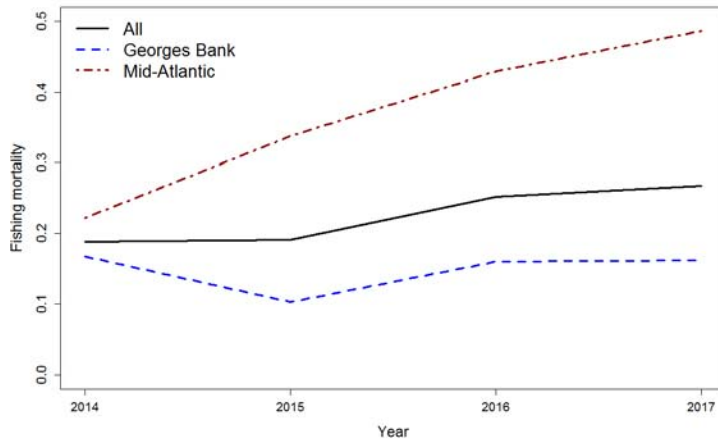
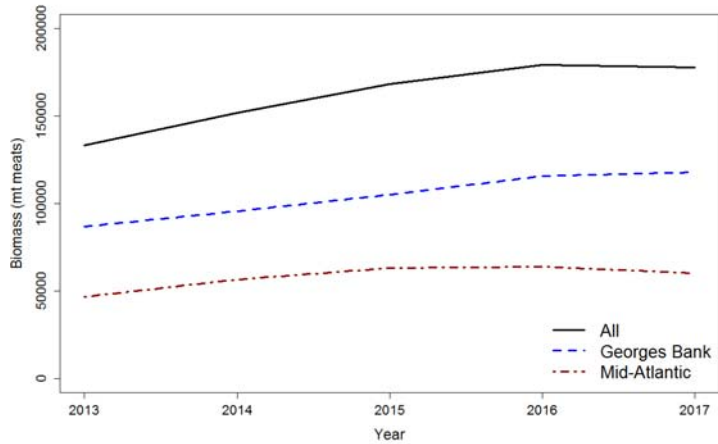


Figure B9.1. Mean projected biomass (top), fishing mortality (middle), and landings (bottom) for sea scallops in the Georges Bank, Mid-Atlantic and combined regions based on an example projection analysis with the SAMS model.

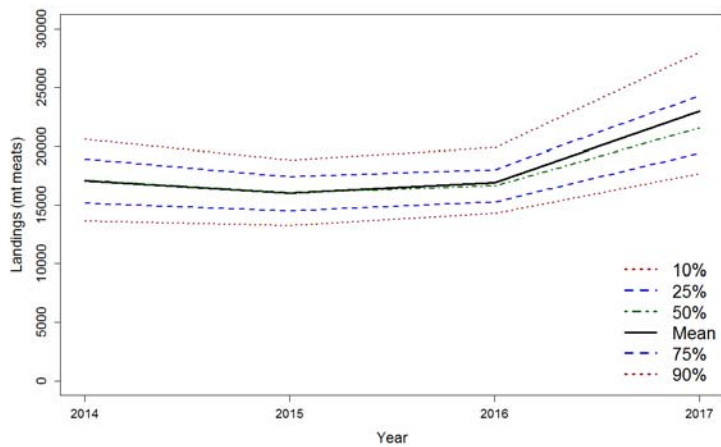
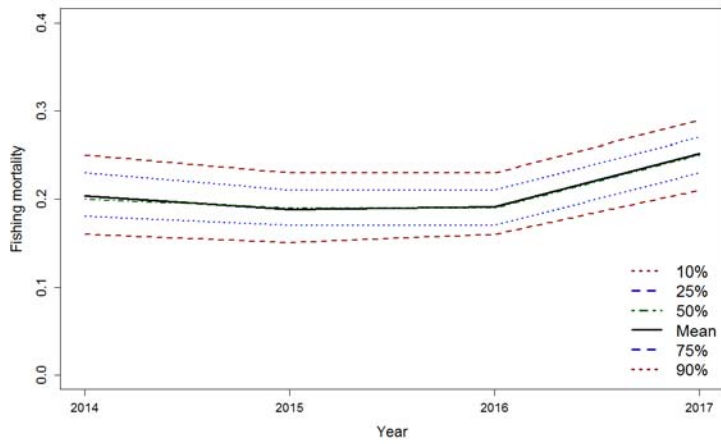
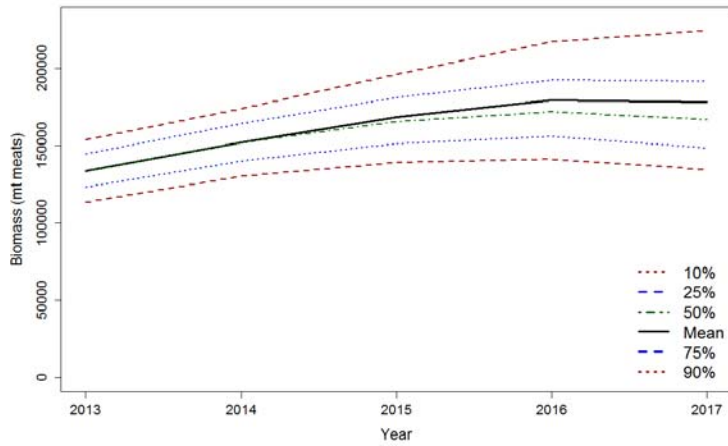


Figure B9.2. Mean and 10th, 25th, 50th, 75th, and 90th percentiles of projected total biomass (top), fishing mortality (middle) and landings (bottom).

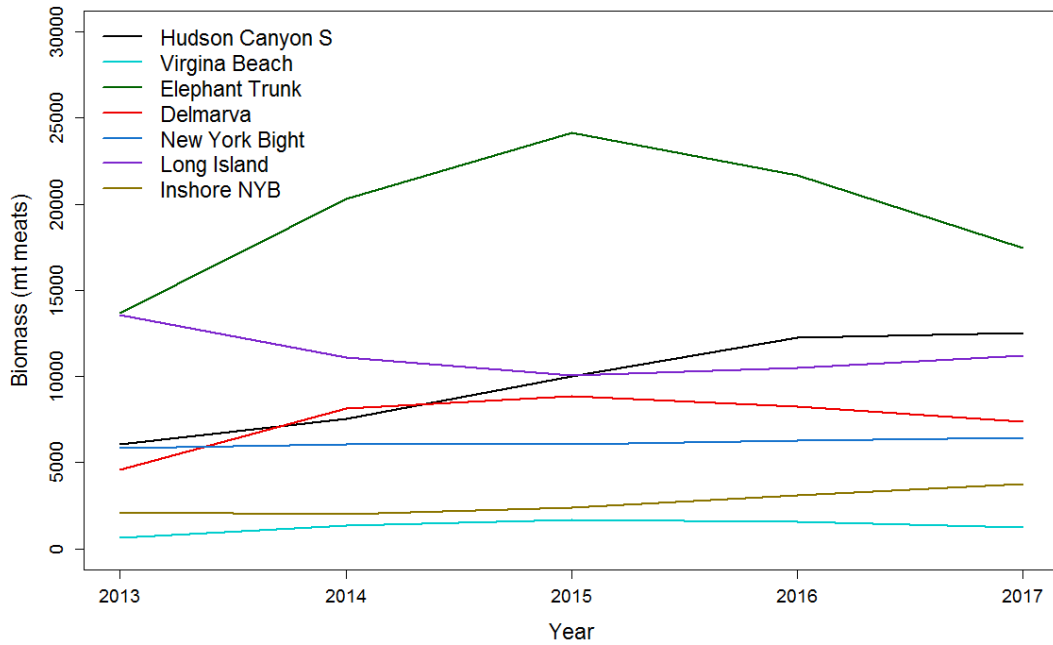
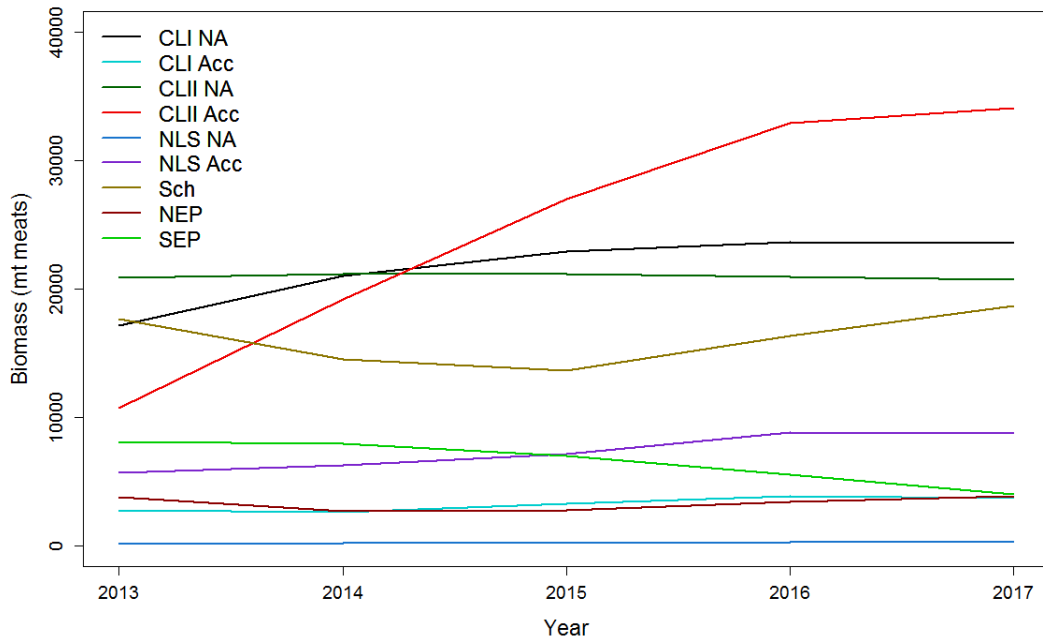


Figure B9.3 Mean projected biomass by subarea in the Georges Bank (top) and Mid-Atlantic (bottom) regions.

B10 – ENVIRONMENTAL EFFECTS ON RECRUITMENT (TOR 3)

Two potential environmental drivers of recruitment were explored: food supply (phytoplankton), and the abundance of a major predator of small scallops, the sea star *Astropecten americanus*. A tentative relationship was found between chlorophyll and scallop recruitment in the Mid-Atlantic Bight. Negative relationships were found between the spatio-temporal abundance of *A. americanus* and scallop recruitment. Both these topics are discussed in Appendix B8.

B11 - RESEARCH RECOMMENDATIONS (TOR 8)

Progress on recommendations from SARC-50 (NEFSC 2010)

1. Look into a way to fit discarded scallops, which have a different length frequency from the rest of the population, into the model. *No progress.*
2. Evaluate the effect of the four-inch rings on incidental mortality. Now that a larger fraction of small scallops are traveling through the mesh, has incidental mortality increased or are the scallops relatively unscathed? *Incidental mortality calculations were improved for this assessment to account for fishery selectivity. Several field projects were funded in 2014 to investigate the extent of incidental mortality from the currently configured fishing gear.*
3. Consider finding a better way to express the variation in the HabCam abundance data (the data were kriged for this assessment, and the variance was calculated by summing the variance of each of the kriged grids). *Two-stage GAM/Kriging models and stratified mean methods were introduced in this assessment, and several methods for calculating variance were investigated and compared in this assessment by simulation and analysis of actual data.*
4. Look at the historical patterns of the “whole stock”; how the spatial patterns of scallops and the fishery have changed over time. *These topics are handled in the description of survey and fishery data to the extent they are relevant.*
5. Estimate incidental mortality by running HabCam or an AUV along dredge tracks. *Several projects were funded this year to do work along these lines.*
6. Effort should be made to make sure the survey dredge is fitted with a camera at some point during the survey to record the movements of the dredge. This will help answer some questions about when the dredge starts and stops fishing, and the determination of tow times. *Five survey dredge tows were conducted with a camera mounted to the dredge that allowed improved interpretation of dredge sensor data.*
7. Seasonal patterns in scallop shell growth need to be analyzed and this data incorporated into the model. *No progress; the assessment team did not feel this is a high priority.*
8. Stock-recruit relationships should be calculated for various sub-sections of the stock, smaller areas than just MAB and GBK to look for possible patterns or relationships. *Appendix B8 examined the relationship between recruitment in the southern Mid-Atlantic and biomass in the entire stock.*
9. Further refine the estimate of the extent of scallop habitat relative to that of the survey. *New VIMS dredge and HabCam and S Mast optical surveys were used to identify stock boundaries and improve understanding of the relationship between the dredge survey and stock areas.*
10. Age archived scallop shells from the 1980s and 1990s. *Archived shells from 1988 and 1993 were used to estimate growth matrices to represent growth when fishing mortality was high in the CASA models. However, additional years should be analyzed as described in a new research recommendation.*
11. Continue to look at patterns of seasonality in weight of the meats and gonads, and timing of spawning. *Annual meat weight anomalies used to adjust mean body weight of individual scallops in the fishery and to compute catch numbers were substantially improved. Shell height-meat weight relationships based on survey data were updated.*

New recommendations

The Invertebrate Subcommittee identified the following research topics while preparing this assessment. The topics listed below are all considered worthwhile and are not listed in order of priority.

1. Investigate methods for better survey coordination between the various survey programs.
2. Evaluate effects of uncertainty in identifying dead scallops in optical surveys and improve procedures for identifying dead scallops.
3. Collect data to refine estimates of incidental mortality. Analytical procedures were improved this assessment but further progress awaits collection of more data.
4. Improve training of annotators used in optical surveys to identify and count specimens. For example, develop and consistently apply criteria for identifying inexact shell height measurements. Formalize QA/QC procedures including reevaluation of annotator accuracy. Develop and maintain reference images for training and testing.
5. Continue work to improve and simplify survey design and analytical procedures for HabCam. Ideally, procedures might be automated to the extent possible and integrated into routine survey operations.
6. Quantify and improve accuracy of SAMS projection models used to specify harvest levels. Recent projections appear to overestimate stock size to some extent.
7. Reduce uncertainty about stock size estimates from surveys and the CASA model. In particular, continue work on density dependent natural mortality for small scallops in stock assessment, reference point and projection models.
8. Collect additional biological data on a regional basis including growth increments from shells collected during historical dredge surveys, seasonality of spawning based on observer data, natural mortality on large scallops due to disease and senescence, and size-specific reproductive output.
9. Refine models that predict scallop recruitment based on chlorophyll and predator data in order to improve estimates from stock assessment and projection models. Investigate statistical approaches to estimating year class strength directly from survey data.
10. Investigate and quantify the utility of multiple scallop surveys.

B. Sea Scallop Assessment Report Appendixes

Appendix B1 - Invertebrate Subcommittee meetings and participants

Appendix B2 - Sea Scallop Discard Estimates

Appendix B3 - Shell Height Meat Weight Relationships

Appendix B4 - Estimation of Dredge efficiency from paired dredge HabCam observations

Appendix B5 - Empirical Assessment

Appendix B6 - NEFSC HabCam survey for sea scallops: survey design, implementation, and data analysis

Appendix B7 - Assessment of the sea scallop resource in the Northern Gulf of Maine management area

Appendix B8 - Relationships between chlorophyll and scallop recruitment potentially useful for stock projections and assessment modeling

Appendix B9 - Technical documentation for the CASA length structured stock assessment model used in the SARC 59 sea scallop stock assessment

Appendix B10 – Forecasting methodology (SAMS Model)

Appendix B1. Invertebrate Subcommittee meetings and participants

The Invertebrate Subcommittee met March 17-21, April 21-25, May 27-30, June 6, June 18 and June 23 during 2014 while preparing the SARC-59 stock assessment for Atlantic sea scallops. Meetings during March-May were held in the Stephen H. Clark Conference Room at the Northeast Fisheries Science Center in Woods Hole, MA with some participation by video conference. Meetings in June were exclusively by video conference. The following members participated in one or more meetings.

Larry Jacobson, NEFSC, chair
Dvora Hart, NEFSC, Assessment Team Lead
Burton Shank, NEFSC
Jia-Han Chang, NEFSC
Jiashen Tang, NEFSC
Toni Chute, NEFSC
Vic Nordahl, NEFSC
Chris Legault, NEFSC
Dan Hennen, NEFSC
Mark Terciero, NEFSC
Kevin Friedland, NEFSC
Paul Rago, NEFSC
Stephen Smith, DFO, Canada
Mary Beth Tooley, NEFMC
Dierdre Boelke, NEFMC
David Rudders, VIMS
Bill DuPaul, VIMS
Carl Huntsberger, Coonamesset Farm Foundation
Ron Smolowitz, Coonamesset Farm Foundation
Katherine Thompson, Coonamesset Farm Foundation
Daphne Munroe, Rutgers U.
Kevin Stokesbury, SMAST
Gregory DeCelles, SMAST
Susan Inglis, SMAST
Karen Bolles, HabCam Group
Richard Taylor, HabCam Group
Trish DeGraaf, Maine DMR
Kevin Kelly, Maine DMR
Matt Camisa, Massachusetts DMR
Sam Truesdell, University of Maine

Appendix B2. Sea Scallop Discard Estimates

Jessica Blaylock (NEFSC, Woods Hole, MA)

This paper presents discard estimates for Atlantic sea scallop (*Placopecten magellanicus*) for scallop dredge, scallop trawl and otter trawl fleets, calculated using the Standardized Bycatch Reporting Methodology (Wigley et al. 2007). This approach was also used in the previous assessment for this stock; however discard estimates were not included as input in the assessment model (NEFSC 2010).

Methods

Estimates of Atlantic sea scallop discards (mt meats) were derived for seven fleets using Northeast Fishery Observer Program (NEFOP) and Northeast Fishery Science Center (NEFSC) commercial landings (i.e., dealer) data for the 1989 to 2013 time period: Georges Bank and Mid-Atlantic Bight scallop dredge, Mid-Atlantic Bight scallop trawl, Georges Bank and Mid-Atlantic Bight small-mesh otter trawl, and Georges Bank and Mid-Atlantic Bight large-mesh otter trawl. Additionally, sea scallop discard estimates were also derived for scallop dredge fleets at a finer stratification level using NEFOP and Vessel Trip Report (VTR) data for the 1994 to 2013 time period. This analysis considered the two scallop dredge fleets above as four fleets: Georges Bank open and closed scallop dredge, and Mid-Atlantic Bight open and closed scallop dredge,

A broad stratification scheme was used with trips partitioned into fleets using the following four classification variables: calendar quarter, gear type, area fished, and mesh. Trips were not partitioned by trip category ('limited' versus 'general', for scallop dredge and scallop trawl) due to small sample size over the time series. Calendar quarter was based on landed date and used to capture seasonal variations in fishing activity. Gear type was based on Northeast gear codes (scallop dredge: negear 132; scallop trawl: negear 052; otter trawl: negear 050). Trips for which gear was unknown were excluded. Two broad geographical regions are defined for area fished based on statistical area: areas 520-562 constituted the Georges Bank (GBK) area, and areas 600 and above constituted the Mid-Atlantic Bight (MAB) area. Two mesh size groups were formed for otter trawl: small (mesh less than 5.5 inches) and large (5.5 inch mesh and greater). The additional analysis considering scallop dredge at a finer scale included access area as another classification variable. Here, two access area categories were used: 'open' and 'closed', where 'closed' includes all trips fishing in one of the scallop access areas (Closed Area I, Closed Area II and Nantucket Lightship in the GBK region; Hudson Canyon, Virginia Beach, Elephant Trunk, and Delmarva in the MAB region). Observer trips were assigned to the access area category based on program code, and VTR trips were assigned based on latitude and longitude.

Discards were estimated using a combined d/k_{all} ratio estimator (Cochran 1963), where d is discarded pounds of sea scallops and k_{all} is kept pounds of all species, calculated from NEFOP data. Discard weight was derived by multiplying the d/k_{all} ratio of each fleet by the corresponding dealer or VTR landings (Wigley et al. 2007). Coefficients of variation (CV) were calculated as the ratio of the standard error of the discards divided by the discards.

In cases where limited observer data were available (i.e. two or less observed trips in a calendar quarter), an imputation approach was used to 'fill in' the missing (or

incomplete) information using data from adjoining strata. In this imputation procedure, the temporal stratification (i.e., calendar quarter) was relaxed to entire year, recognizing that seasonal variations may occur that will thus not be accounted for. Numbers of annual observed trips by fleet are summarized in Tables 1 and 2.

To evaluate the proportion of estimated sea scallop discards to landings, the sum of the current discard estimates for scallop dredge was compared to the sum of estimated landings from Georges Bank, Southern New England, and Mid-Atlantic Bight for the 1992 to 2013 time period.

Results and Discussion

Annual Atlantic sea scallop discard estimates by fleet are presented in Tables 1, 2, and 3. Tables 1A-1D show estimates for the seven fleets without access area classification: Georges Bank and Mid-Atlantic Bight scallop dredge, Mid-Atlantic Bight scallop trawl, Georges Bank and Mid-Atlantic Bight small-mesh otter trawl, and Georges Bank and Mid-Atlantic Bight large-mesh otter trawl. Tables 2A-2B present discard estimates for the scallop dredge fleets at a finer scale that includes access area as a classification variable.

This analysis indicates that during the 1989 to 2013 time period, sea scallops were primarily discarded in the scallop dredge fleets (Tables 1A-1D, Table 3, Figure 1). For 2013, estimated discards from the Georges Bank and Mid-Atlantic Bight scallop dredge were 299 and 128 mt meats, respectively. Discard estimates for the other five fleets for the same year ranged from less than 1 mt meats (Georges Bank small-mesh otter trawl) to 10 mt meats (Mid-Atlantic Bight scallop trawl).

Discard estimates for scallop dredge at the access area classification level (Tables 2A-2B) suggest a higher discarding rate in the ‘open’ category fleets. For 2013, estimated discards from the Georges Bank open and closed scallop dredge fleets were 370 and 8 mt meats, respectively. Estimated discards from the Mid-Atlantic Bight open scallop dredge fleet were 46 mt meats; discards could not be estimated for 2013 for the Mid-Atlantic Bight closed scallop dredge fleet due to VTR trip misclassification.

The discard estimation presented here used a broad stratification approach. In addition, there are inherent limitations in the use of VTR data for trip assignment to the ‘access area’ category because of missing or inaccurate position data. Consequently, the discard estimates from scallop dredge at the access area classification level should be considered as preliminary.

Current estimates of discards and landings from scallop dredge fleets for 1994 to 2013 are presented in Figure 2. Total catch (discards plus landings) averaged 6,814 mt meats between 1993 and 1998. Catch increased in the following six years to peak at 31,435 mt meats in 2004, and averaged 26,560 mt meats from 2005 to 2012. Total catch in 2013 was 18,516 mt meats. Discards generally represent a small portion of total catch, with discard-to-landing ratios ranging from 0.010 in 1997 and 1998 to 0.1233 in 2000.

These results represent estimated sea scallop discards and landings in weight (mt meats). It is likely that discard-to-landing ratios of numbers would be higher because of the different size distribution of discarded scallops compared to that of landed scallops.

Acknowledgements

I wish to thank all the NEFOP observers for their diligent efforts to collect the discard information used in this analysis. Additionally, I would like to thank Toni Chute for her assistance with the classification of VTR trips to access area categories.

References

Cochran, W.L. 1963. Sampling Techniques. J. Wiley and Sons. New York.

Northeast Fisheries Science Center. 2010. 50th Northeast Regional Stock Assessment Workshop (50th SAW) Assessment Report. US Dept Commer., Northeast Fish. Sci. Cent. Ref. Doc. 10-17; 844 p. Available online:
<http://nefsc.noaa.gov/publications/crd/crd1017/>

Wigley, S.E., P.J. Rago, K.A. Sosebee, and D.L. Palka. 2007. The Analytic Component to the Standardized Bycatch Reporting Methodology Omnibus Amendment: Sampling Design, and Estimation of Precision and Accuracy (2nd Edition). US Dep. Commer., Northeast Fish. Sci. Cent. Ref. Doc. 07-09; 156 p. Available online:
<http://www.nefsc.noaa.gov/nefsc/publications/crd/crd0709/index.htm>

Table 1A. Number of observed trips, sea scallop discards (mt meats) and coefficient of variation (CV) for the Georges Bank (GBK) scallop dredge and Mid-Atlantic Bight (MAB) scallop dredge fleets, 1989-2013. Discards were not estimated prior to 1992 due to small sample size.

GBK scallop dredge				MAB scallop dredge			
YEAR	Trips	Discards (mt meats)	CV	YEAR	Trips	Discards (mt meats)	CV
1989				1989			
1990				1990			
1991	1			1991	1		
1992*	11	464	0.48	1992*	7	121	0.00
1993*	12	345	0.32	1993*	10	12	0.80
1994*	7	3	0.89	1994	16	576	0.54
1995*	6	22	0.62	1995*	20	322	0.28
1996	15	116	0.36	1996	23	24	0.71
1997*	11	46	0.73	1997*	18	8	1.14
1998*	9	4	0.57	1998*	16	48	0.66
1999*	63	141	0.28	1999*	8	8	0.56
2000*	228	989	0.09	2000	28	779	0.33
2001*	18	529	0.17	2001*	88	1,955	0.11
2002*	11	105	0.58	2002	87	1,894	0.13
2003*	14	328	0.58	2003	108	2,225	0.10
2004*	46	58	0.20	2004	235	2,446	0.09
2005	107	228	0.27	2005	220	357	0.19
2006	135	347	0.20	2006*	93	78	0.49
2007	180	231	0.21	2007	177	260	0.20
2008	216	334	0.14	2008	425	414	0.15
2009	81	380	0.26	2009	408	923	0.12
2010	98	668	0.18	2010	238	688	0.21
2011	141	668	0.18	2011	251	482	0.14
2012	222	603	0.11	2012	201	237	0.12
2013	269	299	0.14	2013	182	128	0.22

* Imputed data were used for discard estimation for these years.

Table 1B. Number of observed trips, sea scallop discards (mt meats) and coefficient of variation (CV) for the Mid-Atlantic Bight (MAB) scallop trawl fleet, 1989-2013. Discards were not estimated prior to 2004 due to small sample size.

MAB scallop trawl			
YEAR	Discards		CV
	Trips	(mt meats)	
1989			
1990			
1991			
1992			
1993			
1994			
1995			
1996			
1997			
1998			
1999			
2000			
2001	4		
2002	1		
2003			
2004*	44	99	0.25
2005	137	61	0.13
2006*	30	150	0.33
2007	34	17	0.59
2008*	38	6	0.58
2009*	8	49	1.59
2010*	29	12	0.33
2011*	10	12	0.78
2012*	19	<1	0.75
2013*	20	10	0.35

* Imputed data were used for discard estimation for these years.

Table 1C. Number of observed trips, sea scallop discards (mt meats) and coefficient of variation (CV) for the Georges Bank (GBK) small-mesh otter trawl, and Mid-Atlantic Bight (MAB) small-mesh otter trawl fleets, 1989-2013.

GBK small-mesh otter trawl				MAB small-mesh otter trawl			
YEAR	Trips	Discards		YEAR	Trips	Discards	
		(mt meats)	CV			(mt meats)	CV
1989	65	2	0.53	1989	34	213	0.39
1990	31	<1	1.22	1990	47	8	0.44
1991	68	<1	0.80	1991	78	11	2.05
1992	42	<1	0.68	1992	47	6	0.53
1993	25	<1	0.57	1993*	16	8	0.81
1994*	18	7	1.88	1994*	15	29	0.78
1995*	11	<1	1.26	1995	63	71	0.23
1996*	10	0	0.00	1996	80	14	1.70
1997*	20	<1	0.87	1997*	48	1	2.76
1998*	6	<1	1.39	1998*	32	4	1.35
1999*	8	<1	2.62	1999	35	12	1.65
2000*	17	<1	0.49	2000	39	2	0.94
2001*	15	<1	0.64	2001	55	<1	8.75
2002*	33	<1	0.82	2002	32	68	0.34
2003	55	<1	1.11	2003	74	17	0.80
2004	109	2	0.96	2004	257	5	0.42
2005	194	<1	0.47	2005	172	4	0.32
2006	62	<1	0.56	2006	151	13	2.63
2007	60	<1	1.44	2007	218	5	0.56
2008	50	<1	0.49	2008	152	8	0.42
2009	199	<1	0.50	2009	286	23	0.52
2010	217	<1	0.54	2010	361	16	0.48
2011	168	<1	0.49	2011	365	5	0.33
2012	130	<1	0.83	2012	226	3	0.61
2013	186	<1	0.45	2013	395	5	0.35

* Imputed data were used for discard estimation for these years.

Table 1D. Number of observed trips, sea scallop discards (mt meats) and coefficient of variation (CV) for the Georges Bank (GBK) large-mesh otter trawl, and Mid-Atlantic Bight (MAB) large-mesh otter trawl fleets, 1989-2013. Discards were not estimated for MAB large-mesh otter trawl prior to 1992 due to small sample size.

GBK large-mesh otter trawl				MAB large-mesh otter trawl			
YEAR	Discards			YEAR	Discards		
	Trips	(mt meats)	CV		Trips	(mt meats)	CV
1989	27	1	0.88	1989	4		
1990	33	1	0.72	1990			
1991	34	4	0.54	1991	4		
1992	35	<1	1.10	1992*	14	4	0.40
1993	35	<1	1.30	1993*	12	3	1.54
1994	36	<1	1.21	1994*	21	99	0.53
1995	61	<1	0.36	1995	55	102	0.83
1996	38	<1	0.69	1996*	18	<1	0.62
1997	26	<1	1.00	1997*	9	1	0.62
1998*	10	<1	0.89	1998*	13	1	0.69
1999	20	<1	2.48	1999*	8	94	1.16
2000	30	2	0.66	2000*	26	32	0.57
2001	52	1	0.82	2001*	50	13	0.48
2002	83	2	0.61	2002*	39	8	2.36
2003	163	3	0.77	2003*	16	<1	2.26
2004	316	42	0.35	2004	109	9	0.43
2005	959	9	0.18	2005	93	1	0.94
2006	462	30	0.37	2006	71	3	2.39
2007	465	5	0.25	2007	160	12	0.59
2008	563	6	0.21	2008	132	29	0.88
2009	536	9	0.22	2009	167	19	0.22
2010	526	4	0.23	2010	274	9	0.73
2011	782	6	0.17	2011	253	9	1.00
2012	599	6	0.32	2012	169	4	0.78
2013	593	6	0.20	2013	251	7	0.53

* Imputed data were used for discard estimation for these years.

Table 2A. Number of observed trips, sea scallop discards (mt meats) and coefficient of variation (CV) by the Georges Bank (GBK) open scallop dredge and GBK closed scallop dredge fleets, 1994-2013. Discards were not estimated for the GBK open scallop dredge fleet in 2000 and 2001 due to small sample size.

GBK open scallop dredge				GBK closed scallop dredge			
YEAR	Discards		CV	YEAR	Discards		CV
	Trips	(mt meats)			Trips	(mt meats)	
1994*	7	2	0.82	1994	n/a		
1995*	6	23	0.63	1995	n/a		
1996	15	103	0.37	1996	n/a		
1997*	11	41	0.70	1997	n/a		
1998*	9	4	0.57	1998	n/a		
1999*	48	97	0.39	1999*	15	53	0.26
2000	2			2000	226	246	0.03
2001	2			2001	16	26	0.15
2002*	11	99	0.57	2002	n/a		
2003*	14	324	0.58	2003	n/a		
2004*	16	39	0.29	2004	30	25	0.19
2005	41	371	0.36	2005	66	40	0.27
2006*	56	783	0.25	2006	79	41	0.26
2007	53	194	0.30	2007	127	40	0.26
2008	73	202	0.23	2008	140	53	0.12
2009	58	295	0.33	2009*	23	24	0.30
2010	44	576	0.36	2010*	54	117	0.18
2011*	68	603	0.24	2011	71	84	0.20
2012	101	981	0.15	2012	119	48	0.11
2013	202	370	0.16	2013	30	8	0.07

* Imputed data were used for discard estimation for these years.

n/a: not applicable

Table 2B. Number of observed trips, sea scallop discards (mt meats) and coefficient of variation (CV) by the Mid-Atlantic Bight (MAB) open scallop dredge and MAB closed scallop dredge fleets, 1994-2013. Discards were not estimated for the MAB open scallop dredge fleet in 2001 due to small sample size.

MAB open scallop dredge				MAB closed scallop dredge			
YEAR	Trips	Discards (mt meats)	CV	YEAR	Trips	Discards (mt meats)	CV
1994	16	276	0.59	1994	n/a		
1995*	20	341	0.28	1995	n/a		
1996	23	22	0.72	1996	n/a		
1997*	18	8	1.15	1997	n/a		
1998*	16	42	0.66	1998	n/a		
1999*	8	7	0.56	1999	n/a		
2000	28	749	0.33	2000	n/a		
2001	3			2001	85	301	0.09
2002*	13	1,446	0.19	2002	74	151	0.11
2003	62	2,253	0.14	2003	46	120	0.12
2004	143	1,869	0.13	2004	92	510	0.10
2005	166	368	0.29	2005	54	39	0.21
2006*	87	71	0.39	2006*	6	3	0.49
2007	84	65	0.41	2007	93	63	0.22
2008	89	215	0.54	2008	336	97	0.14
2009	118	597	0.15	2009	290	219	0.13
2010	130	583	0.30	2010	108	94	0.20
2011	145	489	0.20	2011	45	22	0.22
2012	100	143	0.20	2012^			
2013	137	46	0.25	2013^			

* Imputed data were used for discard estimation for these years.

^ no discard estimation because of VTR missclassification

n/a: not applicable

Table 3. Summary of sea scallop discard estimates (mt meats) from Table 1 by region, 1989-2013.

Georges Bank (GBK)					Mid-Atlantic Bight (MAB)					
YEAR	scallop dredge	small-mesh otter trawl	large-mesh otter trawl	Total	YEAR	scallop dredge	scallop trawl	small-mesh otter trawl	large-mesh otter trawl	Total
1989	*	2	1	4	1989	*	*	213	*	213
1990	*	<1	1	1	1990	*	*	8	*	8
1991	*	<1	4	5	1991	*	*	11	*	11
1992	464	<1	<1	465	1992	121	*	6	4	131
1993	345	<1	<1	346	1993	12	*	8	3	22
1994	3	7	<1	10	1994	576	*	29	99	703
1995	22	<1	<1	23	1995	322	*	71	102	495
1996	116	0	<1	116	1996	24	*	14	<1	38
1997	46	<1	<1	46	1997	8	*	1	1	11
1998	4	<1	<1	4	1998	48	*	4	1	53
1999	141	<1	<1	142	1999	8	*	12	94	114
2000	989	<1	2	991	2000	779	*	2	32	813
2001	529	<1	1	531	2001	1,955	*	<1	13	1,969
2002	105	<1	2	107	2002	1,894	*	68	8	1,970
2003	328	<1	3	332	2003	2,225	*	17	<1	2,244
2004	58	2	42	102	2004	2,446	99	5	9	2,559
2005	228	<1	9	238	2005	357	61	4	1	424
2006	347	<1	30	378	2006	78	150	13	3	244
2007	231	<1	5	236	2007	260	17	5	12	294
2008	334	<1	6	341	2008	414	6	8	29	457
2009	380	<1	9	389	2009	923	49	23	19	1,013
2010	668	<1	4	672	2010	688	12	16	9	724
2011	668	<1	6	675	2011	482	12	5	9	508
2012	603	<1	6	610	2012	237	<1	3	4	245
2013	299	<1	6	306	2013	128	10	5	7	150

* No discard estimate due to small sample size.

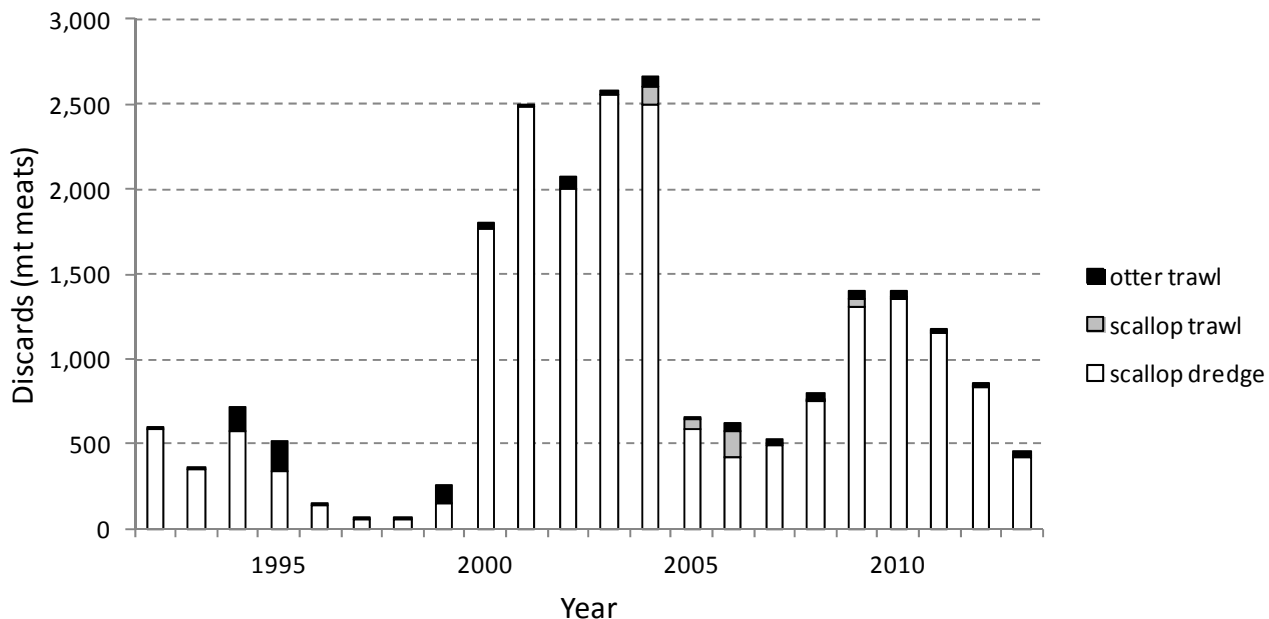


Figure 1. Sea scallop discard estimates (mt meats) from trips using scallop dredge, scallop trawl, and otter trawl gear presented in Table 1, 1992-2013. Discards from scallop trawl were not estimated prior to 2004 due to small sample size.

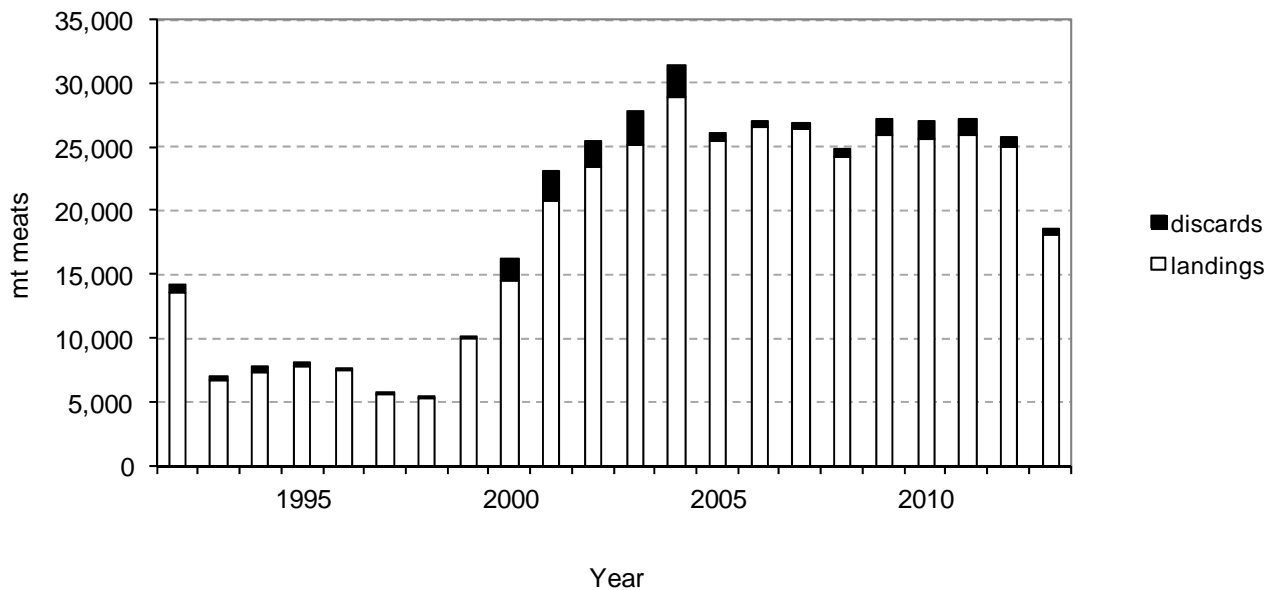


Figure 2. Estimated scallop landings and current estimated sea scallop discards from scallop dredge fleets (mt meats), 1992-2013.

Appendix B3. Shell Height Meat Weight Relationships

Dan Hennen, NEFSC, Woods Hole, MA

1 Methods

Sea scallops (averaging about 6 per station) were selected for analysis on roughly half of all NEFSC survey stations from 2004 to 2013. The scallops were measured to the nearest millimeter, carefully shucked, excess water was removed from the meat, and the meat was weighed to the nearest gram.

Preliminary analysis indicated a residual pattern for those scallops with shell heights less than 70 mm. The small weights of these scallops (1-3 g) combined with the fact that meat weight could only be measured to the nearest gram resulted substantial measurement error. For this reason, the analysis was restricted to scallops that are at least 70 mm shell height (Figure A1).

A generalized linear mixed model (GLMM) with a log link was used to predict meat weight using shell height, depth, density, latitude, and subarea (a finer scale regional division within each broad region). The GLMM used the gamma likelihood with a log link which is appropriate for data (such as these) with "constant CV" error (McCullagh and Nelder [1989]). This method avoids log-transforming the response variable (meat weight) which can lead to biased estimates when the results are back-transformed. The best model was chosen by AIC (Tables 1-5; Burnham and Anderson [2002]). The grouping variable for the random effects was a combination of survey station number and the year in which the survey took place. Survey stations are chosen randomly (though stratified to fit NEFSC survey design specifications) and survey stations numbers are assigned sequentially so that a survey station number in one year does not have any particular relationship to the same station number in the next year. Thus, a grouping variable based on a combination of survey station number and year incorporates random variation in the data that is due to both time (year) and fine scale spatial differences (station number).

Several analyses using simplified versions of the best model were employed to explore the effects of year, subarea, and fishing regulations.

All data analysis was conducted using the R statistical program (v2.13.2).

1.1 Seasonal variation and commercial meat anomalies

The NMFS Observer program provided meat weight estimates from commercial catches that occurred throughout the year. These meat weights are based on meats that are shucked by fishermen. Meats from the observer program are not weighed individually. They are packed into a graduated cylinder and a volume for a sample (typically 100 scallops) is recorded. The meat weight for a sample was calculated using a density estimate of $1.05 \frac{\text{g}}{\text{ml}^3}$ (Caddy and Radley-Walters [1972]; Smolowitz et al. [1989]). These "observed" meat weights are therefore an average weight for all the meats in the cylinder, not a direct observation of the weight of a meat. The observer program does generate approximate shell heights for individual scallops, though they are binned by 5 mm increments. Therefore predicted meat weights can be generated for each shell height represented in the sample. Predicted meat weights were calculated using the best model (by AIC) from the analysis of survey meat weights described above.

It was noted this year that in many cases the number of shells measured was > 100 . Because there were only 100 scallop meats packed into the cylinder and there is no way to determine which of the shells were associated with the meats in the cylinder, all observations in which the shell heights exceeded 100 in number were excluded from this analysis. This

correction reduced the sample size by approximately 52%, but reduced the error in predicted meat weights considerably (compare Figure 9 to Figure 10).

The best model was applied to predict meat weights for observer samples based on shell heights, latitude and longitude recorded for each sample during 2001-2013. Depth outliers were excluded by restricting maximum depths in the observed hauls from each subarea to the maximum depths observed in the survey for that subarea.

Predicted meat weights for each month were compared to the (observed) density derived meat weights for each month by $\frac{\text{pred.}-\text{obs.}}{\text{pred.}}$ (Figure 10). The median of these ratios by month are referred to as the monthly meat weight “anomaly”. A positive anomaly indicates that the observed meat weight was greater than the expected meat weight, while a negative anomaly indicates the opposite is true. Annual meat weight anomalies for use in the CASA stock assessment model were computed by averaging the monthly values within a year using the landings during each month as weights.

2 Results and Discussion

In general, the observed meat weights (from observed volumes) should be less than the survey-based, predicted meat weights (a negative anomaly) because the commercially shucked scallops leave some meat on the shell, and because the surveys occur in late spring or summer (depending on the year), a time of typically high meat weight. The pattern in the anomaly calculated for MAB roughly follows this pattern in that the anomaly is negative in all months excluding April through July, a period that overlaps the survey (Figure 12). On Georges Bank, however, there were months of the year where the observed scallop meats were almost 15% heavier than the predicted meats, resulting in a positive anomaly (Figure 13). The positive anomaly appears in February through July. It is clear from examination of Figure 13 that either observed meat weights were heavier than expected and/or predicted meat weights lighter between January and May since 2009. In 2009, the timing of the survey was shifted to earlier in the year. Predicted meat weights have increased for scallops greater than about 130 mm since the last assessment (Figure 8). Therefore observed meat weights must have increased. In fact, observed meat weights have both increased and stabilized dramatically in the years since 2009 (Figure 14). It is possible that this reflects an increase in efficiency among fishers by selecting areas and time periods when meat weights were high. The early months of the year were not as well sampled by observers relative to the summer months and smaller sample sizes may be influencing this pattern as well (Table 6). There is also some indication of a systemic increase in meat weight for the region generally, based on the shell height to meat weight model estimates reflected in Figure 8, but this result is confounded with the shift in the timing of the survey.

The anomalies refine assessment model estimates of the total annual weight of meats removed by the fishing fleet, based on the lengths recorded by port-side samplers. To make the conversion from port-side shell height to meat weight, the median monthly meat weight anomalies were smoothed by a second order polynomial loess function with a span of 0.25 (months). This short smoothing span provided a modest smooth that allowed the data to strongly influence the model fit (Figures A15). The smooth was applied to a duplicated annual cycle (i.e. 24 months were fit, using identical data in each 12 month period) and the middle 12 months were selected and reordered so that January was the first month in the resulting model fit. This manipulation guaranteed that December and January produced linking estimates and minimized edge effects. The smoothed monthly anomalies were then weighted by the landings in each month in each year for which we have landings data (1975 – 2012) and annual median values

were calculated.

The annual values were somewhat different from similar values calculated for the last assessment (Figures A16 -A17). The anomalies are generally lower (~ 2%) in the MAB and higher (~ 15%) in the GBK. The difference in the GBK region is due to the large shift in the monthly anomalies between the last assessment and the current one, based primarily on the increase in observed meat weight (Figure 14). The shift in the MAB is relatively minor and is likely attributable to a combination of the various manipulations to the observer data and small changes in the shell height to meat weight model.

3 Literature Cited

K.P. Burnham and D.R. Anderson. Model selection and multimodel inference: a practical information-theoretic approach. Springer, 2002.

J.F. Caddy and C. Radley-Walters. Estimating count per pound of scallop meats by volumetric measurement. Technical Report 1202, Fish. Res. Brd. Can. Man. Rep., 1972.

P. McCullagh and J.A. Nelder. Generalized Linear Models, 2nd Ed. Chapman and Hall, Boca Raton, FL, 1989. 511 pp.

R.J. Smolowitz, F.M. Serchuk, and R.J. Reidman. The use of a volumetric measure for determining sea scallop meat count. NOAA Tech. Mem. F/NER-1, Northeast Fisheries Science Center, 166 Water Street, Woods Hole, MA 02543-1026, 1989.

Table 1: AIC results from model fits to predict meat weight.

Formula	AIC	BIC	logLik	deviance
sh+d+sh*d+area+(sh+1)	101114.57	101267.34	-50537.28	101074.57
sh+d+lat+clop+area+(sh+1)	101123.48	101283.90	-50540.74	101081.48
sh+d+area+(sh+1)	101129.14	101274.28	-50545.57	101091.14
sh+d+lat+area+(sh+1)	101130.13	101282.90	-50545.06	101090.13
sh+d+clop+sh*d+(sh+1)	101166.05	101234.80	-50574.02	101148.05
sh+d+lat+clop+(sh+1)	101175.50	101244.25	-50578.75	101157.50
sh+d+clop+(sh+1)	101180.69	101241.80	-50582.35	101164.69
sh+d+sh*d+(sh+1)	101187.51	101248.63	-50585.76	101171.51
sh+d+lat+sh*d+(sh+1)	101188.53	101257.28	-50585.26	101170.53
sh+d+(sh+1)	101202.36	101255.83	-50594.18	101188.36
sh+area+(sh+1)	101288.53	101426.03	-50626.26	101252.53
sh+clop+(sh+1)	101359.04	101412.51	-50672.52	101345.04
sh+lat+(sh+1)	101363.62	101417.09	-50674.81	101349.62
d+(sh+1)	103485.29	103531.13	-51736.65	103473.29
sh+d+sh*d+(1)	105482.86	105528.69	-52735.43	105470.86
sh+d+area+(1)	105660.31	105790.17	-52813.16	105626.31
sh+d+clop+(1)	105750.75	105796.58	-52869.37	105738.75
sh+d+lat+(1)	105769.06	105814.89	-52878.53	105757.06
sh+d+(1)	105773.59	105811.78	-52881.79	105763.59
sh+area+(1)	105824.38	105946.60	-52896.19	105792.38
sh+clop+(1)	105915.93	105954.12	-52952.96	105905.93
sh+(1)	105923.56	105954.12	-52957.78	105915.56
sh+lat+(1)	105925.11	105963.31	-52957.56	105915.11
d+(1)	119777.65	119808.20	-59884.82	119769.65

Table 2: Results from model fits to predict meat weight. The coefficients estimated are: the intercept(int), ln(shell height) (sh), ln(depth) (d), latitude (lat), an interaction between ln(shell height) and ln(depth)(shXd) and an Identifier which is either a marker for a model with subarea coefficients (see Tables 3 and4) or a coefficient for closed vs. open (clop). Random effects are either on the shell height coefficient and intercept (sh+1) or intercept alone (1). The models are listed in order of increasing AIC (lowest AIC model is in the top row).

formula	int	sh	d	lat	shXd	Identifier
sh+d+sh*d+area+(sh+1)	-16.98(0.013)	4.6(0.021)	1.93(0.018)		-0.48(0.087)	1
sh+d+lat+clop+area+(sh+1)	-6.43(0.016)	2.61(0.022)	-0.38(0.019)	-0.02(0.012)		0.09(0.019)
sh+d+area+(sh+1)	-7.45(0.013)	2.61(0.021)	-0.38(0.018)			2
sh+d+lat+area+(sh+1)	-6.55(0.016)	2.61(0.022)	-0.39(0.019)	-0.02(0.012)		3
sh+d+clop+sh*d+(sh+1)	-17.08(0.006)	4.59(0.021)	1.94(0.016)		-0.48(0.087)	-0.06(0.008)
sh+d+lat+clop+(sh+1)	-8.02(0.006)	2.61(0.021)	-0.38(0.016)	0.01(0.003)		-0.07(0.008)
sh+d+clop+(sh+1)	-7.56(0.006)	2.61(0.021)	-0.36(0.016)			-0.06(0.008)
sh+d+sh*d+(sh+1)	-17.38(0.004)	4.64(0.021)	2.01(0.016)		-0.49(0.087)	
sh+d+lat+sh*d+(sh+1)	-17.56(0.004)	4.64(0.021)	2.01(0.016)	0.005(0.003)	-0.49(0.087)	
sh+d+(sh+1)	-9.09(0.004)	2.61(0.021)	-0.34(0.016)			
sh+area+(sh+1)	-9.07(0.013)	2.61(0.022)				4
sh+clop+(sh+1)	-9.04(0.006)	2.61(0.022)				-0.04(0.008)
sh+lat+(sh+1)	-8.63(0.004)	2.61(0.022)		-0.01(0.003)		
d+(sh+1)	4.96(0.005)		-0.36(0.019)			
sh+d+sh*d+(1)	-28.64(0.004)	6.98(0.015)	4.94(0.017)		-1.1(0.064)	
sh+d+area+(1)	-6.38(0.014)	2.38(0.016)	-0.38(0.019)			5
sh+d+clop+(1)	-6.64(0.006)	2.4(0.016)	-0.34(0.017)			-0.06(0.008)
sh+d+lat+(1)	-7.18(0.004)	2.4(0.016)	-0.34(0.017)	0.01(0.003)		
sh+d+(1)	-6.76(0.004)	2.4(0.016)	-0.32(0.017)			
sh+area+(1)	-7.99(0.014)	2.38(0.016)				6
sh+clop+(1)	-8.02(0.006)	2.39(0.016)				-0.04(0.009)
sh+(1)	-8.05(0.004)	2.39(0.016)				
sh+lat+(1)	-7.91(0.004)	2.39(0.016)		-0.003(0.003)		
d+(1)	4.69(0.007)		-0.31(0.028)			

Table 3: Results from model fits to predict meat weight in MAB subareas.

Identifier	VB	DMV	DMV.VB	ET	HC	NYB
1	-0.13(0.023)	-0.06(0.018)	-0.14(0.028)	-0.17(0.022)	-0.08(0.019)	-0.07(0.019)
2	-0.14(0.023)	-0.06(0.018)	-0.15(0.028)	-0.17(0.022)	-0.08(0.019)	-0.07(0.019)
3	-0.14(0.023)	-0.12(0.041)	-0.22(0.05)	-0.23(0.039)	-0.12(0.031)	-0.11(0.028)
4	-0.06(0.024)	0.04(0.018)	-0.03(0.028)	-0.07(0.022)	0.002(0.02)	0.04(0.019)
5	-0.14(0.024)	-0.05(0.019)	-0.2(0.029)	-0.24(0.023)	-0.11(0.02)	-0.07(0.02)
6	-0.07(0.025)	0.05(0.019)	-0.08(0.029)	-0.13(0.023)	-0.03(0.021)	0.04(0.02)

Table 4: Results from model fits to predict meat weight in GBK subareas.

Identifier	NLS	SCH	CA1	SEP	NEP	CA2
1	0.07(0.021)	-0.13(0.018)	0	-0.07(0.023)	-0.13(0.017)	0.004(0.017)
2	0.07(0.021)	-0.13(0.018)	0	-0.07(0.023)	-0.13(0.017)	0.005(0.017)
3	0.06(0.022)	-0.13(0.018)	0	-0.08(0.024)	-0.12(0.018)	0.008(0.017)
4	0.14(0.021)	-0.07(0.019)	0	-0.08(0.024)	-0.12(0.017)	0.05(0.018)
5	0.08(0.021)	-0.12(0.019)	0	-0.06(0.024)	-0.14(0.018)	0.001(0.018)
6	0.14(0.022)	-0.06(0.02)	0	-0.07(0.025)	-0.12(0.018)	0.04(0.018)

Table 5: Results from model fits to predict meat weight. Predictors are ln(shell height) (sh) ln(depth) (d), region (reg) and open vs. closed to fishing (clop). MAB and open coefficients are shown. GBK and closed are assumed to have coefficients equal to 0.

formula	int	sh	d	reg	clop	AIC	BIC
sh+d+reg+clop+(sh+1)	-7.35(0.012)	2.61(0.03)	-0.4(0.028)	-0.05(0.014)	-0.06(0.013)	101171	101240
sh+d+reg+(sh+1)	-7.46(0.009)	2.61(0.03)	-0.38(0.029)	-0.04(0.014)		101195	101256
sh+reg+clop+(sh+1)	-9.07(0.012)	2.61(0.03)		0.04(0.014)	-0.04(0.014)	101353	101414
sh+reg+(sh+1)	-9.09(3e-04)	2.61(4e-04)		0.04(0.01)		101361	101414

Table 6: Sample sizes for observed meat weights by month in GBK.

month	pre2010	post2009	Total
1	142	82	224
2	86	38	124
3	18	62	80
4	32	88	120
5	84	149	233
6	431	333	764
7	433	404	837
8	356	404	760
9	269	174	443
10	201	151	352
11	249	138	387
12	167	58	225
Total	2468	2081	4549

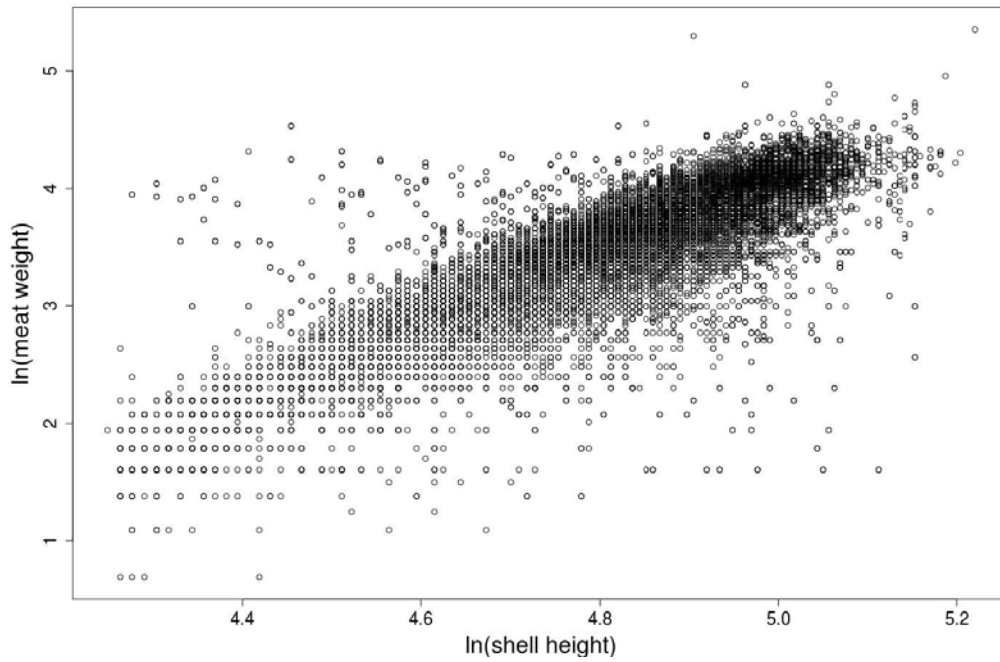


Figure 1: Natural log of shell height against the natural log of meat weights measured on NEFSC scallop surveys between 2003 and 2013.

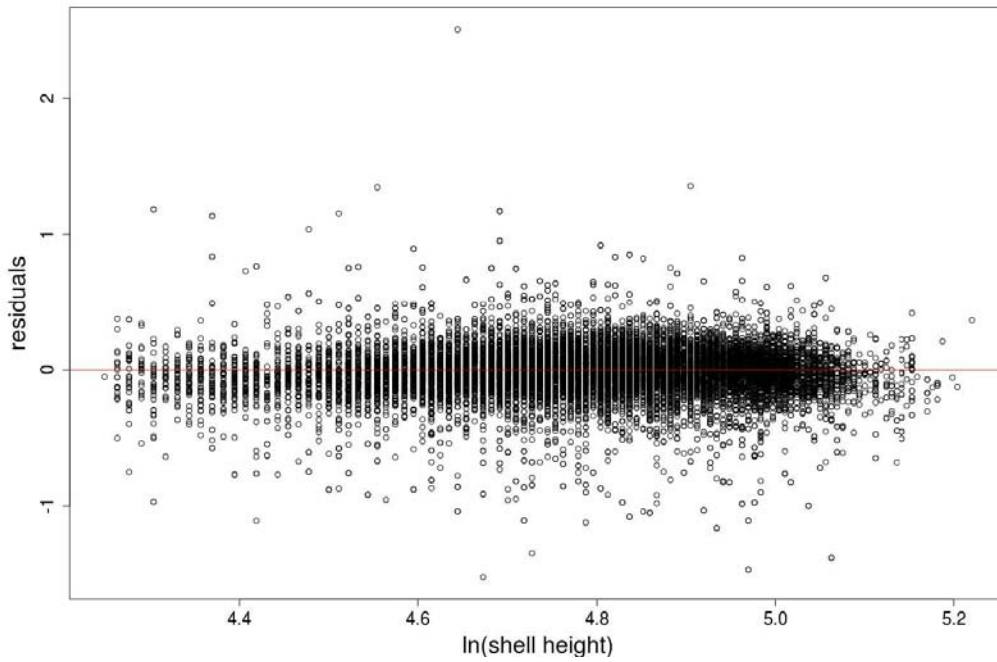


Figure 2: Residuals from the fit of best model predicting meat weight by the natural log of shell height.

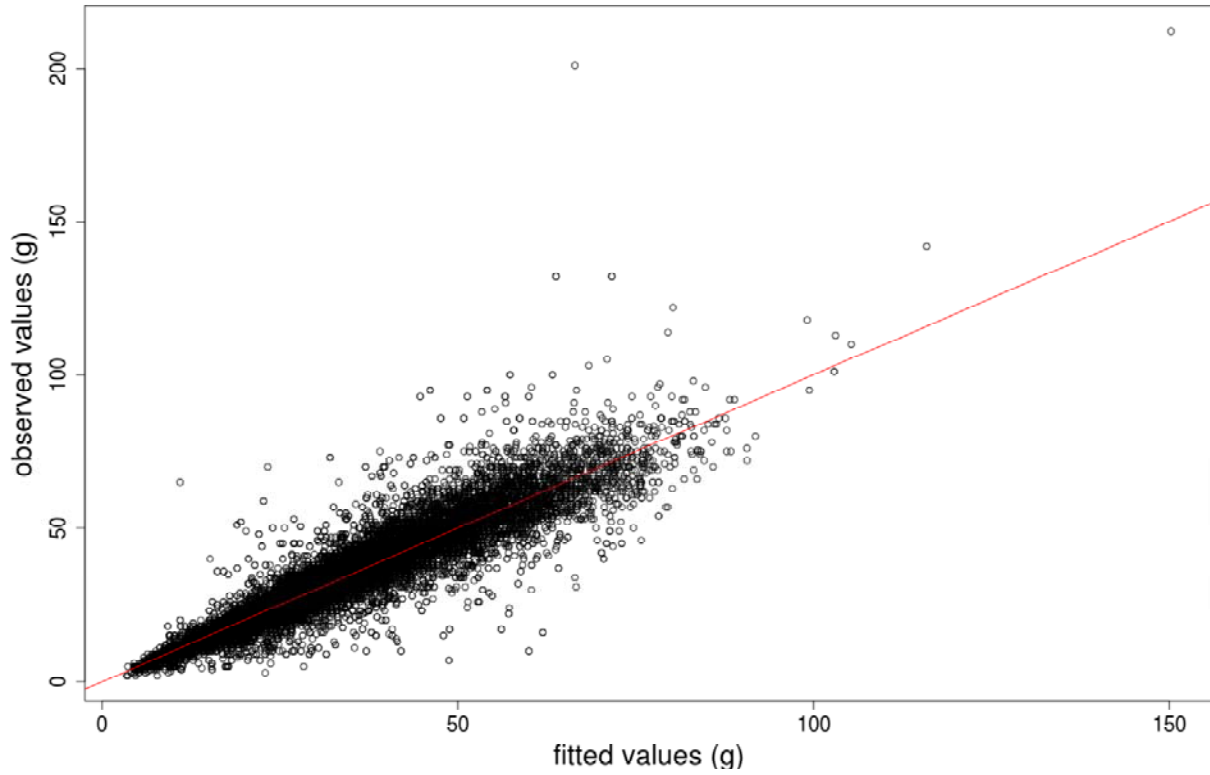


Figure 3: Observed vs. predicted meat weight using the best model by AIC.

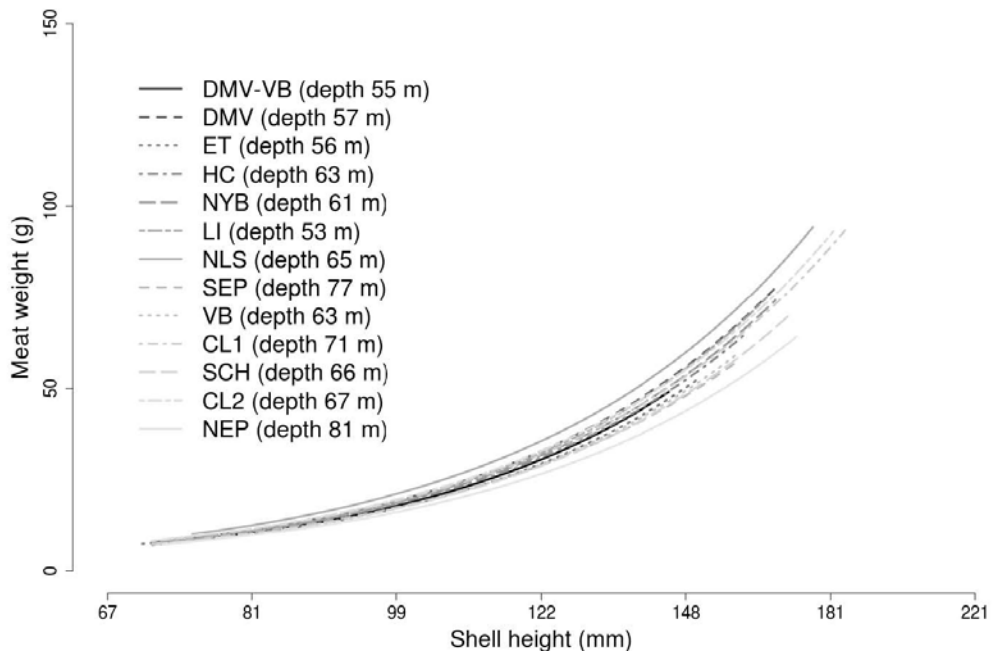


Figure 4: Meat weight curves by subarea. The depths used are the median depths observed in each subarea during all available years of the survey.

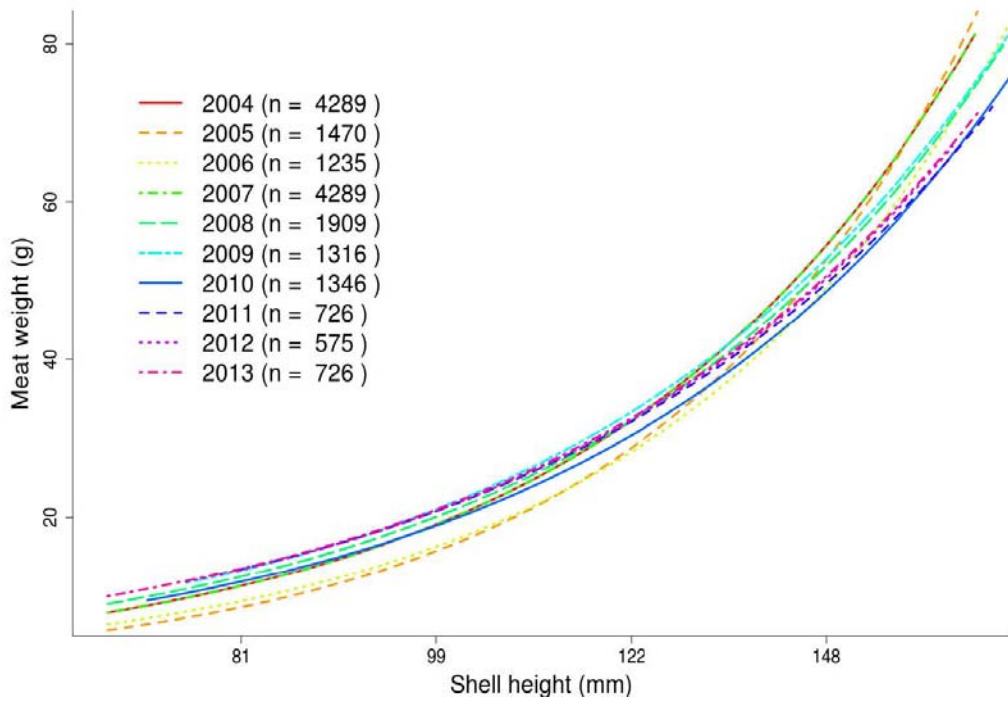


Figure 5: Meat weight curves by year. The curves are fits of the best model to annual subsets of the data. The sample size of each subset are shown in the legend.

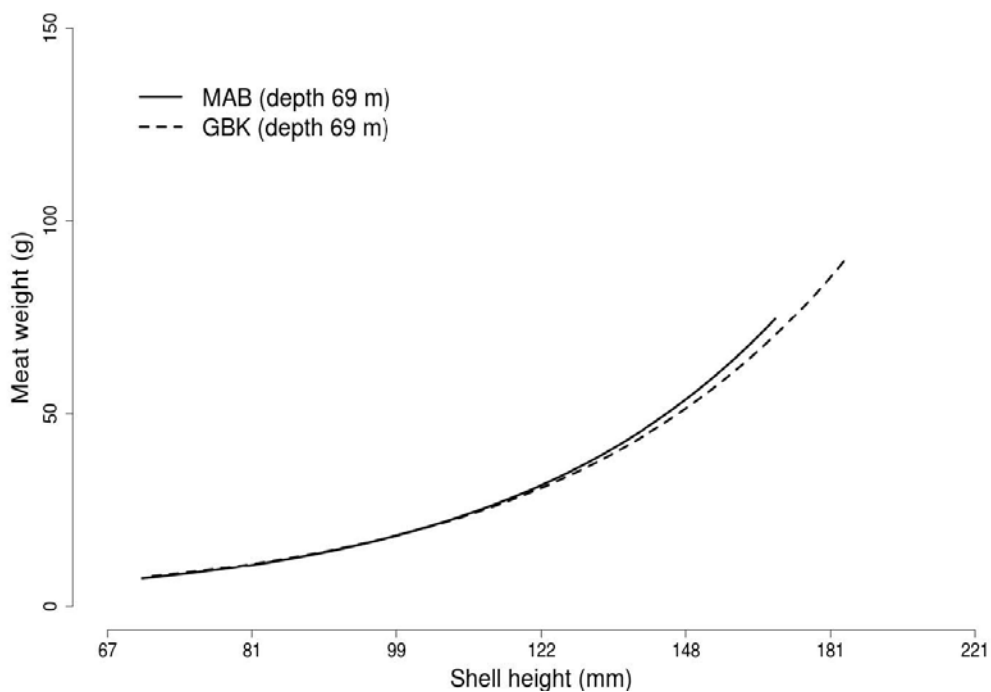


Figure 6: Shell height to meat weight relationship for each region based NEFSC survey data from 2003 -2013. The length of the curves represents the range of shell heights observed in each region.

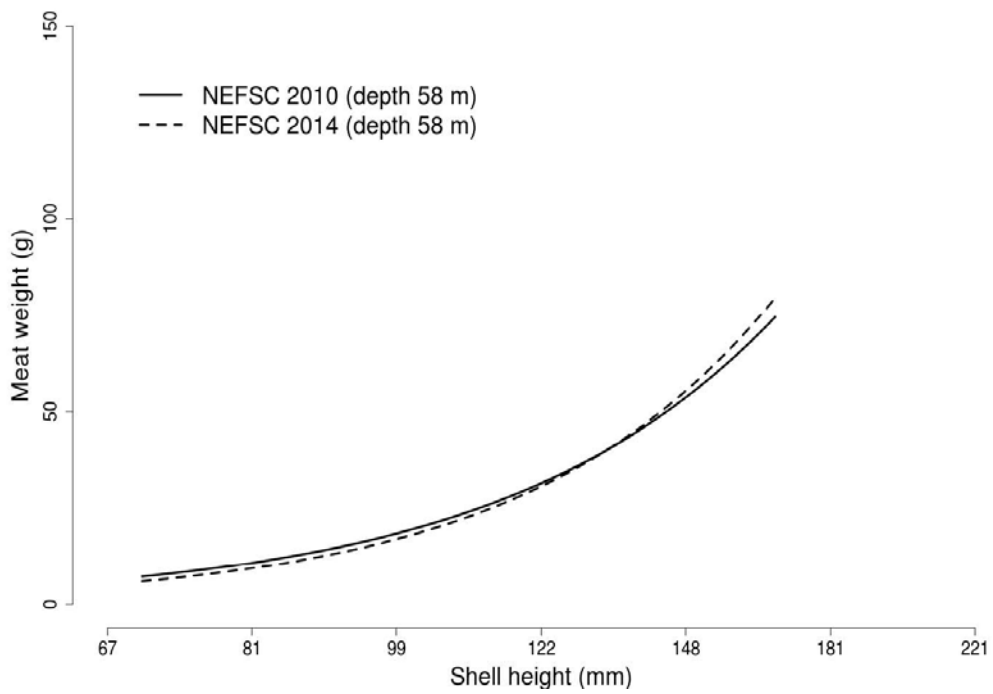


Figure 7: Shell height to meat weight relationship for two time periods in MAB. The length of the curves represents the range of shell heights observed in each period.

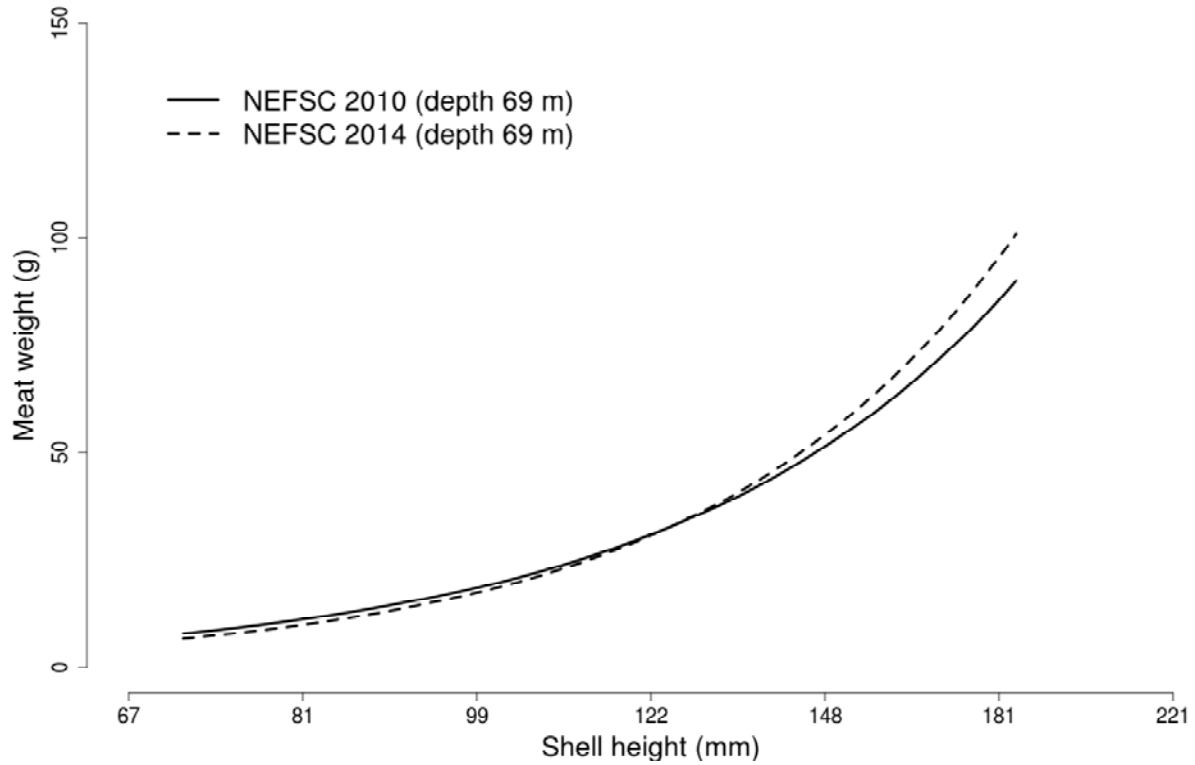


Figure 8: Shell height to meat weight relationship for two time periods in GBK. The length of the curves represents the range of shell heights observed in each period.

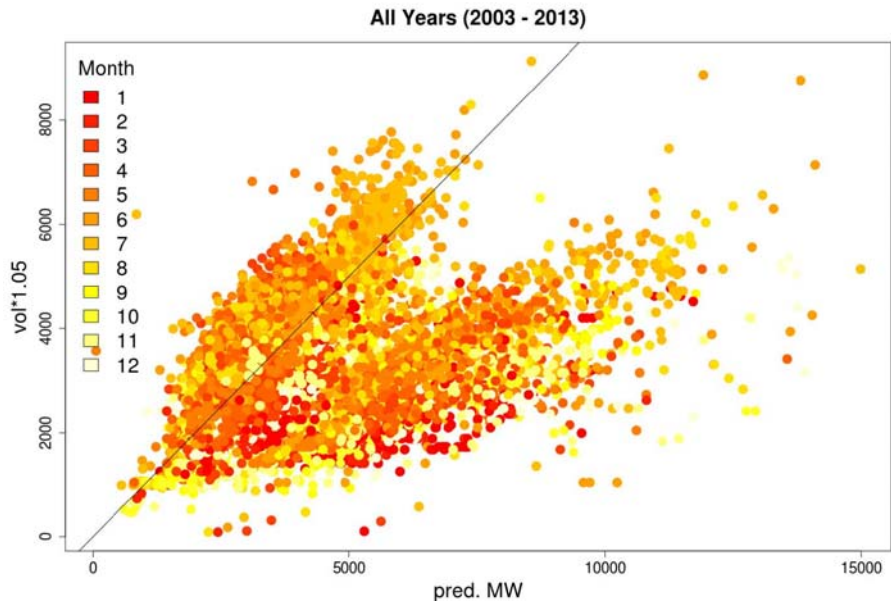


Figure 9: Meat weights estimated using data from the observer program compared to those expected based on NEFSC survey data. The solid line shows one to one correspondence and is for illustrative purposes only. The large cluster of points below the one to one line is an artifact of many more shells being measured for height than were packed into the cylinder for volume determination.

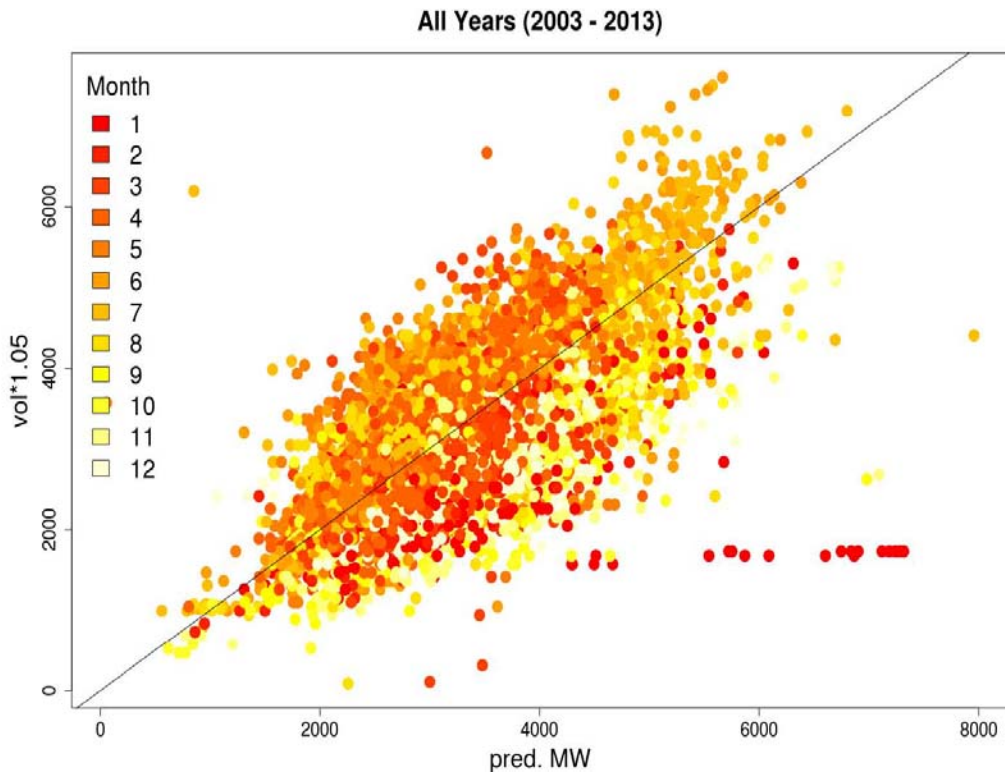


Figure 10: Meat weights estimated using data from the observer program compared to those expected based on NEFSC survey data. The solid line shows one to one correspondence and is for illustrative purposes only. Observations including more than 100 measured shells were excluded.

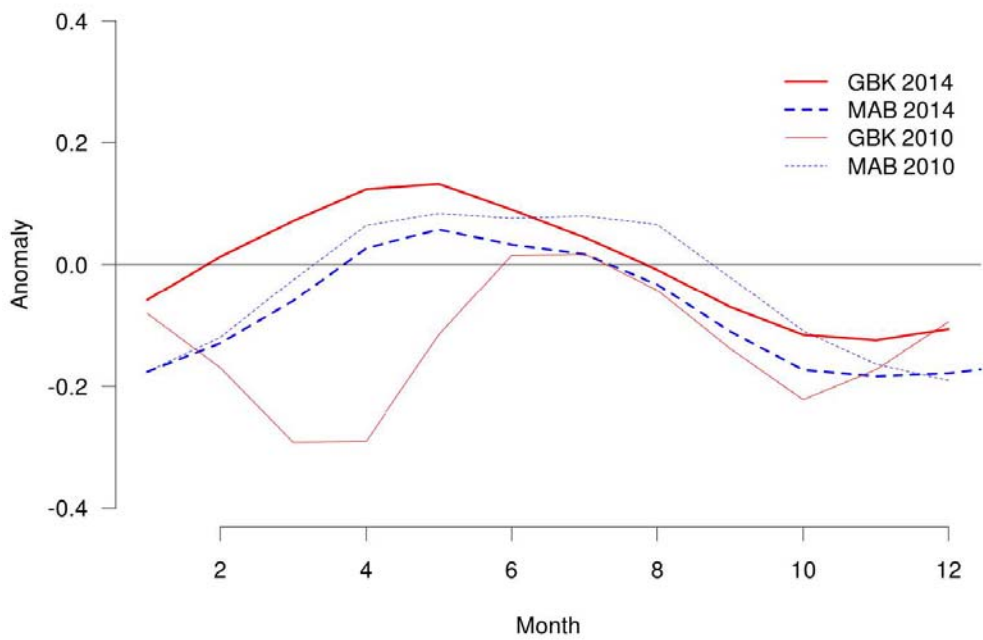


Figure 11: The anomalies estimated in the last assessment compared to the current anomalies.

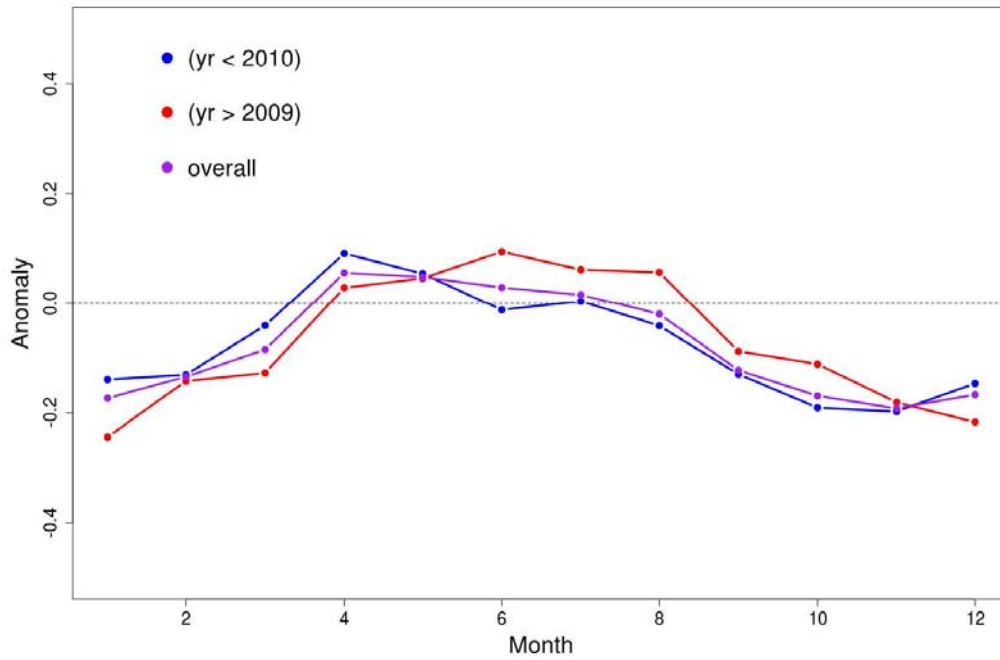


Figure 12: Monthly meat weight anomalies for the period prior to 2010, the period after 2010 and overall in the MAB.

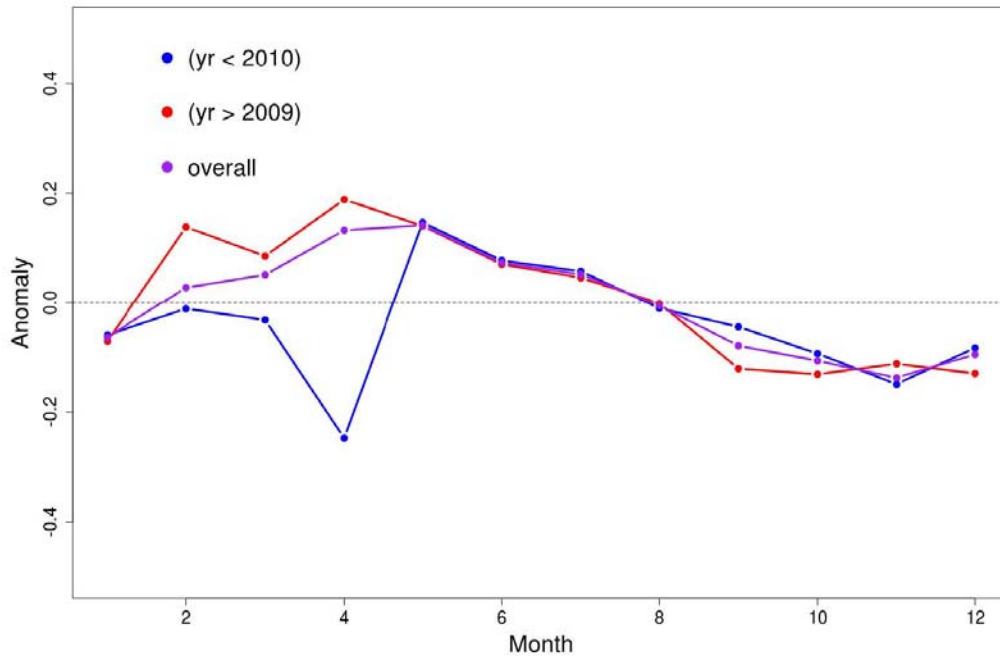


Figure 13: Monthly meat weight anomalies for the period prior to 2010, the period after 2010 and overall on GBK.

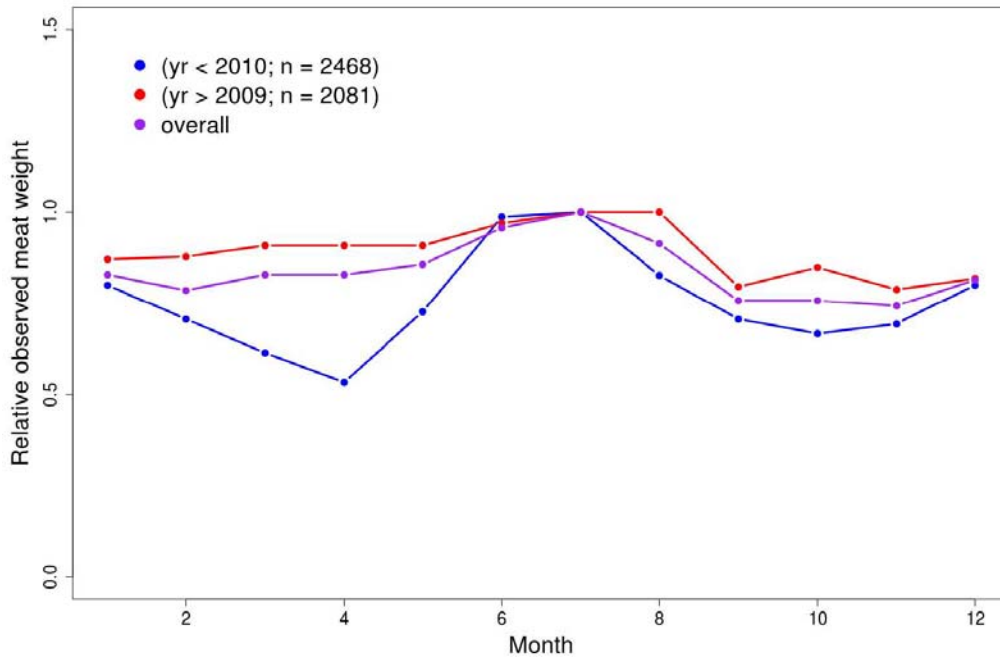


Figure 14: Relative monthly meat weight in observed commercial catches for the period prior to 2010, the period after 2010 and overall on GBK.

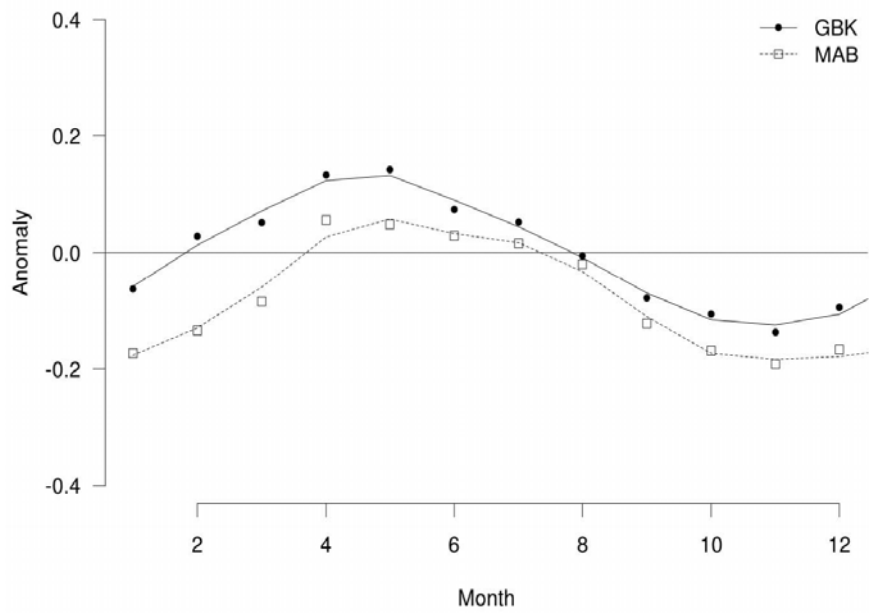


Figure 15: Smoothed anomalies for MAB and GBK.

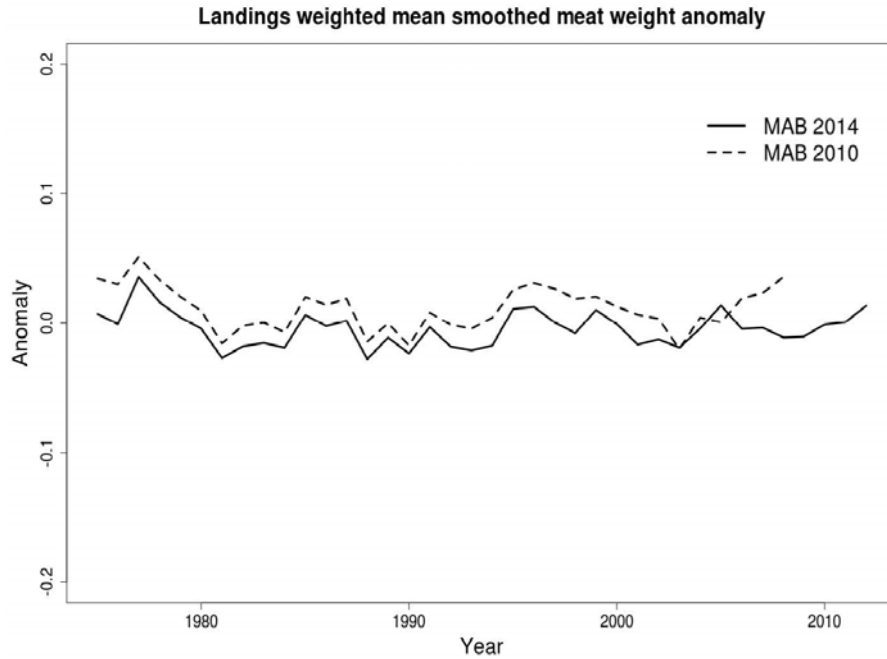


Figure 16: Landings weighted annual anomaly for MAB.

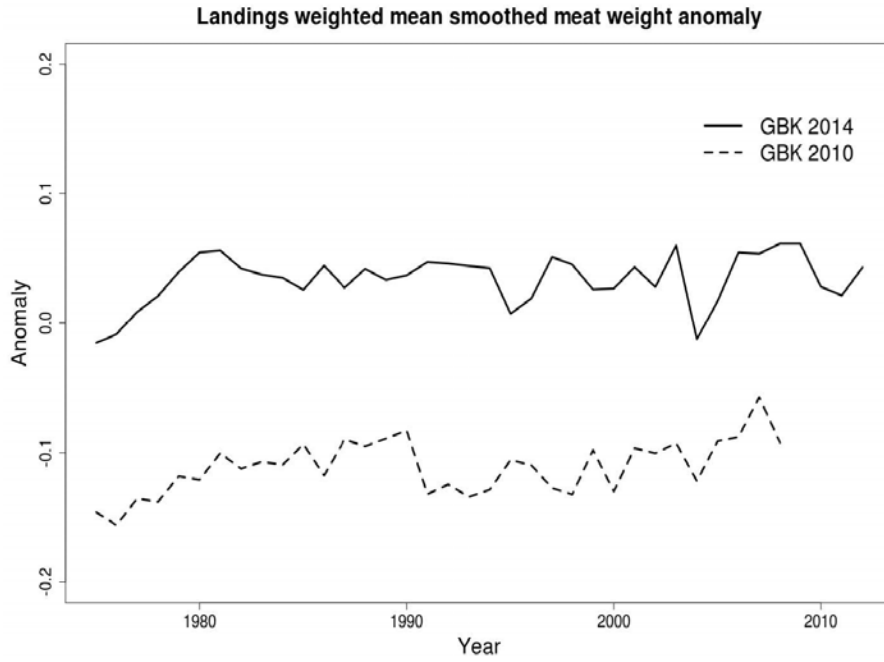


Figure 17: Landings weighted annual anomaly for GBK.

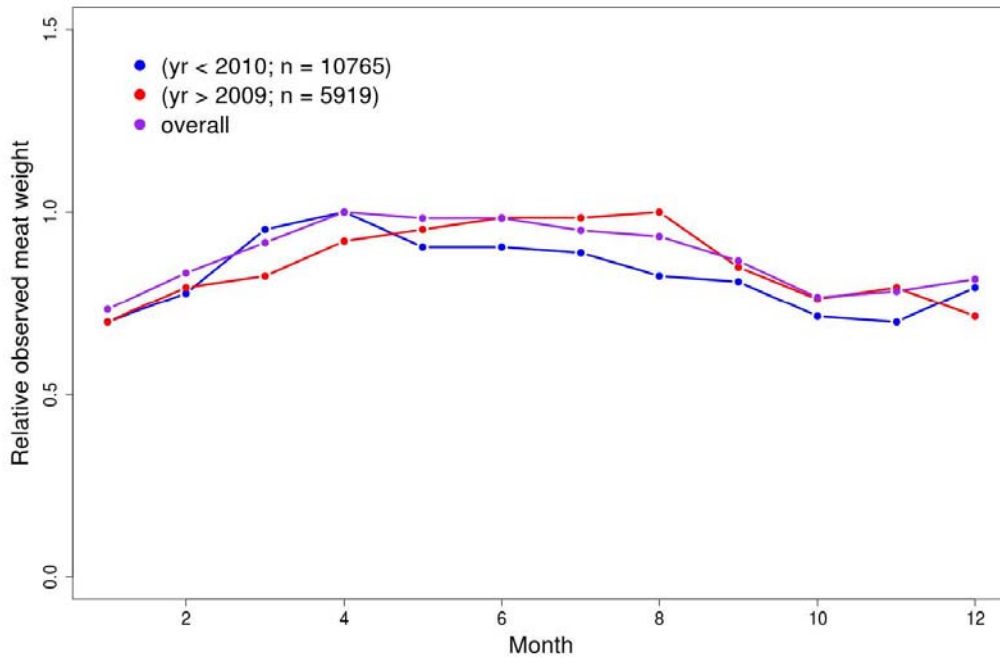


Figure 18: Relative monthly meat weight in observed commercial catches for the period prior to 2010, the period after 2010 and overall for MAB.

Appendix B4. Estimation of Dredge efficiency from paired dredge-HabCam observations

Timothy J. Miller, NEFSC, Woods Hole, MA

We use HabCam optical survey data to estimate capture efficiency of the NEFSC scallop survey dredge where capture efficiency is the probability of capture for a scallop in the path of the dredge. The literature on methods for analysis of comparative gear studies is extensive, but an alternative observation model is used here because HabCam provides hundreds or thousands of observation for each dredge tow. We develop a general hierarchical model for the dredge and HabCam observations, compare relative performance of a set of specific models, assess the statistical behavior of the estimators to determine the best model, and provide relatively precise estimates of the efficiency of the scallop survey dredge on sand and gravel/cobble substrates.

Materials and Methods

A dredge survey is conducted annually by the Northeast Fisheries Science Center to obtain relative abundance indices and other data for sea scallops. The dredge tows are conducted at stations according to a stratified random design. At a subset of these stations in 2008 and 2009, the HabCam optical survey device was also deployed. The HabCam captures images continuously along its track, but a thinned set were used in our analyses to make correlation between successive images within a station analyzed negligible. In all, we had 110 dredge stations where the number of sea scallops and swept area were recorded and where HabCam data including area searched, shell heights and number of scallops observed was recorded. There were 95-1,669 HabCam images used for each station.

The density of scallops differs by substrate type as based on HabCam as may the efficiency of the dredge. Sea scallop density is generally higher in sand than gravel substrates. We observe the substrate in each HabCam image, but the dredge track may cover various substrates which are not directly observed. The lack of these observations for the dredge makes estimation of relative efficiency for specific substrates impossible. However, sand and gravel/cobble substrates are more prevalent in particular survey strata. Sandy bottom is predominant in the Mid-Atlantic strata 6130, 6140, 6150, 6180, and 6190 and Georges Bank strata 6460, 6470, 6530, 6540, 6550, 6610, 6621, and 6670. Rock and gravel substrates are more common in Georges Bank strata 6490, 6500, 6510, 6520, 6651, 6652, 6661, 6662, and 6710. We therefore used stratum to establish proxies for substrate type when estimating dredge efficiency. In all there were 22 stations classified gravel (G) and 88 classified as sand (S).

Observation model

At station i out of n total stations, we have the numbers captured by the dredge ND_i and the total number of sea scallops counted in associated HabCam images n_i . For HabCam, we assume all scallops are observed in each image and that the surface area A_{ij} of the substrate in the field of view is known. We also assume that the area swept by the dredge (determined using inclinometer sensors) is known. Conditional on the density of scallops in the image j at station i

δ_{Hij} , we assume the number of scallops observed in the image is Poisson distributed with mean

$$(1) \quad E(N_{Hij}|\delta_{Hij}, A_{Hij}) = \delta_{Hij}A_{Hij}.$$

Conditional on the density of scallops δ_{Di} and the known area swept by the dredge at station A_{Di} , we assume the number of captured scallops is Poisson distributed with mean

$$(2) \quad E(N_{Hij}|\delta_{Di}, A_{Di}) = q\delta_{Di}A_{Di}$$

where q is the efficiency of the dredge (cf. Paloheimo and Dickie 1964). Note that HabCam images is assumed to be 100% efficient at detecting scallops. More generally, q in Eq. 2 can be viewed as a relative efficiency when the HabCam is less than fully efficient.

We consider two different models for densities in each HabCam image δ_{Hij} . The first simply assumes that the densities within a station are equal $\delta_{Hij} = \delta_{Hi}$ and the second assumes that the densities are gamma distributed with station-specific mean δ_{Hi} and shape σ_{Hi} parameters,

$$f(\delta_{Hij}|\delta_{Hi}, \sigma_{Hi}) = \frac{\delta_{Hij}^{\sigma_{Hi}-1} \exp\left(-\delta_{Hij} \frac{\sigma_{Hi}}{\delta_{Hi}}\right)}{\Gamma(\sigma_{Hi}) \left(\frac{\delta_{Hi}}{\sigma_{Hi}}\right)^{\sigma_{Hi}}}.$$

In the former model the counts in the HabCam images $N_{Hij}|\delta_{Hi}$, are still conditionally Poisson distributed. In the latter model, they are negative binomial distributed in the with mean

$$E(N_{Hij}|\delta_{Hi}) = \delta_{Hi}A_{Hij}$$

and variance

$$V(N_{Hij}|\delta_{Hi}) = E(N_{Hij}|\delta_{Hi}) \left[1 + \frac{E(N_{Hij}|\delta_{Hi})}{\sigma_{Hi}} \right].$$

For models where we assume the HabCam densities are gamma distributed we also consider variants where the shape parameter is constant across stations $\sigma_{Hi} = \sigma_H$ and where the shape parameter is itself gamma distributed with mean σ_H and shape parameter σ_{σ_H} . The former corresponds to an assumption that the variability of the densities observed in each image is constant across stations and the latter allows the variability to change from station to station. For stations where σ_{Hi} is large, the distribution of HabCam image observations is closer to Poisson.

The dredge efficiency q and densities δ_{Di} resulting in the dredge observations and the average densities δ_{Hi} for HabCam observations at a given station are not all estimable as fixed parameters. Estimation of dredge efficiency requires some assumption about the relationship of dredge and HabCam densities both within and across stations. We use a bivariate gamma distribution described by Moran (1969) to relate the densities producing the HabCam and dredge observations at each station (see Attachment B4-1). The distribution is a function of the mean and shape parameters for the marginal gamma distributions and a correlation parameter ($-1 <$

$\rho_\delta < 1$) that defines the relationship of dredge and HabCam densities within a station. The densities are independent when $\rho_\delta = 0$ and identical when $\rho_\delta = 1$. We assume the means of the dredge and HabCam densities are the same, but that these means are a function of the substrate type at a given station. The details for the different components of five plausible models we consider are provided in Table 1.

The general likelihood that we maximize for parameter estimation is

$$(3) \quad L = \prod_{i=1}^n \left\{ \int_0^\infty \int_0^\infty f(N_{Di}|\delta_{Di})f(\delta_{Di}, \delta_{Hi}) \prod_{j=0}^{n_i} \left[\int_0^\infty f(N_{Hij}|\delta_{Hij})f(\delta_{Hij}|\delta_{Hi})d\delta_{Hij} \right] d\delta_{Di}d\delta_{Hi} \right\}.$$

Unobserved densities are treated as random effects and integrated out to obtain the marginal model likelihood. Models such as M_1 where HabCam densities within stations are assumed constant do not require the corresponding integration in Eq. 3. When densities within stations are gamma distributed, the numbers in the HabCam images conditional on δ_{Hi} are negative binomial distributed. The closed form for this marginal sub-model is computationally more efficient. Because the densities are marginally gamma distributed and the dredge counts are Poisson distributed conditional on the realized densities at each station, dredge observations $N_{Di}|\delta$ are marginally negative binomial distributed. The HabCam observations are also marginally negative binomial when the densities within a station are constant. In all models, the correlation of HabCam and dredge observations is defined by ρ .

We used AD Model Builder (Fournier et al. 2012) and the random effects library (Skaug and Fournier 2006) to maximize the marginal likelihood for all models. Parameters θ were estimated on log scale except ρ_δ which was defined as $\rho_\delta = -1 + 2/(1 + e^{-\theta})$. Standard errors were approximated using the delta method and asymmetric 95% confidence intervals were calculated by making the appropriate transformation of $\hat{\theta} \pm z_{1-\frac{\alpha}{2}}SE(\hat{\theta})$ where $\alpha = 0.05$ and $z_{1-\frac{\alpha}{2}}$ is the quantile of the standard normal distribution with cumulative probability $1 - \frac{\alpha}{2}$.

Simulation study

Because the methods were new, we used simulation to evaluate the reliability of the parameter estimates in the best model chosen by AIC. Using the parameter estimates from the best model, we simulated 1000 data sets and fit the same model to each data set. We calculated bias of parameter and standard error estimators and 95% confidence interval coverage.

Results

The best performing model M5 demonstrated that the efficiency of the dredge differed substantially in gravel (0.24) and sandy (0.40) substrates (Table 2). There were dramatic reductions in AIC between M_1 and M_2 and between M_2 and M_3 . The reduction for M_2 implies strong evidence of variability in densities among HabCam observations within stations. The reduction in AIC for model M_3 implies strong evidence of variation among stations in the variance of HabCam observations. The very small difference in AIC values for M_3 and M_4 implies, implies that there is little evidence for differences in variability in mean densities among

stations for both HabCam and dredge observations.

Mean densities were much greater in gravel substrates ($> 0.5 m^2$) than sand substrates ($< 0.5 m^2$) for all models. Because there were fewer stations in the gravel substrate than sand, the relative precision of mean density estimates for gravel was lower for all models (CV about 0.3 for gravel vs. about 0.1 for sand). The precision of the dredge efficiency estimate was lower in gravel also (CV about 0.14 for gravel vs. about 0.06 for sand) for the best performing model M_5 . The correlation of mean densities for dredge and HabCam observations was high ($\rho_\delta > 0.9$) in all models.

Statistical behavior

Seventy file out of 1000 simulations with model M5 did not converge. However, average parameter estimates for the unconverged fits were similar to averages for simulations where the model did converge. The relative bias for estimates from converged model fits was negligible for most parameters except that the shape parameter σ_{σ_H} which determines the variability of HabCam densities at each station was biased high by about 12% (Table 3). Standard error estimates were negligible for most parameters except σ_{σ_H} (SE approximately -15%) and the efficiency of the dredge in gravel substrates (SE approximately 6%). Bias of coverage for 95% confidence intervals was also small with the exception of the parameter σ_{σ_H} (bias about -9%).

References

- Fournier, D. A., Skaug, H. J., Ancheta, J., Ianelli, J., Magnusson, A., Maunder, M., Nielsen, A., and Sibert, J. 2012. AD Model Builder: using automatic differentiation for statistical inference of highly parameterized complex nonlinear models. *Optimization Methods and Software* 27(2): 233-249.
- Moran, P. A. P. 1969. Statistical inference with bivariate gamma distributions. *Biometrika* 56(3): 627-634.
- Paloheimo, J. E. and Dickie, L. M. 1964. Abundance and fishing success. *Rapports et Procès-Verbaux des Réunions. Conseil Permanent Internationale pour l'Exploration de la Mer* 155: 152-163.
- Skaug, H. J. and Fournier, D. A. 2006. Automatic approximation of the marginal likelihood in non-Gaussian hierarchical models. *Computational Statistics & Data Analysis* 51(2): 699-709.

Table 1. Details of the fixed effects and random effects sub-models in the hierarchical models we fitted to paired HABCAM and dredge data.

Model	$E(N_{Di} \delta_{Di}, q)$	$E(N_{Hij} \delta_{Hij})$	δ_{Hij}	σ_{Hi}	δ_{Di}, δ_{Hi}	n_p
M ₁	$q\delta_{Di}A_{Di}$	$\delta_{Hij}A_{Hij}$	δ_{Hi}	—	BGamma($\delta(G, S), \sigma_\delta, \rho_\delta$)	5
M ₂	$q\delta_{Di}A_{Di}$	$\delta_{Hij}A_{Hij}$	Gamma(δ_{Hi}, σ_{Hi})	σ_H	BGamma($\delta(G, S), \sigma_\delta, \rho_\delta$)	6
M ₃	$q\delta_{Di}A_{Di}$	$\delta_{Hij}A_{Hij}$	Gamma(δ_{Hi}, σ_{Hi})	Gamma($\sigma_H, \sigma_{\sigma_H}$)	BGamma($\delta(G, S), \sigma_\delta, \rho_\delta$)	7
M ₄	$q\delta_{Di}A_{Di}$	$\delta_{Hij}A_{Hij}$	Gamma(δ_{Hi}, σ_{Hi})	Gamma($\sigma_H, \sigma_{\sigma_H}$)	BGamma($\delta(G, S), \sigma_{D\delta}, \sigma_{H\delta}, \rho_\delta$)	8
M ₅	$q(G, S)\delta_{Di}A_{Di}$	$\delta_{Hij}A_{Hij}$	Gamma(δ_{Hi}, σ_{Hi})	Gamma($\sigma_H, \sigma_{\sigma_H}$)	BGamma($\delta(G, S), \sigma_\delta, \rho_\delta$)	8

Table 2. AIC and parameter estimates for each fitted model. Parameters denoted with (G) and (S) are specific to observations from gravel and sand substrates, respectively and (D) and (H) denote parameters specific to dredge and HABCAM observations, respectively.

Model	$\Delta(AIC)$	q	δ	σ_δ	ρ_δ	σ_H	σ_{σ_H}
M ₁	6724.0	0.376 (0.020)	5.048 (1.476) (G) 0.470 (0.056) (S)	0.621 (0.084)	0.905 (0.022)	—	—
M ₂	986.6	0.376 (0.020)	5.041 (1.480) (G) 0.469 (0.056) (S)	0.622 (0.084)	0.905 (0.022)	1.576 (0.044)	—
M ₃	8.20	0.376 (0.020)	5.085 (1.505) (G) 0.469 (0.056) (S)	0.620 (0.084)	0.906 (0.022)	3.419 (0.625)	0.880 (0.207)
M ₄	8.60	0.383 (0.021)	5.448 (1.653) (G) 0.461 (0.054) (S)	0.586 (0.084) (D) 0.647 (0.091) (H)	0.910 (0.021)	3.418 (0.624)	0.880 (0.207)
M ₅	—	0.243 (0.034) (G) 0.400 (0.022) (S)	5.771 (1.708) (G) 0.458 (0.054) (S)	0.630 (0.085)	0.912 (0.020)	0.630 (0.624)	0.880 (0.207)

Table 3. Relative bias of parameter and standard error estimators and coverage probability of approximate 95% confidence interval for 925 simulated data sets with parameters specified from the best performing model M₅.

Parameter	Value	Relative Bias	SE	Relative Bias of SE	95% CI coverage
q (G)	0.24	0.01	0.03	-0.06	0.93
q (S)	0.40	0.00	0.02	-0.01	0.94
δ (G)	5.77	-0.01	1.33	0.00	0.94
δ (S)	0.46	0.00	0.06	-0.03	0.93
σ_δ	0.63	0.03	0.09	-0.03	0.94
ρ_δ	0.91	0.00	0.02	-0.04	0.94
σ_H	3.42	-0.03	0.53	-0.02	0.91
σ_{σ_H}	0.88	0.12	0.19	-0.15	0.86

Attachment B4-1. Bivariate gamma distribution.

This is the same formulation described by Moran (1969). Let Y_1 and Y_2 be bivariate standard normal distributed with correlation parameter ρ ,

$$f(Y_1, Y_2) = \frac{1}{2\pi(1 - \rho^2)^{\frac{1}{2}}} \exp \left[-\frac{1}{2(1 - \rho^2)} (y_1^2 - 2\rho y_1 y_2 + y_2^2) \right].$$

Then letting the marginal distributions $F(X_1) = F(Y_1)$ and $F(X_2) = F(Y_2)$, where

$$F(X_i) = \int_0^{X_i} \frac{1}{\Gamma(\sigma_i)\beta_i^{\sigma_i}} w_i^{\sigma_i-1} \exp(-w_i\beta_i^{-1}) dw_i,$$

X_1 and X_2 have a bivariate gamma distribution with means $\sigma_i\beta_i$ and marginal variances $\sigma_i\beta_i^2$, but correlation defined by ρ . When $\rho = 0$, X_1 and X_2 are independent and when $\rho = 1$, X_1 and X_2 are identically distributed.

Appendix B5. Empirical assessment

Larry Jacobson, NEFSC, Woods Hole, MA

Introduction

The empirical assessment used simple techniques to estimate sea scallop stock abundance, biomass and fishing mortality in the MAB, GBK and combined stock areas. The purpose was to evaluate the accuracy of CASA estimates as independently as possible. However, empirical results could be used in place of CASA model estimates if the later were unavailable. The data and various parameters used in the empirical analysis are a subset of those also used in the CASA model and were all obtained independently in field studies or other analyses rather than from a stock assessment model.

Materials and methods

Survey swept-area abundance data used in the empirical analysis were the best available estimates of total 40+ mm stock abundance and considered reliable. Abundance from the dredge and optical surveys (HabCam and SMAST large camera) were the same as used in CASA except that SMAST data were adjusted for logistic size selectivity using externally estimated selectivity curves (Appendix B7 in NEFSC 2007). In CASA, the same selectivity curves are applied in the model after data input. In addition abundance estimates were not rescaled for comparison to a prior distribution as in CASA although this had no impact on results. Size selectivity was assumed to be flat in the dredge and HabCam surveys.

Updated capture efficiency estimates were used in expansion of the dredge survey to calculate swept-area abundance prior to their use in this analysis (Appendix B4). Additional variance due to uncertainty about dredge efficiency was included (see below). Capture efficiency was assumed to be 100% in the dredge and HabCam surveys for scallops 40+ mm SH in calculating swept-area abundance for this analysis. Thus, capture efficiency was factored in to all of the survey abundance data prior to use here.

As in the CASA model analysis, dredge survey abundance estimates were adjusted to account for scallops in deep or shallow water areas not sampled by the dredge but no adjustments were made for areas of poor habitat within the survey area. Survey abundance at length data were not adjusted for errors in measuring shell height as in the CASA model although such errors are appreciable in the optical surveys because the adjustment requires information available in a simulation based stock assessment model. These type of errors smooth size composition estimates making modes lower, valleys higher and proportions in the largest and smallest length groups larger (Jacobson et al. ???).

Five mm length groups (40-45, 45-50 ...) were used and the last length group was always a plus group. Intermediate calculations included all of the size groups in the original data but results are summarized using a 140+ mm size group, which is roughly the same as von Bertalanfy L_{max} (asymptotic mean size) estimates. Only years 2003-2013 were included because at least two surveys (dredge+SMAST, dredge+HabCam, or dredge+SMAST+HabCam) were conducted each year. Using multiple independent surveys helps smooth estimates without using a population dynamics model like CASA.

Total abundance in each year and for each size group ($N_{y,L}$) was estimated by averaging swept-area abundance estimates from each survey:

$$N_{y,L} = \frac{\sum_s N_{s,y,L}}{n_{s,y}}$$

where $N_{s,y,L}$ was swept area abundance data for year y and survey s while $n_{s,y}=2$ or 3 was the number of surveys. Total survey stock abundance was $N_y = \sum_L N_{y,L}$. Stratified random CVs for mean total number per tow and the number of positive tows by year in the dredge survey provide some information about precision of abundance data (Table 1 and Figure 1).

Variances for $N_{y,L}$ were calculated from length specific average CVs for mean number per tow in the dredge survey. Length specific variances were not easily available for the SMAST and HabCam surveys. In particular:

$$Var(N_{s,y,L}) = (CV_L N_{s,y,L})^2$$

where CV_L is the average CV at length in the dredge survey for either Georges Bank or the Mid-Atlantic (Figure 2). CVs for total abundance N_y were from the CVs for total catch per tow in each survey (Figure 1):

$$Var(N_{s,y}) = CV_{s,y} N_{s,y}$$

and:

$$Var(N_y) = \sum_s Var(N_{s,y})/n_s^2.$$

Dredge survey abundance CVs were increased to account for uncertainty in capture efficiency. CVs for dredge survey capture efficiency were $0.034/0.243=0.14$ (gravel/cobble) and $0.022/0.4=0.05$ (sand, Appendix B4). Therefore, the adjusted CV for a dredge survey abundance estimate was $\sqrt{CV_{s,y}^2 + 0.1^2}$ where 0.1 is close to the average CV for gravel/cobble and sand.

Uncertainty about stock area, area sampled, and other factors were ignored in calculating survey abundance. However, variance from these factors was probably modest relative to the variance in mean catch per tow and capture efficiency for the dredge survey. Uncertainty about stock area is relatively small because scallops are sessile with a static spatial distribution that is well defined by the optical surveys and covered effectively by each survey after the dredge data are adjusted for area not surveyed. Uncertainty about size selectivity in the experimentally derived size selectivity curve for the SMAST survey was ignored for lack of time but could have been included.

For plotting, mean abundance at length estimates were smoothed with GAM models fit assuming gamma errors using the mgcv library in the R programming language (Wood 2006):

$$\text{gam}(y \sim s(x), \text{family}=\text{Gamma}(\text{link}=\text{log}), \text{weights}=\text{wts})$$

The variances used for weights were, for example, $Var(N_{y,L}) = [N_{y,L} CV(N_{y,L})]^2$. Assuming predicted values were gamma distributed, 95% percent confidence intervals were calculated for means equal to the fitted values and variances $Var(\hat{N}_{y,L}) = [\hat{N}_{y,L} CV(F_{y,L})]^2$. The variance of the fitted values calculated in the GAM was not used because it grossly underestimated uncertainty. Better confidence intervals might have been obtained by combining the CV above with the CV for uncertainty in the smooth trend calculated by the GAM software.

Fishing mortality rates by year and length ($F_{y,L}$) were approximated by dividing catch numbers by estimated abundance:

$$F_{y,L} = \frac{C_{y,L}}{N_{y,L}}$$

Where $C_{y,L}$ is catch number at length. This approximation is reasonable because the instantaneous rate of fishing mortality is exactly $F = C/\bar{N}$ (Ricker 1975) and because scallop surveys tend to occur near the middle of the year when abundance may be similar to average abundance (Table 2).

Catch numbers at length in each year ($C_{y,L}$) were calculated:

$$C_{y,L} = \frac{W_y}{m_y} p_{y,L}$$

where W_y is total meat weight for landings, m_y is mean weight of scallops in the catch and $p_{y,L}$ is a size-specific proportion of the total commercial catch. The mean weight (m_y) was calculated from commercial size composition data, survey shell height-meat weight parameters and annual commercial meat weight anomalies as in the CASA model.

Variances for fishing mortality were approximated based on CVs for average survey abundance and an assumed CV=10% for catch to give $CV(F_{y,L}) = \sqrt{CV(N_{y,L}) + 0.1^2}$.

Abundance weighted fishing mortality (all sizes combined) was approximated $F_y = C_y/N_y$ with $(F_y) = \sqrt{CV(N_y) + 0.1^2}$.

CASA models include a correction for incidental mortality which is highest on the smallest size groups. This adjustment was not made in the empirical analysis because it requires an a-priori estimate of fishing mortality and fishery selectivity not available in the empirical analysis. Therefore, fishing mortality $F_{y,L}$ and F_y are underestimated relative to total fishery mortality. Fishing mortality attributable to landings and fully recruited fishing mortality are unaffected.

GAM models were used to smooth fishing mortality at size estimates and confidence intervals were estimated in a manner similar to abundance at size. The variances used for weights were $Var(F_{y,L}) = [F_{y,L} CV(F_{y,L})]^2$ and the variances used to calculate confidence intervals were $Var(\hat{F}_{y,L}) = [\hat{F}_{y,L} CV(F_{y,L})]^2$. Fully recruited fishing mortality was estimated using the gam model to predict $F_{y,L}$ over a wide range of narrowly spaced shell height values and selecting the largest value of predicted $F_{y,L}$.

Commercial size selectivity estimates are useful although not required in the empirical assessment or in projections which are handled independently in the SAMS model. However, for illustration, size selectivity by year and size $s_{y,L}$ was estimated by rescaling fishing mortality at size:

$$s_{y,L} = \frac{F_{y,L}}{\max(F_{y,L})}$$

and then smoothing the rescaled estimates using a model for proportions:

$$\text{gam}(y \sim s(x), \text{family} = \text{quasibinomial}, \text{weights} = \text{wts})$$

The weights were one when estimating selectivity at size in individual years. Weights equal n_s were used when selectivity estimates for multiple years were combined to estimate average fishery selectivity. After the GAM model was fit, predicted selectivity were rescaled again to a maximum value of one. Fishable abundance (available to the fishery) in each year A_y can be calculated using abundance at size and a fishery selectivity estimate although the estimates are not required for this empirical assessment. For example:

$$A_y = \sum_L s_L N_{y,L}$$

Results

Empirical abundance at size estimates appear reasonably precise and smooth although the smoothness is due partly to measurement errors in survey size data (Figure 3). The progression of two large year classes is clear during 2003-2006 in the Mid-Atlantic and during 2012-2013 in

both regions. There are clear differences between the two regions in population size composition (e.g. the 140+ mm size group) seem clear. Important aspects of the fishery (relatively low exploitation rates and targeting large animals) are evident in comparing abundance and catch numbers at size (Figure 4).

Empirical fishing mortality at length data show that fishing pressure is higher in the Mid-Atlantic than on Georges Bank (Figure 5). The working group concluded that the variation over time in fishery selectivity between domed and ascending patterns could be explained in terms of management measures that: 1) increased the minimum ring size on commercial vessels and decreased selectivity of small scallops during 1994-1995, 2) recruitment events, and 3) management measures that opened and closed rotational harvest areas where large scallops were common. Average fishery selectivity curves for 2003-2013 illustrate how selectivity for particular time periods can be estimated as needed for management related or other analyses (Figure 6).

Empirical abundance and fishing mortality for the combined Mid-Atlantic and Georges Bank regions were calculated by summing catch numbers and abundance for the Mid-Atlantic and Georges Bank regions and then computing approximate fishing mortality rates from the ratio of the sums. CVs and were calculated using standard formulas for sums of random variables.

Empirical and CASA model estimates of abundance and fishing mortality show similar trends in all regions (Tables 3-4 and Figure 7). However, empirical abundance estimates were generally higher reflecting the tension in CASA models between matching the scale of the abundance data (matching the prior on Q) versus fitting the survey and fishery data. As expected, fishing mortality show the inverse pattern with empirical generally lower than CASA estimates.

Fully recruited fishing mortality estimates from empirical calculations were usually lower than from CASA the CASA model as well (Figure 8). However, the comparison may not be very useful because of fully recruited F depends on fishery selectivity assumptions which differed in the two assessment approaches.

Status determination and catch advice

No special provisions are necessary for providing catch advice to the scallop fishery using the empirical methods. Catch advice is generated using a simulation models (SAMS) which is initialized using best estimates of abundance at length from surveys (i.e. using the empirical method).

Reference points used to determine if the scallop stock is overfished or if overfishing is occurring are more difficult. For this assessment, it would be reasonable to compare empirical fishing mortality estimates to reference points calculated in terms of landings divided by 1 July abundance from the SYM reference point model. The CASA model may be problematic due to the tension between scale of the model estimates and general fit to the data. However, the current condition of the stock (not overfished and overfishing not occurring) is clear based on both sets of models and common sense. Empirical and CASA results are broadly similar. If the trend in B/B_{MSY} estimates from the CASA and SYM models are roughly correct, then the ratio for 2013 should be sufficient to determine if the stock is overfished despite uncertainty about scale.

Advantages and disadvantages

It was advantageous to use both empirical and the complex CASA modeling approach for CASA, if only for comparison and to determine if the CASA model results were plausible. Empirical estimates depend almost entirely on data while the CASA model depends on data, biological assumptions (e.g. about growth and natural mortality) and modeling techniques. The empirical approach requires fewer assumptions about growth, natural mortality, size selectivity, etc. and uses most of the data also used in CASA. However, the empirical approach is sensitive to survey measurement errors which are relatively high in the Georges Bank area. It is therefore necessary to have multiple surveys each year for empirical estimation. The empirical approach cannot be applied in all years and the CASA model may give a clearer long term perspective on stock size and productivity.

In theory, the CASA model should do a better job of balancing goodness of fit to survey, catch and size composition data to estimate realistically smooth population trends. However, experience with many real stocks and models indicates that stock assessment models often have pathological problems that may be difficult to resolve due to many potential causes including inaccurate catch data, changes in natural mortality, etc..

An assessment model like CASA makes it easier to calculate reference points. Empirical reference point methods were not evaluated in this assessment but there are a number of methods that could be applied.

Empirical estimates do not suffer from retrospective patterns, which are usually blamed on model structure or assumptions about the data which may remain hidden in empirical analyses. CASA model results did not show retrospective error in this assessment but this was probably due to the proximity of the estimates to priors for survey capture efficiency with tension in the model pulling abundance estimates low enough so that implied capture efficiency estimates were trapped near the upper prior bound. The empirical estimates in this assessment for 2003-2013 are less sensitive to errors in historical catch which are often suspected when modeling problems occur.

Reference:

NEFSC. 2007. 45th Northeast Regional Stock Assessment Workshop (45th SAW): 45th SAW assessment report. US Dep Commer, Northeast Fish Sci Cent Ref Doc 07-16.

Table 1. Numbers of tows in which at least one scallop was caught in the MAB and GBK areas during dredge surveys during 2003-2013 by size group. For example, the 40 mm size group is 40-44.9 mm SH. The last size bin (140+ mm SH) is a plus group. The number of positive tows is a lower bound estimate for the effective sample size in each year/size group category..

Year	Size group (mm)																				
	40	45	50	55	60	65	70	75	80	85	90	95	100	105	110	115	120	125	130	135	140+
MAB																					
2003	110	113	120	127	145	146	145	151	147	145	152	158	160	159	156	157	135	122	91	56	39
2004	124	132	145	137	150	146	154	170	187	192	191	188	187	186	192	187	169	150	120	84	41
2005	157	160	170	161	147	152	142	168	188	205	215	217	220	224	224	223	216	210	194	164	127
2006	111	139	160	176	196	232	222	231	242	235	239	240	246	250	248	252	246	234	211	163	117
2007	70	97	130	148	150	172	186	204	209	218	237	249	250	257	250	249	244	237	203	168	131
2008	168	183	179	178	176	158	154	159	172	180	199	214	217	222	215	217	207	202	175	149	125
2009	77	88	104	97	114	108	121	147	152	151	160	152	157	153	162	157	156	150	130	103	86
2010	141	156	156	135	131	117	122	134	171	199	219	227	240	236	234	241	233	227	196	132	100
2011	119	149	151	146	123	111	96	117	165	191	223	214	219	225	232	230	238	238	225	187	163
2012	155	165	158	141	131	120	126	149	156	174	185	187	192	211	208	201	213	217	204	171	119
2013	99	129	164	167	213	216	229	227	222	232	231	238	224	220	220	216	213	214	203	161	140
GBK																					
2003	64	72	76	84	99	92	95	99	96	110	115	116	124	137	137	131	131	139	128	114	122
2004	83	94	96	105	102	92	95	108	120	141	140	145	148	156	153	164	166	169	163	141	140
2005	46	57	98	94	108	101	106	109	133	142	164	177	205	229	245	254	267	277	276	256	248
2006	67	74	88	103	108	96	103	96	93	112	127	138	138	144	154	154	170	172	173	165	172
2007	153	181	217	215	240	222	204	189	190	185	199	202	210	212	208	246	271	276	277	274	284
2008	111	114	129	146	156	145	131	141	138	148	158	174	178	183	168	170	159	176	169	180	196
2009	95	107	135	132	128	126	119	117	130	145	158	160	156	162	164	162	160	161	152	148	168
2010	81	77	92	88	111	108	117	130	152	150	170	161	185	193	214	215	219	223	224	206	216
2011	44	44	43	50	68	72	85	92	119	132	146	138	154	148	155	176	177	184	180	176	184
2012	61	86	100	105	100	94	107	107	125	133	144	155	151	157	168	174	176	181	181	178	177
2013	81	106	115	123	138	139	118	108	112	116	122	126	134	133	141	142	155	153	163	156	161

Table 2. Dates (Julian) for sea scallop surveys during 2003-2013 in the MAB and GBK regions.

Survey	Mid-Atlantic			Georges Bank			Comment
	Min	Max	Mid	Min	Max	Mid	
Dredge	130	215	173	163	230	197	1979-2013
SMAST	130	194	162	165	233	199	2003-2009
HabCam	153	201	177	159	210	184	2011-2012 for the Mid-Atlantic and 2011-2013 for Georges Bank

Table 3. Abundance and fishing mortality (estimates from the empirical approach and CASA model for the Georges Bank (top) and Mid-Atlantic (bottom) regions).

Year	Empirical					CASA	
	Abundance (Mid-year, 40+ mm, 10 ⁶)	CV	Landings	Aprox. F	CV	Abundance (1 July, 40+ mm, 10 ⁶)	Landings/ Abundance
Georges Bank							
2003	4,145	0.10	173	0.04	0.14	3,517	0.05
2004	3,788	0.12	133	0.04	0.15	3,159	0.04
2005	3,660	0.11	267	0.07	0.15	3,132	0.09
2006	3,216	0.11	448	0.14	0.15	2,769	0.16
2007	3,979	0.11	249	0.06	0.15	3,219	0.08
2008	3,941	0.10	179	0.05	0.14	3,300	0.05
2009	5,332	0.12	221	0.04	0.15	3,690	0.06
2010	4,883	0.17	170	0.03	0.19	3,801	0.04
2011	4,169	0.12	217	0.05	0.15	4,194	0.05
2012	3,498	0.08	316	0.09	0.13	4,607	0.07
2013	4,073	0.14	365	0.09	0.17	5,620	0.06
Mid-Atlantic							
2003	13,601	0.31	807	0.06	0.33	5,511	0.15
2004	7,324	0.21	918	0.13	0.23	4,036	0.23
2005	6,154	0.15	545	0.09	0.18	4,811	0.11
2006	6,261	0.15	272	0.04	0.18	4,226	0.06
2007	5,521	0.15	503	0.09	0.18	4,310	0.12
2008	6,340	0.13	463	0.07	0.16	4,647	0.10
2009	5,312	0.11	664	0.13	0.15	3,202	0.21
2010	3,794	0.11	687	0.18	0.15	2,458	0.28
2011	2,747	0.10	598	0.22	0.14	1,606	0.37
2012	4,617	0.10	365	0.08	0.14	3,387	0.11
2013	4,163	0.14	219	0.05	0.17	2,648	0.08

Table 4. Abundance and fishing mortality (estimates from the empirical approach and CASA model to the combined Georges Bank plus Mid-Atlantic regions (whole stock).

Year	Empirical			CASA			
	Abundance (Mid-year, 40+ mm, 10 ⁶)	CV	Landings	Aprox. F	CV	Abundance (1 July, 40+ mm, 10 ⁶)	Landings/ Abundance
Whole stock							
2003	17,746	0.24	980	0.06	0.26	9,028	0.11
2004	11,112	0.14	1,051	0.09	0.17	7,195	0.15
2005	9,814	0.11	812	0.08	0.15	7,942	0.10
2006	9,477	0.11	720	0.08	0.15	6,994	0.10
2007	9,500	0.10	752	0.08	0.14	7,529	0.10
2008	10,281	0.09	643	0.06	0.13	7,946	0.08
2009	10,644	0.08	885	0.08	0.13	6,891	0.13
2010	8,677	0.11	857	0.10	0.15	6,259	0.14
2011	6,915	0.08	815	0.12	0.13	5,799	0.14
2012	8,115	0.07	681	0.08	0.12	7,995	0.09
2013	8,237	0.10	584	0.07	0.14	8,269	0.07

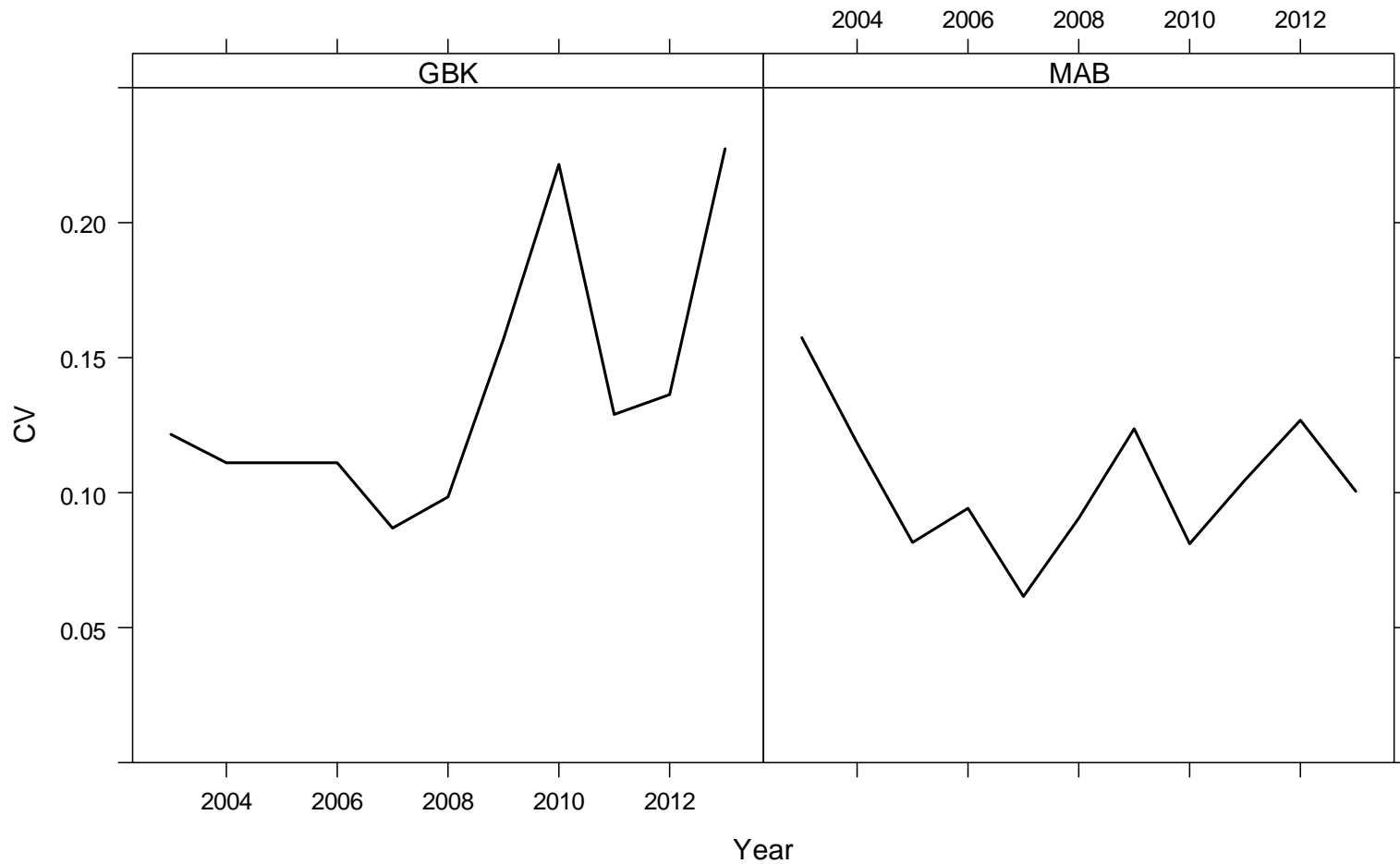


Figure 1. CVs for total mean catch per tow (all sizes) in the dredge survey during 2003-2013.

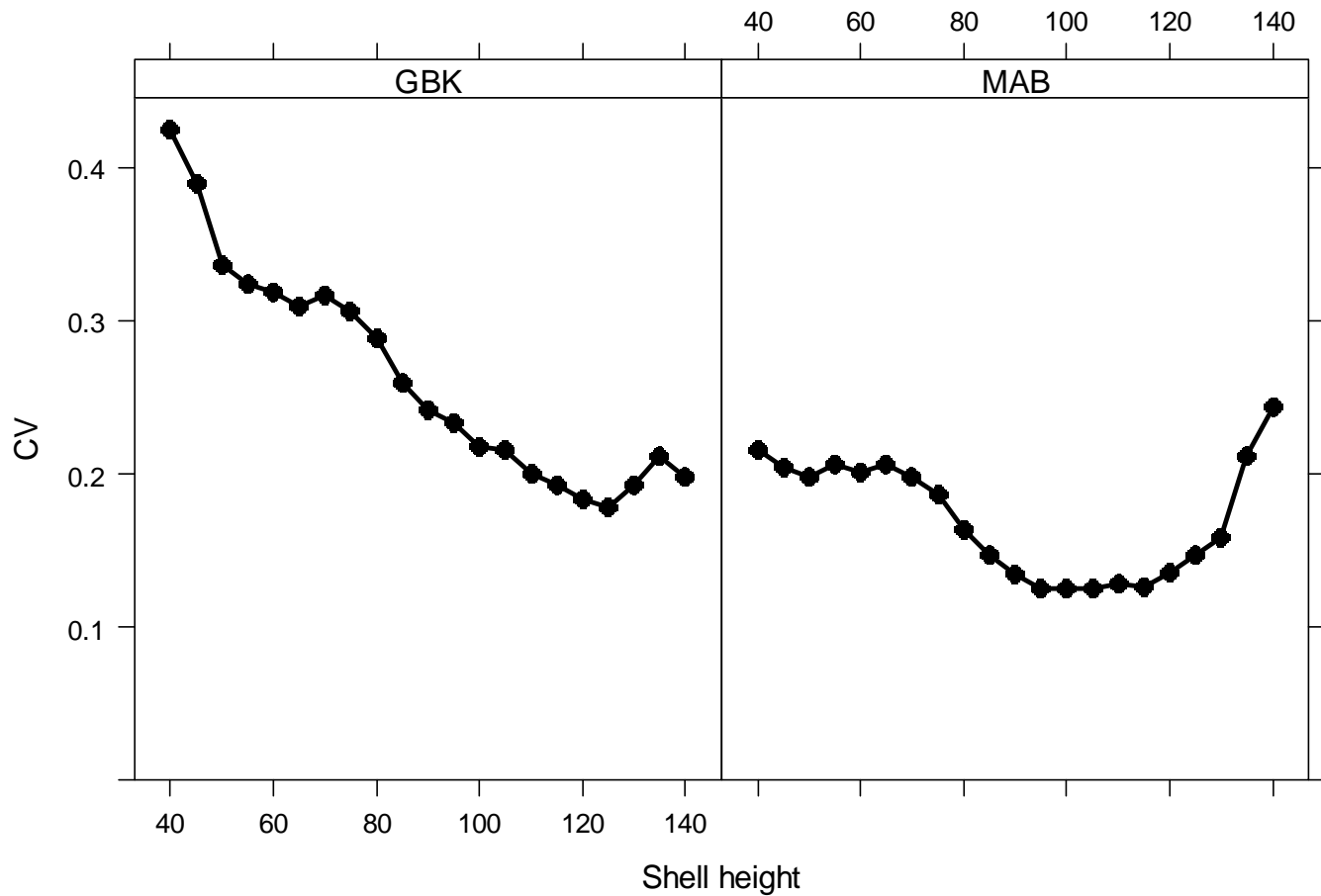


Figure 2. Average CVs for mean scallop catch per tow in the dredge survey during 1978-2013 by shell height size group and stock area.

MAB empirical population abundance and 95% CI (y-axis varies)

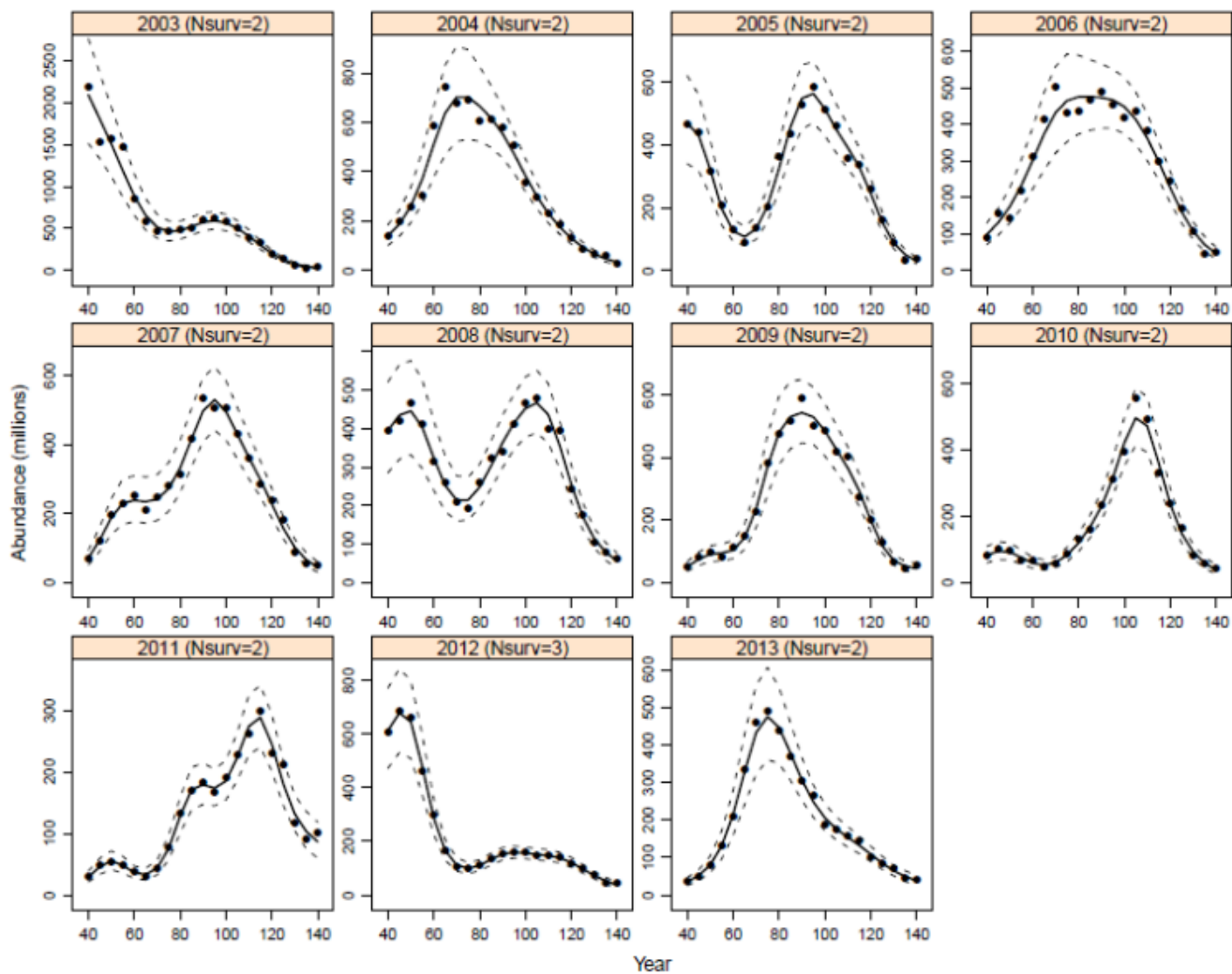


Figure 3a. Empirical abundance at length during 2003-2013 in the Mid-Atlantic region with approximate 95% confidence intervals. Note that the scales on the y-axis vary.

GBK empirical population abundance and 95% CI (y-axis varies)

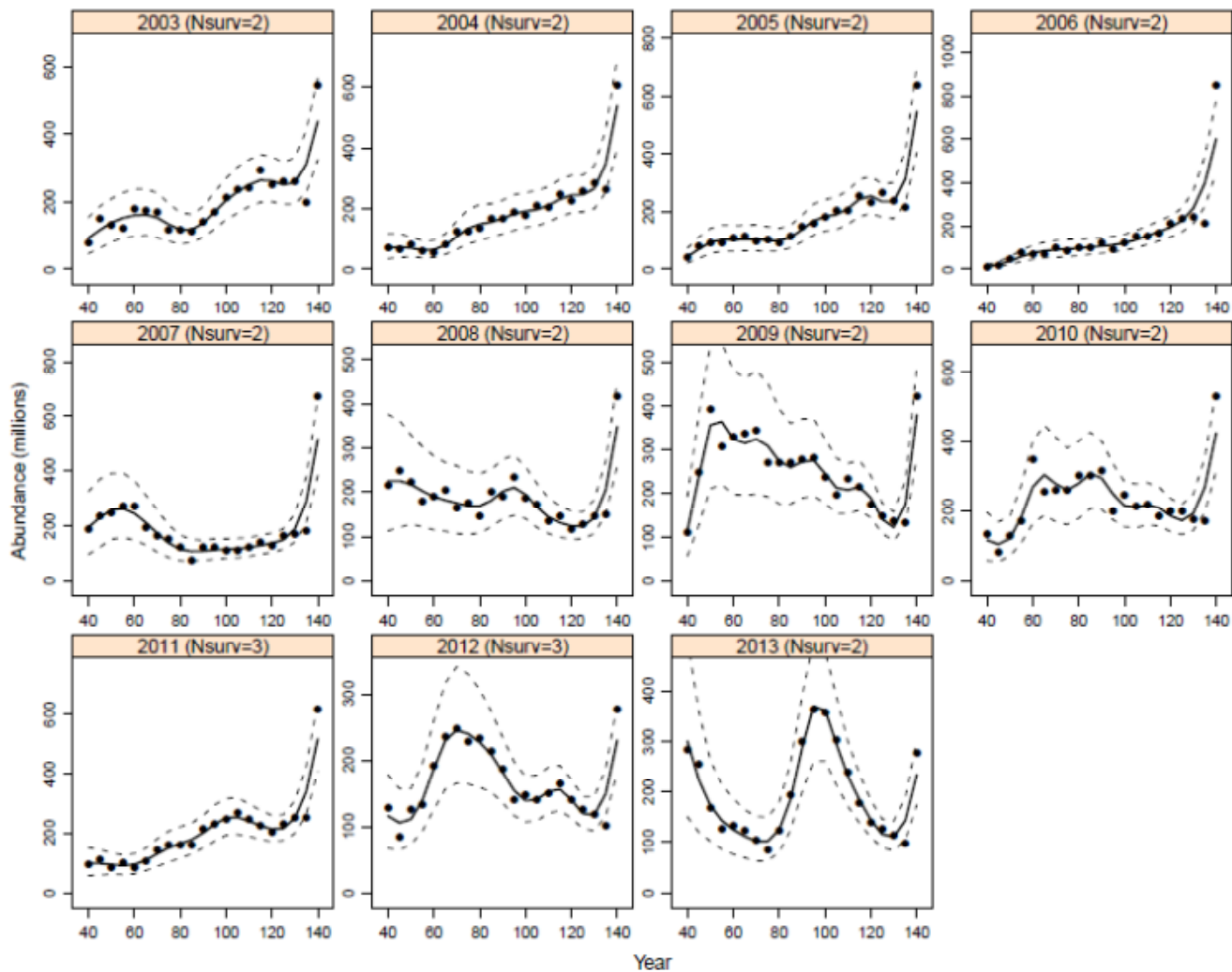


Figure 3b. Empirical abundance at length during 2003-2013 in the Georges Bank region with approximate 95% confidence intervals. Note that the scales on the y-axis vary.

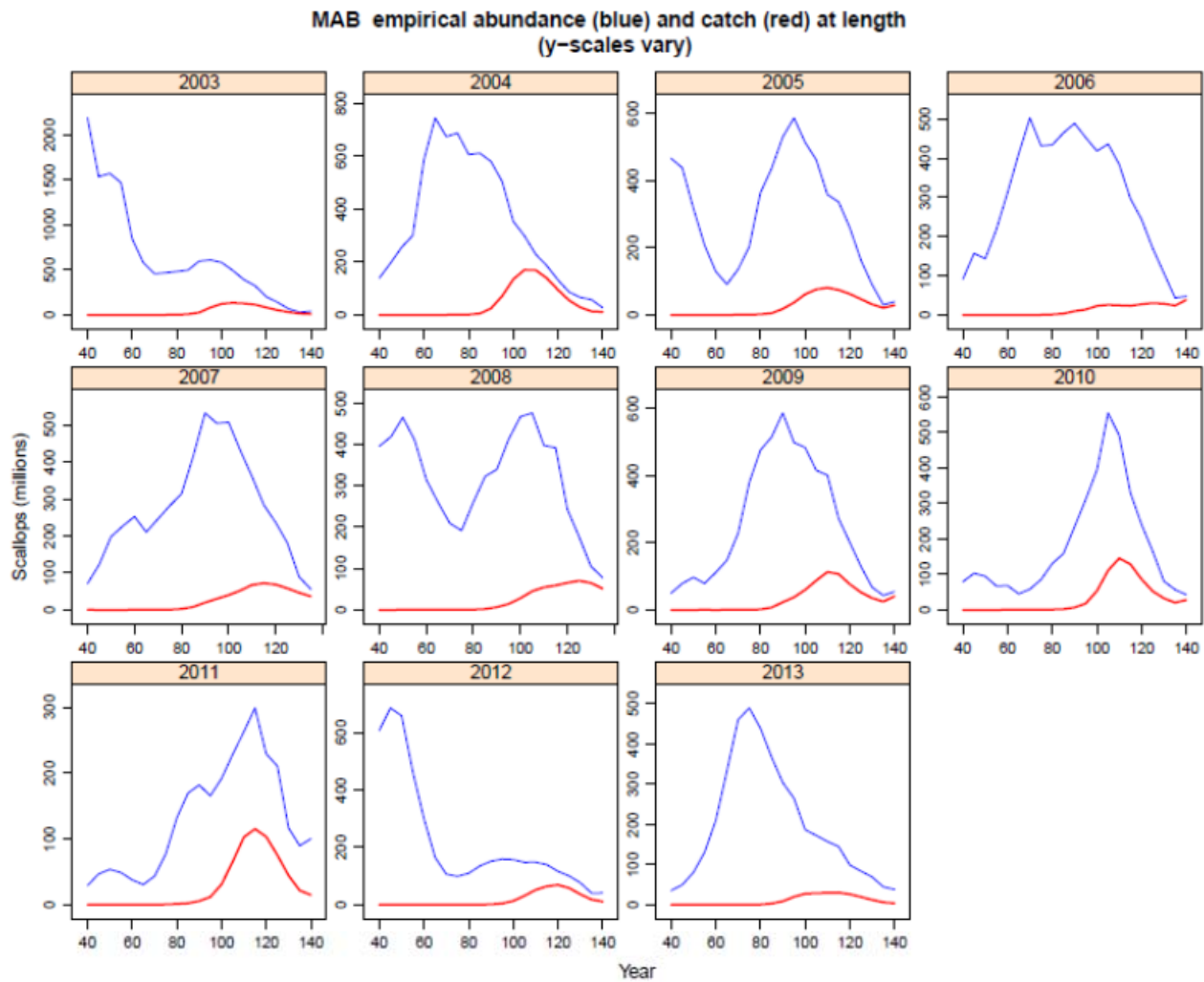


Figure 4a. Empirical abundance and catch at length during 2003-2013 in the Mid-Atlantic region. Note that the scales on the y-axis vary.

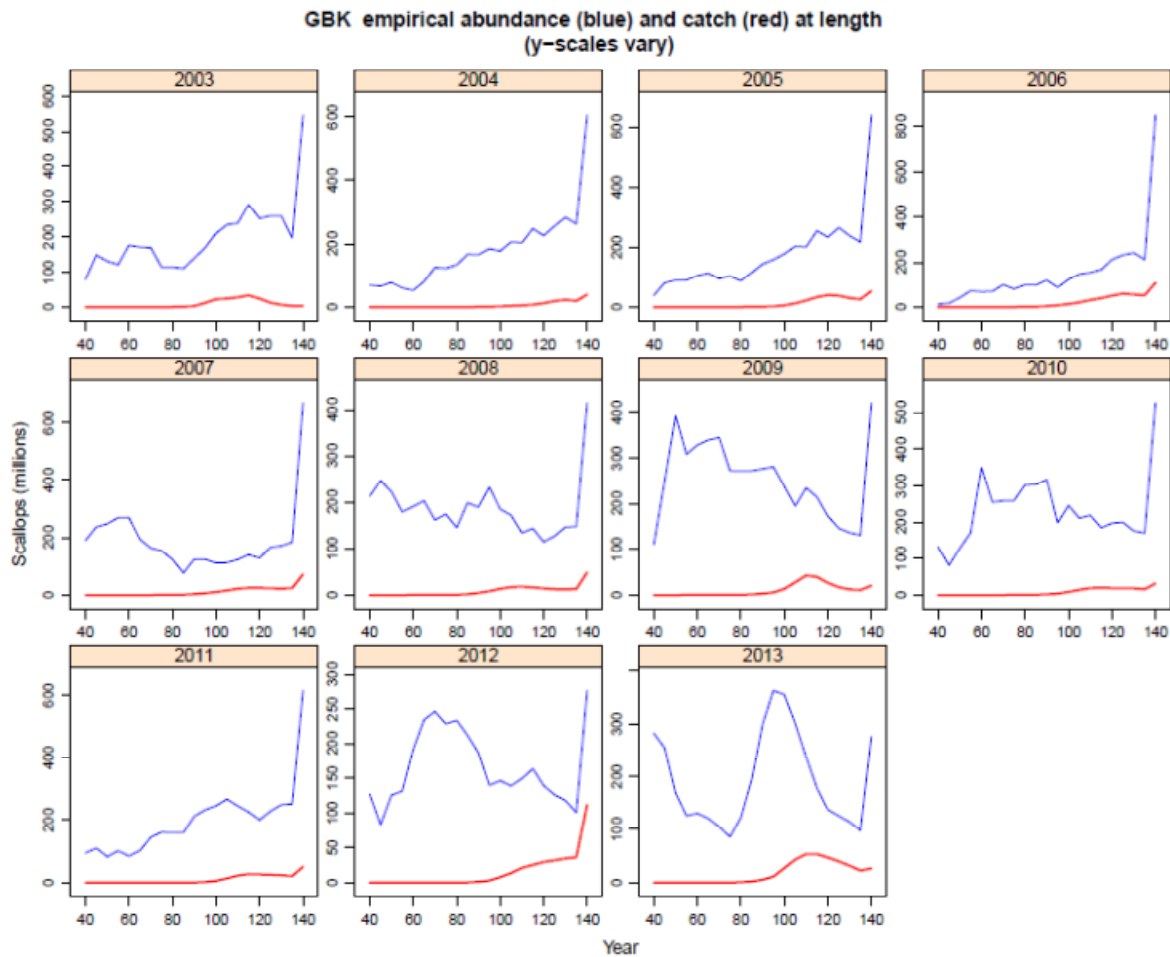


Figure 4b. Empirical abundance and catch at length during 2003-2013 in the Georges Bank region. Note that the scales on the y-axis vary.

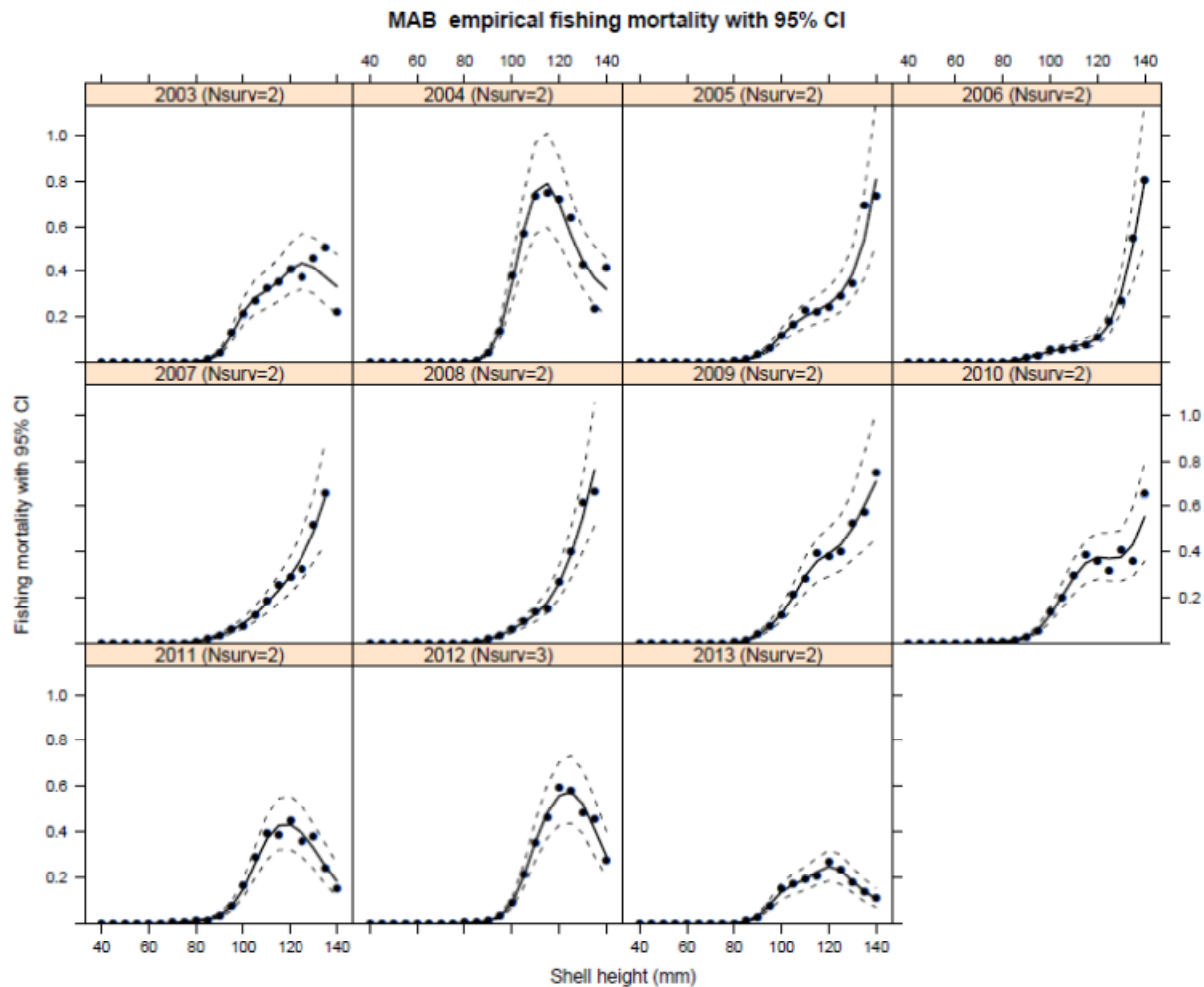


Figure 5a. Empirical fishing mortality at length during 2003-2013 in the Mid-Atlantic region with approximate 95% confidence intervals. Note that the scales on the y-axis differ (fishing mortality was typically higher in the Mid-Atlantic region).

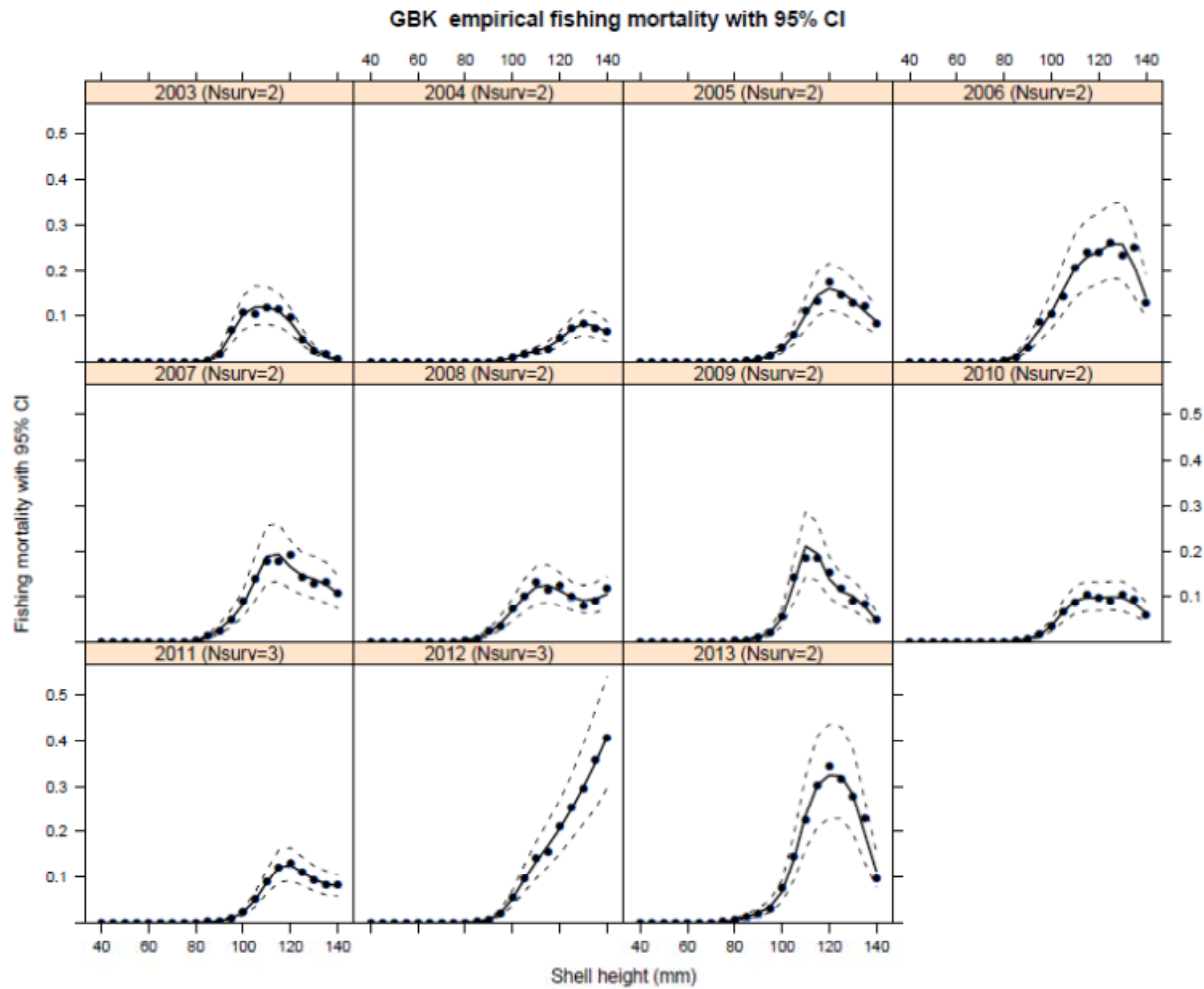


Figure 5b. Empirical fishing mortality at length during 2003-2013 in the Georges Bank region with approximate 95% confidence intervals. Note that the scales on the y-axis differ (fishing mortality was typically higher in the Mid-Atlantic region).

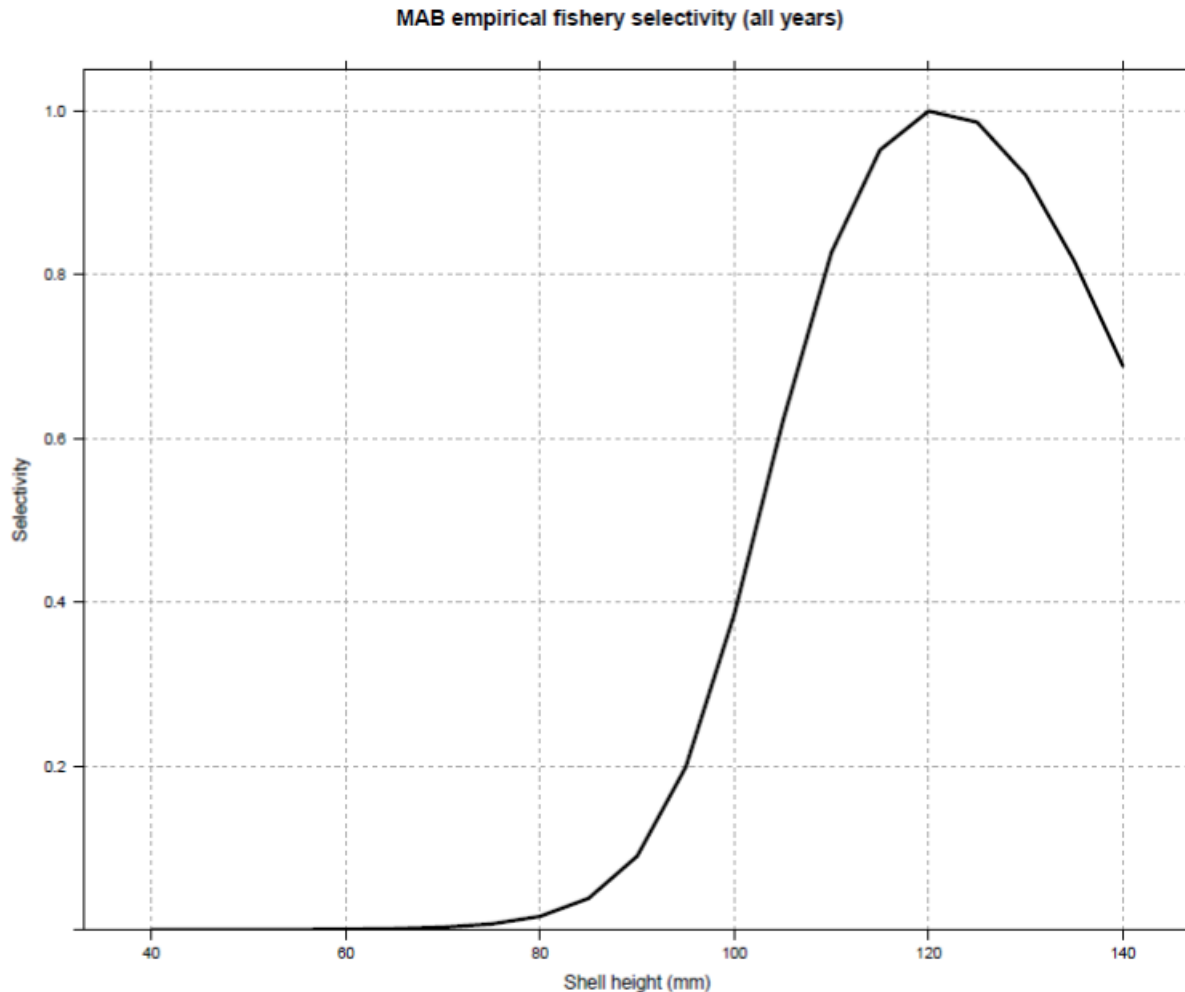


Figure 6a. Empirical estimates of average size selectivity for the scallop fishery during 2003-2013 in the Mid-Atlantic region. This curve was calculated by pooling data for different years and fitting a single line to show the trend. Another approach is to average the fitted selectivity curves for each year.

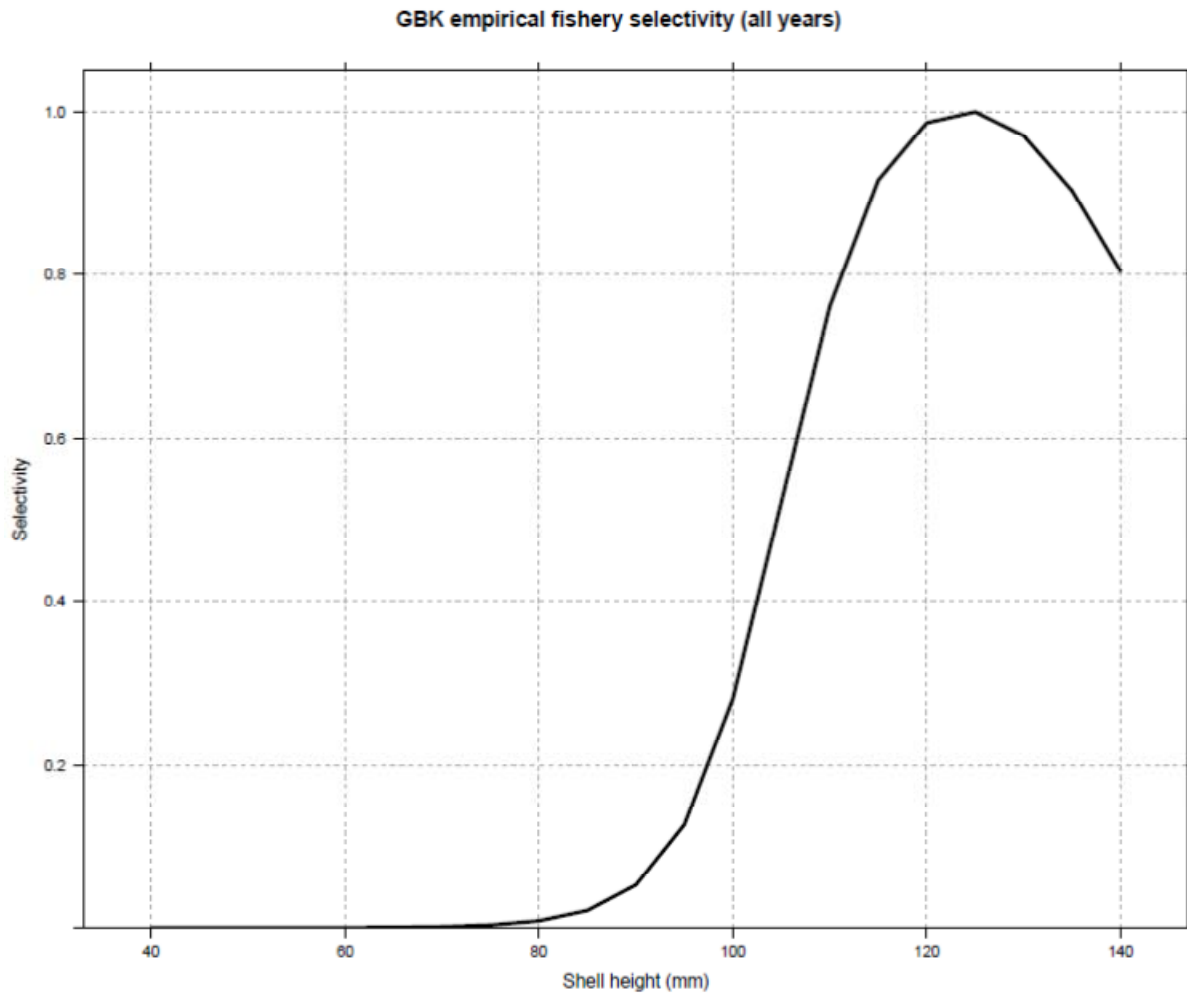


Figure 6b. Empirical estimates of average size selectivity for the scallop fishery during 2003-2013 in the Georges Bank region. This curve was calculated by pooling data for different years and fitting a single line to show the trend. Another approach is to average the fitted selectivity curves for each year.



Figure 7. Abundance (left) and fishing mortality estimates (right) from the empirical method and the CASA model during 2003-2013 for the Georges Bank (top), Mid-Atlantic (middle) and combined (bottom) regions.

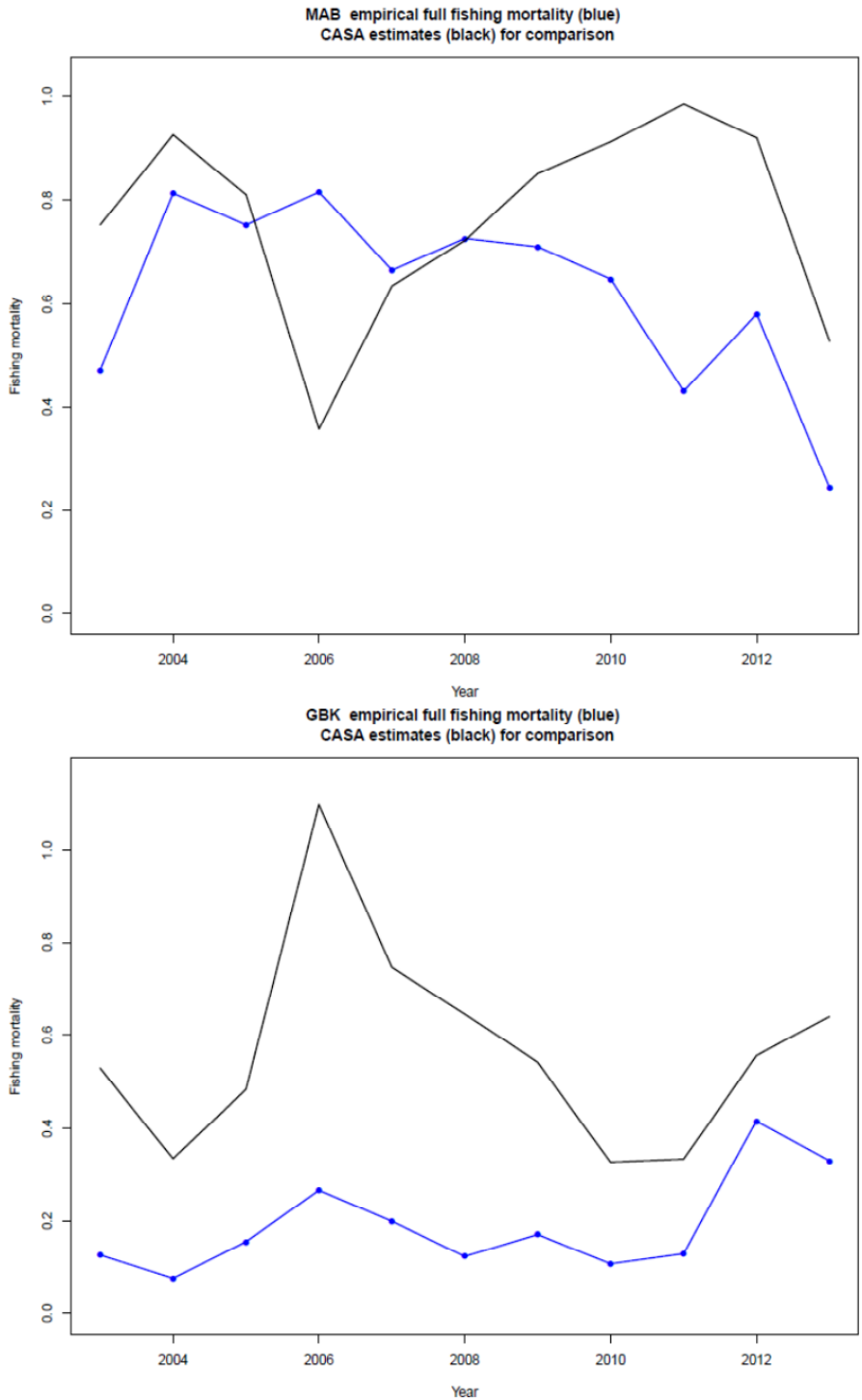


Figure 8. Fully recruited fishing mortality estimates for the Mid-Atlantic (top) and Georges Bank (bottom) regions. The empirical estimates are in blue, CASA estimates are black.

Appendix B6. NEFSC HabCam survey for sea scallops: survey design, implementation, and data analysis.

Jui-Han Chang, Burton Shank, and Dvora Hart. Northeast Fisheries Science Center, Woods Hole MA.⁴

This report contains five stand-alone sections that together describe HabCam gear and operations, simulation work used to develop and test survey designs, how the actual surveys during 2011-2013 were carried out, and how abundance estimates and size composition for 2011-2013 used in assessment models were made.

1. Introduction to the HabCam survey

HabCam is an underwater vehicle that was originally developed through collaboration of commercial fishermen, independent scientists, and staff at the Woods Hole Oceanographic Institute as a vehicle for documenting the size and abundance of benthic / demersal organisms and mapping sea floor habitats. The vehicle is towed behind a vessel, while actively “flown” ~2m off the bottom by a pilot. It collects overlapping, downward facing digital still imagery. Between 2005 and 2010, the HabCam group developed and improved this technology and successfully performed a number of surveys on the Mid-Atlantic continental shelf, Georges Bank and in the Gulf of Maine, primarily using the HabCam_V2 vehicle which preceded the current design. The development of the vehicle and many of these surveys were supported by the Sea Scallop Research Set-Aside program and the vehicle proved to be appropriate technology for assessing sea scallops (NEFSC 2010). In 2009 a paired HabCam / dredge experiment was conducted to determine the capture efficiency of the NEFSC survey dredge (probability of catching a scallop in the path of the dredge) and in 2011 the HabCam_V2 was used in the NEFSC scallop survey to get an estimate of the entire scallop resource on Georges Bank.

With an interest in making a HabCam-type survey a standard part of the sea scallop assessment survey, NEFSC secured funds from NOAA Office of Science and Technology and contracted WHOI to build a vehicle for NEFSC’s use. This vehicle, (HabCam_V4 or NOAA HabCam), completed resource-wide surveys in 2012 and 2013, beginning a new assessment time series for sea scallops that is used for the first time in this assessment. The HabCam_V4 vehicle is equipped with stereo digital still cameras, altimeters, and a compliment of oceanographic sensors including temperature, salinity, water spectrometer, 3D side-scan sonar, and optical sensors for dissolved oxygen, cdom, and turbidity.

2. Survey Design

Because the HabCam vehicle collects a constant track of images, data derived from the images are autocorrelated and not appropriate for analysis as a random or stratified survey. Resource assessments from such data are typically use spatial models including Generalized Linear Models (GLMs) and Generalized Additive Models (GAMs) or geostatistical methods

⁴ First and second coauthors alphabetical.

such as kriging (Rivoird et al. 2008). Literature on sampling designs for this type of survey comes primarily from literature on acoustic surveys. With geostatistical methods, the uncertainty in the estimate at any given location increases with distance from the survey track. As a result, evenly spaced grids are optimal for acoustic surveys as the distance from the survey track is minimized with even spacing. A second common survey design is a two-stage approach where a low resolution survey is first performed to determine the location of high-density aggregations and a second high-resolution survey is conducted on the aggregations. The results from two-stage surveys are post-stratified to account for spatial heterogeneity in survey effort. In both cases, geostatistical methods assume that the mean and variance is homogeneous throughout a survey stratum.

The HabCam sea scallop survey differs from these situations because adult sea scallops are relatively easy to detect and intensively surveyed, do not move long distances, and because spatial heterogeneity is primarily driven by management measures and known habitat affinities. While geostatistical methods assume a landscape with a stationary mean (Figure 1a), a landscape with a higher mean along the center of the landscape (Figure 1b) is more realistic for sea scallops because densities typically decrease in habitats deeper and shallower than the optimal habitat for a region (Figure 1c). In this case, it may be advantageous to increase sampling effort in the core habitats along the center of the survey area. Given a survey track of evenly-spaced transects of equal length (Figure 2a) and assuming an underlying variogram model, we can derive a map of kriging variances for the survey at each location in the landscape (Figure 2b). If the mean density is higher in the center of the landscape instead of stationary, we may assume that the standard deviation of the mean is proportional to the mean (similar to a Gamma distribution) and calculate an adjusted kriging variance for each location as:

$$\text{AdjVar}_{x,y} = \text{KrVar}_{x,y} * [e^{(\text{CE})}]^2 \quad (2.1)$$

Where $\text{AdjVar}_{x,y}$ is the adjusted variance of the estimate at a given location, $\text{KrVar}_{x,y}$ is the unadjusted variance at the location and $e^{(\text{CE})}$ is the magnitude of the center effect from Figure 1c.

As a proof of concept, we used geostatistical simulation to examine the effect of allowing the mean (and variance) to vary across the shelf and longitudinally along the shelf. We first simulated varying the mean across the shelf and examined how the survey variances were affected by varying (1) the proportion of the effort concentrated along the center of the survey area and (2) the length of the survey track. We modeled the cross-shelf gradient as a double-logistic with higher densities along the center of the study area and the amplitude of the center effect varying from 0 (no effect) to 1 (variance is e^2 or 7.38 times higher along the center of the study area (Figure 3). To assess the effect of increasing sampling intensity along the center of the study area, we decreased the length of alternating transects (range from 0 – 100% of the total width of the study area) and increased the total number of transects to keep the total survey track length constant (Figure 4). We then varied the total survey track length from 1,000 to 4,000 pixels. For each simulation, we examined the resulting variance maps (i.e. Figure 5) and used the sum of the adjusted kriging variance (eq. 2.1) as a relative proxy for the variance of the survey. While this is not the true variance of the survey, as the variances are correlated across the landscape, we are not aware of established methods for calculating a kriging variance for survey areas with non-stationary variances and this should be an effective relative measure for

comparison purposes.

The adjusted kriging variances varied across center effects and transect lengths (Figure 6). Optimal short transect lengths decreased as center effects increased and increased as total track length increased. The center effect and total track length interacted to produce an optimal short transect length. With a track length of 1,000 pixels, increasing the center effects from 0 and 1 decreased optimal short transect length from 67% to 30%. However, for track lengths of 4,000 pixels, varying the center effect from 0 to 1 only decreased optimal short transect length from 92% to 85%.

For a second simulation, we examined the effect of the mean and variance varying longitudinally along the survey area (i.e. zonal anisotropy, Figure 7). The zonal effect was implemented by dividing the landscape into two zones (upper and lower) and adding an additional, longitudinally-oriented logistic trend to the landscape. We then varied the amplitude of the longitudinal effect (Zone effect) the spacing of adjacent transects between the two zones, and total track length (Figure 8).

The optimal solutions for landscapes with Zone effects placed more transects in the zone with higher underlying means and variances (Figure 9). The effect was most notable for shorter total track lengths, increasing transect density in the higher mean zone by as much as 300% over the lower mean zone.

3. Survey Area and Design for Actual HabCam surveys

The above simulations indicate that the variance of a survey can be decreased by alternating the length of survey transects and increasing transect density in areas with known higher abundances. These simulation results are used informally in the design of each year's survey but actual survey design is based on researchers' knowledge of where the current stock biomass and incoming cohorts are.

The two stock areas (MAB and GB) are each divided into multiple subregions, based on changes in habitat type, habitat orientation (anisotropy), and management boundaries (Figure 10 and 11). These subregions are used both for designing the survey and for abundance estimation from the resulting survey data.

The extent of the survey area is based on an updated analysis of biomass patterns from the NMFS dredge and RSA surveys, Vessel Trip Reports, sea scallop observer trips, and Vessel Monitoring System data. In general, the current extent of the dredge survey was found to be very adequate for covering the scallop resource, though small areas were added to the extent of the HabCam survey to capture areas where there was evidence of adequate scallop densities or commercial activity.

The survey tracks are constructed in one long track for the MAB and three separate tracks for GB. Each track is bounded by a set of subregions. A midline, drawn along the center of biomass, runs through each set of subregions. Survey transects are centered around and oriented orthogonal to the midline.

3.1 Software and procedures used in designing HabCam surveys

In designing actual surveys, specialized software prompts a user to enter the total effort (survey days) to allocate to a track, the relative lengths of the short transects on the track, and the transect density offset for each subregion along the track. The software varies the relative transect densities and provides a number of alternative tracks of similar lengths for the user to choose among, based on appropriate allocation of effort across the subregions, how well each track works around complex bathymetric structures, and other logistical considerations.

4. Image Acquisition, Processing and Annotation.

The HabCam vehicle is towed along the survey track at speeds from 6 – 7 knots while a pilot maintains the unit at an altitude of ~2m off the bottom. Digital still images are generally collected at a sufficiently high frequency that ~35% of adjacent images overlap. Collected images are initially stored as raw TIFF-formatted images. The raw TIFFs are then light-field and color corrected to improve image quality and saved in processed PNG format. Each image is named with a unique identifier and metadata for each image is recorded including longitude, latitude, time, vehicle depth, bottom depth, and vehicle altitude, roll, and pitch as well as the data from the oceanographic sensors. The altitude of each image is critical for determining the field of view of the image and measuring objects in the images. As altitude can be measured in multiple ways, the value used for a particular image is based on the following list ordered by expected accuracy:

1. Altitude as measured via disparity mapping (parallax) from the stereo images
2. Altitude as measured by the altimeters on the vehicle
3. Altitude inferred from the side-scan sonar

The metadata associated with each image is then stored in a PostgreSQL database and used for selecting images for annotation.

We select blocks of images for annotation, termed “assignments”, based on the spatial extent of the image set and a target image density. Based on the desired density of images to be annotated, we break the survey track into equal length segments and select one image from each segment. Individual image selection is biased towards preferred vehicle heights (Gaussian-weighted, based on known issues with water turbidity or other factors that affect image quality) but image selection is otherwise random within each segment.

The selected image list is uploaded to the Postgres database for direct observation and annotation using a web-based annotation tool. Additional assignments may be created once an assignment is completed if additional images are desired from the same region. In such cases, we first remove all images from a buffered region around each image that has already been annotated from the pool of available images before the next random subset of images is selected. The goal of this is to keep the density of annotated images consistent within subregions along the track.

Data on the abundance, size and behavior of scallops are extracted from each image using an online annotation tool developed by collaborators at WHOI (Figure 12). Only scallops where

the center of the scallop is judged to be inside the image are enumerated. Scallops larger than about 35mm (age 2+) are measured by drawing a line over the shell while smaller scallops are only marked with a point and counted. Additional data are recorded including confidence in identification, swimming, dead, clappers, etc. Image quality may be poor due to turbid waters, extremely high or low altitudes, image corruption, or other objects obscuring the bottom. In this case, the image can be noted as poor quality and data from this image excluded from derived data sets. All annotations, as well as comments on image quality and sediment types, are recorded directly to the Postgres database by the annotation tool.

Because scallops are not always oriented normal to the camera or may be partially obscured, scallops measurements are either shell heights (umbo to opposite margin) or widths (lateral margins), whichever is judged to be more accurate. Shell widths are converted to shell heights using a statistical model derived from paired measurements of scallops that were well oriented to the camera:

$$\text{Shell_height} = 3.538 + 1.034 * (\text{Shell_width}) - 0.0003502 * (\text{Shell_width})^2 \quad (4.1)$$

Shell height is calculated in pixels based on the start and end coordinates of the annotated line. The size of each pixel in an image is calculated from the altitude of the associated image, based on tank calibration experiments, and this pixel size is used to convert the shell height to actual millimeters. The altitude is also used to calculate the field of view for each image for density calculations.

For estimating size frequency distributions and abundance for each year, we constructed standardized data sets from the database and posted them to a common location on a network drive. The annual data sets include data from both the NEFSC HabCam surveys and from the HabCam group RSA surveys, which have to be drawn from multiple databases and corrected individually for problems in altitude measurements or other issues. The data sets include the metadata from all annotated images of acceptable quality, plus the classification of all scallops observed in each image and calculated lengths of for any scallop measured with a line segment.

5. Model-based estimation of sea scallop abundance and biomass

5.1 Introduction and summary

The goal of this section is to assess different model-based methods for estimating total abundance and biomass from HabCam and then apply these methods to HabCam data for 2011 - 2013 data to estimate abundance, biomass and size composition of sea scallops in the Georges Bank (GB) and Mid-Atlantic Bight (MAB) assessment regions (Figures 14 and 15). We also present design-based method (stratified mean) for this data set as an alternative to model-based methods and use it to validate the model-based estimates and CV's.

Scallop abundance or biomass data from HabCam are highly spatially autocorrelated and zero inflated, reflecting the patchiness of scallop distributions and the continuous nature of the observations. Thus, model-based estimation methods might be required to extrapolate observations along the observed track to larger areas. We used 2013 HabCam biomass data to

test 3 geostatistical models: (1) ordinary kriging on spatially averaged data (OK), (2) zero-inflated Generalized Additive Models on spatially averaged data with kriged model residuals (GAM+OK), and (3) zero-inflated Generalized Additive Mixed Models where small scale variations are treated as random effects, combined with kriged model residuals (GAMM+OK). Effects of scale (neighborhood) size to average the data or scale of random effects was also evaluated. Co-located survey data from other gear types (dredge surveys from NEFSC and VIMS and video surveys from SMAST) were used for model validation. No single modeling approach and scale was consistently superior but GAM+OK performed better than OK and GAMM+OK in general.

We then conducted a simulation to evaluate performance of the 3 model-based methods along with a design-based method (stratified mean method, SM) and effects of scale size for data averaging and random effects. The GAM+OK method with small scale size outperformed the other 2 model-based methods and scale sizes in the simulation in terms of accuracy and precision of estimating mean and CV in most cases. SM estimates were more accurate and precise than the model-based estimates but only when the study region was stratified more correctly than might be expected in practice.

Based on the results of 2013 HabCam biomass data analysis and simulations, we selected the GAM+OK method to estimate scallop abundance and biomass for the GB and MAB stock for 2011 to 2013. SM estimates estimated with careful stratifications are also provided to back up the model-based estimates. Following are detailed descriptions of the simulation design, model- and design-based methods, simulation results, and procedures to estimate GB and MAB scallop abundance and biomass for 2011 to 2013.

5.2 Simulation Design

The area covered (domain) of simulated scallop populations was 50 km longitude and 100 km latitude (roughly the size of Hudson Canyon subregion, Figure 2) with a 100 m grid size. The scallop spatial distributions are non-stationary due to the influences of physical and biological environment including current, depth, and predator distributions (Brand, 1991). The simulated scallop population is therefore assumed to be heterogeneous in global trend (first-order effect), combined with stationary second-order effects. We simulated different first-order and second-order effects in order to test whether the abundance and biomass estimation methods are robust to the type of spatial distributions of the underlying population.

Variations in global mean quantity were simulated using a double logistic function

$$p_{i,j} = \frac{1}{1+\exp(-a(i-b))} + \frac{1}{1+\exp(a(i-b+\frac{\max(i)}{2}))}, \quad (5.1)$$

where a and b parameters determine the shape of the logistic curve, and i and j are the longitude and latitude, respectively. The simulated first-order effects are high in the middle and decrease logistically toward the left and right edge of the simulation domain (Figure 16). Two types of first-order effects were simulated, one narrow but highly dense and the other wide and less dense (Figure 16).

Second-order effects were simulated as stationary Gaussian random fields with a spherical isotropic covariance structure (Cressie 1993)

$$\gamma(h) = \begin{cases} 0 & h = 0 \\ c_0 + c_1 \left\{ \frac{3h}{2r} - \frac{1}{2} \left(\frac{h}{r} \right)^3 \right\} & 0 < h \leq r, \\ c_0 + c_1 & h \geq r \end{cases} \quad (5.2)$$

where c_0 , c_1 , and r are the nugget, partial sill, and range parameter, respectively. The nugget/sill ratio ($\frac{c_0}{c_0+c_1}$) determines randomness and r determines aggregations size of the second-order effects. We simulated combinations of 2 levels of nugget/sill ration and 2 levels of the range parameter resulting in 4 types of second-order effects: small aggregation, large aggregation, small aggregation with a large random noise, and large aggregation with a large random noise (Figure 17). We chose the parameter values based estimates from actual HabCam data.

Scallop distributions are patchy, resulting in HabCam data being highly zero-inflated (Table 1). To reflect the patchiness of scallop distribution, for each second-order realization, densities smaller than 90th percentile were set to zero. The zero-inflated second-order effects were combined with first-order effects to produce realistic simulated scallop distributions (Figure 18).

We simulated combinations of 2 first-order and 4 second-order effects resulting in 8 types of simulated population distributions. Thirty realizations were generated for each population type. Total abundance and biomass of each realization was scaled to equality across realizations. Each realization was surveyed using 30 different tracks. Shape and direction of tracks was designed to mimic the actual HabCam survey design.

Model-based and designed-based methods were used to estimate total biomass and abundance for the simulated populations. These estimation methods were evaluated using percent bias and percent root mean square error (RMSE)

$$\% \text{ Bias} = \frac{\sum_{i=1}^n (\hat{T}_i - \mu)}{n \mu} \quad (5.3)$$

$$\% \text{ RMSE} = \sqrt{\frac{\sum_{i=1}^n (\hat{T}_i - \mu)^2}{n \mu^2}}, \quad (5.4)$$

where \hat{T}_i is the estimated total biomass or abundance for sample set i , μ is the true population size, and n is the total number of sample sets analyzed. Percent bias and percent RMSE of CVs for the precision of model estimates were also evaluated. The method that produced the least biased and most precise estimates was selected to analyze the actual HabCam data.

5.3 Model-Based Estimation

Kriging is one of the most widely used geostatistical method for spatial interpolation (Webster and Oliver 2001). We tested performance of 3 different kriging methods including

OK, GAM+OK, and GAMM+OK on the simulated scallop populations. OK is a standard version of the kriging models with the assumption of a constant mean and consideration of variation and distance between sample points (Hengl 2009, Webster and Oliver 2001). Although the constant mean assumption might not be reasonable for scallops, the simulation tests are necessary to determine whether the observed non-stationary pattern can be modeled as an autocorrelation among errors with a constant mean or a trend with mean changing with variance.

Isotropy and anisotropy is the variation of scallop abundance or biomass being identical or directionally dependent. It is not clear whether the samples are isotropic or anisotropic although actual observations indicate that first-order effects the simulated populations should have the largest variations along the horizontal axis. Therefore, we built both the isotropic and anisotropic models and selected the final OK model using RMSE

$$\text{RMSE} = \sqrt{\frac{\sum_{i=1}^n (\hat{z}_i - z_i)^2}{n}} \quad (5.5)$$

Total abundance or biomass (T) and its variance were estimated as

$$\hat{T} = A \sum_{i=1}^n \hat{z}_i \quad (5.6)$$

$$\text{Var}(\hat{T}) = A^2 \sum_{i=1}^n \sum_{j=1}^n \text{Cov}(\hat{z}_i, \hat{z}_j), \quad (5.7)$$

where \hat{z}_i is the kriging estimates at location i and A is the grid size.

Regression kriging (RK) extends the OK to account for a global trend, which can be estimated by apply a regression model (e.g. GAM or GLM) to a series of ancillary variables (e.g. depth, latitude or longitude) then applying OK to the residuals of the regression model (Hengl 2009, Odeh et al. 1995). The final predictions of RK are obtained by summing the regression predicted values and the kriged residuals. This approach was criticized by Cressie (1993) and Lark et al. (2006) because the variogram estimates of the random component of spatial variation are theoretically biased. Generalized least squares and residual maximum likelihood-empirical best linear unbiased predictor are two potential solutions (Lark et al. 2006). However, Kitanidis (1993) and Minasny and McBratney (2007) showed that although these methods are theoretically preferable to RK, they did not substantially improve model predictions. We therefore used the RK approach.

Scallop data from the HabCam survey are highly spatially autocorrelated and zero inflated, reflecting the patchiness of scallop distributions. Therefore, we estimated the first order effects (over relatively large geographic areas) using a two-stage hurdle model which models the probability that scallops are found in a sample (presence/absence) separately from the density given that at least one scallop was found (Barry and Welsh, 2002). Predictions from the two models are combined to make the complete estimates of abundance and biomass. Hurdle model results were usually modified further to account for second order effects over smaller geographic areas as described below. We tested a hurdle GAM on data averaged within segments along the tracks (to reduce the autocorrelation and zero-inflation) and a hurdle GAMM where the fine-scale variations within track segments were treated as random effects. A quasi-binomial distribution was assumed for the presence/absence model and a quasi-Poisson distribution for the

positive model. The first-order effects were estimated using an interaction term of latitude and longitude for both GAM and GAMM. OK was performed on the residuals using the same algorithm described above. Total abundance and biomass of GAM+OK and GAMM+OK model estimates were estimated using

$$\hat{T} = A \sum_{i=1}^n \hat{x}_i \hat{y}_i + \hat{z}_i, \quad (5.8)$$

where \hat{x}_i is the probability of presense estimate, y_i is the positive estimate, \hat{z}_i is the kriged residual at location i . By assuming that \hat{x} and \hat{y} are independent, the variance of the \hat{T} was calculated using

$$\text{Var}(\hat{T}) = A^2 (\sum_{i=1}^n E^2 \hat{x}_i \text{Var}(\hat{y}_i) + E^2 \hat{y}_i \text{Var}(\hat{x}_i) + \text{Var}(\hat{x}_i) \text{Var}(\hat{y}_i) + \sum_{i=1}^n \sum_{j=1}^n \text{Cov}(\hat{x}_i, \hat{y}_i)) \quad (5.9)$$

Effects of segment length to average the data or determine random effects along the tracks was evaluated. The dense scallop aggregations occurred at approximately 400 to 900 m (NESFC 2010) and therefore we tested 3 segment lengths, 750, 1500, and 2,250 m. These segment lengths were also used to define the grid size A.

5.4 Design-Based Estimation

We tested a SM method to estimate total abundance and biomass from the simulated data. Only horizontal transects were used in the SM estimation because variance of these transects were different from the vertical transects. Horizontal transects were post-stratified into 2 strata based on high and low first-order effects (Figure 19). Mean and its variance of the simulated scallops (t) by segment (j) and stratum (i) were calculated by

$$\bar{t}_{i,j} = \frac{\sum_{k=1}^{n_{i,j}} t_{i,j,k}}{n_{i,j}} \quad (5.10)$$

$$\text{Var}(\bar{t}_{i,j}) = \frac{\text{Var}(t_{i,j,k})}{n_{i,j}}, \quad (5.11)$$

where $n_{i,j}$ is the number of images by segment and stratum. Total abundance and biomass estimates (\hat{T}) and variance were estimated as

$$\hat{T} = A \sum_{i=1}^2 S_i \frac{\sum_{j=1}^{n_i} \bar{t}_{i,j}}{n_i} \quad (5.12)$$

$$\text{Var}(\hat{T}) = A^2 \sum_{i=1}^2 S_i^2 \sum_{j=1}^{n_i} \frac{\text{Var}(\bar{t}_{i,j})}{n_i^2}, \quad (5.13)$$

where n_i is the number of segments by stratum i , and S_i is the size of stratum i .

The simulation domain was well-stratified based on the first-order trend; however, we do not have the same information when dealing with the real data which tend to complicated as

shown below using real data. We tested whether the SM estimates are sensitive to the stratification by enlarging (Stratified Mean Wide, SMW) and shrinking (Stratified Mean Narrow, SMN) the central high density stratum by 20% (Figure 19) and estimated total abundance and biomass under the original (incorrect) assumptions about stratum size.

5.5 Simulation Results

Proportion of converged model runs was 99% for GAM+OK and OK but 80-93% for GAMM+OK (Table 2). Percent bias and percent RMSE showed that GAM+OK with data averaged by 750 m (scale) is the best way to estimate the scallop biomass among all the model-based methods. For abundance, the method that produce the least biased estimates is GAM+OK with 1500 m scale, though it only outperformed the GAM+OK with 750 m scale by 0.006%. When both the bias and precision of the estimates are taking into account, GAM+OK with 750 m is the best way to estimate the scallop abundance (lowest percent RMSE, Table **Error! Reference source not found.**). The GAM+OK with 750 m segments also produce the least biased CV estimates for both biomass and abundance estimates (Table 2).

Percent bias and percent RMSE of the SM estimates are smaller than all the model-based estimates (except for the percent RMSE of the abundances estimated using GAM+OK with 750 m) but the CVs were highly underestimated. Beside the problems of estimating CVs, SM estimates were sensitive to the quality of post stratification. SMW and SMN estimates were biased and worse than all the model-based estimates.

Based on the simulation results, we concluded that GAM+OK method with data averaged over 750 m segments was the best way to estimate total abundance and biomass using HabCam data. SM estimates with careful stratifications were also provided in order to validate the model-based estimates although variances for the SM method are probably understated.

5.6 Analysis of actual HabCam data for 2011-2013

The HabCam data were collected during 2011-2013 in GB and during 2012-2013 in MAB. We divided the GB and MAB stock region into 14 subregions based on geographic characteristics and management areas and analyzed them separately because their topology, orientation and covariance structures differ (Figures 14 and 15).

Images with altitudes higher than 4 m and scallops with measured shell heights smaller than 40 mm were excluded for estimating scallop abundance and biomass. The shell height (SH) measures were converted to meat weights (g) (MW) based Hennen and Hart (2012)

$$\text{MAB: } MW = -16.88 + 4.64 \log(SH) + 1.57 \log(D) - 0.43 \log(SH) \log(D) \quad (5.14)$$

$$\text{GB: } MW = 14.38 + 2.826 \log(SH) - 0.529 \log(D) - 5.98 \log(L), \quad (5.15)$$

where D is depth and L is latitude. The counts and weight data were summed by image and standardized into abundance and biomass per m^2 by field of view of the image. A summary of the HabCam data used by subregion for 2011-2013 is listed in Table 1.

As described above and based on the simulation results, the GAM+OK method with 750 m segments was used to estimate total abundance and biomass for each subregion. For estimation purposes, we constructed a 1-km buffer zone around each subregion and used the data within the buffered region to build the subregional models. An average of weight or count (t) by image (j) and distance group (i) weighted by field of view (f) was calculated for every 750 m segment along the tracks

$$\bar{t}_i = \sum_{j=1}^{n_i} \frac{f_{i,j} t_{i,j}}{\sum_{j=1}^{n_i} f_{i,j}}, \quad (5.16)$$

The \bar{t}_i was weighted by both variation (s) and number of images (n) in the hurdle GAM using

$$w_i = \frac{s_i - s_{(1)}}{2(s_{(n_i)} - s_{(1)})} + \frac{n_i - n_{(1)}}{2(n_{(n_i)} - n_{(1)})} \quad (5.17)$$

A hurdle GAM with a quasi-binomial distribution for the presence/absence model and quasi-Poisson distribution for the positive model was used to estimate the first-order trend with respect to latitude, longitude, and depth. Depth is correlated with latitude and / or longitude in some of the subregions. To prevent potential problems cause by collinearity, latitude and longitude were transformed into composite variables: latitude plus longitude and half of the latitude or longitude plus longitude/latitude. A list of models with the different combination of covariates is supplied in Table 3. Depth is included in all of the candidate models because it is one of the most important variables that affecting scallop distributions. The maximum amount of knots for interactions between covariates in GAM models was limited to 15 (reduced to 10 for some of the subregions) and 10 for the single terms to prevent over-fitting. We selected the final first-order model using the RMSE from a 10-fold cross validation.

OK were performed on the GAM residuals. We tested isotropic and a series of anisotropic (from 0 to 180 by 20 degrees) residual OK models and selected the final OK model using the median standard error (MedSE).

$$\text{MedSE} = \sum_{i=1}^n \text{Median}(\hat{\bar{t}}_i - \bar{t}_i) \quad (5.18)$$

GAM and OK final models by subregion and year are listed in Table 4.

For the SM analysis we used only the data within the subregion. The transects were separated into segments based on the following criteria: parallel or perpendicular to depth contour, distance between points (2 km), depth strata, and distance along the transect (10 km). We first separated transects into segments at locations where the direction of the transects changed between parallel and perpendicular to the depth contour. These segments were further separated into smaller ones by depth strata or any location where the distance of any two points in the segment was greater than 2 km. The resulting segments were again broken into smaller ones if length where segments were longer than 10 km. An example of segmentations of the HabCam data (abundance data for 2013) is in Figure 20.

Thresholds for the depth strata were estimated using a maximum likelihood based change

point analysis (Killick et al. 2010). A GAM with a quasi-Poisson error distribution was built for each subregion. The depth partial residuals from the GAM were used in the change point analysis to estimate the depth thresholds. The thresholds were detected based on changes in mean or variance or both mean and variance of the partial residuals. Each subregion is post-stratified into a maximum of 3 depth strata. The depth stratification was done for each year by subregion and separately for abundance and biomass data.

The mean count or weight and its variance was estimated by segment and stratum using equations 10 and 11 and weighted by total field of view (f) and length of the segment (d) to estimate the total abundance or biomass and its variance

$$\hat{T} = A \sum_{i=1}^3 S_i \sum_{j=1}^{n_i} w_{i,j} \bar{t}_{i,j} \quad (5.19)$$

$$\text{Var}(\hat{T}) = A^2 \sum_{i=1}^3 S_i^2 \sum_{j=1}^{n_i} w_{i,j}^2 \text{Var}(\bar{t}_{i,j}), \quad (5.20)$$

where n_i is number of segments within depth stratum i , S_i is the size of depth stratum i , and $w_{i,j}$ is the weighting factor

$$w_{i,j} = \frac{d_{i,j} - d_{i,(1)}}{2(d_{i,(n_i)} - d_{i,(1)})} + \frac{f_{i,j} - f_{i,(1)}}{2(f_{i,(n_i)} - f_{i,(1)})} \quad (5.21)$$

The resulting GAM+OK and SM abundance and biomass estimates and CV's by subregion are listed in Table 5 and by stock in Table 6 for 2011-2013.

5.7 Size composition data for assessment modeling

Calculating scallop size frequency distributions from HabCam data for use in this assessment required re-stratifying Georges Bank for each year for appropriate spatial expansions because inclusion of the RSA surveys resulted in very high densities of annotated images in localized areas (Figure 13). A simple union of the sea scallop strata and HabCam estimation areas was sufficient for the Mid Atlantic in 2012 and 2013 as there were no RSA surveys in this region. Based on these stratifications, we derived stratified size frequency distributions by calculating the density of scallops within each strata and size class, weighted these densities by strata area, and averaging across the region. No adjustments for measurement errors were made although such measurement errors in the two optical surveys for sea scallops (HabCam and SMAST) may have standard deviations on the order of 1 cm. Instead, this type of error is accommodated in the CASA stock assessment model as predicted population length distributions are transformed into predicted length composition observations (Jacobson et al. 2010).

References

- Barry, S. C., Welsh, A. H. (2002) Generalized additive modeling and zero inflated count data. *Ecological Modeling*, 157(2), 179–188
- Brand, A. R. 1991. Scallop ecology: distributions and behavior. In: Shumway, S. (Ed.), *Scallops: Biology, Ecology, and Aquaculture*, Elsevier, Amsterdam, p. 517-584.
- Cressie, N. A. C. 1993. *Statistics for Spatial Data*, revised edition. 68 John Wiley and Sons, New York, p. 416.
- Hengl, T. 2009. *A practical guide to geostatistical mapping*. University of Amsterdam, Amsterdam, p. 291.
- Hennen, D.R., Hart, D.R. 2012. Shell height-to-weight relationships for Atlantic sea scallops (*Placopecten magellanicus*) in offshore U.S. waters. *J. Shellfish Res.* 31:1133-1144.
- Jacobson, L.D., Stokesbury, K.D.E., Allard, M.A., Chute, A., Harris, B.P., Hart, D., Jaffarian, T., Marino, M.C., Nogueira, J.I., and Rago, P. 2010. Quantification, effects, and stock assessment modeling approaches for measurement errors in body size data using sea scallops (*Placopecten magellanicus*) as an example. *Fish. Bull.* 108: 233–247.
- Killick, R., Eckley, I. A., Jonathan, P., Ewans, K. 2010. Detection of changes in the characteristics of oceanographic time-series using statistical change point analysis. *Ocean Engineering*, 37(13), 1120-1126.
- Kitanidis, P. K. 1993. Generalized covariance functions in estimation. *Mathematical Geology*, 25(5), 525-540.
- Lark, R. M., Cullis, B. R., Welham, S. J., 2006. On spatial prediction of soil properties in the presence of a spatial trend: the empirical best linear unbiased predictor (E-BLUP) with REML. *European Journal of Soil Science*, 57(6), 787-799.
- Minasny, B., McBratney, A. B. 2007. Spatial prediction of soil properties using EBLUP with the Matérn covariance function. *Geoderma*, 140(4), 324-336.
- Northeast Fisheries Science Center (NEFSC) 2010. 50th Northeast Regional Stock Assessment Workshop (50th SAW): Assessment Report. Northeast Fisheries Science Center Reference Document 10-17.
- Odeh, I. O. A., McBratney, A. B., Chittleborough, D. J. 1995. Further results on prediction of soil properties from terrain attributes: heterotopic cokriging and regression-kriging. *Geoderma* 67(3), 215-226.
- Rivoirard, J., Simmonds, J., Foote, K. G., Fernandes, P., Bez, N. 2008. *Geostatistics for estimating fish abundance*. John Wiley & Sons.
- Webster, R., Oliver, M. A. 2001. *Geostatistics for Environmental Scientist*. John Wiley and Sons, Chichester, England, p. 149.

Table 1: Sample size, percent zero, mean weight and count per m² of for HabCam data by regions during 2011-2013.

Stock	Year	Subregion	Sample Size	% Zero	Meat Wt (g/m ²)	Meat Ct (m ²)
GB	2011	CA1	1942	0.86	15.09	0.39
GB	2011	CA2_N	213	0.91	26.93	1.11
GB	2011	CA2_S	614	0.96	3.22	0.1
GB	2011	GSC_NW	1022	0.83	21.31	0.56
GB	2011	GSC_SE	677	0.97	24.67	0.42
GB	2011	NF	797	0.96	7.77	0.24
GB	2011	NLS	349	0.94	8.48	0.25
GB	2011	SF	554	0.99	2.34	0.08
GB	2012	CA1	660	0.91	6.18	0.35
GB	2012	CA2_N	1382	0.52	27.95	0.91
GB	2012	CA2_S	1415	0.93	3.34	0.12
GB	2012	GSC_NW	735	0.77	8.5	0.47
GB	2012	GSC_SE	276	0.94	5.42	0.23
GB	2012	NF	1486	0.82	22.84	0.75
GB	2012	NLS	298	0.87	5.85	0.26
GB	2012	SF	982	0.96	3.83	0.14
GB	2013	CA1	2054	0.95	1.54	0.07
GB	2013	CA2_N	1015	0.61	21.83	0.51
GB	2013	CA2_S	476	0.86	2.14	0.29
GB	2013	GSC_NW	953	0.86	2.99	0.15
GB	2013	GSC_SE	676	0.95	1.77	0.07
GB	2013	NF	1818	0.93	11.34	0.28
GB	2013	NLS	322	0.85	2.8	0.13
GB	2013	SF	491	0.84	2.05	0.3
MAB	2012	DMV_VB	753	0.9	0.84	0.11
MAB	2012	ET	665	0.85	1.28	0.19
MAB	2012	HC	1159	0.9	1.66	0.15
MAB	2012	HCnr	732	0.93	1.45	0.1
MAB	2012	HCsr	619	0.92	1.86	0.14
MAB	2012	LI	486	0.95	1.24	0.07
MAB	2013	DMV_VB	561	0.91	1.93	0.17
MAB	2013	ET	922	0.87	4.25	0.35
MAB	2013	HC	1114	0.96	2.02	0.18
MAB	2013	HCnr	657	0.95	1.55	0.08
MAB	2013	HCsr	585	0.96	1.7	0.14
MAB	2013	LI	608	0.96	1.55	0.08

Table 2: Percent bias, CV, percent RMSE, estimated CV and number of converged sample runs for biomass and abundance estimates by segment sizes and estimation methods.

Model Type	Scale	% Bias	CV	% RMSE	Estimated CV	# Runs	% Bias	CV	% RMSE	Estimated CV	# Runs
GAM	750	0.048	0.194	0.209	0.191	7194	0.038	0.167	0.177	0.16	7187
GAMM	750	0.088	0.19	0.225	0.308	6699	0.069	0.165	0.189	0.249	6106
OK	750	0.136	0.195	0.26	0.289	7196	0.098	0.173	0.214	0.241	7182
GAM	1500	0.052	0.276	0.295	0.173	7198	0.033	0.188	0.197	0.154	7195
GAMM	1500	0.088	0.192	0.227	0.465	6305	0.066	0.167	0.19	0.507	5774
OK	1500	0.173	0.385	0.484	0.272	7184	0.113	0.288	0.34	0.225	7194
GAM	2250	0.056	0.227	0.246	0.16	7199	0.036	0.206	0.198	0.156	7199
GAMM	2250	0.09	0.193	0.228	0.559	6342	0.063	0.206	0.19	0.651	5953
OK	2250	0.178	0.339	0.438	0.259	7199	0.126	0.206	0.415	0.213	7199
SM		-0.002	0.193	0.193	0.09	7200	0.001	0.206	0.181	0.064	7200
SMN		0.219	0.233	0.359	0.091	7200	0.168	0.206	0.294	0.068	7200
SMW		0.13	0.201	0.262	0.094	7200	0.085	0.206	0.216	0.067	7200

Table 3: List of GAMs tested in the 10-fold cross validation.

GAM Models
s(Longitude, Latitude, k=15)+s(Depth)
s(Latitude, Depth, k=15)
s(Longitude, Depth, k=15)
s(LatPlusHalfLong, Depth, k=15)
s(HalfLatPlusLong, Depth, k=15)
s(LatPlusLong, Depth, k=15)
s(Latitude)+s(Depth)
s(Longitude)+s(Depth)
s(LatPlusHalfLong)+s(Depth)
s(HalfLatPlusLong)+s(Depth)
s(LatPlusLong)+s(Depth)
s(Latitude)+Depth

Table 4: List of first-order and second-order models for the biomass and abundance estimates of GB and MAB subregions for 2011 to 2013.

Stock	Year	Subregion	GAM (Biomass)	GAM (Abundance)	OK (Biomass)	OK (Abundance)
GB	2011	CA1	s(HalfLatPlusLong) + s(Depth)	s(HalfLatPlusLong) + s(Depth)	No angle	Angle: 100
GB	2011	CA2_N	s(LatPlusLong) + s(Depth)	s(LatPlusLong) + s(Depth)	Angle: 0	No angle
GB	2011	CA2_S	s(Longitude, Depth, k = 15)	s(Longitude, Depth, k = 15)	No angle	Angle: 160
GB	2011	GSC_NW	s(Longitude, Latitude, k = 15) + s(Depth)	s(LatPlusLong) + s(Depth)	No angle	No angle
GB	2011	GSC_SE	s(Latitude, Depth, k = 10)	s(Latitude, Depth, k = 15)	No angle	Angle: 140
GB	2011	NF	s(LatPlusLong) + s(Depth)	s(Longitude, Latitude, k = 15) + s(Depth)	Angle: 60	No angle
GB	2011	NLS	s(Longitude, Latitude, k = 15) + s(Depth)	s(Longitude, Latitude, k = 15) + s(Depth)	Angle: 120	Angle: 160
GB	2011	SF	s(Latitude) + Depth	s(LatPlusHalfLong, Depth, k = 15)	Angle: 160	No angle
GB	2012	CA1	s(HalfLatPlusLong) + s(Depth)	s(HalfLatPlusLong) + s(Depth)	Angle: 160	No angle
GB	2012	CA2_N	s(Longitude, Latitude, k = 15) + s(Depth)	s(Longitude, Latitude, k = 15) + s(Depth)	Angle: 100	Angle: 60
GB	2012	CA2_S	s(Latitude, Depth, k = 15)	s(Latitude, Depth, k = 15)	Angle: 40	No angle
GB	2012	GSC_NW	s(Latitude) + s(Depth)	s(LatPlusLong) + s(Depth)	No angle	Angle: 0
GB	2012	GSC_SE	s(HalfLatPlusLong) + s(Depth)	s(Longitude, Latitude, k = 15) + s(Depth)	Angle: 60	Angle: 20
GB	2012	NF	s(Longitude, Latitude, k = 15) + s(Depth)	s(Longitude, Latitude, k = 15) + s(Depth)	No angle	No angle
GB	2012	NLS	s(HalfLatPlusLong) + s(Depth)	s(HalfLatPlusLong) + s(Depth)	Angle: 120	Angle: 80
GB	2012	SF	s(LatPlusLong, Depth, k = 15)	s(Longitude, Latitude, k = 15) + s(Depth)	No angle	Angle: 40
GB	2013	CA1	s(Longitude, Latitude, k = 15) + s(Depth)	s(Longitude, Depth, k = 15)	Angle: 120	No angle
GB	2013	CA2_N	s(Longitude, Latitude, k = 15) + s(Depth)	s(Longitude, Latitude, k = 15) + s(Depth)	No angle	No angle
GB	2013	CA2_S	s(Longitude, Latitude, k = 15) + s(Depth)	s(Latitude, Depth, k = 10)	Angle: 0	Angle: 160
GB	2013	GSC_NW	s(Latitude) + s(Depth)	s(Longitude, Latitude, k = 15) + s(Depth)	Angle: 0	Angle: 0
GB	2013	GSC_SE	s(Longitude, Latitude, k = 15) + s(Depth)	s(Longitude, Latitude, k = 15) + s(Depth)	Angle: 160	Angle: 20
GB	2013	NF	s(Longitude, Latitude, k = 15) + s(Depth)	s(Longitude, Latitude, k = 15) + s(Depth)	Angle: 160	Angle: 160
GB	2013	NLS	s(Longitude, Latitude, k = 15) + s(Depth)	s(Longitude, Latitude, k = 15) + s(Depth)	Angle: 0	Angle: 160
GB	2013	SF	s(LatPlusLong, Depth, k = 15)	s(Longitude, Latitude, k = 15) + s(Depth)	Angle: 20	No angle
MAB	2012	DMV_VB	s(Longitude, Latitude, k = 15) + s(Depth)	s(Longitude, Latitude, k = 15) + s(Depth)	Angle: 60	Angle: 60
MAB	2012	ET	s(Longitude, Latitude, k = 15) + s(Depth)	s(Longitude, Latitude, k = 15) + s(Depth)	Angle: 80	No angle
MAB	2012	HC	s(Longitude, Latitude, k = 15) + s(Depth)	s(Longitude, Latitude, k = 15) + s(Depth)	Angle: 160	No angle
MAB	2012	HCnr	s(LatPlusHalfLong, Depth, k = 15)	s(Longitude, Latitude, k = 15) + s(Depth)	Angle: 140	Angle: 100
MAB	2012	HCsr	s(Longitude, Latitude, k = 15) + s(Depth)	s(Longitude, Latitude, k = 15) + s(Depth)	Angle: 0	Angle: 60
MAB	2012	LI	s(Latitude) + s(Depth)	s(Latitude) + s(Depth)	Angle: 100	Angle: 0
MAB	2013	DMV_VB	s(LatPlusLong) + s(Depth)	s(LatPlusLong) + s(Depth)	No angle	Angle: 20
MAB	2013	ET	s(Longitude, Latitude, k = 15) + s(Depth)	s(Longitude, Latitude, k = 15) + s(Depth)	Angle: 60	No angle
MAB	2013	HC	s(Longitude, Latitude, k = 15) + s(Depth)	s(LatPlusHalfLong) + s(Depth)	No angle	Angle: 120
MAB	2013	HCnr	s(Latitude) + s(Depth)	s(Latitude) + s(Depth)	Angle: 100	Angle: 40
MAB	2013	HCsr	s(Longitude, Latitude, k = 15) + s(Depth)	s(LatPlusHalfLong, Depth, k = 10)	No angle	No angle
MAB	2013	LI	s(LatPlusLong, Depth, k = 15)	s(Longitude, Latitude, k = 15) + s(Depth)	Angle: 0	Angle: 40

Table 5: Abundance and biomass and its CVs estimated using GAM+OK and SM methods by subregions for 2011 to 2013.

Stock	Year	Subregion	Number (million)				Weight (mt)			
			SM	GAM+OK	SM CV	GAM+OK CV	SM	GAM+OK	SM CV	GAM+OK CV
GB	2011	CA1	1151.70	1220.70	0.02	0.92	41772.14	42648.48	0.01	0.05
GB	2011	CA2_N	406.92	409.21	0.05	0.07	8325.85	12797.17	0.05	0.06
GB	2011	CA2_S	215.35	338.48	0.08	0.35	8882.94	10237.32	0.07	0.29
GB	2011	GSC_NW	1480.93	1289.01	0.04	0.17	32578.17	21675.43	0.04	0.15
GB	2011	GSC_SE	79.21	75.00	0.12	0.77	3578.14	2051.35	0.14	1.50
GB	2011	NF	336.35	201.78	0.10	0.09	5002.90	4631.38	0.08	1.70
GB	2011	NLS	218.19	159.66	0.07	0.06	7285.42	6224.57	0.07	0.17
GB	2011	SF	103.55	138.22	0.12	1.86	2778.85	2553.07	0.20	3.05
GB	2012	CA1	489.46	763.04	0.08	0.13	10102.43	11744.98	0.08	0.29
GB	2012	CA2_N	659.49	568.81	0.02	0.09	19660.00	21527.78	0.02	0.02
GB	2012	CA2_S	257.40	372.81	0.09	0.07	9803.77	9590.06	0.08	0.16
GB	2012	GSC_NW	1401.52	1721.65	0.05	0.04	25584.05	26266.07	0.05	0.22
GB	2012	GSC_SE	97.12	65.23	0.30	0.23	2390.65	4359.93	0.60	0.30
GB	2012	NF	375.65	259.75	0.05	0.09	8809.68	5919.12	0.05	0.23
GB	2012	NLS	275.23	256.81	0.14	0.44	8139.02	7111.74	0.16	0.14
GB	2012	SF	447.59	634.37	0.11	1.00	9534.90	7519.81	0.12	0.17
GB	2013	CA1	223.26	434.47	0.07	0.05	4479.75	6313.61	0.09	1.09
GB	2013	CA2_N	358.69	279.35	0.03	0.03	15818.66	12027.82	0.03	0.04
GB	2013	CA2_S	545.50	1026.61	0.04	0.09	5594.88	5445.98	0.10	0.05
GB	2013	GSC_NW	471.15	501.50	0.05	0.47	8518.39	8875.60	0.06	0.31
GB	2013	GSC_SE	78.82	57.64	0.16	0.90	1934.28	2281.77	0.21	0.08
GB	2013	NF	135.35	175.20	0.06	1.40	3413.10	4206.02	0.09	2.87
GB	2013	NLS	227.46	188.51	0.12	0.07	4519.21	4039.83	0.11	0.03
GB	2013	SF	1521.91	1385.35	0.06	0.05	10405.12	6480.77	0.09	0.18
MAB	2012	DMV_VB	487.11	340.30	0.06	0.09	3563.73	2657.57	0.08	0.08
MAB	2012	ET	1069.29	1431.26	0.06	0.02	7872.55	7455.85	0.06	0.68
MAB	2012	HC	1056.73	1417.64	0.05	0.02	12865.32	13196.17	0.07	0.10
MAB	2012	HCnr	497.09	616.72	0.11	0.99	8320.79	8607.06	0.12	0.03
MAB	2012	HCsr	418.46	435.87	0.13	0.15	6398.27	6531.35	0.12	0.03
MAB	2012	LI	637.03	660.37	0.11	0.04	11553.18	10748.32	0.11	0.25
MAB	2013	DMV_VB	594.70	529.23	0.07	0.09	5928.37	5742.01	0.05	0.05
MAB	2013	ET	1607.36	1555.18	0.04	0.04	20500.36	19429.08	0.04	0.05
MAB	2013	HC	1324.67	1091.30	0.08	0.16	9953.54	10758.67	0.09	0.05
MAB	2013	HCnr	644.33	502.73	0.26	0.48	8899.89	9953.83	0.14	0.78
MAB	2013	HCsr	262.77	266.72	0.27	0.40	5107.50	4946.65	0.26	0.11
MAB	2013	LI	630.57	665.43	0.09	0.10	11925.31	10655.17	0.10	0.06

Table 6: Abundance and biomass and its CVs estimated using GAM+OK and SM methods by stocks for 2011 to 2013.

Stock	Management Area	Year	Number (million)				Weight (mt)			
			SM	GAM+OK	SM CV	GAM+OK CV	SM	GAM+OK	SM CV	GAM+OK CV
GB	Close	2011	1992.16	2128.05	0.02	0.53	66266.35	71907.54	0.02	0.06
GB	Close	2012	1681.58	1961.46	0.04	0.08	47705.22	49974.57	0.04	0.08
GB	Close	2013	1354.91	1928.94	0.03	0.05	30412.50	27827.24	0.03	0.25
GB	Open	2011	2000.04	1704.01	0.04	0.20	43938.06	30911.23	0.03	0.39
GB	Open	2012	2321.88	2681.00	0.04	0.24	46319.28	44064.93	0.05	0.14
GB	Open	2013	2207.23	2119.68	0.04	0.17	24270.90	21844.16	0.05	0.57
GB	Total	2011	3992.20	3832.06	0.02	0.31	110204.42	102818.77	0.02	0.12
GB	Total	2012	4003.46	4642.46	0.03	0.14	94024.50	94039.50	0.03	0.08
GB	Total	2013	3562.13	4048.62	0.03	0.09	54683.40	49671.39	0.03	0.29
MAB	Total	2012	4165.70	4902.15	0.03	0.13	50573.84	49196.34	0.04	0.12
MAB	Total	2013	5064.39	4610.57	0.05	0.07	62314.98	61485.41	0.04	0.13

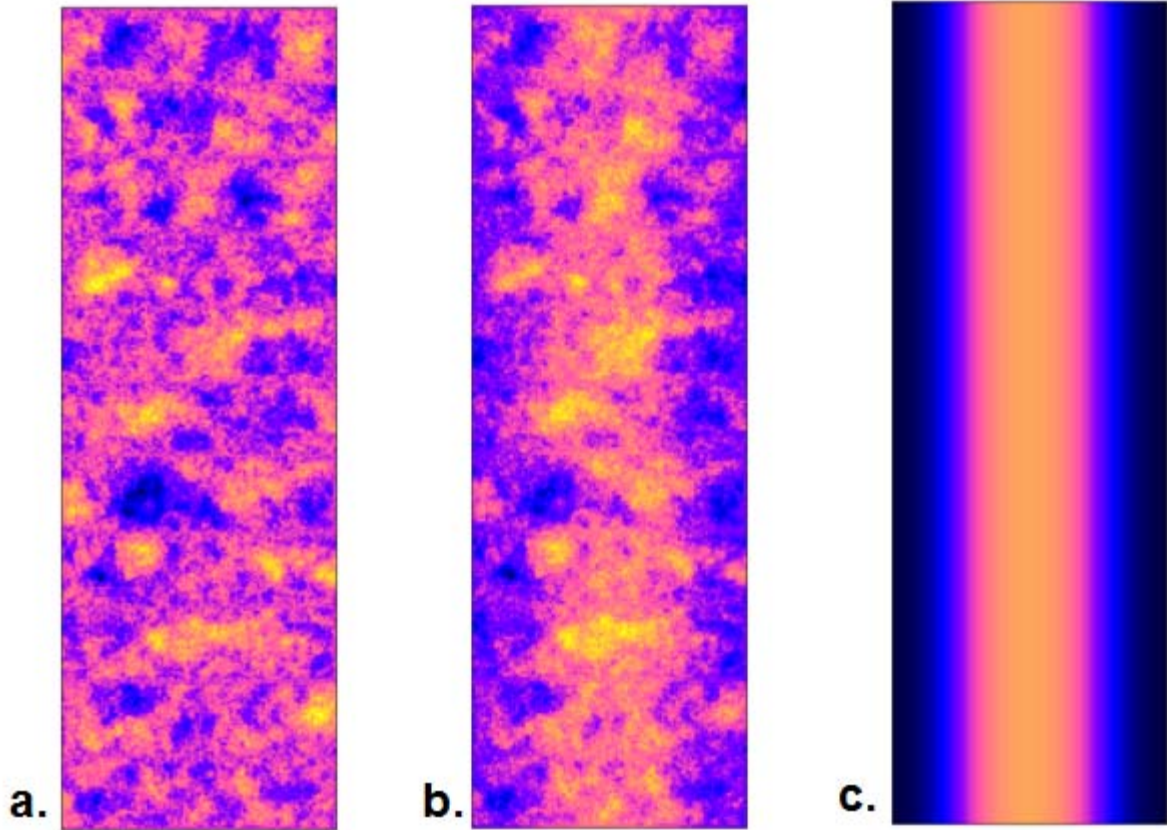


Figure 1. Hypothetical landscapes for (a) a landscape with a stationary mean, (b) a biased landscape with a higher mean along the center, and (c) the bias applied to landscape a to produce landscape b. In all plots, densities are higher in lighter-colored pixels.

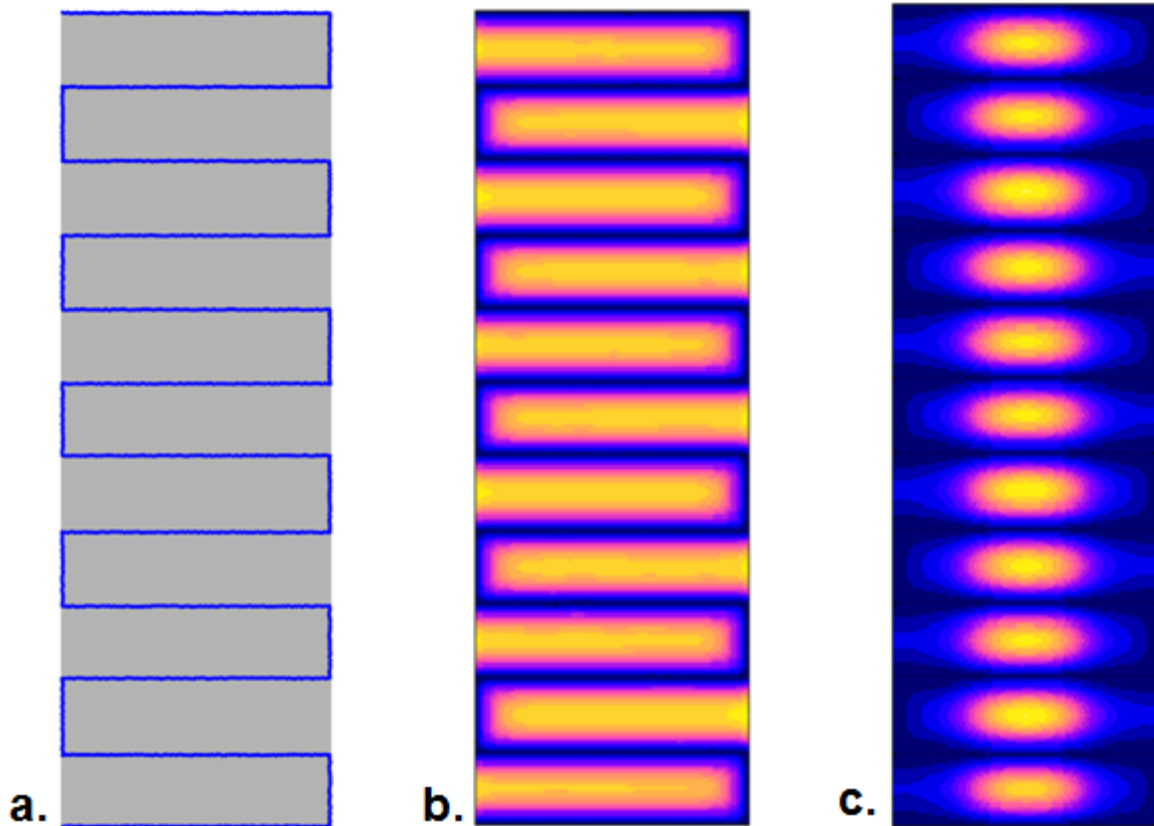


Figure 2 (a) A regularly spaced survey track across a rectangular survey area, (b) map of kriging variance derived from the survey track and an assumed underlying variogram model describing the data, (c) adjusted kriging variances resulting from applying the underlying trend from Figure 1c to (b).

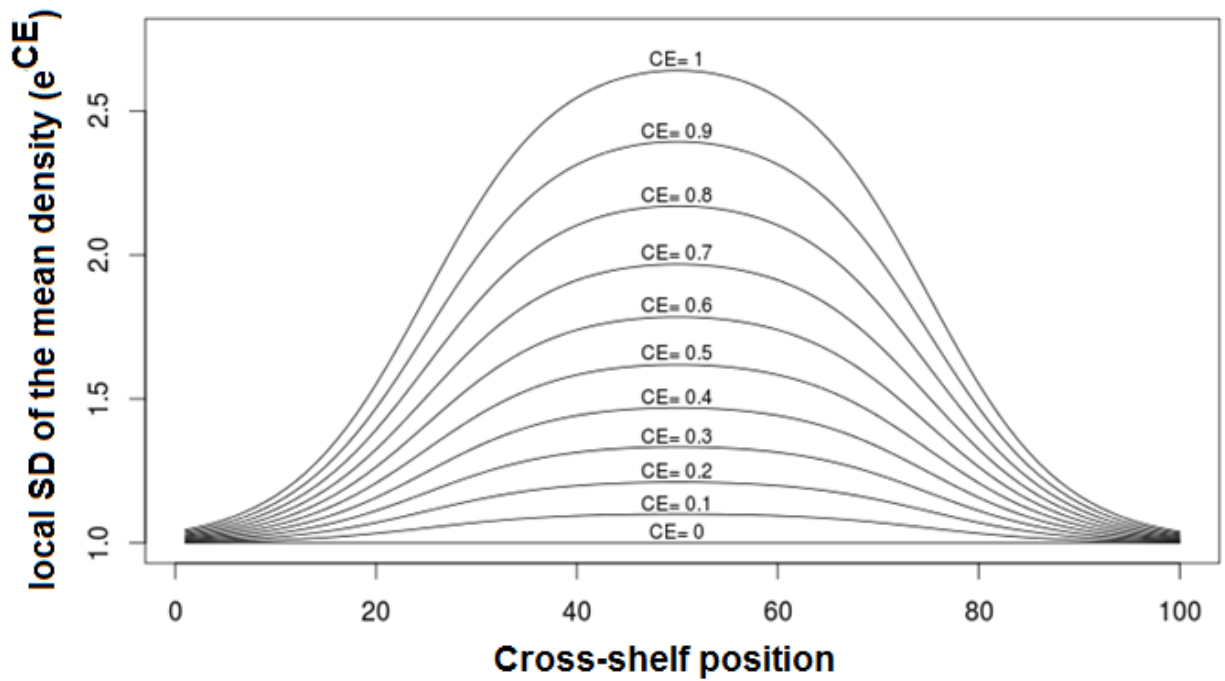


Figure 3. Levels of center effect used in simulations and resulting effects on the local standard deviation of the mean.

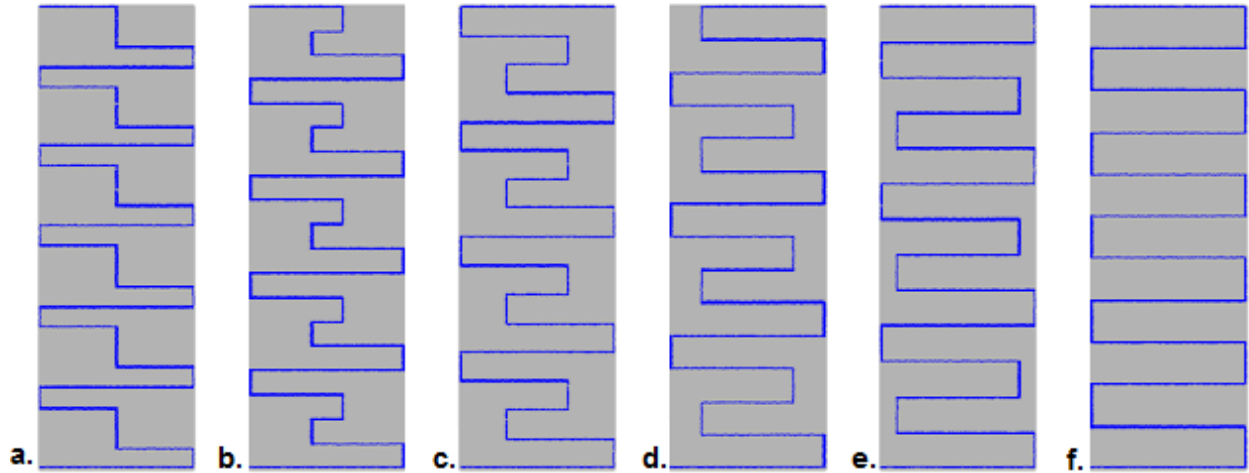


Figure 4a. Alternative survey configurations, alternating the length of transects along the track and keeping total survey length constant. Short transect lengths are (a) 0%, (b) 20%, (c) 40%, (d) 60%, (e) 80%, and (f) 100% of the length of the long transects.

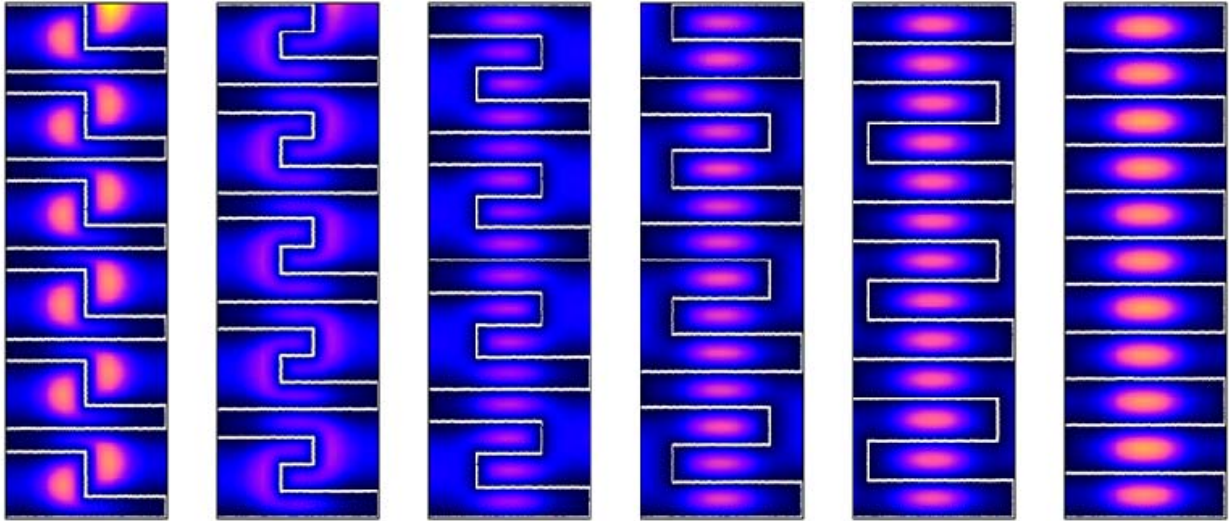


Figure 5. Variance maps for the survey tracks in Figure 4 with an applied center effect. Lighter colors indicate higher areas of variance.

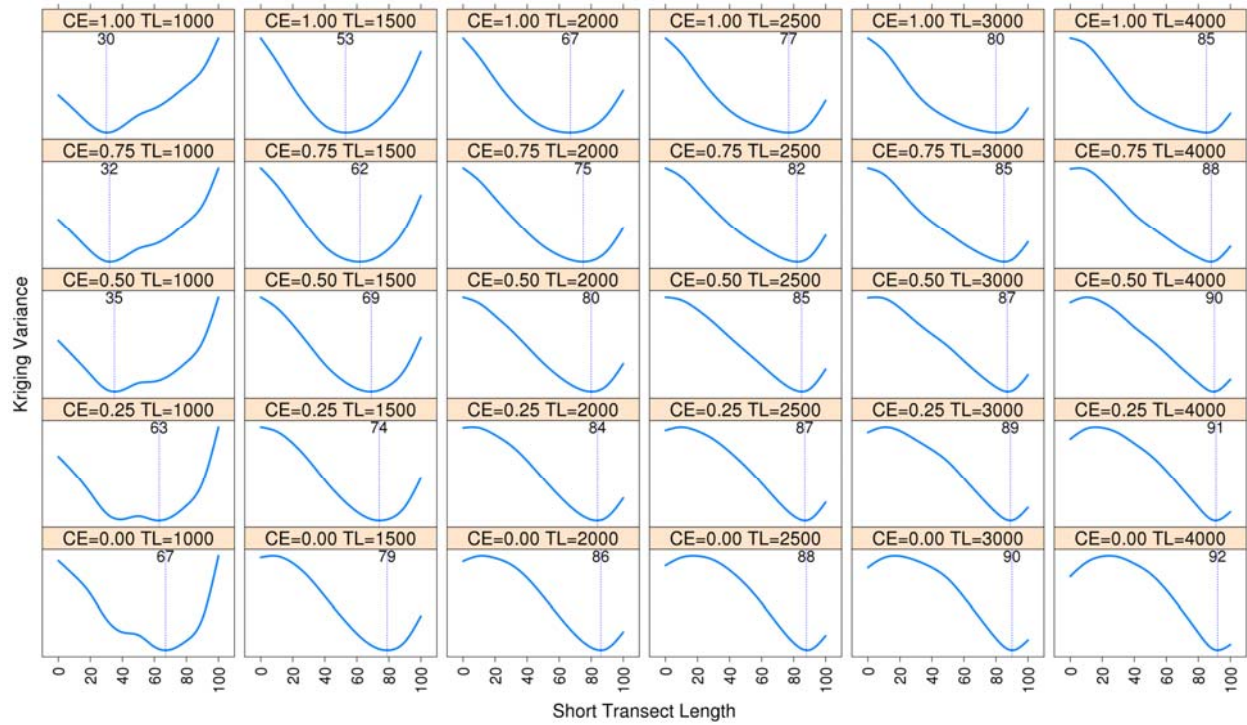


Figure 6. Adjusted kriging variances for different center effects (CE), short transect lengths and total survey track lengths (TL). Optimal solutions for each combination are marked with a dotted vertical line and labeled.

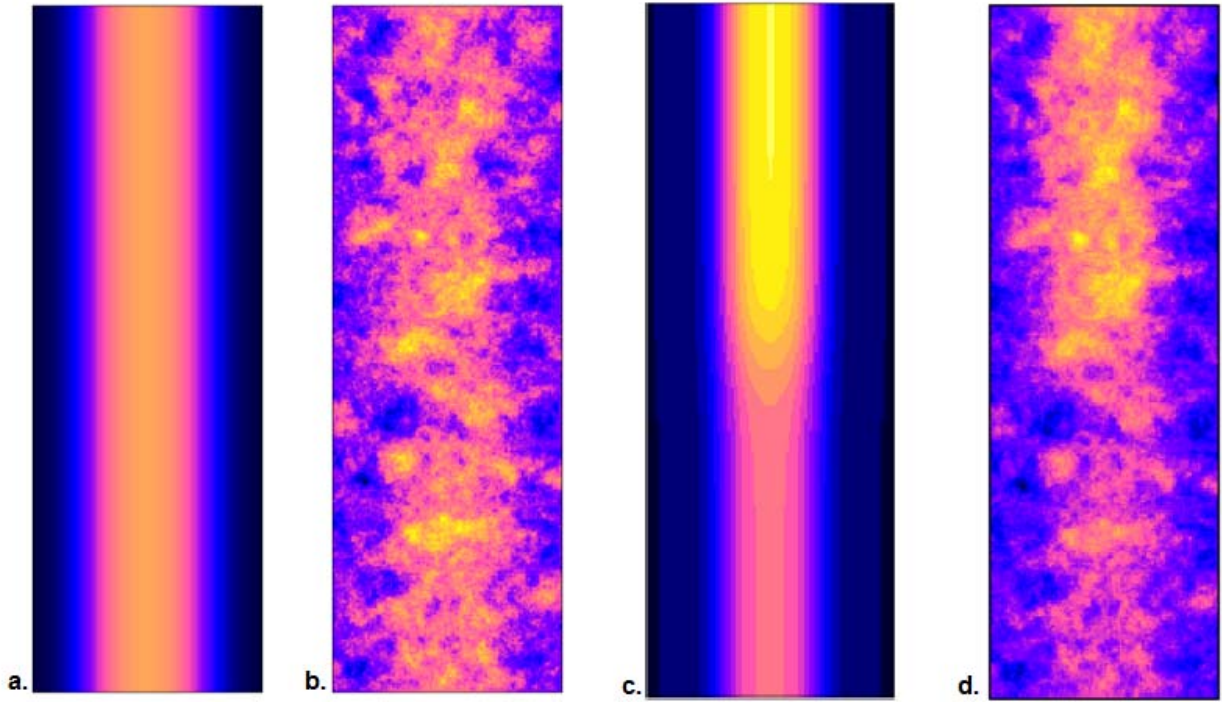


Figure 7. Comparison of survey landscapes without (a and b) and with (c and d) zonal anisotropy effects. Figures a and c represent the underlying trend in the mean while b and d represent the resulting simulated landscapes.

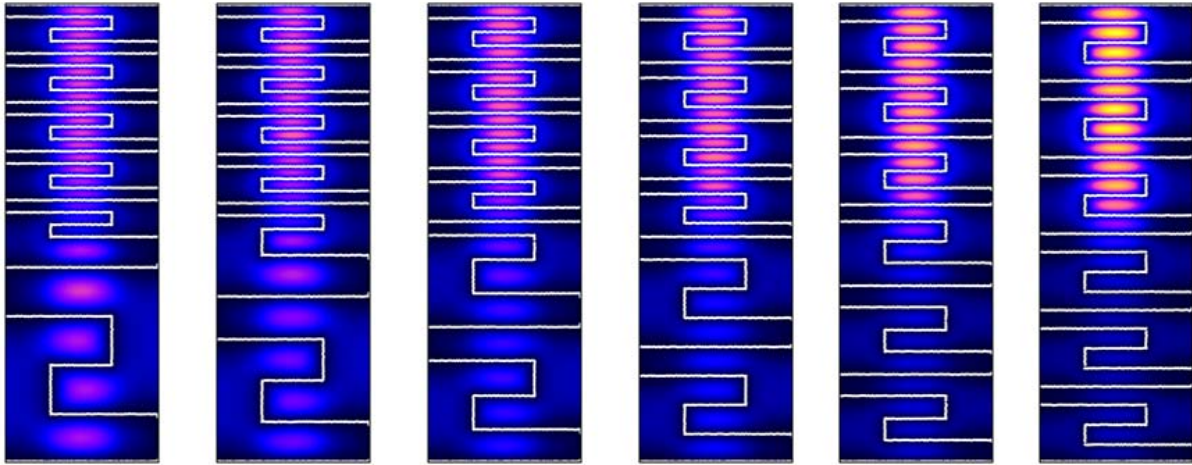


Figure 8. Example of varying transect density between zones and resulting variance maps for a simulated landscape with an underlying trend similar to C-7c. The survey track is represented in white. Lighter colors indicate higher variances.

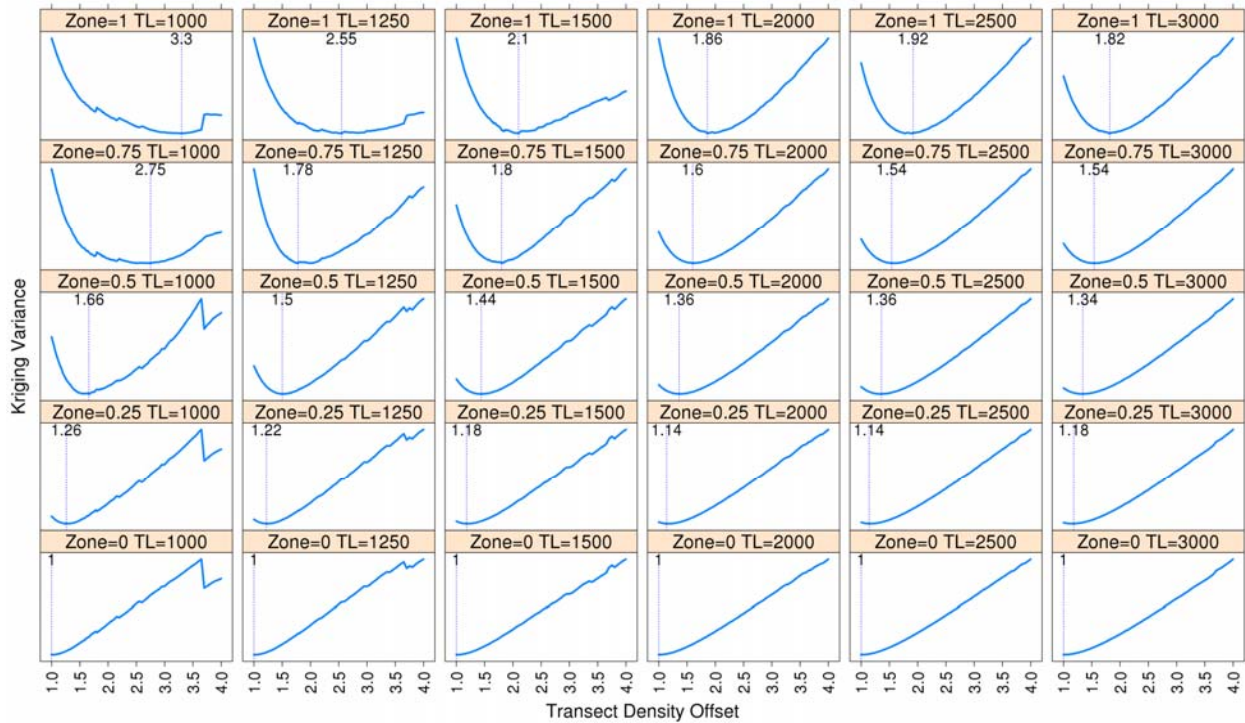


Figure 9. Zonal effects on transect density allocation. Higher “Transect Density Offsets” represent the placement of proportionally more transects in the high density zones. Optimal solutions for each simulation set are labeled and marked with a dotted line.

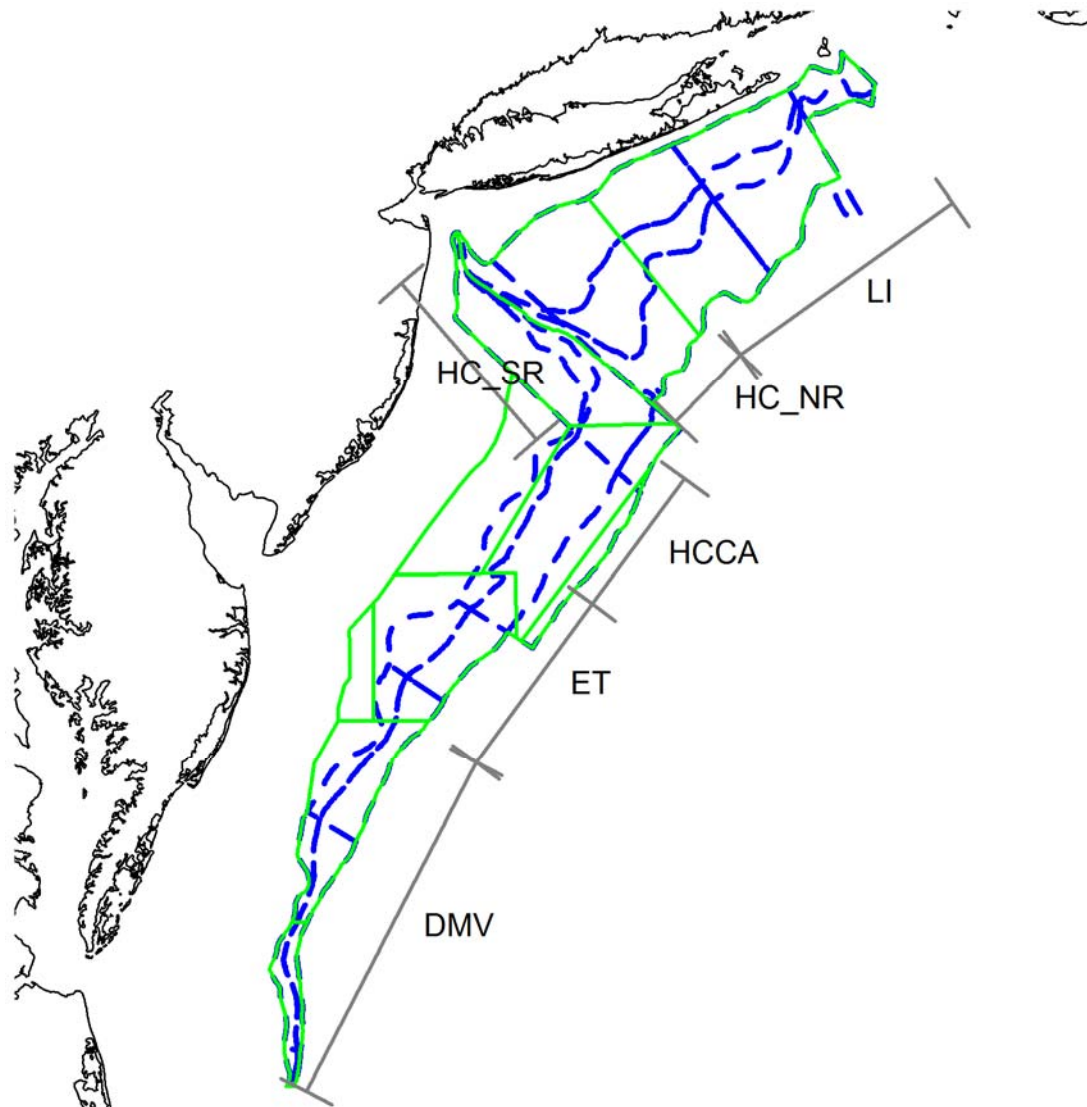


Figure 10. HabCam survey area (solid green line) compared to NEFSC scallop survey core strata (dashed blue line) in the MAB region. Subregions used for allocating survey effort and abundance estimation are: LI – Long Island, HC_NR – Hudson Canyon North Rim, HC_SR Hudson Canyon South Rim, HCCA – Hudson Canyon Closed Area, ET – Elephant Trunk, and DMV – DelMarVa.

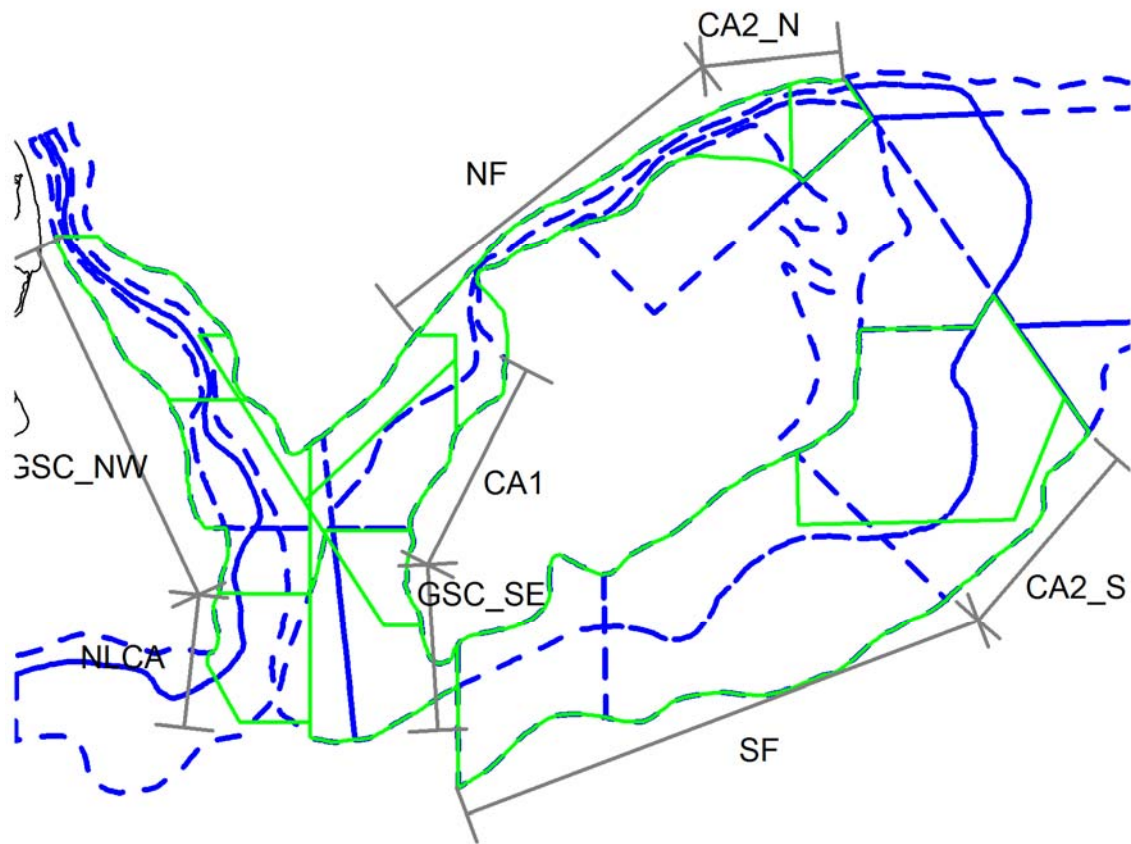


Figure 11. HabCam survey area (solid green line) compared to NEFSC scallop survey core strata (dashed blue line) for Georges Bank. Subregions used for allocating survey effort and abundance estimation are: GSC_NW – Great South Channel Northwest, NLCA – Nantucket Lightship Closed Area, GSC_SE – Great South Channel Southeast, CA1 – Closed Area 1, NF – Northern Flank, CA2_N – Closed Area 2 North, CA2_S – Closed Area 2 South, and SF – Southern Flank.

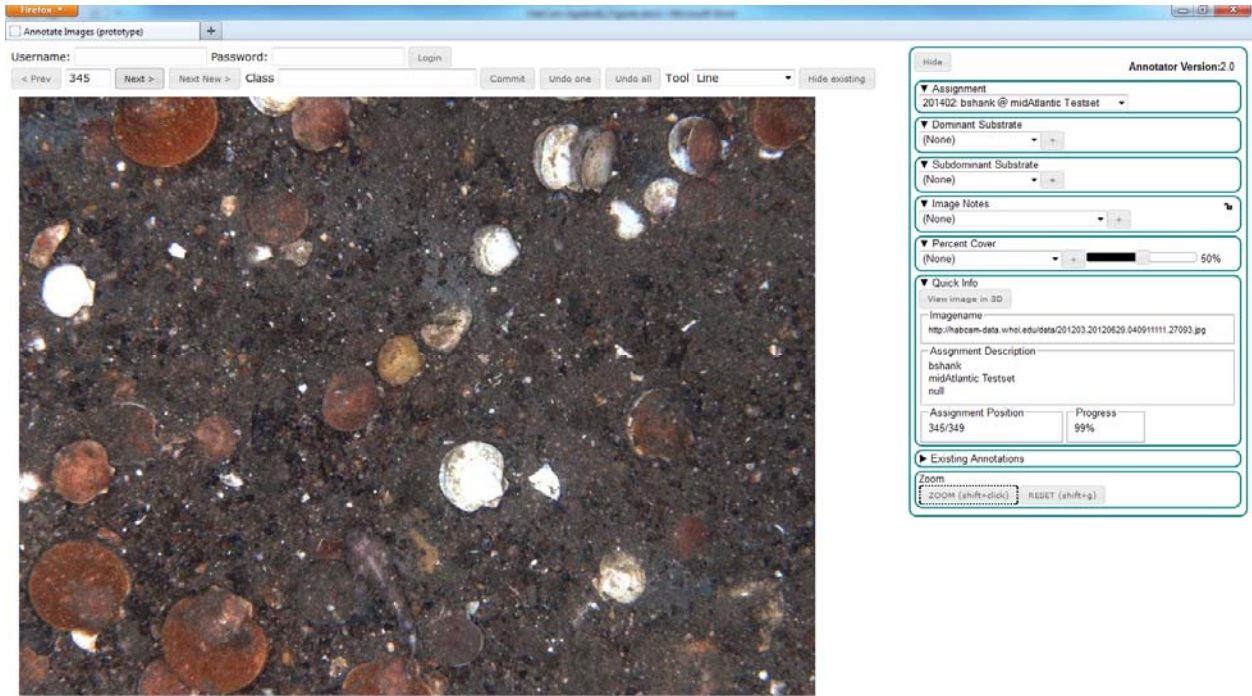


Figure 12. Screen image showing the web-based annotation tool for counting and measuring scallops from HabCam images.

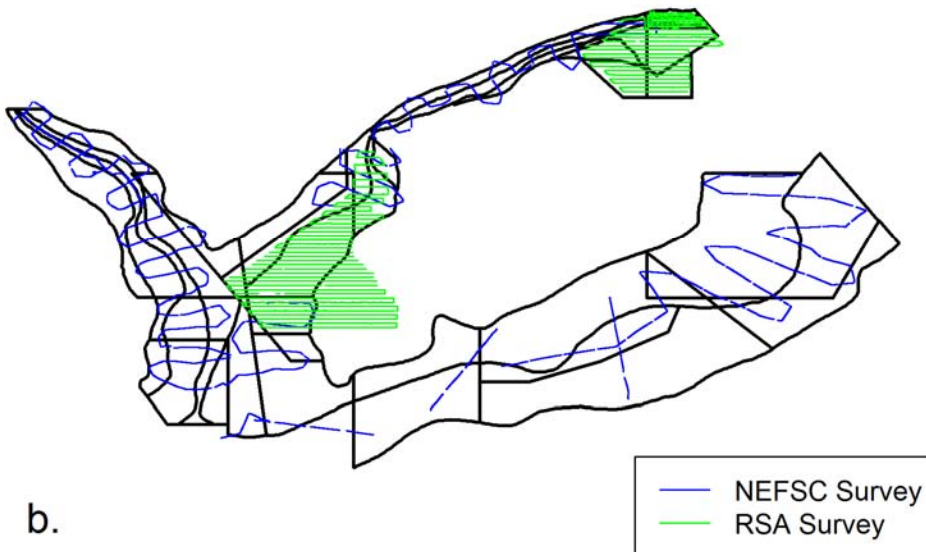
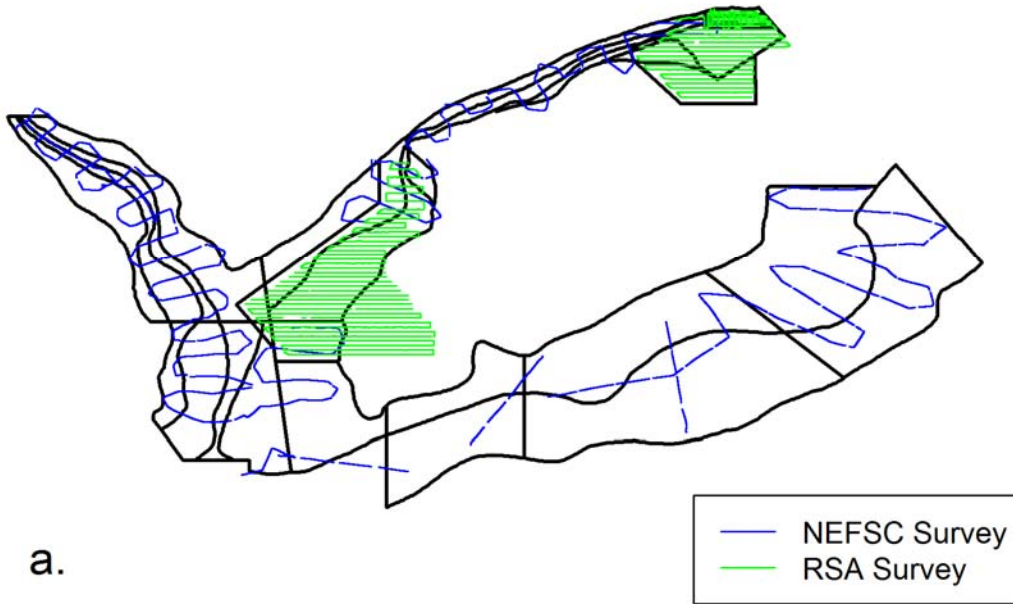


Figure 13 Example re-stratification of Georges Bank used for 2013 size frequencies: (a) open and closed areas combined and (b) open and closed areas separate.

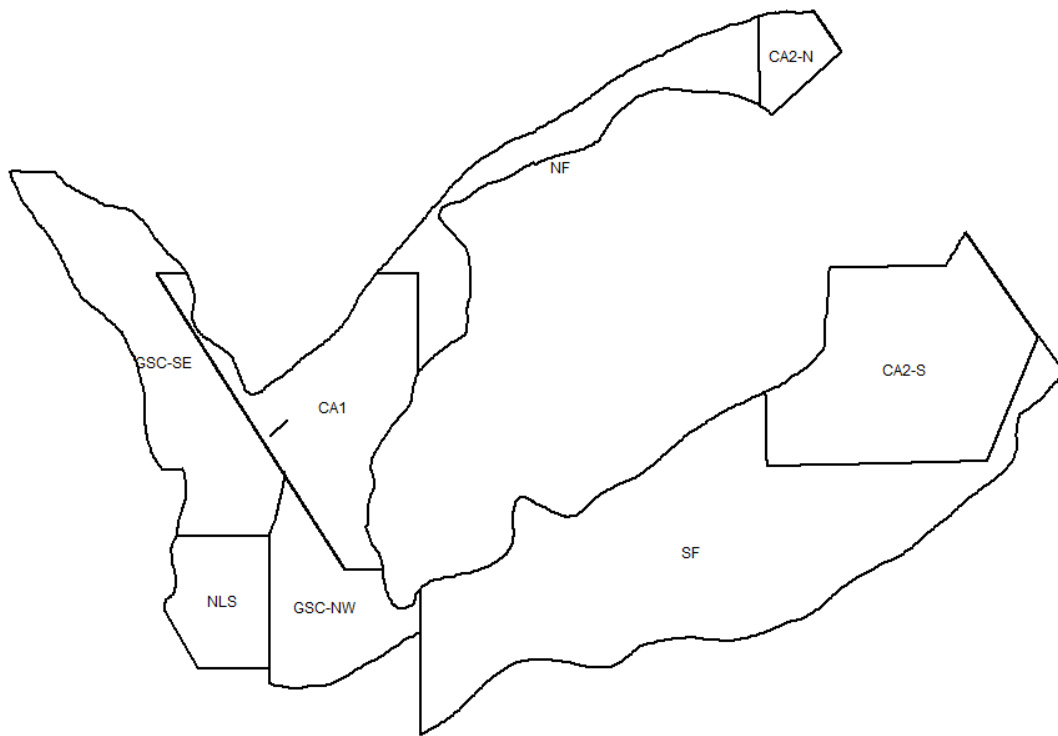


Figure 14: Subregions of the GB scallop stock area used in the HabCam survey.

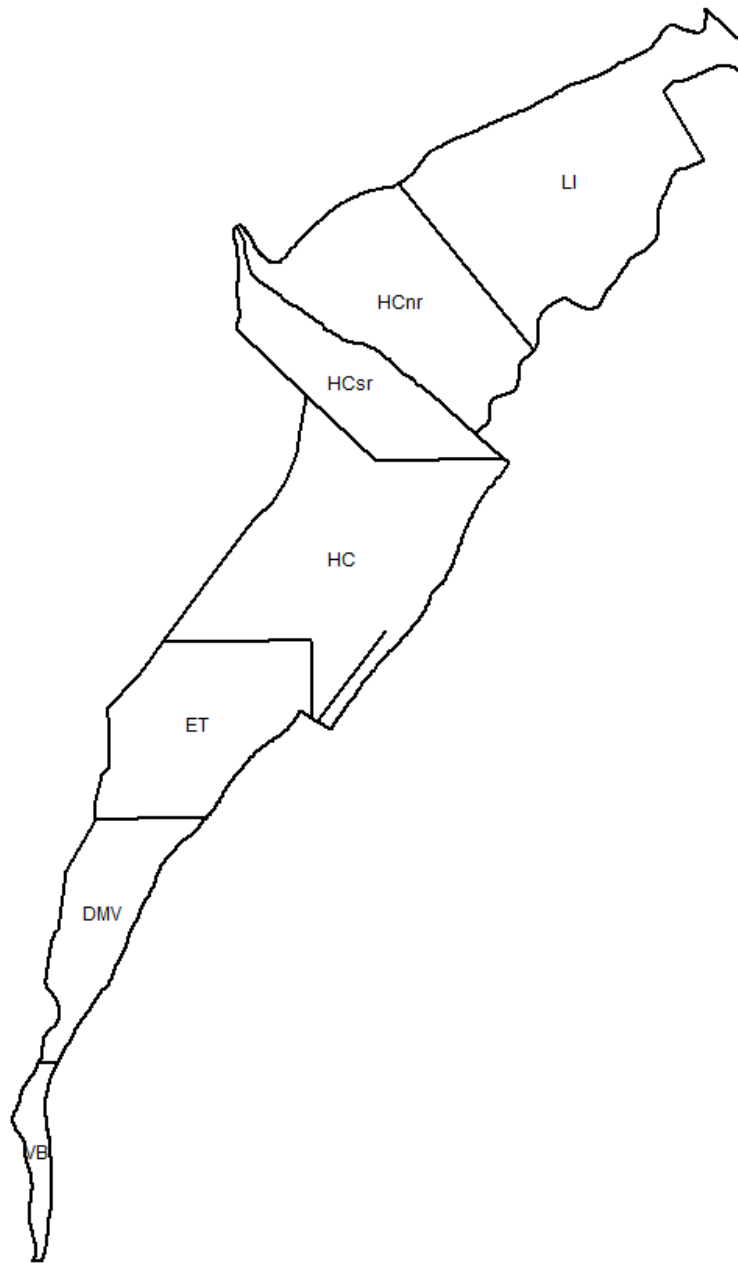


Figure 15: Subregions of the MAB scallop stock area used for the HabCam survey.

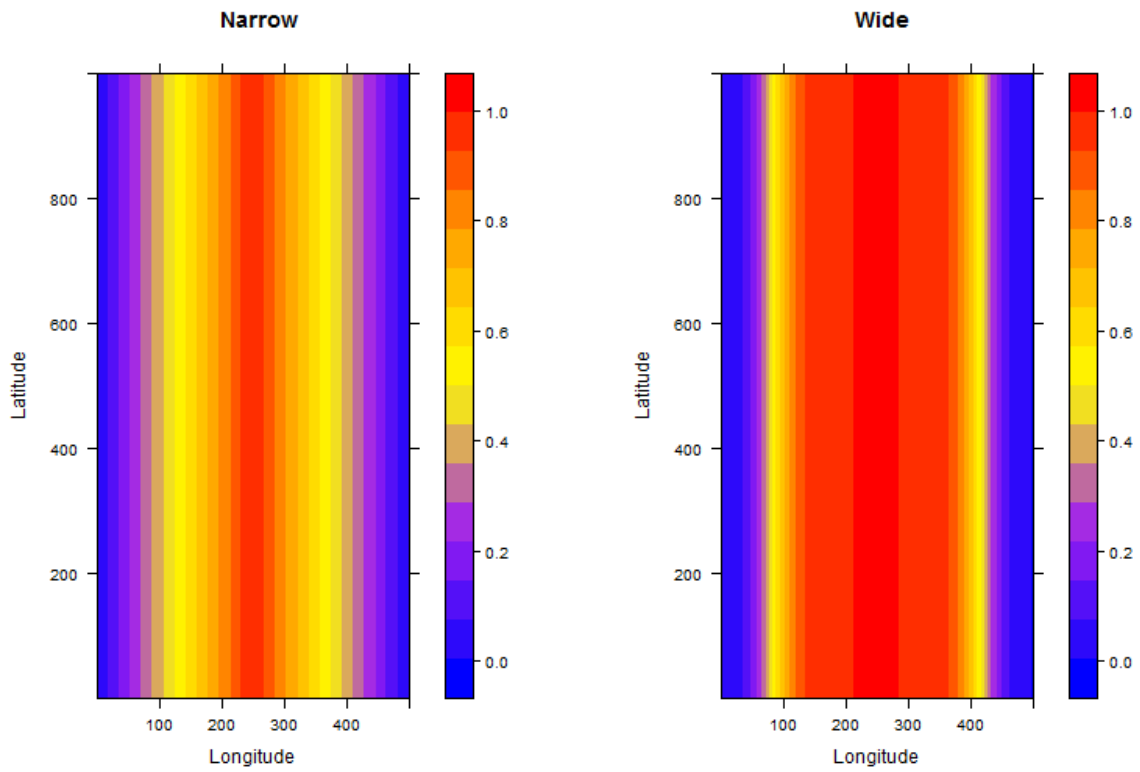


Figure 16: The two types of first-order effects used to simulate scallop populations: a narrow but highly dense first-order effect (left) and a wide but relatively less dense first-order effect (right).

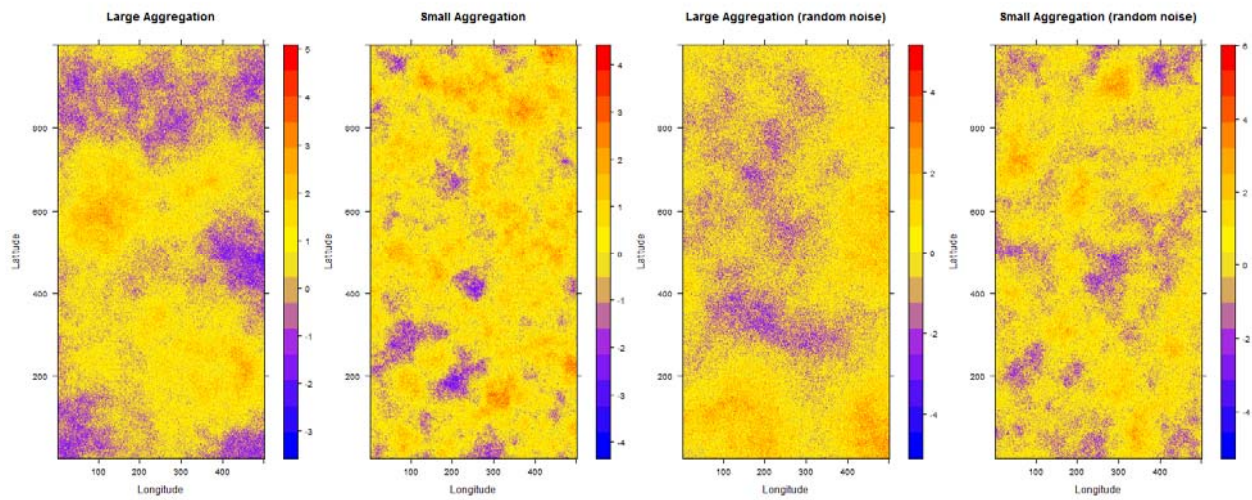


Figure 17: The four types of second-order trends tested to simulate scallop populations: large aggregations, small aggregations, large aggregations with a high random noise, and small aggregations with a high random noise (from left to right).

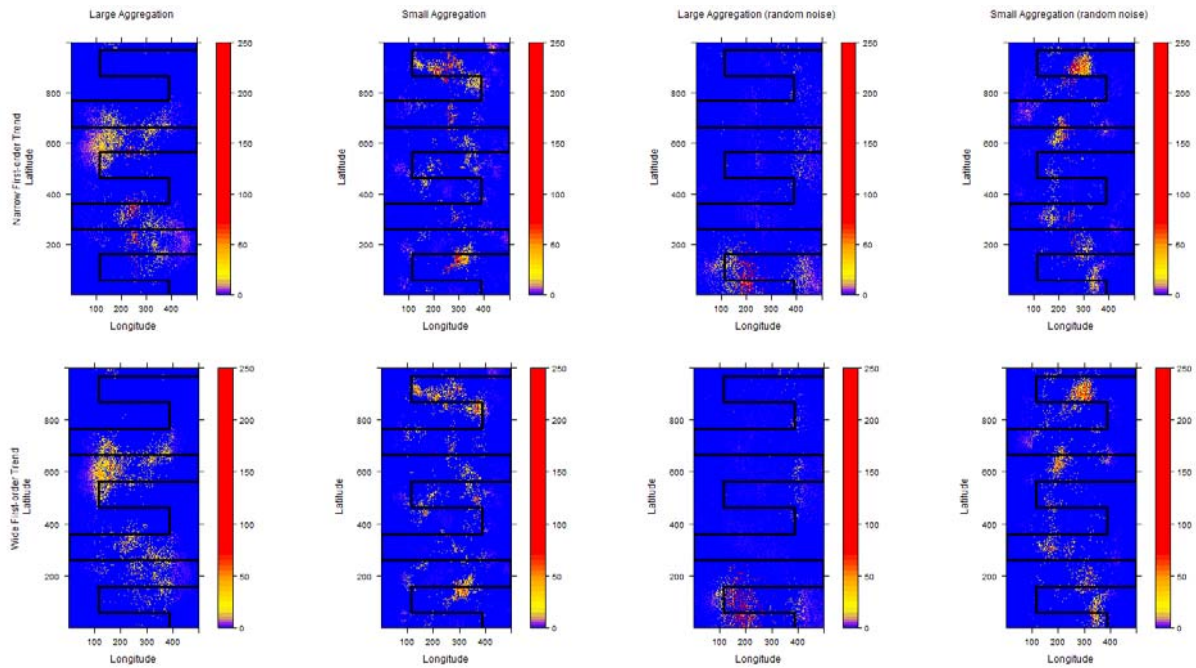


Figure 18: Example simulated scallop population distributions with an over-layed sampling track.

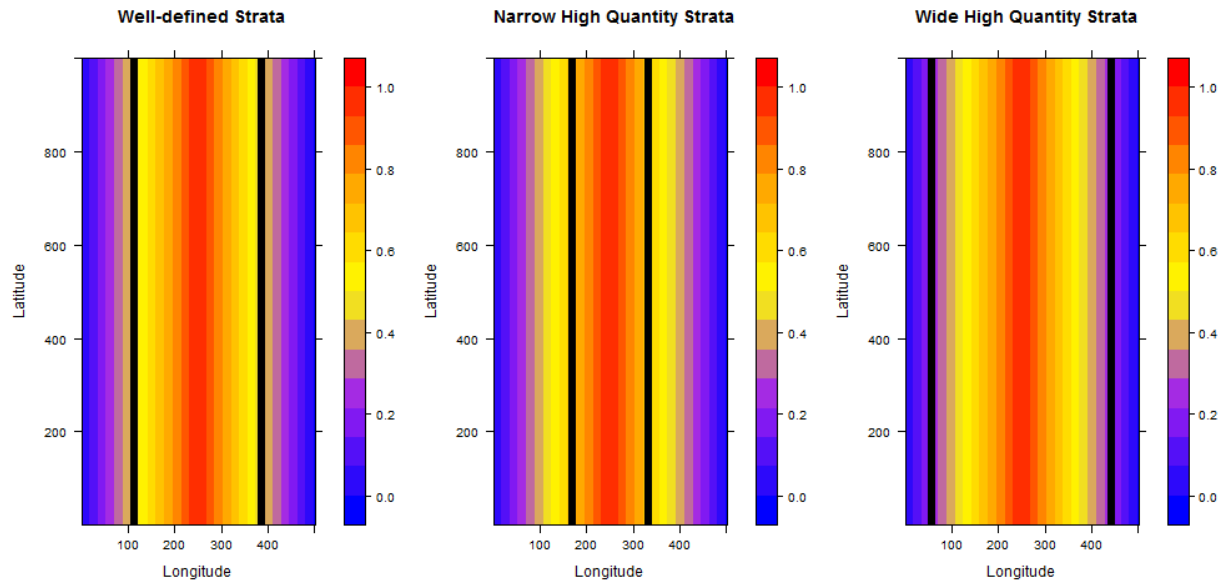


Figure 19: Alternative types of stratifications used for stratified mean estimations.

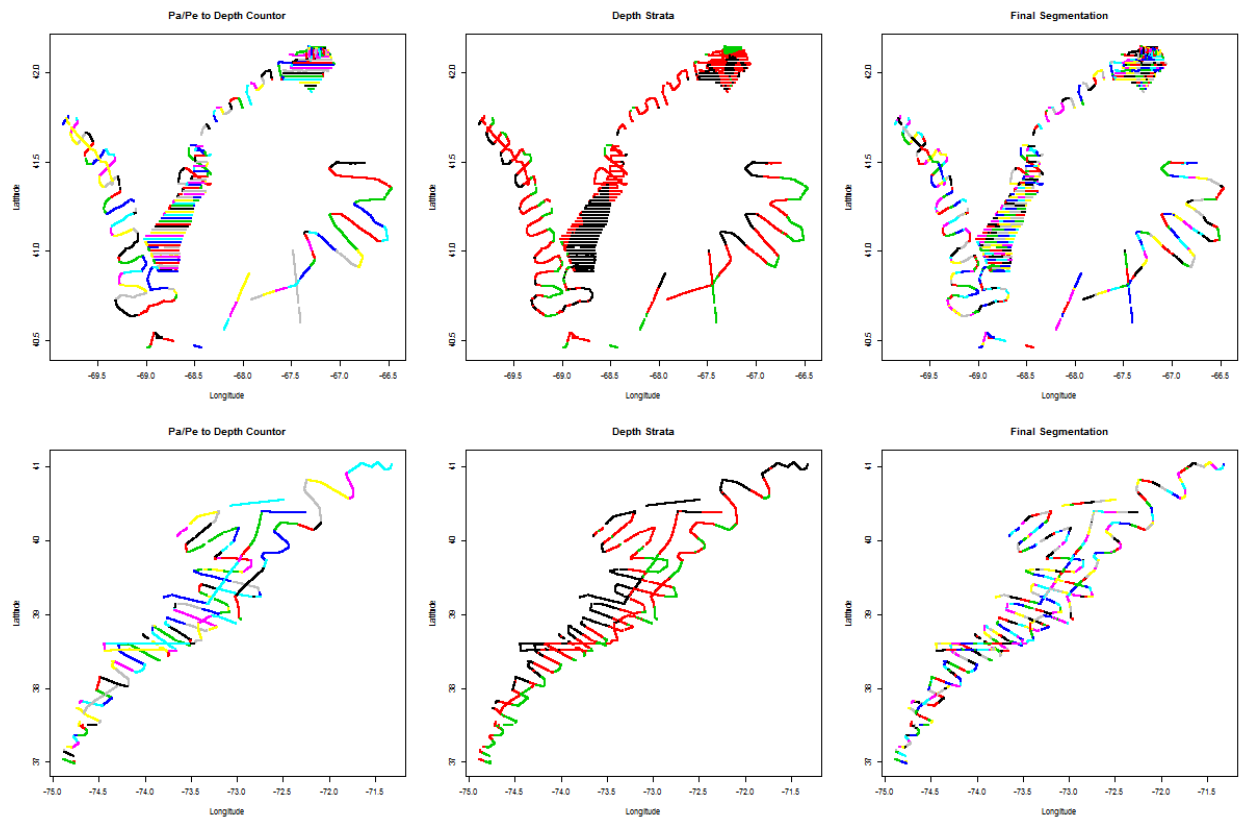


Figure 20: Transect segmentation for stratified mean estimation and the 2013 survey based on orientation to depth contours and distance between points (2 km) (left) and depth strata (center). The final combined segmentation is on the far right for GB (upper panels) and MAB (lower panels).

Appendix B7. Assessment of the sea scallop resource in the Northern Gulf of Maine management area

Samuel B. Truesdell (University of Maine, Orono, ME); Kevin H. Kelly (Maine Department of Marine Resources, W. Boothbay Harbor, ME); and Yong Chen (University of Maine, Orono, ME).

Summary

The sea scallop (*Placopecten magellanicus*) fishery in the Northern Gulf of Maine management area (NGOM) occurs in federal waters and is managed by the New England Fishery Management Council. The NGOM resource and associated fishery are locally important but amount to a small portion of the total stock and less than 0.1% of total landings. The fishery is managed by a TAC independently of the rest of the EEZ sea scallop stock. Management of the NGOM fishery does not involve biological reference points as targets or thresholds.

A cooperative survey was carried out by the Maine Department of Marine Resources and University of Maine during May-June of 2012. Based on survey results, estimated biomass of NGOM sea scallops targeted by the fishery (102+ mm or 4+ in shell height) was approximately 164.19 MT (90% confidence interval from 74.35 to 278.91), an increase from 115.40 MT (66.05 to 173.31) in 2009. These estimates are based on density estimates from the survey assuming a capture efficiency of 43.6%. The previous survey in 2009 noted a large year class of 10-50 mm scallops on Platts Bank; this year class was still evident in 2012 and had grown to approximately 65-90 mm.

Based on these biomass estimates the exploitation rate in weight (landings/stock biomass, assuming harvested scallops greater than 102 mm shell height and a dredge efficiency of 43.6%) during 2012 was 2.1% with a 90% confidence interval from 1.3% to 4.7%.

Several analyses were performed to determine how representative the survey was of the NGOM to determine applicability of survey results to management of the NGOM. The fraction of the NGOM covered by the survey area is 0.11, however using information regarding habitat preferences of scallops, the fraction of the suitable habitat area for the stock within the NGOM covered by the survey is 0.37. The survey extent was designed to ensure coverage of the primary fishing areas, and the fraction of fishing locations within the survey bounds was greater than 50% since 2006 and greater than 70% since 2011. Thus, the survey probably encompasses most of the areas with scallop concentrations high enough to support fishing activity indicating that survey results should be useful information for management of the NGOM scallop stock.

Introduction

The Gulf of Maine scallop fishery that occurs in federal waters is managed by the New England Fishery Management Council. Amendment 11 to the New England Fishery Management Council Sea Scallop Fishery Management Plan (NEFMC 2008) created a separate limited entry program for general category fishing in the Northern Gulf of Maine management area (NGOM; Fig. 1). The area is managed under an annual total allowable catch (TAC; currently 31.75 MT) and a daily possession limit of 90.7 kg (NEFMC 2008). Scallop dredge ring size must be greater than 102 mm, but there are currently no regulations regarding shell size (as in Maine state waters) or meat count.

Landings in the NGOM are low relative to the rest of the scallop stock, averaging just over 7 MT from 2008 to 2013 (total sea scallop landings have been over 20,000 MT in recent

years). In 2013 the most landings since the management area's inception in 2008 (over 18 MT) were reported, more than double any other year.

The region has limited fishery-independent data available. There was an offshore survey administered by the Maine Department of Marine Resources in 1974 (Spencer 1974), and in 1983 and 1984 NMFS sampled some areas in this region on their annual survey (Serchuk 1983; Serchuk and Wigley 1984), but no broad-scale surveys were completed between the early 1980s and 2008 when the region was first managed under a TAC. Given the lack of recent fishery-independent data, the initial allowable catch was determined using historical federal Gulf of Maine landings (NEFMC 2008). More recently, Maine Department of Marine Resources/University of Maine scallop surveys in 2009 and 2012, along with UMass Dartmouth video scallop surveys that occasionally sample in this area (e.g., Stokesbury et al. 2010) have offered fishery-independent sources of information to aid in generating the TAC.

The only management area-wide biomass estimate previously available was based on the Maine Department of Marine Resources/University of Maine scallop survey in 2009. This was a point estimate that used swept area to expand the survey results to a subset of the NGOM (this subset is discussed below; Fig. 1). This analysis estimated 103 MT of scallops greater than 102 mm shell height, with a confidence interval that ranged from 53 to 186 MT (Truesdell et al. 2010). This estimate was revised (see Results/Discussion section) during the current analysis and the new estimate for 2009 is 115.40 MT (90% confidence interval from 66.05 to 173.31). The best estimate based on the 2012 survey results indicates that the biomass of NGOM sea scallops over 102 mm shell height was approximately 164.19 MT of meats with a 90% confidence interval ranging from 74.35 to 278.91 MT.

Methods

Survey area identification and delineation

The NGOM management area is bounded by Cape Ann, Massachusetts in the west and the Canadian border in the east (Fig. 1). Prior to 2009 when the first survey was conducted, the NGOM had limited fishery dependent and no recent fishery-independent data available to help design the survey. Scallops are not found uniformly throughout this region so sampling efforts were focused on a subset of areas in the NGOM. To determine this subset, fishing locations from National Marine Fisheries Service vessel trip reports (VTRs) from 2000 to 2008 were reviewed as well as three historical surveys of the region from the 1970s and 1980s (Spencer 1974; Serchuk 1983; Serchuk and Wigley 1984). In addition to the information available, two fishermen with a history of scalloping in the Gulf of Maine were interviewed to help identify current and historical fishing grounds. These sources of information were used qualitatively to determine the five sampling areas: Machias-Seal Island (MSI), Mount Desert Rock (MDR), Platts Bank (PB), Northeast of Cape Ann (NCA) and Northern Stellwagen Bank (NSB; Fig. 1).

To increase sampling precision, the two western strata off the Massachusetts coast (where most fishing occurs), NCA and NSB, were further divided into substrata of expected high, medium and low scallop density.

Survey coverage area

Although the survey is intended to represent the NGOM scallop management area, the entirety of the NGOM was not sampled (Fig. 1); as such it is necessary to document the survey coverage area relative to total stock area, total stock biomass and the area fished. This was accomplished most simply by calculating the ratio of the sampling area (A_{SURVEY}) to the area of the NGOM (A_{NGOM})

$$R_{BASE} = \frac{A_{SURVEY}}{A_{NGOM}} \quad \text{Eqn. 1}$$

where R_{BASE} is the proportion of survey coverage. This baseline ratio is only one approach to estimating the coverage area of the survey, and it assumes that scallops are as likely to be found within the survey area as they are outside. However, the survey was designed specifically to sample the areas where scallops are distributed within the NGOM, so R_{BASE} is likely to be an underestimate of the survey's coverage of the scallop stock. Two additional methods were used to arrive at a more realistic approximation: one based on the depths at which scallops are typically found and another based on fishing effort data.

Sea scallops are typically more abundant at shallower depths (Merrill 1972; Posgay 1979; Serchuk et al. 1979); a depth threshold was employed as one way to estimate the effective coverage proportion of the survey. Serchuk et al. (1979) note that most commercial quantities of scallops are found in depths less than 100 m; this is corroborated by analyses of the NMFS bottom trawl survey from 1982 to 2010 and the NMFS bottom trawl survey from 2010 to 2012.

Employing a depth threshold DTh to determine an effective coverage proportion for the survey can be

$$R_{DTh} = \frac{A_{SURVEY}^*}{A_{DTh}} \quad \text{Eqn. 2}$$

where R_{DTh} stands for the ratio at a particular depth threshold (100 m in this analysis), A_{SURVEY}^* is the survey area shallower than the threshold and A_{DTh} is the area of the NGOM shallower than the depth threshold.

Alternatively, an effective coverage proportion can be estimated using fishing effort data. This assumes that the Gulf of Maine scallop fleet follows an ideal free distribution (Fretwell and Lucas 1969; i.e., fishing activity is directly related to abundance). Vessel monitoring system (VMS) data from 2006 to 2013 were used to determine the effort-based effective coverage proportion R_{VMS} as

$$R_{VMS} = \frac{P_{SURVEY}}{P_{NGOM}} \quad \text{Eqn. 3}$$

where R_{VMS} is the coverage proportion with respect to VMS observations (satellite location records), P_{SURVEY} is the number of VMS observations within the survey areas and P_{NGOM} is the total number of VMS observations within the NGOM.

Two resolutions of VMS data were considered: 1km and 3km. The advantage to the finer resolution is that the locations were more accurate, which is important near the boundaries of the areas. The disadvantage is that for confidentiality reasons less VMS data was available at higher resolutions. At the 1 km resolution 83% of VMS observations were available and at 3 km resolution 91% were available.

Survey design

Surveys were carried out in June and July of 2009 and in May and June of 2012. Dredge tow stations were selected from a grid overlying each stratum. The dimensions of each grid unit were 1 km². Each survey followed a two-stage random stratified design in the NCA and NSB strata. Station allocation in the first stage was based on fishing intensity from 2000-2008 vessel trip report (VTR) data and the size of each substratum. Forty stations in each stratum were assigned to the first stage and distributed among substrata according to the formula

$$N_s = 40 * \frac{M(V_s)A_s}{\sum_{s=1}^S M(V_s)A_s} \quad \text{Eqn. 4}$$

where N_s (rounded) is the number of stations to be sampled in substratum s , $M()$ is the median function, V_s is the VTR landings from 2000 to 2008 for substratum s and A_s is the area of substratum s . VTR data is assumed to be a proxy for scallop density and so was used to help allocate survey sample size. Such commercial data have also been used in the design of Canadian scallop surveys (Robert and Jamieson 1986; Serchuk and Wigley 1986). Area size was included in the weighting to ensure sufficient effort in the larger substrata.

In the NCA and NSB strata, which were further divided into substrata, a two-stage survey was employed. The approach taken by Francis (1984) was used to allocate tows to the second survey stage. His formula to assign one additional station among strata is:

$$G'_s = \frac{A_s^2 M_s^2}{n_s(n_s + 1)} \quad \text{Eqn. 5}$$

where G'_s is the assumed reduction in variance from adding a single station to a particular substratum s , A_s is the area, M_s is the mean catch rate (when squared, a proxy for the variance suggested by Francis (1984)) and n_s is the number of additional stations. Twenty stations were available for the second stage and were apportioned among the substrata. They were assigned one-by-one (by repeated use of Eqn. 5) according to whichever substratum would gain the most in terms of reduced variance from receiving one additional station. As such, the assignment of the j^{th} station can be written

$$G'_s = \frac{A_s^2 M_s^2}{(n_s + j - 1)(n_s + j)} \quad \text{Eqn. 6}$$

A single stage design was used for the remaining three strata in the eastern GOM.

In 2012 206 stations were sampled using a 2.13 m New Bedford style dredge with 51 mm rings, 4.4 cm head bale, 8.9 cm twine top, 25.4 cm pressure plate and rock chains. This gear was identical to that used in the 2009 survey. The target tow duration in 2009 was 7 minutes at a speed of 6.5km/h (a distance of approximately 750m). This was reduced to 5 minutes and about 540m in 2012, though fixed gear in some locations forced shorter tows.

Data Analyses

Historically, meat count by shell height has been found to vary regionally within the Gulf of Maine (Serchuk and Rak 1983), so separate models predicting meat weight using shell height were employed for each stratum. Depth was included because it has been shown to influence many aspects of scallop life history (Naidu and Robert 2006) and has been used in this type of analysis by Hennen and Hart (2012). These models also included a random effect (as in Hennen and Hart 2012) to account for repeated sampling within a station. The mixed effects models were produced using R (v. 2.15.1, R Core Team 2012) with the package lme4 (Bates et al. 2013). The form of the model within each stratum was

$$\ln(W_{i,t}) = \beta_1 \ln(H_{i,t}) + \beta_2 D_t + R_t + \varepsilon_{i,t} \quad \text{Eqn. 7}$$

where $W_{i,t}$ is the meat weight of individual i at station t , $H_{i,t}$ is its respective shell height, D_t is the depth, R_t is a random effect term associated with each station, β_1 and β_2 , are the coefficients of the explanatory variables, and $\varepsilon_{i,t}$ is the error term for each sample. Depth was important to include as a covariate because although meat weights were sampled whenever possible, the samples were not always evenly distributed throughout the depth range of a stratum, though the results were extrapolated across all depths. PB had a low number of meat weight samples in 2009 so the 2009 samples were combined with those from 2012 for the 2009 PB meat weight

model.

Prior to analyzing length frequency distributions, the number of scallops in each 5 mm size class belonging to a particular station was standardized to the mean swept area per station in the relevant stratum or substratum according to the formula:

$$Z_{l,s,c} = \frac{R_{l,s}}{\bar{R}_s} N_{l,s,c} \quad \text{Eqn. 8}$$

where $Z_{l,s,c}$ is the standardized count for scallops at station l within stratum (or substratum for strata 4 and 5) s in 5 mm size class c , $R_{l,s}$ is the swept area of the station tow, \bar{R}_s is the mean swept area for samples in area s , and $N_{l,s,c}$ is the number of scallops of size class c in tow l of area s . In these analyses the middle of the size bin was always used as the reference size for estimation.

The mean number of scallops within each stratum was estimated and uncertainty was addressed using bootstrapping and percentile confidence limits. Survey sample counts were bootstrapped 50,000 times. Bootstrapping was chosen to estimate confidence bounds because it requires few distributional assumptions (Efron and Tibshirani 1986) and avoids unrealistic confidence bounds that drop outside the range of observation (such as below zero).

To estimate the biomass and confidence limits for each stratum, the predicted meat weights from the mixed effects models at each location (1 km^2) within each stratum were estimated by size class and combined with the (sub)stratum length frequency distribution and the number of scallops per station to calculate the overall biomass per stratum such that

$$B_s = \sum_{g=1}^G \sum_{c=1}^C W_{s,c,g} P_{s,c} N_s \quad \text{Eqn. 9}$$

where B_s is the estimated biomass in stratum s , G is the number of 1 km^2 grids in stratum s , c is the number of 5 mm size classes over 102 mm (4 in; assumed to be harvestable size), W is the expected weight per scallop from Eqn. 7, $P_{s,c}$ is the proportion of scallops in stratum s within size class c , and N is the bootstrapped standardized mean count per station in stratum s . The upper and lower confidence limits were estimated by substituting the upper and lower percentile estimates for N in each substratum.

The dredge efficiency (vulnerability coefficient) used in this study was 43.6% which was estimated experimentally in Maine state waters (Kelly 2007). The Maine value was used because it was generated near the survey area and is close to other estimates of dredge efficiency (e.g., Gedamke et al. 2004).

Weight-based exploitation rates for the NGOM were estimated for 2009 and 2012 as

$$E = \frac{L}{B} \quad \text{Eqn. 10}$$

where E is the exploitation rate, L is the landings in weight and B is the total estimated biomass in the NGOM of scallops larger than 102 mm shell height. A 90% confidence interval for the exploitation rate was computed using the 5th and 95th percentiles for biomass, derived from the bootstrapping. Landings were assumed to be error-free.

Results and Discussion

Survey coverage area

The Northern Gulf of Maine management area encompasses a region of 23,470 km². Although this entire management area is under the regulations outlined in Amendment 11 to the sea scallop Fishery Management Plan (NEFMC 2008), scallops are not found throughout the region. The survey region (Fig. 1) has an area of 2,652 km² and the ratio of this region to the total area in the Northern Gulf of Maine regulatory region is 0.11 (Eqn. 1). While this areal coverage appears low, the effective survey coverage is larger in terms of both potential scallop habitat with respect to depth as well as the realized fishery area according to vessel monitoring system data.

The coverage proportion assuming a depth threshold of 100 m (Eqn. 2) is 0.37 (Fig. 2). This represents an estimate of the survey's coverage of the NGOM stock area, assuming depth is related to the probability of scallop occurrence. Using VMS data to determine the fraction of the fishery that occurs within the survey extent, the effective coverage proportion (Eqn. 3) was greater than 0.9 using either low or high resolution VMS data (Table 1). The proportion of total VMS observations by year (with no data excluded for confidentiality) was calculated by Burton Shank (NMFS NEFSC) for 2006-2013. Since 2009, the first year of the survey, the minimum coverage proportion was 0.69 (in 2010) and in 2013, the most recent year available, it was 0.87 (Table 2).

Scallop demographics within the NGOM

The most heavily fished area within the NGOM is the southwestern part, within survey areas NCA and NSB. In the NCA area, most scallops were found north of Cape Ann near the state waters boundary in both 2009 and 2012 (Fig. 3A). In the NSB area there were some scallops at the northern boundary (especially in 2012) and in both years scallops were found on the northern part of Stellwagen Bank near the southern-central part of the NSB area (Fig. 3A). Both NCA and NSB had wide, multimodal shell height distributions in both years (Figs. 4A-B). NSB was noteworthy in 2012 because it had signs of recent recruitment as well as some of the largest scallops seen on the survey.

In both years scallops were found on the southwest part of PB (Fig. 3B). The growth of the cohort first observed in 2009 was evident (Fig. 4C); the mode shell height grew from 32.5 mm in 2009 to 72.5 mm in 2012. In both years there was a small proportion of scallops that were between 125 and 150 mm. The survey in MDR encountered almost no scallops in both years (Fig. 3C). There were scallops to the south of this area near Mount Desert Rock in both years, but this small region is within Maine state waters and not part of the NGOM. The scallops that were caught in 2009 were mainly less than 100 mm (Fig. 4D). In 2012 only a single scallop was caught in this area. In the MSI area there was no obvious coherence between the spatial distribution of catch in the 2009 and 2012 surveys; scallops within this area appear from these surveys to be fairly evenly distributed relative to the patchiness observed in NCA and NSB to the south (Fig. 3D). The only persistent aggregation was near Machias Seal Island, again within state waters. Little signs of recruitment were seen in this region in either 2009 or 2012 and most scallops were between 110 and 150 mm (Fig. 4E).

The relationship between shell height and meat weight varied by area, as in 2009 (Fig. 5). The best condition meats were in NSB and NCA, while the meats in MSI were clearly smaller for their size. Few samples of larger scallops were taken on PB, but those greater than 100 mm were of similarly poor condition to the scallops sampled in MSI.

Biomass and exploitation rate estimates

Analysis of the surveys produced estimates indicating that the NGOM had overall harvestable biomass in 2009 and 2012 of 115.40 MT (90% confidence interval from 66.05 to

173.31) and 164.19 MT (74.35 to 278.91), respectively. The 2009 estimate was revised slightly since 2010 because of the new meat weight estimates for Platts Bank, a slightly different approach to the bootstrapping (previously a bootstrapping with replacement method was used along with bias corrected confidence intervals; see Truesdell et al. 2010), and the correction of an error that was found in the standardization of length frequencies. The original estimate given was 103 (53 to 186) MT (Truesdell et al. 2010). In addition, the assumed dredge efficiency in 2009 was 40%, but this was changed to 43.6%, which is based on a dredge efficiency study by the Maine Department of Marine Resources.

Harvestable biomass was distributed disproportionately across the areas surveyed. In the eastern half of the NGOM, the MSI area was found to have consistently high biomass (Fig. 6), though the density of biomass was lower than in some regions of the western NGOM (Fig. 7). Further west and offshore, PB was estimated to contain 5.6 harvestable MT in 2009 and 2.1 MT in 2012. However, this assumes that none of the large year class on PB is yet available to fishing since these scallops are under the assumed harvestable size of 102 mm used in this study (Fig. 4C). Given the increased activity on Platts Bank evident in VMS data however, it is likely that some fishermen are targeting this year class though its biomass is not included in the calculations presented here. Still further west in the two strata where most of the fishing currently occurs, NCA and NSB, the mean biomass available for harvest was 17.0 and 43.55 MT in 2009 and 55.6 and 67.2 MT in 2012. Despite their relatively small areas (Fig. 1), the high expected density strata within these regions supported considerable biomass of harvestable scallops in both survey years relative to the other areas surveyed (Fig. 6).

These biomass estimates are dependent on some fixed parameters. Survey dredge efficiency was assumed to be 43.6%, which was determined experimentally in Maine waters. No uncertainty is attached to this estimate however. Gadamke et al. (2004) estimated the efficiency of a dredge with 89 mm rings to be 42.7%, with a potential range based on sensitivity analyses from 35.5 to 52.5%. The gear was different (this study used 51 mm rings), but the mean estimate was similar to the Maine study. The approximate sensitivity range from Gadamke et al.'s study was used as a sensitivity range for the 2012 biomass estimates presented here. If dredge efficiency is assumed to be 35% the 2012 estimate is 207.51 MT (with a 90% confidence interval ranging from 93.35 to 353.29; Table 3). If dredge efficiency is 50% the estimate is 143.14 MT (65.00 to 242.88). No uncertainty was considered for the shell height to meat weight relationships or the length frequency distributions. These sources of uncertainty should be considered in subsequent analyses, though they are probably better estimated than sampling variability which is likely the main source of uncertainty and was quantified by bootstrapping.

Landings were low from 2008 to 2012, though increased notably in 2013 (Fig. 8). To determine the source of this change it would be necessary to examine vessel trip report data; however that information is not currently available to the authors. One possible reason for the higher landings, is the increased fishing effort on PB as the year class first observed in 2009 may have become targeted by the fishery.

The estimated exploitation rate during 2012 was 2.14% (90% confidence interval from 1.26% to 4.72%; Table 3), which is lower than the 6.1% (4.1% to 10.7%) estimated during 2009. The reduced exploitation rate was a function of both a decrease in landings (Figure 8) and the increase in estimated biomass from 115.40 MT in 2009 to 164.16 MT in 2012.

Characterization of scallops in the Gulf of Maine

The Maine Department of Marine Resources mid-1970s survey report (Spencer 1974) noted that most scallops encountered were older and there was no evidence of recent recruitment,

leading Spencer to conclude that “only in widely separated years do scallops set in these offshore waters.” The report stated that only near-shore fishing was tenable at present, though it was noted that in the 1960s the beds around Jeffereys Ledge were commercially viable. In the early 1980s scallop sets were recorded in the GOM: Serchuk (1984) and Serchuk and Wigley (1984) reported large quantities of small scallops offshore on Fippennies Ledge and Jeffereys Ledge. High densities of commercial size scallops, however, were not found in either of these surveys (Serchuk and Wigley 1984). The Maine Department of Marine Resources/University of Maine 2009 survey identified a large set of scallops on Platts Bank. Another 2009 Gulf of Maine survey corroborated these findings and also observed small scallops on Fippennies Ledge, Jeffereys Ledge and Cashes Ledge (Stokesbury et al. 2010). No such recruitment event was seen in the Maine Department of Marine Resources/University of Maine 2012 survey however.

While the fishery-independent data are not extensive for this region, it is clear that scallop sets in the NGOM are intermittent. In most years recruitment is limited or non-existent, but occasionally large recruitment events do occur. This is supported by the history of the commercial fishery in the region, which is highly variable (Dow 1971; Kelly 2012). The exception may be the western NGOM, in particular the NSB and NCA areas. It is evident from the length frequency distributions (Figs. 4A-B) that recruitment is more stable in this region than to the east where not all size classes are evident. This discrepancy may indicate environmental differences between the eastern and western NGOM, in particular how local oceanography interacts with the early life history of scallops.

Conclusions

Scallops in the NGOM represent a small but locally important fishery. Landings have been low since the inception of the NGOM management area, though they more than doubled in 2013. The best estimates from 2009 and 2012 indicate that scallop biomass increased by about 40% over that period. The exploitation rate in weight (landings/stock harvestable biomass) during 2009 was 6.1% with a 90% confidence interval from 4.1% to 10.7%, and during 2012 was 2.1% (1.3% to 4.7%). Given the region’s low biomass relative to the rest of the stock along with its intermittent recruitment in eastern areas, it is probably not necessary to survey the NGOM every year. However, periodic surveys that provide point biomass estimates are likely to be helpful to managers for determining a TAC.

Acknowledgements

We would like to thank Wallace and Steve Gray and the late Wallace Gray Jr. and Wayne Young of the *F/V Foxy Lady II*, and Glenn Nutting, Anna Henry, and Mike Kersula who assisted as scientific observers. The National Marine Fisheries Service Sea Scallop Research Set-Aside Program and the NMFS-Sea Grant fellowship program in population dynamics funded this study.

References

- Bates, Douglas, Maechler, M., Bolker, B. and Walker, S. 2013. lme4: Linear mixed-effects models using Eigen and S4. R package version 1.0-4. <http://CRAN.R-project.org/package=lme4>
- Dow, R.L. 1971. Periodicity of Sea Scallop Abundance Fluctuations in the Northern Gulf of Maine. Bulletin of the Department of Sea and Shore Fisheries. Research Bulletin No. 31.
- Efron, B., and Tibshirani, R. 1986. Bootstrap methods for standard errors, confidence intervals, and other measures of statistical accuracy. *Statistical science* 1: 54–75.
- Francis, R.I.C.C. 1984. An adaptive strategy for stratified random trawl surveys. *New Zealand Journal of Marine and Freshwater Research* 18: 59–71.
- Fretwell, S.D., and Lucas, H.L. 1969. On territorial behavior and other factors influencing habitat distribution in birds. *Acta biotheoretica* 19: 16–36.
- Gedamke, T., DuPaul, W.D., and Hoenig, J.M. 2004. A Spatially Explicit Open-Ocean DeLury Analysis to Estimate Gear Efficiency in the Dredge Fishery for Sea Scallop *Placopecten magellanicus*. *North American Journal of Fisheries Management* 24: 335–351.
- Hennen, D.R., and Hart, D.R. 2012. Shell height-to-weight relationships for Atlantic sea scallops (*Placopecten magellanicus*) in offshore US waters. *Journal of Shellfish Research* 31: 1133–1144.
- Kelly, K.H. 2007. Results from the 2006 Maine Sea Scallop Survey. Maine Department of Marine Resources; West Boothbay Harbor, Maine.
- Kelly, K.H. 2012. Results from the 2011 Maine Sea Scallop Survey. Maine Department of Marine Resources; West Boothbay Harbor, Maine.
- Merrill, A.S. 1960. Abundance and distribution of sea scallops off the Middle Atlantic coast. *Proceedings of the National Shellfisheries Association* 51: 74–80.
- Naidu, K.S., and Robert, G. 2006. Chapter 15 Fisheries sea scallop, *Placopecten magellanicus*. *In* *Scallops: Biology, Ecology and Aquaculture*. Elsevier. pp. 869–905.
- New England Fisheries Management Council (NEFMC). 2008. Fisheries of the Northeastern United States; Atlantic Sea Scallop Fishery; Amendment 11; Final Rule.
- Posgay, J.A. 1979. Sea scallop *Placopecten magellanicus* (Gmelin). *In* *Fish distribution*. Edited by M.D. Grosslein and T. Azarovitz. New York Sea Grant Institute. pp. 130–133.
- R Core Team. 2012. R: A language and environment for statistical computing. R Foundation for Statistical Computing, Vienna, Austria. ISBN 3-900051-07-0, URL <http://www.R-project.org/>.

- Robert, G., and Jamieson, G.S. 1986. Commercial fishery data isopleths and their use in offshore sea scallop (*Placopecten magellanicus*) stock evaluations. *In* Proceedings of the North Pacific Workshop on Stock Assessment and Management of Invertebrates. Can. Spec. Publ. Fish. Aquat. Sci. pp. 76–82.
- Serchuk, F.M. 1983. Results of the 1983 USA Sea Scallop research survey: distribution and abundance of Sea Scallops in the Georges Bank, Mid-Atlantic and Gulf of Maine Regions and biological characteristics of Iceland Scallops off the coast of Massachusetts. Northeast Fisheries Science Center Reference Document 83-37, Woods Hole, Massachusetts.
- Serchuk, F.M., and Rak, R.S. 1983. Biological characteristics of offshore Gulf of Maine sea scallop populations: size distributions, shell height meat weight relationships and relative fecundity patterns. Northeast Fisheries Science Center Reference Document 83-07, Woods Hole, Massachusetts.
- Serchuk, F.M., and Wigley, S.E. 1984. Results of the 1984 USA sea scallop research vessel survey: status of sea scallop resources in the Georges Bank, Mid-Atlantic and Gulf of Maine regions and abundance and distribution of Iceland scallops off the southeastern coast of Cape Cod. Northeast Fisheries Science Center Reference Document 84-34, Woods Hole, Massachusetts.
- Serchuk, F.M., and Wigley, S.E. 1986. Evaluation of USA and Canadian Research Vessel Surveys for Sea Scallops (*Placopecten magellanicus*) on Georges Bank. *Journal of Northwest Atlantic Fisheries Science*. 7: 1–13.
- Serchuk, F.M., Wood, P.W., Posgay, J.A., and Brown, B.E. 1979. Assessment and status of sea scallop (*Placopecten magellanicus*) populations off the northeast coast of the United States. *Proceedings of the National Shellfisheries Association* 69: 161–191.
- Spencer, F. 1974. Final report: offshore scallop survey - Cape Ann, Massachusetts to Maine-Canadian border. Maine Department of Marine Resources.
- Stokesbury, K.D., Carey, J.D., Harris, B.P., and O’Keefe, C.E. 2010. High densities of juvenile Sea Scallop (*Placopecten magellanicus*) on banks and ledges in the central Gulf of Maine. *Journal of Shellfish Research* 29: 369–372.
- Truesdell, SB, KH Kelly, CE O’Keefe and Yong Chen. 2010. An assessment of the sea scallop resource in the Northern Gulf of Maine management area. Appendix B6 to the 50th Northeast Regional Stock Assessment Workshop (50th SAW) assessment report. Northeast Fisheries Science Center Reference Document 10-17, Woods Hole, Massachusetts.

Table 1: Survey coverage proportion calculated using three methods (See Eqns. 1-3). Num. stands for numerator, den. stands for denominator and prop. stands for proportion.

Type	Num. descriptor	Num. value	Den. descriptor	Den. value	Prop. inside
Area	Total survey area (km ²)	2,652	NGOM	23,470	0.11
Depth thresh.	Survey area < 100m	2,652	NGOM < 100m	7,132	0.37
VMS – low res.	VMS inside survey area	26,661	Total VMS within NGOM	27,217	0.98
VMS – high res.	VMS inside survey area	21,901	Total VMS within NGOM	23,555	0.93

Table 2: Proportion of VMS observations within the NGOM survey area. All VMS observations were included (i.e., none were excluded for confidentiality). Table provided by Burton Shank (NMFS NEFSC).

Year	Proportion inside
2006	0.94
2007	0.94
2008	0.55
2009	0.84
2010	0.69
2011	0.74
2012	0.81
2013	0.87
Overall	0.86

Table 3: Best estimates for 2012 NGOM harvestable biomass (HB) and corresponding exploitation rates (ER) under three assumptions of dredge efficiency.

Assumed Dredge Efficiency	5 th percentile		Mean		95 th percentile	
	HB	ER %	HB	ER %	HB	ER %
35%	93.35	3.76	207.51	1.69	353.29	0.99
43.6%	74.35	4.72	164.19	2.14	278.91	1.26
50%	65.00	5.40	143.14	2.45	242.88	1.44

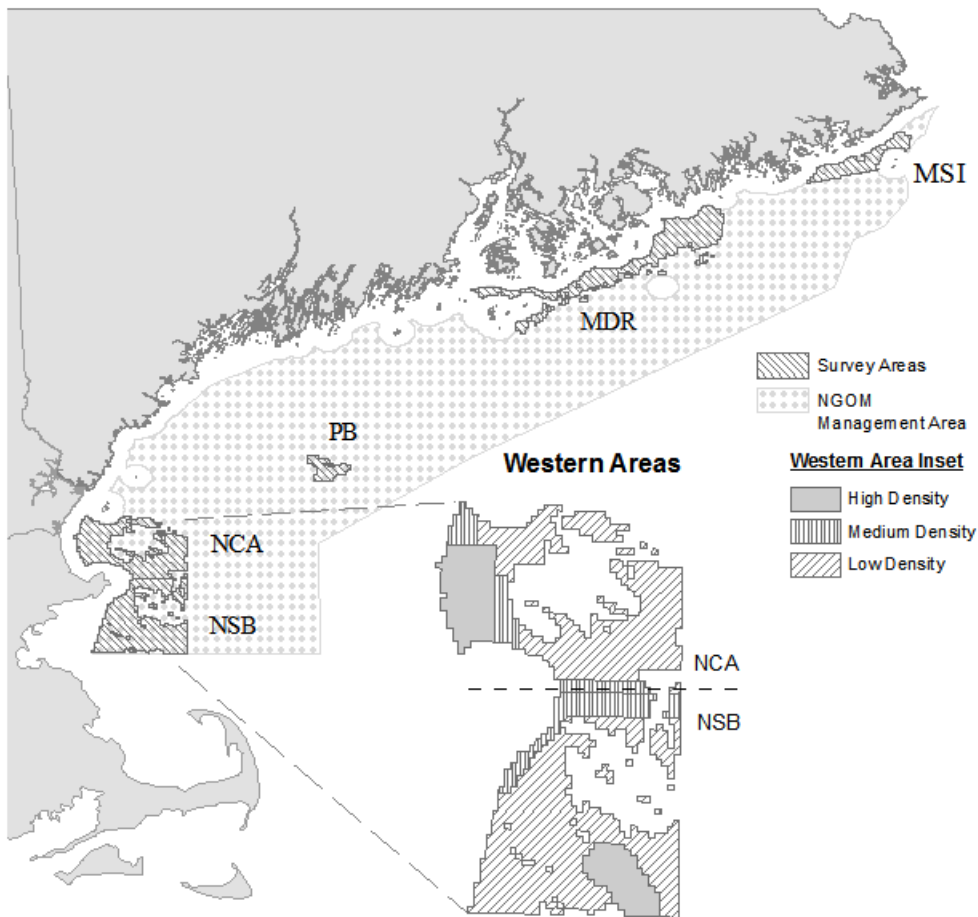


Figure 1: The NGOM and the 5 strata selected for the survey, with substrata of differing expected scallop density appearing in the western areas inset. MSI: Machias-Seal Island; MDR: Mount Desert Rock; PB: Platts Bank; NCA: Northeast of Cape Ann; NSB: Northern Stellwagen Bank.

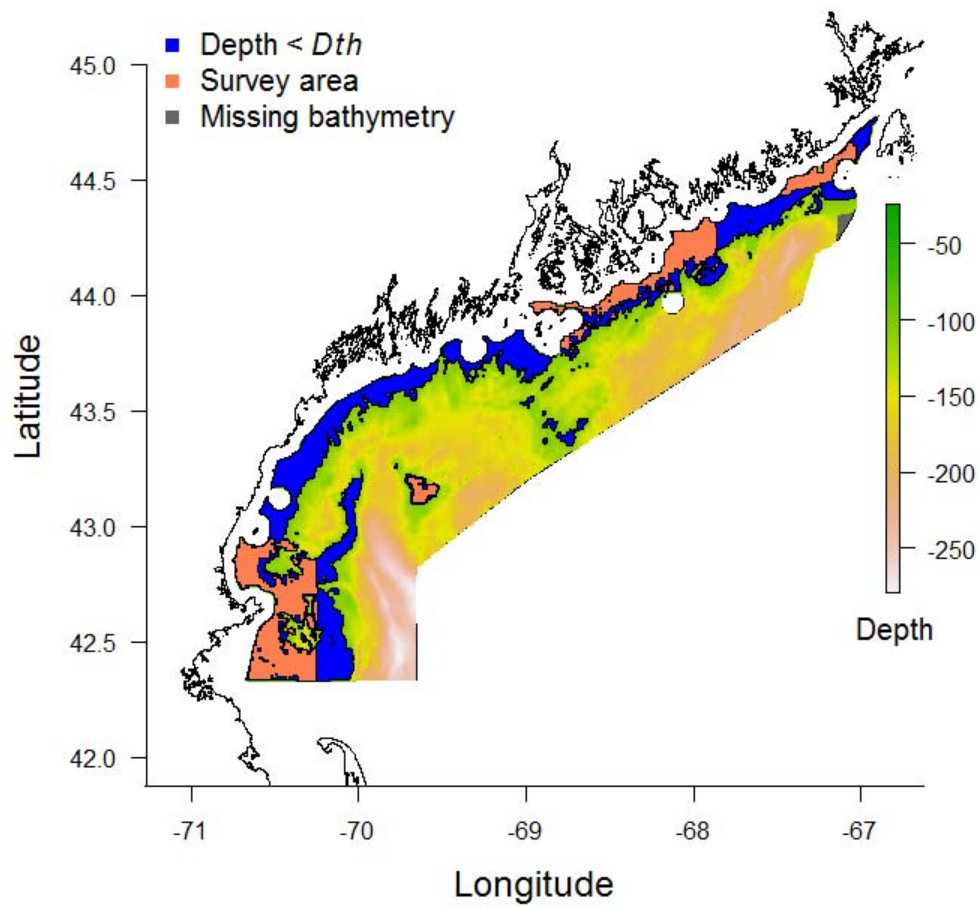


Figure 2: Survey area (pink) relative to the NGOM shallower than 100 m (*Dth*; blue). The survey area accounts for 37% of the NGOM shallower than 100 m.

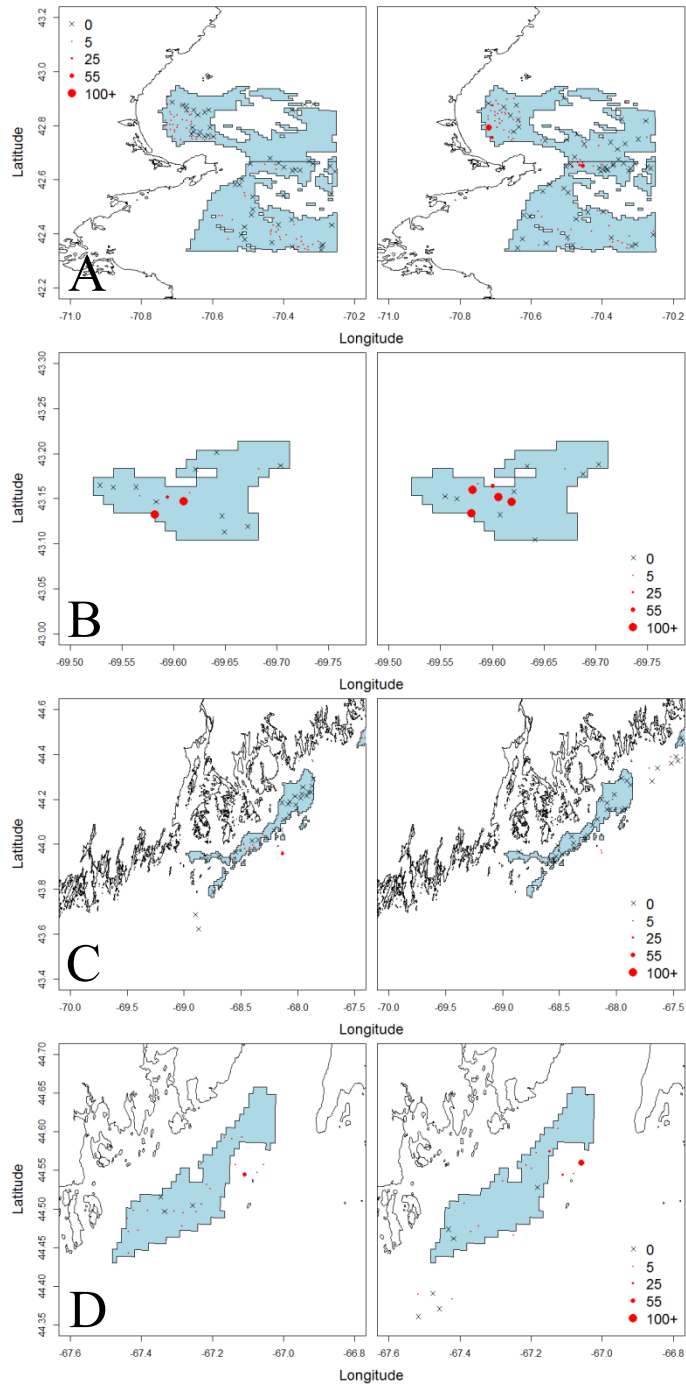


Figure 3: Distribution of survey scallop catch (all sizes) in 2009 (left panels) and 2012 (right panels). A: NCA and NSB; B: PB; C: MDR; and D: MSI.

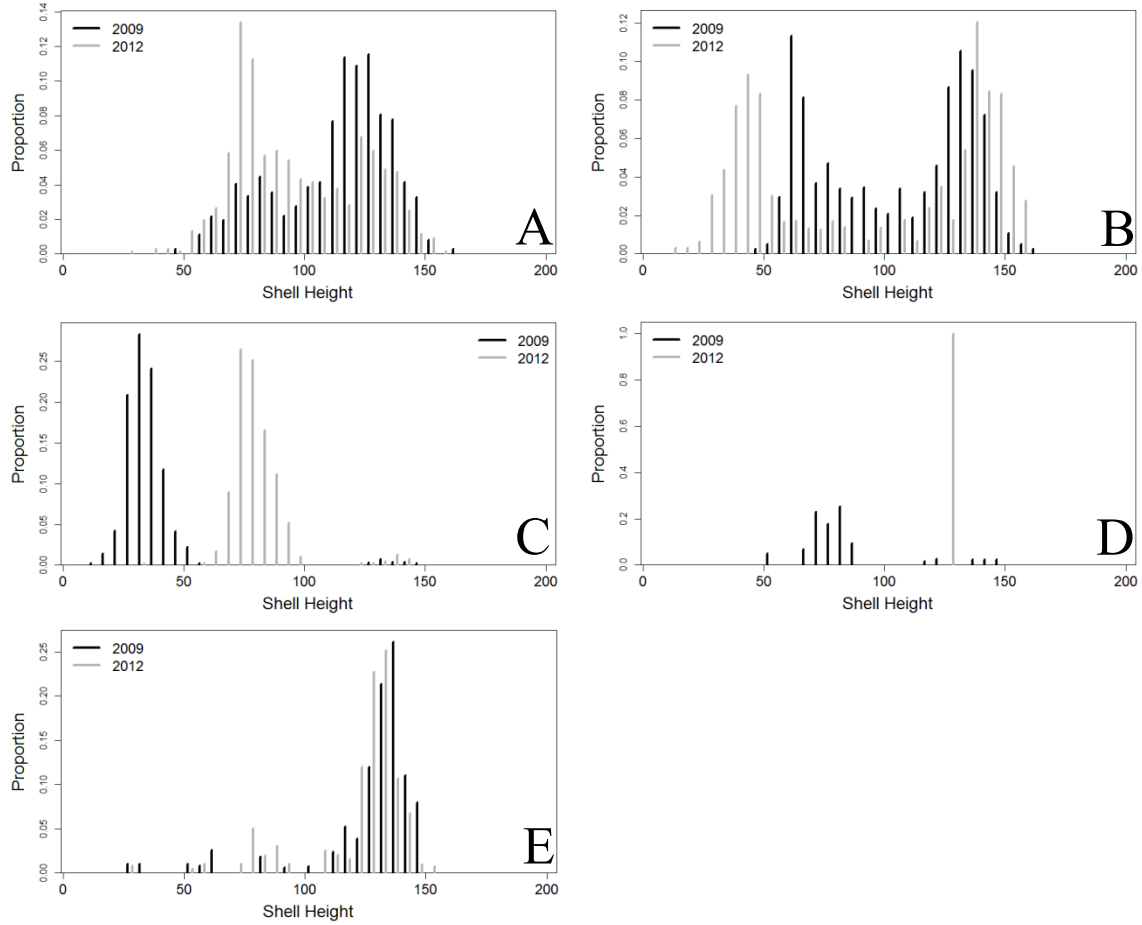


Figure 4: Shell height distribution in mm for each of the areas in 2009 and 2012. A: NCA; B: NSB; C: PB; D: MDR; E: MSI.

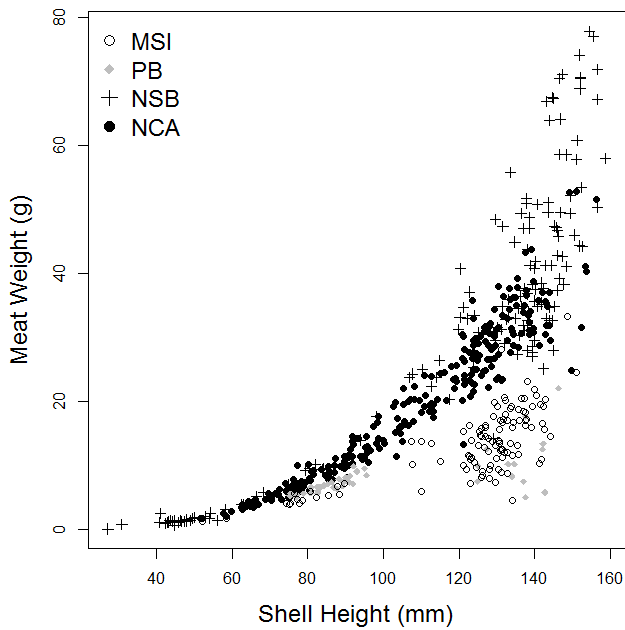


Figure 5: Relationship between shell height and meat weight in 2012 for the survey areas (excluding MDR).

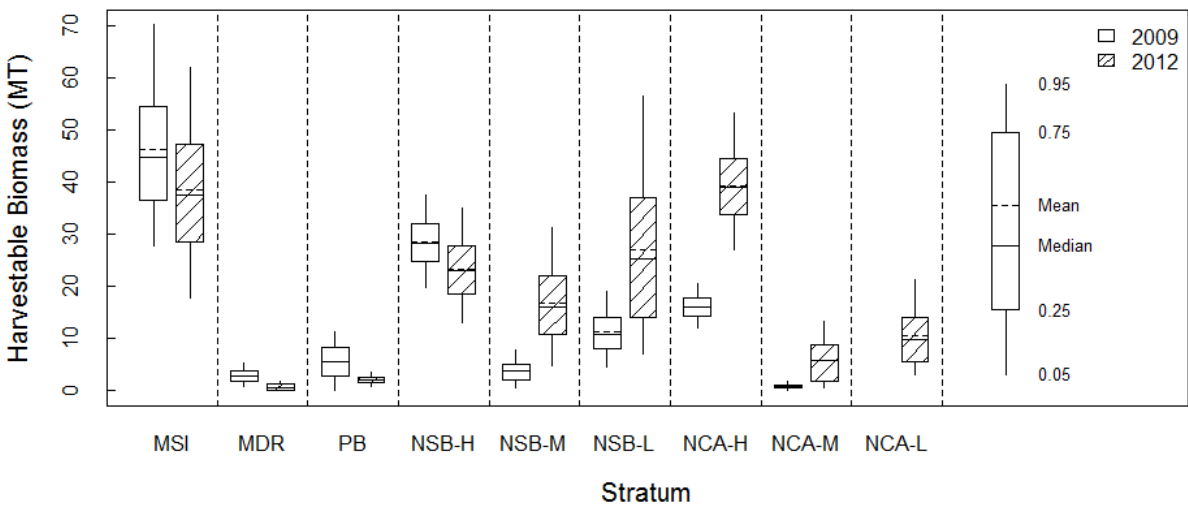


Figure 6: 2009 and 2012 harvestable biomass in NGOM survey strata (and substrata in the western region). H, M and L indicate expected high, medium and low density substrata.

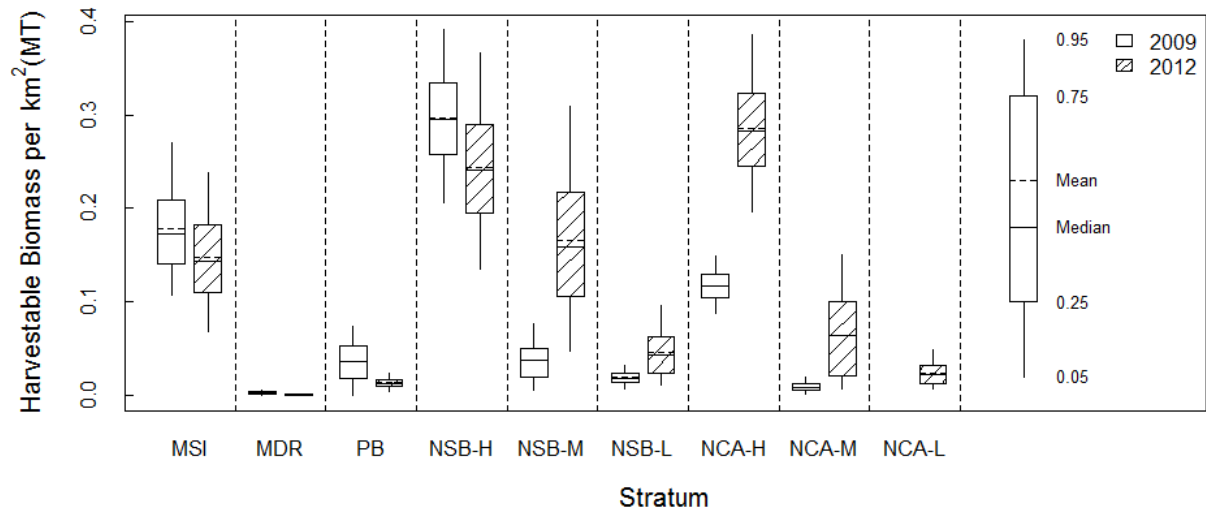


Figure 7: 2009 and 2012 harvestable density (in biomass per km²) in NGOM survey strata (and substrata in the western region). H, M and L indicate expected high, medium and low density substrata.

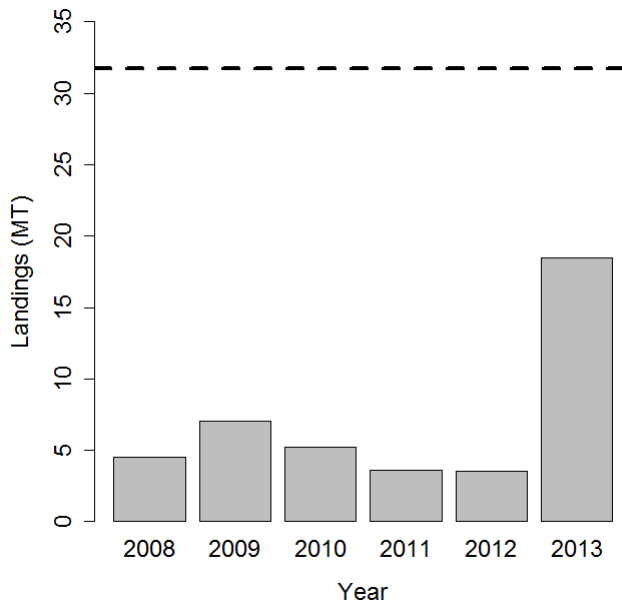


Figure 8: Landings history for the NGOM management area since its inception in 2008. Dashed line is the 31.75 MT quota.

Appendix B8. Relationships between chlorophyll and scallop recruitment potentially useful for stock projections and assessment modeling

Kevin Friedland (NEFSC, Narragansett, RI), Deborah Hart and Burton Shank (NEFSC, Woods Hole, MA)

Summary

Preliminary analyses of remote sensing and scallop dredge data suggest that recruitment to the yearling stage is influenced by summer phytoplankton bloom activity. Blooms in areas likely to influence Middle Atlantic spawning aggregations occur just prior to spring and summer spawning periods with larger bloom levels associated with high yearling settlement. The results of this analysis are encouraging and indicate further work developing techniques for predicting regional recruitment patterns based on chlorophyll concentrations is warranted. Such predictions are at spatial scales of interest to managers (e.g. rotational management areas) and might be used to improve management and profitability of the fishery.

Introduction

This appendix describes an analysis of spring and summer bloom activity and scallop recruitment in the Middle Atlantic Bight during 1998 to 2012. The topic is important because uncertainty about recent and near-term scallop recruitment reduces the accuracy of stock projection analyses used to set harvest levels and to open rotational fishing areas. Recruitment of scallops in the region was represented by two indices based on survey data: i) a yearling index based on the abundance of 1-year old scallops, and ii) a 2-year old index. The two indices generally agree but there are notable disagreements for some year classes, indicating potential measurement errors in the survey data and/or variable survival between age-1 and 2. For the purpose of this summary, we will concentrate on the results of modeling recruitment to the yearling stage.

There are two spawning periods for Middle Atlantic Bight scallops. Spring spawning occurs mostly during May and fall spawning occurs in September. In line with these putative spawning periods, the spring and summer bloom dynamics of the Middle Atlantic Bight were characterized using chlorophyll *a* concentrations based on remote sensing data. The distribution of blooms was evaluated over a 0.5° spatial grid. Chlorophyll *a* concentrations were based on remote-sensing measurements made with the Sea-viewing Wide Field of View (SeaWiFS) and Moderate Resolution Imaging Spectroradiometer (MODIS) sensors. The level-3 processed data, at 9 km and 8-day spatial and temporal resolutions, respectively, were obtained from the Ocean Color website (oceancolor.gsfc.nasa.gov). These two sensors provide an overlapping time series of chlorophyll *a* concentrations during the period 1998 to 2013. An analysis restricted to the overlapping period of data from both sensors revealed a systemic and consistent difference (relative bias) between them. We corrected for this bias with simple correction factors applied to MODIS data to approximate the mean levels of the SeaWiFS data. Chlorophyll *a* concentrations (mg m^{-3}) were calculated by taking the average of the constituent pixel elements for each spatial-temporal cell.

The sequential averaging algorithm called STARS or “sequential *t*-test analysis of regime shifts” (Rodionov, 2004, 2006) was used to find the beginning and end of blooms (change

points) in the chlorophyll time series. A detected bloom could not exceed nine sample periods (approximately 2.4 months) based on analyses of climatological bloom patterns. Periods bracketed by positive and negative change points exceeding nine 8-day periods were considered to be ecologically different from discrete blooms. This method has been used in previous analyses of Northeast Shelf bloom patterns (Friedland et al., 2008, 2009) and elsewhere (Friedland and Todd, 2012).

We extracted statistics to characterize timing and magnitude of each bloom. Bloom start was defined as the day of initiation, which was the first day of the 8-day bloom period that exhibited bloom conditions. Bloom magnitude was the integral of the chlorophyll concentrations during the bloom period. In some years and locations, no distinct bloom period was detected by the STARS algorithm; when this occurred, bloom magnitude was taken as the integral of chlorophyll concentrations during the climatological (long-term average) bloom period based on average start and end dates for years with blooms.

Results

Yearling scallop recruitment appears to be related to spring and summer phytoplankton blooms in the Middle Atlantic Bight. The area of highest correlation between spring chlorophyll concentrations and yearling recruitment was on the continental shelf off Long Island (Fig. 1a). In contrast, the area of the greatest correlative density between summer chlorophyll concentrations and yearling recruitment was off the New Jersey coast (Fig. 1b). Mean seasonal surface currents suggest that these blooms contributed to both water column chlorophyll and depositional particulate organic carbon in the areas of spawning scallops. These observations are consistent with the hypotheses that blooms either stimulate scallop spawning or support larval survival. Recruitment to age two was not related to the same spring and summer bloom patterns as yearling scallops due primarily to the change in population size of the 2011 year class between year-1 and 2.

Future research

Refine models that predict scallop recruitment based on chlorophyll and predator data to improve estimates from stock assessment and projection models. Investigate statistical approaches to refine yearling recruitment indices. Develop complimentary models of bloom driven settlement and spatio-temporal predation pressure to ultimately stimulate recruitment of scallops to the fishery.

References

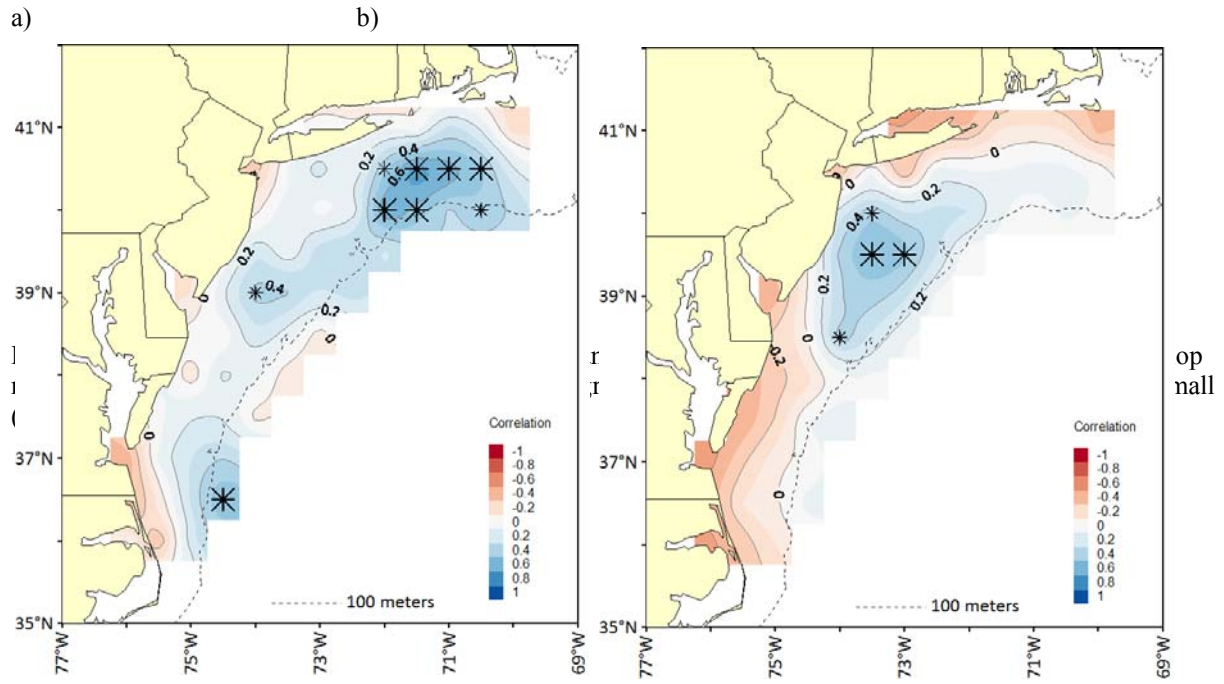
- Friedland, K.D., Hare, J.A., Wood, G.B., Col, L.A., Buckley, L.J., Mountain, D.G., Kane, J., Brodziak, J., Lough, R.G., Pilskaln, C.H., 2008. Does the fall phytoplankton bloom control recruitment of Georges Bank haddock, *Melanogrammus aeglefinus*, through parental condition? *Can J Fish Aquat Sci* 65, 1076-1086.
- Friedland, K.D., Hare, J.A., Wood, G.B., Col, L.A., Buckley, L.J., Mountain, D.G., Kane, J., Brodziak, J., Lough, R.G., Pilskaln, C.H., 2009. Reply to the comment by Payne et al. on "Does the fall phytoplankton bloom control recruitment of Georges Bank haddock, *Melanogrammus aeglefinus*, through parental condition?". *Can J Fish Aquat Sci* 66, 873-

877.

Friedland, K.D., Todd, C.D., 2012. Changes in Northwest Atlantic Arctic and Subarctic conditions and the growth response of Atlantic salmon. *Polar Biology* 35, 593-609.

Rodionov, S.N., 2004. A sequential algorithm for testing climate regime shifts. *Geophys Res Lett* 31, Doi 10.1029/2004gl019448.

Rodionov, S.N., 2006. Use of prewhitening in climate regime shift detection. *Geophys Res Lett* 33, Doi 10.1029/2006gl025904.



Appendix B9. Technical documentation for the CASA length structured stock assessment model used in the SARC-59 sea scallop stock assessment.

Larry Jacobson, Northeast Fisheries Science Center, Woods Hole, MA.

[*This technical description is current through CASA version nc246.*]

The stock assessment model described here is based on Sullivan et al.'s (1990) CASA model.⁵ CASA is entirely length-based with population dynamic calculations in terms of the number of individuals in each length group during each year. Age is almost completely irrelevant in model calculations. Unlike many other length-based stock assessment approaches, CASA is a dynamic, non-equilibrium model based on a forward simulation approach. CASA incorporates a very wide range of data with parameter estimation based on maximum likelihood. CASA can incorporate prior information about parameters such as survey catchability and natural mortality in a quasi-Bayesian fashion and MCMC evaluations are practical. The implementation described here was programmed in AD-Model Builder (Otter Research Ltd.).⁶

Population dynamics

Time steps in the model are years, which are also used to tabulate catch and other data. Recruitment occurs at the beginning of each time step. All instantaneous rates in model calculations are annual (y^{-1}). The number of years in the model n_y is flexible and can be changed easily (e.g. for retrospective analyses) by making a single change to the input data file. Millimeters are used to measure body size (e.g. sea scallop shell heights). Length-weight relationships should generally convert millimeters to grams. Model input data include a scalar that is used to convert the units for length-weight parameters (e.g. grams) to the units of the biomass estimates and landings data (e.g. mt). The units for catch and biomass are usually metric tons.

The definition of length groups (or length “bins”) is a key element in the CASA model and length-structured stock assessment modeling in general. Length bins are identified in CASA output by their lower bound and internally by their ordinal number. Calculations requiring information about length (e.g. length-weight) use the mid-length ℓ_j of each bin. The user specifies the first length (L_{min}) and the size of length bins (L_{bin}). Based on these specifications, the model determines the number of length bins to be used in modeling as $n_L = 1 + \text{int}[(L_\infty - L_{min})/L_{bin}]$, where L_∞ is maximum asymptotic size supplied by the user, and $\text{int}[x]$ is the integer part of x . The last length bin in the model is always a “plus-group” containing individuals L_∞ and larger. Specifications for length data used in tuning the model are separate (see below).

⁵ Original programming in AD-Model Builder by G. Scott Boomer and Patrick J. Sullivan (Cornell University), who bear no responsibility for errors in the current implementation.

⁶ AD-Model Builder can be used to calculate variances for any estimated or calculated quantity in a stock assessment model, based on the Hessian matrix with “exact” derivatives and the delta method.

Growth

In population dynamics calculations, individuals in each size group grow (or not) at the beginning of the year, based on the annual growth transition matrix $P_0(b,a)$ which measures the probability that a survivor in size bin a at the beginning of the previous year will grow to bin b at the beginning of the current year (columns index initial size and rows index subsequent size).⁷ Growth probabilities do not include any adjustments for mortality and are applied to surviving scallops based on their original size in the preceding year.

There are two options for growth transition matrices. Under Option 1, a single annual growth matrix is calculated internally based on raw shell increment data:

$$P_0(b,a) = \frac{n(b|a)}{\sum_{j=a}^{n_L} n(j|a)}$$

where $n(b|a)$ is the number of individuals that started at size a and grew to size b after one year in the raw size increment data.

Under option 2, the user specifies the number of transition matrices to be supplied in the input file and then assigns one of the matrices to each year in the model. All such growth matrices must have the same number of length groups. The number and size groups in the model and in the growth matrices should be large enough to accommodate the largest maximum size in any year. If growth varies such that maximum size in some time period is lower the maximum value, then the growth transition probabilities for that period of maximum size are set to one along the diagonal. For example, if there were five length groups in the model: [20,25), [25,30), [30,35), [35,40) and [40,45+] mm SH and the maximum size was 34 mm SH in period one and 44 mm SH in period two, the growth transition matrices might look like:

Growth matrix for period 1

		Starting size				
		[20, 25)	[25, 30)	[30, 35)	[35, 40)	[40, 45)
Ending size	[20, 25)	0.7	0	0	0	0
	[25, 30)	0.2	0.7	0	0	0
	[30, 35)	0.1	0.3	1	0	0
	[35, 40)	0	0	0	1	0
	[40, 45)	0	0	0	0	1

Growth matrix for period 2

		Starting size				
		[20, 25)	[25, 30)	[30, 35)	[35, 40)	[40, 45)
Ending size	[20, 25)	0.7	0	0	0	0
	[25, 30)	0.2	0.7	0	0	0
	[30, 35)	0.1	0.2	0.7	0	0
	[35, 40)	0	0.1	0.2	0.7	0
	[40, 45)	0	0	0.1	0.3	1

Abundance, recruitment and mortality

Population abundance in each length bin during the first year of the model is:

⁷ For clarity in bookkeeping, mortality and annual growth calculations are always based on the size on January 1.

$$N_{1,L} = N_1 \pi_{1,L}$$

where L is the size bin, and $\pi_{1,L}$ is the initial population length composition expressed as

proportions so that $\sum_{L=1}^{n_L} \pi_L = 1$. $N_1 = e^\eta$ is total abundance at the beginning of the first modeled

year and η is an estimable parameter. It is not necessary to estimate recruitment in the first year because recruitment is implicit in the product of N_1 and π_L . The current implementation of CASA takes the initial population length composition as data supplied by the user, typically based on survey size composition data and a preliminary estimate of survey size-selectivity.

Abundance at length in years after the first is calculated:

$$\vec{N}_{y+1} = P_0 (\vec{N}_y \circ \vec{S}_y) + \vec{R}_{y+1}$$

where \vec{N}_y is a vector (length n_L) of abundance in each length bin during year y , P_0 is the matrix ($n_L \times n_L$) of annual growth probabilities $P_0(\mathbf{b}, \mathbf{a})$, \vec{S}_y is a vector of length-specific survival fractions for year y , \circ is the operator for an element-wise product, and \vec{R}_y is a vector holding length-specific abundance of new recruits at the beginning of year y .

Survival fractions are:

$$S_{y,L} = e^{-Z_{y,L}} = e^{-(M_{y,L} + F_{y,L} + I_{y,L})}$$

where $Z_{y,L}$ is the total instantaneous mortality rate and $M_{y,L}$ is the instantaneous rate for natural mortality (see below). Length-specific fishing mortality rates are $F_{y,L} = F_y s_{y,L}$ where $s_{y,L}$ is the size-specific selectivity⁸ for fishing in year y (scaled to a maximum of one at fully recruited size groups), F_y is the fishing mortality rate on fully selected individuals. Fully recruited fishing mortality rates are $F_y = e^{\phi + \delta_y}$ where ϕ is an estimable parameter for the log of the geometric mean of fishing mortality in all years, and δ_y is an estimable “dev” parameter.⁹ The instantaneous rate for “incidental” mortality ($I_{y,L}$) accounts for mortality due to contact with the fishing gear that does not result in any catch on deck (see below).¹⁰ The degree of variability in dev parameters for fishing mortality, natural mortality and for other variables can be controlled by specifying variances or likelihood weights $\neq 1$, as described below.

Natural mortality rates are calculated:

$$M_{y,L} = u_L e^{\zeta + \xi_y} + p_L \psi_y g$$

where \vec{u} holds length-specific adjustments to the natural mortality rate for each length group (input by the user and assumed constant over time), ζ is an estimable parameter measuring the mean log natural mortality rate during all years and ξ_y is an estimable year-specific dev parameter. The r.h.s. deals with density-dependent natural mortality which may be important in the population dynamics of small scallops after large recruitment events. In particular, p_L is a

8 In this context, “selectivity” describes the combined effects of all factors that affect length composition of catch or landings. These factors include gear selectivity, spatial overlap of the fishery and population, size-specific targeting, size-specific discard, etc.

9 Dev parameters are a special data type for estimable parameters in AD-Model Builder. Each set of dev parameters (e.g. for all recruitments in the model) is constrained to sum to zero. Because of the constraint, the sums $\phi + \delta_y$ involving $n_y + 1$ terms amount to only n_y parameters.

10. See the section on per recruit modeling below for formulas used to relate catch, landings and incidental mortality.

descending logistic function based on size (larger size groups experience less density dependent mortality), ψ_y is abundance of sea scallops used to calculate density dependent natural mortality, $g=e^\alpha$ is a multiplier that converts from units of abundance to units of instantaneous mortality, and α is an estimable scaling parameter. The logistic function is used to calculate the abundance that controls maximum density dependent mortality while reducing the importance of large individuals:

$$\psi_y = \sum_l p_L N_{y,L}$$

Where $N_{y,L}$ is on January 1.

The logistic function in density dependent mortality calculations is calculated:

$$p_L = 1 - \frac{1}{1 + e^{-b(L-a)}}$$

where b is the slope parameter and a is the L_{50} parameter. The logistic curve is flat or decreasing with size because $b=e^\alpha$ is > 0 where α is an estimable parameter. The L_{50} parameter is parameterized so that it automatically falls between the first and last sizes in the model:

$$a = L_{min} + (L_{max} - L_{min}) * \frac{e^\alpha}{1 + e^\alpha}$$

where L_{min} is the size at the bottom of the first size bin in the population model, L_{max} is the top of the last size bin, and α is an estimable parameter.

Incidental mortality $I_{y,L} = F_y u_L i$ is the product of fully recruited fishing mortality (F_y , a proxy for effective fishing effort, although nominal fishing effort might be a better predictor of incidental mortality), relative incidental mortality at length (u_L) and a scaling parameter i , both of which are supplied by the user and not estimable in the model. Incidental mortality at length is supplied by the user as a vector (\vec{u}) containing a value for each length group in the model. The model rescales the relative mortality vector so that the mean of the series is one.

Given abundance in each length group, natural mortality, and fishing mortality, predicted fishery catch-at-length in numbers is:

$$C_{y,L} = \frac{F_{y,L} (1 - e^{-Z_{y,L}}) N_{L,y}}{Z_{y,L}}$$

Total catch number during each year is $C_y = \sum_{j=1}^{n_L} C_{y,L}$. Catch data (in weight, numbers or as

length composition data) are understood to include landings (L_y) and discards (d_y) but to exclude losses to incidental mortality (i.e. $C_y=L_y+d_y$).

Discard data are supplied by the user in the form of discarded biomass in each year or a discard rate for each year (or a combination of biomass levels and rates). In the current model, discards have the same selectivity as landed catch and size composition data for discards are not included in the input file.¹¹ It is important to remember that discard rates in CASA are defined the ratio of discards to landings (d/L). The user may also specify a mortal discard fraction between zero and one if some discards survive. If the discard fraction is less than one, then the discarded biomass and discard rates in the model are reduced correspondingly. See the section on per recruit modeling below for formulas used to relate catch, landings and incidental mortality.

¹¹ The model will be modified in future to model discards and landing separately, and to use size composition data for discards.

Recruitment (the sum of new recruits in all length bins) at the beginning of each year after the first is calculated:

$$Ry = e^{\rho + \gamma_y}$$

where ρ is an estimable parameter that measures the geometric mean recruitment and the γ_y are estimable dev parameters that measure inter-annual variability in recruitment. As with natural mortality devs, the user specified variance or likelihood weight $\neq 1$ can be used to help estimate recruitment deviations (see below).

Proportions of recruits in each length group are calculated based on a beta distribution $B(w, r)$ over the first n_r length bins that is constrained to be concave down.¹² Proportions of new recruits in each size group are the same from year to year. Beta distribution coefficients must be larger than one for the shape of the distribution to be unimodal. Therefore, $w=1+e^\omega$ and $r=1+e^\rho$, where ω and ρ are estimable parameters. It is presumably better to calculate the parameters in this manner than as bounded parameters because there is likely to be less distortion of the Hessian for w and r values close to one and parameter estimation is likely to be more efficient.

Surplus production during each year of the model can be computed approximately from biomass and catch estimates (Jacobson et al., 2002):

$$P_t = B_{t+1} - B_t + C_t$$

In future versions of the CASA model, surplus production will be more calculated more accurately by projecting the population at the beginning of the year forward one year assuming only natural mortality.

Weight at length¹³

The assumed body weight for size bins except the last is calculated using user-specified length-weight parameters and the middle of the size group. Different length-weight parameters are used for the population and for the commercial fishery. Mean body weight in the last size bin is read from the input file and can vary from year to year. Typically, mean weight in the last size bin for the population would be computed based on survey length composition data for large individuals and the population length –weight relationship. Mean weight in the last size bin for the fishery would be computed in the same manner based on fishery size composition data.

In principle, these calculations could be carried out in the model itself because all of the required information is available. In practice, it seems better to do the calculations externally and supply them to the model as inputs because of decisions that typically have to be made about smoothing the estimates and years with missing data.

Population summary variables

Total abundance at the beginning of the year is the sum of abundance at length $N_{y,L}$ at the beginning of the year. Average annual abundance for a particular length group is:

¹² Standard beta distributions used to describe recruit size distributions and in priors are often constrained to be unimodal in the CASA model. Beta distributions $B(w, r)$ with mean $\mu = w/(w+r)$ and variance

$\sigma^2 = wr/[(w+r)^2(w+r+1)]$ are unimodal when $w > 1$ and $r > 1$. See

http://en.wikipedia.org/wiki/Beta_distribution for more information.

¹³ Model input data include a scalar that is used to convert the units for length-weight parameters (e.g. grams) to the units of the biomass estimates and landings data (e.g. mt).

$$\bar{N}_{y,L} = N_{y,L} \frac{1 - e^{-Z_{y,L}}}{Z_{y,L}}$$

The current implementation of the assessment model assumes different weight-at-length relationships for the stock and the fishery. Average stock biomass is computed using the population weight at length information.

Total stock biomass is:

$$B_y = \sum_{L=1}^{n_L} N_{y,L} w_L$$

where w_L is weight at length for the population on January 1. Total catch weight is:

$$W_y = \sum_{L=1}^{n_L} C_{y,L} w'_L$$

where w'_L is weight at length in the fishery.

F_y estimates for two years are comparable only when the fishery selectivity in the model was the same in both years. A simpler exploitation index is calculated for use when fishery selectivity changes over time:

$$U_y = \frac{C_y}{\sum_{j=x}^{n_L} N_{y,L}}$$

where x is a user-specified length bin (usually at or below the first bin that is fully selected during all fishery selectivity periods). U_y exploitation indices from years with different selectivity patterns may be relatively comparable if x is chosen carefully.

Spawner abundance in each year is (T_y) is computed:

$$T_y = \sum_{L=1}^{n_L} N_{y,L} e^{-\tau Z_{y,L}} g_L$$

Where $0 \leq \tau \leq 1$ is the fraction of the year elapsed before spawning occurs (supplied by the user). Maturity at length (g_L) is from an ascending logistic curve:

$$g_L = \frac{1}{1 + e^{a-bL}}$$

with parameters a and b supplied by the user. Spawner biomass is computed using the population length-weight values.

Egg production (S_y) in each year is computed:

$$S_y = \sum_{L=1}^{n_L} N_{y,L} e^{-\tau Z_{y,L}} g_L x_L$$

where:

$$x_L = cL^v$$

Where the fecundity parameters (c and v) for fecundity are supplied by the user. Fecundity parameters per se include no adjustments for maturity or survival. They should represent reproductive output for a spawner of given size.

Fishery and survey selectivity

The current implementation of CASA includes six options for calculating fishery and survey selectivity patterns. Fishery selectivity may differ among “fishery periods” defined by

the user. Selectivity patterns that depend on length are calculated using lengths at the mid-point of each bin (ℓ). After initial calculations (described below), selectivity curves are rescaled to a maximum value of one.

Option 1 is a flat with $s_L=1$ for all length bins. Option 2 is an ascending logistic curve:

$$s_{y,\ell} = \frac{1}{1 + e^{A_Y - B_Y \ell}}$$

Option 3 is an ascending logistic curve with a minimum asymptotic minimum size for small size bins on the left.

$$s_{y,\ell} = \left(\frac{1}{1 + e^{A_Y - B_Y \ell}} \right) (1 - D_Y) + D_Y$$

Option 4 is a descending logistic curve:

$$s_{y,\ell} = 1 - \frac{1}{1 + e^{A_Y - B_Y \ell}}$$

Option 5 is a descending logistic curve with a minimum asymptotic minimum size for large size bins on the right:

$$s_{y,\ell} = \left(1 - \frac{1}{1 + e^{A_Y - B_Y \ell}} \right) (1 - D_Y) + D_Y$$

Option 6 is a double logistic curve used to represent “domed-shape” selectivity patterns with highest selectivity on intermediate size groups:

$$s_{y,\ell} = \left(\frac{1}{1 + e^{A_Y - B_Y \ell}} \right) \left(1 - \frac{1}{1 + e^{D_Y - G_Y \ell}} \right)$$

The coefficients for selectivity curves A_Y , B_Y , D_Y and G_Y carry subscripts for time because they may vary between fishery selectivity periods defined by the user. All options are parameterized so that the coefficients A_Y , B_Y , D_Y and G_Y are positive. Under options 3 and 5, D_Y is a proportion that must lie between 0 and 1.

Depending on the option, estimable selectivity parameters may include α , β , δ and γ . For options 2, 4 and 6, $A_Y = e^{\alpha_Y}$, $B_Y = e^{\beta_Y}$, $D_Y = e^{\delta_Y}$ and $G_Y = e^{\gamma_Y}$. Options 3 and 5 use the same conventions for A_Y and B_Y , however, the coefficient D_Y is a proportion estimated as a logit-transformed parameter (i.e. $\delta_Y = \ln[D_Y/(1-D_Y)]$) so that:

$$D_Y = \frac{e^{\delta_Y}}{1 + e^{\delta_Y}}$$

The user can choose, independently of all other parameters, to either estimate each fishery selectivity parameter or to keep it at its initial value. Under Option 2, for example, the user can estimate the intercept α_Y , while keep the slope β_Y at its initial value.

Per recruit modeling

The per recruit model in CASA uses the same population model as in other model calculations under conditions identical to the last year in the model. It is a standard length-based approach except that discard and incidental mortality are accommodated in all calculations. In per recruit calculations, fishing mortality rates and associated yield estimates are understood to include landings and discard mortality, but to exclude incidental mortality. Thus, landings per recruit L are:

$$L = \frac{C}{(1 + \Delta)}$$

where C is total catch (yield) per recruit and Δ is the ratio of discards D to landings in the last year of the model. Discards per recruit are calculated:

$$D = \Delta L$$

Losses due to incidental mortality (G) are calculated:

$$G = \frac{I(1 - e^{-Z})B}{Z}$$

$$= IK$$

where $I = Fu$ is the incidental mortality rate, u is a user-specified multiplier (see above) and B is stock biomass per recruit. Note that $C = FK$ so that $K = C/F$. Then,

$$G = \frac{FuC}{F}$$

$$G = uC$$

The model will estimate a wide variety ($F_{\%SBR}$, F_{max} and $F_{0.1}$) of per recruit model reference points as parameters. For example,

$$F_{\%SBR} = e^{\theta_j}$$

where $F_{\%SBR}$ is the fishing mortality reference point that provides a user specified percentage of maximum SBR. θ_j is the model parameter for the j^{th} reference point.

A complete per recruit output table is generated in all model runs that can be used for evaluating the shape of YPR and SBR curves, including the existence of particular reference points.

Per recruit reference points are time consuming to estimate and it is usually better to estimate them after other more important population dynamics parameters are estimated. Phase of estimation can be controlled individually for %SBR, F_{MAX} and $F_{0.1}$ so that per recruit calculations can be delayed as long as possible. If the phase is set to zero or a negative integer, then the reference point will not be estimated. As described below, estimation of F_{max} always entails an additional phase of estimation. For example, if the phase specified for F_{max} is 2, then the parameter will be estimated initially in phase 2 and finalized the last phase (phase ≥ 3). This is done so that the estimate from phase 2 can be used as an initial value in a slightly different goodness of fit calculation during the latter phase.

Per recruit reference points should have no effect on other model estimates. Residuals (calculated – target) for %SBR, $F_{0.1}$ and F_{max} reference points should always be very close to zero. Problems may arise, however, if reference points (particularly F_{max}) fall on the upper bound for fishing mortality. In such cases, the model will warn the user and advise that the offending reference points should not be estimated. *It is good practice to run CASA with reference point calculations turned on and then off to see if biomass and fishing mortality estimates change.*

The user specifies the number of estimates required and the target %SBR level for each. For example, the target levels for four %SBR reference points might be 0.2, 0.3, 0.4 and 0.5 to estimate $F_{20\%}$, $F_{30\%}$, $F_{40\%}$ and $F_{50\%}$. The user has the option of estimating F_{max} and/or $F_{0.1}$ as model parameters also but it is not necessary to supply target values.

Tuning and goodness of fit

There are two steps in calculating the negative log likelihood (NLL) used to measure how well the model fits each type of data. The first step is to calculate the predicted values for data. The second step is to calculate the NLL of the data given the predicted value. The overall goodness of fit measure for the model is the weighted sum of NLL values for each type of data and each constraint:

$$\Lambda = \sum \lambda_j L_j$$

where λ_j is a weighting factor for data set j (usually $\lambda_j=1$, see below), and L_j is the NLL for the data set. The NLL for a particular data is itself is usually a weighted sum:

$$L_j = \sum_{i=1}^{n_j} \psi_{j,i} L_{j,i}$$

where n_j is the number of observations, $\psi_{j,i}$ is an observation-specific weight (usually $\psi_{j,i}=1$, see below), and $L_{j,i}$ is the NLL for a single observation.

Maximum likelihood approaches reduce the need to specify *ad-hoc* weighting factors (λ and ϕ) for data sets or single observations, because weights can often be taken from the data (e.g. using CVs routinely calculated for bottom trawl survey abundance indices) or estimated internally along with other parameters. In addition, robust maximum likelihood approaches (see below) may be preferable to simply down-weighting an observation or data set. However, despite subjectivity and theoretical arguments against use of *ad-hoc* weights, it is often useful in practical work to manipulate weighting factors, if only for sensitivity analysis or to turn an observation off entirely. Observation specific weighting factors are available for most types of data in the CASA model.

Missing data

Availability of data is an important consideration in deciding how to structure a stock assessment model. The possibility of obtaining reliable estimates will depend on the availability of sufficient data. However, NLL calculations and the general structure of the CASA model are such that missing data can usually be accommodated automatically. With the exception of catch data (which must be supplied for each year, even if catch was zero), the model calculates that NLL for each datum that is available. No NLL calculations are made for data that are not available and missing data do not generally hinder model calculations.

Likelihood kernels

Log likelihood calculations in the current implementation of the CASA model use log likelihood “kernels” or “concentrated likelihoods” that omit constants. The constants can be omitted because they do not affect slope of the NLL surface, final point estimates for parameters or asymptotic variance estimates. For data with normally distributed measurement errors, the complete NLL for one observation is:

$$L = \ln(\sigma) + \ln(\sqrt{2\pi}) + 0.5 \left(\frac{x-u}{\sigma} \right)^2$$

The constant $\ln(\sqrt{2\pi})$ can always be omitted. If the standard deviation is known or assumed known, then $\ln(\sigma)$ can be omitted as well because it is a constant that does not affect derivatives. In such cases, the concentrated NLL is:

$$L = 0.5 \left(\frac{x - \mu}{\sigma} \right)^2$$

If there are N observations with possible different variances (known or assumed known) and possibly different expected values:

$$L = 0.5 \sum_{i=1}^N \left(\frac{x_i - \mu_i}{\sigma_i} \right)^2$$

If the standard deviation for a normally distributed quantity is not known and is estimated (implicitly or explicitly) by the model, then one of two equivalent calculations is used. Both approaches assume that all observations have the same variance and standard deviation. The first approach is used when all observations have the same weight in the NLL:

$$L = 0.5N \ln \left[\sum_{i=1}^N (x_i - u)^2 \right]$$

The second approach is equivalent but used when the weights for each observation (w_i) may differ:

$$L = \sum_{i=1}^N w_i \left[\ln(\sigma) + 0.5 \left(\frac{x_i - u}{\sigma} \right)^2 \right]$$

In the latter case, the maximum likelihood estimator:

$$\hat{\sigma} = \sqrt{\frac{\sum_{i=1}^N (x_i - \hat{x})^2}{N}}$$

(where \hat{x} is the average or predicted value from the model) is used explicitly for σ . The maximum likelihood estimator is biased by $N/(N-d_f)$ where d_f is degrees of freedom for the model. The bias may be significant for small sample sizes, which are common in stock assessment modeling, but d_f is usually unknown.

If data x have lognormal measurement errors, then $\ln(x)$ is normal and L is calculated as above. In some cases it is necessary to correct for bias in converting arithmetic scale means to log scale means (and *vice-versa*) because $\bar{x} = e^{\bar{\chi} + \sigma^2/2}$ where $\chi = \ln(x)$. It is often convenient to convert arithmetic scale CVs for lognormal variables to log scale standard deviations using $\sigma = \sqrt{\ln(1 + CV^2)}$.

For data with multinomial measurement errors, the likelihood kernel is:

$$L = n \sum_{i=1}^n p_i \ln(\theta_i) - K$$

where n is the known or assumed number of observations (the “effective” sample size), p_i is the proportion of observations in bin i , and θ_i is the model’s estimate of the probability of an observation in the bin. For surveys, θ_i is adjusted for mortality up to the date of the survey and for growth up to the mid-point of the month in which the survey occurs. For fisheries, θ_i accommodates all of the mortality during the current year and is adjusted for growth during January 1 to mid-July. The constant K is used for convenience to make L easier to interpret. It measures the lowest value of L that could be achieved if the data fit matched the model’s expectations exactly:

$$K = n \sum_{i=1}^n p_i \ln(p_i)$$

For data x that have measurement errors with expected values of zero from a gamma distribution:

$$L = (\gamma - 1) \ln\left(\frac{x}{\beta}\right) - \frac{x}{\beta} - \ln(\beta)$$

where $\beta > 0$ and $\gamma > 0$ are gamma distribution parameters in the model. For data that lie between zero and one with measurement errors from a beta distribution:

$$L = (p - 1) \ln(x) + (q - 1) \ln(1 - x)$$

where $p > 0$ and $q > 0$ are parameters in the model.

In CASA model calculations, distributions are usually described in terms of the mean and CV. Normal, gamma and beta distribution parameters can be calculated mean and CV by the method of moments.¹⁴ Means, CV's and distributional parameters may, depending on the situation, be estimated in the model or specified by the user.

The NLL for a datum x from gamma distribution is:

$$L = (1 - k) * \ln(x) + \frac{x}{\theta} + \ln[\Gamma(k)] + k \ln(\theta)$$

where k is the shape parameter and θ is the scale parameter. The last two terms on the right are constants and can be omitted if k and θ are not estimated. Under these circumstances,

$$L = (1 - k) * \ln(x) + \frac{x}{\theta}$$

Robust methods

Goodness of fit for survey data may be calculated using a “robust” maximum likelihood method instead of the standard method that assumes lognormal measurement errors. The robust method may be useful when survey data are noisy or include outliers.

Robust likelihood calculations in CASA assume that measurement errors are from a Student's t distribution with user-specified degrees of freedom d_f . Degrees of freedom are specified independently for each observation so that robust calculations can be carried out for as many (or as few) cases as required. The t distribution is similar to the normal distribution for $d_f \geq 30$. As d_f is reduced, the tails of the t distribution become fatter so that outliers have higher probability and less effect on model estimates. If $d_f = 0$, then measurement errors are assumed in the model to be normally distributed.

The first step in robust NLL calculations is to standardize the measurement error residual $t = (x - \bar{x})/\sigma$ based on the mean and standard deviation. Then:

¹⁴ Parameters for standard beta distributions $B(w,r)$ with mean $\mu = w/(w+r)$ and variance

$\sigma^2 = wr/[(w+r)^2(w+r+1)]$ are calculated from user-specified means and variances by the method of moments. In particular, $w = \mu[\mu(1-\mu)/\sigma^2 - 1]$ and $r = (1-\mu)[\mu(1-\mu)/\sigma^2 - 1]$. Not all combinations of μ and σ^2 are feasible. In general, a beta distribution exists for combinations of μ and σ^2 if $0 < \mu < 1$ and $0 < \sigma^2 < \mu(1-\mu)$. Thus, for a user-specified mean μ between zero and one, the largest feasible variance is $\sigma^2 < \mu(1-\mu)$. These conditions are used in the model to check user-specified values for μ and σ^2 . See http://en.wikipedia.org/wiki/Beta_distribution for more information.

$$L = \ln\left(1 + \frac{t^2}{d_f}\right) \left(1 - \frac{1-d_f}{2}\right) - \frac{\ln(d_f)}{2}$$

Catch weight data

Catch data (landings plus discards) are assumed to have normally distributed measurement errors with a user specified CV. The standard deviation for catch weight in a particular year is $\sigma_y = \kappa \hat{C}_y$, where “^” indicates that the variable is a model estimate and errors in catch are assumed to be normally distributed. The standardized residual used in computing NLL for a single catch observation and in making residual plots is $r_y = (C_y - \hat{C}_y) / \sigma_y$.

Specification of landings, discards, catch

Landings, discard and catch data are in units of weight and are for a single or “composite” fishery in the current version of the CASA model. The estimated fishery selectivity is assumed to apply to the discards so that, in effect, the length composition of catch, landings and discards are the same.

Discards are from external estimates (d_t) supplied by the user. If $d_t \geq 0$, then the data are used as the ratio of discard to landed catch so that:

$$D_t = L_t \Delta_t$$

where $\Delta_t = D_t / L_t$ is the ratio of discard and landings (a.k.a. d/K ratios) for each year. If $d_t < 0$ then the data are treated as discard in units of weight:

$$D_t = \text{abs}(d_t).$$

In either case, total catch is the sum of discards and landed catch ($C_t = L_t + D_t$). It is possible to use discards in weight $d_t < 0$ for some years and discard as proportions $d_t > 0$ for other years in the same model run.

If catches are estimated (see below) so that the estimated catch \hat{C}_t does not necessarily equal observed landings plus discard, then estimated landings are computed:

$$\hat{L}_t = \frac{\hat{C}_t}{1 + \Delta_t}$$

Estimated discards are:

$$\hat{D}_t = \Delta_t \hat{L}_t.$$

Note that $\hat{C}_t = \hat{L}_t + \hat{D}_t$ as would be expected.

Fishery length composition data

Data describing numbers or relative numbers of individuals at length in catch data (fishery catch-at-length) are modeled as multinomial proportions $c_{y,L}$:

$$c_{y,L} = \frac{C_{y,L}}{\sum_{j=1}^{n_L} C_{y,j}}$$

The NLL for the observed proportions in each year is computed based on the kernel for the multinomial distribution, the model’s estimate of proportional catch-at-length (\hat{c}_y) and an

estimate of effective sample size cN_y supplied by the user. Care is required in specifying effective sample sizes, because catch-at-length data typically carry substantially less information than would be expected based on the number of individuals measured. Typical conventions make ${}^cN_y \leq 200$ (Fournier and Archibald, 1982) or set cN_y equal to the number of trips or tows sampled (Pennington et al., 2002). Effective sample sizes are sometimes chosen based on goodness of fits in preliminary model runs (Methot, 2000; Butler et al., 2003).

Standardized residuals are not used in computing NLL fishery length composition data. However, approximate standardized residuals $r_y = (c_{y,L} - \hat{c}_{y,L}) / \sigma_{y,L}$ with standard deviations $\sigma_{y,L} = \sqrt{\hat{c}_{y,L}(1 - \hat{c}_{y,L}) / {}^cN_y}$ based on the theoretical variance for proportions are computed for use in making residual plots.

Survey index data

In CASA model calculations, “survey indices” are data from any source that reflect relative proportional changes in an underlying population state variable. In the current version, surveys may measure stock abundance at a particular point in time (e.g. when a survey was carried out), stock biomass at a particular point in time, or numbers of animals that dies of natural mortality during a user-specified period. For example, the first option is useful for bottom trawl surveys that record numbers of individuals, the second option is useful for bottom trawl surveys that record total weight, and the third option is useful for survey data that track trends in numbers of animals that died due to natural mortality (e.g. survey data for sea scallop “clappers”). Survey data that measure trends in numbers dead due to natural mortality can be useful in modeling time trends in natural mortality. In principle, the model will estimate model natural mortality and other parameters so that predicted numbers dead and the index data match in either relative or absolute terms.

In the current implementation of the CASA model, survey indices are assumed to be linear indices of abundance or biomass so that changes in the index (apart from measurement error) are assumed due to proportional changes in the population. Nonlinear commercial catch rate data are handled separately (see below). Survey index and fishery length composition data are handled separately from trend data (see below). Survey data may or may not have corresponding length composition information.

In general, survey index data give one number that summarizes some aspect of the population over a wide range of length bins. Selectivity parameters measure the relative contribution of each length bin to the index. Options and procedures for estimating survey selectivity patterns are the same as for fishery selectivity patterns, but survey selectivity patterns are not allowed to change over time.

NLL calculations for survey indices use predicted values calculated:

$$\hat{I}_{k,y} = q_k A_{k,y}$$

where q_k is a scaling factor for survey index k , and $A_{k,y}$ is stock available to the survey. The scaling factor is computed using the maximum likelihood estimator:

$$q_k = e^{\frac{\sum_{i=1}^{N_k} \left[\ln \left(\frac{I_{k,i}}{A_{k,i}} \right) / \sigma_{k,i}^2 \right]}{\sum_{j=1}^{N_k} \left(1 / \sigma_{k,j}^2 \right)}}$$

where N_v and $\sigma_{k,j}^2$ is the log scale variance corresponding to the assumed CV for the survey observation.¹⁵

Available stock for surveys measuring trends in abundance or biomass is calculated:

$$A_{k,y} = \sum_{L=1}^{n_L} s_{k,L} N_{y,L} e^{-Z_{y,L} \tau_{k,y}}$$

where $s_{k,L}$ is size-specific selectivity of the survey, $\tau_{k,y} = J_{k,y} / 365$, $J_{k,y}$ is the Julian date of the survey in year y , and $e^{-Z_{y,L} \tau_{k,y}}$ is a correction for mortality prior to the survey. Available biomass is calculated in the same way except that body weights w_L are included in the product on the right hand side.

Available stock for indices that track numbers dead by natural mortality is:

$$A_{k,y} = \sum_{L=1}^{n_k} s_{k,L} \tilde{M}_{y,L} \bar{N}_{y,L}$$

where $\bar{N}_{y,L}$ is average abundance during the user-specified period of availability and $\tilde{M}_{y,L}$ is the instantaneous rate of natural mortality for the period of availability. Average abundance during the period of availability is:

$$\bar{N}_{y,L} = \frac{\tilde{N}_{y,L} (1 - e^{-\tilde{Z}_{y,L}})}{\tilde{Z}_{y,L}}$$

where $\tilde{N}_{y,L} = N_{y,L} e^{-Z\Delta}$ is abundance at elapsed time of year $\Delta = \tau_{k,y} - \nu_k$, $\nu_k = j_k / 365$, and j_k is the user-specified duration in days for the period of availability. The instantaneous rates for total $\tilde{Z}_{y,L} = Z_{y,L} (\tau_{k,y} - \nu_k)$ and natural $\tilde{M}_{y,L} = M_{y,L} (\tau_{k,y} - \nu_k)$ mortality are also adjusted to correspond to the period of availability. In using this approach, the user should be aware that the length based selectivity estimated by the model for the dead animal survey ($s_{k,L}$) is conditional on the assumed pattern of length-specific natural mortality (\bar{u}) which was specified as data in the input file.

NLL calculations for survey index data assume that log scale measurement errors are either normally distributed (default approach) or from a t distribution (robust estimation approach). In either case, log scale measurement errors are assumed to have mean zero and log scale standard errors either estimated internally by the model or calculated from the arithmetic CVs supplied with the survey data.

¹⁵ Scaling factors in previous versions were calculated $q_s = e^{\varpi_s}$ where ϖ_s is an estimable and survey-specific parameter. However, prior distributions were shown to have a strong effect on the parameters such that the relationship $N=qA$ did not hold. The approach in the current model avoids this problem.

The standardized residual used in computing NLL for one survey index observation is $r_{k,y} = \ln(I_{k,y}/\hat{I}_{k,y})/\sigma_{k,y}$ where $I_{k,y}$ is the observation. The standard deviations $\sigma_{k,y}$ will vary among surveys and years if CVs are used to specify the variance of measurement errors. Otherwise a single standard deviation is estimated internally for the survey as a whole.

Survey length composition data

Length bins for fishery and survey length composition data are flexible and the flexibility affects goodness of fit calculations in ways that may be important to consider in some applications. The user specifies the starting size (bottom of first bin) and number of bins used for each type of fishery and survey length composition. The input data for each length composition record identifies the first/last length bins to be used and whether they are plus groups that should include all smaller/larger length groups in the data and population model when calculating goodness of fit. Goodness of fit calculations are carried out over the range of lengths specified by the user. Thus length data in the input file may contain large or small size bins that are ignored in goodness of fit calculations. As described above, the starting size and bin size for the population model are specified separately. In the ideal and simplest case, the minimum size and same length bins are used for the population and for all length data. However, as described below, length specifications in data and the population model may differ.

For example, the implicit definitions of plus groups in the model and data may differ. If the first bin used for length data is a plus group, then the first bin will contain the sum of length data from the corresponding and smaller bins of the original length composition record. However, the first bin in the population model is never a plus group. Thus, predicted values for a plus group will contain the sum of the corresponding and smaller bins in the population. The observed and predicted values will not be perfectly comparable if the starting sizes for the data and population model differ. Similarly, if the last bin in the length data is a plus group, it will contain original length composition data for the corresponding and all larger bins. Predicted values for a plus group in the population will be the sum for the corresponding bin and all larger size groups in the population, implicitly including sizes $> L_{\infty}$. The two definitions of the plus group will differ and goodness of fit calculation may be impaired if the original length composition data does not include all of the large individuals in samples.

In the current version of the CASA model, the size of length composition bins must be $\geq L_{bin}$ in the population model (this constraint will be removed in later versions). Ideally, the size of data length bins is the same or a multiple of the size of length bins in the population. However, this is not required and the model will prorate the predicted population composition for each bin into adjacent data bins when calculating goodness of fit. With a 30-34 mm population bin and 22-31 and 32-41 mm population bins, for example, the predicted proportion in the population bin would be prorated so that 2/5 was assigned to the first data bin and 3/5 was assigned to the second data bin. This proration approach is problematic when it is used to prorate the plus group in the population model into two data bins because it assumes that abundance is uniform over lengths within the population group. The distribution of lengths in a real population might be far from uniform between the assumed upper and lower bounds of the plus group.

The first bin in each length composition data record must be $\geq L_{min}$ which is the smallest size group in the population model. If the last data bin is a plus group, then the *lower* bound of the last data bin must be \leq the upper bound of the last population bin. Otherwise, if the last data bin is not a plus group, the *upper* bound of the last data bin must be \leq the upper bound of the

population bin.

NLL calculations for survey length composition data are similar to calculations for fishery length composition data. Surveys index data may measure trends in stock abundance or biomass but survey length composition data are always for numbers (not weight) of individuals in each length group. Survey length composition data represent a sample from the true stock which is modified by survey selectivity, sampling errors and, if applicable, errors in recording length data. For example, with errors in length measurements, individuals belonging to length bin j , are mistakenly assigned to adjacent length bins $j-2, j-1, j+1$ or $j+2$ with some specified probability. Well-tested methods for dealing with errors in length data can be applied if some information about the distribution of the errors is available (e.g. Methot 2000).

Prior to any other calculations, observed survey length composition data are converted to multinomial proportions:

$$i_{k,y,L} = \frac{n_{k,y,L}}{\sum_{j=L_{k,y}^{first}}^{L_{k,y}^{last}} n_{k,y,j}}$$

where $n_{k,y,j}$ is an original datum and $i_{k,y,L}$ is the corresponding proportion. As described above, the user specifies the first $L_{k,y}^{first}$ and last $L_{k,y}^{last}$ length groups to be used in calculating goodness of fit for each length composition and specifies whether the largest and smallest groups should be treated as “plus” groups that contain all smaller or larger individuals.

Using notation for goodness of fit survey index data (see above), predicted length compositions for surveys that track abundance or biomass are calculated:

$$A_{k,y,L} = \frac{s_{k,L} N_{y,L} e^{-Z_{y,j} \tau_{k,y}}}{\sum_{L=L_{k,y}^{first}}^{L_{k,y}^{last}} s_{k,j} N_{y,j} e^{-Z_{y,j} \tau_{k,y}}}$$

Predicted length compositions for surveys that track numbers of individuals killed by natural mortality are calculated:

$$A_{k,y} = \frac{s_{k,L} \tilde{M}_{y,L} \bar{N}_{y,L}}{\sum_{L=L_{k,y}^{first}}^{L_{k,y}^{last}} s_{k,L} \tilde{M}_{y,L} \bar{N}_{y,L}}$$

Considering the possibility of structured measurement errors, the expected length composition $\bar{A}'_{k,y}$ for survey catches is:

$$\bar{A}'_{k,y} = \bar{A}_{k,y} E_k$$

where E_k is an error matrix that simulates errors in collecting length data by mapping true length bins in the model to observed length bins in the data.

The error matrix E_k has n_L rows (one for each true length bin) and n_L columns (one for each possible observed length bin). For example, row k and column j of the error matrix gives the conditional probability $P(k|j)$ of being assigned to bin k , given that an individual actually belongs to bin j . More generally, column j gives the probabilities that an individual actually belonging to length bin j will be recorded as being in length bins $j-2, j-1, j, j+1, j+2$ and so on. The columns of E_k add to one to account for all possible outcomes in assigning individuals to observed length bins. E_k is the identity matrix if there are no structured measurement errors.

In CASA, the probabilities in the error matrix are computed from a normal distribution with mean zero and $CV = e^{\pi_k}$, where π_k is an estimable parameter. The normal distribution is truncated to cover a user-specified number of observed bins (e.g. 3 bins on either side of the true length bin).

The NLL for observed proportions at length in each survey and year is computed with the kernel for a multinomial distribution, the model's estimate of proportional survey catch-at-length ($\hat{i}_{k,y,L}$) and THE effective sample size ${}^L N_y$ supplied by the user. Standardized residuals for residual plots are computed as for fishery length composition data.

Effective sample size for length composition data

Effective sample sizes that are specified by the user are used in goodness of fit calculations for survey and fishery length composition data. A post-hoc estimate of effective sample size can be calculated based on goodness of fit in a model run (Methot 1989). Consider the variance of residuals for a single set of length composition data with N bins used in calculations. The variance of the sum based on the multinomial distribution is:

$$\sigma^2 = \sum_{j=1}^N \left[\frac{\hat{p}_j (1 - \hat{p}_j)}{\varphi} \right]$$

where φ is the effective sample size for the multinomial and \bar{p}_j is the predicted proportion in the j^{th} bin from the model run. Solve for φ to get:

$$\varphi = \frac{\sum_{j=1}^N [\hat{p}_j (1 - \hat{p}_j)]}{\sigma^2}$$

The variance of the sum of residuals can also be calculated:

$$\sigma^2 = \sum_{j=1}^N (p_j - \hat{p}_j)^2$$

This formula is approximate because it ignores the traditional correction for bias. Substitute the third expression into the second to get:

$$\varphi = \frac{\sum_{j=1}^N [\hat{p}_j (1 - \hat{p}_j)]}{\sum_{k=1}^N (p_j - \hat{p}_j)^2}$$

which can be calculated based on model outputs. The assumed and effective sample sizes will be similar in a reasonable model when the assumed sample sizes are approximately correct. Effective sample size calculations can be used iteratively to manually adjust input values to

reasonable levels (Methot 1989).

Variance constraints on dev parameters

Variability in dev parameters (e.g. for natural mortality, recruitment or fishing mortality) can be limited using variance constraints that assume the deviations are either independent or that they are autocorrelated and follow a random walk. When a variance constraint for independent deviations is activated, the model calculates the NLL for each log scale residual γ_y / σ_γ , where γ_y is a dev parameter and σ is a log-scale standard deviation. If the user supplies a positive value for the arithmetic scale CV, then the NLL is calculated assuming the variance is known. Otherwise, the user-supplied CV is ignored and the NLL is calculated with the standard deviation estimated internally. Calculations for autocorrelated deviations are the same except that the residuals are $(\gamma_y - \gamma_{y-1}) / \sigma_\gamma$ and the number of residuals is one less than the number of dev parameters.

LPUE data

Commercial landings per unit of fishing effort (LPUE) data are modeled in the current implementation of the CASA model as a linear function of average biomass available to the fishery, and as a nonlinear function of average available abundance. The nonlinear relationship with abundance is meant to reflect limitations in “shucking” capacity for sea scallops.¹⁶ Briefly, tows with large numbers of scallops require more time to sort and shuck and therefore reduce LPUE from fishing trips when abundance is high. The effect is exaggerated when the catch is composed of relatively small individuals. In other words, at any given level of stock biomass, LPUE is reduced as the number of individuals in the catch increases or, equivalently, as the mean size of individuals in the catch is reduced.

Average available abundance in LPUE calculations is:

$${}^a\bar{N}_y = \sum_{L=1}^{n_L} s_{y,L} \bar{N}_{y,L}$$

and average available biomass is:

$${}^a\bar{B}_y = \sum_{L=1}^{n_L} s_{y,L} w_L^f \bar{N}_{y,L}$$

where the weights at length w_L^f are for the fishery rather than the population. Predicted values for LPUE data are calculated:

$$\hat{L}_y = \frac{{}^a\bar{B}_y \eta}{\sqrt{\phi^2 + {}^a\bar{N}_y^2}}$$

Measurement errors in LPUE data are assumed normally distributed with standard deviations $\sigma_y = CV_y \hat{L}_y$. Standardized residuals are $r_y = (L_y - \hat{L}_y) / \sigma_y$.

¹⁶ D. Hart, National Marine Fisheries Service, Northeast Fisheries Science Center, Woods Hole, MA, pers. comm.

Per recruit (SBR and YPR) reference points¹⁷

The user specifies a target %SBR value for each reference point that is estimated. Goodness of fit is calculated as the sum of squared differences between the target %SBR and %SBR calculated based on the reference point parameter. Except in pathological situations, it is always possible to estimate %SBR reference point parameters so that the target and calculated %SBR levels match exactly. Reference point parameters should have no effect on other model estimates and the residual (calculated – target %SBR) should always be very close to zero.

Goodness of fit for $F_{0.1}$ estimates is calculated in a manner similar to %SBR reference points. Goodness of fit is calculated as the squared difference between the slope of the yield curve at the estimate and one-tenth of the slope at the origin. Slopes are computed numerically using central differences if possible or one-sided (right hand) differences if necessary.

F_{max} is estimated differently in preliminary and final phases. In preliminary phases, goodness of fit for F_{max} is calculated as $(1/Y)^2$, where Y is yield per recruit at the current estimate of F_{max} . In other words, yield per recruit is maximized by finding the parameter estimate that minimizes its inverse. This preliminary approach is very robust and will find F_{max} if it exists. However, it involves a non-zero residual $(1/Y)$ that interferes with calculation of variances and might affect other model estimates. In final phases, goodness of fit for F_{max} is calculated as (d^2) where d is the slope of the yield per recruit curve at F_{max} . The two approaches give the same estimates of F_{MAX} but the goodness of fit approach used in the final phases has a residual of zero (so that other model estimates are not affected) and gives more reasonable variance estimates. The latter goodness of fit calculation is not used during initial phases because the estimates of F_{MAX} tend to “drift down” the right hand side of the yield curve in the direction of decreasing slope. Thus, the goodness of fit calculation used in final phases works well only when the initial estimate of F_{MAX} is very close to the best estimate.

Per recruit reference points should have little or no effect on other model estimates. Problems may arise, however, if reference points (particularly F_{max}) fall on the upper bound for fishing mortality. In such cases, the model will warn the user and advise that the offending reference points should not be estimated. *It is good practice to run CASA with and without reference point calculations to ensure that reference points do not affect other model estimates including abundance, recruitments and fishing mortality rates.*

Growth data

Growth data in CASA consist of records giving initial length, length after one year of growth, and number of corresponding observations. Growth data may be used to help estimate growth parameters that determine the growth matrix P . The first step is to convert the data for each starting length to proportions:

$$P(b, a) = \frac{n(b, a)}{\sum_{j=n_L-b+1}^{n_L} n(j, a)}$$

where $n(b, a)$ is the number of individuals starting at size a that grew to size b after one year. The NLL is computed assuming that observed proportions $p(a|b)$ at each starting size are a sample from a multinomial distribution with probabilities given by the corresponding column in the

¹⁷ This approach is not currently estimated because of performance problems. The user can, however, estimate per recruit reference point from a detailed table written in the main output file (nc.rep). However, variances are not available in the table.

models estimated growth matrix P . The user must specify an effective sample size $^P N_j$ based, for example, on the number of observations in each bin or the number of individuals contributing data to each bin. Observations outside bin ranges specified by the user are ignored. Standardized residuals for plotting are computed based on the variance for proportions.

Survey gear efficiency data

Survey gear efficiency for towed trawls and dredges is the probability of capture for individuals anywhere in the water column or sediments along the path swept by the trawl. Ideally, the area surveyed and the distribution of the stock coincides so that:

$$I_{k,y} = q_k B_{k,y}$$

$$q_k = \frac{a_k e_k u_k}{A}$$

$$e_k = \frac{A q_k}{a_k u_k}$$

$$K_t = \frac{A}{a_k u_k}$$

$$e_k = K_t q_t$$

Where $I_{k,y}$ is a survey observation in units equivalent to biomass (or numerical) density (e.g. kg per standard tow), $B_{k,y}$ is the biomass (or abundance) available to the survey, A is the area of the stock, a_k is the area swept during one tow, $0 < e_k \leq 1$ is efficiency of the survey gear, and u_k is a constant that adjusts for different units.

Efficiency estimates from studies outside the CASA model may be used as prior information in CASA. The user supplies the mean and CV for the prior estimate of efficiency, along with estimates of A_k , a_k and u_k . At each iteration if the model, the gear efficiency implied by the current estimate of q_k is computed. The model then calculates the NLL of the implied efficiency estimate assuming it was sampled from a unimodal beta distribution with the user-specified mean and CV.

If efficiency estimates are used as prior information (if the likelihood weight $\lambda > 0$), then it is very important to make sure that units and values for the survey data (I), biomass or abundance (B), stock area (A), area per tow (a), and adjustments for units (u) are correct (see Example 1). The units for biomass are generally the same as the units for catch data. In some cases, incorrect specifications will lead to implied efficiency estimates that are ≤ 0 or ≥ 1 which have zero probability based on a standard beta distribution used in the prior. The program will terminate if $e \leq 0$. If $e \geq 1$ during an iteration, then e is set to a value slightly less than one and a penalty is added to the objective function. In some cases, incorrect specifications will generate a cryptic error that may have a substantial impact on estimates.

Implied efficiency estimates are useful as a model diagnostic even if very little prior information is available because some model fits may imply unrealistic levels of implied efficiency. The trick is to down weight the prior information (e.g. $\lambda = 1e^{-6}$) so that the implied efficiency estimate has very little effect on model results as long as $0 < e < 1$. Depending on the situation, model runs with e near a bound indicate that estimates may be implausible. In

addition, it may be useful to use a beta distribution for the prior that is nearly a uniform distribution by specifying a prior mean of 0.5 and variance slightly less than $1/12=0.083333$.

Care should be taken in using prior information from field studies designed to estimate survey gear efficiency. Field studies usually estimate efficiency with respect to individuals on the same ground (e.g. by sampling the same grounds exhaustively or with two types of gear). It seems reasonable to use an independent efficiency estimate and the corresponding survey index to estimate abundance in the area surveyed. However, stock assessment models are usually applied to the entire stock, which is probably distributed over a larger area than the area covered by the survey. Thus the simple abundance calculation based on efficiency and the survey index will be biased low for the stock as a whole. In effect, efficiency estimates from field studies tend to be biased high as estimates of efficiency relative to the entire stock.

Maximum fishing mortality rate

Stock assessment models occasionally estimate absurdly high fishing mortality rates because abundance estimates are too small. The NLL component used to prevent this potential problem is:

$$L = \lambda \sum_{t=0}^N (d_t^2 + q^2)$$

where:

$$d_t = \begin{cases} Ft - \Phi & \text{if } Ft > \Phi \\ 0 & \text{otherwise} \end{cases}$$

and

$$q_t = \begin{cases} \ln(Ft/\Phi) & \text{if } Ft > \Phi \\ 0 & \text{otherwise} \end{cases}$$

with the user-specified threshold value Φ set larger than the largest value of F_t that might possibly be expected (e.g. $\Phi=3$). The weighting factor λ is normally set to a large value (e.g. 1000).

References

- J.L. Butler, L.D. Jacobson, J.T. Barnes, and H.G. Moser. 2003. Biology and population dynamics of cowcod (*Sebastes levis*) in the southern California Bight. *Fish. Bull.* 101: 260-280.
- Fournier, D., and Archibald, CP. 1982. General theory for analyzing catch at age data. *Can. J. Fish. Aquat. Sci.* 39: 1195-1207.
- Jacobson, L.D., Cadrin, S.X., and J.R. Weinberg. 2002. Tools for estimating surplus production and F_{MSY} in any stock assessment model. *N. Am. J. Fish. Mgmt.* 22: 326-338.
- Methot, R. D. 2000. Technical description of the stock synthesis assessment program. NOAA Tech. Memo. NMFS-NWFSC-43: 1-46.
- Pennington, M., Burmeister, L-M., and Hjellvik, V. 2002. Assessing the precision of frequency distributions estimated from trawl-survey samples. *Fish. Bull.* 100: 74-80.
- Press, W.H., Flannery, B.P., S.A. Teukolsky, and W.T. Vetterling. 1990. Numerical recipes. Cambridge Univ. Press, NY.
- Sullivan, P.J., Lai, H.L., and Gallucci, V.F. 1990. A catch-at-length analysis that incorporates a stochastic model of growth. *Can. J. Fish. Aquat. Sci.* 47: 184-198.

Appendix B10. Forecasting methodology (SAMS model)

Dvora Hart, Northeast Fisheries Science Center, Woods Hole, MA.

The model presented here is a version of the SAMS (Scallop Area Management Simulator) model used to project sea scallop abundance and landings as an aid to managers since 1999. Subareas were chosen to coincide with current management. In particular, Georges Bank was divided into four open areas (two portions of the South Channel, Northern Edge and Peak, and Southeast Part), the three access portions of the groundfish closures, and the three no access portions of these areas. The Mid-Atlantic was subdivided into seven areas: Virginia Beach, the Delmarva, Elephant Trunk Closed Area and Hudson Canyon South Rotational Areas, New York Bight, Inshore New York Bight, and Long Island.

Methods

The model tracks population vectors $\mathbf{p}(i,t) = (p_1, p_2, \dots, p_n)$, where $p_j(i,t)$ represents the density of scallops in the j th size class in area i at time t . The model uses a difference equation approach, where time is partitioned into discrete time steps t_1, t_2, \dots , with a time step of length $\Delta t = t_{k+1} - t_k$. The landings vector $\mathbf{h}(i,t_k)$ represents the catch at each size class in the i th region and k th time step. It is calculated as:

$$h(i,t_k) = [I - \exp(\Delta t H(i,t_k))] p(i,t_k),$$

where I is the identity matrix and H is a diagonal matrix whose j th diagonal entry h_{jj} is given by:

$$h_{jj} = 1/(1 + \exp(s_0 - s_1 * s))$$

where s is the shell height of the mid-point of the size-class.

The landings $L(i,t_k)$ for the i th region and k th time step are calculated using the dot product of landings vector $\mathbf{h}(i,t_k)$ with the vector $\mathbf{m}(i)$ representing the vector of meat weights at shell height for the i th region:

$$L(i,t_k) = A_i \mathbf{h}(i,t_k) \bullet \mathbf{m}(i)$$

where e_i represents the dredge efficiency in the i th region.

Even in the areas not under special area management, fishing mortalities tend not to be spatially uniform due to the sessile nature of sea scallops (Hart 2001). Fishing mortalities in open areas were determined by a simple “fleet dynamics model” that estimates fishing mortalities in open areas based on area-specific catch rates, and so that the overall DAS or open-area F matches the target. Based on these ideas, the fishing mortality F_i in the i th region is modeled as:

$$F_i = k * f_i * L_i$$

where L_i is the estimated LPUE (landings per day charged) in the i th region, f_i is an area-specific adjustment factor to take into account preferences for certain fishing grounds (due to lower costs, shorter steam times, ease of fishing, habitual preferences, etc.), and k is a constant adjusted so that the total DAS or fishing mortality meets its target. For these simulations, $f_i = 1$ for all areas.

Scallops of shell height less than a minimum size s_d are assumed to be discarded, and suffer a discard mortality rate of d , taken here, as in the rest of the assessment to be 20%. There is also evidence that some scallops not actually landed may suffer mortality due to incidental damage from the dredge. Let F_L be the landed fishing mortality rate and F_I be the rate of incidental mortality on scallops not caught. For Georges Bank, which is a mix of sandy and hard bottom, we used $F_I = 0.2F_L$. For the Mid-Atlantic (almost all sand), we used $F_I = 0.1F_L$. Incidental mortality for a given shell height bin was then calculated using equations (4.3) and (4.4) of the main document.

Growth in each subarea was specified by a growth transition matrix G , based on area-specific growth increment data from 2001-2012. Recruitment was modeled stochastically, and was assumed to be log-normal in each subarea. The mean, variance and covariance of the recruitment in a subarea was set to be equal to that observed in the historical time-series between 1979-2013. New recruits enter the first size bin at each time step at a rate r_i depending on the subarea i , and stochastically on the year. These simulations assume that recruitment is a stationary process, i.e., no stock-recruitment relationship is assumed. This may underestimate recruitment in the Mid-Atlantic if the recent strong recruitment there are due to a stock-recruit relationship.

The population dynamics of the scallops in the present model can be summarized in the equation:

$$p(i, t_{k+1}) = \rho_i + G \exp(-M\Delta t H) p(i, t_k),$$

where ρ_i is a random variable representing recruitment in the i th area. The model was run with 10 time steps per year. The population and harvest vectors are converted into biomass by using the shell-height meat-weight relationship:

$$W = \exp[a + b \ln(s)],$$

where W is the meat weight of a scallop of shell height s . These relationships are subarea-specific; see Appendix B3 for details. For calculating biomass, the shell height of a size class was taken as its midpoint.

Commercial landing rates (LPUE, landed meat weight per day) were estimated using an empirical function based on the observed relationship between annual landing rates, expressed as number caught per day (NLPUE) and survey exploitable numbers per tow. At low biomass levels, NLPUE increases roughly linearly with survey abundance. However, at high abundance levels, the catch rate of the gear will exceed that which can be shucked by a seven-man crew. This is similar to the situation in predator/prey theory, where a predator's consumption rate is limited by the time required to handle and consume its prey (Holling 1959). The original Holling Type-II predator-

prey model assumes that handling and foraging occur sequentially. It predicts that the per-capita predation rate R will be a function of prey abundance N according to a Monod functional response:

$$R = \frac{\alpha N}{\beta + N},$$

where α and β are constants. In the scallop fishery, however, some handling (shucking) can occur while foraging (fishing), though at a reduced rate because the captain and one or two crew members need to break off shucking to steer the vessel during towing and to handle the gear during haulback.

The fact that a considerable amount of handling can occur at the same time as foraging means that the functional response of a scallop vessel will saturate quicker than predicted by the above equation. To account for this, a modified Holling Type-II model was used, so that the landings (in numbers of scallops) per unit effort (DAS) L (the predation rate, i.e., NLPUE) will depend on scallop (prey) exploitable numbers N according to the formula:

$$L = \frac{\alpha N}{\sqrt{\beta^2 + N^2}}.$$

The parameters α and β to this model were fit to the observed fleet-wide LPUE vs. exploitable biomass relationship during the years 1994-2012 (previous years were not used because of the change from port interviews to logbook reporting). The number of scallops that can be shucked should be nearly independent of size provided that the scallops being shucked are smaller than about a 20 count. The time to shuck a large scallop will go up modestly with size. To model this, if the mean meat weight of the scallops caught, g , in an area is more than 20 g, the parameters α and β in the above equation are reduced by a factor $\sqrt{20/g}$. This means, for example, that a crew could shuck fewer 10 count scallops per hour than 20 count scallops in terms of numbers, but more in terms of weight.

An estimate of the fishing mortality imposed in an area by a single DAS of fishing in that area can be obtained from the formula $F_{\text{DAS}} = L_a/N_a$, where L_a is the NLPUE in that area obtained as above, and N_a is the exploitable abundance (expressed as absolute numbers of scallops) in that area. This allows for conversion between units of DAS and fishing mortality.

Initial conditions for the population vector $\mathbf{p}(i,t)$ were estimated using the 2013 surveys, with the overall estimates scaled to match the 2013 biomass as estimated by CASA. The 2013 initial conditions were varied depending on the survey standard errors in each subarea, and scaled so that the initial standard error in biomass was about 15,000 mt, a figure that the working group considered a fair measure of the true uncertainty in the initial estimates.